

TRIUMF



ANNUAL REPORT SCIENTIFIC ACTIVITIES 1998

CANADA'S NATIONAL MESON FACILITY
OPERATED AS A JOINT VENTURE BY:

MEMBERS:

UNIVERSITY OF ALBERTA
SIMON FRASER UNIVERSITY
UNIVERSITY OF VICTORIA
UNIVERSITY OF BRITISH COLUMBIA

ASSOCIATE MEMBERS:

UNIVERSITY OF MANITOBA
UNIVERSITÉ DE MONTRÉAL
UNIVERSITY OF TORONTO
UNIVERSITY OF REGINA
CARLETON UNIVERSITY
QUEEN'S UNIVERSITY

UNDER A CONTRIBUTION FROM THE
NATIONAL RESEARCH COUNCIL OF CANADA

APRIL 1999

TRIUMF

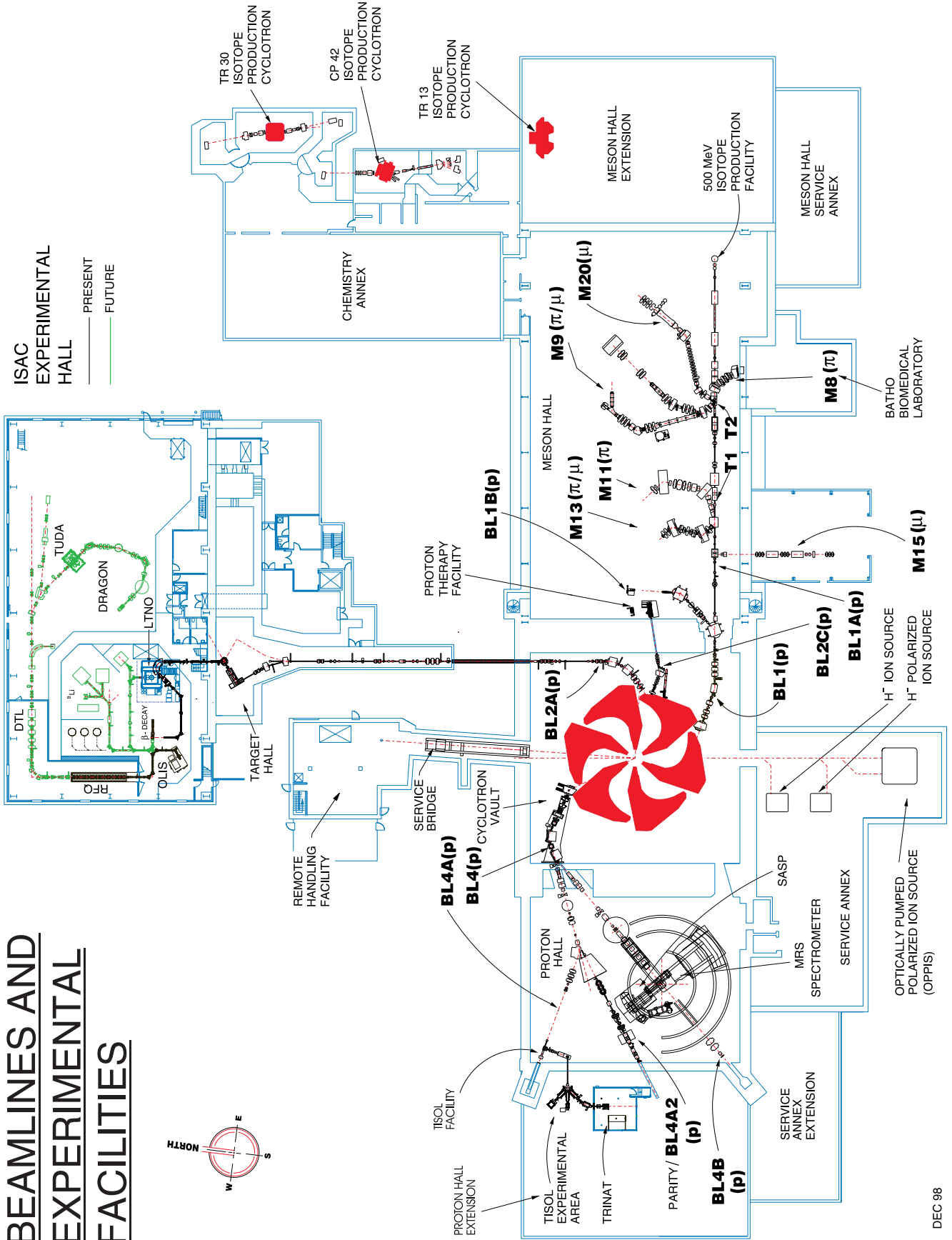
ANNUAL REPORT SCIENTIFIC ACTIVITIES 1998

Postal Address:

TRIUMF
Publications Office
4004 Wesbrook Mall
Vancouver, B.C.
Canada
V6T 2A3

<http://www.triumf.ca/annrep>

BEAMLINES AND EXPERIMENTAL FACILITIES



The contributions on individual experiments in this report are outlines intended to demonstrate the extent of scientific activity at TRIUMF during the past year. The outlines are not publications and often contain preliminary results not intended, or not yet ready, for publication. Material from these reports should not be reproduced or quoted without permission from the authors.

FOREWORD

The year 1998 was one of outstanding achievement for TRIUMF and the laboratory fully met its goals across a broad front.

On November 30, ISAC delivered its first radioactive beam. The target set for the ISAC project was to achieve a low energy beam before the end of 1998. The isotope $^{38\text{m}}\text{K}$ was detected at the TRINAT beam stop in the early evening of the last day of November. This was a superb effort for all concerned, and accolades showered onto TRIUMF as news of the event reached the world's laboratories.

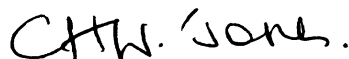
TRIUMF's "in kind" contribution to the Large Hadron Collider (LHC) project at CERN has provided Canada with a seat "on the stage" in what is truly a global scientific endeavour. High quality, high-tech equipment has been provided on time, mostly from within Canadian industry, and TRIUMF has emerged as a highly valued collaborator in accelerator physics.

Through the year, TRIUMF made good progress towards becoming a truly national laboratory for nuclear and particle physics in Canada. Both Carleton University and Queen's University were admitted as associate members, joining Regina, Manitoba, Toronto, and Montreal. In addition, terms have been agreed to for the admission of Carleton as a full member of TRIUMF beyond April, 2000.

The culmination of the year in many senses was the review of TRIUMF's past program and future plans by a NRC-appointed, international peer-evaluation committee. The review provided a very strong endorsement of TRIUMF's progress to date and the plans for 2000-2005. This applied to all areas of TRIUMF's program including nuclear and particle physics, condensed matter studies and the life sciences program. Of particular note, the review committee was also full of praise for TRIUMF's technology transfer activities, pointing out the very considerable economic benefits which flow to Canada from a basic research facility.

This record of achievement, coupled with the very strong peer-evaluation conducted by the NRC, has positioned TRIUMF exceptionally well to make the case for funding for the full program beyond 2000. Soon these efforts will be in the political arena, where unfortunately nothing is certain. However, the excellent peer review will allow a very strong case to be made at the political level.

The staff of TRIUMF can look back with pride on 1998. The hard work and dedication have paid off, and TRIUMF has achieved excellent visibility across Canada and internationally. I know I speak for all the members of the Board of Management when I say to all of the staff, "Well done — this was a great year!"



C.H.W. Jones
Chair, Board of Management

TRIUMF was established in 1968 as a laboratory operated and to be used jointly by the University of Alberta, Simon Fraser University, the University of Victoria and the University of British Columbia. The initial consortium has been expanded to include the University of Manitoba, the Université de Montréal, the University of Toronto, the University of Regina, Carleton University and Queen's University as associate members. The facility is also open to other Canadian as well as foreign users.

The experimental program is based on a cyclotron which is capable of producing four simultaneous beams of protons, two of which are individually variable in energy from 180–520 MeV, the third from 472–510 MeV, and the fourth between 70 and 110 MeV. The potential for high beam currents – 100 μA at 500 MeV to 300 μA at 400 MeV – qualified this machine as a ‘meson factory’.

Fields of research include basic science, such as particle and nuclear physics and condensed matter research, as well as life sciences based primarily on isotope research. There are also biomedical research facilities which used π mesons and now use protons in cancer research and treatment.

The ground for the main facility, located on the UBC campus, was broken in 1970. Assembly of the cyclotron started in 1971. The machine produced its first full-energy beam in 1974 and its full current in 1977.

The laboratory employs approximately 325 staff at the main site in Vancouver and 19 based at the participating universities. The number of university scientists, graduate students and support staff associated with the present scientific program is about 625.

CONTENTS

INTRODUCTION	1
SCIENCE DIVISION	3
Introduction and Overview	3
Particle Physics	5
(Expt. 497) Measurement of the flavour conserving hadronic weak interaction	5
(Expt. 614) Precision measurement of the Michel spectrum from muon decay	9
(Expt. 705) BNL Experiments 813, 885 and 906: Strange physics at BNL: a search for the H particle (BNL 813); a search for $\Lambda\Lambda$ hypernuclei (BNL 885) using gas microstrip chambers (705); an experiment to detect $\Lambda\Lambda$ hypernuclei via characteristic π -mesonic decays (BNL 906)	13
(ATLAS) The ATLAS experiment at the LHC	17
(BNL787) Study of rare K decays	21
(FINUDA) Hypernuclear spectroscopy at DAΦNE	23
(HERMES) Spin structure of the nucleon	23
(KEK246) Search for T violation in $K_{\mu 3}$ decay	27
(TJNAF91-017) Measurement of the flavour singlet form factors of the proton	28
Nuclear and Atomic Physics	32
(Expt. 560) Low energy $\pi^{\pm}\bar{p}$ analyzing powers with CHAOS	32
(Expt. 613) Reactions of muonic hydrogen isotopes	33
(Expt. 624) The $H(\pi, 2\pi)$ reaction, a tool to determine scattering lengths and coupling constants	35
(Expt. 700) Measuring cross sections of long-lived radionuclides produced by 200–500 MeV protons in elements found in lunar rocks and meteorites	37
(Expt. 704) Charge symmetry breaking in $np \rightarrow d\pi^0$ close to threshold	37
(Expt. 715) Weak interaction symmetries in β^+ decay of optically trapped $^{37,38\text{m}}\text{K}$	45
(Expt. 719) $^4\text{He}(\pi^+, \pi^-pp)$ invariant mass measurement with CHAOS	47
(Expt. 725) Pionic double charge exchange on ^4He	49
(Expt. 741) Beta-delayed proton decay of ^{17}Ne to α -emitting states in ^{16}O	49
(Expt. 742) Scattering of muonic hydrogen isotopes	52
(Expt. 778) $\pi^{\pm}p$ differential cross sections in the Coulomb-nuclear interference region	56
(Expt. 781) Investigations of the $\pi\pi$ invariant mass distributions of nuclear ($\pi^+, \pi^-\pi^+$) reactions with the CHAOS detector	58
(Expt. 785) Pion double charge exchange on ^3He with CHAOS	59
(Expt. 823) Pure Fermi decay in medium mass nuclei	60
(Expt. 824) Measurement of the astrophysical rate of the $^{21}\text{Na}(p, \gamma)^{22}\text{Mg}$ reaction rate	62
(Expt. 837) Pion induced soft error upsets in 64 Mbit DRAM chips	63
(Expt. 838) Two-photon capture mode of pionic hydrogen	64
(YEN) Undergraduate/graduate teaching beam time	64
Research in Chemistry and Solid-State Physics	65
(Expt. 684) μSR spin relaxation studies of small molecules in the gas phase	65
(Expt. 691) The vortex cores in type-II superconductors	66
(Expt. 713) Muonium chemistry in supercritical water	67
(Expt. 717) Muonic hyperfine transition rates in light nuclei	68
(Expt. 720/750) Muonium as a light isotope of hydrogen	69
(Expt. 724) Effects of dilute (Cu,Zn) substitution in spin gap system SrCu_2O_3	70
(Expt. 746) Muonium in Si	71
(Expt. 749) Muonium-substituted free radicals	71
(Expt. 751) μSR measurements of off-axis internal magnetic fields in anisotropic superconductors	73
(Expt. 774) Muonium dynamics in GaAs	75
(Expt. 776) Rare-earth materials with disordered spin structures	76
(Expt. 777) Vortex state of s -wave superconductors investigated by muon spin rotation	77
(Expt. 782) Non-fermi-liquid behaviour and other novel phenomena in heavy-fermion alloys	78
(Expt. 784) The μSR studies of spin-singlet states in oxides	80
(Expt. 791) Electronic structure and dynamics of charged muonium centres in semiconductors	81

(Expt. 792) Muonium in III-V semiconductors	82
(Expt. 804) Muonium in gallium nitride	84
(Expt. 809) Muonium localization in solid methanes	86
(Expt. 814) μ SR studies of unconventional superconductivity in Sr_2RuO_4	88
(Expt. 831) Magnetic properties of $\text{REBa}_2\text{Cu}_3\text{O}_x$	89
(Expt. 832) Study of the non-magnetic-magnetic transition in the $\text{YB}(\text{Cu}_{1-x}\text{Ni}_x)_2\text{Si}_2$ system	90
Life Sciences Research	92
Introduction	92
(Expt. LS0) PET facilities	92
(Expt. LS2) Synthesis of radiohalogenated carbohydrates	93
(Expt. LS3) PET radiopharmaceuticals	93
(Expt. LS4) TR13 targets for PET radioisotope production	93
(Expt. LS8) Radiotracers for the physical and biosciences	94
(Expt. LS6/LS21) Accelerator mass spectrometry for trace element analysis in living organisms	95
(Expt. LS10) Aptamer imaging agents	95
(Expt. LS23/LS34) Radioisotope production targets	95
(Expt. LS24) PET of breast cancer in a community hospital: a study of advanced disease using a coincidence gamma camera	95
(Expt. LS25) 3D PET in human neuroreceptor studies: quantification and reconstruction	96
(Expt. LS26) A gaseous planar positron source for routine 3D PET normalization	97
(Expt. LS28) Evaluation of potentially viable myocardium with dobutamine myocardial SPECT imaging	97
(Expt. LS29) Production and distribution of FDG for clinical studies	97
(Expt. LS30) Life Sciences five year plan	97
(Expt. LS33) Evaluation and improvement of a dual head coincidence camera	98
(Expt. LS35) ^{18}F -nitroimidazole hypoxia agents	99
Theoretical Program	100
Introduction	100
Miscellaneous	100
Nuclear Structure and Reactions	100
Effective Field Theories and Chiral Perturbation Theory	102
Hadronic Structure	103
The Standard Model and Beyond	104
Experimental Facilities	106
Proton Therapy Facility	106
Proton Irradiation Facility	106
μ SR User Facility	106
Detector Facility	109
Cryogenic Targets	110
Computing Services	110
Data Acquisition Systems	113
Scientific Services	114
GEANT4	116
Sudbury Neutrino Observatory	117
The BaBar Experiment	117
Low Temperature Nuclear Orientation Facility at ISAC	118
DRAGON at ISAC: A Status Report	119
Gamma-ray Detectors for DRAGON and Industrial Applications	123
Expt. 715 Off-line Laser Development Lab: Optical Pumping of ^{41}K	123
An Ultra-sensitive Radioactivity Monitoring Station on UBC Campus and Its Relation to TRIUMF	125
CYCLOTRON OPERATIONS DIVISION	127
Introduction	127
Beam Production	127

Beam Schedule 92	131
Spring Shutdown	132
Beam Schedule 93	132
Fall Shutdown	132
Beam Schedule 94	133
Beam and Cyclotron Development	133
Short Bunches from the Cyclotron	133
Multipactoring in the RFB Coupling Loop	133
Cyclotron Beam Dynamics	133
Stripping Foils for the Parity Violation Experiment	134
Radio Frequency Systems	134
RF Operations	134
RF Support	134
Radio Frequency Controls	134
Cyclotron Probes and Diagnostics	135
Probes and Diagnostics Mechanical MRO	135
Probes MRO	135
Monitor MRO	135
Vacuum and Engineering Physics	135
ISIS and POLISIS	135
ISIS	135
POLISIS	136
Primary Beam Lines	137
2C	137
Controls	137
CCS Operation	137
Beam Line 2A	138
Year 2000 Issues	138
Other Systems	138
CCS Facilities	138
Miscellaneous	139
Operational Services	139
Remote Handling	139
Magnet Power Supplies	140
Electrical Systems	140
Mechanical Systems	141
 ISAC PROJECT	 142
Introduction	142
Schedule and Planning	142
Beam Line 2A	142
Target Areas	143
RFQ	143
Separator System	143
Drift Tube Linac (DTL)	143
DRAGON	143
Manpower	143
Contract Administration	143
Personnel Resources	144
Conventional Facilities and Infrastructures	145
Data and Ethernet Communication	146
Electrical Services	146
Mechanical Services	147
Voice and Telephone Communication	147

ISAC-I Experimental Facilities	148
Target Hall	149
Shielding	150
Target Station Modules	150
ISAC Diagnostics	151
Safety and Radiation Control	151
Licensing	151
Access Control and Radiation Monitoring	151
Commissioning	152
Remote Handling	152
Service Shielding	152
Beam Lines Servicing	152
Hot Cell Facility	152
Remote Crane Handling System	152
Alignment	152
Beam Line 2A	153
Ion Source Test Stand	154
Surface Ionization Source	154
Electron Cyclotron Resonance Source	154
Polarized ^8Li Beam	154
Target/Ion Source	154
On-line Targets	154
ISAC Mass Separator	155
Target Station and Matching Section	155
Pre-separator Stage	156
Mass Separator Stage	156
Diagnostics	156
Beam Commissioning	156
RF Systems	156
LEBT Pre-buncher	156
MEBT Rebuncher	158
DTL Triple Gap Buncher	159
RF Amplifiers	159
RF Controls	159
Other Developments	160
RFQ Task Force	160
OLIS, LEBT and Pre-buncher Commissioning	160
The RFQ Interim Beam Test	161
Medium Energy Beam Transport	165
DTL Quadrupole Triplet	165
High Energy Beam Transport	166
Beam Diagnostics	166
ISAC Controls	168
Hardware	168
Software	168
ISAC-II	170
ACCELERATOR TECHNOLOGY DIVISION	172
Introduction	172
Magnets	172
Magnet Measurements	173
Mechanical Engineering	173
ISAC	173
ISAC – University of Victoria	175

Engineering – Other	175
Planning	176
Shutdown Activities	177
Design Office	178
Machine Shop	178
Building Program	178
Electronics Services	178
Overview	178
Technical Support	179
Experimental and Target Support	179
Electronics Shop	179
Microprocessor Support	179
Electronics Development	180
ISAC Support	180
CERN Support	181
CDS	181
Nordion TR30	181
CERN COLLABORATION	182
Introduction	182
Beam Dynamics	183
Second Harmonic in PSB	183
Injection and Collimation in the PSB	184
Beam Stability	184
Beam Optics and Collimation	185
Simulation Tool for LHC/SPS Tune Control	185
Controls and Instrumentation	186
Fast Blade Profile Monitor	186
Fast Wire Scanner	187
Upgrading SPS Orbit Observation System	187
Design and Production of VME TSM	188
Power Supplies	188
Booster Transfer Line Power Supplies	188
Booster Magnet Power Supply Transformers	188
Reactive Power Compensator	188
Magnet Development	188
Transfer Line Magnets	188
Cleaning Insertion Magnets	189
Kicker Magnets	189
LHC Injection Power Supply and PFN	189
Radio Frequency Systems	191
Coordination/Project Planning	191
40 MHz Cavity Structure	191
80 MHz Structure and HOMs	191
High Voltage Power Supplies	192
TECHNOLOGY TRANSFER DIVISION	193
Introduction	193
Technology Transfer	193
Applied Technology Group	193
500 MeV Isotope Production Facility	193
CP42 Facility	193
TR30 Facility	195

ATG Research Projects	195
Radioisotope Processing (MDS Nordion)	195
ADMINISTRATION DIVISION	196
Introduction	196
Operational Safety	196
Safety Organization	196
AECB Licensing	196
Site Security	196
WCB and Site Environmental	196
Interlocks and Monitoring	196
Personnel Dosimetry	197
Administration Computing	197
Data Processing	197
Word Processing	197
Telephones and Telecommunications	197
CONFERENCES, WORKSHOPS AND MEETINGS	199
ORGANIZATION	203
APPENDICES	
A. Publications	207
B. Seminars	222
C. Users Groups	224
D. Experiment Proposals	225
E. Life Sciences Proposals	271

INTRODUCTION

In 1998 the TRIUMF laboratory achieved major successes in all of the components of its program. Perhaps the most visible and outstanding highlight was the delivery of the first radioactive beam from ISAC on November 30. Under normal circumstances this may have been sufficient for a banner year, but 1998 brought an additional crop of achievements at CERN, in our infrastructure role, and in the basic program at the cyclotron.

In the first phase of TRIUMF's "in kind" contribution to the Large Hadron Collider (LHC) at CERN there had been a concentration on the provision of components for the CERN PS complex, involving an upgrade to the energy of the PS Booster and refurbishing of ageing components in general; all in preparation for PS operation as a part of the injector chain of LHC. The delivery schedules set by CERN were tight, with components required for installation into the CERN accelerator complex during the 1997/98 winter shutdown. All of the Canadian components were operational for the machine startup in March, 1998, and have operated without fault throughout the year. The degree of professionalism exhibited by the TRIUMF accelerator physicists and engineers has been much appreciated by their CERN counterparts, who eagerly pursue continued collaboration on other aspects of the LHC project.

The role of TRIUMF as a provider of infrastructure to Canadian subatomic physicists also produced some notable successes, which provided TRIUMF with excellent visibility in some of the world's major laboratories. The drift chamber for the BaBar experiment on the B-Factory at the Stanford Linear Accelerator Centre (SLAC) was delivered to SLAC in March, actually on the day promised a year earlier. The chamber has had a successful commissioning run on cosmic rays and has managed to remain one of the "most ready" subsystems in the BaBar detector. First collisions are currently anticipated for May, 1999. The stringing of this chamber was an excellent example of collaboration between Canadian university physicists, their collaborators from the US and Italy, and TRIUMF staff.

As the BaBar chamber moved out of the clean-room at TRIUMF, the ATLAS experiment moved in. ATLAS is a large collaboration at LHC, which includes Canadian physicists from the University of Alberta, Carleton University, CRPP, UBC, University of Toronto, University of Victoria, York University and TRIUMF. TRIUMF engineers were responsible for the mechanical design of the hadronic end-cap calorimeter (HEC) and modules of this calorimeter will be built and tested in TRIUMF over the next three and a half

years. During 1998 all aspects of tooling and quality assurance have been put in place and module production is scheduled to commence early in 1999.

TRIUMF has had a long-standing engagement in the rare decay experiment BNL E787, which has been performed at the AGS in Brookhaven National Laboratory. This experiment set out to determine the branching ratio for the process $K^+ \rightarrow \pi^+ + \nu\bar{\nu}$. A result was reported last year which is consistent with the prediction of the standard model in the region of 10^{-10} . There was the possibility of revealing new physics had the branching ratio been larger than predicted. Sadly this seems not to be the case. BNL E787 collected its final data in 1998 and will re-emerge in a modestly upgraded version known as BNL E949, which will aim to measure the $|V_{td}|$ element of the Cabibbo-Kobayashi-Maskawa quark mixing matrix. The single event sensitivity of the proposed measurement is in the region of $(8 - 14 \times 10^{-12})$. BNL E949 measures again the decay $K^+ \rightarrow \pi^+ \nu\bar{\nu}$ but with a target of obtaining some 10 events.

In addition to providing infrastructure support for experiments performed away from TRIUMF, the laboratory is providing significant support to two major projects at TRIUMF. One of these is the experiment aimed at making precise measurements of the Michel decay parameters of the muon, Expt. 614, and the other is DRAGON, the recoil spectrometer which is an essential tool for the nuclear astrophysics program which will commence at ISAC towards the end of the year 2000.

At the cyclotron the so-called parity experiment achieved an initial result. The experiment measures the parity-violating longitudinal analyzing power in $p - p$ elastic scattering at 221 MeV, using a 200 nA beam which is $\sim 80\%$ polarized. Enormous demands have been placed on the operating characteristics of the machine and the group has clearly demonstrated that systematic errors are understood and under control at the level of less than 10^{-7} . The early result is in line with theoretical predictions, and a further good data run in 1999 should complete the long and challenging program. The other workhorse at the cyclotron has been the CHAOS spectrometer which has pursued a series of experiments using pions, both elastic and inelastic scattering, with particular emphasis on tests of chiral perturbation theory. The spectrometer is working well and producing good science. Sadly, during 1998, the assigning of priorities within the overall TRIUMF scientific program impinged upon the CHAOS program. This should not be the case in 1999.

Experiments in condensed matter physics and

chemistry, using the μ SR technique, have continued vigorously in the laboratory with no signs of a diminishing appetite for beam time. The menu of the basic program continues to include a small but extremely interesting series of experiments in the life sciences.

As mentioned at the beginning, 1998 was really the year that ISAC “came to life”. When the first radioactive beam of $^{38\text{m}}\text{K}$ was delivered to two experiments before the shutdown at the end of the year. TRINAT, which completed a very successful run at TISOL, was moved, rebuilt, and trapped potassium in its new location at ISAC. TRINAT will continue its search for evidence of scalar currents in the decay of $^{38\text{m}}\text{K}$ through a study of $\beta - \nu$ correlations in the detection trap, where the positron and argon recoils are measured. A second experiment received beam briefly at ISAC. It aims to make precision measurements of half lives of nuclei which are of interest in the study of super allowed Fermi transitions in β -decay. Initially $^{36\text{m}}\text{K}$ will be studied but later ^{74}Rb becomes the nucleus of interest.

The production of an exotic beam at ISAC was a superb performance by the ISAC project team. Many aspects of the facility had to work reliably in order to achieve the end result, and the science program with the low energy beams can now be confidently anticipated. In parallel, significant progress was made on the accelerator front; for example, very successful tests of the RFQ proved the validity of the design and alignment procedures. These elements can now move into production and accelerated beams of 1.5 MeV/u will be available for experiments before the end of the year 2000.

When TRIUMF received its five years of funding in 1995 a review procedure was put in place such that during the fourth year of the plan a major review of the work of the laboratory would take place. TRIUMF would be assessed on how it had performed in all aspects, and also would receive a critical appraisal of the laboratory’s plans for the next five years – on this occasion 2000–2005. In the late summer, with input from the TRIUMF Users and the broader subatomic physics community including IPP, the manage-

ment produced a plan which initially was presented to the Advisory Committee on TRIUMF (ACOT). The main ingredients of the proposal were an increase in the energy of ISAC to around 6.5 MeV/u, a further contribution “in kind” to the LHC at CERN, and also a modest “in kind” contribution to the ATLAS detector. In order to achieve the goals of the first five years much of the laboratory’s infrastructure, including refurbishing of main systems at the cyclotron, had been hit. In the new plan these steps would be slowly reversed. The raising of the energy of ISAC above the Coulomb barrier will provide TRIUMF with an unparalleled position in North American radioactive beam physics.

NRC selected the international review group under the chairmanship of Professor Stewart Smith of Princeton University. The group met at TRIUMF, October 21–23.

Initial indications are that the report on TRIUMF’s past performance and future plans will be extremely positive. This will give TRIUMF an excellent platform from which to seek additional funding and all of the laboratory staff who have contributed to this strong position should feel very proud.

In July TRIUMF enjoyed a very important, but pleasant privilege. For the first time Canada was host to the Rochester Conference. This is a very prestigious series of meetings where over the years practically every major discovery in high energy physics has been announced. The UBC campus was the selected venue for the XXIX International Conference on High Energy Physics. The speakers and weather cooperated to make the meeting a memorable occasion for delegates who had come from all over the world. The TRIUMF staff who were engaged in the local organization have, in essence, set new standards for the series of meetings.

It is hard to imagine a better year for TRIUMF. It would be easy to lapse. We cannot possibly maintain the peak achieved in 1998 over the long term, but we can sustain the excellence of performance which we learned to enjoy and which is bringing us world recognition for our achievements.



A. Astbury,
Director

SCIENCE DIVISION

INTRODUCTION AND OVERVIEW

This year, TRIUMF and the physics community said goodbye to one of their greatest experimenters when Professor Otto Häusser lost his battle with cancer in March. He had embraced the TRIUMF science program since 1983 and was leading the scientific group promoting opportunities offered by ISAC, TRIUMF's radioactive beam facility. While we all knew of that inevitable ending, we were motivated by his strength and intellectual leadership displayed until the very last moment. To a large extent, his vision of the role of radioactive beams for the future of nuclear physics at TRIUMF is being carried forward, and by the end of 1998 the ISAC team had delivered the first potassium beams from the new source. Not surprisingly, the TRIUMF neutral atom trap (TRINAT) facility, which Otto had established in 1994, was the first recipient of this new beam.

Considerable efforts were expended this year to develop the initial program at ISAC with its required experimental facilities. In fact, before Christmas, two set-ups saw beams from ISAC: TRINAT and the β -decay tape station which will measure half-lives of nuclei involved in $0^+ \rightarrow 0^+$ superallowed transitions.

Also on the ISAC front, the layout of the low energy area was established, with the low temperature nuclear orientation set-up (LTNO) acquired from Oak Ridge being recommissioned, and a unique polarized ion beam delivery system for condensed matter studies developed.

For the accelerated beams which will be available in the fall of 2000, the backbone facility for the science program will be the DRAGON spectrometer. It will be used to measure radiative capture cross sections for reactions of interest in supernovae explosions.

1998 saw the transition between the TISOL program and the beginning of ISAC. Developed in the late 1980's, the TISOL test facility on beam line 4 served not only as a development tool for defining what ISAC is now, but also serviced a large number of experiments including a series of measurements on the $^{12}\text{C}(\alpha, \gamma)$ cross section, studies of light exotic nuclei like ^9Li and ^9C , the development of the TRINAT, and the initial measurements of $\beta - \nu$ correlations on $^{38\text{m}}\text{K}$ decays, to mention just a few. It is planned to maintain TISOL as a development station for the ISAC targets and ion sources using modest ($<1 \mu\text{A}$) proton beam currents.

While the main focus of the Science Division was on the preparation of ISAC's future scientific program, a number of important milestones were achieved in the non-ISAC program as well. As documented in this Annual Report, the parity experiment had very suc-

cessful data-taking runs in the winter and summer polarized beam periods. The charge symmetry breaking experiment, Expt. 704, entered the data-taking phase with good control of its systematic uncertainties. The CHAOS program generated more than 10 publications this year and, were it not for our failure to operate the new thin cryogenic target, it would be starting its low energy measurement of the forward differential πp scattering cross section in the Coulomb-Nuclear interference region. No dibaryons were seen in the data taken previously and the data on $\pi\bar{p}$ asymmetries will anchor the new phase shift analyses. Tests of chiral perturbation theory predictions for the pion scattering length $a_{\pi\pi}^0$ were published recently. Towards year-end, the RMC spectrometer together with its associated proutium target was recommissioned and about 300 events were collected on the rare process $\pi^- p \rightarrow \gamma\gamma n$ in a region of phase space which should eventually allow for a test of the pion polarizability. The high precision study of muon decay entered the decisive construction phase with the purchase of the 2T superconducting coil and preparations for stringing of the wire chambers.

For off-site programs, the BaBar drift chamber was strung in 1997 and delivered to SLAC on time. All 28,000 wires survived the trip to San Francisco and the chamber has been commissioned at SLAC with cosmic rays without too many problems.

An important milestone was achieved at year-end when the search for the rare decay $K \rightarrow \pi\nu\bar{\nu}$ under BNL E787 ended its data-taking at the AGS (15 years after the initial approval of the proposal, one event seen and published and perhaps a few more on tape). It will be replaced by an upgraded version under BNL E949 which is approved for running at the AGS by 2001.

TRIUMF infrastructure is now being used to build the liquid argon hadronic calorimeters for ATLAS. This is a pan-Canadian effort to join the experimental program at LHC in 2005. TRIUMF also continues to support the Canadian effort on the HERMES experiment at DESY and the SNO effort in Sudbury.

The Condensed Matter program at TRIUMF is still mainly based on the μSR techniques with emphasis on high temperature superconductivity, semiconductors, magnetism and chemistry. Major advances were made on the development of new instruments for the μSR facility taking advantage of a fast timing spectrometer and of multiple muon tracking systems to improve the data-taking quality and efficiency. These instruments will keep our μSR facility at the forefront as evidenced by the large number of requests for muon beams.

Preparations are being made to take advantage of

the opportunities presented by the light polarized ions at ISAC to study thin structures, and by the LTNO set-up to use NMR techniques on oriented samples.

The Life Sciences program is still dominated by the effort on positron emission tomography. The dedicated TR13 cyclotron produced a record number of irradiations and radiotracers were dispatched to three local hospitals. Although considerable effort went into the development of an attractive proposal to build a state-

of-the-art processing facility at TRIUMF (TRIPL) to supply Canadian researchers with innovative tracers, no funding was received from the Canadian Foundation for Innovation and our plan to develop a Centre of Excellence in radiotracer imaging will have to be revised.

1998 will be remembered as a year of major achievements, particularly in ISAC, and this is the best tribute TRIUMF could deliver to the memory of Otto Häusser.

PARTICLE PHYSICS

Experiment 497

Measurement of the flavour conserving hadronic weak interaction

(*J. Birchall, S.A. Page, W.T.H. van Oers, Manitoba*)

The ongoing parity violation experiment at TRIUMF will determine the parity-violating longitudinal analyzing power $A_z = (\sigma^+ - \sigma^-)/(\sigma^+ + \sigma^-)$ in $p-p$ elastic scattering at 221 MeV, where σ^+ and σ^- are the scattering cross sections for positive and negative helicity.

The 221 MeV energy of Expt. 497 is chosen so that the measured A_z , accounting for the finite acceptance of the detectors, arises exclusively from the ${}^3P_2-{}^1D_2$ parity mixed partial wave. (At this energy the contribution to A_z from the ${}^1D_2-{}^3F_2$ partial wave is only 5% of that from ${}^3P_2-{}^1D_2$.) The ability to measure at this energy is an advantage of the TRIUMF measurement, as it simplifies the interpretation of the result. For example, if A_z is calculated using a meson exchange model with ρ and ω exchange, then the TRIUMF experiment is sensitive only to the effects of ρ exchange [Simonius, *Can. J. Phys.* **66**, 548 (1988)] and can be used to extract the weak ρ -meson-nucleon coupling constant. In the context of the weak meson exchange model [Desplanques *et al.*, *Ann. Phys.*

(N.Y.) **124**, 449 (1980)], the proposed measurement of A_z to $\pm 0.2 \times 10^{-7}$ will provide a $\pm 25\%$ determination of the weak ρ -nucleon coupling constant $h_{\rho}^{pp} = (h_{\rho}^0 + h_{\rho}^1 + h_{\rho}^2/\sqrt{6})$.

A major effort to minimize and understand systematic error contributions is required to successfully perform an experiment to this level of precision. The first significant data set for Expt. 497 was acquired in February, 1997, with a raw statistical error of $\pm 0.4 \times 10^{-7}$ and most systematic errors at or below the 10^{-7} level. That result represented a major milestone for the experiment, the culmination of many years of effort to reduce both the helicity correlated beam modulations and the sensitivities to them. The February, 1997 data set is fully described in Araz Hamian's Ph.D. thesis [Hamian, *The measurement of parity violation in proton-proton scattering at 221 MeV*, Ph.D. thesis (University of Manitoba, 1998)].

Beam line and instrumentation

In addition to the measuring apparatus, the optically pumped polarized ion source (OPPIS), cyclotron, and transport beam lines are critical components of the experimental set-up, as illustrated in Fig. 1. A 5 μA transversely polarized beam is transported to the

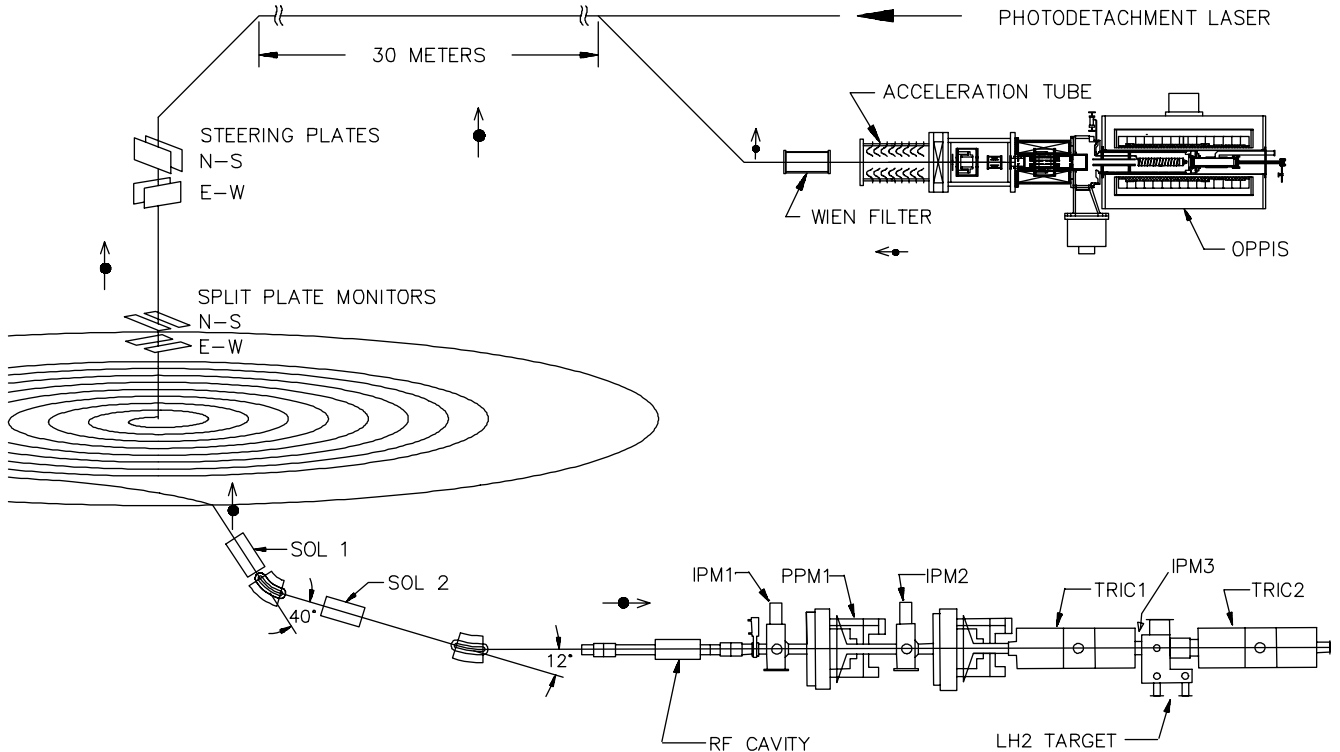


Fig. 1. General layout of the TRIUMF parity experiment. (OPPIS: optically pumped polarized ion source; SOL: spin precession solenoid; IPM: intensity profile monitor; PPM: polarization profile monitor; TRIC: transverse field ionization chamber.)

cyclotron through an approximately 50 m long injection beam line. The ion source Wien filter is tuned to produce vertical polarization at the entrance to the cyclotron. A 200 nA beam at 75–80% vertical polarization is extracted at 221 MeV. Spin precession through a pair of solenoid and dipole magnets results in delivery of a longitudinally polarized beam to the 40 cm liquid hydrogen target, which scatters 4% of the beam. Transverse field parallel plate ion chambers TRIC1 and TRIC2 measure the beam current incident on and transmitted through the target. The parity violation signal is derived from the helicity-correlated difference between the beam currents measured by the two TRICs. Upstream of the target are two polarization profile monitors (PPMs) to measure the distributions of transverse polarization $P_y(x)$ and $P_x(y)$ across the beam, and two intensity profile monitors (IPMs) to measure the intensity distribution of beam current in x and y . The IPMs are coupled to a pair of servo magnets which lock the beam path on the optimum axis through the equipment.

Target upgrade

To correct marginal cooling power experienced during 1996 and 1997, two new CTI cryogenerator units were added at the end of 1997. This upgrade was very successful and the runs in 1998 enjoyed excellent target performance with approximately 15 W of excess cooling power.

Data

The full parity data set now consists of three major (1 month) data runs, taken in February–March, 1997, in December–January, 1998, and July–August, 1998, plus a short run (1 week) taken in August, 1997. The long runs have a raw statistical error of approximately $\pm 0.4 \times 10^{-7}$ each, while the short August, 1997 run has a raw statistical error of $\pm 1 \times 10^{-7}$. Systematic error corrections, however, limit the final precision of the overall result in all cases. A major effort has been under way to analyze these data sets; very significant progress made recently which sheds new light on the dominant systematic error contribution is discussed below.

Data analysis

Every 200 ms, the longitudinal analyzing power A_z is deduced from an 8-state data cycle with spin sequence (+ – – + – + +–) or its complement. The width of the A_z distribution is determined mainly by detector noise and random beam and cyclotron instabilities (the normal ‘counting statistics’ contribution is negligible). Random noise is minimized by aligning the beam along the symmetry or ‘neutral axis’ of the apparatus and ensuring that the two TRICs are as identical as possible in their response to the beam. The mean

of the A_z distribution can be displaced from zero either by real parity violation or by a false signal from other helicity-correlated changes in beam properties. These false signals are studied in a series of calibration measurements in which small spin-state-correlated modulations of beam current, energy, position, angle, and transverse polarization are purposely introduced. Interspersed data acquired in the frequent spin-off cycles provide an important zero asymmetry check of the apparatus and electronics.

February, 1997 data re-analysis

A thorough re-analysis of the February, 1997 data has recently been completed [Hamian, *op. cit.*], leading to revised conclusions regarding the systematic data offset and sensitivity to polarization moments, the two largest corrections to the data.

In correcting for the effects of transverse polarization we consider **intrinsic** moments of transverse polarization $\langle xP_y \rangle$ and $\langle yP_x \rangle$ resulting from a non-uniform distribution of transverse polarization within the beam envelope, as distinct from the corresponding **extrinsic** polarization moments $\langle x \rangle \langle P_y \rangle$ and $\langle y \rangle \langle P_x \rangle$ which arise when a beam with finite transverse polarization is displaced from the polarization neutral axis. The polarization neutral axis, which defines $\langle x \rangle = 0$, $\langle y \rangle = 0$, is determined from routine calibration scans of the sensitivity to **extrinsic** polarization moments, several times per data run. These scans yield a set of coefficients which are used to correct the raw asymmetries for non-zero average polarization components $\langle P_y \rangle$ and $\langle P_x \rangle$. These extrinsic calibration coefficients also determine the optimum beam convergence at the LH₂ target to minimize the sensitivity to **intrinsic** polarization moments $\langle xP_y \rangle$ and $\langle yP_x \rangle$, as described in previous reports.

It is important to emphasize that the sensitivities of the apparatus to both intrinsic and extrinsic polarization moments should be identical, so that in principle only the extrinsic polarization scans are required to determine the sensitivity coefficients for both effects. However, the distribution of corrected A_z is much broader than that of the raw A_z measurements when the extrinsic coefficients are combined with the intrinsic moments at each PPM to correct the data, since the resolution of the PPMs is significant compared to the intrinsic polarization moments that they measure. For this reason, previous analyses instead relied on a regression analysis to determine the sensitivity to intrinsic moments from correlations of the measured A_z values with the intrinsic first moments.

During the re-analysis of the 1997 data it was discovered that the regression analysis program had been systematically underestimating the sensitivity to intrinsic first moments of transverse polarization. This

was due to the small size of the intrinsic polarization moments relative to the measurement resolution for small data samples. When the data are bundled into samples of 5000 or more event pairs (approx. 1/2 hour acquisition time), the intrinsic moment sensitivities obtained from the regression analysis are in agreement with the sensitivities obtained from the extrinsic coefficients scaled by the average ratio of intrinsic first moments measured by PPM1 and PPM2. It hence seems clear that the sensitivities extracted from the re-analysis are the correct ones.

In examining the problem of the increased noise in the corrected data using the extrinsic polarization moments sensitivities at each PPM, it was realized that corrections for intrinsic polarization moments could be made to greater precision by combining the extrinsic correction coefficients with measurements of the **ratio** of intrinsic moments at PPM1 and PPM2, i.e. $\langle xP_y \rangle_2 / \langle xP_y \rangle_1$ and similarly for $\langle yP_x \rangle$, averaged over the entire parity data sample. This reduces the uncertainty in the overall correction, provided that the ratio is consistent over the data sample it is calculated from. This latter requirement implies extremely stable and reproducible beam tune conditions are needed over the course of a 4 week data run, which can be verified by independent measurements with the parity IPMs and other beam line diagnostic monitors. The uncertainty in the overall correction using this method is reduced because the effective sensitivity obtained by scaling the extrinsic correction coefficients by the average intrinsic moments ratio is significantly smaller than the sensitivity at each PPM. If the cyclotron and beam line tune produce precisely the right ratio of intrinsic moments at PPM1 and PPM2, the effective sensitivity to intrinsic moments vanishes.

The results of the re-analysis of the February, 1997 data are shown in Fig. 2. The upper figure shows the data corrected based on extrinsic sensitivity coefficients for transverse polarization moments at each PPM. The lower figure shows the data corrected based on intrinsic polarization moment sensitivities deduced from the regression analysis of the raw A_z data. The corrected A_z values are consistent in both cases; the spread in the data is dramatically reduced using the latter technique. Note that the regression analysis approach requires that the beam tune be constant over the entire set of runs, since it assumes a constant net intrinsic first moment sensitivity, while the approach based on extrinsic coefficients alone is beam tune independent. In any case, there is only one significant correction to the data, corresponding to the intrinsic first moment of transverse polarization $\langle xP_y \rangle$. The corrected A_z values have a reduced χ^2 of 0.5 per degree of freedom, as compared with 10.8 for the raw A_z values

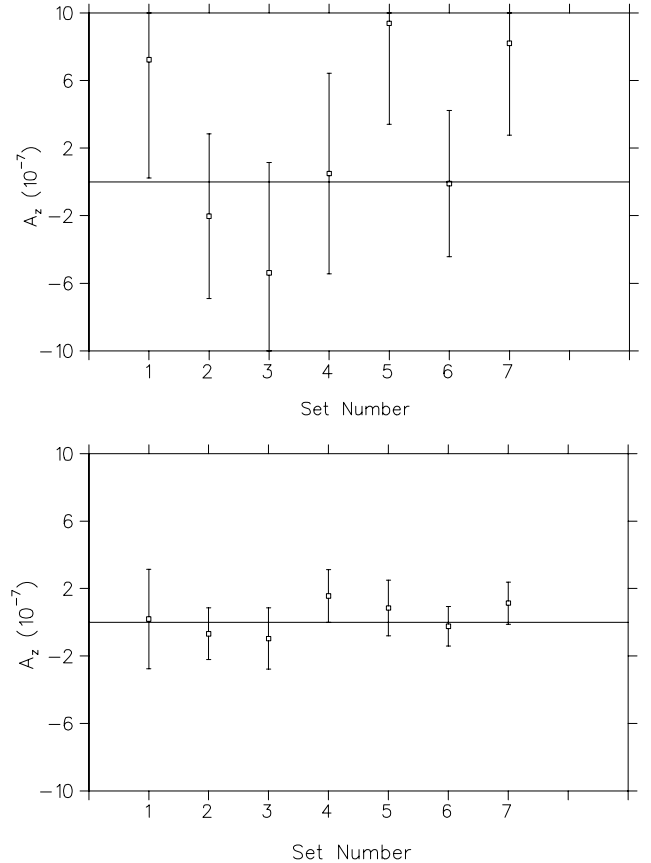


Fig. 2. Corrected A_z from February, 1997 re-analysis. The data are grouped into 7 sets with different relative orientations of the spin in the cyclotron and the parity beam line. The upper figure shows the data corrected based on the extrinsic sensitivity coefficients for transverse polarization moments at each PPM. The lower figure shows the data corrected based on intrinsic moment sensitivities deduced from the regression analysis of the raw A_z data. The corrected A_z values are consistent in both cases; the spread in the data is dramatically reduced using the latter technique.

for the same 7 data sets.

The excellent consistency of the February, 1997 data sets after correcting for all known effects indicates that unmeasured systematic errors correlated with both the direction of spin at the ion source and the direction of spin in the cyclotron are consistent with zero at the level of precision in A_z , approximately $\pm 0.7 \times 10^{-7}$. Thus, the apparent systematic offset associated with the direction of spin in the cyclotron reported in the preliminary analysis of this data set has been shown to be explained by an underestimated sensitivity to the intrinsic polarization moment $\langle xP_y \rangle$. This is a very encouraging result for future work.

The final corrected result from the February, 1997 data set is found to be:

$$A_z = (0.33 \pm 0.57 \pm 0.31) \times 10^{-7} = (0.33 \pm 0.65) \times 10^{-7}$$

where the first error is derived from the standard de-

viation of the corrected A_z distribution (“statistical”) and the second is the contribution from the uncertainties in the sensitivity coefficients (“systematic”). The statistical error includes the uncertainty in ΔA_z due to the spread of the helicity correlated beam property measurements, but is dominated by the spread of the raw A_z values. The systematic error, since it is due almost entirely to the uncertainty in the $\langle xP_y \rangle$ sensitivity as determined from the regression analysis of the parity data, is in fact statistics dominated.

August, 1997 data

These data were acquired in two main sets, one in each of the beam line helicity configurations. Unfortunately, much of the running period was lost to technical problems, and the statistical uncertainty is $\pm 1.0 \times 10^{-7}$ for approximately 20 hours of polarized data. This uncertainty will be further increased by corrections for systematic error, giving this data set little weight.

December, 1997 – January, 1998 data

During the December, 1997 – January, 1998 running period, approximately 150 hours of polarized data were acquired in addition to systematic error calibrations and other tests. Although the liquid hydrogen target performed excellently, a failure of the HE2 probe control mechanism prevented the August, 1997 cyclotron tune from being re-established with the ultrathin stripping foil. The thin foil was used for the first half of the run, with the holder shadowed with the beam line 1 extraction foil instead of HE2, but the arrangement was not optimal, and a great deal of extra time was spent in attempting to achieve acceptable beam profiles to keep polarization moments small at the parity apparatus. Relatively large raw asymmetries obtained from the on-line analysis indicated that the beam convergence was not appropriate to reduce the intrinsic first moment sensitivity to zero.

A delayed start was experienced after the Christmas break due to problems with the cyclotron cooling water system. The beam line 1 combination magnet also failed during this period, severely limiting the ability to shadow the ultrathin ($200 \mu\text{g}/\text{cm}^2$) stripping foil holder with the beam line 1 stripping foil. The remainder of the run was therefore carried out using a much thicker $2.5 \text{ mg}/\text{cm}^2$ stripping foil which was freely hanging and therefore did not require the holder to be shadowed inside the machine. Relatively large and variable systematic offsets were found in the raw data, and extra time was spent experimenting with different beam tunes to try to identify the source of the effects.

Analysis of these data is currently under way. The raw data have a statistical error of $\pm 0.4 \times 10^{-7}$ grouped

into 14 main data sets according to the beam line helicity tune, but the consistency of the **raw** A_z values on a set-by-set basis is about an order of magnitude worse than this.

Because the December–January data were acquired with a variety of beam tune conditions and two drastically different cyclotron stripping foils, the data sets do not have a consistent net sensitivity to intrinsic first moments of transverse polarization $\langle xP_y \rangle$ and $\langle yP_x \rangle$. For this reason, it is very difficult to take advantage of the technique applied to the re-analysis of the February, 1997 data to reduce the uncertainty in the correction for intrinsic moments using the measured extrinsic moment sensitivities obtained in calibration measurements. Thus far, corrections for intrinsic polarization moments have only been made with the ‘tune independent’ method using external calibration sensitivities at each PPM. The corrected values are consistent with each other. A reduced χ^2 of 0.8 for 13 degrees of freedom results from this analysis, but unfortunately the correction introduces additional noise in each data set.

The preliminary result for the December–January data from this analysis is:

$$A_z = (0.8 \pm 1.8) \times 10^{-7}$$

where the error bar is dominated by the uncertainty in the correction for intrinsic polarization moments. No residual correlations of the corrected A_z are found with any other helicity correlated beam properties for these data, and the data are consistent with zero systematic offsets associated with the spin direction at the ion source and at the cyclotron stripping foil. It must be emphasized that this result is very preliminary, and the reason for the relatively large error bar is entirely due to the fact that a large enough data set was not obtained with a fixed set of beam and cyclotron tune conditions to utilize the error reduction approach taken with the February, 1997 data. Work is continuing to examine subsets of the data and attempt to apply the latter approach to reduce the systematic error uncertainty.

July–August, 1998 data

The raw results of the most recent July–August, 1998 run are presented in Fig. 3 and Table I. The experimental asymmetries ε_{\pm} are defined as: $\varepsilon = \pm(A_z \pm \delta A_z)$ for positive and negative beam line helicity tunes; a total of approximately 250 data hours were acquired, roughly equally shared between states of opposite beam line helicity tune. The beam line helicity tune reversal allows some systematic error contributions such as beam energy modulation to be cancelled by averaging the data. Analysis is now concentrating on extracting the sensitivities to polarization

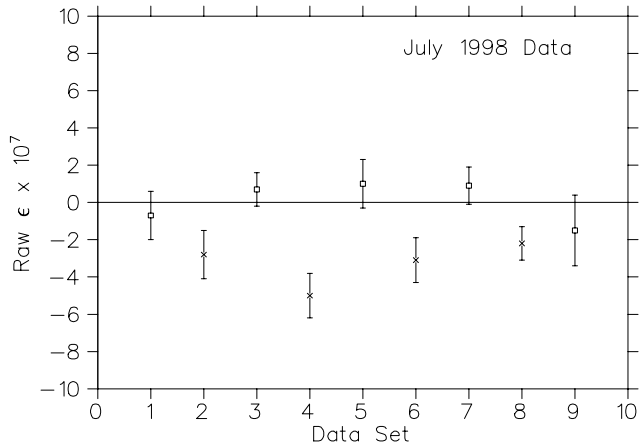


Fig. 3. Raw data from July–August, 1998 parity run. The squares are for positive helicity beam line tunes and the crosses are for negative helicity. The agreement between the data sets is poor compared to Fig. 2 because corrections for first moments of transverse polarization have not yet been applied.

Table I. Raw data summary, July–August, 1998 run. Once sensitivities to $\langle yP_x \rangle$ and $\langle xP_y \rangle$ have been determined, the raw asymmetries can be corrected.

Set	Raw ε ($\times 10^7$)	$\langle yP_x \rangle$ (μm)	$\langle xP_y \rangle$ (μm)
1 +	-0.7 ± 1.3	10.7 ± 4.1	1.7 ± 2.3
2 -	-2.8 ± 1.3	1.0 ± 1.3	10.0 ± 1.8
3 +	0.7 ± 0.9	14.1 ± 1.7	3.0 ± 1.6
4 -	-5.0 ± 1.2	8.5 ± 2.4	1.9 ± 1.4
5 +	1.0 ± 1.3	9.6 ± 3.2	-2.6 ± 1.8
6 -	-3.1 ± 1.2	3.3 ± 2.2	4.6 ± 1.7
7 +	0.9 ± 1.0	15.2 ± 2.4	0.5 ± 2.0
8 -	-2.2 ± 0.9	7.4 ± 2.6	0.2 ± 1.4
9 +	-1.5 ± 1.9	2.2 ± 4.5	6.8 ± 3.5

moments, and correcting in a way which introduces the least noise.

Summary and outlook

Major progress on data analysis has been made during 1998, resulting in an improved understanding of the sensitivity to intrinsic polarization moments and their effect on the A_z data. It has been shown that the large apparent systematic offset observed in February, 1997 and subsequently in December, 1997 – January 1998 can be understood as a correction due to intrinsic moments of transverse polarization. An analysis technique has been developed to minimize the uncertainty in this correction procedure, but this relies on achieving optimal cyclotron and beam tune conditions over extended periods of time, as experienced in February, 1997. While a data set of comparable size was obtained in December, 1997 – January, 1998, preliminary analysis has thus far been limited to an overall uncertainty that is some $2.5 \times$ larger than in February, 1997 due

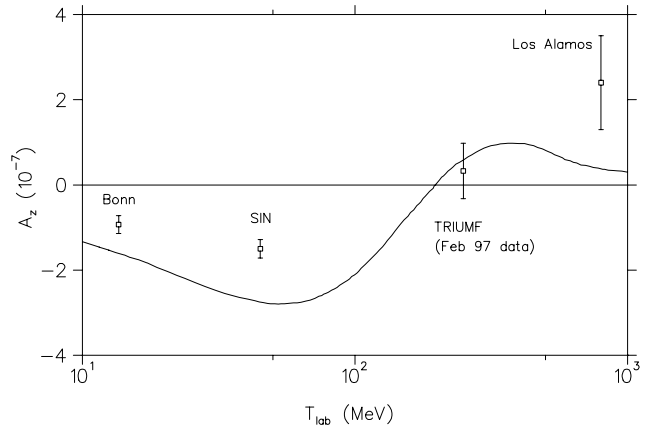


Fig. 4. Theoretical prediction for A_z in pp scattering, calculated by Driscoll and Miller using DDH predictions for the weak meson-nucleon coupling constants, shown with the highest precision existing experimental data. The TRIUMF data point is preliminary, based on the re-analysis of the February, 1997 data set.

to difficulties in assessing the sensitivity to intrinsic polarization moments with sufficient accuracy. Work in progress could substantially reduce the error bar in the most recent data set to the 10^{-7} level, but this remains to be demonstrated. Work is also in progress to re-analyze data taken in 1996 using the new technique.

The result from the re-analysis of the February, 1997 data is shown in Fig. 4 together with a meson exchange model prediction for A_z in the range of $T_{\text{lab}} = 10 - 1000$ MeV calculated by Driscoll and Miller [Phys. Rev. **C39**, 1951 (1989)], with weak meson nucleon coupling constants h_{ρ}^{pp} and h_{ω}^{pp} taken from the original prediction by Desplanques, Donoghue and Holstein (DDH)[Desplanques *et al.*, *op. cit.*]. Also shown are the highest precision existing experimental data in this energy range. The TRIUMF data point supports the meson exchange prediction at the level of this first result. Preliminary analysis has already indicated that the existing parity data set should be accurate at the $\pm 0.4 \times 10^{-7}$ level (total error bar) or better. An additional 6 week run is planned for summer, 1999, which is expected to complete the experiment. The final result should be available in 2000 and should be of high enough precision to determine uniquely for the first time an experimental constraint on the weak meson nucleon coupling constant h_{ρ}^{pp} .

Experiment 614

Precision measurement of the Michel spectrum from muon decay

(D.R. Gill, TRIUMF)

As tests of the standard model continue to support its veracity, the need for higher and higher precision measurements increases in importance. Historically one of the best laboratories for testing the electroweak sector of the standard model has been the

decay of the μ . With this in mind a new round of muon decay experiments, with considerable improvement over previous undertakings, is about to get under way at the meson factories, TRIUMF and PSI. At TRIUMF the Expt. 614 collaboration proposes to measure with high precision the differential spectrum, $d^2\Gamma/dXd(\cos\theta)$ of positrons from the decay, $\mu^+ \rightarrow e^+\nu_e\bar{\nu}_\mu$ for polarized muons. Here X is the positron energy ($X = 1$ corresponds to the maximum positron energy $E_{\max} = 52.83$ MeV), θ is the angle between the muon spin direction and the positron momentum. The ‘‘surface’’ muon beam with a momentum of 29.8 MeV/c from the M13 beam line at TRIUMF will be used as the muon source.

During 1998 the Expt. 614 collaboration achieved several important milestones. The first of these was the delivery to TRIUMF of all the high precision components of the planar drift chambers (PDC) that the Russian team had undertaken to provide. Following closely were the funding of the U.S. members of the collaboration by DOE and the first substantial project grant for the Canadian team from NSERC. Other milestones include: the completion of the analysis of the 1997 test data on the performance of the prototype PDCs, several Monte Carlo studies and the purchase of the superconducting solenoid required for the experiment.

Full scale prototypes of the Expt. 614 PDCs were constructed and tested in M13 in August, 1997. The analysis of this data was completed in early 1998. The analysis of an event consisted of a search for hits identifiable with a track, an iterative procedure to determine the hit position on the drift circle and the angle of the track relative to the chamber planes, construction of the track and calculation of an average tracking residual. The width of the tracking residuals reflects the intrinsic resolution of the chamber as well as all other factors that may contribute to inaccuracies in the tracking. This includes ingredients such as wire positions and drift distance. In addition, it reflects any biases in the fitting process, as well as the weighting used in the fit. The reasonably narrow width obtained and the level of symmetry of the results provides reasonable confidence in all these factors.

To determine the resolution as a function of position across a wire chamber cell, the widths of the tracking residuals were determined in 10 bins (each 200 μm wide). Employing an iterative procedure, the residuals as a function of drift distance were established. Figure 5 shows the result.

The chamber resolution improves as a function of drift radius due to the increase in ionization statistics. Our result is generally consistent with others (see for example Cindro *et al.* [Nucl. Instrum. Methods **A309**, 411 (1991)]).

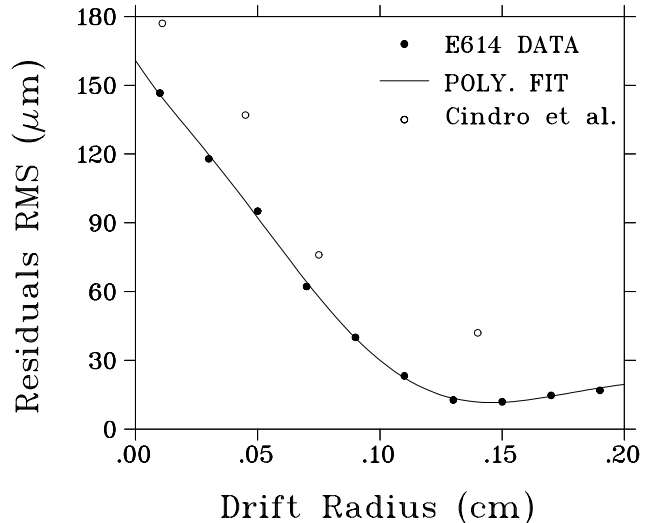


Fig. 5. Chamber resolution as a function of drift radius. The dots are computed from data acquired at 1850 V and a chamber orientation of 0° ; the curve is an eight parameter polynomial fit to the data. The circles are data from Cindro *et al.* [*op. cit.*] obtained with a drift chamber that had a cell size of 10.4 mm \times 11.4 mm and filled with pure DME gas.

One of the prime purposes of this prototype test was an important decision regarding the final chamber design, whether field wires are required between the sense wires. Installing field wires introduces disadvantages in terms of chamber construction and stability, as well as increasing multiple scattering in the chamber. The no field wire option is, therefore, desired based on this criteria. The lack of field wires, however, results in a weak electric field region away from the sense wires (zero at the midpoint between any two sense wires), and hits may therefore be lost due to poor electron collection from this region. This weak field region raises a concern about the chamber efficiency as a function of distance from the sense wire. To examine this effect the efficiency was calculated as a function of distance from the sense wire for 0° runs resulting in Figure 6. As expected, the lower threshold runs (140 mV) provide the best result, since signals arriving from the weak field region are expected to be small and therefore the most likely to be cut out by a high threshold. This result indicates that the chambers will have a negligible volume of slightly reduced efficiency if constructed without field wires. Construction of the PDCs along the design of those of the prototype tested will therefore begin in early 1999. Another conclusion reached is that the front end electronics of the detector function as expected. Construction of the required complement of these electronics will also begin in early 1999.

The construction of the seven planes and their assembly into the prototype detector for use in this test provided much needed experience in this procedure.

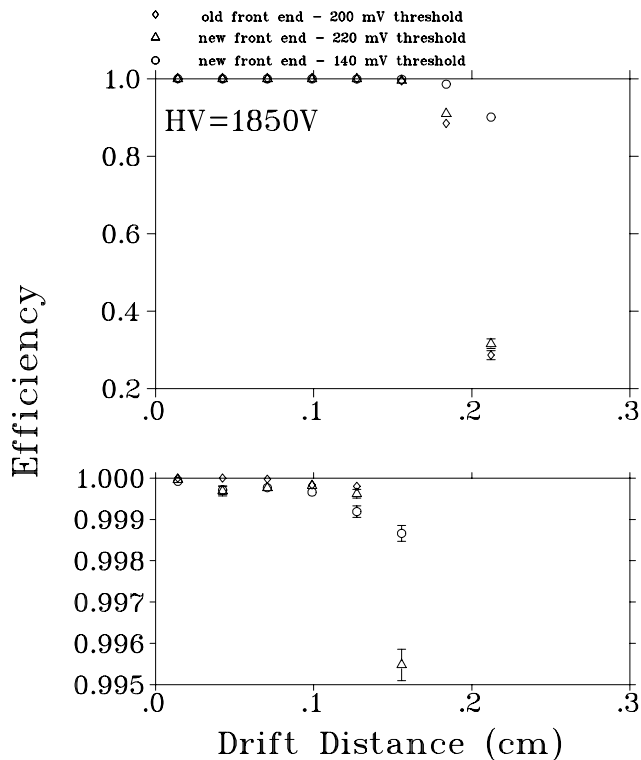


Fig. 6. Chamber cell efficiency as a function of distance from the sense wire for data acquired at 1850 V with a) the old front end at a threshold of 200 mV, b) the new front end at a threshold of 220 mV, and c) the new front end at a threshold of 140 mV. The bottom histogram is an enlarged copy of the top histogram.

As a result several changes were made in the detector design and in the assembly procedure. One of these changes may make it possible to assemble the chambers on a time scale of one year rather than the previously estimated 18 months to two years.

During 1998 several design decisions were made on the basis of Monte Carlo studies of the Expt. 614 detector system. One of those involved the tracking of the incoming muon. A central goal of Expt. 614 is to measure the product $P_\mu \xi$ to a precision of less than three parts in 10^4 . The mean depolarization ($\langle 1 - P_\mu^z \rangle$) must therefore also be less than this in magnitude. The approach used in a previous experiment [Jodidio *et al.*, Phys. Rev. **D34**, 1967 (1986); *ibid.*, **D37**, 237 (1988); Balke *et al.*, Phys. Rev. **D37**, 587 (1988)] at TRIUMF, to measure the muon trajectory before the muon encounters the fringe field (i.e. where the trajectory is linear) was examined via Monte Carlo. To determine if such a measurement would provide the desired information on the stopped muon polarization, two simulated PDCs were placed in the beam line, upstream of the fringe field. The multiple scattering in these detectors modified the relationship between the muon momentum and the muon spin so much that the results could not be used to make a selection. It was therefore

decided to study the employment of a very low mass device, such as a time expansion chamber (TEC), in this position. In Monte Carlo simulations, such a chamber was placed upstream of the solenoid fringe field. This chamber, designed to be operated at 20 torr, will be positioned so that the xz and yz measuring sections are just before the entry port in the spectrometer steel, which is ~ 160 cm upstream of the stopping target. In the simulation of the TEC the output of the chamber was used to reconstruct the incoming muon track. Correlations between the reconstructed angle with the spin direction of the muon as it stopped in the target were studied. A cut on the polar angle of the initial muon track as measured by the TEC was found which retained $\sim 12\%$ of all muons stopping in the target while reducing the mean depolarization $\langle 1 - P_\mu^z \rangle$ of the retained events to $\sim 2 \times 10^{-4}$. This result was obtained using a standard M13 beam with a focus at the fringe field region, 160 cm upstream of the target. For such a tune $\sim 78\%$ of the M13 flux stops in the target so that the above selection means that only 10% of the incoming muons are finally useful. This success of the TEC concept has led to the decision to complete the design work with the aim of testing a prototype in the summer of 1999. Monte Carlo studies to search for an M13 tune that optimizes the percentage of muons with mean depolarization $\langle 1 - P_\mu^z \rangle \leq 2 \times 10^{-4}$ will be carried out.

Another design decision, the implementation of pulse height measurements on signals from the proportional chambers (PC) near the muon stopping target was made based on Monte Carlo studies.

μ depolarization in detector materials will occur through the formation of muonium with subsequent spin exchange occurring between the electron and muon. This does not occur in general in pure metals where the lifetime of any muonium that is formed is too short to allow the spin exchange to happen. Obviously the target material will be the highest grade Al possible.

On the other hand muonium can form in many of the materials that make up the detector and may last sufficiently long enough for this spin exchange process to occur. It is necessary to prevent muons stopping in such materials or to be able to “cut” such events during the analysis stage. This issue will be addressed by the use of the proportional chambers adjacent to the stopping target. Nominally the condition that the two upstream PCs see the passing muon while there is no signal from those downstream of the target removes such events. However, this simple scheme may not account for those muons that could lose all their energy and stop in the last upstream PC. The addition of ADCs to the PCs will solve this problem by allow-

ing for a measurement of the energy loss. Monte Carlo simulations were performed to determine the efficacy of this extra information. In the simulation a beam of 29.7 MeV/c μ^+ s was tracked until they stopped. As muons entered and exited the PCs, their kinetic energy was recorded and their energy loss in each chamber was entered into a histogram. The mean energy loss per muon in the chambers was ~ 0.1 MeV. It was found that, in 10,000 entries, the smallest energy loss recorded by PC(+1) was ~ 20 keV. Providing the chamber thresholds can be kept low (≤ 5 keV), it is therefore unlikely that muons will pass through the target and not be recorded by PC(+1). With the pessimistic assumption that the PC(+1) energy threshold is 25 keV, ~ 2 stops in PC(+1) will be missed by a cut at this level per 10^4 stops in the target.

A scatterplot of energy losses in PC(-2) and PC(-1) is shown in the upper-left of Fig. 7 and exhibits two main features: a dense locus of points with a positive slope and a less dense locus with a negative slope. The dense locus with positive slope is due to muons stopping in the target (Fig. 7, bottom left), and the low energy end of this locus is due to those that pass through the target (Fig. 7, bottom right). The less dense locus of negative slope is due to muons stopping in PC(-1). A two dimensional cut along the lower edge of the locus of PC(-1) stops reduced such stops to $2 \cdot 10^{-4}$ of the incident flux while more than 97% of the muons stopping in the target were kept.

The measured P_μ value for muons stopped in $CF_4(ISO)(80 : 20)$ gas at $B = 2T$ is $P_\mu > 0.985$.

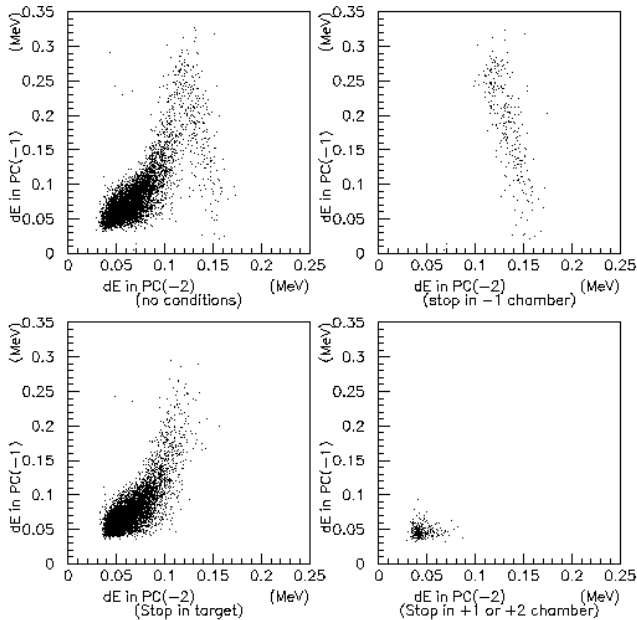


Fig. 7. Energy loss in PC(-1) vs. PC(-2) chambers for various muon stopping conditions. Top left: no conditions; top right: stop in PC(-1); bottom left: stop in target; bottom right: stop in PC(+1) or PC(+2).

According to the above Monte Carlo calculations $\leq 2 \cdot 10^{-4}$ muons stop in PC(-1) and in PC(+1). The shift of $(1 - P_\mu \xi)$ is therefore pessimistically estimated to be $(1 - 0.985) \times 5 \cdot 10^{-4} = 7.5 \cdot 10^{-6}$.

A monitor of the stopping distribution in the target is required. A simple method is merely to count the number of muons passing through the proportional chambers. A Monte Carlo study in which the material determining the range of muons was altered showed that the ratio of the number of muons recorded by PC(+2) to those recorded by PC(-2), $N_{PC(+2)}/N_{PC(-2)}$, and the ratio of PC(+1) to PC(-1), $N_{PC(+1)}/N_{PC(-1)}$, were found to be sensitive to changes in the stopping distribution. These ratios should not be affected significantly by factors such as PC efficiency or muons stopping in PC(-1). For a stopping distribution that was symmetric in the target the ratios $N_{PC(+1)}/N_{PC(-1)}$, and $N_{PC(+2)}/N_{PC(-2)}$ were 0.054 and 0.0173, respectively. Deviations of $\pm 20 \mu\text{m}$ in degrader thickness produced a significant change in these ratios. It has thus been concluded that the central PCs will provide a reliable monitor of stopping distribution.

The geometry of the original (baseline) detector had equal, 4.8 cm, centre to centre spacings of the PDC pairs (x, y) . This geometry presents the possibility that the wavelengths of certain helical tracks would coincide with the period of the chamber pairs, thus producing poor fits in the x or y projection. A Monte Carlo study was therefore made of alternating these spaces such that the distances between the centre of each pair was either 4.8 or 6.8 cm. It was found that this change substantially improved the momentum resolution (see Fig. 8) by increasing the lever arm over which the track position is measured. Little difference was found in the angular resolution for the two cases. The detector will be assembled with spaces between pairs that are not all identical and on average that are larger than the baseline design.

The Expt. 614 solenoid magnet is a used NMR coil, "sister" to a magnet used in an experiment at LAMPF. The LAMPF magnet was not available to Expt. 614. The Expt. 614 magnet was tested at the site of the company from which it was purchased. These tests were observed by TRIUMF personnel sent for that purpose. It was then shipped, at liquid helium temperature, to TRIUMF in September where further tests were performed. The solenoid has no return yoke for the very large field so design work has begun, with construction of this shield scheduled for mid 1999. The field of the shielded magnet will then be mapped in detail.

During 1998 Expt. 614 took possession of a new clean room in the office building. This facility, the old CCD lab modified by TRIUMF to meet the

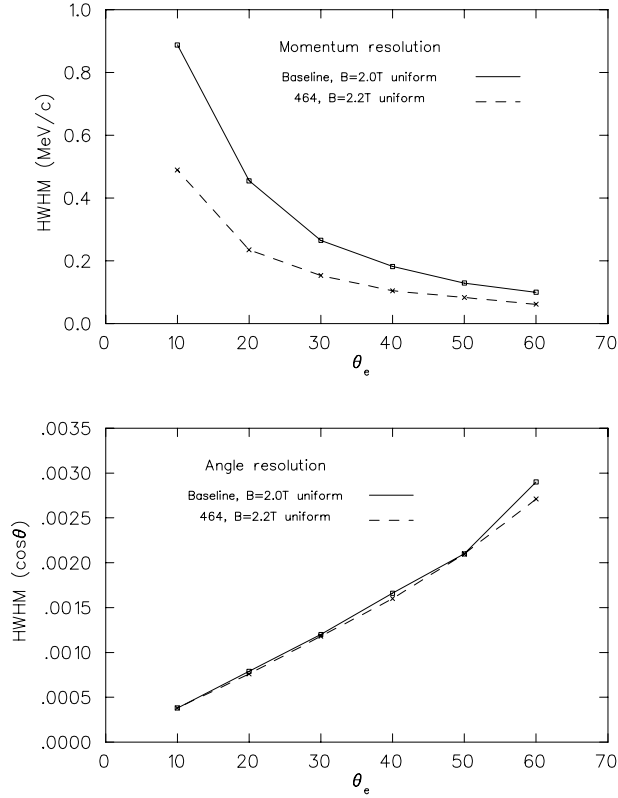


Fig. 8. Top: momentum resolution for baseline spectrometer (solid line), and spectrometer modified to include alternating 4.8 and 6.8 centre to centre spaces (464 option, dashed line). Bottom: angle resolution for same two options.

requirements of Expt. 614, will be used for the assembly of the drift chambers and the proportional chambers. As stated above, this work is to begin in early 1999. The goal of the Expt. 614 collaboration is to assemble these chambers so that it will be possible to be on the floor in late 2000 to begin data accumulation.

Also in 1998 the Expt. 614 collaboration undertook to examine the M11 channel as a potential source of surface muons. The “old wives’ tale” was that no surface muons could be found emanating from M11. This undertaking turned out to be non-trivial. The largest changes that were required to make this hunt for polarized muons possible fell to the TRIUMF Power Supply group. Alterations to the power supplies had to be made in order that they would operate at the low currents required for a 30 MeV/c tune. In fact it was found that the septum supply would not operate at the required current so another supply had to be substituted for it. The hunt was a success, M11 is a source of surface muons. The flux is lower than that in M13 but should be useful for tests of Expt. 614 detectors. The μ SR people are now considering the possibility of doing some of their work on M11.

In summary, for Expt. 614 1998 was another busy and productive year.

Experiment 705

BNL Experiments 813, 885 and 906

Strange physics at BNL: a search for the H particle (BNL 813); a search for $\Lambda\Lambda$ hypernuclei (BNL 885) using gas microstrip chambers (705); an experiment to detect $\Lambda\Lambda$ hypernuclei via characteristic π -mesonic decays (BNL 906) (C.A. Davis, TRIUMF)

Experiment BNL 813

In 1998, Manitoba graduate student Liping Gan completed her Ph.D. thesis [Gan, *A study of the sensitivity of the H dibaryon search experiment E813 at BNL through $(\Sigma^-, p)_{\text{atom}} \rightarrow \Lambda + n$* , Ph.D. thesis (University of Manitoba, 1998)] on the analysis of calibration data for BNL Expt. 813. This experiment searches for the six-quark (uuddss) H particle [Jaffe, Phys. Rev. Lett. **38**, 195 (1977)] by looking for H particle production by means of Ξ^- capture on the deuteron ($\Xi^- + d \rightarrow H + n$). Ξ^- particles are stopped in liquid deuterium (see Fig. 9) and the signal of H particle production is monoenergetic neutrons in coincidence with “tagged” Ξ^- s. To interpret our results quantitatively, we have to know both the “tagging efficiency” – that is, the probability that a Ξ^- which we identify as entering the deuterium with the right energy and at the right angle to stop will, in fact, stop – and the neutron detection efficiency. These quantities can be calculated by Monte Carlo simulation, but the work described in Gan’s thesis provides an independent check on the Monte Carlo. Instead of Ξ^- s stopping in liquid deuterium, she looked at Σ^- particles stopping in liquid hydrogen, producing a Λ particle and a monoenergetic neutron. The Σ^- particles are tagged in the same

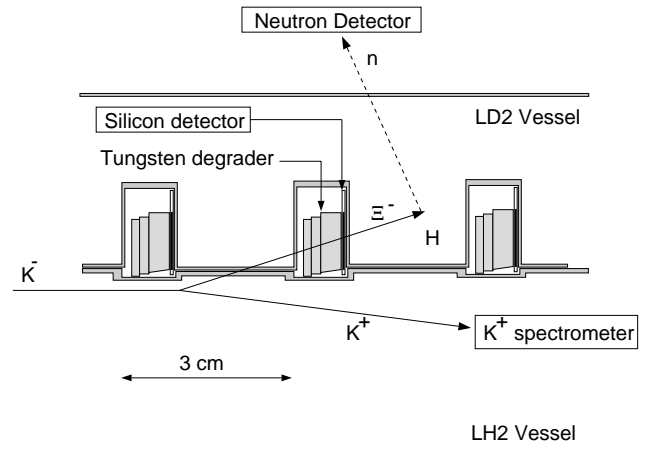


Fig. 9. The BNL E813 version of the H search. Ξ^- particles produced in the liquid hydrogen of the lower chamber of the target are brought to rest in liquid deuterium in the upper chamber. Only three of the twenty target cells are shown.

way as the Ξ^- particles of the main experiment and the monoenergetic neutrons are detected in the same neutron detector. The target and detector geometry is the same and the kinematics of the two reactions are adjusted to be the same. The difference is that the fraction of stopped Σ^- particles which will be captured and form a Λ particle and a neutron is known quite accurately, so the calibration reaction gives us the product of the tagging efficiency and the neutron detection efficiency.

About 10% of the BNL E813 data were taken in 1992. The balance was split between 1993 and 1995. The 1992 and 1993 data have already formed the basis of Ph.D. theses. The 1995 data are now being added to the 1992 and 1993 data and an overall analysis is being done. We expect the final result will be published in 1999.

Details

The H dibaryon is a hypothetical six-quark particle with the same quark content (uuddss) as two Λ s. In 1977, Jaffe [*op. cit.*] predicted that the H might be lighter than the $\Lambda\Lambda$ mass of 2231 MeV/c², and hence not be able to decay without a change in strangeness – i.e. it would be bound against strong decay. BNL E813 and E836 are experiments designed to look directly for the signature of H formation. As such, these experiments have the advantage that they are insensitive to decay modes and lifetime of the H . BNL E813 looks for H formation through Ξ^- capture on the deuteron and is most sensitive to a lightly bound or slightly unbound H in the mass range from about 15 MeV/c² above to 100 MeV/c² below the $\Lambda\Lambda$ mass. BNL E836 looks for H formation via the (K^-, K^+) reaction on ³He and is most sensitive to a more tightly bound H in the mass range from about 50 to 380 MeV/c² below the $\Lambda\Lambda$ mass.

BNL E836 was completed in 1997 and the result is published in Physical Review Letters [Stotzer *et al.*, Phys. Rev. Lett. **78**, 3646 (1997)]. No evidence for H -production was seen in the mass range from 50 to 380 MeV/c² below the $\Lambda\Lambda$ threshold. The upper limit on H -production cross section in this region is approximately an order of magnitude below the theoretical prediction [Aerts and Dover, Phys. Rev. **D28**, 450 (1983)].

BNL E813 uses the two step process, $K^- + p \rightarrow K^+ + \Xi^-, \Xi^- + d \rightarrow (\Xi^-d)_{\text{atom}} \rightarrow H + n$ (see Fig. 9). The 1.8 GeV/c K^- beam enters the lower, liquid hydrogen, part of the target where the Ξ^- are produced. The outgoing K^+ enter a magnetic spectrometer while the Ξ^- pass through an energy degrader and a silicon detector into the upper, liquid deuterium, part of the target where they stop, forming Ξ^- -deuteron atoms. A

$(\Xi^-, d)_{\text{atom}}$ is predicted [Aerts and Dover, Phys. Rev. **D29**, 433 (1984)] to have a substantial probability of forming an H particle and a neutron. Ξ^- s in the right angular range and having the right energy to stop in the liquid deuterium are tagged. The signature of the production of H particles is the detection of monoenergetic neutrons in coincidence with the tagged Ξ^- s.

In order to interpret the BNL E813 data properly and set a quantitative upper limit on the production cross section, it is necessary to know the product of the tagging efficiency and the neutron detection efficiency. At present, these have been calculated by Monte Carlo simulation. For example, the tagging efficiency was estimated at 0.136 stops per tag [Merrill, Ph.D. thesis (Carnegie Mellon University, 1995)]. The neutron detection efficiency depends on the energy of the neutron and on the pulse height cut. A typical value, for $\beta^{-1} = 3.0$ (57 MeV) and 3 MeV_{ee} threshold, is 38% [Merrill, *op. cit.*], which, when multiplied by the 21% of 4π solid angle of the neutron arrays, gives an overall neutron detection efficiency of 8%.

To check the Monte Carlo calculations experimentally, a (π^-, K^+) calibration run was made. During the 1995 run, data were taken for approximately 7 weeks with a π^- beam and with both the top and bottom chambers of the BNL E813 target filled with liquid hydrogen. The momentum (1.4 GeV/c) of the π^- beam was selected so that the kinematics of the Σ^- particles from $\pi^- + p \rightarrow K^+ + \Sigma^-$ would match that of the Ξ^- s from $K^- + p \rightarrow K^+ + \Xi^-$. The Σ^- s pass through the degraders and silicon detectors between the upper and lower target chambers and stop in the LH₂ of the upper chamber, forming monoenergetic neutrons by means of $\Sigma^- + p \rightarrow \Lambda + n$. This simulates the case in the normal H search configuration, with LD₂ in the upper target chamber, in which the Ξ^- s pass through the degraders and silicon detectors and stop in the LD₂, producing H particles by means of $(\Xi^-d)_{\text{atom}} \rightarrow H + n$. Since a stopping Σ^- in the calibration experiment deposits the same energy in the silicon detectors as a stopping Ξ^- in BNL E813, and since it is known that $(45 \pm 3)\%$ ¹ of the stopped Σ^- s will give a neutron, analysis of the calibration data will give us the product of the stops per tag and the neutron detection efficiency, allowing us to confirm the Monte Carlo simulation.

The analysis of the calibration data is presented in the Ph.D. thesis of Liping Gan. Figure 10 is taken from her thesis and shows the results of the 1995 (π^-, K^+) run. 1650 events satisfied the tag definition shown. Also shown are two methods of estimating the background under the peak. The polynomial fit is better at low β^{-1} than the background estimated from the untagged neutron spectrum. The monoenergetic neutron peak from

¹The uncertainty is mainly due to uncertainty in ν , the fraction of stopped Σ^- which will actually form a $(\Sigma^-, p)_{\text{atom}}$.

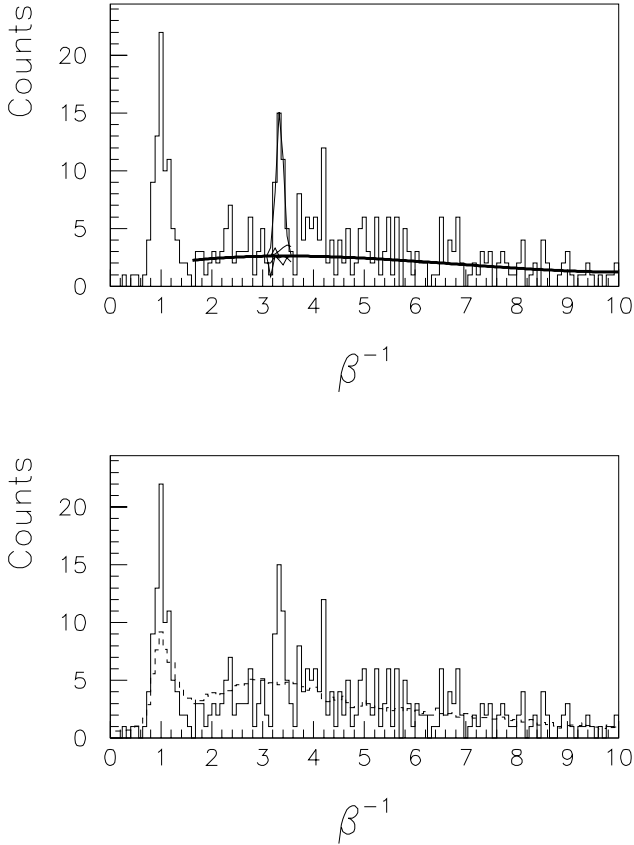


Fig. 10. Neutron β^{-1} spectrum of tagged Σ^{-} events from the 1995 $\pi^{-} + p \rightarrow K^{+} + \Sigma^{-}$ running. The tag definition is $7.5^{\circ} \leq \Theta_{K^{+}} \leq 10^{\circ}$, and $1.2 \text{ MeV} \leq E_{SI} \leq 2.2 \text{ MeV}$. The neutron detector threshold is 3 MeV. The background in the top plot was fitted with a third order polynomial, and the background in the bottom plot was fitted with the untagged neutron spectrum.

43.5 MeV neutrons is clearly seen at a β^{-1} of 3.4. The number of neutrons in the peak can be expressed

$$N_{\text{neutron}} = N_{\text{tag}} \eta_{\text{stop}} \nu R_{\Lambda} \eta_{nd},$$

where $N_{\text{tag}} = 1650$ is the number of tagged Σ^{-} events, η_{stop} is the number of stops per tag, $\nu = (85 \pm 5)\%$ is the fraction of stopped Σ^{-} which form a $(\Sigma^{-}, p)_{\text{atom}}$, $R_{\Lambda} = (53.2 \pm 1)\%$ is the branching ratio for the $(\Sigma^{-}, p)_{\text{atom}} \rightarrow \Lambda + n$ reaction [Hepp and Schleich, Z. Phys. **214**, 71 (1968)], and η_{nd} is the product of the neutron detector efficiency and solid angle. The number of neutrons in the peak (in the upper spectrum of Fig. 10) is 28 ± 6 , which gives $\eta_{\text{stop}} \eta_{nd} = 0.0375 \pm 0.0084$.

Based on this calibration, estimates can be made of the number of neutrons which would be expected from the full BNL E813 data set if H particles are really being formed. By taking the fraction of stopped Ξ^{-} which will form a $(\Xi^{-}, d)_{\text{atom}}$ from Batty [private communication] and the branching ratio for $(\Xi^{-}, d)_{\text{atom}} \rightarrow H + n$

from Aerts and Dover [*op. cit.*], Liping Gan estimates that a peak of about 80 neutrons at 0 MeV H binding or 40 neutrons at 50 MeV H binding would be expected. Such a peak would stand out much more clearly than the calibration peak shown in Fig. 10, and would be easily seen.

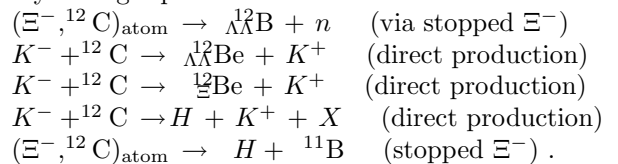
All the BNL E813 data from 1992, 1993, and 1995 are now being combined using a consistent set of cuts. At the present time it appears that no statistically significant H production peak will be seen, and that the experiment will set an upper limit. We expect the final result to be published in 1999.

Experiment BNL 885

Experiment BNL 885 is a search for exotic $S = -2$ systems, namely $\Lambda\Lambda$ -hypernuclei, Ξ -hypernuclei, and the H particle, a hypothetical six quark state (uudds) below the mass of two Λ particles. BNL E885 is a high statistics experiment, necessitated by the lack of data in this sector. For instance, the three candidate events for $\Lambda\Lambda$ -hypernuclei [Danysz *et al.*, Phys. Rev. Lett. **11**, 29 (1963); Prowse, Phys. Rev. Lett. **17**, 782 (1963); Aoki *et al.*, Phys. Rev. Lett. **69**, 1729 (1990)] are kinematically incomplete and appear to give inconsistent $\Lambda\Lambda$ binding energies. Experiment BNL 885 was carried out in 1996 at the D6 2 GeV K beam line [Pile *et al.*, Nucl. Instrum. Methods **A321**, 48 (1992)] at Brookhaven National Laboratory. The beam line was created for the BNL E813/E836 H particle searches, and is characterized by an excellent K/π ratio ($\sim 2-3$) and large acceptance (0.065 sr).

During the initial running of BNL E885, kaons incident on a CH_2 target produced Ξ^{-} hyperons. The Ξ baryons then left the production target, were degraded and stopped in a scintillating fibre array (SciFi), which acted as an active target. The Ξ hyperons are then free to form $S = -2$ exotic systems with target nuclei. After several weeks of running with CH_2 , a target switch was made. The majority of the running time then utilized a chemical vapour-deposited diamond target, in which the Ξ^{-} is created, stopped, and captured to form $\Lambda\Lambda^{12}\text{B}$ or other $S = -2$ objects. A diamond target ($\rho = 3.3 \text{ g/cm}^3$) was selected given the high density would result in more Ξ^{-} stops in the target, relative to graphite ($\rho = 2.3 \text{ g/cm}^3$) or CH_2 ($\rho = 1.1 \text{ g/cm}^3$).

BNL E885 is sensitive to a variety of channels in the $S = -2$ sector. Data analysis will search for evidence of the formation and decay of the following doubly strange species:



The AGS delivered beam to the D6 line from March 1, 1996 – June 28, 1996. In this time new apparatus was commissioned, experimental startup problems were ironed out, and production data were gathered. After commissioning and running several weeks with the CH_2 production target, we switched to diamond and received $0.807 \times 10^{12} K^-$ on this target, with 7.75×10^8 triggers accepted. The DAQ live time was approximately 75%. Over half of the data were reduced on-line and the cascade production rate was monitored (typically $\sim 600 \Xi^- / 10^9 K^-$, live-time corrected). Reduction of the data set was necessary to eliminate events in which the secondary particle is a proton misidentified by the hardware triggers as a K^+ , for example.

Micro-strip gas chambers

Microstrip gas chambers (MSGC) with an active area of $80 \times 50 \text{ mm}^2$ were instrumented and operated as a vertex detector in the experiment. While MSGC were first introduced a decade ago [Oed, Nucl. Instrum. Methods **A263**, 351 (1988)], they have rarely been used in experiments [Angelini *et al.*, Nucl. Instrum. Methods **A315**, 21 (1992); Geijsberts *et al.*, NIKHEF-H/94-12 (1994); Henkes *et al.*, Proc. Int. Workshop on Micro-Strip Gas Chambers (Lyon, 1995) p.143]. Furthermore, two distinct types of microstrip prints were utilized in these chambers. Prints manufactured with integrated circuit (IC) photolithographic technology have fine tolerances and thin minimum trace widths, but can suffer from a high rate of defects per print and are more costly. Prints constructed with printed circuit (PC) photolithographic technology have coarser tolerances but relatively few defects per print, and are extremely cost-effective. BNL E885 marks the first use, worldwide, of the inexpensive and simple microstrip printed circuit process, “PC-based” MSGC.

In-beam MSGCs are mounted upstream (IM1) and downstream (FM1 and FM2) of the target (see Fig. 11), which consists of an array of chemically vapour-deposited industrial diamond wafers. Drift chambers ID1-3 and FD0-3 provide tracking for beam and scattered particles upstream and downstream of the target; the MSGCs were used to improve knowledge of the interaction vertex. The gas mixture used in the MSGCs at BNL was argon:dimethyl ether (DME) (80:20).

PC x and IC y prints were mounted in the upstream MSGC IM1. Downstream of the target, chambers FM1 and FM2 contained only IC prints (IC x and IC y). Commissioning of the detectors was lengthy due to the difficulties in eliminating oscillations in the on-board microstrip preamplifier, the QPA02, and shielding against rf noise sources.

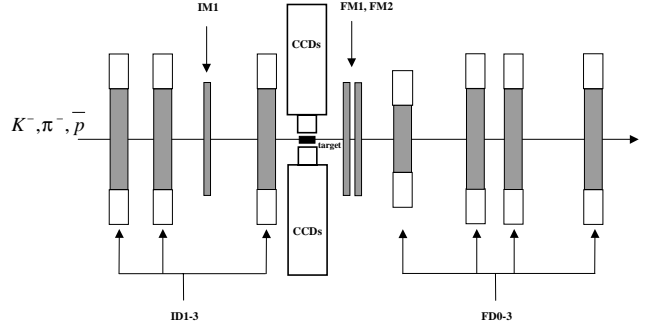


Fig. 11. Position sensitive detectors in BNL E885. For clarity, not all detectors in the target region are shown. MSGCs are IM1 and FM1-2. Drift chambers include ID1-3, FD0-3 (diagram not to scale).

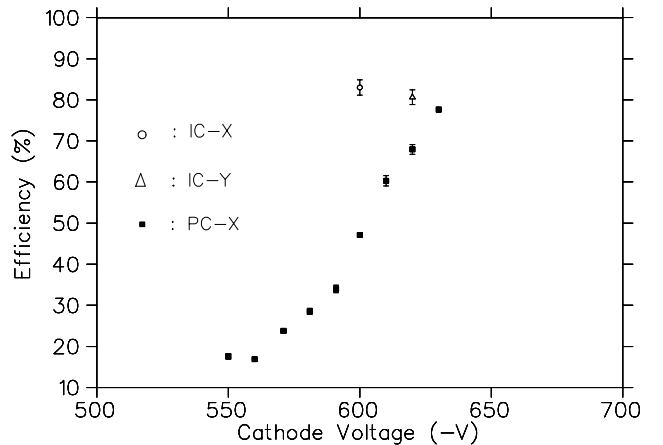


Fig. 12. An efficiency curve for a PC x print in the D6 area at BNL. Higher voltages were not attained due to sparking on the print. Also depicted are operating points for the IC x and y prints.

Figure 12 shows efficiency data for a PC x print, taken during the BNL 885 experiment, with the entire print instrumented. For comparison, the operating point for IC x and y prints is shown. The PC x microstrip will plateau at a higher operating voltage (plateau voltages could not be achieved due to breakdown beyond $V_{x,\mu} = 640 \text{ V}$), largely due to the thicker metal layer deposited on PC-based microstrip prints, versus that of IC-based prints. The experimental results include known defects due to lithography and high thresholds due to rf noise and are therefore reduced in efficiency. Efficiencies of the MSGCs reached $\sim 99\%$ in beam tests on sub-sections of microstrip prints, but were reduced in the experiment due to localized lithographic defects on prints, and high discriminator threshold settings.

A paper describing the experience designing, testing and operating the MSGC will be published [Landry *et al.*, Nucl. Instrum. Methods (in press)].

Analysis

BNL E885 analysis is carried out concurrently at Carnegie Mellon University (CMU), Kyoto University, and TRIUMF/University of Manitoba. Analysis efforts at CMU have concentrated on observing the monoenergetic neutron from $\Lambda\Lambda^12\text{B}$ formation, as well as analyses of the missing mass spectrum. At Kyoto, ten students have been employed to review the images obtained in the scintillating fibre (SciFi) arrays. Manitoba efforts have concentrated on the MSGC data and the missing mass spectrum.

A missing mass plot for the carbon data set can be used to indicate the production of Ξ^- hypernuclei, expected to be formed in various nuclei [Dover *et al.*, Ann. Phys. **146**, 309 (1983)]. Bound Ξ^- states would be observed as an enhancement in a missing mass spectrum below the quasi-free Ξ^- production peak. Similarly, this spectrum could be cast in terms of binding energy, in which bound states occur below $E = 0$.

A reduced data set of the entire BNL 885 data set has been selected and a time-of-flight alignment performed on a run-by-run basis. A binding energy spectrum can be obtained, making reasonable cuts on kinematic variables such as DCA (distance of closest approach of beam and scattered tracks), Chi-squared of track fits, outgoing kaon mass, etc. Figure 13 shows a preliminary binding energy spectrum, produced including kinematic variable cuts, for the reduced carbon data set. The binding energy is defined as the missing mass minus the sum of the ^{11}B and Ξ^- masses, or missing mass $- 11.5738 \text{ GeV}/c^2$. No clear indication of a peak in the bound region is seen. However, there are a significant number of counts in the bound region which have to be accounted for, and cleaned up through further calibration and energy-loss corrections.

Final analyses in the form of Ph.D. theses and publications are expected in 1999.

Experiment BNL 906

The D6 line at the Alternating Gradient Synchrotron at Brookhaven National Laboratory, the most intense and pure source of $\sim 2 \frac{\text{GeV}}{c}$ kaons available, was again used this year to explore the double strangeness frontier. The (K^-, K^+) reaction is used to transfer two units of strangeness ($S = -2$) to a nuclear or two-baryon system.

Another search for doubly strange hypernuclei using a cylindrical drift chamber and a beryllium target (BNL E906) was run on the D6 line in September–November. BNL E906 also serves as an H search and as a search for hyperfragments. Though several weeks of data were taken, additional data will be required in the near future as less than half of the proposed data set was realized.

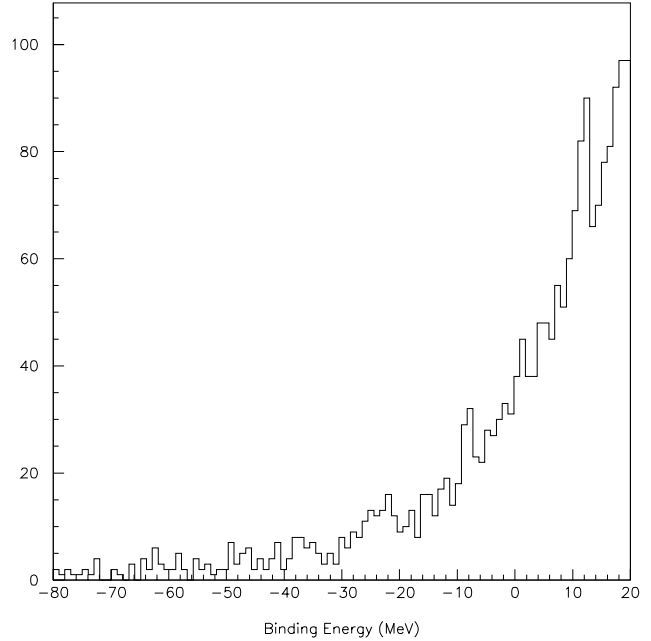


Fig. 13. Preliminary binding energy spectrum for carbon data set.

The ATLAS experiment at the LHC

(C. Oram, TRIUMF)

As described in detail in the 1996 Annual Report, ATLAS is building a general purpose pp detector which is designed to exploit the full discovery potential of the Large Hadron Collider (LHC) at CERN. The TRIUMF group is responsible for the engineering of the hadronic endcap (HEC) calorimeter, and the feedthroughs for the endcap cryostat. For the HEC, this year has seen the end of prototype and pre-production construction and the beginning of module production, while for the feedthrough project, at the University of Victoria, the project is completing the prototype stage. The simulation of the HEC, previously done using GEANT 3, is being re-written in the GEANT 4 framework by a collaboration between ATLAS and the GEANT 4 group headed by TRIUMF personnel.

Physics goals

The present theoretical understanding of elementary particles is in the context of the standard model. The standard model is a remarkably successful model, providing predictions which have been consistently confirmed by experiment for over two decades. Its agreement with experimental results, to enormous accuracy in some cases, makes it the most accurately verified model in science. Of the many elementary particles contained in the standard model, only the Higgs remains to be discovered. The central goal of ATLAS is the search for the Higgs particle.

There are good theoretical reasons to believe that the discovery of the Higgs will at least contain hints at, and more likely direct evidence of, what lies beyond the standard model. If the Higgs is composite, its existence requires as yet unknown ultra-strong forces. If it is elementary, it would be the only spinless particle to be discovered so far. There is a theoretical ‘naturalness’ problem for the masses of spinless particles. In the standard model, which is a highly nonlinear dynamical system, the elementary particles tend to take on the heaviest of all possible mass scales which in such a model are at inaccessible energies and inconsistent with other requirements of the model. All other particles discovered thus far have natural mechanisms, such as gauge and chiral symmetries, for protecting their masses so that they can lie in the observable range. For the Higgs particle, there is no such symmetry in the present model. The only theoretical scenarios which leave the Higgs particle light enough to observe are hypothetical ones, either technicolour or supersymmetry, both radical departures from the present structure of the standard model. If Higgs is seen at LHC, one of these scenarios should be seen at the same time.

Particle theory has progressed enormously over the last few decades with many appealing scenarios for physics beyond the standard model. The most likely of these is supersymmetry and the boldest of these is superstring theory. These theories are intimately related and are both radical ideas which promise a new conceptual framework for understanding elementary particles. Though far from being complete theories so far, there are superstring models which resemble the standard model in their low energy limit. These models have a great appeal as they contain a unification of fundamental forces which includes gravity. They have already had substantial impact on gravitational physics where, for example, in addition to the long sought reconciliation of gravity with quantum mechanics, they have been used to derive a fundamental understanding of black hole thermodynamics. Superstring theory is still in its infancy, but progress has been dramatic and the promise of great things to come has captured the imagination of a substantial fraction of the world’s theoretical particle physicists.

The present theoretical view is that the conventional grand unification of the strong, weak and electromagnetic forces can only work in the supersymmetric extension of the standard model. In that model, the grand unified energy scale is only two decades below the Planck scale, the ultimate energy where spacetime itself has quantum fluctuations. It is not out of the realm of imagination that, at energy scales where supersymmetry would be observed, evidence for an ultimate theory of everything, at least everything that can

exist once spacetime is formed, is within human grasp.

Experiments at LHC, where the ATLAS detector will take data, will probe the energy region where the Higgs particle, possibly supersymmetry, or other structures will be visible. This will be the first experimental probe of an energy region where fundamentally new physics is expected to occur in many years. There is every reason to believe that the results will be among the most dramatic ever.

Basic ATLAS design considerations

The most prominent issue for the LHC is the quest for the origin of the spontaneous symmetry-breaking mechanism in the electroweak sector of the standard model (SM). This is related to one of the most fundamental questions of physics: What is the origin of the different particle masses? New direct experimental insight is required to answer this question.

One of the possible manifestations of the spontaneous symmetry-breaking mechanism could be the existence of a SM Higgs boson (H), or of a family of Higgs particles (H^\pm , h , H and A) when considering the minimal supersymmetric extension of the standard model (MSSM). The Higgs search is therefore used as a first benchmark for the detector optimization. For the SM Higgs, the detector has to be sensitive to the following processes ($\ell = e$ or μ) in order to cover the full mass range above the expected discovery limit of LEP of about $m_H > 90$ GeV:

$H \rightarrow b\bar{b}$ from WH , ZH and $t\bar{t}H$ using a ℓ^\pm and b -tagging,
mass range $80 < m_H < 100$ GeV;

$H \rightarrow \gamma\gamma$ mass range $90 < m_H < 150$ GeV;

$H \rightarrow ZZ^* \rightarrow 4\ell^\pm$
mass range $130 \text{ GeV} < m_H < 2m_Z$;

$H \rightarrow ZZ \rightarrow 4\ell^\pm, 2\ell^\pm + 2\nu$
mass range $m_H > 2m_Z$;

$H \rightarrow WW, ZZ \rightarrow \ell^\pm\nu + 2 \text{ jets}, 2\ell^\pm + 2 \text{ jets}$
from WW, ZZ fusion using tagging of forward jets for m_H up to about 1 TeV.

The sensitivity of ATLAS to the standard model Higgs is displayed in Fig. 14.

In addition to signatures similar to these, the MSSM Higgs searches also require sensitivity to processes such as:

$A \rightarrow \tau^+\tau^- \rightarrow e\mu + \nu$'s
 $\rightarrow \ell^\pm + \text{hadrons} + \nu$'s;

$H^\pm \rightarrow \tau^\pm\nu$ from $t\bar{t} \rightarrow H^\pm W^\mp b\bar{b}$ and using
 ℓ^\pm tag and b -tagging.
 $\rightarrow 2\text{jets}$

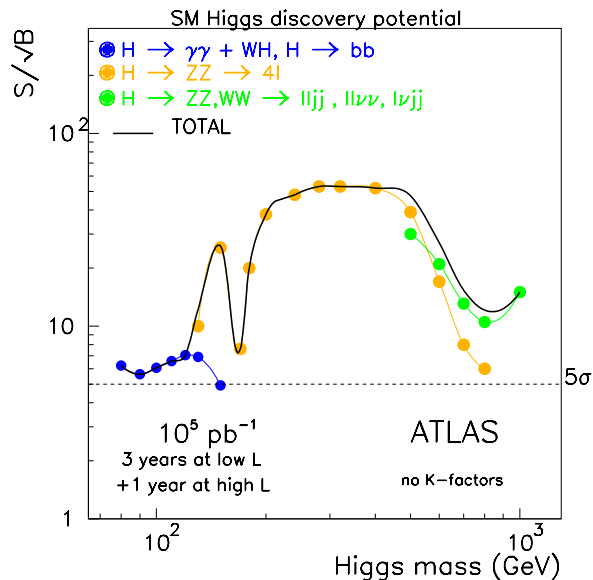


Fig. 14. Expected significance in ATLAS of standard model Higgs boson signal, as a function of Higgs mass, for integrated luminosity of 10^5pb^{-1} for several decay channels.

The observable cross sections for most of these processes are small over a large part of the mass range to be explored at the LHC. Hence it is important to operate at high luminosity, and to maximize the detectable rates above backgrounds by high-resolution measurements of electrons, photons, and muons.

Canada's participation in ATLAS

The Canadian group consists of 35 grant eligible physicists from TRIUMF, University of Alberta, Carleton University, CRPP, UBC, University of Toronto, University of Victoria, and York University. We are strongly involved in three construction projects centred around detecting hadrons in the endcap region: the hadronic endcap project, the hadronic portion of the forward calorimeter project, and the pipeline electronics for calorimetry. In addition we are committed as part of our common project contribution to providing the feedthroughs for the two endcap cryostats. TRIUMF is directly involved in all these projects and in the physics simulations.

The hadronic endcap project

The hadronic endcap calorimeter (HEC) is a liquid argon sampling calorimeter with copper absorbers [ATLAS Collab., ATLAS Liquid Argon Technical Design Report (1996)]. A concise overview of this design was provided in the TRIUMF 1996 Annual Report.

Hadronic endcap module production

This year saw the major milestone of successfully passing the Production Readiness Review process at CERN. This process reviews the design and quality control aspects of the design, its aim is to provide ATLAS with a confidence that the sub-detectors will all

be of high quality and reliability. Successful completion authorizes the series production to proceed at the HEC sites. The successful completion by the HEC group allowed production to start this fall at all the HEC sites (in Germany, Russia, and Canada). Mechanical aspects of the construction project are overseen by the TRIUMF group. To pass this review the design had to be finalized. While only minor engineering changes had to be made from the pre-production module, the choice had to be made of the technical realization of the high resistive coating. A review committee from Mainz and MPI (Munich) was struck, and the decision was made to use carbon loaded kapton rather than a carbon loaded paint technique. The carbon loaded kapton technique was originally proposed by the detector group at TRIUMF.

Starting in November, the clean room in the MESA was fully in use manufacturing the production readout boards for the HEC. The brake press in the TRIUMF Machine Shop has been heavily used, cutting out components of the detector. Using the brake press and an adaptation of a technology called a steel rule die, commonly used to cut out boxes and shoe leathers, we stamp out nearly all the materials that go in the liquid argon gaps of the HEC. These materials are then either shipped to module stacking sites (including TRIUMF), to Russia for assembly into EST boards, or stay at TRIUMF for assembly into readout boards.

Also in November, copper plate production started at the University of Alberta, for absorber plates for modules to be stacked at TRIUMF. This production is undertaken on a milling machine purchased using a loan from TRIUMF. First plate delivery to TRIUMF will be in early 1999, when module stacking will start in the meson hall clean room. Final manufacture of tooling for this clean room area was proceeding through the fall. Module stacking should start in early 1999.

Test beam measurements of hadronic endcap modules

Two test beam periods on the CERN H6 beam line this year have tested the performance of the pre-production modules of the calorimeter. The H6 beam line provides beams from 20 to 180 GeV. The April test beam data has been analyzed, while analysis of the second period is on-going.

The layout of the beam defining collimators, beam position measuring MWPCs, the collimator and liquid argon cryostat is shown in Fig. 15. In the cryostat are 4 modules of the HEC. Because of limited space they are orientated with their plates perpendicular to the test beam, rather than pointing in a pseudo-rapidity geometry as they will be in ATLAS. This causes the beam to impinge on significantly more readout channels than will be the case in ATLAS, thus increasing

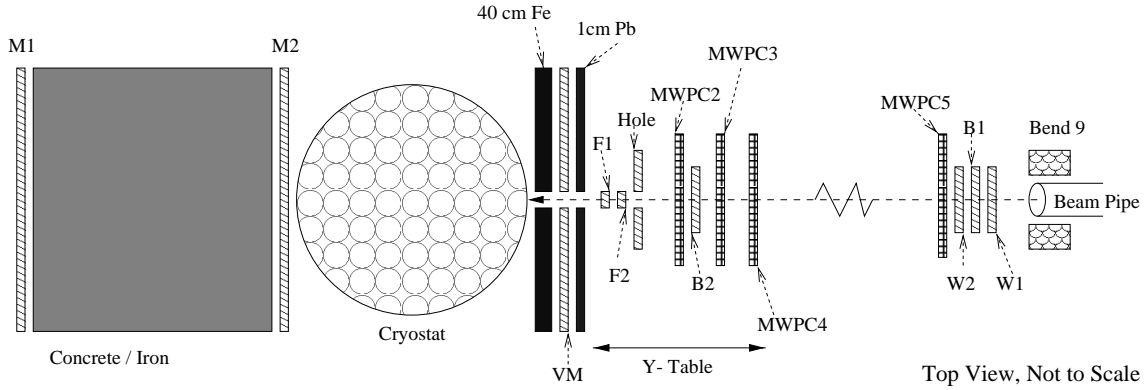


Fig. 15. Set-up of the HEC test beam area at the CERN SPS H6 beam line.

the observed electronic noise to the energy resolution. The impact points of the centre of the beam on the front face of the calorimeter are shown in Fig. 16, along with the transverse readout segmentation on the front face. The longitudinal (or depth) segmentation of the calorimeter is in three depths, the first 20 cm, the next 40 cm, and finally the last 80 cm of copper.

The pulse height from each readout segment is collected in 25 ns time slices. In a typical event there are about 6 adjacent time slices significantly above the noise. Digital filtering [Cleland and Stern, Nucl. Instrum. Methods **A338**, 467 (1994)] is used to optimize the signal-to-noise ratio. Results of this analysis, as analyzed by the University of Victoria group [Dobbs *et al.*, ATL-COM-LARG-98-009], are shown in Figs. 17 and 18 for electrons and pions respectively. Comparison of these results with Monte Carlo simulations shows the calorimeter is performing as expected, and meets ATLAS design requirements.

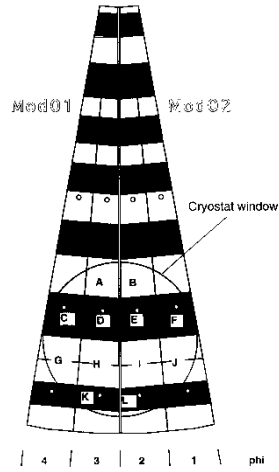


Fig. 16. The geometric layout of the four beam impact positions (D, E, H, and I) on the front face of the HEC calorimeter modules.

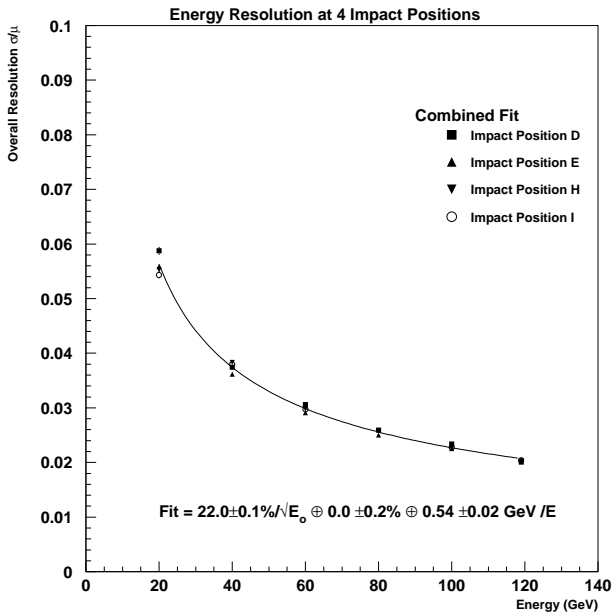


Fig. 17. Measured electron energy resolution: 20–120 GeV.

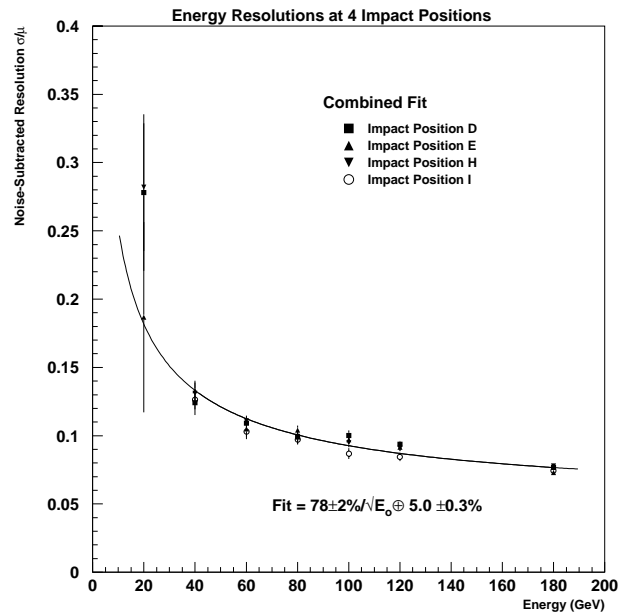


Fig. 18. Pion energy resolution from 20 to 180 GeV, fit over the four beam impact positions.

Study of rare K decays

BNL 787

(D. Bryman, TRIUMF/Victoria)

The rare kaon decays $K^+ \rightarrow \pi^+ \nu \bar{\nu}$ and $K_L \rightarrow \pi^0 \nu \bar{\nu}$ offer unique opportunities to scrutinize phenomena associated with quark mixing and the origin of charge-parity (CP) non-invariance.

BNL 787 has presented evidence for the decay $K^+ \rightarrow \pi^+ \nu \bar{\nu}$ [Adler *et al.*, Phys. Rev. Lett. **79**, 2204 (1997)] based on the observation of a single clean event from data collected in the 1995 run of the AGS. The branching ratio indicated by this observation ($4.2_{-3.5}^{+9.7} \times 10^{-10}$) is consistent with the standard model expectation although the central experimental value exceeds it by a factor of four.

The expected sensitivity from data currently under analysis (taken in 1995–97) is ~ 2.5 times that of the 1995 data alone. Subsequent to the initial publication, improvements in the analysis have resulted in background rejection that is ~ 3 times greater (a background level of 1×10^{-11}), with no loss in acceptance and results of the analysis of the larger data set are expected shortly. BNL 787 is expected to reach an ultimate single event sensitivity below 10^{-10} by the end of the 1998 running period.

The results presented so far relate only to the relatively clean phase space region above the $K^+ \rightarrow \pi^+ \pi^0$ ($K_{\pi 2}$) peak. Progress is also being made to access the region below the $K_{\pi 2}$ peak in order to roughly double the sensitivity, but here the background rejection is much more difficult. Using 1989 data, the published upper limit for this was 1.7×10^{-8} (90% C.L.) [Atiya *et al.*, Phys. Rev. **D48**, R1 (1993)] based on no candidate events. The most serious background comes from the decay $K_{\pi 2}$, where the π^+ loses its energy in the target by a nuclear scattering while the detector fails to detect either of the two photons from the π^0 decay. In addition to substantial upgrading of the photon veto system, π/μ identification has since been improved by three orders of magnitude due to the better momentum resolution and demultiplexed range stack scintillators. At present, the analysis of 1995–97 data is in progress in parallel with the analysis of the region above the $K_{\pi 2}$ peak. The expected sensitivity from the 1995–97 data is at the level of the SM prediction with $S/N \approx 1$.

In 1998 the first published limit on the decay $K^+ \rightarrow e^+ \nu \mu^+ \mu^-$ was obtained by the BNL 787 collaboration [Adler *et al.* Phys. Rev. **D58**, 012003 (1998)]. The result $B < 5.0 \times 10^{-7}$ is consistent with predictions from chiral perturbation theory. This decay mode is a particularly good test of the chiral expansion because the structure dependent terms dominate over the inner bremsstrahlung term due to helicity suppression.

BNL 949 – $K^+ \rightarrow \pi^+ \nu \bar{\nu}$

If the branching ratio is as high as the central value of the current result (although there is a large statistical uncertainty), new physics would be indicated. To fully explore this possibility or to make a precise measurement of the $t-d$ quark coupling $|V_{td}|$ (assuming the SM value for the branching ratio), a new measurement has been proposed. BNL 949 has been designed to obtain a single event sensitivity of $(8-14) \times 10^{-12}$ by means of modest upgrades of the present BNL 787 detector.

The detection of $K^+ \rightarrow \pi^+ \nu \bar{\nu}$ (a single incident K^+ followed by the decay to a single π^+ of momentum $P < 227$ MeV/c and no other observable products) requires suppression of all backgrounds to well below the sensitivity for the signal. The two most significant backgrounds are the two-body decays $K_{\mu 2}$ and $K_{\pi 2}$. The other significant background comes from either a π^+ in the beam scattering into the detector or from K^+ charge exchange (CEX).

The primary requirement for the improved experiment BNL 949 is to stop more K^+ mesons near the centre of the detector without increasing the instantaneous rates in the detector. This requires more proton flux from the AGS, but by using an increased duty factor and a lower kaon momentum, the instantaneous beam rate is essentially unchanged. At lower kaon momentum the efficiency for stopping kaons in the target increases while the instantaneous rates due to other sources decrease. Additional improvement arises from longer running time and from increased trigger and DAQ efficiencies. Modest upgrades to the BNL 787 detector and DAQ are needed, primarily to reduce backgrounds in the region below the $K_{\pi 2}$ peak and to satisfy the increased DAQ bandwidth requirements corresponding to the increased sensitivity.

Additional photon veto detectors will be installed, principally a ‘barrel veto liner’ (BVL), between the range stack and present barrel photon veto, and new photon detectors along the beam axis. The BVL system consists of 48 modules of Pb scintillator arranged in 48 azimuthal sectors. This system is complete and installation will commence after BNL 787 completes data-taking at the end of 1998. The BVL adds critical live material in a thin region of the detector near 45° , and thus is expected to improve the photon vetoing power of the entire detector. It will be especially effective in reducing the $K_{\pi 2}$ background in the region below the peak.

The BNL 787 photon veto thickness is ≤ 7 radiation lengths (X_0) along the beam line in the forward and backward directions. For photons at the low end of our energy range this implies a pass-through inefficiency as high as a few percent. It is important to

reduce this inefficiency in order to suppress the $K_{\pi 2}$ background below the peak. This can be partly accomplished by adding a small supplemental veto counter downstream of the scintillating fibre stopping target. In the upstream direction, three strategies will be used to improve the photon veto efficiency: (i) add several radiation lengths to the existing lead glass detector and increase the radius, (ii) replace the lucite hodoscope light guides by wavelength shifting (WLS) fibres (this allows the installation of active photon veto elements. Another improvement will be the use of triangular-shaped hodoscope elements which will result in better hodoscope position resolution by up to a factor of 5.); and, (iii) modify the beam instrumentation support structure to allow the addition of an annular calorimeter of up to 10 radiation lengths of pure CsI or CeF₃.

The DAQ is FASTBUS based, with front-end read-out into SLAC scanner processors (SSP). The data are transferred via the FASTBUS cable segment to VME processors (200 MHz Power PCs). The data are transferred between spills from the VME processors to a 4-CPU SGI Origin 200. The data transfer capability was demonstrated to be >50 Mbytes per spill. The system as currently configured can maintain 80 Mbytes/spill. The dead time was $\sim 17\%$ per MHz of stopped kaons (KB) (down from 28% in 1995). The DAQ system has been substantially upgraded already. The addition of a fourth cable segment and VME processor are needed for 10^{14} protons/pulse running. Other modest trigger and DAQ efficiency improvements should provide an additional 15% gain. We can also make improvements of $\sim 10\%$ in the efficiency of our off-line production software. Other more extensive improvements to the trigger/DAQ system using extended programmable logic devices (ELPD) to implement a level 0 pattern finder and a pipelined trigger transmitter are presently under study and may yield up to a factor of 2 gain in sensitivity.

The net increase in sensitivity per year for BNL 949 (relative to the published 1995 result) is expected to be a factor of ~ 13 .

BNL 926 – $K_L \rightarrow \pi^0 \nu \bar{\nu}$

During 1998, some effort began aimed at prototype detector development for a new experiment designed to detect and study $K_L \rightarrow \pi^0 \nu \bar{\nu}$ for the first time. The goal of AGS experiment 926 is to observe and definitively measure the rate of this decay. We aim to unambiguously detect a large sample of events so that η , the SM CP violation parameter, can be determined to better than 15% accuracy without serious interference from background or systematic effects. We have scoped the experiment for a sensitivity of approximately 6×10^{-13} allowing for nearly an order of magnitude contingency to meet the goal of a successful measurement if the

branching ratio is at least 10^{-11} as predicted by the SM.

In order to make a measurement at the level expected in the SM, the most important means of eliminating unwanted events will be to determine that nothing other than one π^0 was emitted in the decay, i.e. to veto any extra particles. The most difficult mode to suppress is $K_L^0 \rightarrow 2\pi^0$. Good photon veto detection efficiency comparable to what has been achieved in BNL 787 will be required. However, to increase the probability that the source of the observed signal is truly the $\pi^0 \nu \bar{\nu}$ mode, additional information is needed. The K_L^0 momentum will be measured using time-of-flight by employing very low momentum kaons produced by a highly time-structured proton beam. Finally, angular and energy measurements for each photon from π^0 decay will be obtained from a preradiator/calorimeter. Such a system imposes kinematic constraints allowing event-by-event reconstruction in the K_L^0 centre of mass frame making a large fraction of the phase space available for detection.

A GEANT Monte Carlo study of the proposed BNL 926 detector has been done at TRIUMF. The simulation included the effects of the varying position of the K_L decay vertex, solid angle acceptance (including the beam hole), and reconstruction efficiency in the photon preradiator. The existing simulation includes photon conversion and reconstruction, phase space acceptance and cuts designed to suppress the major backgrounds (e.g. missing energy, missing mass and photon energy sharing). Preradiator angular resolution from the detector simulation is approximately 25 mrad. The inefficiency due to accidental spoiling of good events is estimated to be $< 10\%$ for a threshold of a few MeV and a timing window of 2 ns. The expected number of events to be accumulated is about 50. The single event sensitivity of the experiment would be approximately 6×10^{-13} if not limited by background.

At TRIUMF we are designing and constructing preradiator prototypes. The requirements of the preradiator include a photon angular resolution of approximately 0.02 r, a photon conversion efficiency of about 0.7 ($1.5 X_0$), a good measurement of the deposited energy and as short as possible linear extent. The principle we will employ is to measure the x and y positions and directions of the first electrons in the shower in a series of thin converter/detector modules. To keep multiple scattering of these electrons at the 0.02 r level each detector module will be $\leq 0.05 X_0$. Since our position resolution will be roughly 200 μm , the detector modules must then be separated by about 1 cm.

The full preradiator will employ 42 layers. Each layer consists of a 2 mm thick \times 16 cm wide scintillator (either scintillator plate or arrays of fibres), a layer

of drift chambers or straw tubes with sense wires separated by 10 mm and 5 mm wide cathode strips running perpendicular to the wires, and a 0.035 X_0 thick metal radiator. Mechanical rigidity may be given to a module by pleating the metallic radiator, thus avoiding the need for heavy frame structures around the beam region. The thicknesses of scintillators and radiators are similar to that of the calorimeter so that the energy resolution will be largely unaffected by the preradiator.

To confirm the expectations for the preradiator performance a 10-layer preradiator prototype module is under development. The prototype detectors will be tested at TRIUMF and at the National Synchrotron Light Source (NSLS) at BNL in conjunction with calorimeter prototypes.

Hypernuclear spectroscopy at DAΦNE FINUDA

(T. Bressani, Torino)

TRIUMF has been involved in the FINUDA experiment at DAΦNE for several years. Our contributions have included construction at TRIUMF of the 20 low-mass drift chambers, and tests using TRIUMF beams of the prototype neutron counters, silicon microstrips, and straw tubes. An extension of the experiment to study the reaction $K_L n \rightarrow K^+ p$ has been accepted by the DAΦNE Scientific Committee.

The experiment has been delayed due to the delayed startup of DAΦNE and due to problems with the FINUDA solenoid magnet.

DAΦNE status

In 1998 the accelerator has been commissioned in the “Day One” configuration, i.e. without solenoid magnets in the interaction regions. First collisions were observed in March with the collider in single bunch mode; a luminosity of 2×10^{28} was achieved. Following replacement of a defective dipole magnet, single bunch luminosities exceeding 10^{30} were achieved in October. In November multibunch collisions were observed with a luminosity of 10^{31} . The initial experiments are presently being installed in the collision regions.

FINUDA status

The FINUDA solenoid field was extensively mapped and finally declared acceptable. It has been delivered to Frascati and will be installed in early 1999. Installation of the detector elements is scheduled for summer, 1999. The full detector system, sans magnet, is being commissioned using cosmic rays.

TRIUMF/Univ. Victoria contributions

The outermost tracking layer is an array of 2424 aluminized mylar straw tubes arranged in three super-

layers (one axial and two approximately $\pm 13^\circ$), each superlayer with two sub-layers of staggered straws. The inner radius is 110 cm with a full length of about 255 cm for axial superlayers. The basic array element is a 0.03 mm-thick mylar straw, with a 15 mm inner diameter, for a total of 2424 straws. In this year, we have assisted with the installation and commissioning of the straw tube chambers in the clepsydra, which will be subsequently mounted in the solenoid.

The initial experimental program for FINUDA has stressed high resolution hypernuclear spectroscopy. However, there is also the possibility to study the hadronic weak interaction through the observation of the $\Lambda N \rightarrow NN$ and $\Lambda NN \rightarrow NNN$ interactions. This allows us to address the parity-conserving amplitudes as well as the parity-violating amplitudes studied by Expt. 497 at TRIUMF. The present data have large errors and do not agree well with theory.

At TRIUMF we have incorporated into the FINUDA simulation an event generator for weak decays based on a code obtained from A. Ramos. Briefly, the probabilities for $\Lambda N \rightarrow NN$ and $\Lambda NN \rightarrow NNN$ reactions are calculated using the one-pion-exchange mechanism, and then the propagation of these nucleons through the nucleus are considered. This results in the generation of nucleons fully correlated in energy and angle which can be tracked through the detector. The very thin targets used in FINUDA allow us to observe efficiently the low energy nucleons which are most sensitive to the different model predictions.

FINUDA collaborators (Canada only) are: Art Olin, George Beer, and Pierre Amaudruz.

Spin structure of the nucleon

HERMES

C.A. Müller, TRIUMF; M.C. Vetterli, TRIUMF/SFU; M.G. Vincter, Alberta)

Deep inelastic lepton-nucleon scattering (DIS) experiments have been crucial in the development of our current understanding of the quark-gluon structure of nucleons. In the last decade, intense interest has focused on how the spins of the quarks and gluons contribute to the spin of the nucleon. Information about this spin structure can be obtained from the cross section asymmetry measured in deep inelastic scattering of longitudinally polarized leptons from polarized nucleons with their spins parallel or anti-parallel. A series of such inclusive DIS experiments at CERN, SLAC and DESY on both proton and ‘neutron’ targets, recently culminating in remarkable precision, present a coherent picture. Early indications of the relatively small net contribution of the quark spins to the nucleon spin have been confirmed. Newly published data from HERMES, together with new data from SLAC at 50 GeV,

are adding to the inclusive data set as a function of Q^2 , thereby improving global fits of polarized quark distribution functions. However, it is now realized that inclusive measurements are intrinsically limited in what more they can offer.

Semi-inclusive measurements involving the detection of a leading hadron in coincidence with the scattered lepton offer a means of ‘flavour-tagging’ the struck quark to help isolate the contributions to the nucleon spin of the individual quark flavours, including the sea quarks. This is a central theme of the HERMES experiment, which is unique among polarized DIS experiments in two important respects. The targets are atomically pure nuclear-polarized H, D or ^3He gas in a high energy polarized electron storage ring. Hence the targets are undiluted by unpolarized nucleons in ‘extraneous’ materials. Also, the spectrometer detecting the scattered lepton, often in coincidence with hadron(s), combines substantial acceptance with hadron identification capability. Pion identification was included from the beginning, and kaon identification has been added for 1998. A schematic diagram of the experiment is shown in Fig. 19 and a detailed description can be found in [HERMES collaboration, Nucl. Instrum. Methods **A417**, 230 (1998), hep-ex/9806008].

While data on semi-inclusive hadron production have been produced by SMC, their statistical precision is limited and SMC does not identify the hadron type. HERMES is substantially improving the precision of data on semi-inclusive processes because of the experimental advantages mentioned above. Preliminary results of similar quality for the polarized quark distributions have already been released, from an analysis of only the 1995 ^3He and 1996 proton data. Twice as many proton data exist from the 1997 running, and a similar amount of deuteron data will be acquired in 1998/99. Kaon identification by the new RICH detector will provide flavour-tagging of strange quarks, for example through the identification of $K^-(\bar{u}s)$. Thus

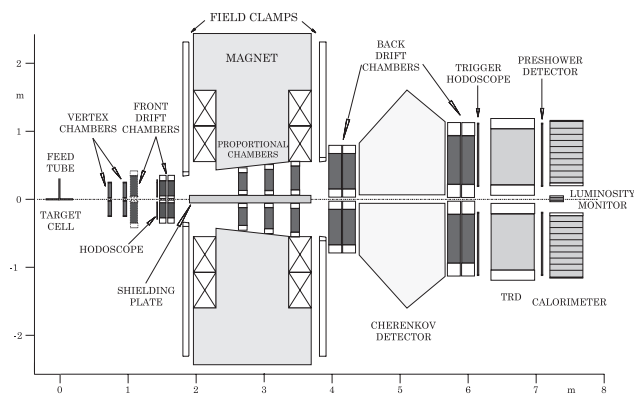


Fig. 19. Schematic side view of HERMES spectrometer.

the full database from HERMES will provide good precision on polarized quark distribution functions. Since precise data from two targets are required to exploit the power of this technique, the definitive HERMES precision will not be available until 2000.

In summary, HERMES will give unique results on semi-inclusive processes while remaining competitive for measurements of $g_1(x)$.

Canadian contribution to the experiment

Discrimination between e^\pm and hadrons is provided by the combination of a transition radiation detector (TRD) and electromagnetic shower counters. The Canadian group took the responsibility for the design and construction of the TRD, together with its complex xenon gas recirculation system, relying heavily on the expertise and infrastructure at TRIUMF. The Canadian group has also played a central role in the design and management of the rest of the experiment, including the design of all the wire chambers as well as the design and commissioning of the electron polarimeter at HERA. The demonstration of a high degree of beam polarization ($> 40\%$) was a pre-requisite for the approval of the experiment by DESY.

The experiment was commissioned in the spring/summer of 1995. Data were taken in 1995 on a ^3He target and in 1996–97 on H. A few weeks were also spent on high luminosity running with unpolarized targets. The TRD has worked very well over the first three years of operation. The design goal was to provide a pion rejection factor of 100 at 5 GeV with a e^\pm efficiency of 90% (PRF= total # of pions/hadrons divided by the # of misidentified pions/hadrons). This was achieved quasi-on-line early in the 1995 run, with typical PRFs of 120 integrated over all energies. Improvements to the interpretation of the TRD data using a probability-based analysis have increased the PRF by a factor of up to 10. More details on TRD performance can be found in [HERMES collaboration, *op. cit.*; R. Kaiser (for the PID group), *Particle identification at HERMES*, HERMES internal note 97-025], and in last year’s Annual Report.

The TRIUMF group is also responsible for PID (particle identification) algorithms. Progress was made this year on improving the description of the detector responses (parent distributions) used in the probability analysis of the PID detectors. This work is the basis for the technical portion of the thesis of Mr. J. Wendland (SFU) and is the subject of a HERMES internal note which will be submitted early in 1999 [Wendland, *A new simple Monte Carlo for PID analysis*, Simon Fraser University].

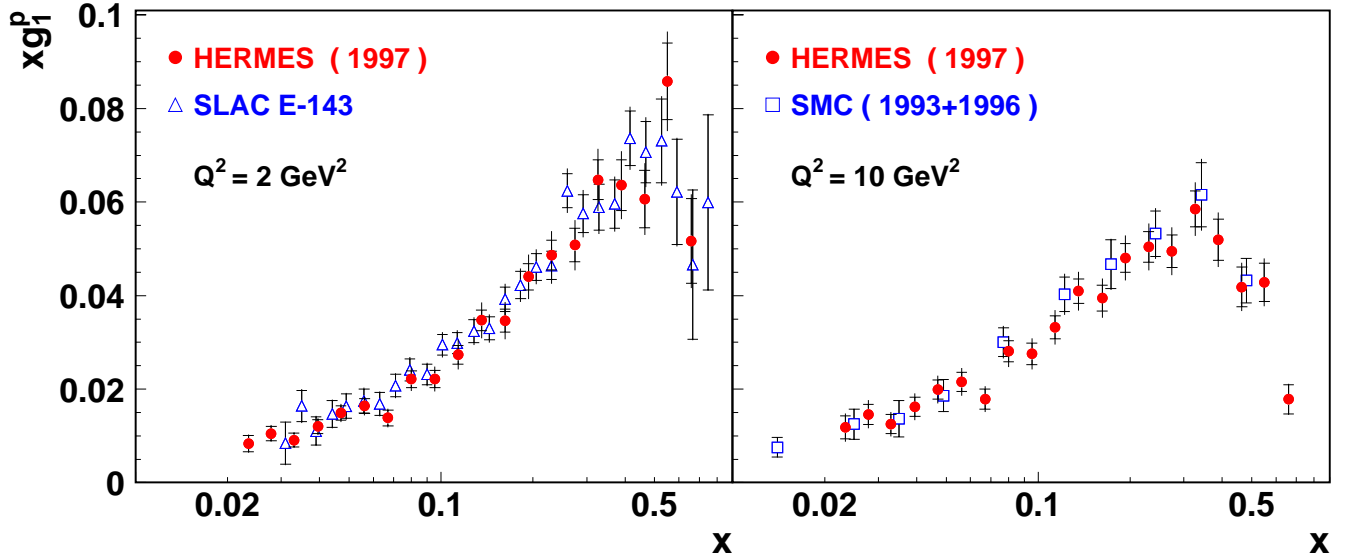


Fig. 20. The spin structure function $g_1^p(x)$ of the proton, multiplied by x , as a function of x . The HERMES data are evolved to a) $Q_0^2 = 2 \text{ GeV}^2$ and b) $Q_0^2 = 10 \text{ GeV}^2$, assuming g_1^p/F_1^p to be independent of Q^2 . This measurement is compared to recent results for $Q^2 > 1 \text{ GeV}^2$ from E-143 and from SMC, the latter for $x > 0.011$ only. The error bars show both statistical and systematic contributions.

Physics results

Inclusive scattering and spin structure functions

The spin structure function $g_1(x)$ can be determined from data on the deep inelastic scattering of longitudinally polarized leptons from polarized nucleon targets. The integral of g_1 is a measure of the contribution of the quark spins to the nucleon spin. Results for $g_1^n(x)$ from the 1995 data set on ^3He have been published [HERMES collaboration, Phys. Lett. **B404**, 383 (1997)] and formed the basis for the Ph.D. thesis of a Canadian student (R. Kaiser, SFU). However, given that 1995 was a commissioning year, the number of events collected does not represent the full data set on the neutron which will be accumulated by HERMES. On the other hand, the final results for $g_1^p(x)$ from the 1997 data set are at least as precise as any published data. They have now been published [HERMES collaboration, Phys. Lett. **B442**, 484 (1998), hep-ex/9807015] and are shown in Fig. 20, compared to results from SLAC-E143 and SMC at the appropriate Q^2 . It is clear that the systematic uncertainties are very well understood in all these experiments, which are based on quite different techniques.

Semi-inclusive scattering and polarized quark distribution functions

In parallel with the inclusive measurements, HERMES has been designed to measure polarized semi-inclusive DIS. This unique data set (with identified π 's and K 's) will significantly improve the determination of the individual spin-dependent quark distribution functions. Figure 21 shows that the preliminary

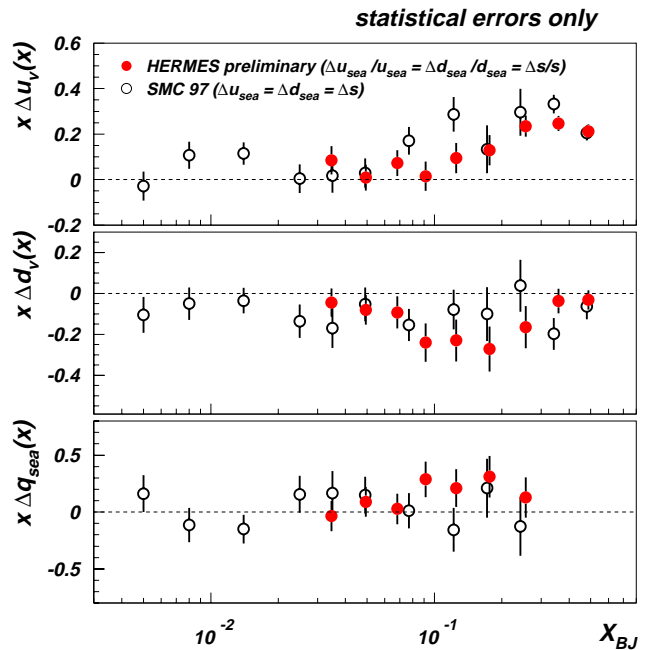


Fig. 21. Preliminary results from 1995/96 for the quark spin distributions of the valence $x\Delta u_v, x\Delta d_v$ and the sea $x\Delta q_{\text{sea}}$ as a function of x , and at the measured Q^2 values. They are compared to the results from SMC at a Q^2 of 10 GeV^2 .

results for the polarized quark distributions, based on only undifferentiated hadrons in the 1995 ^3He and the 1996 proton data sets, are already competitive with the only previous information on these quantities. A paper based on the full H data set (1996-97) and the 1995 ^3He data is in the final stages of preparation.

Physics with unpolarized targets

Although HERMES is primarily a *polarized* deep inelastic scattering experiment, data on *unpolarized* DIS are also taken during short dedicated runs when the density of the target is increased significantly for H₂, D₂, ³He, and N₂. These measurements provide good statistics on processes which do not require polarization (fragmentation functions, light quark sea asymmetry, ρ -meson production, etc.). Some of these processes have been well studied in previous experiments and can be used as consistency checks of the HERMES apparatus and analysis chain. Beyond providing these checks, the unpolarized data set can be used to determine quantities of great current interest such as the flavour asymmetry in the light quark sea. Measurements by NMC at CERN have shown that the Gottfried sum rule is violated significantly. This can be explained as an excess of $d\bar{d}$ pairs over $u\bar{u}$ pairs in the proton. HERMES unpolarized data are sensitive to this asymmetry through a particular combination of observables in hadron production. Results for the ratio $(\bar{d}(x) - \bar{u}(x))/(u(x) - d(x))$ are shown in Fig. 22 and have been published

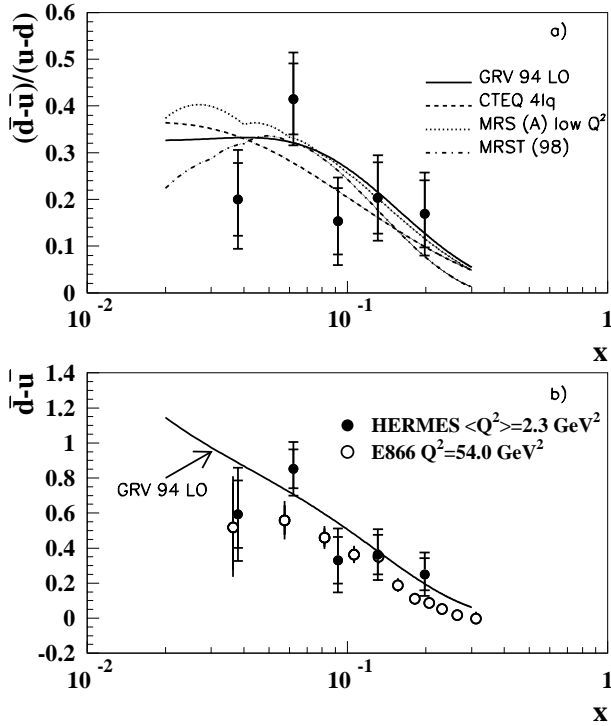


Fig. 22. (a) $(\bar{d} - \bar{u})/(u - d)$ as a function of x . Also included are the GRV 94 LO, CTEQ 4lq, MRS (A) low Q^2 , and MRST (98), parameterizations calculated at the appropriate Q^2 for each x -bin. (b) $\bar{d} - \bar{u}$ as a function of x . The curve is the GRV 94 LO parameterization. The open circles represent the E866 determination of $\bar{d} - \bar{u}$ using the Drell-Yan process. The inner error bars represent the statistical uncertainty while the total error bars represent statistical and systematic uncertainties added in quadrature.

[HERMES collaboration, Phys. Rev. Lett. **81**, 5519 (1998), hep-ex/9807013]. This quantity is clearly non-zero and positive showing that there are indeed more $d\bar{d}$ pairs in the proton sea than $u\bar{u}$ pairs. Note that these E866 results are derived from data on \bar{d}/\bar{u} . E866 and HERMES provide complementary data on \bar{d}/\bar{u} and $\bar{d} - \bar{u}$ respectively.

ρ meson production

Data on ρ -meson production can be used to study diffractive processes, in particular the spin characteristics of this interaction. Data with very high statistics have been taken on ³He. The angular distribution of the pions from ρ decay can be analyzed to yield the spin density matrix of the ρ , and hence its coupling to that of the virtual photon. The quantity r_{00}^{04} is a measure of the longitudinal polarization of the ρ and varies with Q^2 . It is directly related to the ratio $R \equiv \sigma_L/\sigma_T$ of longitudinal to transverse photon cross sections, which is shown as a function of Q^2 in Fig. 23. The HERMES results are the most precise in the lower energy range, and lend support to the previous hypothesis that R is dependent on energy as well as Q^2 .

ρ -meson production can also be used to probe the space-time evolution of a virtual quantum state – the quark-antiquark pair ($q\bar{q}$) fluctuation of a photon – by studying its propagation through a perturbing medium. The kinematics of the scattering can be adjusted to vary the *coherence length* l_c , the distance travelled by the off-shell $q\bar{q}$ pair during which it is vulnerable to hard interactions inside the nucleon, and both the *size* and the *expansion time* of the point-like configuration after it has been put on-shell by the Pomeron. By varying the energy ν of the virtual photon, HERMES is able to separate these two effects, since $l_c = 2\nu/(Q^2 + M_{q\bar{q}}^2)$, while the expansion time during which the size and hence the final state

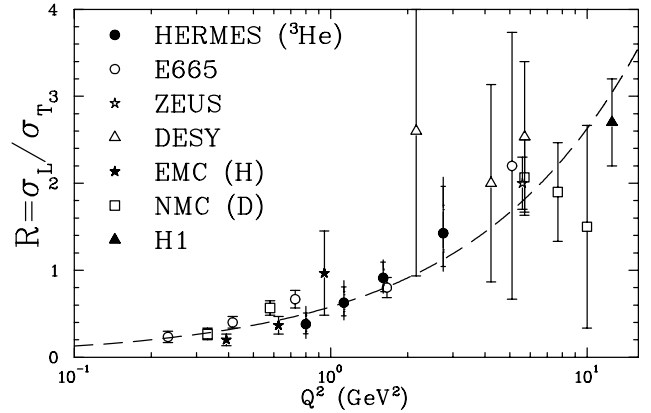


Fig. 23. The ratio $R \equiv \sigma_L/\sigma_T$ of longitudinal to transverse photon cross sections as a function of Q^2 , compared to previous data. The dashed line represents a simultaneous power-law fit to all data.

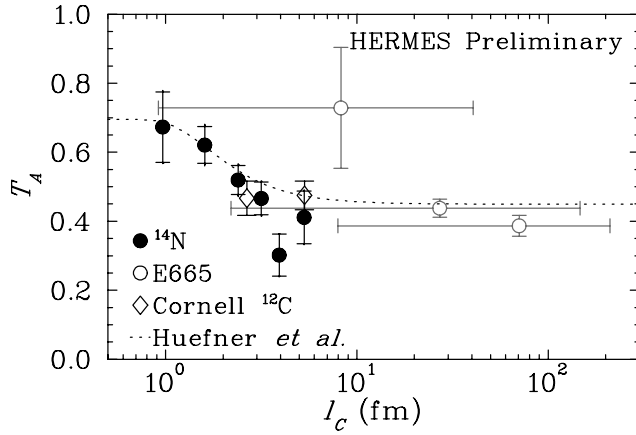


Fig. 24. Nuclear transparency T_A – the ratio of the measured cross section per nucleon in the medium of the nucleus A to that in the nucleon where initial and final state interactions are assumed to be minimal, as a function of coherence length l_c . The HERMES data are for the ^{14}N nucleus, for which the 6% systematic uncertainty in the overall normalization is not shown. The curve is a Glauber calculation. Also shown are previous photoproduction (open diamonds) and muoproduction (open circle) results.

interaction probability remains small is proportional to ν . (The size depends inversely on Q^2 , the negative mass squared of the virtual photon, leading to a similar Q^2 dependence of both initial and final state interactions.) Figure 24 shows the first explicit demonstration that the interactions of the photon with the nuclear medium depends on the propagation distance l_c of the $q\bar{q}$ pair. These results have been submitted for publication [HERMES collaboration, hep-ex/9811011].

Fragmentation functions

The Canadian group is also analyzing the unpolarized semi-inclusive data to extract the fragmentation functions (D_q^h), which represent the probability that a quark of flavour q will produce a hadron of type h . These functions are not only interesting in their own right, but are crucial input to semi-inclusive analyses at HERMES. Preliminary results for the so-called favoured (e.g. $D_u^{\pi^+}$, $D_d^{\pi^-}$, ...) and disfavoured (e.g. $D_u^{\pi^-}$, $D_d^{\pi^+}$, ...) fragmentation functions are shown in Fig. 25 where they are compared to previous measurements by EMC. The fact that there is reasonable agreement between the two experiments, done at very different energies, is further proof that the HERMES semi-inclusive data at relatively low energy can be interpreted in a straightforward manner. In more formal terms, factorization of the hard scattering process ($\gamma^* - q$) and the subsequent hadronization process is valid. Furthermore, this shows that it is possible to separate the so-called current fragments (coming from the struck quark) from the target fragments (coming from the spectator quarks) for HERMES kinematics.

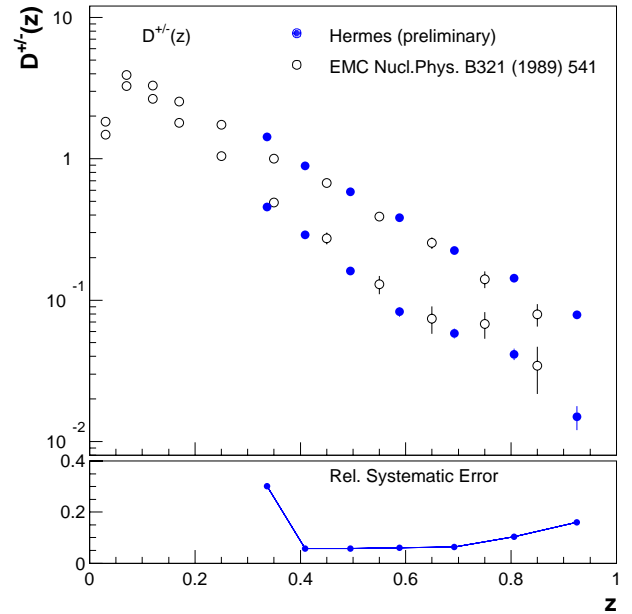


Fig. 25. Favoured (D^+ ; upper set of points) and disfavoured (D^- ; lower set of points) fragmentation functions from HERMES data compared to results from EMC. The latter have been evolved to the HERMES Q^2 of 2.3 GeV^2 .

Outlook

The HERMES collaboration has undertaken several upgrades to the spectrometer and the targets: upgrade of the Čerenkov detector to a RICH for kaon identification giving access to the strange sea, the addition of a muon filter wall and improved acceptance to increase our sample of J/ψ 's through the detection of the $\mu^+\mu^-$ decay channel, a *forward quadrupole spectrometer* (FQS) to detect the scattered e^\pm at very small angles and thus tag the energy of 'real' photons producing vector mesons such as the J/ψ and ϕ , a silicon tracker in the target chamber mostly to improve the acceptance for Λ particles, and an improved rf dissociator for the atomic beam source which will provide increased target thickness. The RICH and muon filter wall are now operational for 1998 running, and FQS and silicon detector prototypes are installed and under test. A Canadian (A. Miller) is spearheading the development of the FQS. All these upgrades will result in enhanced productivity as the polarized program continues for a few more years, starting with the polarized deuterium target in 1998–99.

Search for T violation in $K_{\mu 3}$ decay

KEK Expt. 246 (Japan-Russia-Canada-Korea-U.S.A. collaboration)

(M.D. Hasinoff, UBC; J.A. Macdonald, TRIUMF; B. Shin, Saskatchewan)

A search for transverse polarization (P_T) of muons in $K^+ \rightarrow \pi^0 \mu^+ \nu_\mu$ ($K_{\mu 3}^+$) decay at the $\sim 10^{-3}$ level is being carried out at the High Energy Accelerator

Research Organization (KEK) in Japan by a collaboration from Canada, Japan, Korea, Russia and the U.S.A. For a weak interaction in the absence of electromagnetic final state interactions, such a component of the muon polarization normal to the decay plane would be an indication of the violation of time-reversal invariance. A feature of P_T in $K_{\mu 3}$ decay is that it does not have contributions from the standard model and consequently, this measurement has the potential to reveal new CP violation physics, given CPT invariance. Motivation to search for additional sources of CP violation arises from the observed baryon asymmetry in the universe, which cannot be explained by the CP violation in the standard model alone. Furthermore, recent theoretical progress of electroweak baryogenesis suggests that new CP violation sources might exist at the electroweak scale which can be accessible experimentally.

In $K_{\mu 3}^+$ decay, the hadronic matrix element can be described as

$$\langle \pi | J | K \rangle = f_+^K(q^2)(\tilde{p}_K + \tilde{p}_\pi) + f_-^K(q^2)(\tilde{p}_K - \tilde{p}_\pi)$$

where \tilde{p}_K and \tilde{p}_π are the four momenta of the kaon and pion, respectively. $f_+^K(q^2)$ and $f_-^K(q^2)$ are the form factors of the hadronic matrix elements as a function of momentum transfer squared (q^2). Time-reversal invariance requires that the phases of f_+^K and f_-^K are relatively the same; in other words, if the parameter $\xi(q^2) \equiv f_-^K(q^2)/f_+^K(q^2)$ is defined, ξ should be a real number. Conversely, a non-zero value of $\text{Im}\xi$ would indicate T violation.

The experiment is being carried out at the low energy kaon beam line (K5) of the KEK 12 GeV Proton Synchrotron (PS) and has been described in previous Annual Reports. Briefly, the technique uses stopped kaons in conjunction with a 12-gap superconducting toroidal spectrometer, a finely segmented CsI photon calorimeter, and a muon polarimeter capable of a measurement with low backgrounds and small systematic errors at the 10^{-3} level for ΔP_T .

P_T of the muons stopped in the polarimeter manifests itself as either a clockwise (cw) or counter clockwise (ccw) asymmetry in the decay positron distribution, depending on the emission angle of the pion relative to the beam axis. By summing over the 12 spectrometer gaps, several systematics, such as the effect of an asymmetric kaon stopping distribution in the target and unequal detection efficiency of positron counting, can be cancelled. Moreover, by taking the double ratio for events with the π^0 going into the forward and the backward directions, further cancellation of systematic errors is possible because our experiment uses stopped kaons.

Good $K_{\mu 3}$ events are selected by cutting on the muon momentum and mass (from time of flight), on

the π^0 invariant mass spectrum from photon total energy and direction in the calorimeter, and on the kaon decay time spectrum. A kinematic cut on the opening angle between the muon and the pion is very useful for rejecting any $K_{\pi 2}$ pions remaining after the momentum cut. Finally, the missing-mass cut is tuned to reject events from kaon decay-in-flight. The clean π^0 events consist of 2-photons in the CsI. In order to recover some of the π^0 acceptance lost due to the ‘‘muon’’ holes in the CsI array, we also accept events with only 1-photon cluster satisfying a high energy threshold (70 MeV), for which most of the π^0 kinematic information is preserved.

By June we accumulated a total of 3.6 million events in the π^0 -forward and π^0 -backward regions. We are performing two independent analyses in the group in order to check consistency and estimate systematic errors associated with the analysis. The major differences in the two analyses lie in the charged particle tracking algorithm and in the photon clustering algorithm in the CsI(Tl) array. The near equivalence of the two analyses was checked by comparing good final events in both analyses and their correlations. However, some fraction of the good events are uncommon and the difference between their central values is attributed to the statistical fluctuations of this part. Both analyses have finished processing all the 1996 and 1997 data. The two results are consistent with null T violation within the statistical error,

$$P_T = (-2.55 \pm 5.68) \times 10^{-3}, \quad \text{Im}\xi = (-0.77 \pm 1.86) \times 10^{-2}$$

for one analysis, and

$$P_T = (-0.25 \pm 5.72) \times 10^{-3}, \quad \text{Im}\xi = (-0.01 \pm 1.80) \times 10^{-2}$$

for the other. We are currently engaged in a discussion how best to combine these two results. When the 1998 data have been analyzed, a statistical limit of $\Delta \text{Im}\xi = 0.01$ is expected.

Because the result from existing data will be statistics limited, KEK E246 will benefit from further data-taking and has been granted 200 shifts of additional beam time starting in the fall of 1999.

Measurement of the flavour singlet form factors of the proton

TJNAF Experiment E91-017

(*W.T.H. van Oers, Manitoba*)

The structure of the nucleon at low energies in terms of the quark and gluon degrees of freedom is not well understood. The G_0 experiment is to measure two proton ground state matrix elements which are sensitive to point-like strange quarks and hence to the quark-antiquark sea in the proton. The matrix elements of interest are the elastic scattering vector

weak neutral current ‘charge’ and ‘magnetic’ form factors, G_E^Z and G_M^Z , respectively. These can be extracted from a set of parity violating electron-proton scattering measurements. If one assumes a relationship between the proton and neutron structure in that the proton and neutron differ only by the interchange of up and down quarks, i.e., isospin symmetry, the strange quark (as well as the up and down quark) contribution to the charge and magnetic form factors of the nucleon can be determined. This would result from taking appropriate linear combinations of the weak neutral form factors and their electromagnetic counterparts.

Determinations of both the charge and magnetic strange quark form factors are of fundamental interest, as they would constitute the first direct evidence of the quark sea in low energy observables. The objective of the $G0$ experiment is to determine these contributions to the proton form factors at the few percent level. Observations at high energy suggest that the strange quarks carry about 1/2 as much momentum as up and down quarks in the sea. It is important to determine both the role of the quark sea and the relevance of strange quarks at low energy where there are voids in understanding the theory of the strong interaction (quantum chromodynamics, QCD). Even if the strange quark contributions do not amount to the level of sensitivity of the experiment, upper limit determinations at this level are as valuable as non-zero results. The matrix elements, G_E^Z and G_M^Z , are also relevant to discussions of the Ellis-Jaffe sum rule and the pion-nucleon sigma term; there is uncertainty in both of these about the strange quark contributions. The $G0$ experiment will allow the determination of the strange quark contributions to the proton charge and magnetic form factors in a much more straightforward manner than is possible with regard to the corresponding observables in the above two determinations.

In the $G0$ experiment parity violating longitudinal analyzing powers will be measured in electron-proton scattering in the range $0.1 \leq Q^2 \leq 1.0 \text{ GeV}^2$ at both forward and backward angles. The longitudinal analyzing power is defined as

$$A_z = \frac{1}{P} [\sigma^+(\theta) - \sigma^-(\theta)] / [\sigma^+(\theta) + \sigma^-(\theta)] ,$$

with P the polarization of the incident electron beam and the $+$ and $-$ signs indicating the helicity state. Making pairs of measurements at forward and backward angles will allow the separation of G_E^Z and G_M^Z . Predicted longitudinal analyzing powers range from about $(-3 \text{ to } 35) \times 10^{-6}$; it is planned to measure the longitudinal analyzing powers with statistical uncertainties of $\Delta A/A = 5\%$ and systematic uncertainties related to helicity correlated effects of $\Delta A/A \leq$

2.5×10^{-7} . In the first phase of the experiment longitudinal analyzing powers will be measured concurrently at seven values of the momentum transfer in the range $0.1 \leq Q^2 \leq 1.0 \text{ GeV}^2$. With an electron beam polarization of 0.49, the time required to reach this precision in the first phase measurement will be about 700 hours. It now appears highly probable that by the time of data-taking for the $G0$ experiment higher beam polarizations will have been reached, reducing the data-taking time by close to a factor of two. However, it must be realized that it is not the actual data-taking time that governs the length of the experiment but rather making elaborate control measurements to determine the corrections that have to be made to the measured asymmetries and to understand systematic errors. Using the result for G_M^Z at $Q^2 = 0.1 \text{ GeV}^2$ from the SAMPLE experiment now being performed at the MIT-Bates Laboratory, it would be possible to separate the charge and magnetic form factors at the lowest Q^2 bin after the first phase measurement. In the second phase experiment each subsequent backward angle analyzing power measurement would require from 0.5 to 1 month of running time. It should be noted that the overall uncertainties of a few times 10^{-8} quoted for the recent parity violation experiments at PSI and the University of Bonn and quoted for the systematic uncertainties in the parity violation experiments at MIT-Bates and Mainz suggest that systematic uncertainties of a few times 10^{-7} should be attainable in the $G0$ experiment. The preliminary result of the HAPPEX experiment shows that there exists no barrier at Jefferson Lab to successfully perform the $G0$ experiment.

The $G0$ collaboration

The $G0$ experiment will be carried out by a collaboration of scientists from Canada, France, and the United States, with funding provided through NSERC (Canada), IN2P3 (France), and DOE/NSF (US).

The experiment underwent a Cost and Schedule Review in February, and the conclusions of the Review Committee included a very strong statement in support of the experiment, as well as recommendations for an updated budget, schedule, and implementation of a Project Management Plan. In early spring, both the Canadian and French subgroups of the collaboration received notification of the successful outcomes of their funding requests. Over the course of the spring and summer, much effort was put into developing and finalizing the $G0$ Management Plan. This Management Plan was submitted to the US DOE and NSF agencies in late summer, and the updated funding level and profile was successfully defended and accepted.

Canadian contribution to the *G0* experiment

The Canadian members of the *G0* collaboration, based at the universities of Manitoba, Northern British Columbia, and at TRIUMF, have been asked to : (i) develop and produce specialized photomultiplier tube bases for the main detector arrays; (ii) machine and produce the cryostat-exit detector arrays for the backward angle measurements; (iii) develop and test specialized beam monitors, control apparatus, and “parity” type electronics to read out these monitors; and (iv) design, build and test an automated magnetic field measuring apparatus complete with its own data acquisition system.

This past year has seen much progress in the designing and building of many of the various components/subsystems listed above.

The *G0* main detector array

The heart of the *G0* detection system is a spectrometer which consists of an 8 sector toroidal magnet, with an array of scintillation detectors located at the focal surface of each sector (see Fig. 26). Due to geometry, resolution, and rates considerations, the shapes of both the prototype scintillators and their associated light-guides have become quite elaborate. Since data will not be acquired in event-by-event mode in this experiment, and since the scintillator arrays are the only detectors to measure the scattered particles in the forward angle mode, the performance of these focal-plane detectors (FPD) are of critical importance. The timing and pulse shape characteristics of this system must be fine-tuned at the hardware level because it will not be possible to reconstruct individual events. Furthermore, the “real signal” rates associated with many of the FPD segments will be quite high (1 MHz) and the photon yields may be quite large. As such, special demands will be

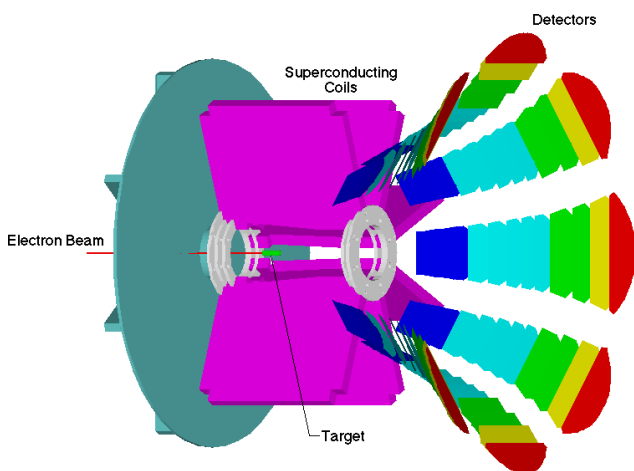


Fig. 26. View of the *G0* superconducting toroidal spectrometer with one sector and the spectrometer housing removed.

made on the photomultiplier tubes (PMT) and especially on their associated divider/base circuit.

Much progress has been made in the design, development, and building of the *G0* bases at TRIUMF. In 1997, 4 prototype “high-rates” bases were constructed and delivered to TJNAF for tests. Based on these studies, modifications were made and a second set of prototype bases were constructed and delivered to TJNAF in early 1998. In the early summer, 12 final prototype bases were constructed and delivered to TJNAF to be used in conjunction with the first set of prototype focal-plane detectors, and fabrication of the actual “production” bases began in earnest. With the help of summer students (funded partly through the TRIUMF Summer/Co-op Students program and partly through the *G0* NSERC grant), the assembling of the electrical components for all of the production bases has been completed. The remaining tasks for this subsystem are related to the fabrication and assembly of the mechanical housing for the PMT and base.

As well, the Canadian subgroup is responsible for the testing and characterizing of all of the photomultiplier tubes to be used with the TRIUMF/*G0* high-rates bases. With the help of summer students at TJNAF, the primary testing and characterization of the PMTs was completed in late summer.

The cryostat-exit detector array

For the backward angle measurements, simulation results indicate that the elastic and inelastic electrons could be more cleanly separated with the addition of a second array of scintillation detectors, located near the spectrometer-cryostat exit-windows. The geometry of these cryostat-exit detector (CED) arrays is still being studied at present. Due to the resident expertise at TRIUMF in producing high quality scintillation detectors and lightguides, the Canadian subgroup has been asked to play a main role in the prototyping and production of the CEDs. Once the preliminary shapes have been optimized, it is expected that several prototypes will be produced at TRIUMF and delivered to TJNAF or Louisiana Tech for further studies. Full scale production of the CEDs would then follow shortly after these studies are completed. The CEDs will also make use of the same types of photomultiplier tubes and specialized TRIUMF/*G0* bases as the focal-plane detectors.

Resonant cavity position and current monitors

Five sets of “XYQ” monitors will be required in order to measure the beam current (charge) and trajectory (positions and angles) at several critical locations (directly upstream of the target, at an upstream dispersed focus, and further upstream in the beam line). The proposed current monitor will be of the resonant

cavity type. Presently, the design consists of a cylindrical cavity operating in the TM₀₁₀ mode at 1497 MHz. A beam current sensitivity of $\pm 4 \times 10^{-5}$ measured in a 33 ms integration-time sample will be required to monitor and correct for possible helicity correlated intensity modulations. For the beam position monitors (BPM), there are two designs under consideration. The presently existing BPMs consist of stripline monitors operating in a special “switched electrode electronics” (SEE) mode. An alternate proposal involves the use of a pair of cylindrical resonant cavities (X and Y) operating in the TM₁₁₀ mode. In either case, a spatial resolution of better than 25 μm at an integration time of 33 ms will be required.

The beam current and the stripline position monitors were tested during an engineering run in July, 1997 at TJNAF. The run was organized by members of the G0 Canadian subgroup and personnel from TJNAF (Hall C), with much of the readout electronics provided by the Canadian subgroup. Precision analog subtractor/divider modules and voltage-to-frequency converters from the TRIUMF parity experiment were readily adapted to the TJNAF beam monitors. Helicity correlated properties of the TJNAF polarized electron beam and noise characteristics of some of the beam monitors were successfully measured. Analysis of the data indicates that the beam current monitors will meet the specification requirements of $\Delta Q/Q \leq 4 \times 10^{-5}$ (in 33 ms). The stripline SEE monitors were able to provide position determinations with $\Delta X \leq 1 \mu\text{m}$ (in 33 ms), which will also meet the specification requirements. Further test-beam time is planned for the future.

To read out the analog signals from the various beam current and position monitors, and to provide feedback control signals, specialized parity type electronics will be required for the G0 experiment. Much of this electronics, such as precision analog subtractors/dividers and precision voltage-to-frequency converters, has already been designed and used by members of the Canadian subgroup in their parity experiments at TRIUMF. Modifications, driven by the requirements of the G0 experiment, were made to some of these electronics modules and they were operated successfully at the July, 1997 engineering run at TJNAF, as mentioned above. Since that time, several voltage-to-frequency converters of the TRIUMF/parity variety have been requested by TJNAF for the G0 experiment. Construction of these 32-channel precision V-to-Fs was completed at TRIUMF and delivery was made to TJNAF in early 1998.

Magnetic field measuring apparatus

An automated field measuring apparatus will be used to provide a magnetic verification of the G0 super-

conducting toroid by measuring the zero-crossing locations of specific field components at selected points of symmetry. This will be carried out by scanning a predefined set of “contour” lines, and determining where specific field components reverse signs. The system must be capable of providing a position determination of 0.2 mm and a field determination of 0.2 G. A partially-automated carriage will be used in conjunction with precision hall probes to meet these requirements.

The present design concept is illustrated in Fig. 27. Here, the magnetic verification device will consist of a small carriage which mounts to the spectrometer cryostat and can be rotated from sector to sector. Located on the carriage will be a movable magnetic field probe, positioned via a high-precision position or shaft encoder. The mapping of the zero-crossing points will be carried sector by sector, and the field data will be acquired via a precision DVM and a GPIB/PC-based data acquisition system. This first order conceptual design for the field measuring apparatus is presently being completed.

Canadian subgroup of the G0 collaboration: J. Birchall, W.R. Falk, L. Lee, S.A. Page, W.D. Ramsay, W.T.H. van Oers, R.J. Woo (Manitoba); E. Korkmaz, G. O’Reilly (University of Northern British Columbia); C.A. Davis (TRIUMF).

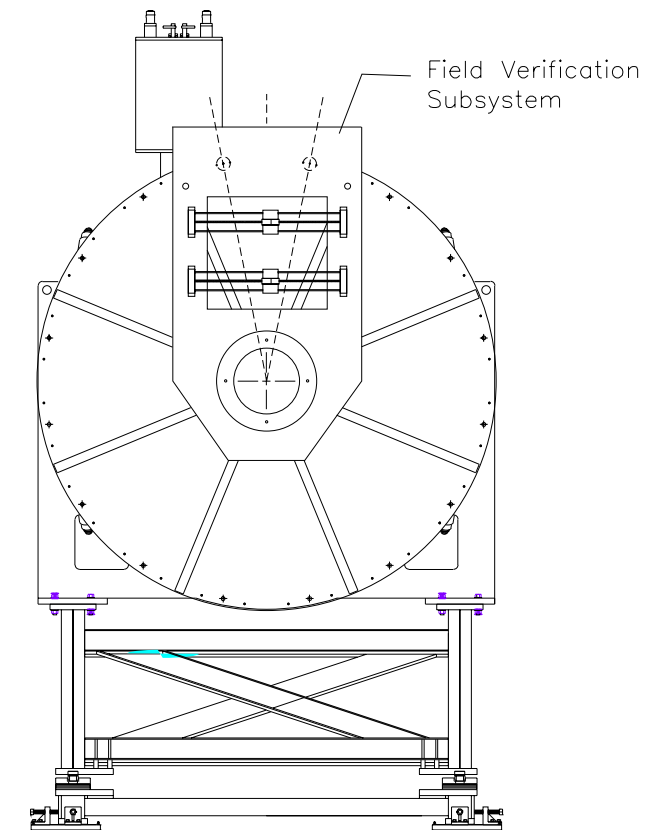


Fig. 27. Schematic layout of the magnetic verification apparatus, mounted to the spectrometer cryostat.

NUCLEAR AND ATOMIC PHYSICS

Experiment 560

Low energy $\pi^\pm p$ analyzing powers with CHAOS
(*G.R. Smith, K. Raywood, TRIUMF; J. Patterson, Colorado*)

This experiment made use of the CHAOS spectrometer and a specially designed CHAOS polarized proton target (CPPT). The experimental goals of Expt. 560 were to measure the analyzing power (A_y) for $\pi^\pm p$ scattering to better than ± 0.05 between angles of $\sim 60^\circ$ and 180° at several bombarding energies between 30 and 140 MeV. The 1995/1996 beam periods were aimed at resonance energies due to persistent problems with the polarized target. The running period which took place in the fall of 1997, however, enjoyed flawless operation of the target (and spectrometer), and the low energy region was successfully explored with incident π^- down to 51 MeV, although the statistics obtained at this lowest energy were marginal. Unfortunately, the beam time available to this experiment in fall, 1997 was insufficient to pursue the π^+ part of the low energy program. Since the Polarized Target group is committed to ISAC experiments for the foreseeable future, data acquisition for Expt. 560 is finished.

Using the technique of single energy partial wave analysis (PWA), the data obtained in this experiment will be used to filter out differential cross section ($d\sigma/d\Omega$) measurements which are inconsistent with the A_y data. At present the low energy $d\sigma/d\Omega$ data base contains a number of gross inconsistencies between experiments. In order to determine the πN partial wave amplitudes with precision, reliable and precise $d\sigma/d\Omega$ data (which fix the larger amplitudes) must be combined with reliable and precise A_y data (which fix the smaller amplitudes). Analyzing power results in the forward angle (Coulomb-nuclear interference) region for $\pi^+ p$ scattering, and in the S-P interference region at backward angles near 50 MeV for $\pi^- p$ scattering are especially useful in this regard. With accurate πN partial wave amplitudes, in particular at low energies, the physics goals of Expt. 560 are then to provide improved values for the πN coupling constant, to extrapolate to threshold where the πN scattering lengths can be obtained, and to extrapolate below threshold as well to obtain a more accurate measure of the πN sigma term. The πN sigma term is an explicit measure of chiral symmetry breaking from which the strange sea quark content of the proton can be deduced.

In 1997 the analysis of the resonance energy experiments was completed, and a Ph.D. thesis [Hofman] was obtained based on those data. In 1998 the resonance energy results were published [Hofman *et al.*, Phys.

Rev. **C58**, 3484 (1998)]. In this year's progress report, we focus on the analysis of the low energy $\pi^- p$ data obtained in the fall, 1997 Expt. 560 running period.

As a result of the many previous problems with the CPPT, the fall, 1997 effort took place in the M11 channel rather than the (low energy) M13 channel. This was because in M11 the target polarization could be checked by comparison to previous measurements of the analyzing power at resonance energies. This check was performed at the start of the measurement (140 MeV incident π^+) and verified the target polarization determined by NMR techniques was indeed ~ 0.80 .

Due to the fact that data were acquired with CHAOS at $\pm\theta$ simultaneously, the only other quantity that had to be measured was the πp scattering yield. Measurements of other factors, such as the relative flux of incident pions, etc., were unnecessary due to the powerful self-normalizing features of analyzing power measurements with CHAOS. Another crucial feature was that complete angular distributions were measured simultaneously. Without this feature, the experiment would not have been practical due to the extremely low cross sections involved and subsequent long running times associated with standard angle-by-angle measurements.

As a result, in what turned out to be a very successful run, data were acquired for incident π^- at 51, 57, 67, 87, 98, 117, and 140 MeV. Graphite background data were also collected. The resulting data base spans the S-P interference region which is 'centered' at 57 MeV, 180° . Most of the beam time was devoted to the 57 MeV measurement. There the backward angle cross sections are less than $1 \mu\text{b}/\text{sr}$, more than 3 orders of magnitude less than the corresponding cross sections at 140 MeV. However, it has been shown that the greatest sensitivity to the scattering lengths is right at the S-P interference minimum, so enough time was spent collecting data in this most difficult region to obtain approximately ± 0.08 uncertainty at the most backward angle, with uncertainties at almost all other angles (and energies) typically ± 0.02 or less.

In order to obtain data in to the smallest possible scattering angles at the lowest three energies in particular, the CHAOS first level trigger (1LT) was programmed for 'singles' mode so that any scattered pion could generate a 1LT. This would have led to an overwhelming background of quasi-elastic $\pi^- n$ scattering (the polarized target consists of butanol, $\text{C}_4\text{H}_9\text{OH}$) were it not for innovative changes which were made to the second level trigger (2LT). The 2LT was programmed to recognize 'short tracks', i.e. protons which were observed in the correct angular region and with

the expected curvature based exclusively on information from only the inner two wire chambers. Events with (recoil) protons whose trajectories stopped outside of WC2 were not lost; if the protons failed to make it out to WC3 their trajectories were determined by combining the pion vertex with the proton hits registered in WC1/2. Events with protons which made it at least to WC2 were required in the (second level) trigger, which reduced trigger rates to manageable levels (typical live times were $\sim 90\text{--}95\%$) without having to resort to a doubles 1LT, which would have considerably abbreviated the measured angular distributions at the lowest energies.

An example of preliminary analyzing powers obtained in the fall, 1997 running period is shown in Fig. 28 for the case of 117 MeV incident π^- . These are on-line results. Two error bars are plotted, one based on the on-line statistics, the other based on what the error is projected to be after recovering the full statistics available in off-line replay. For most points, this latter error is smaller than the plotted point (smaller than ± 0.01) and is thus not visible. The on-line data were acquired with very loose software requirements so it is usual that after more careful analysis the points can move, in particular the forward angle points where the background requires more careful treatment than that given on-line. Having said this, however, the agreement of these preliminary, on-line results with the prediction of the partial wave solution SM95 is remarkable.

The analysis efforts in 1998 focused first on the treatment of the polarized target NMR signals, from which the absolute target polarization was deduced for each run in the experiment. This effort was completed in the summer. At that point programming effort was directed towards implementing the CERN

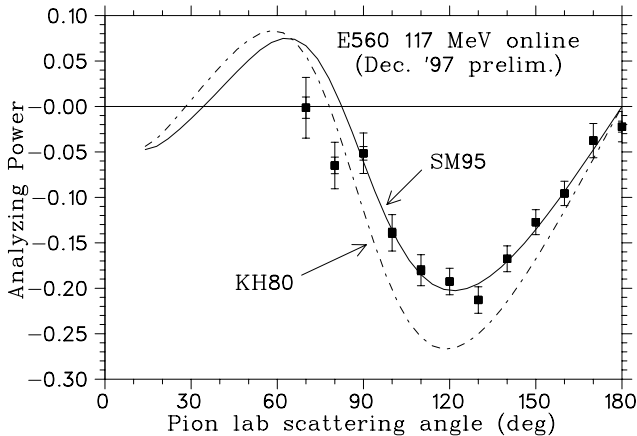


Fig. 28. Preliminary on-line angular distribution of the π^-p analyzing power measured with CHAOS in the fall of 1997 at 117 MeV. Also shown are the results of two partial wave analyses: SM95 (solid line) and KH80 (dashed line).

ROOT system for analysis of the scattering data. The ROOT implementation was completed late in 1998 and now the scattering data are being analyzed, and analyzing powers are being extracted. We anticipate that the data analysis should be completed by fall, 1999.

Experiment 613

Reactions of muonic hydrogen isotopes

(G.M. Marshall, TRIUMF)

The very striking characteristic of certain muonic molecular hydrogen ion formation reactions is that they are resonant. This was first postulated and described for the $dd\mu$ system by Vesman [Pis'ma Zh. Eksp. Teor. Fiz. **5**, 113 (1967) (JETP Lett. **5**, 91 (1967))], following experimental observation [Dzhelepov *et al.*, Zh. Eksp. Teor. Fiz. **50**, 1235 (1966) (Sov. Phys. JETP **23**, 820 (1966))]. It also prevails in the $dt\mu$ system [Bystritsky *et al.*, Phys. Lett. **94B**, 476 (1980); Jones *et al.*, Phys. Rev. Lett. **56**, 588 (1986); Breunlich *et al.*, Phys. Rev. Lett. **58**, 329 (1987)], and is discussed in several reviews [see for example Ponomarev, Contemp. Phys. **31**, 219 (1990); Cohen, *Atomic and molecular processes in muon-catalyzed fusion*, in Review of Fundamental Processes and Applications of Atoms and Ions, ed. C.D. Lin (World Scientific, Singapore, 1993); Breunlich *et al.*, Ann. Rev. Nucl. Part. Sci. **39**, 311 (1989)].

It is experimentally challenging to verify the recent results of calculations for $dt\mu$ resonant formation [Faifman and Ponomarev, Phys. Lett. **B265**, 201 (1991); a subsequent calculation, including effects of quadrupole interactions, can be found in Faifman *et al.*, Hyp. Int. **101/102**, 179 (1996); Petrov *et al.*, Phys. Lett. **B331**, 266 (1994)], especially for muonic atom kinetic energies above 0.1 eV corresponding to the highest predicted molecular formation rates. One method is to use the time-of-flight (TOF) technique to estimate the muonic atom's energy as it travels between two layers of solidified hydrogen isotopes, separated by a known distance. This has advantages, but also some disadvantages. Since the first considerations of the technique [Forster *et al.*, Hyp. Int. **65**, 1007 (1990)], much has been learned about how to optimize the quality of the data, and about the magnitude of the systematic limitations. Some of the inconsistencies reported in earlier preliminary results [Marshall *et al.*, Hyp. Int. **101/102**, 47 (1996)] have been resolved. Largely through the use of simulations, the sensitivity to some critical rates and cross sections has been estimated. Quantitative comparisons with experimental data are now in progress [Mulhauser *et al.*, Hyp. Int. (in press); Fujiwara *et al.*, Hyp. Int. (in press)], and final results are expected soon [Fujiwara, Ph.D. thesis, University of British Columbia (in preparation); Porcelli, Ph.D. thesis, University of Victoria (in preparation)].

Resonant muonic molecular ion formation

Resonant muonic molecular ion formation occurs when the kinetic energy in a collision of a muonic atom with a hydrogen molecule can be absorbed in the rotational and vibrational excitations of a neutral muonic molecular complex. The excitations are of two types. One is of the muonic molecular ion (such as $dt\mu$) which forms one massive, positively charged, relatively localized constituent of the complex. The second is of the entire neutral complex molecule itself (such as $[(dt\mu)^+d^+e^-e^-]$ or $[(dt\mu)^+p^+e^-e^-]$, produced in collisions of $t\mu$ with D_2 or HD respectively). Deexcitation of the muonic molecular ion leads to fusion, but it is also possible for the molecular complex to dissociate (or “back decay”) into the systems from which it was formed.

Calculations for the resonant processes [Faifman and Ponomarev, *op. cit.*] have been modified for a low temperature target at 3 K, ignoring any possible solid-state effects, for the cases of $t\mu$ and D_2 or HD. These calculations do not include possible effects of subthreshold resonances as discussed in Petrov *et al.* [*op. cit.*]. In certain cases, it is expected that the formation rate at low energy will influence the results of solid target experiments.

Review of experimental techniques

The target and its use has been described elsewhere [Knowles *et al.*, Nucl. Instrum. Methods **A368**, 604 (1996); Fujiwara *et al.*, Nucl. Instrum. Methods **A395**, 159 (1997)]. A beam of typically $5 \times 10^3 \text{ s}^{-1}$ negative muons of momentum near 27 MeV/c (kinetic energy 3.4 MeV) originates from pion decays near a production target in a proton beam; when produced this way, they are sometimes known as “cloud muons”. The beam is transported to the cryogenic solid hydrogen target through a crossed-field velocity separator or Wien filter, and on entering the target is $\sim 3 \text{ cm}$ in diameter with a momentum spread of $\sim 5.5\%$ (fwhm). Muons must pass through a 0.25 mm beam-defining scintillator, a 0.025 mm stainless steel vacuum isolation window, a 0.013 mm copper thermal isolation window, and a 0.051 mm 3.5 K gold foil before arriving at a layer of solid hydrogen frozen onto the gold foil. The momentum of the muon beam is tuned for maximum stop rate in hydrogen. A substantial fraction of the beam can be stopped in a layer of less than 1 mm thickness. The cryogenic target is surrounded by a thermal shield in which silicon detectors are mounted, and is contained within a cube at ultra-high vacuum, viewed by detectors for fusion neutrons, muon decay electrons, and muonic x-rays, as shown in Fig. 29.

The time of flight technique is applied to test predictions for the energy dependence of resonant muonic

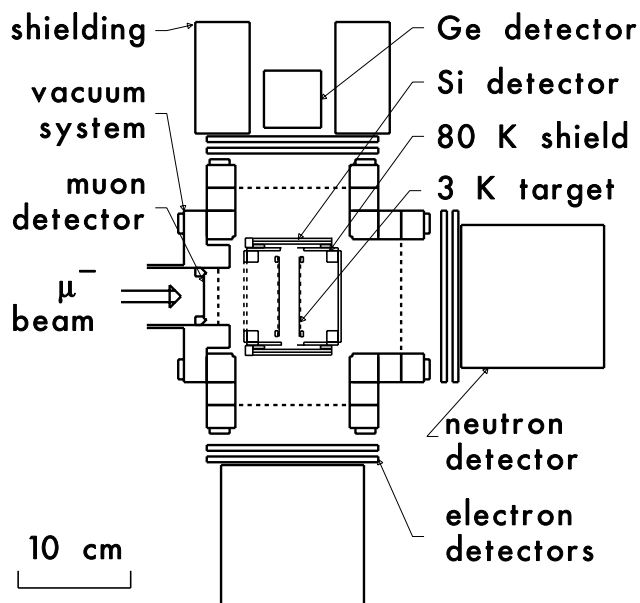


Fig. 29. Arrangement for time of flight experiments, showing the cryogenic solid hydrogen target and vacuum system, with detectors for incident muons, muon decay electrons, muonic x-rays, and fusion products (α , p , n).

molecule formation. A second gold foil is used to support a reaction layer of D_2 or HD. The time for a muonic atom to travel between the hydrogen isotope layers on the first foil to the adjacent reaction layer on the second foil is compared with a simulation to confirm the predicted resonance structure. A fraction of the muons stops in a production layer of protium ($^1\text{H}_2$) containing 0.1% tritium, of thickness 3.5 mg cm^{-2} , almost always forming muonic protium ($p\mu$). Transfer to the small tritium concentration occurs with a characteristic time of about 10^{-7} s , and the increase in binding energy corresponding to the greater reduced mass results in a typical $t\mu$ energy of 45 eV. The Ramsauer-Townsend scattering cross section of $t\mu$ by H_2 is low enough that the muonic atom can escape the layer before thermalization. In fact, a moderation layer of D_2 (0.1 mg cm^{-2}), in which $t\mu$ energy loss is much greater, is added to the surface of the production layer to optimize the energy distribution for TOF experiments. After traversal of the 18 mm separation between the first and second foils, the $t\mu$ atoms of energies for which the rate is high may form muonic molecular ions in the reaction layer of thickness 0.02 mg cm^{-2} . In this case, fusion follows almost immediately, in about 10^{-12} s . It is also possible that the $t\mu$ atoms scatter and lose energy before formation and fusion, so that the time of flight is not correlated with the energy of molecular ion formation. This indirect process leads to an unavoidable background. In either case, a fusion product such as an alpha particle at 3.5 MeV can be detected, while other muonic atoms pass through the reaction layer

into the supporting gold foil, giving no fusion signal. The interval between muon arrival and fusion is dominated by the time of flight between the foils. Lower energy resonances near 0.5 eV appear with times greater than $3 \mu\text{s}$, while higher energy resonances are in the range $2\text{--}3 \mu\text{s}$. Emission from the moderation layer at different angles implies different lengths of flight path, smearing the resonant time-of-flight structures and necessitating comparison via simulations.

Computer simulations have been performed and compared with experiment to aid the understanding of different quantities, such as hydrogen target thickness and uniformity [Fujiwara *et al.*, Nucl. Instrum. Methods **A395**, 159 (1997)], muon stopping distributions in the hydrogen layers, and solid angles and efficiencies of detectors [GEANT 3.21, CERN Program Library Long Writeup W5013, CERN, Geneva (1993)]. Modelling of the evolution of muonic states requires complex and specialized programs [Markushin *et al.*, Hyp. Int. **101/102**, 155 (1996); Huber *et al.*, Hyp. Int. (in press); Woźniak *et al.*, Hyp. Int. **101/102**, 573 (1996)]. Preliminary results show approximate agreement of data with the simulation (Figs. 30 and 31), with only a few of the many theoretical rates and cross sections requiring adjustment. Although the strength is roughly correct, the structure predicted for molecular formation, especially for HD (Fig. 31), is absent in the data. This may indicate a solid-state effect in the formation mechanism which is not included in the theoretical model.

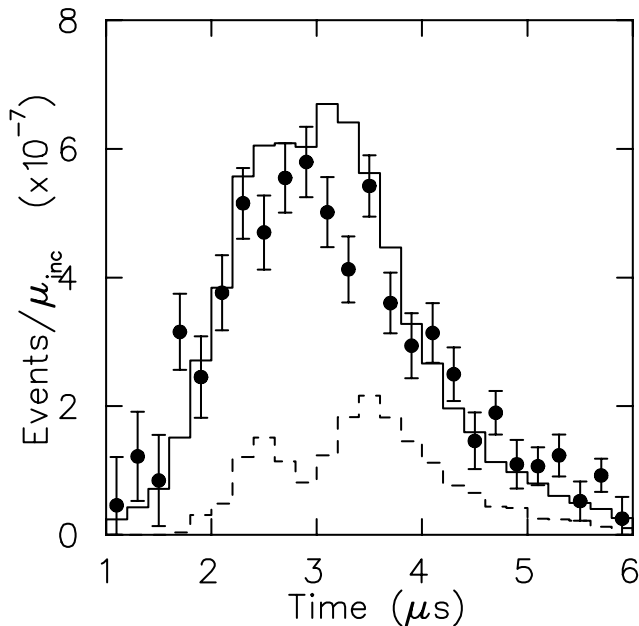


Fig. 30. Preliminary comparison of fusion product (α) time distributions for a reaction layer of D_2 , normalized to incident muons (μ_{inc}). Points with error bars (statistical only) are experimental, while histograms are from a simulation; the dashed histogram shows direct interactions only.

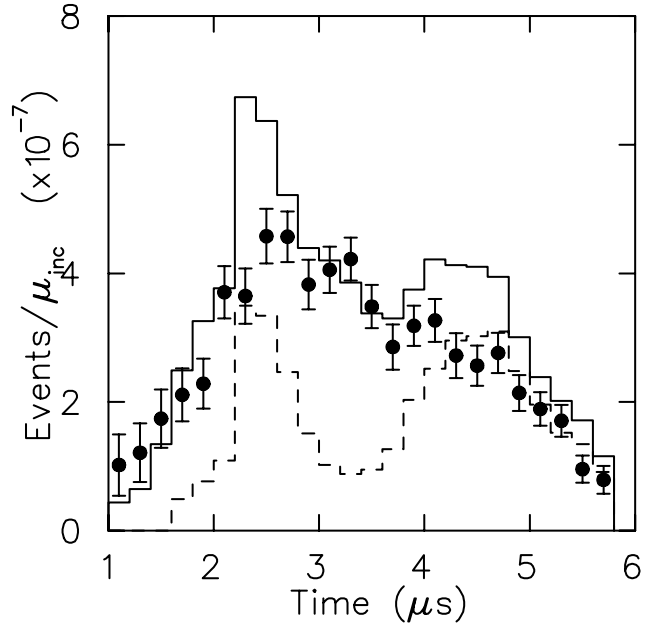


Fig. 31. As Fig. 30, but for a reaction layer of HD. The theoretical resonant muonic molecular formation rate has been scaled by 0.5 to account for the assumed normalization to fractional proton atomic concentration.

Final analysis is nearly complete, with two Ph.D. students (M.C. Fujiwara and T.A. Porcelli) in the final stages of thesis preparation.

Experiment 624

The $\text{H}(\pi, 2\pi)$ reaction, a tool to determine scattering lengths and coupling constants

(G.R. Smith, TRIUMF)

This experiment received beam time during the high intensity periods of TRIUMF operation between January, 1994 and August, 1994. A liquid hydrogen target was employed with the CHAOS spectrometer in the TRIUMF M11 beam line.

The experiment consisted of a systematic investigation of the $\text{H}(\pi^\pm, \pi^\pm \pi^\pm)n$ reactions in a series of exclusive measurements. For incident π^- , the $\text{H}(\pi^-, \pi^+ \pi^-)n$ and the $\text{H}(\pi^-, \pi^- \pi^0)p$ channels were measured simultaneously by detecting the two charged particles in the final state in coincidence. Likewise for incident π^+ , the $\text{H}(\pi^+, \pi^+ \pi^+)n$ and the $\text{H}(\pi^+, \pi^+ \pi^0)p$ channels were measured simultaneously. Pion bombarding energies of 220, 240, 260, 280, and 300 MeV were studied and approximately 10,000 $(\pi, 2\pi)$ events were recorded at each energy for the channels with two charged pions in the final state. In addition, πp elastic data were acquired at each energy and pion polarity in order to provide checks on the absolute normalization.

The $(\pi, 2\pi)$ reaction at a given energy can be completely described in terms of four variables: the dipion invariant mass squared ($m_{\pi\pi}^2$), the four-momentum transfer to the nucleon squared (t), the an-

gle between the two π^- in the dipion rest frame (θ), and an out-of-plane angle (ψ). The first three of these variables are well covered by the CHAOS acceptance. Although only about 10% of the latter variable is covered, the out-of-plane departures from phase space are small in the energy regime covered by this experiment [Ortner *et al.*, Phys. Rev. **C47**, 447 (1993)]. In fact, the total cross sections obtained at each of the five energies studied agree well with previously published results obtained mostly with (4π sr) bubble chambers.

The results of the experiment were loaded into a three dimensional lattice consisting of ten bins in each of $m_{\pi\pi}^2$, t , and $\cos(\theta)$, with each node in the lattice weighted according to the acceptance determined from the simulations. The $\cos(\theta)$ dependence was integrated out, yielding double differential cross sections $d^2\sigma/dm_{\pi\pi}^2 dt$. Single and total cross sections were obtained by successive integration.

Some aspects of the experimental results have been described in previous Annual Reports. The Ph.D. thesis (Kermami) associated with this work was completed in 1997. In 1998, we performed a novel, global Goeble-Chew-Low analysis in order to extract a more accurate measure of the isospin 0 S -wave $\pi\pi$ scattering length a_0^0 . In 1998 we also published the work in back-to-back publications.

In the first article [Phys. Rev. **C58**, 3419 (1998)] we described the experimental method in detail, and presented single and total differential cross sections, as well as phase space comparisons and fits to the $m_{\pi\pi}^2$ distributions in the $\pi^+\pi^-$ channel at all five energies. For the latter we made use of an extended model [Sossi *et al.*, Nucl. Phys. **A548**, 562 (1992)] of Oset and Vicente-Vacas. Besides providing best-fit values for several Δ and N^* coupling constants, this (model-dependent) approach was used to provide the chiral perturbation theory parameters L_1 and L_2 . The best-fit parameters of the model were then used to predict the behaviour of the $m_{\pi\pi}^2$ distributions in the $\pi^+\pi^+$ channel as well as the total cross sections in both channels. Although the quality of the fits was very good, the predictions for the $\pi^+\pi^+$ channel were poor, indicating that the model still lacks essential ingredients.

The second article [Phys. Rev. **C58**, 3431 (1998)] dealt exclusively with the double differential cross sections $d^2\sigma/dtdm_{\pi\pi}^2$, global Goeble-Chew-Low analysis, and extraction of a_0^0 . The Goeble-Chew-Low formalism is a model-independent technique for isolating the one-pion-exchange (OPE) diagram of interest (and consequently on-shell $\pi\pi$ scattering cross sections) by extrapolating the 2-fold differential cross sections to the (unphysical) pion pole at $t=+1$ (in units of m_π^2). The physical threshold is at $t=0$. Since the CHAOS data fell primarily into the near threshold, small $m_{\pi\pi}^2$, small t

region needed for an accurate extrapolation, our results were well suited for this type of analysis. Although the Chew-Low method is model-independent, it does assume OPE dominance in the extrapolation region. Unfortunately, the influence of the Δ diagrams rendered the extrapolation unreliable for the $H(\pi^+, \pi^+\pi^+)n$ results. However, the $H(\pi^-, \pi^+\pi^-)n$ analysis was successful. For this reaction channel several arguments necessary for (but not sufficient to prove) OPE dominance could be made. In addition we were able to explain why this channel is more amenable to Goeble-Chew-Low analysis than the $\pi^+\pi^+$ channel.

Several independent analyses were performed based on different selections of the available CHAOS data, and using different threshold expansions and fitting functions, in order to explore the sensitivity of the results to these choices. The results of the analysis of the CHAOS data are summarized in Fig. 32, which shows the on-shell $\pi\pi$ cross sections extracted from the global Goeble-Chew-Low analysis as a function of $m_{\pi\pi}^2$. Threshold expansions were used to deduce the scattering length from the results in this figure, and led to the result $a_0^0 = 0.204 \pm 0.014$ (statistical) ± 0.008 (systematic) in units of the inverse pion mass. This is the most precise measure to date of a_0^0 , and compares favourably with the predicted value of 0.20 ± 0.01 from chiral perturbation theory. The best previous experimental value for a_0^0 (determined from K_{e4} decay) is 0.28 ± 0.05 [Rosselet *et al.*, Phys. Rev. **D15**, 574 (1976)].

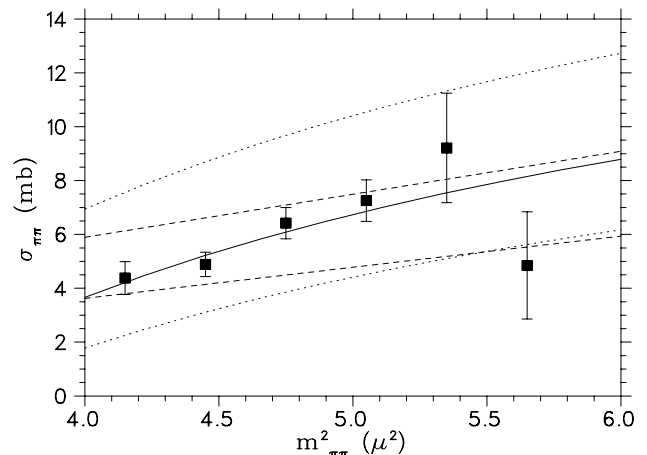


Fig. 32. The on-shell $\pi\pi$ scattering cross sections obtained in this experiment plotted against $m_{\pi\pi}^2$. The solid points denote the extrapolated values from the global Goebel-Chew-Low analysis. The solid line is the result of a threshold expansion fit. The dotted lines indicate the results of fixing a_0^0 at the K_{e4} result of 0.26 (upper) or to the Weinberg result of 0.16 (lower), and are provided to highlight the sensitivity to the scattering length in this kinematic regime. The dashed lines represent constraints from a dispersion analysis using the Roy equations, with the present results as well as higher momenta data included as input.

Experiment 700

Measuring cross sections of long-lived radionuclides produced by 200–500 MeV protons in elements found in lunar rocks and meteorites

(*J. Sisterson, Harvard*)

Small quantities of radionuclides and stable isotopes are produced in lunar rocks and meteorites by cosmic ray interactions. Interpreting this cosmic ray record gives information about the average solar proton flux over the past million years and the history of the irradiated object. Most cosmic rays are protons and good proton production cross section measurements are essential input to the theoretical models used to interpret the cosmogenic nuclide archive preserved in lunar rocks and meteorites. The cross section measurements made at TRIUMF are part of an overall program – funded in part by NASA – to measure all of the needed cross sections. Data analysis continues for samples irradiated in both February, 1996 and August, 1997. By August, 1998, all the needed gamma-ray spectroscopy measurements were completed at the Harvard Cyclotron Laboratory and the ^{14}C determinations using accelerator mass spectrometry (AMS) at the University of Arizona. In February, 1996, many of the irradiations were designed to produce neon isotopes in targets of magnesium, aluminum, silicon, iron and nickel, and argon in iron and nickel targets. The irradiations made at TRIUMF were part of the overall program to measure the excitation functions for the production of ^{20}Ne , ^{21}Ne and ^{22}Ne (and ^{22}Na) in these targets from threshold to 500 MeV. ^{22}Na produced in the target must be measured to correct for the ^{22}Ne produced from ^{22}Na decay. Irradiations were made at the Harvard Cyclotron Laboratory and at the Crocker Nuclear Laboratory, U.C. Davis at lower proton energies in 1998. Mass spectroscopy (MS) is used to measure neon isotopes at the Lawrence Livermore National Laboratory. In 1998, we reported preliminary results for the following cross sections: $\text{Mg}(p, x)^{20}\text{Ne}$, $\text{Mg}(p, x)^{21}\text{Ne}$, $\text{Mg}(p, x)^{22}\text{Ne}$, $^{27}\text{Al}(p, x)^{20}\text{Ne}$, $^{27}\text{Al}(p, x)^{21}\text{Ne}$, $^{27}\text{Al}(p, x)^{22}\text{Ne}$, $\text{Si}(p, x)^{20}\text{Ne}$, $\text{Si}(p, x)^{21}\text{Ne}$, and $\text{Si}(p, x)^{22}\text{Ne}$ at the 29th Lunar and Planetary Science meeting held in Houston, Texas in March [Sisterson and Caffee, in Lunar and Planet. Sci. XXIX, Abstract 1234 (Houston, 1998)]. Few modern measurements had been made for these cross sections before our new measurements and those of the European collaboration [Leya *et al.*, Nucl. Instrum. Methods **B145**, 449 (1998)]. We have compared our measurements with theoretical calculations. We expect to report on the comparison to model calculations, our recently completed measurements of these cross sections, and revised values for the earlier measurements in March, 1999 at the 30th Lunar Planetary

Science meeting. In August, 1997, irradiations made at TRIUMF included those designed to produce Kr isotopes in targets of RbMnF_3 (for Rb), SrF_2 (for Sr) and Y; and to produce ^{14}C in Ti. Short lived activities have been measured in these targets. ^{22}Na produced in the Rb, Sr and Y targets has been measured. These targets will be sent for the determination of noble gases by MS at the Centre d'Etudes Nucleaires de Bordeaux-Gradignan, France after the residual activity in the targets has reached acceptable levels – probably within the next few months. ^{14}C in the Ti targets has been measured using AMS at the University of Arizona. We report all current cross sections for ^{14}C production in oxygen, magnesium, aluminum, silicon, iron and nickel in the paper *^{14}C depth profiles in Apollo 15 and 17 cores and lunar rock 68815* [Jull *et al.* (Geochim. et Cosmochim. Acta, in press)]. Additional cross sections for $\text{Ti}(p, x)^{14}\text{C}$ were measured after this paper was accepted, and these new data will be presented in March, 1999 at the 30th Lunar Planetary Science meeting.

Experiment 704

Charge symmetry breaking in $np \rightarrow d\pi^0$ close to threshold

(*A.K. Opper, Ohio; E.J. Korkmaz, UNBC*)

Experiment 704, a high precision measurement of charge symmetry breaking (CSB) in the strong interaction, has been set up and taking production data in the proton hall at TRIUMF through 1998. The CSB observable being measured is the forward-backward asymmetry (A_{fb}) in $np \rightarrow d\pi^0$, which must be zero in the centre-of-mass if charge symmetry is conserved. Recent calculations by Niskanen [nucl-th/9809009] give an angle integrated value of approximately -35×10^{-4} for A_{fb} near 280 MeV with the dominant contributions being an order of magnitude larger than those of the elastic scattering CSB measurements carried out at TRIUMF [Abegg *et al.*, Phys. Rev. Lett. **56**, 2571 (1986); Phys. Rev. **D39**, 2464 (1989); Phys. Rev. Lett. **75**, 1711 (1995)] and IUCF [Vigdor *et al.*, Phys. Rev. **C46**, 410 (1992)]. These contributions are due to $(\pi^0 - \eta)$ and $(\pi^0 - \eta')$ mixing, which are linearly dependent on the ηNN coupling constant and the $\eta - \pi$ ($\eta' - \pi$) mixing amplitude. As a measure of *inelastic* np scattering, Expt. 704 complements the existing data set in that it has contributions that don't exist in elastic np scattering. The mixing matrices are well known from analysis of η and η' decay [Coon *et al.*, Phys. Rev. **D34**, 2784 (1986); Alde *et al.*, Sov. J. Nucl. Phys. **40**, 918 (1984); Binon *et al.*, *ibid.* **39**, 903 (1984)] but the value of the η -nucleon coupling constant ranges from $(g_{\eta NN}^2/4\pi=)$ 0.2 to 6.2 [Bennhold, private communication; Benmerrouche *et al.*, Phys. Rev. **D51**, 3237 (1995)].

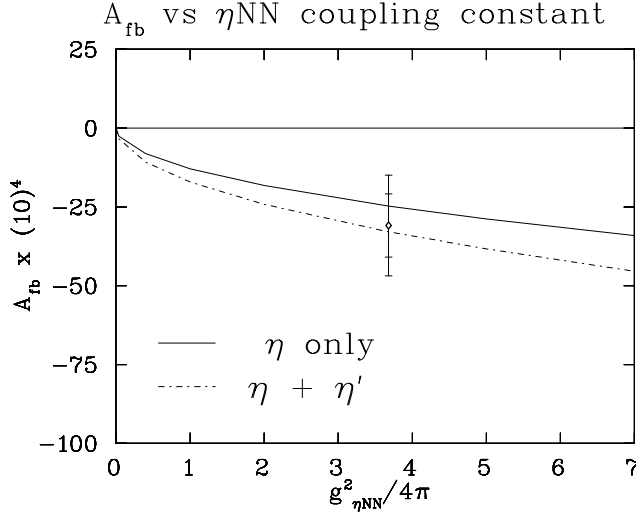


Fig. 33. A_{fb} as a function of the ηNN and $\eta' NN$ coupling constants. The solid (dashed) curve is the value of A_{fb} assuming $g_{\eta' NN} = 0$ ($= g_{\eta NN}$). The open diamond indicates the *predicted* value of A_{fb} at the energy of this experiment with *anticipated* error bars.

Figure 33 shows Niskanen's calculation of A_{fb} as a function of $g_{\eta NN}^2/4\pi$ and $g_{\eta' NN}^2/4\pi$ [Niskanen, private communication]. Given that the interpretations of the electromagnetic η production are controversial and that the strong production of η is complicated by final state interactions, this measurement of A_{fb} may be the best way to determine $g_{\eta NN}$.

The experiment is carried out with a 279.5 MeV neutron beam, a liquid hydrogen target, and the SASP spectrometer positioned at 0° . With these kinematics and the large acceptance of SASP the full deuteron distribution is detected in one setting of the spectrometer thereby eliminating many systematic uncertainties. This experiment requires a measurement of the $pp \rightarrow d\pi^+$ distribution as a test case to verify the analysis and simulation codes, since the deuteron distribution from $pp \rightarrow d\pi^+$ must be symmetric in the centre of mass due to the indistinguishability of the two protons. Figures 34 and 35 show schematic layouts for these two measurements.

Any difficulties related to hardware have been resolved and the experimental layout and equipment have become standardized. The resources of the collaboration have focused on understanding the CSB contributions to A_{fb} , analyzing data, understanding the acceptance of SASP, and understanding the systematic uncertainties using a simple Monte Carlo simulation and a GEANT simulation of the experiment. With over two million $np \rightarrow d\pi^0$ events on tape at the end of 1998 the statistical (systematic) uncertainty of A_{fb} is $\pm 17 \times 10^{-4}$ ($\pm 20 \times 10^{-4}$); the ultimate goal is to have the systematic and statistical uncertainties add in quadrature to $\pm 16 \times 10^{-4}$.

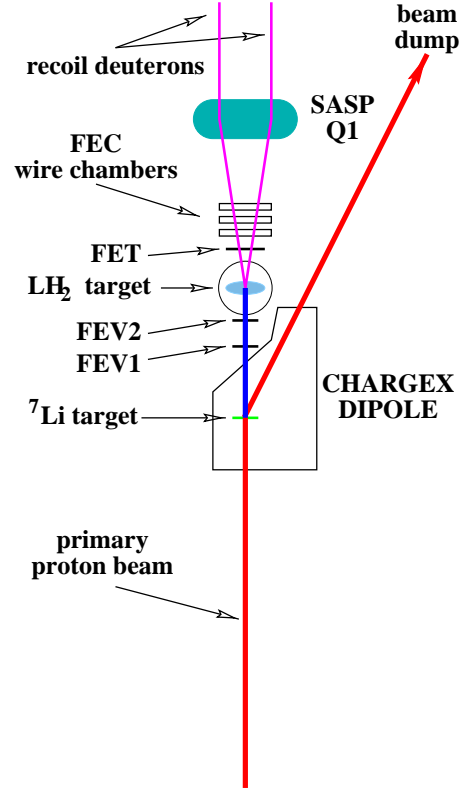


Fig. 34. Experimental layout for the $np \rightarrow d\pi^0$ measurement mode.

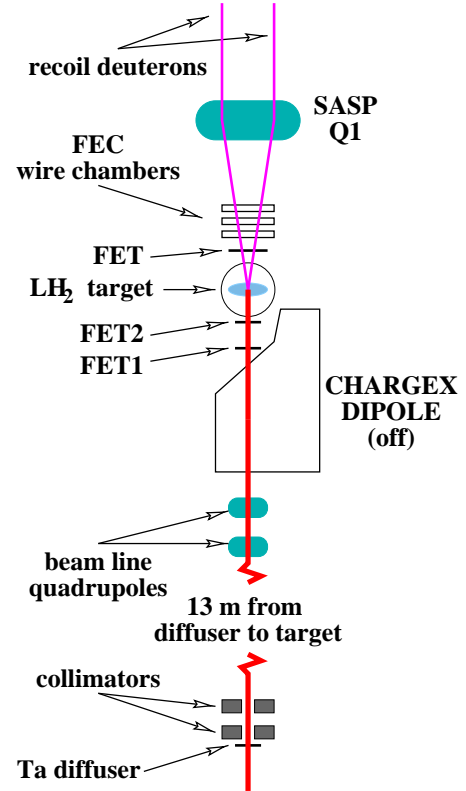


Fig. 35. Experimental layout for the $pp \rightarrow d\pi^+$ measurement mode.

Hardware issues

Front end wire chambers (FECs)

The FECs were designed to run with “magic gas”, an argon-isobutane mix with an additional 2% freon-13B1. This small percentage of this freon allows the chambers to run at a relatively lower voltage and still have a high gain. Due to concerns regarding freon-13B1 and the UV shielding ozone layer in the upper atmosphere, legislation now exists that strongly regulates the use of freon. Consequently, TRIUMF cannot acquire more of this gas. As the amount of freon existing on site was estimated to last no longer than mid-summer, we investigated the possibility of running with an environmentally friendly freon.

Several proposed substitutes passed bench tests during the spring only to fail under running conditions. Note that a replacement gas was sought in the spring of 1997 with a similar result. A 55% Ar, 30% isobutane, and 15% freon 134A mixture eventually proved to be acceptable. With both the magic gas and the new gas mixture, the FECs typically run at greater than 98% efficiency.

The FASTBUS TDC readout system for the FECs has been highly unreliable since we received it. At the end of 1997 we were using TDC PROMs (Rev. F) which had FAST CLEAR capability but could only be reset on power-up of the FASTBUS crate. To eliminate time lost to access the proton hall we installed hardware to remotely power cycle the FASTBUS system. LeCroy issued a further revision of the PROM (Rev. J), which was tested in the spring and found to be capable of resetting with fewer sessions of power-cycling. These PROMs are currently being used in the data acquisition system.

FEC alignment and beam axis definition

Track information from the FECs establishes the position and direction of particles exiting the target. The treatment of the FEC coordinate system in data analysis may be divided naturally into two steps: (1) specifying the FEC coordinate system with respect to the SASP acceptance; and (2) measuring the trajectory of the incident beam in this coordinate system to permit calculation of the true reaction angle.

Ensuring consistency of the FEC coordinate system over the course of several running periods is complicated by the unavoidable necessity of removing and re-positioning the chambers for maintenance. Early measurements of the reproducibility of the FEC positioning using a transit suggested that the chambers could be removed and re-inserted to an accuracy of 1 mm or better. This alignment method is not practical for repeated use due to the fact that sighting along the beam line to the chambers requires the removal of a

significant portion of the front end hardware (in particular, the LH₂ target). The horizontal positions of the FECs are much more susceptible to misalignment than the vertical positions due to the degree of freedom in the horizontal direction in the mounting frame. In contrast, the mechanical alignment in the vertical direction is estimated to be stable at the sub-mm level due to the combined limitations of FEC stand rigidity and reproducibility of the FEC positions with respect to the FEC stand. Thus a fiducial provided by flange slots of the FEC stand was used for mechanical alignment in the horizontal direction up to July. Evidence from analysis of data taken before and after the FECs and FEC stand were removed (so that a different experiment could use the beam line) and from observations of installation procedures indicated that this fiducial was not sufficient to ensure sub-mm position reproducibility.

In response to this horizontal shift evidence, a more stringent alignment procedure was adopted during the summer running period. The new mechanical alignment of the FECs relies upon comparison of the positions of the chamber edges with a fiducial on the front face of the first SASP quadrupole, Q1, so that the chambers are now manifestly aligned to better than 1 mm with respect to the entrance of the SASP spectrometer. Alignment of the Q1 fiducial with the axis of the beam is done with a narrow “pencil” beam, produced by a “pinhole” collimator temporarily inserted in the entrance of Q1, and steering the proton beam until standard positions of the pinhole beam focal plane distributions (in particular the non-dispersive variables Y_{fp} and ϕ_{fp}) are reproduced. This reproducibility, in conjunction with the reproducibility of the SASP dipole field at the level of 1 part in 10⁴, ensures that the FEC pinhole peak positions have not been significantly shifted by changes in the beam angle.

Analysis of pinhole collimator data from running periods prior to July suggests that software chamber alignment at the sub-mm level can still be achieved prior to the use of the improved mechanical protocol described above. The pinhole collimator measurements were originally introduced in the summer, 1997 running period in order to determine the energy spread of the incident proton beam with the pinhole collimator located at the downstream between two of the FECs. This collimator position is not as stable as that in the entrance of Q1 due to uncertainties in the horizontal positions of the mounting scheme. However, by comparing the focal plane Y -position and angle for the pinhole events as predicted by the FEC information with the measured values of these variables, shifts in the horizontal positions of the FECs can be deduced. The typical statistical precision of the centroid deter-

minations for the Y_{fp} and ϕ_{fp} difference distributions in the various data sets then permits detection of shifts in the horizontal FEC positions with a statistical precision well below 1 mm.

Reconstruction of the true deuteron scattering angle in each reaction requires knowledge of the incident beam direction as measured in the FEC reference frame. Two methods are used to determine the incident beam direction in the $np \rightarrow d\pi^0$ mode. The first method provides a “direct” measurement of the beam direction by using slightly different trigger conditions and replacing the primary ${}^7\text{Li}$ target with a Pb target foil target to produce a “neutral hydrogen” beam, i.e. protons which pick up an electron in the Pb foil. These pass undeflected through the CHARGEEX magnetic field and when the hydrogen atom traverses the CHARGEEX exit window its electron is stripped off, leaving a proton that proceeds through SASP as if it had not been altered by the primary target. From the centroids of the measured Y_I , ϕ_I target distributions, the angle of the incident proton beam – and thus the mean direction of the secondary neutron beam – and its horizontal position at the ${}^7\text{Li}$ target can then be deduced. In practice, small corrections due to the CHARGEEX fringe field must be applied.

The second method uses the angular distribution of the $np \rightarrow d\pi^0$ data itself to determine the mean neutron beam direction. In this method, data are first replayed with nominal values of beam trajectory and ${}^7\text{Li}$ target position parameters. A two-dimensional histogram of the horizontal and vertical components of the reaction angle is produced with a cut on a small range of focal plane momenta in order to select deuterons emitted near 90° in the centre-of-mass system. The resulting “smoke ring” pattern (Fig. 36) represents the azimuthal distribution of the $np \rightarrow d\pi^0$

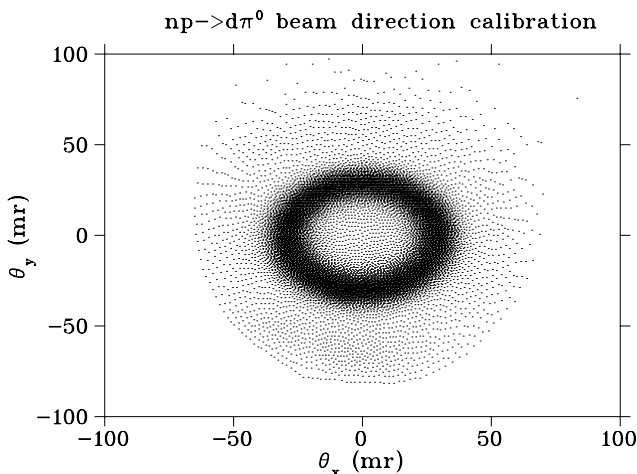


Fig. 36. Horizontal and vertical components of the reaction angle for deuterons emitted near 90° in the centre of mass from $np \rightarrow d\pi^0$.

events with the assumed incident beam trajectory. Software parameters describing the incident beam direction are adjusted to centre this pattern on the origin.

The same smoke ring calibration method is also applied to the $pp \rightarrow d\pi^+$ data. In the proton beam mode, the only relevant incident beam parameter is its direction. In the proton beam case, a small fraction of the protons from the low energy tail of the incident beam “leak” through the hardware deuteron trigger. These protons show up as a “bull’s-eye” at the centre of the smoke ring reaction angle pattern described above, and can be used in conjunction with the edges of the pattern to determine the angular offset of the beam in the FEC coordinate system.

SASP acceptance

Understanding the acceptance of SASP has been an ongoing challenge, complicated by many effects being negligible until sufficient data are in hand. Early analysis of $np \rightarrow d\pi^0$ data taken in the fall of 1996 indicated three general features of the SASP acceptance. (1) The angular acceptance for fixed target position is roughly “lozenge” or “cruciform”-shaped, reflecting the boundaries imposed by the face and internal surfaces of the first quadrupole, Q1. (2) The ϕ_I acceptance featured a momentum dependence at horizontal positions, Y_I , beyond roughly ± 1 cm. (3) To the statistical accuracy of the data in hand at that time, there was no discernible momentum dependence to the acceptance as a function of the vertical position variable, X_I .

By the end of 1997, a new quad tune had been established to minimize the severity of the Y_I effect, and the acceptance of SASP with that tune mapped out with a series of np elastic scattering data. Data were collected at three beam energies (leaving the SASP magnetic fields constant) to cover roughly the same portion of the focal plane occupied by the deuterons from $np \rightarrow d\pi^0$ and $pp \rightarrow d\pi^+$. Roughly 2 to 3 million counts in the np elastic peak were acquired at each of the three beam energies. The three sets are referred to as the “+4%”, “-4%”, and “0%” sets, according to the approximate value of δ for the np elastic peak relative to the region of the focal plane occupied by deuterons at the centre of the $np \rightarrow d\pi^0$ locus.

Off-line analysis of the np elastics data was used to determine appropriate target angle cuts defining the software SASP angular acceptance. A lozenge-shaped polygon in the (θ_I, ϕ_I) plane was determined from each of these distributions which “trims off” extreme portions of the angular acceptance where the SASP response is expected to be least stable as a function of momentum.

The primary tool for investigating instrumental asymmetries in the $np \rightarrow d\pi^0$ and $pp \rightarrow d\pi^+$ data

has thus far been the count ratio of high momentum to low momentum particles in the sub-10 mr (laboratory scattering angle) portion of the kinematic locus, referred to as R . For zero A_{fb} , the transformation of centre of mass to lab solid angles for a neutron beam energy of 279.5 MeV gives a predicted deuteron count ratio of 1.142. The raw and acceptance-corrected ratios for the extremes of Y_I (the central Y_I strip is essentially uncorrected in this scheme) are given in Table II.

Table II. High/low count ratios for $8/97\ np \rightarrow d\pi^0$.

Y_I Strip (cm)	Raw	Corrected
(-2.0, -0.66)	1.41 ± 0.06	1.14 ± 0.05
(0.66, 2.0)	1.33 ± 0.05	1.19 ± 0.04

Thus for this limited statistics $np \rightarrow d\pi^0$ data set the correction scheme has reproduced the expected (zero A_{fb}) ratio within statistical uncertainty for the negative Y_I strip, and within 1.3 sigma for the positive Y_I strip.

The “ θ_I effect” and np elastic data analysis

The acceptance in the vertical target angle, θ_I , also exhibits a small apparent variation with momentum. Figure 37 shows the $(\delta = -4\%)/(\delta = +4\%)$ np elastic count ratio distributions as a function of θ_I . The three curves correspond to cuts on X_I ranges of (-2.0,-0.6), (-0.6,0.6), and (0.6,2.0) cm in the central Y_I strip of -0.6 to 0.6 cm, for horizontal angles ϕ_I in the range (-10,10) mr. Note that any Y_I dependence is expected to be negligible in this central strip. Linear fits to the central “plateau” regions of the three curves yield slopes which are 6σ , 2σ , and 3σ away from 0 for the top, middle, and bottom graphs, respectively. These slopes correspond to changes in the count ratios of 12%, 3.5%, and 5.8%, respectively, over the range (-50,50) mr. Note that the slope in the relative θ_I acceptance distributions shows up even in the central X_I range. Thus it has not yet been possible to identify a “flat” region of the acceptance with θ_I over any portion of the standard 16 cm² target area. The SASP optics correlate θ_I with the focal plane dispersive angle, θ_{fp} . Thus one source of the apparent slope in “acceptance” may actually be an angle-dependent detector inefficiency. Investigations of the VDC tracking efficiency as a function of focal plane angle over the range of angles relevant to the $np \rightarrow d\pi^0$ locus have failed to reveal systematic trends at anything above the 0.1% level, however, and the angle-integrated efficiencies of the focal plane scintillators are stable at above 99%. Thus the source of this slope is still under investigation.

X_I dependence in acceptance

An apparent X_I dependence in the momentum acceptance of SASP was discovered in December, 1997.

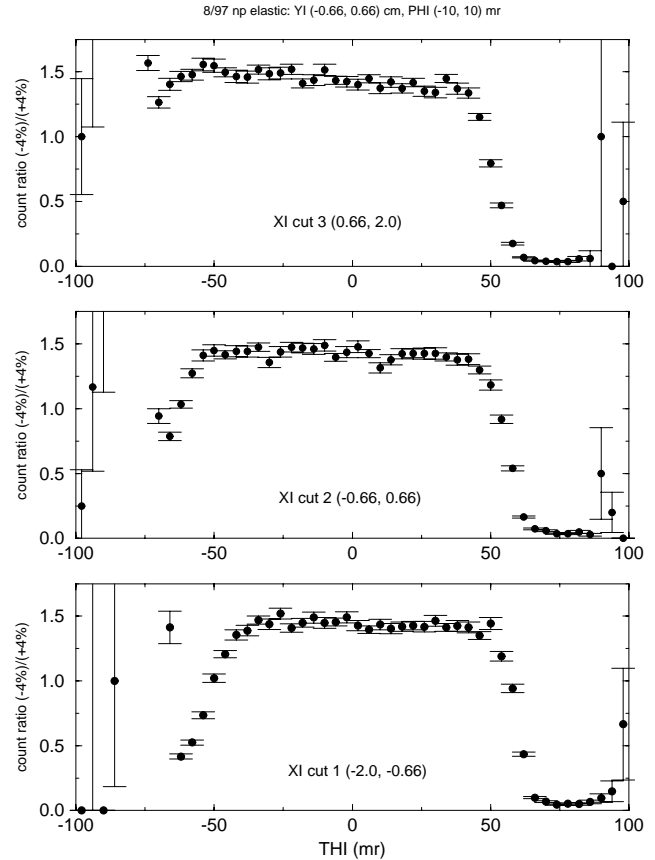


Fig. 37. The θ_I , X_I acceptance correlation.

Investigating several possible sources of the X_I dependence (including front end and focal plane detector efficiency variations as a function of position and momentum, scintillator thresholds, etc.), revealed no obvious “smoking gun”. It was then noted that, for fixed particle momentum, the average angle through the focal plane VDCs varies with X_I . Thus apparent variations in the SASP response as a function of the target variable X_I can, in fact, reflect variations in the response of the VDCs as a function of focal plane angle. This realization led to a thorough investigation of the VDC plane decoding and track reconstruction programs.

A new VDC decoding routine was developed which incorporates a line-fit approach to the problem of determining tracks from wire hit clusters. The primary advances of the new routine are the following: (1) a 25% improvement in single-plane angular resolution over the old routine; (2) careful control of the VDC internal angle reconstruction as a function of the number of wires occurring in a hit cluster; (3) provision for convenient calibration of drifts in the VDC response with time due to small changes in voltage, gas flow, etc.; (4) improved wire-hit pattern recognition capability over the previous routine, resulting in an increase in the track reconstruction efficiency of each plane.

The np elastic data were replayed with the new VDC track reconstruction method and the previously observed fall-off in acceptance in X_I was eliminated. The $np \rightarrow d\pi^0$ data from summer and fall, 1997 were then replayed using the new VDC track reconstruction routines. The sub-10 mr count ratio (high momentum)/(low momentum) is listed in the following table. Recall that the value expected for the ratio of solid angles for forward and backward-going deuterons (lab scattering angle < 10 mrad) is 1.142. The ratios with the new tracking codes are all in agreement with the expected ratio at the 1-sigma level.

Table III. Ratio of high to low momentum deuteron yields for different slices of X_I , using the two sets of tracking codes.

X_I bin	Old tracking codes	New tracking codes
	High-p/Low-p	High-p/Low-p
1	1.06 ± 0.03	1.11 ± 0.03
2	1.15 ± 0.03	1.16 ± 0.03
3	1.10 ± 0.03	1.14 ± 0.03

Analysis of $pp \rightarrow d\pi^+$ from 1997

A first-pass analysis of the 1997 $pp \rightarrow d\pi^+$ data incorporated “one track” cuts, namely requiring events to have one track in the VDCs and one track in the FECs. This was done to minimize background and increase our confidence in the correlation of tracks observed at the target with those in the focal plane of SASP. However, the one track cuts cannot be used for further stages in analysis of the $pp \rightarrow d\pi^+$ data.

The low momentum deuterons from this reaction are accompanied by forward-going charged pions which pass through the front end detectors, while the pions associated with the high momentum deuterons either have insufficient energy to exit the target, or emerge at larger lab angles and are not detected. The size of the effect may be gauged by the value of the ratio of yields of high momentum vs. low momentum deuterons at sub-10 mrad angles, R . With the one track condition $R = 1.94 \pm 0.03$, which is to be compared to an expected value of 1.166 (due to differing CM to lab solid-angle transformations at forward vs. backward CM angles) at our proton beam energy.

To eliminate this source of momentum dependent asymmetry we developed a multi-track analysis method to “loop over all tracks” and count every combination with an acceptable chi-squared, thereby avoiding suppression of deuteron tracks. The method will lead to some double counting, but this is estimated to be small (0.5% effect) and readily simulated by Monte Carlo. The analyses of the July, 1997 and November, 1997 data were repeated, this time with the looping over all possible tracks in effect. The re-

sults with this analysis method show a dramatic improvement in the value of R with the average value for the summer, 1997 (fall, 1997) data being 1.33 ± 0.013 (1.40 ± 0.011).

These results were obtained with background corrections similar to those used for the $np \rightarrow d\pi^0$ data. Data-from-data background subtraction is not a straightforward procedure in that the background deuterons generated upstream of the LH₂ target suffer different energy losses and multiple scattering when the target is empty than when it is full. Thus a target-empty measurement does not produce a locus which can be subtracted in the familiar way from the target-full locus to produce a “foreground-only” spectrum, and various prescriptions for attempting to do so are rough approximations only. Different prescriptions were tried and gave ratios ranging from $R = 1.14 \pm 0.01$ to 1.19 ± 0.01 (statistical errors only), compared to the anticipated value of 1.166. Clearly, the uncertainty inherent in “direct subtraction” of background is much larger than can be tolerated in this experiment. The ultimate analysis for this calibration reaction will thus rely on comparison of target-full and target-empty spectra with a detailed simulation of energy loss and multiple scattering by proton beam and reaction deuterons.

Full simulation in GEANT

By the end of 1997 the GEANT simulation of Expt. 704 was modelling an “ideal” experiment and comparisons with data could be used as a guide. Since then a number of features have been added that make for a more realistic simulation and the results for both the $np \rightarrow d\pi^0$ and $pp \rightarrow d\pi^+$ reactions can be compared to data. The primary improvements are:

- tracks the pion and its decay products
- allows deuteron production on hydrogen in non-LH₂ materials
- produces $C(N, d)$ background. The deuteron distribution in the lab frame has the form $\frac{d\sigma}{d\Omega} = B_0(1 + B_1\theta + B_2\theta^2)(1 + C_1\delta + C_2\delta)$ where the constants B_0, B_1, B_2, C_1 and C_2 are determined by fitting the GEANT output to graphite data and target empty data at sub-threshold.
- uses the energy deposition on the FE scintillators to reproduce on-line trigger conditions
- has a generator for np elastic events derived from SAID; this has not been used yet
- describes the focal plane detectors

- describes all the interior surfaces of the various vacuum boxes and pole faces of the spectrometer between the top and front end.
- models the SASP dipole field as an “ideal” dipole from RAYTRACE with corrections from a measured field map.
- models the two entrance quads with a RAYTRACE description.

The energy distribution of the incident nucleon is described by a double Gaussian if the nucleon is a neutron or a single Gaussian if the nucleon is a proton. By simultaneously fitting these functions to the deuteron locus and the scattered nucleon band we expect to determine the average incident beam energy to better than ± 5 keV.

The centre-of-mass cross section for $np \rightarrow d\pi^0$ is given by

$$d\sigma/d\Omega = A_0 + A_1P_1(\theta^*) + A_2P_2(\theta^*),$$

where θ^* is the deuteron c.m. angle and P_i are Legendre polynomials. This is the function used to generate the deuterons in the simulation. In this expression, the second term describes any charge symmetry breaking with the coefficient A_1 giving the asymmetry. The ratio of $A_2/A_0 = 0.1134$ was obtained in Expt. 466 [Hutcheon *et al.*, Nucl. Phys. **A535**, 618 (1991)]; ultimately we will determine the value of A_2/A_0 that best reproduces the data. Figure 38 shows the kinematic locus for the GEANT simulated $pp \rightarrow d\pi^+$ reaction.

Planned improvements

Several effects have not yet been incorporated into the Monte Carlo simulation. We estimate that, when completed, they will result in significantly improved agreement between the observed and simulated data.

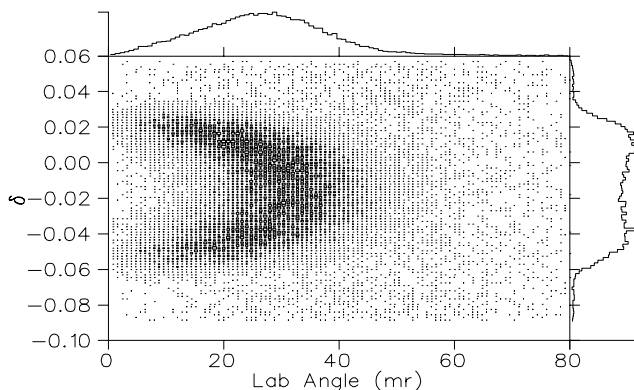


Fig. 38. Kinematic locus of $pp \rightarrow d\pi^+$, generated by GEANT.

Planned improvements include:

- Deuteron reaction losses. Between 1% and 2% of the deuterons are lost due to nuclear reactions in the target and detectors. As the cross sections for these losses are energy dependent, the effect within the $\pm 4\%$ momentum range of the deuteron locus must be determined.
- Accidental coincidences. The simulation must track all particles in $pp \rightarrow d\pi^+$ and include the effects these particles have on the track reconstruction. These problems are much smaller in the neutron-beam measurements.
- Simulation of elastic $np \rightarrow pn$ data. In a cycle of production data-taking, elastic $np \rightarrow pn$ scattering data are taken almost simultaneously with the $Np \rightarrow d\pi$ data. By comparing the simulated data and the real data we should be able to further constrain the input parameters to the fit.

Sensitivity of χ^2 tests

$pp \rightarrow d\pi^+$

A study of the $pp \rightarrow d\pi^+$ interaction has been done as a test of the suitability of using the GEANT model to extract the value of A_{fb} with the δ vs. θ binning scheme. This study involves varying the initial proton beam energy and the central momentum p_0 of the spectrometer so as to find the values of these parameters which will minimize the χ^2 of the fit of the GEANT output and the data. Other parameters such as the initial beam energy spread and the signal-to-noise ratio were held constant.

In the study for target full, a 29 mm target was used instead of the nominal 20 mm target to simulate the effect of bulging target windows. Two independent methods were used to optimize both the beam energy and p_0 , the results of which are given in Table IV.

Table IV. Beam energy and p_0 yielding minimum χ^2 .

Method	Beam energy (MeV)	p_0 (MeV/c)
1	295.20 ± 0.01	730.74 ± 0.06
2	295.21 ± 0.02	730.59 ± 0.11

The consistency of the beam energy and central momentum for these two techniques suggests that the values are quite reliable. A second scan was done with target empty. The χ^2/DoF was extracted for each of these runs and averaged with the χ^2/DoF from the target full scans.

Using the values for beam energy and p_0 found from the combined χ^2 fit, the value of A_1/A_0 was varied in steps of 0.1 through the range of -0.2 to 0.2 . The minimum in the plot of χ^2 vs. A_1/A_0 will yield

the best estimate of the value for A_1/A_0 . The width of this plot leads to the sensitivity in A_{fb} . From the GEANT runs, the minimum was determined to be at $A_1/A_0 = 0.102$. The GEANT model does not currently include the effects of multiple tracks in the FECs, thus it is expected that the fit for A_1/A_0 should predict an abnormally large positive value for A_1/A_0 . The plot of χ^2 vs. A_1/A_0 for full target data is shown in Fig. 39.

The statistical uncertainty in the fit of A_1/A_0 is determined as

$$\sigma^2 = \frac{1}{N} \frac{1}{2} \frac{d^2(A_1/A_0)}{d(\chi^2)^2}$$

where N is the number of degrees of freedom in the fit. With 137 degrees of freedom, we obtain an uncertainty in the estimate of A_1/A_0 of $\pm 1/\sqrt{(137 \times 112)} = \pm 0.0081$. It must be noted that the GEANT runs were short, thus their statistics limited the present sensitivity. Increasing the number of events in the GEANT runs to that which is comparable to the number of events in the data, the statistical sensitivity to A_1/A_0 should increase greatly and limit the instrumental A_1/A_0 to just over ± 0.002 .

$np \rightarrow d\pi^0$

A similar study of the $np \rightarrow d\pi^0$ interaction has also been done as a further test of the suitability of the GEANT model. Obtaining the best fit value for A_1/A_0 followed the same procedure as that for the $pp \rightarrow d\pi^+$ study. The plots of $np \rightarrow d\pi^0$ χ^2 vs. A_1/A_0 are similar to those for $pp \rightarrow d\pi^+$ as shown in Fig. 39. The best fit value for A_1/A_0 , was determined to be 0.06 with an uncertainty in the estimate of A_1/A_0 of $\pm 1/\sqrt{(137 \times 93)} = \pm 0.0089$.

As was the case with the $pp \rightarrow d\pi^+$ simulation, the typical $np \rightarrow d\pi^0$ GEANT runs were shorter than the

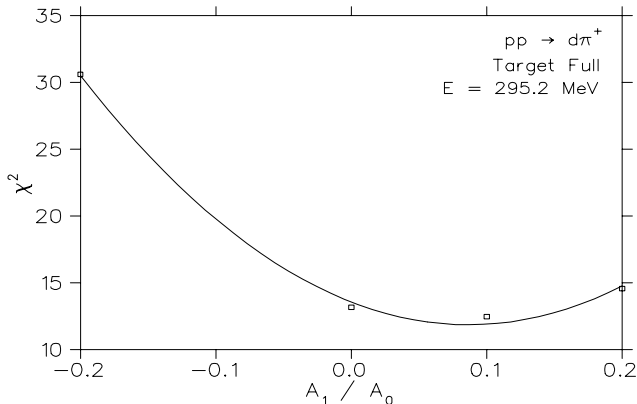


Fig. 39. Plot of χ^2 vs. A_1/A_0 for $pp \rightarrow d\pi^+$ target full at a beam energy of 295.20 MeV. The minimum value for χ^2 occurs at $A_1/A_0 = 0.087 \pm 0.010$. The χ^2 for the empty target runs have not been combined with the values shown. As a result, the estimated best fit for A_1/A_0 differs from that in the text.

actual amount of data on tape. Thus, increasing the number of events in the GEANT runs to be comparable to the number of events in the data should reduce the fit uncertainty on A_1/A_0 to just over ± 0.002 .

Systematic effects

It is important to note that the total number of events influences both the statistical uncertainty and the constraints on the systematic uncertainties.

Limit from systematic errors

To summarize the sources of uncertainty in A_{fb} discussed in the previous sections, it is convenient to first broadly categorize the various error sources as follows:

- statistical error as represented in the fit sensitivity to A_{fb} , given simultaneous fitting of other kinematic parameters which determine the locus shape;
- efficiency uncertainties (VDC tracking, FEC tracking, front end trigger scintillator);
- acceptance uncertainties;
- uncertainty in energy dependence of reaction loss/multiple scattering for deuterons passing from the LH₂ target to the focal plane.

Table V. A_{fb} error budget.

Source	Reaction	Uncertainty (10^{-4})
$pp \rightarrow d\pi^+$		
Statistics		8
Efficiencies		2
Tracking		5
Total		± 10
$np \rightarrow d\pi^0$		
Statistics		10
Efficiencies		2
Acceptance		8
Reaction losses		10*
Total		± 16

* (from $pp \rightarrow d\pi^+$)

Data collection

Expt. 704 had two extended running periods in 1998, both of which were highly productive in spite of situations which greatly handicapped the experiment. The May through July period was interrupted by a period in which the LH₂ target had to be removed and repaired due to a leak in an interior window. Effects of the target leak were observed during $pp \rightarrow d\pi^+$ running and made that portion of a run cycle unusable.

The fall running period was interrupted by a malfunctioning pump in the cyclotron cooling system which affected the whole lab.

The number of $np \rightarrow d\pi^0$ ($pp \rightarrow d\pi^+$) events taken in 1998 was 1.9 million (2.9 million), which brings our total number of $np \rightarrow d\pi^0$ events to approximately 2.4 million. With full analysis of these data the statistical (systematic) uncertainty will be $\pm 17 \times 10^{-4}$ ($\pm 20 \times 10^{-4}$).

Future activities

While acquisition of more data is needed, it is crucial that the simulation of the experiment be at a level such that the systematic uncertainties are at the same level as the statistical uncertainties. With the hardware and running procedures firmly established, the collaboration will direct its resources to bringing the χ^2/N of our fit down to ~ 2 , which will indicate that the systematic effects are understood.

A total of 130–150 shifts are required to obtain a statistical (systematic) uncertainty of $\pm 10 \times 10^{-4}$ ($\pm 13 \times 10^{-4}$), and complete this experiment. Data collection should be nearing completion by fall, 1999.

Experiment 715

Weak interaction symmetries in β^+ decay of optically trapped $^{37,38}\text{K}$

(*J.A. Behr, TRIUMF; K.P. Jackson, TRIUMF/SFU*)

In the last year, TRINAT (TRIUMF neutral atom trap) has made considerable progress. Running at TISOL in June we transferred sufficient atoms to our nuclear detection magneto-optical trap (MOT) for a viable measurement of the $\beta^+-\nu$ correlation coefficient a_F in the superallowed Fermi decay of ^{38}K . We trapped approximately 2,000 ^{37}K atoms and 5,000 ^{38}K atoms at a time, the latter for approximately 1 week. The result was over 500,000 Ar- β^+ coincidence events from the decay of ^{38}K , and 75,000 from ^{37}K , approximately 100x our data sample from 1997. Analysis is in progress. If systematic errors prove to be small, this data set will produce a measurement of the $\beta^+-\nu$ correlation coefficient a_F with statistical error 0.005.

The TRINAT lab has now been moved to the ISAC facility, and first data from trapped atoms were taken there in December.

The status of the off-line magneto-optical trap development for polarizing ^{41}K in preparation for ^{37}K spin correlation measurements can be found on page 123 of this Annual Report.

Search for scalar currents with $\beta-\nu$ correlation in ^{38}K

For β -decay studies, the magneto-optical trap (MOT) provides a sample of atoms in a localized volume with virtually zero source thickness, so unperturbed nuclear recoils can be detected in coincidence

with the β , allowing the determination of the ν momentum. In the $0^+ \rightarrow 0^+$ Fermi decay of ^{38}K , the angular distribution is given by $W[\theta] = 1 + a_F \frac{v}{c} \cos\theta$, with $a_F = 1$ in the standard model and $a_F = -1$ for a hypothetical scalar boson exchange. We measure back-to-back coincidences between β^+ and ^{38}Ar neutral atom recoils; the recoils will have lower energy – hence longer time of flight – if the leptons are emitted back-to-back. In addition, we collect charged Ar recoils with high efficiency with a uniform electric field, and implicitly reconstruct their angular distribution; for a given E_{β^+} , $\cos(\theta_{\beta\nu})$ decreases monotonically with increasing recoil TOF.

Limits on the scalar interaction are poor, both from β decay [Adelberger, Phys. Rev. Lett. **70**, 2856 (1993); Erratum, Phys. Rev. Lett. **71**, 469 (1993)] and from particle physics. For example, direct limits on the couplings and masses of the charged Higgs were (as of 1995) such that a charged Higgs could in principle have a contribution to β decay as large as the standard model weak interaction [Herzceg, in *Precision tests of the standard model*, ed. Langacker (1995)]. Garcia and Adelberger have now reached precision 0.005 in a_F in ^{32}Ar [Adelberger, WEISS Workshop (1997)]. Fermilab D0 lower limits on scalar leptoquark masses have now reached 225 GeV [Abbott *et al.*, Phys. Rev. Lett. **80** 2051 (1998)], approximately the limit attainable from a measurement of a_F to precision 0.01 (with complementary model dependence in each case).

Present results

Figure 40 shows a scatter plot of E_{β^+} vs. recoil TOF from ^{38}K decays. The various charge states of the Ar recoils can be seen, separated in TOF by the electric field.

Figure 41 shows the TOF projection of Fig. 40 on a log scale. Note the background between Ar^{+1} and Ar^0 in TOF (which can be seen to be kinematically forbidden in Fig. 40) is at the level of $\approx 1\%$ of the data.

For fixed β^+ energy, $\cos(\theta_{\beta\nu})$ decreases monotonically as time of flight increases for Ar^{+1} in the presence of the electric field. We have begun fitting TOF spectra for several simultaneous E_{β^+} cuts to a Monte Carlo, varying a_F to minimize χ^2 . The difficulty in this analysis is that it requires accurate knowledge of the β^+ energy and response function; e.g. an uncertainty in a creates similar changes in slope to an uncertainty in energy calibration, with an error in a of 0.01 corresponding approximately to an energy calibration uncertainty of 10 keV at 3 MeV. We are working to include the angle information (i.e. position information in both β^+ and recoil detectors) to alleviate this.

Using the present analysis, the statistical uncertainty in a is ≈ 0.005 , using the Ar^{+1} data; systematic errors are still being evaluated.

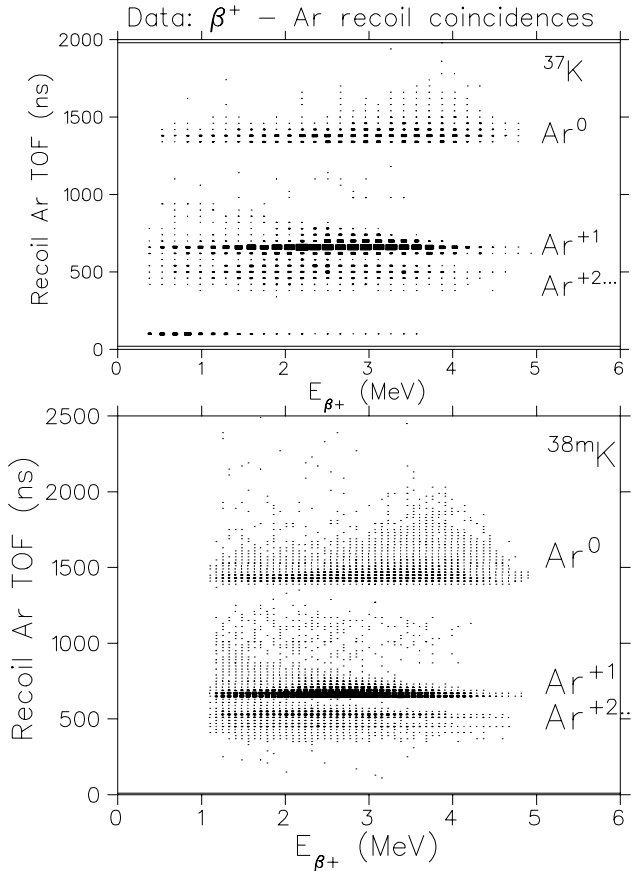


Fig. 40. Scatter plot of Ar recoil TOF vs. kinetic E_{β^+} : $\approx 20\%$ of the data. $|\vec{E}| = 800$ V/cm cleanly separates Ar^0 from $\text{Ar}^{+1, \dots, +6}$

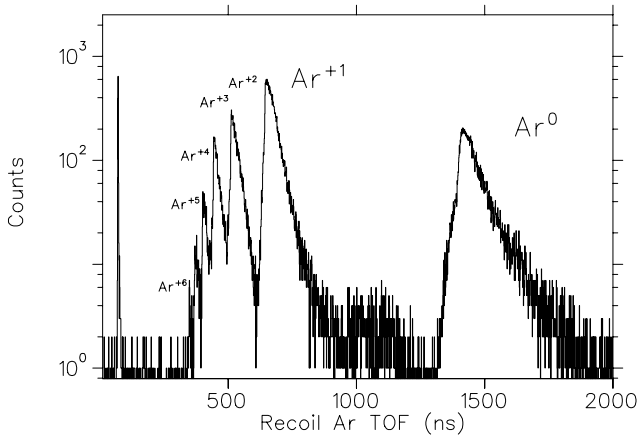


Fig. 41. TOF projection of Fig. 40. Note log scale.

Backgrounds

In Fig. 41 kinematically forbidden events appear in TOF between the Ar^{+1} and Ar^0 peaks. They constitute $\approx 1\%$ of all events, in two distinct TOF peaks. Since they are kinematically forbidden, they can be excluded; the question is whether similar smaller backgrounds can contaminate the allowed kinematic data.

We have taken data in two modes to try to establish the nature of this background. We can deliberately release atoms to the walls; the result was a similar number of background events in the lower TOF background peak, and $<0.1\%$ background appearing under the Ar^{+1} peak, with no other backgrounds apparent. In addition, we ran with the electric field with opposite sign, removing all ions but allowing Ar^0 events; the result was a background in the Ar ion region flat in TOF at 0.2% of the real coincidence rate per nsec, consistent with accidental coincidences.

For $^{38\text{m}}, ^{37}\text{K}$ atoms stuck on the electrostatic rings or the chamber walls, the uniform electric field is such that Ar ions from their decay cannot reach the microchannel plate (MCP). A possible background source is atoms that are not properly trapped and are deflected, and reach the large 1 mg/cm^2 Al foil in the direction of the β^+ detector which defines an equipotential, as events from it would reach the MCP.

The γ -ray background from ^{38}K ground state decays in the collection trap has been greatly reduced. They now constitute 50% of the MCP singles rate.

The deliberate release tests suggest a 2% background in the β^+ telescope ‘singles’ from atoms on walls; again, this background is almost completely removed by the MCP coincidence requirement. This does suggest that the addition of wire chambers for tracking β^+ ’s to exclude the wall backgrounds would enable accurate β^+ asymmetry measurements in ^{37}K in singles in future measurements, in addition to the coincidence measurements planned.

Technical improvements

Target

The target used at TISOL was made from pressed CaO disks, producing higher density and mechanical stability. The target ran for several weeks with minimal degradation, producing yields (2×10^7 /sec of $^{38\text{m}}\text{K}$) similar to those of the best previous CaO powder targets with much lower oven temperatures. The same target material was used at ISAC; the ISAC yields are in the ISAC section of this Annual Report.

Neutralizer

Emulating success at Los Alamos in trapping ^{82}Rb [Gückert *et al.*, Phys. Rev. **A58** R1637 (1998)], the TRINAT neutralizer is now a Zr 0.001 in. conical foil at the back of the cube. The ion beam travels through the trap region to the neutralizer (Fig. 42). There are many more metals and materials with work functions lower than the ionization potential of K, so it is possible to choose a material with fast enough release times at lower temperatures than the previous Re ionizer. As a diagnostic for release of ^{37}K , $1/8$ in. stainless steel

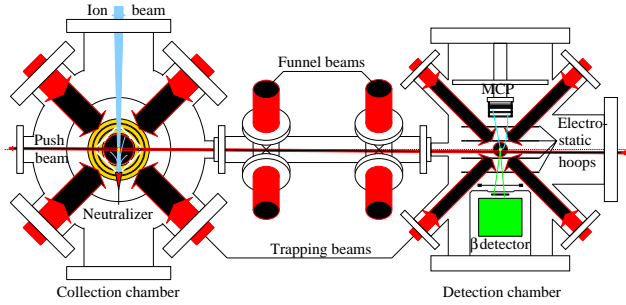


Fig. 42. Plan view of Expt. 715 apparatus.

positron stoppers surround the Zr cone; when the neutralizer is cold, the ^{37}K decays while in the cone, the β^+ s stop in the stainless steel and annihilate, and their back-to-back γ decays are detected in two NaI detectors. When the neutralizer is heated, the coincidence rate becomes smaller, due to the ^{37}K fraction that has escaped into the trap cell volume. Many materials, including low temperature melting point materials like Li, Al, and In, were tested on TISOL beam line A using this technique, and Zr was found to be the best combination of release time, temperature, and vapour pressure. At 900°C , Zr releases $>70\%$ of 12 keV implanted ^{37}K .

The resulting trapping efficiency in the collection trap was $\approx 1 \times 10^{-3}$ for $^{38\text{m}}\text{K}$, and the overall efficiency for trapping and transfer to the detection trap was $\approx 7 \times 10^{-4}$.

Energy calibration

The energy calibration from Compton edges of γ -rays has now been established to be linear from 0.6 to 1.6 MeV with residuals of less than 5 keV. Our feedback PMT gain stabilization system (locking electronics from Y. Holler at DESY [Holler, Nucl. Instrum. Methods **204**, 485 (1983)], 450 nm blue LED to match photocathode response, and temperature controlled photodiode) reliably locks the gain to sufficient accuracy. A remaining question is whether the scintillator response to β^+ s will be close enough to γ s (e.g., non-uniformity of light collection will be different), and we are testing this by fitting the β^+ ‘singles’ spectrum from the telescope from the on-line trap data.

Cloud size

Recoil TOF resolution is limited by cloud size; 1 mm FWHM implies 7 ns timing for the Ar^{+1} ions. The cloud size was 1.5 mm FWHM for the bulk of the data. We have made this as small as 0.7 mm FWHM for the last 20% of the data, done by first transferring the atoms using the frequency optimized for transfer, then shifting the trap light closer to resonance. Atomic theory for Doppler-limited cooling suggests that the cloud can be made much smaller, and we have now set

up continuously tunable light in frequency and power which we will scan at the next opportunity.

Admixture of ν_e with a massive ν

In addition to quantitative measurements of the $\beta^+-\nu$ correlation, our kinematic reconstruction of β^+ -recoil coincidences allows us to look for kinematically forbidden peaks in recoil TOF. Using the same $^{38\text{m}}\text{K}$ data, we can set upper limits on the admixture of ν_e with hypothetical heavy neutrinos for masses of $\approx 1\text{--}4$ MeV/ c^2 . The kinematic signature would in principle be striking, events near the fast Ar^0 recoil branch with longer time of flight. The best direct limits in this range are $< 2 \times 10^{-3}$ from a ^{20}F β spectrum ‘kink’ search [Deutsch *et al.*, Nucl. Phys. **A518**, 149 (1990)], while indirect limits from the $(\pi \rightarrow e\nu)/(\pi \rightarrow \mu\nu)$ branching ratio vary from 1×10^{-3} to 1×10^{-4} [Bryman, Comm. Nucl. Part. Physics **21**, 101 (1993); Boehm and Vogel, *Physics of massive neutrinos* (Cambridge, 1992) p.66]. For $^{38\text{m}}\text{K}$, where the slow-going Ar recoils are suppressed, we estimate from the present raw TOF data we should reach upper limits of better than 2×10^{-3} . Analysis is proceeding on using the full kinematic reconstruction to remove the finite detector size, which along with a proper peak search should reach better limits. A ν_τ with mass of a few MeV/ c^2 – the scale of nuclear binding energies – would solve certain possible problems in Big Bang nucleosynthesis [Kawasaki *et al.*, Phys. Lett. **B430**, 132 (1998); Fields *et al.* Astroparticle Phys. **6**, 169 (1997)].

Experiment 719

$^4\text{He}(\pi^+, \pi^- pp)$ invariant mass measurement with CHAOS

(R. Meier, Tübingen; M.E. Sevier, Melbourne; G.R. Smith, TRIUMF)

This experiment received beam time during the high intensity beam periods of TRIUMF operation in January, July and December, 1996. The CHAOS spectrometer with a ^4He gas target was used in the TRIUMF M11 area. Measurements were done at pion kinetic energies of 115 and 105 MeV.

The experiment is searching for the hypothetical d' dibaryon, which is a possible explanation for the enhancement in the total cross section of pion double charge exchange (DCX) to discrete final states in nuclei around $T_\pi = 50$ MeV. From the analysis of DCX, the mass of the d' has been derived to be about 2065 MeV, with a width of about 0.5 MeV. The quantum numbers were suggested to be $J^P = 0^-$ and $T = 0, 2$. With these quantum numbers, the d' can not couple to the two nucleon channel, but will decay into a pion and two nucleons.

Experiment 719 searches for the d' by investigating the double charge exchange reaction $\pi^+ ^4\text{He} \rightarrow$

$\pi^- pppp$. If the d' exists, a large part of the DCX cross section in a region above the d' production threshold should be due to the reaction $\pi^+ {}^4\text{He} \rightarrow d' pp \rightarrow (\pi^- pp) pp$.

CHAOS was set up to simultaneously detect the π^- and at least two protons. From the measured momenta of the three detected particles, the invariant mass of the $\pi^- pp$ system can be calculated; the d' should show up as a peak in the invariant mass spectrum. As only two of the four protons in the final state can possibly come from the d' , the peak will be accompanied by a combinatorial background from detecting one or two protons not from the d' . Additionally, there will be background from non-resonant DCX.

Although the DCX mechanism via the d' is predicted to dominate the DCX cross section just above the d' threshold (at about $T_\pi = 80$ MeV), the measurements were done at 25 and 35 MeV above threshold. Simulations showed that near threshold for acceptance reasons the signature expected from the d' is indistinguishable from the behaviour of conventional DCX.

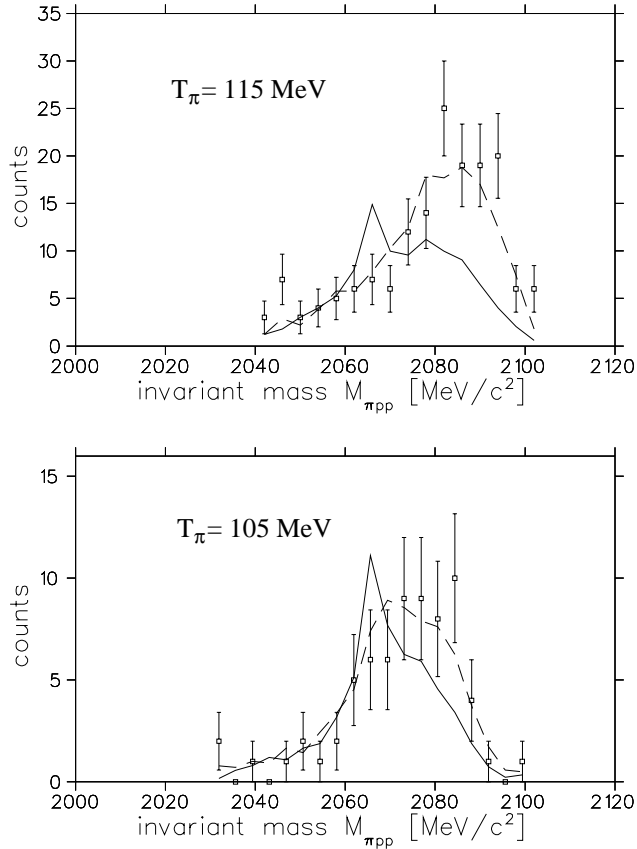


Fig. 43. Experimental results for the invariant mass of the outgoing π^- and the two protons detected in CHAOS at 105 and 115 MeV, compared to predictions from the d' model (solid lines) and from a conventional sequential single charge exchange model (dashed curves).

The data have been analyzed at the University of Melbourne and the University of Tübingen. A publication is being prepared for submission to Physics Letters B.

Figure 43 shows the experimental result for the invariant mass of the pion and the two detected protons; Fig. 44 the result for the invariant mass for the pion and the two protons not detected in the spectrometer, at both incident energies. The invariant mass of the two unobserved protons is deduced from the missing mass of the observed particles. The data are compared to predictions from the d' model and from a conventional sequential single charge exchange model. We note that collision damping $d'N \rightarrow 3N$ has not been taken into account in the d' simulations. It would lead to a broadening of the d' curves. In all cases the sequential single charge exchange model gives a good description of the data. Upper limits for a possible contribution of the d' to the DCX process will be extracted from the data.

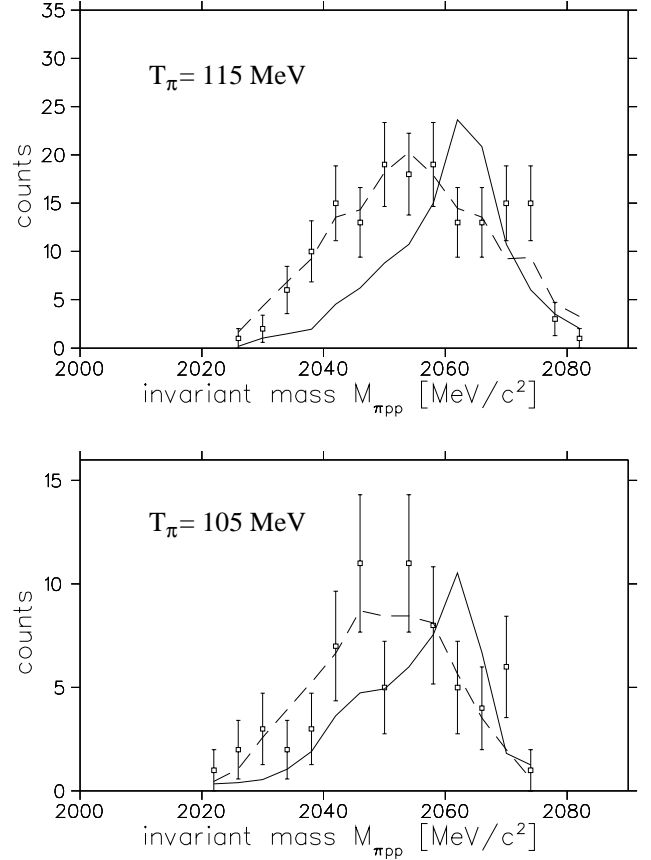


Fig. 44. Same as Fig. 43, but for the invariant mass of the π^- and the two protons *not* detected in CHAOS.

Experiment 725

Pionic double charge exchange on ${}^4\text{He}$

(E. Friedman, Jerusalem; G.J. Wagner, Tübingen)

This experiment of the CHAOS collaboration received beam time during the high intensity beam period of TRIUMF operation in February, 1996. The experiment employed a liquid ${}^4\text{He}$ target with the CHAOS spectrometer in the TRIUMF M11 beam line. The data analysis has been completed and the results have been published [Gräter *et al.*, Phys. Lett. **B420**, 37 (1998); *ibid.*, Phys. Rev. **C58**, 1576 (1998)].

In the energy region of the Δ -resonance, the reaction mechanism of pionic double charge exchange (DCX) on nuclei seems to be fairly well understood. In contrast, around 50 MeV the forward angle excitation function for DCX to well-defined final states on light and medium weight nuclei shows a resonance-like structure which is difficult to describe by conventional reaction mechanisms.

The hypothetical πNN resonance d' was proposed as a possible explanation of this peculiar energy dependence in DCX to discrete final states in nuclei. According to this hypothesis the observed behaviour corresponds to the formation of the d' in the course of the DCX process. The parameters of the d' deduced from DCX to final states in nuclei are $m \approx 2.06 \text{ GeV}/c^2$, $\Gamma_{\pi NN} \approx 0.5 \text{ MeV}$ and $I(J^P) = \text{even}(0^-)$.

We measured the total cross section for DCX on ${}^4\text{He}$ for incoming pion kinetic energies between 70 and 130 MeV and momentum spectra of the outgoing negative pions. While at 70 and 130 MeV only small d' contributions are expected, conventional models differ significantly from predictions including the d' mechanism around 90 MeV. There, the d' hypothesis predicts cross sections that exceed conventional calculations by almost one order of magnitude. Also the predicted momentum distributions provide a means of testing the reaction mechanism. With the mass of the hypothetical d' being around 2.06 GeV the maximum kinetic energy of the decay protons is 25 MeV in the centre of mass system of the d' . At such low energies an attractive final state interaction (FSI) between the participating nucleons is effective. Due to this FSI the d' hypothesis predicts a structure for the momentum distributions of the outgoing pions which is significantly peaked towards higher momenta compared to conventional predictions.

Figure 45 shows the results for the total DCX cross section compared to previous data and predictions. Calculations using a sequential single charge exchange model by Gibbs and Rebka (dot-dashed curve) yield only qualitative agreement with the data at energies above 120 MeV and are an order of magnitude smaller than our data at lower energies. A semi-classical model

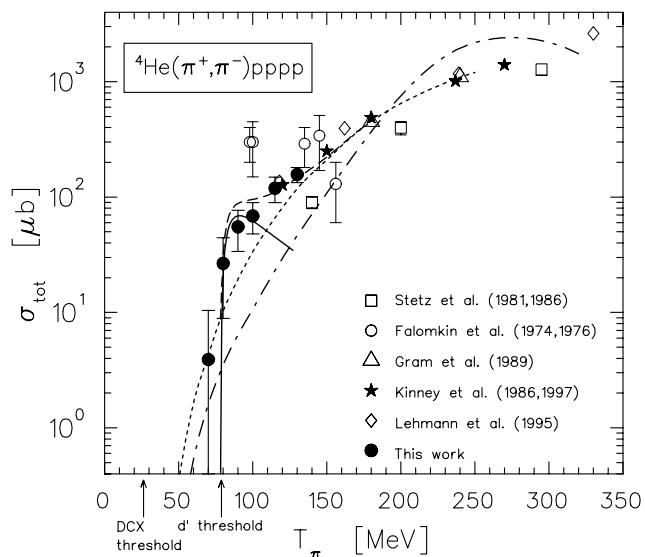


Fig. 45. ${}^4\text{He}(\pi^+, \pi^-)$ total cross sections. The dot-dashed curve shows results from the Gibbs-Rebka model, the dotted curve represents the MC model, the full curve the d' mechanism and the dashed curve the incoherent sum of the MC model and the d' mechanism.

(MC), calculating the DCX as sequential single charge exchange in a Monte Carlo approach, gives a good description of the data at higher energies when normalized at 150 MeV. However, it is a factor of 3 below the data around 90 MeV. A good description of the data is achieved when the result of the MC model is added incoherently to the result of a calculation assuming DCX via the d' mechanism (solid curve and dashed curve). This finding supports the d' hypothesis, although it cannot be construed as definitive proof due to the model dependence in the prediction of the conventional mechanism, which is illustrated by the variation represented by the two conventional calculations shown in Fig. 45. We note that collision damping $d'N \rightarrow 3N$ has not been taken into account in the d' calculations. It would lead to a substantial damping of the predicted d' cross sections.

Experiment 741

Beta-delayed proton decay of ${}^{17}\text{Ne}$ to α -emitting states in ${}^{16}\text{O}$

(J.D. King, Toronto)

The goal of this experiment is to obtain an α -particle spectrum from the break-up of ${}^{16}\text{O}$ following the β -delayed proton decay of ${}^{17}\text{Ne}$, and to use this spectrum to reduce the uncertainty in the ${}^{12}\text{C}(\alpha, \gamma){}^{16}\text{O}$ reaction rate, which is of prime importance in determining the ratio of ${}^{16}\text{O}$ to ${}^{12}\text{C}$ at the end of helium burning in stars. In Expt. 589 we measured the α -particle spectrum from the break-up of ${}^{16}\text{O}$ following the β decay of ${}^{16}\text{N}$. Through simultaneous R - and K -matrix fits to this spectrum, to the ${}^{12}\text{C}(\alpha, \gamma){}^{16}\text{O}$ data

sets, and to $^{12}\text{C}(\alpha, \alpha)$ scattering data, we were able to reduce considerably the uncertainty in the $E1$ component of the astrophysical S -factor for the $^{12}\text{C}(\alpha, \gamma)^{16}\text{O}$ reaction, which is determined primarily by the tail of the sub-threshold 1^- state at 7.117 MeV. Since the 2^+ state at 6.917 MeV is not populated in the decay of ^{16}N , the effect of the tail of this sub-threshold state on the $E2$ component was not determined, and a very large uncertainty in this component, which could be as large as the $E1$, still exists. However, 2^+ states in ^{16}O are populated in the β -delayed proton decay of ^{17}Ne and the feasibility of using this decay is being explored in this experiment.

In last year's Annual Report we described the preliminary results of a study of the three-particle breakup of ^{17}Ne through the isobaric analog state (IAS) of ^{17}F via proton decay to the 9.59 MeV state in ^{16}O , and via α decay to excited states in ^{13}N . A kinematic procedure has been developed to remove background from the triple coincidence spectrum due to coincidences involving a true two-particle coincidence plus a random third particle. This procedure will be described below. Additional runs in November and December of 1998 were carried out using the same strip and PIPS detectors as for the 1997 runs, but with the strip detectors moved back from 6 to 10 cm from the collector foil to reduce the solid angle subtended at the collector foil by the detector pixels. This was expected to reduce the random coincidence background and to provide better identification of proton vs. α events through time of flight. The detector array was surrounded by plastic scintillators covering approximately 25% of 4π so that a quadruple coincidence spectrum could be obtained, again as a method to reduce the random background. These data are now being analysed.

Kinematic procedure

A software procedure has been developed to investigate the kinematics of triple coincidence events on an event-by-event basis. The objective was to discriminate against background by eliminating events which were not kinematically reasonable based on the observed energy and position information.

We define the centre of the collector foil as the origin and the beam axis as the x -axis of the system. A triple coincidence event can be visualized as a simultaneous 3-body decay taking place within the beam spot (8 mm diameter) from which the trajectories of the 3 daughter particles intercept 3 detector elements. Assuming that the particle identities are known, it takes 11 parameters to completely determine the kinematics, viz., the azimuthal and polar angles of the 3 tra-

jectories, the kinetic energies of the particles, and the 2 coordinates on the collector foil which specify the location of the decay vertex. The locations of the detector elements help to constrain the directions of the trajectories, and the three observed energies together with their uncertainties constrain the energies of the particles. With 6 angles and 3 observed energies, each event in the data contains only 9 measured parameters. Therefore, the problem is not well-determined in the sense that we have 2 fewer measured parameters than would be needed to completely constrain the kinematics. Our approach was to minimize a function, S , which would be small for physically reasonable events. We constructed the function S with five components,

$$S = \sum_{i=1}^5 S_i,$$

where

$$\begin{aligned} S_1 &= \sum_{i=p,\alpha,c} \frac{(E_i - e_i)^2}{\sigma_i^2}, \\ S_2 &= A \sum_{j=x,y,z} \left(\sum_{i=p,\alpha,c} p_{ij} \right)^2, \\ S_3 &= B \sum_{i=p,\alpha,c} W(\mathbf{r}_i, R_i, d_B), \\ S_4 &= CW \left(\left(\sum_{i=p,\alpha,c} E_i \right), Q, d_C \right) \\ &\quad + C \sum_{i=p,\alpha,c} W(E_i, 0, d_C), \\ S_5 &= DW(\sqrt{a^2 + b^2}, R_t, d_D). \end{aligned}$$

In S_1 , E_i (e_i) is the fitted (observed) energy of particle i , and σ_i ¹ is the energy resolution for the detection of particle i . This term is simply a χ^2 . In S_2 , p_{ij} is the j^{th} component of the momentum of particle i and A is an arbitrary constant which determines the weight given to momentum conservation in the minimization. This term becomes non-zero when momentum conservation is violated and will be large for events which are not physical. In S_3 , $W(\mathbf{r}_i, R_i, d_B)$ is a Woods-Saxon function of \mathbf{r}_i with radius R_i and surface diffusiveness d_B ; \mathbf{r}_i is a vector representing the distance between the fitted trajectory of particle i and the centre of the detector element in which the particle is observed, R_i is the size of the detector element, and B and d_B are

¹We use 10, 25, and 55 keV for σ_p , σ_α , and σ_c , respectively. σ_p was obtained from the IAS peaks in singles spectra; σ_α was deduced from the observed width of the 2.3 MeV alpha peak from the decay $\text{IAS} \rightarrow 2.37(^{13}\text{N})$; σ_c was deduced from the IAS triple-energy-sum peak assuming that the 3 σ s could be added in quadrature.

constants. S_3 is non-zero when the fitted direction of travel of any of the particles does not intercept the detector element in which that particle is observed. S_4 forces the energies to be positive, and their sum to be less than Q , the total energy available in the beta decay (determined by the mass difference between the ground state of ^{17}Ne and the 3-body final state), and C and d_C are constants. This term forces the energies to remain physical. In S_5 , a and b are the x - and y -coordinates of the location of the decay vertex on the beam spot, R_t is the size of the beam spot and D and d_D are constants. This term becomes large when the decay vertex moves out of the beam spot.

The function S thus depends on 11 variables – the 3 energies and 6 angles of the particles and the 2 coordinates of the decay vertex – and involves 7 arbitrary parameters ($A, B, C, D, d_B, d_C, d_D$). We chose physically reasonable numbers for the diffusiveness parameters (d_B, d_C, d_D) while the values of the four multiplicative constants (A, B, C , and D) are arbitrary.

The geometry of the set-up dictates that triple coincidence events which involve both PIPS detectors are not favoured kinematically since most of the active regions of the detectors lie in one hemisphere. Therefore, we can safely ignore events which involve both PIPS. For those which involve both silicon strip detectors (SSD), there are four possible combinations of particle identities – the proton and alpha can be detected by either one of the two SSD in coincidence with a carbon recoil detected by either of the two PIPS – assuming that carbon ions can only be observed with the PIPS. Furthermore, the SSD at 160° to the PIPS which detects a carbon ion will most likely be hit by an alpha – in fact, this is the reason behind our choice of the geometry, based on results of a Monte Carlo study, and the hit pattern of the alpha particles observed by SSD-L in Fig. 46 supports this assertion. In this sense, two of the combinations are much more probable than the other two.

The function S was minimized with respect to 11 variables for each event in the data set, and for each possible combination of particle identities – twice (four times) for events in which one (both) PIPS was (were) involved². The combination that gave the minimum value of S was retained for each event. The process was repeated whereby we required the trajectory of the carbon recoil to lie on the plane defined by the trajectories of the proton and alpha, thus decreasing the number of fitting variables to 10. The two fitting methods were found to generate very similar results and we have adopted the one with fewer variables to generate the final results. For a subset of the entire data set, the multiplicative parameters (A, B, C, D) were varied

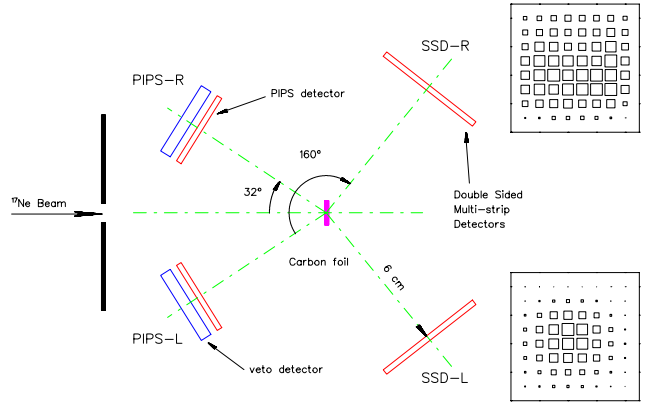


Fig. 46. Set-up for July, 1997 run using double-sided strip detectors for protons and α s and PIPS detectors for ^{16}O and ^{13}N recoils. The hit patterns were obtained with the strip detectors in triple coincidence with PIPS-R, and with a gate set on the IAS triple-energy-sum peak at 3.43 MeV.

over several orders of magnitude and very little dependence on these parameters was found. Ultimately, they were chosen so that the χ^2 term (S_1) was generally dominant. S can therefore be viewed as a quantity like a χ^2 . However, since the problem is not well constrained, S cannot be used as a measure of goodness-of-fit; S should only be treated as a quantity the relative magnitude of which reflects the likelihood that an event is kinematically reasonable – the smaller, the more reasonable.

The triple-energy-sum spectrum before and after the implementation of kinematic constraints is shown in Fig. 47. Requiring that S has a value < 8 reduces the background in the region of the IAS peak considerably. The alpha spectrum obtained by putting a gate on the IAS peak of Fig. 47 is shown in Fig. 48(a), while the α spectrum from the August, 1996 run is shown in Fig. 48(b).

Present status of the experiment

We have developed software procedures to handle a large number of detector elements and to carry out the energy calibration automatically. We have also developed a kinematic procedure to handle background events more systematically. A final alpha spectrum has been generated and compared with the one obtained from the August, 1996 data. We believe that the use of the kinematic procedure just described makes the recent spectrum superior to the previous one. In the previous analysis of the August, 1996 data, we extracted the relative branching ratio between two 3-body decay modes of the IAS, viz., via the 9.59 MeV state in ^{16}O and the first excited state in ^{13}N ; we plan to extend this work using the more recent alpha spectrum and include the mode via the second/third excited state in ^{13}N .

²Events in which both PIPS are involved amount to about 4% of the entire data set.

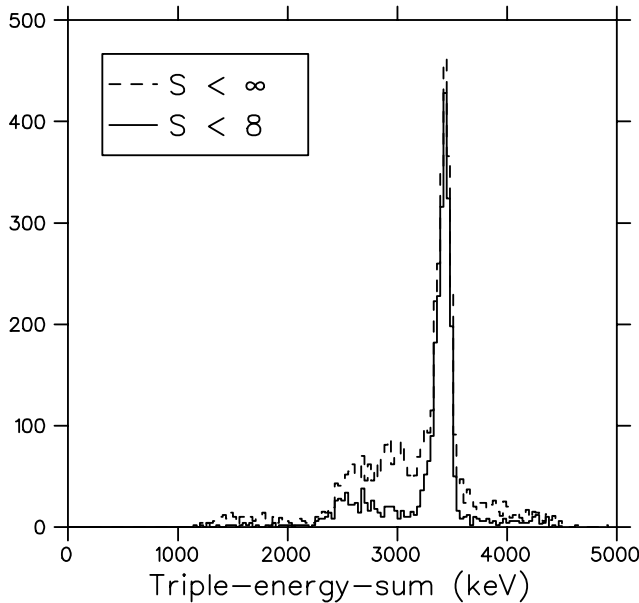


Fig. 47. Triple-energy-sum spectrum before and after implementation of kinematic constraints.

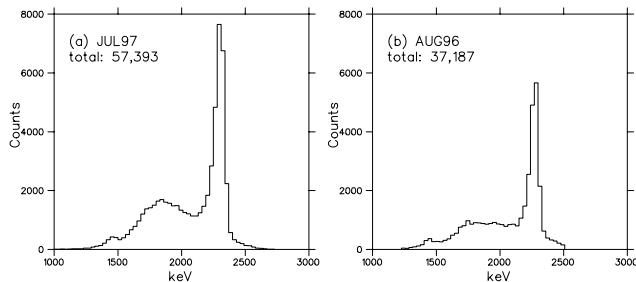


Fig. 48. Final alpha spectra: (a) data from the July, 1997 run; (b) data from the August, 1996 run.

The fact that the false triple coincidences could not be completely removed can be attributed to the fact that the large solid angle covered by the detector elements resulted in loose constraints in the kinematic procedure. In the November/December, 1998 runs, we improved this situation by increasing the distance between the detectors and the collector foil. This increase in distance also allowed us to obtain better time-of-flight information for the particles. We anticipate that the smaller solid angle coverage of the detector elements, together with the requirement of quadruple coincidence with a β -particle, should remove most of the false triple coincidences. On-line analysis showed a considerable reduction in the background; off-line analysis is now under way.

Experiment 742

Scattering of muonic hydrogen isotopes

(V.M. Bystritsky, JINR; R. Jacot-Guillarmod, F. Mulhauser, Fribourg)

Our measurement studies the energy dependence of the scattering cross sections of muonic hydrogen atoms on hydrogen molecules for collisions in the energy range 0.1 – 45 eV. A time-of-flight (TOF) method was used to measure the scattering cross section as a function of the muonic atom beam energy and shows clearly the Ramsauer-Townsend effect. The experimental results are compared with theoretical calculations by using Monte Carlo simulations. The molecular $pd\mu$ formation creates background processes. We have measured the formation rates as well as the fusion rates in solid hydrogen by detecting the subsequent nuclear fusion processes.

Ramsauer-Townsend effect

μ^- are stopped in an upstream (US) layer (target and procedures have been described in [Knowles *et al.*, Nucl. Instrum. Methods **A368**, 604 (1996); Fujiwara *et al.*, Nucl. Instrum. Methods **A395**, 159 (1997)]) made of H_2 with a small admixture of D_2 or T_2 , form mainly μp atoms, and then transfer with 70–75% efficiency to form μd (μt) atoms. At formation, the muonic deuterium (tritium) atoms have a kinetic energy of about 45 eV which they subsequently lose via elastic collisions, mainly with protium, until they reach 20–30 eV, when the scattering cross section falls below 10^{-20} cm^2 . The mean distance between collisions becomes very large, especially at 4–20 eV, and the hydrogen layer becomes effectively transparent to the muonic atoms. The muonic atoms are then emitted from the solid hydrogen into the adjacent vacuum and may reach the downstream layer of neon covered with protium of variable thickness.

The measurements were made for deuterium and tritium during two different run periods. The upstream (US) layer is the source of muonic deuterium or tritium atoms. They travel toward the downstream (DS) gold foil, located at a distance of 17.9 mm, which itself supports the protium and neon layers. The time of flight (also used for other measurements with the same TRIUMF target [Marshall *et al.*, Hyp. Int. (in press); Fujiwara *et al.*, Hyp. Int. (in press)]) of the μd (μt) atoms delays their DS arrival time as a function of their incident energy, resulting in delayed neon x-rays after muon transfer to neon. The emitting layer is the same for a series of DS H_2 thicknesses and thus the energy distribution of the muonic atom incident beam does not change. The comparison between measurements with and without DS protium layers shows the effect of μd (μt) scattering on H_2 , with specific sensitivity to the Ramsauer-Townsend effect.

Experimental time spectra of neon x-rays for each measurement have been obtained. Figures 49 a) and b) show the time spectra for μd and μt scattering with 300 and 350 torr $\cdot l$, respectively, of H_2 on the DS neon layer. One clearly observes delayed neon x-rays due to muonic atoms emitted from the US layer eventually reaching the DS neon. The time corresponding to the maximum delayed x-ray intensity is different for μd and μt , as expected from the theoretical calculations of the Ramsauer-Townsend minima. Therefore, the TOF measurement gives time spectra in which the transfer intensity maximum is located at a later time for μd than for μt .

A Monte Carlo code (FOW) written by Woźniak *et al.* [Hyp. Int. **101/102**, 573 (1996)] is used to simulate all processes occurring after a μ^- stop in the different layers. The FOW simulations agree very well with the experimental data for μd scattering, while a deviation of the Ramsauer-Townsend maximum is visible in the μt case. By comparing Figs. 49 b) and d), one sees, for times greater than 1.5 μs , a strong reduction of neon x-rays, due to low energy μt stopped in the DS H_2 layer and thus not reaching the neon layer.

A χ^2 analysis has been performed to fit the FOW input parameters to the experimental data. The theoretical cross sections are varied in two different ways. Position of the zero of the S -wave amplitude and the P -wave cross section at the Ramsauer-Townsend minimum are determined by scaling the theoretical cross sections with an energy shift, ΔE , and a depth factor, d . Preliminary results have been obtained and are given in Table VI.

Table VI. Preliminary results for the Ramsauer-Townsend scattering cross section in terms of energy shift, ΔE , and depth factor, d .

Run	ΔE (eV)	d
Deuterium	0.00 ± 0.05	-0.03 ± 0.05
Tritium	-0.40 ± 0.05	-0.05 ± 0.05

The agreement between experimental results and the theoretical cross section is excellent for $\mu d + H_2$, whereas the theoretical energy of the Ramsauer-Townsend minimum is about 5% higher than the experimental results in $\mu t + H_2$. However, our last result is in disagreement with a measurement of μt emitted into vacuum [Fujiwara *et al.*, Hyp. Int. (in press)]. The discrepancy between the two preliminary results, obtained by the same collaboration and apparatus, may indicate systematic effects which have not yet been investigated.

New effects in low energy scattering of μp atoms

In our experiment we have observed an emission of the low energy μp atoms from the solid hydrogen

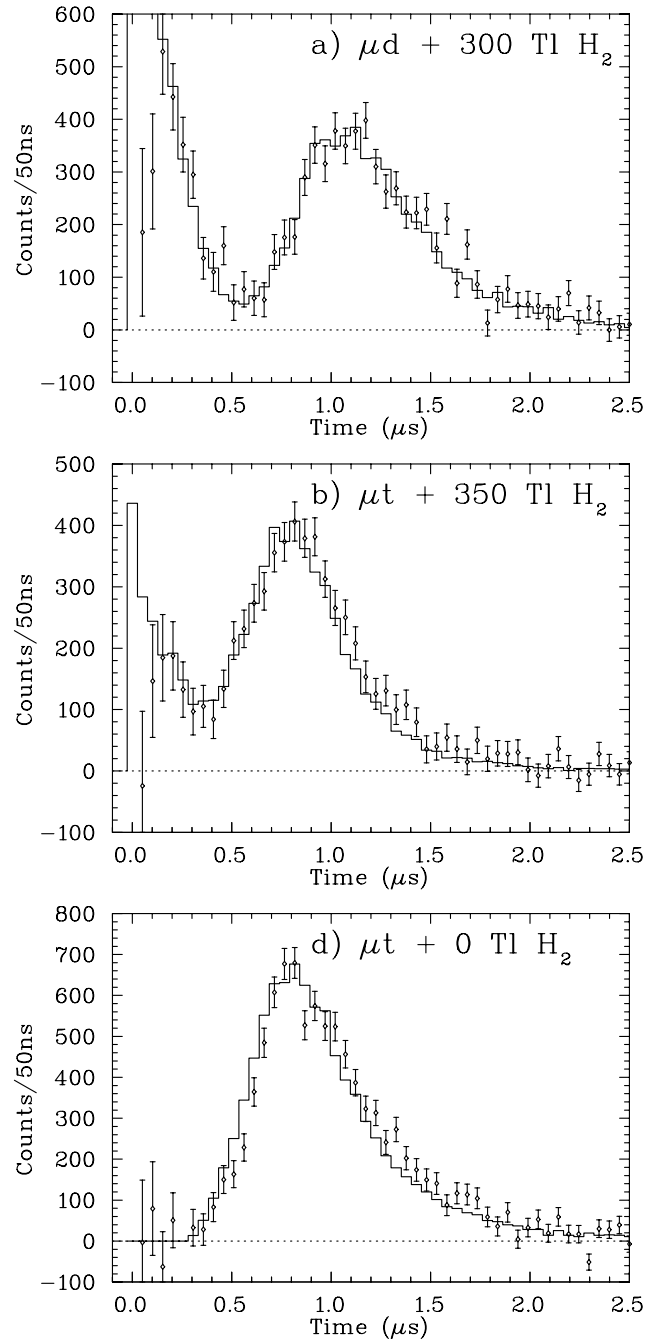


Fig. 49. Comparison between FOW simulation (solid line) and experimental (points with error bars) time spectra of neon x-rays obtained for a) μd incident on 300 torr $\cdot l$ of H_2 on the DS foil, for b) μt incident on 350 torr $\cdot l$ of H_2 on the DS foil, and d) without H_2 on the DS foil.

layer into the adjacent vacuum. The emission was much higher than expected based on calculations which ignored the solid structure of the hydrogen.

The most accurate calculations of the elastic and inelastic scattering cross sections of the reaction $p\mu(F) + p \rightarrow p\mu(F') + p$ (where F is a total spin of μ -atom) are numerically

performed by solving the multichannel scattering problem [Bracci *et al.*, Muon Catal. Fusion **4**, 247 (1989)]. The modifications to nuclear scattering phase shifts and cross sections for the case of scattering from hydrogen molecules are calculated mainly by Adamczak *et al.* [Z. Phys. **D4**, 153 (1986); Adamczak, Muon Catal. Fusion **4**, 31 (1989); *ibid.*, Hyp. Int. **82**, 91 (1993)]. Such cross sections are called “gas” cross sections. Total and differential cross sections for scattering from solid hydrogen (so-called “solid” cross sections) have also been recently calculated by Adamczak [Hyp. Int. **101/102**, 113 (1996); *ibid.*, Hyp. Int. (in press)].

The measured TOF spectrum is shown in Fig. 50 together with the Monte Carlo simulations performed with two sets of scattering cross sections: “gas” and “solid”. The events occurring a short time (before ~ 600 ns) are due to μp atoms formed in the DS hydrogen and diffused to neon. The peak in TOF spectrum corresponds to delayed μd atoms which travel the distance between foils and are not stopped in DS hydrogen due to the Ramsauer-Townsend effect. As one can see from this comparison both types of cross sections equally well describe the Ramsauer-Townsend part of the spectrum. It is a consequence of the fact that solid state effects are negligible for the energies of μd which correspond to the Ramsauer-Townsend minimum in cross sections (~ 7 eV). On the contrary there is a big difference between spectra in the μp diffusion part where an agreement with the experiment is obtained only for “solid” cross sections. The solid state effects in the scattering of low energy μp atoms strongly enhance (factor ~ 3) the emission of μp .

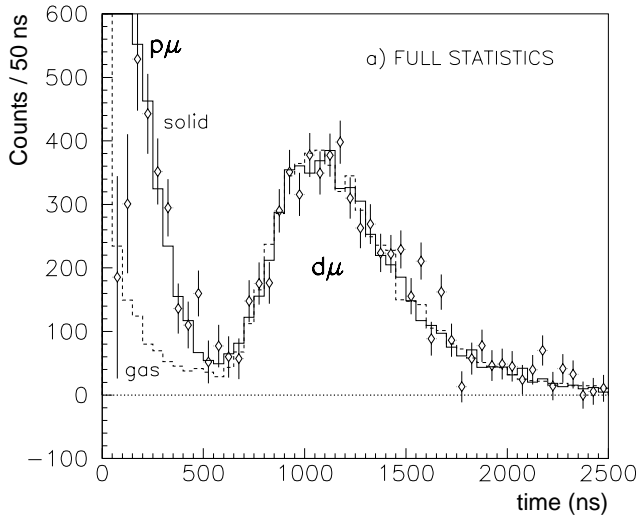


Fig. 50. Experimental (points with error bars) and Monte Carlo (lines) TOF spectra obtained for a standard measurement. Monte Carlo simulations were performed using “solid” scattering cross sections (solid line) and “gas” cross sections (dashed line).

The main contributions to the low energy scattering of μ -atoms in solid hydrogen come from the coherent processes: elastic Bragg scattering and phonon scattering. The first process is possible only at collision energies greater than the Bragg cut-off limit which is 1.9 MeV in the case of μp scattering in protium. The incoherent elastic cross section is negligible there since the amplitude of $p\mu(F=0) + \text{H}_2$ scattering does not depend on the total spin of this system. For very small energies (less than 10^{-4} eV) a phonon incoherent scattering becomes important. The details of the method used in the calculations of scattering cross sections for solid hydrogen can be found in [Adamczak, Hyp. Int. (in press)].

Figure 51 shows an example of calculated total cross sections for the scattering of μp in the lower spin state ($F=0$) from solid polycrystalline hydrogen. At μp energies just above the Bragg cut-off the total cross section is much higher than the doubled nuclear cross section, but is dominated by elastic scattering on the lattice. Such scattering does not practically cause any loss of the μp energy, because of the very large mass of the recoiling crystal. As a result, the μ -atoms undergo many collisions in the solid target without efficient deceleration, since the probability of a phonon creation, which is the process responsible for the energy loss, is very small in this energy region. At energies above ~ 0.1 eV the total cross section is dominated by the inelastic processes (multi-phonon scattering and excitations of H_2 molecules) and can be approached by the doubled nuclear cross section.

The presence of Bragg cut-off gives the most interesting effect. Since below the energy 1.9 MeV the

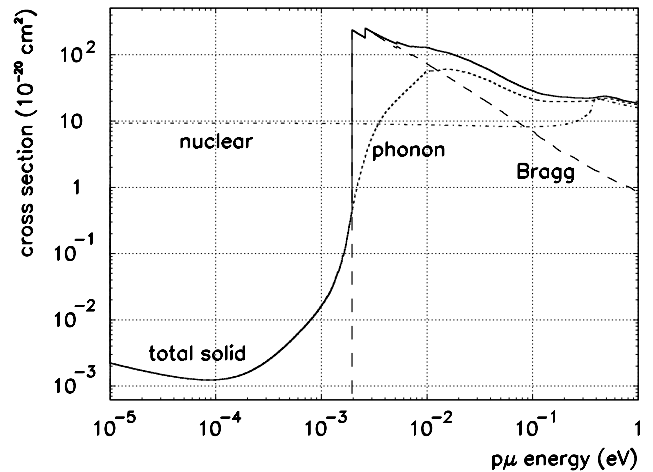


Fig. 51. Total cross section (solid line) for $p\mu(F=0)$ scattering in solid polycrystalline (*fcc*) hydrogen (for orthopara statistical mixture). Dashed line represents the coherent elastic Bragg scattering, dotted line the inelastic phonon scattering. The doubled nuclear cross section of the $p\mu(F=0) + p$ process is also shown for comparison.

elastic coherent scattering on the hydrogen lattice disappears, the phonon processes determine here the magnitude of the total cross section. In effect the total cross section falls by several orders of magnitude, and the target becomes almost transparent and the emission of ultra cold μp takes place. This phenomenon (which is similar to the previously described Ramsauer-Townsend effect but for completely different physical reasons) is responsible for the enhancement of the μp emission seen in Fig. 50.

In order to investigate it more precisely with higher statistics, a separate measurement with only one layer of pure solid hydrogen on the upstream foil as μp emission target has been performed. A 1000 torr $\cdot l$ (H_2) layer has been covered with a thin (10–20 torr $\cdot l$) neon layer. The time spectrum of Ne x-rays (see Fig. 52) describes the diffusion of μp atoms in hydrogen from the moment of muon stop to the emission moment. The simulated MC spectrum presented also in the figure describes well the experimental data when a set of “solid” cross sections is used (solid lines). The calculation with the “gas” cross sections (dashed lines) gives the suppressed yield although the slopes representing diffusion time are not dramatically different. Diffusion times obtained from the one-exponential fit of the data ($60 < t < 900$ ns) are presented in Table VII.

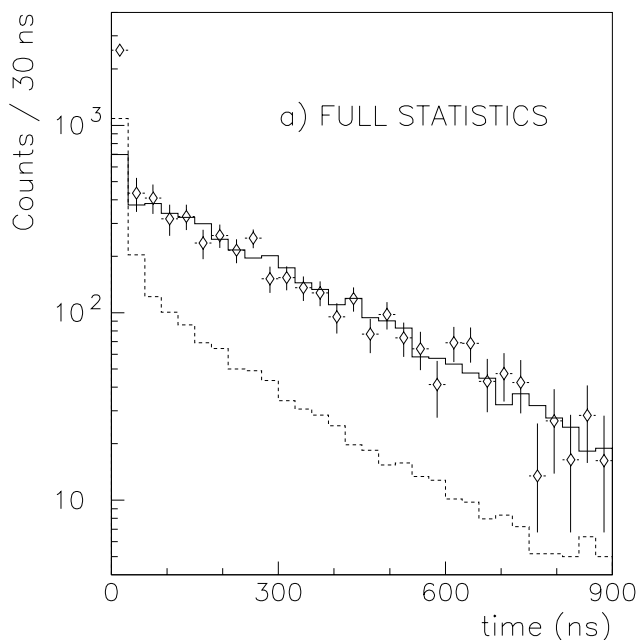


Fig. 52. Experimental (points with error bars) and simulated (lines) time spectrum of μp emitted from 1000 torr $\cdot l$ H_2 layer. Solid line: calculation with the “solid” cross sections used, dashed line: calculation result for the “gas” cross sections.

Table VII. Mean diffusion times (ns) of μp atoms emitted from 1000 torr $\cdot l$ solid hydrogen layer.

Experiment	274 (17)
MC, “solid” cross sections	278 (20)
MC, “gas” cross sections	207 (11)

Study of $pd\mu$ fusion rates

Muon-catalyzed fusion was first observed in the $pd\mu$ system, and remains a good test of our understanding of the underlying molecular and nuclear processes. In contrast to the $dd\mu$ and $dt\mu$ systems, no resonant behaviour is expected, which considerably simplifies the dynamics. We will discuss data taken with solid H–D mixtures of 0.05%, 2%, 15%, and 75% D_2 . In these measurements we observed simultaneously muons from $pd\mu \rightarrow \mu + {}^3He$ and γ 's from $pd\mu \rightarrow \mu^3He + \gamma$. The systematics of the fusion rates are strongly dependent on the total nuclear spin $S = S_p + S_d$ of the muonic molecular system. This in turn is dependent on the μd hyperfine state carried through the molecular formation process. The μd spin flip reaction, induced by $\mu d + d$ collisions, alters the ratio of intensities of these two observables in a non-trivial way depending on the deuterium concentration in a dense mixture [Gershtein, Zh. Eksp. Teor. Fiz. **40**, 698 (1961) (Sov. Phys. JETP **13**, 488 (1961))]; this has become known as the Wolfenstein-Gershtein effect.

Our analysis uses a simulation code to describe the various physics processes. Included are the relevant $pd\mu$ and $dd\mu$ fusion and molecular formation rates, initial atomic capture probabilities, and μp emission probability into vacuum. Fusion rates for the $pd(S = \frac{3}{2}\mu)$ and $pd(S = \frac{1}{2}\mu)$ states were obtained from fits to the timing spectra.

Preliminary conversion muon intensities are shown in Fig. 53 together with simulation results and other measurements. A similar picture for the fusion γ is shown in Fig. 54. There is an additional uncertainty in the normalization of the intensities of 15% coming mainly from the estimated fraction of muons which stop in the target.

In Figs. 53 and 54 can be seen the dependence of the different yields with deuterium concentration. The uncertainties on the yields include a 3% systematic uncertainty which was determined from the reproducibility of the yield as measured on a series of nominally 0.4 mm protium targets. These variations set a limit on possible small differences in the target thickness and beam tune.

The absolute yield of conversion μ depends linearly on $\lambda_{f,\mu}^{1/2}$ so we can determine it directly from the conversion μ yield data. The leading systematic error is 15% in the normalization, arising from uncertainties in the stopping distribution.

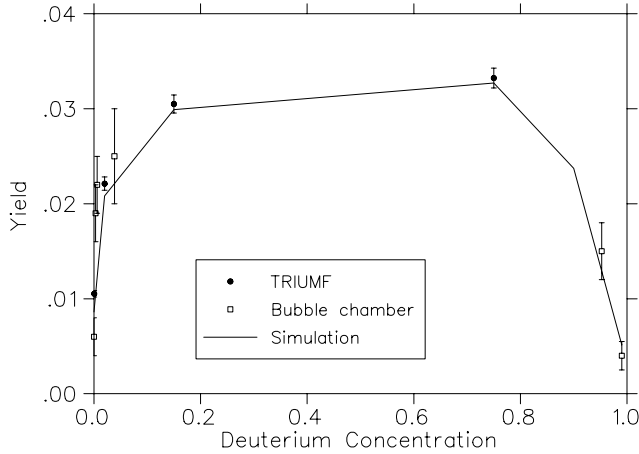


Fig. 53. Conversion μ yields. The TRIUMF data have an additional overall normalization error of 15%.

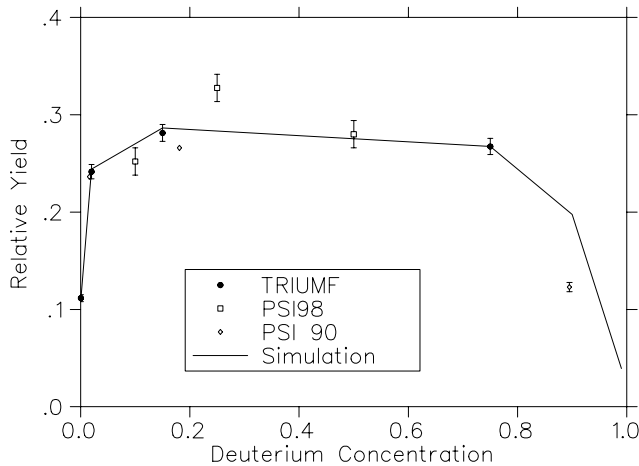


Fig. 54. Muon catalyzed fusion γ relative yields for solid and liquid hydrogen data from Petitjean *et al.* [Muon Catal. Fusion **5/6**, 199 (1990/91)] (PSI90) and Lauss *et al.* [Hyp. Int. (in press)] (PSI98).

Values used in the simulation are given in Table VIII, where they are compared to previous work. The fits to the TRIUMF data have a χ^2 of 5 or 6 degrees of freedom using the rates in Table VIII with only the normalizations allowed to vary. This is a sensitive confirmation of the Wolfenstein-Gershtein effect.

The S -wave astrophysical factor for $p+d \rightarrow {}^3\text{He}+\gamma$ can be obtained from our measurements. In the $pd\mu$ molecule the effective reaction energy is the muon binding energy of 8 keV, which is approximately the same as the Gamow peak in stellar interiors. This relationship has been calculated by Friar using a Faddeev calculation for the $pd\mu$ molecule [Friar *et al.*, Phys. Rev. Lett. **66**, 1827 (1991)]. Using those values, we obtain $S = 0.128 \pm 0.008$ eV barns. This is to be compared with measurements of pd scattering: $S = 0.109 \pm 0.010$ eV barns [Schmidt *et al.*, Phys. Rev. Lett. **76**, 3088 (1996)] and $S = 0.12 \pm .03$ eV barns [Griffiths *et al.*, Can. J. Phys. **41**, 734 (1963)].

Table VIII. $pd\mu$ process rates (in 10^6s^{-1}) used in the simulation: preliminary.

Parameter	This measurement 10^6s^{-1}	Previous measurement 10^6s^{-1}	Ref.
$\lambda_{pd\mu}$	5.46 ± 0.1	5.60 ± 0.2	[1]
$\lambda_f^{1/2}$	0.426 ± 0.014	0.41 ± 0.02	[1]
$\lambda_{f,\gamma}^{3/2}$	0.14 ± 0.02	0.11 ± 0.01	[1]
$\lambda_{f,\mu}^{1/2}$	0.050 ± 0.005	0.056 ± 0.006	[2]
Rates fixed from $dd\mu$ and other measurements			
$\lambda_{pp\mu}$	3.21		[3]
$\lambda_{p \rightarrow d}$	17500 ± 1400		[4]
$\lambda_{\mu d \frac{3}{2} \rightarrow \frac{1}{2}}$	34.0		[5]
$\lambda_{\mu d \frac{3}{2} \rightarrow dd\mu}$	3.21		[5]
$\lambda_{\mu d \frac{1}{2} \rightarrow dd\mu}$	0.052		[5]

- [1] Petitjean *et al.*, Muon Catal. Fusion **5/6**, 199 (1990/91).
 [2] Bogdanova, Muon Catal. Fusion **3**, 359 (1988).
 [3] Mulhauser *et al.*, Phys. Rev. **A53**, 3069 (1996).
 [4] Jacot-Guillarmod *et al.*, Hyp. Int. **101/102**, 239 (1996).
 [5] Knowles *et al.*, Phys. Rev. **A56**, 1970 (1997);
 erratum in Phys. Rev. **A57**, 3136 (1998).

Experiment 778

$\pi^\pm p$ differential cross sections in the Coulomb-nuclear interference region

(*G.R. Smith, TRIUMF*)

The primary goals of the CHAOS physics program to date have been to test predictions and measure parameters of chiral perturbation theory. To this end, we have performed measurements in the $\pi^\pm p$ sector of pion induced pion production (Expt. 624) and elastic analyzing powers (Expt. 560). Experiment 778 deals with the next stage of this program, namely the measurement of $\pi^\pm p$ absolute differential cross sections in the very forward angle region where Coulomb scattering interferes destructively (constructively) with $\pi^\pm p$ ($\pi^- p$) hadronic scattering amplitudes.

The experimental goals of the proposed measurements are to provide absolute differential cross sections to a precision of $\leq 5\%$ for both $\pi^\pm p$ elastic scattering at angles greater than 5° , for pion bombarding energies between 20 and 70 MeV.

The physics goals are to use these data to provide information missing in the current partial wave analyses on the real part of the isospin-even forward scattering amplitude. The real part of the isospin even amplitude D^+ at $t=0$ will be measured in this experiment

to a precision of a few percent. This will greatly improve the determination of πN scattering amplitudes, and as a result would improve the determination of the πN coupling constant and πN scattering lengths, in addition to the $\pi N \Sigma$ term, all observables of crucial importance. In addition, the proposed measurements are important in the context of understanding isospin breaking due to the u-d quark mass difference.

In the Expt. 778 proposal (see <http://www.triumf.ca/chaos/cni.ps>) we showed, in addition to providing $\text{Re}(D^+)$ at $t=0$ for partial wave analysis (PWA) improvements, how a systematic set of measurements in the Coulomb-nuclear interference (CNI) region can be used to measure the isospin even, S -wave scattering length a_{0+}^+ and the isospin even P -wave scattering length a_{1+}^+ *directly*. This new, direct information can then be used for an independent determination of the $\pi N \Sigma$ term. The Σ term is of fundamental importance, it is a direct measure of chiral symmetry breaking, and can be used to provide a measure of the strange sea quark content of the proton. The CNI measurements proposed here can be used to measure $\Sigma_{\pi N}$ in a manner less dependent on the results of PWA.

Early in 1998 the CHAOS spectrometer was moved for the first time from the M11 pion channel to the M13 low energy pion channel in preparation for Expt. 778. A large auxiliary access platform was installed adjacent to the spectrometer as well to facilitate access to the top of the spectrometer in its new location. Several changes to the spectrometer itself were also made. An 18° wide section of the outermost drift chamber was removed where the beam enters the spectrometer to reduce multiple scattering of the incident beam and thereby control the size of the focus at the target. In addition, the in-beam trigger counter, which counts the beam and provides the primary trigger for the readout electronics, was replaced with a thinner, 1 mm thick counter and was moved closer to the target, just outside the WC3 radius, for the same reason. The counter was also redesigned to accommodate a beam pipe extension which brought pions in vacuum all the way into the WC4 radius. To improve the cathode and resistive wire pulse heights which are used in CHAOS for vertical tracking, all 2000 FASTBUS ADC channels were converted to 50Ω quasi-differential input mode and a more efficient pedestal subtraction scheme was implemented. All 2400 channels of our 2735 amplifier/discriminator cards were altered with a low-noise modification. The data acquisition computer was upgraded from a DEC station to a Pentium PC running LINUX, writing directly to disk, and logging to 8 mm tape in the background. All the acquisition software (MIDAS), control, test, and initialization software which ran on the DEC station was ported to

LINUX, as was the complete CHAOS analysis package.

One of the crucial pieces of new equipment required for this experiment is a π/μ particle identification stack, capable of operating in conjunction with CHAOS in the angular region $5^\circ < \theta < 30^\circ$ with equal efficiency for both beam polarities. The stack is a joint venture of our collaborators from INFN Trieste and the University of Tübingen. In the fall of 1997 a prototype stack was tested and was described briefly in last year's Annual Report. Based on the experience with the prototype, the large final version was fabricated and assembled early in 1998. It was installed in M13 with CHAOS in the configuration required for Expt. 778 and the readout electronics were set up prior to the start of the spring, 1998 Expt. 778 beam time.

The other special piece of equipment required for Expt. 778 is a planar cryogenic LH_2 target, which was supposed to be provided by the TRIUMF Target group by the start of the spring beam time (April 22). Unfortunately, the Cryogenic Target group has been winnowed to a single person, and the administration was faced with a variety of competing demands for the remaining resource. Work on the CHAOS target did not begin until mid-February, during a period when competition in the Machine Shop was stiff. As a result, the target was not ready for initial testing until nearly the end of the summer beam period. These tests showed that the target did not have sufficient cooling power and that a new, larger refrigerator was required. At that point a replacement refrigerator was ordered, the target specialist was again assigned to other targets, and the scheduled fall beam time for this experiment was cancelled. Work began anew on the CHAOS LH_2 target only in late November, in preparation for beam time starting March 22, 1999.

Without the cryogenic target required for Expt. 778, many of the goals of the spring/summer beam time had to be dropped. However, progress was achieved in a number of areas. Due to its size, CHAOS had to be positioned downstream of the canonical M13 focus. Therefore considerable effort was devoted to tuning the M13 beam to achieve an optimum focus at the centre of the spectrometer. Beam properties including rates, spot size, and composition were measured over the entire momentum range envisioned for Expt. 778.

The π/μ stack was calibrated and trained in an exhaustive series of measurements in which the beam was swept across the stack in 8 positions, for 8 momenta, for both channel polarities, and for several triggers selecting different particle species. This information was later used to train a neural network which now provides particle identification based on all the information provided by the stack.

After the move to M13, noise problems in the wire chambers were severe. A considerable effort was directed towards noise reduction. To make a long (and excruciating) story short, eventually the noise problems were completely eliminated.

Data were collected for $\pi/\mu/e$ scattering on a graphite target at several incident momenta, with trigger conditions close to what we expect for the real experiment. This permitted some progress to be made on tuning the trigger, improving rate estimates, etc. These data were used off-line during the second half of 1998 to develop new algorithms required for Expt. 778, including 3D scattering angle and event reconstruction, new techniques for handling vertex and scattering angle reconstruction in the extreme forward angle regime where the tracks used for these calculations are nearly parallel to the incident beam, and development of more sophisticated decay recognition algorithms for pions which decay inside the spectrometer. We also used the unexpected time out of the counting room to publish some of our earlier work: nine CHAOS papers were accepted for publication in calendar year 1998.

To summarize, despite bitter disappointments in 1998, we stand even more prepared than we were a year ago to begin Expt. 778. With target modifications scheduled for completion in February, 1999 should be a very productive year for this experiment.

Experiment 781

Investigations of the $\pi\pi$ invariant mass distributions of nuclear ($\pi^+, \pi^-\pi^+$) reactions with the CHAOS detector

(M. Sevier, Melbourne)

Experiment 781 is a continuation of CHAOS Expt. 653. In this experiment we measured 4-fold differential cross sections at incident pion energy 280 MeV for the reactions:

${}^2\text{H}(\pi^+, \pi^+\pi^-)X$ and ${}^2\text{H}(\pi^+, \pi^+\pi^+)X$,
 ${}^{12}\text{C}(\pi^+, \pi^+\pi^-)X$ and ${}^{12}\text{C}(\pi^+, \pi^+\pi^+)X$,
 ${}^{40}\text{Ca}(\pi^+, \pi^+\pi^-)X$ and ${}^{40}\text{Ca}(\pi^+, \pi^+\pi^+)X$, and
 ${}^{208}\text{Pb}(\pi^+, \pi^+\pi^-)X$ and ${}^{208}\text{Pb}(\pi^+, \pi^+\pi^+)X$.

We found a marked enhancement just above threshold for the isospin 0 channel $\pi^+\pi^-$ on carbon, calcium and lead compared to deuterium. No such enhancement was present in the $\pi^+\pi^+$ isospin 2 channel for the reaction on any nucleus.

We do not understand the origin of this enhancement. It could be due to:

1. An enhancement of the one pion exchange diagram in a nuclear medium;
2. The existence of a new 2 nucleon reaction mechanism for pion induced pion production;

3. A final state interaction between the outgoing pions due to a greatly increased attraction between the $\pi^+\pi^-$ within the nuclear medium.

Since the interaction between pions is governed by the properties of the QCD vacuum state, explanations (1) and (3) may imply that QCD has a vastly different vacuum structure within the nuclear medium. Explanation (2) would require some interesting new reaction dynamics.

The 1996 summer EEC committee awarded this experiment 20 shifts of high intensity running at medium priority to investigate the energy dependence of the effect. We completed the data-taking phase of the experiment in August, 1997. We ran on a CD_2 target at 280 MeV and on a ${}^{45}\text{Sc}$ target at incident π^+ energies of 320, 300, 280, 260 and 240 MeV.

Figure 55 shows very preliminary histograms

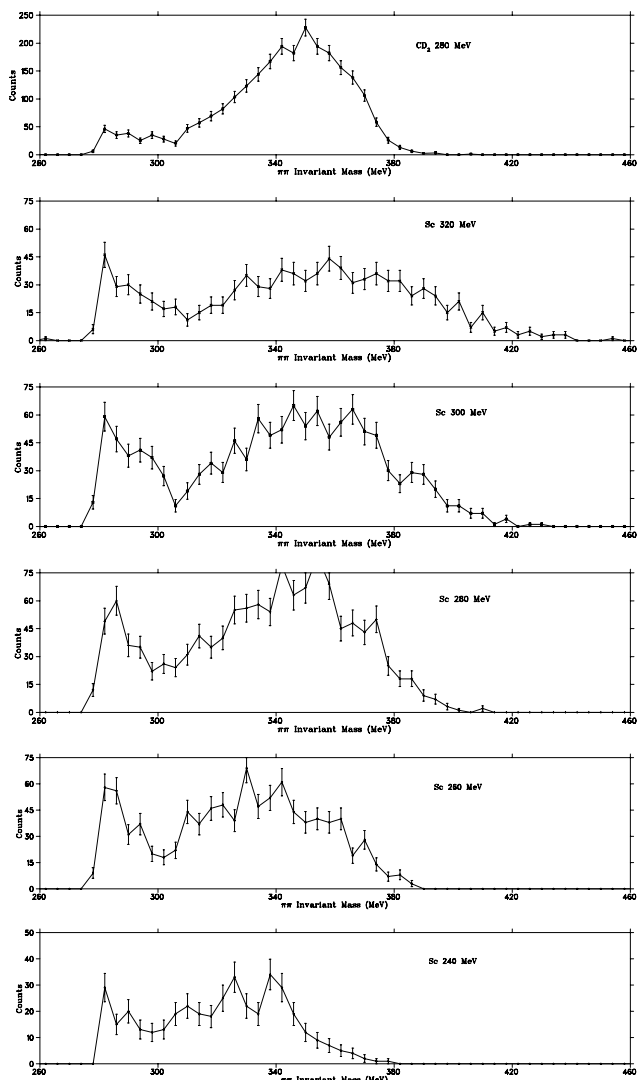


Fig. 55. Preliminary histograms of the $\pi-\pi$ invariant mass distributions.

of the invariant mass distributions from the $^{45}\text{Sc}(\pi^+, \pi^+\pi^-)X$ and $\text{CD}_2(\pi^+, \pi^+\pi^-)X$ reactions at energies of 320, 300, 280, 260 and 240 MeV.

It is clear that the region of the invariant mass distributions below 300 MeV provides far less of the yield from the CD_2 target than the ^{45}Sc target. Moreover the enhancement in yield below 300 MeV is present at all energies.

All the data (including the 240 MeV) have now been skimmed and the calibrations needed for accurate particle identification have been completed.

Unfortunately progress on Expt. 781 has been slower than anticipated because of other demands on our man-power. However, it is the top priority for the Melbourne group in 1999. We hope to complete the analysis this year.

Experiment 785

Pion double charge exchange on ^3He with CHAOS

(R. Tacik, TRIUMF/Regina)

This experiment was run in M11 in the summer of 1997. It involved the measurement of both the inclusive $^3\text{He}(\pi^-, \pi^+)$ and semi-exclusive $^3\text{He}(\pi^-, \pi^+n)$ double charge exchange (DCX) reaction channels, at low incident pion energies. It is complementary to earlier experiments 719 and 725, which are currently being analyzed by the CHAOS collaboration.

One particularly novel feature of Expt. 785 was that it involved the simultaneous operation of CHAOS and an external time-of-flight neutron detector array. The hardware coincidence between the neutron array and CHAOS was made at the CHAOS second level trigger stage. Calibration data for the neutron array was obtained using charged particles from the incident and scattered beams, cosmic rays, and events from the $^3\text{He}(\pi^-, dn)$ reaction, where the deuteron was detected in CHAOS. Experiment 785 employed the same basic Regina/TRIUMF liquid helium target as had been previously used for Expt. 725, but modified for L^3He instead of L^4He .

The general aim of Expt. 785 was to obtain high quality DCX data for ^3He with which to confront all models of the DCX process. No other measurements have been performed below $T_\pi = 120$ MeV. A more specific aim of Expt. 785 was to search for the existence of a narrow resonance in the πNN subsystem, called the d' . The effect of the d' has been proposed as the source of the otherwise unexplained behaviour of the total DCX cross sections near $T_\pi = 50$ MeV, as measured on virtually all heavier nuclear targets which have been studied. Use of the helium isotopes as targets provides the best potential for separating the influences of nuclear structure and the underlying DCX reaction mechanism.

Most of the Expt. 785 running time was spent on accumulating statistics in the neutron time-of-flight spectra for the semi-exclusive $^3\text{He}(\pi^-, \pi^+n)$ reaction. The analysis of this part of the experiment constitutes the Ph.D. thesis project of Mr. G. Tagliente from UBC, and is still ongoing. Measurements were taken at $T_\pi = 65$ and 75 MeV, since the total DCX cross section is larger at the higher energy, and the signal from a d' was predicted to be larger at the lower energy. Within the d' model, the reaction proceeds via the two-step process: $\pi^- ^3\text{He} \rightarrow d'n \rightarrow (\pi^+nn)n$. The detection of the π^+ in CHAOS serves as the signature of DCX. Because of the two-body intermediate state, the existence of the d' should manifest itself as a narrow peak in the neutron energy spectrum measured at a particular angle, above a combinatorial background arising from the detection of one of the neutrons from d' decay, rather than the one which recoiled against it in the intermediate state. Model calculations predict a smooth energy dependence for this background. The same holds true for neutrons produced via conventional mechanisms. There was a large experimental background associated with electrons in the beam which must still be dealt with properly. However, preliminary results do not show a sharp peak in the measured neutron energy distributions. Detailed comparisons with model simulations must still be performed in order to set an upper limit on any possible d' contribution.

A relatively smaller part of the Expt. 785 running time was spent on the inclusive $^3\text{He}(\pi^-, \pi^+)$ reaction. Measurements were taken at several incident pion energies between 65 and 120 MeV. The analysis of this part of the experiment formed part of the Ph.D. thesis project of Mr. J. Graeter from the University of Tübingen, and is almost complete.

Figure 56 shows the preliminary total cross sections for the $^3\text{He}(\pi^-, \pi^+)$ reaction measured in Expt. 785. The dotted curve in Fig. 56 represents the results of a Monte Carlo calculation which models the reaction with the conventional assumption that it proceeds via two sequential single charge exchange scatterings. The curve has been normalized to the existing data point at 120 MeV [Yuly *et al.*, Phys. Rev. **C55**, 1848 (1997)]. It is evident that the dotted curve provides a good description of the observed energy dependence. The solid line in Fig. 56 represents a prediction [Clement *et al.*, Phys. Lett. **B337**, 43 (1194)] for the total cross section based on the assumption that the reaction proceeds entirely via d' formation. Clearly, the solid line overestimates the data. In an attempt to explain this discrepancy, it has been pointed out by Schepkin that the solid line calculation does not account for the fact that the d' , once formed, can interact via the $d'N \rightarrow NNN$ reaction.

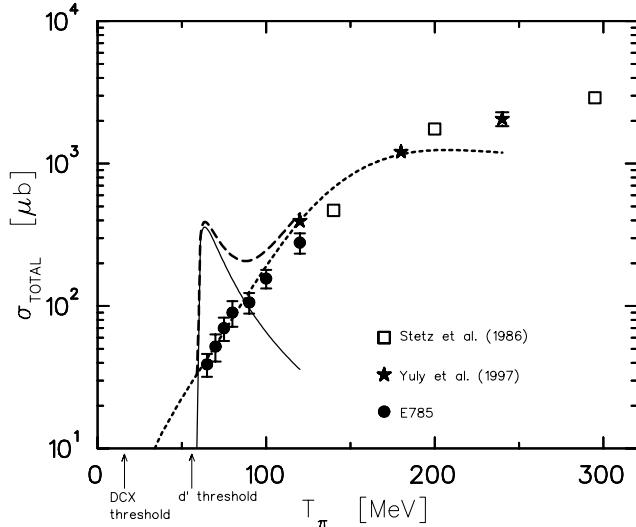


Fig. 56. Total cross section for the ${}^3\text{He}(\pi^-, \pi^+)$ reaction measured in Expt. 785. The dotted line represents the results of a conventional calculation for the DCX process, while the solid line represents the prediction for the d' mechanism.

The data from the inclusive ${}^3\text{He}(\pi^-, \pi^+)$ reaction have also been analyzed searching for the possible production of a bound trineutron state. From the momenta of the incoming π^- and the outgoing π^+ , the invariant mass M_{nnn} of the final state three-neutron system has been reconstructed. Results are shown in

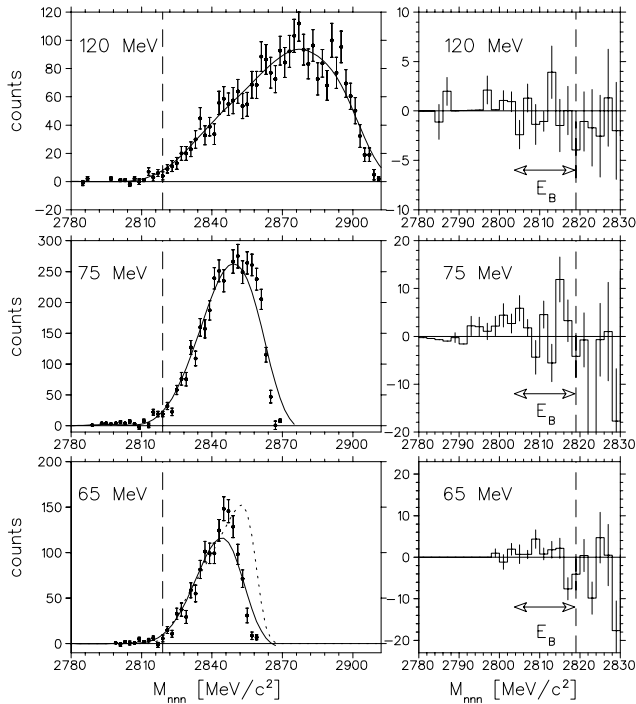


Fig. 57. On the left: Invariant mass distribution of the three-neutron system following the ${}^3\text{He}(\pi^-, \pi^+)$ reaction, as measured in Expt. 785. The solid lines are cubic spline fits to the data. On the right: The difference between the data and the fitted curves.

Fig. 57. The measured M_{nnn} distributions were fit with smooth curves for $M_{nnn} > 2818.7$ MeV, which were then extrapolated to lower invariant masses. A bound trineutron would manifest itself as a peak in M_{nnn} above the smooth curve. No evidence for the existence of the 3n was found, and an upper limit of 30 nb/sr was obtained. Full details can be found in an article by J. Grater *et al.*, which will appear in *Europhysics Journal*.

Experiment 823 Pure Fermi decay in medium mass nuclei (G.C. Ball, TRIUMF; D.M. Moltz, LBL)

Precise measurements of the intensities for super-allowed Fermi $0^+ \rightarrow 0^+$ β decays provide demanding and fundamental tests of the properties of the weak interaction. In particular, since the axial vector decay strength is zero for such decays the intensities are directly related to the weak vector coupling constant. Presently, nine transitions have been determined with sufficient precision [Towner *et al.*, Proc. WEIN'95 (World Scientific, Singapore, 1995) p.313] to confirm the conserved vector current (CVC) hypothesis at the level of 3×10^{-4} . These data, together with the muon lifetime, also provide the most accurate value for the up-down quark mixing matrix element of the Cabibbo-Kobayashi-Maskawa (CKM) matrix, V_{ud} . However, the resulting unitarity test of the first row of the CKM matrix differs from unity by more than two standard deviations [Towner and Hardy, Proc. WEIN'98 (to be published)]. Since there is no known reason to question the uncertainties in the small calculated Coulomb and radiative corrections that have been applied to these data, additional measurements are required to study this discrepancy.

At ISAC a program has been initiated to measure the half-lives and branching ratios for $T_z = 0$ nuclei with $A \geq 62$. These data together with more accurate Q-values will test the theoretical calculations for analogue symmetry breaking which are predicted to be much larger for these nuclei [Ormand and Brown, Phys. Rev. **C52**, 2455 (1995)]. The nucleus ${}^{74}\text{Rb}$ has been chosen for the initial experiment since it should be the easiest to produce.

Although the measurements are simple in principle, the required precision ($\sim 0.05\%$) demands great care in the technique. In addition, since the Q-value is large, several significant branches to excited states will need to be accurately determined. The measurements are further challenged by the very short half-life of ${}^{74}\text{Rb}$ (~ 69 ms) and limited beam intensity.

Initial measurements

At the 1997 December meeting of the EEC it was proposed to start by measuring the half-lives of the first

beams available from ISAC, namely $^{38\text{m}}\text{K}$ and ^{37}K . The measurement of $^{38\text{m}}\text{K}$, a well known superallowed β transition ($t_{1/2} = 923.95 \pm 0.64$ ms) will provide an important test of the experimental apparatus. In addition, a more precise measurement of the half-life for ^{37}K is required for the high priority TRINAT experiment 715. Precision measurements that would test the standard model can be made by measuring polarization asymmetries in the β -decay of non-zero spin nuclei. The decay probability dW is given by

$$dW = dW_0 \xi (1 + a\beta \cos \Theta_{e\nu} + AP\beta \cos \Theta_{ej} + BP \cos \Theta_{j\nu} + cc_P \beta [\cos \Theta_{j\nu} \cos \Theta_{ej} - \cos \Theta_{e\nu}/3])$$

where $dW_0 \xi$ is the rate in the absence of correlations, β is p/E with p the electron momentum and E the electron energy, c_P is the polarization parameter $[-J(J+1) + 3P^2 J^2]/J(2J-1)$ which varies strongly with the nuclear polarization P and \vec{j} is a unit vector in the direction of the vector polarization $\langle J \rangle$. The $\beta - \nu$ correlation parameter a , the β and ν asymmetry parameters A and B , respectively and the polarization coefficient c depend on the nuclear spin, J , and the ratio of the matrix elements $\lambda = g_A M_{GT}/g_V M_F$.

Estimates of the non-zero correlation parameters in ^{37}K can be calculated using the known branching ratio, $97.89 \pm 0.11\%$ and β -decay half-life 1226 ± 7 ms. The standard model predictions for a, A, B , and c are shown in Table IX. The quoted error in these data is dominated by the uncertainty in the β -decay half-life. In the present experiment it should be possible to reduce this error to < 1 ms.

Table IX. Observables in ^{37}K positron decay^{a)}.

	a	A	B	c
value	0.6608	-0.5731	-0.7765	0.2035
error ^{b)}	0.0058	0.0021	0.0056	0.0035
	(0.0021)	(0.0007)	(0.0020)	(0.0013)

a) calculated within the standard model with $\lambda = -0.5841 \pm 0.0067$

b) errors in (–) were calculated for an error in λ of ± 0.0024 , corresponding to an error in the ^{37}K half-life of ± 2 ms.

Description of experiment

The experiment will be carried out at ISAC using techniques that were developed by members of this collaboration in previous high-precision β -decay half-life measurements [Koslowsky *et al.*, Nucl. Instrum. Methods **A401**, 289 (1997)]. The low energy (60 keV) radioactive beams from ISAC will be implanted into a 25 mm wide aluminized mylar tape of a fast tape transport system. After a collection period of ~ 3 half-lives,

the ISAC beam will be interrupted and the samples will be moved out of the vacuum chamber through two stages of differential pumping and positioned in a 4π continuous-gas-flow proportional counter. After multiscaling the signals from the 4π counter for about 20 half-lives the data will be stored and the cycle repeated continuously. The experiment will be controlled using a Jorway 221 12-channel timing and sequencing CAMAC module. A Stanford Research DS335 function generator was obtained to provide a $100 \text{ kHz} \pm 0.2$ Hz time standard for the experiment. An instantly retriggerable gate generator will be used to give a well-defined non-extendable dead time ($\sim 3\text{--}4 \mu\text{s}$) that is significantly longer than any series dead time preceding it. Systematic errors introduced by the measurement techniques (for example, as a result of electronic dead times, discriminator thresholds, or detector bias) will be determined in off-line measurements, and by making on-line measurements under a variety of different conditions. A total of about 10 runs, each with about 2×10^6 events, will be required for a complete set of measurements on each isotope of interest.

Sample purity will be monitored by measuring the γ -ray spectrum using an HPGe detector located close to the 4π counter. The surface ion source used to produce the radioactive beams of interest is very specific to alkali elements but small quantities of alkaline-earth elements may be produced at high temperatures.

Technical progress

The experiment has been set up initially at a temporary location in the low energy experimental area. The low energy beam transport (LEBT) was completed to this location in early December. An electrostatic quadrupole triplet is used to focus the radioactive ion beam from the surface ion source to a 2–3 mm diameter spot on the mylar tape. The design, fabrication and installation of the differentially pumped slit system has been completed. The fast tape transport system used at TASCC (Chalk River) was refurbished, and the TASCC 4π β -counter with associated electronics were installed, tested and repaired. The data acquisition computer system provided by TRIUMF consists of a Pentium/LINUX PC interfaced to a CAMAC crate running the new data acquisition software MIDAS.

The LEBT was commissioned with stable ^{39}K beam on 16 December and a ^{37}K radioactive beam was available for ~ 30 minutes. During this time it was possible to determine that the experimental equipment is ready for the initial measurements on ^{37}K and $^{38\text{m}}\text{K}$ during the next scheduled beam time in the spring of 1999.

Experiment 824

Measurement of the astrophysical rate of the $^{21}\text{Na}(p, \gamma)^{22}\text{Mg}$ reaction rate

(N. Bateman, TRIUMF/SFU/Toronto)

The first experiment with the DRAGON facility will be a measurement of the $^{21}\text{Na}(p, \gamma)^{22}\text{Mg}$ reaction rate. The rate of this reaction determines operation of the NeNa cycle during explosive hydrogen burning. As a result it is important to know this rate to determine the production of ^{22}Na in novae [José *et al.* (submitted to *Astrophys. J.*)]. This nucleus is interesting because its decay can be detected by gamma ray telescopes, and because it has been shown to be present in pre-solar grains from meteorites (e.g. [Ott, *Nature* **364**, 25 (1993)]).

At ISAC, the DRAGON recoil separator will be used to measure the resonance strengths of the astrophysically important resonances for this reaction. The ^{21}Na beam will be tuned at the resonance energy and the yield measured. These measurements will allow an accurate determination of the reaction rate at the appropriate temperatures.

Unfortunately the resonance energies are not well known. In particular the third resonance ($E_x = 4.965$ MeV) is uncertain by 25 keV [Endt, *Nucl. Phys.* **A521**, 1 (1990)], and the radioactive beam will lose considerably less energy than this in the gas target that will be used with the DRAGON. Unless the resonance energy is measured more accurately we will have to run multiple beam energies until the resonance is located. We have used the $^{24}\text{Mg}(p, t)^{22}\text{Mg}$ reaction to accurately measure the relevant resonance energies.

Experiment

The experiment was performed from the 9th-11th of June at CNS-Tanashi, Japan with the QDD spectrograph. Data were taken at 8° , 16° , and 20.5° . At each angle targets of (enriched) ^{24}Mg , ^{26}Mg , and ^{12}C were measured. At these angles we were able to observe lines in the triton, deuteron and alpha spectra, all of which are useful for calibration purposes. The 8° triton spectrum is shown in Fig. 58. All observed lines have been identified, and the (p, γ) threshold is marked.

Preliminary results

Although the data analysis is still ongoing, we can make some preliminary remarks. We have observed a previously unknown state at about 5.08 MeV. The level scheme of ^{22}Mg is well established at this energy; as a result this new state cannot fit in the level scheme of Endt [*op. cit.*]. This suggests that the current level scheme for ^{22}Mg is wrong. Obviously, this has implications for the mirror identities of the higher-lying states, which determine the astrophysical reaction rate. We

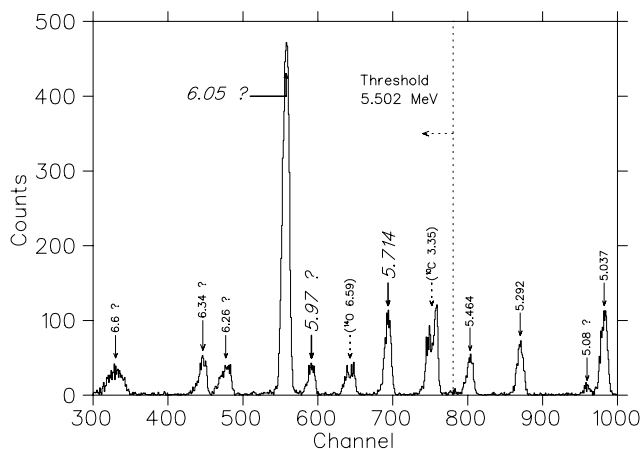


Fig. 58. Triton spectrum at 8° . The threshold for $^{21}\text{Na}(p, \gamma)^{22}\text{Mg}$ is shown. The states that correspond to resonances of astrophysical interest are labelled in italics, with bold arrows. States marked with ‘?’ are listed with the experimental excitation energies. The 6.05 state is strongly forward peaked, so it ought to be the 0^+ state, though the observed energy is 90 keV higher than the literature value. The state at 5.97 may be a previously unobserved resonance.

observe the first 0^+ state at about 6.05 MeV, some 90 keV higher than it has been observed in $(^3\text{He}, n)$ measurements [McDonald and Adelberger, *Nucl. Phys.* **A144**, 593 (1970); Alford *et al.*, *Nucl. Phys.* **A457**, 317 (1986)]. As this is one of the resonances that will be measured at ISAC this is also an important result. If our energy is correct the astrophysical importance of this resonance will be reduced. We have also observed a state at 5.97 MeV. This energy agrees with the $(^3\text{He}, n)$ measurements for the 0^+ state, but the state that we observe is not strongly populated by (p, t) , and Paddock [*Phys. Rev.* **C5**, 485 (1972)] measured strong population of the 0^+ by this reaction. If this is a previously unknown resonance, it should be taken into account in estimating the $^{21}\text{Na}(p, \gamma)^{22}\text{Mg}$ reaction rate, and it will need to be measured with the DRAGON. Finally, we have observed a broad ($\Gamma \simeq 25$ keV) state at 6.26 MeV. While this resonance is unlikely to be of astrophysical importance, it may provide a very useful crosscheck for radioactive beam work.

Conclusion

While final conclusions must await the completion of the data analysis, some discussion is warranted at this point. Before we made this measurement the level structure of ^{22}Mg near the proton threshold appeared to be well understood. As a result, determination of the $^{21}\text{Na}(p, \gamma)^{22}\text{Mg}$ reaction rate seemed to be straightforward [Wiescher and Langanke, *Z. Phys.* **A325**, 309 (1986)]. In this measurement we have observed three new states between 500 keV below and 1 MeV above threshold. We have not observed three of the known states, but unnatural parity states should be weakly

populated by the (p, t) reaction. In order to perform the radioactive beam experiment that will put the $^{21}\text{Na}(p, \gamma)^{22}\text{Mg}$ reaction rate on a firm experimental basis we need to know enough about the spectroscopy of ^{22}Mg to be able to say with confidence which resonances need to be measured, and what the energies of these resonances are. Hopefully, our $^{24}\text{Mg}(p, t)^{22}\text{Mg}$ measurement will do this for the $^{21}\text{Na}(p, \gamma)^{22}\text{Mg}$ reaction, but other radioactive beam experiments will require similar work.

Experiment 837

Pion induced soft error upsets in 64 Mbit DRAM chips

(R.J. Peterson, G.J. Hofman, Colorado)

In November of this year we carried out the first cross section measurements for pion induced soft error upsets (SEU) in commercial 64 Mbit memory chips. The measurement spanned the Δ resonance (40–240 MeV incident pion energy). This experiment continues the work on 16 Mbit chips performed at Los Alamos [Gelderloos *et al.*, IEEE Trans. Nucl. Sci. **44** (1997)] and will be compared to recent measurements of proton induced reactions on 64 Mbit chips done at the Harvard Cyclotron.

As the amounts of charged stored in microelectronics becomes less, the stray charge deposited by the ambient ionizing radiation can easily corrupt the information, leading to a temporary (or ‘soft’) readout error. Radiation damage in microcircuits has become a problem for avionics at commercial aircraft altitudes. Much information has been gathered on SEU induced by neutrons and protons but a significant portion of the cosmic ray flux at 35,000 ft are pions ($\approx 36\%$ [Ziegler, IBM J. Res. and Dev. **40**, 19 (1996)]). Moreover, pions at a relatively low energy can be produced by cosmic ray reactions on aircraft hulls.

Pions may be particularly effective at causing upsets. Unlike protons and neutrons, pions can be absorbed by a nucleus, effectively depositing the total rest mass and kinetic energy in the nucleus. Such an excited nucleus may decay by emitting nucleons or heavily ionizing alpha particles.

All the present measurements were carried out in the M11 beam line. Two scintillators, mounted behind the testing box counted the number of pions incident on the chip. Time-of-flight measurements were performed to calculate the pion/proton fraction of the beam. The monitoring electronics continuously read and wrote a bit pattern to the chip under test and displayed the number of readout errors. A full read write cycle typically takes several seconds. The experimental cross section is defined as

$$\sigma(\text{SEU}) = \frac{\text{errors}}{\text{bits} \times \pi/\text{cm}^2}$$

This experiment showed a variation of almost three orders in magnitude across the various (9) manufacturers, reflecting a strong dependence on the design of the chip. For a given chip, the cross sections followed the rise of the Δ resonance. Measurements at π^- energies of 60, 150, 240 MeV confirmed [Gelderloos *op. cit.*] the charge independence of the SEU cross section. Typical values at 150 MeV π^+ ranged from $1\text{--}400 \times 10^{-16}/\text{cm}^2$. For one chip we investigated the possible angular dependence of the cross section by rotating the silicon wafer with respect to the incidence beam. No variations were found within the statistical errors.

The data obtained at 150 MeV π^+ were also compared to those obtained with incident protons (see Fig. 59). The straight line on the graphs indicates a $3\times$ scaling behaviour for pions and protons. As for the previously measured 16 Mbit chips, pions are much more likely to induce SEUs than protons (or neutrons) at these energies. One hypothesis on how pions deposit damaging charge is via the production of α particles. In order to quantify this we made measurements of the α production cross section on aluminum using CR-39 plastic detectors. The α particles leave tracks in the plastic which were later counted by the supplier. Preliminary results show cross sections near 100 mb for alpha particles from about 1 to 20 MeV. Monte Carlo calculations are in progress to correct for target thickness effects on the final cross sections. These alpha particle yields are large enough to indicate that their production is likely to be the cause of SEU induced in silicon circuit elements. This work is being prepared for publication in several appropriate journals.

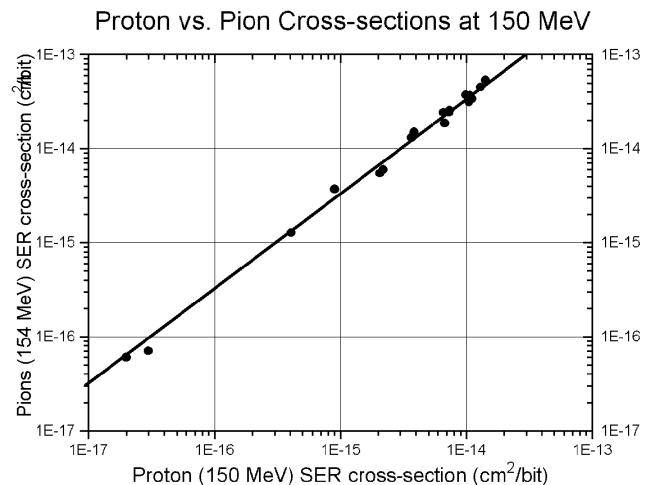


Fig. 59. 154 MeV positive pion versus 150 MeV proton SEU cross sections for the 64 Mb DRAM samples.

Experiment 838

Two-photon capture mode of pionic hydrogen

(*T. Gorringer, Kentucky*)

When negative pions are stopped in liquid hydrogen pionic hydrogen atoms are formed. These pionic hydrogen atoms subsequently disintegrate via one of several capture modes. While the capture modes $\pi^-p \rightarrow \pi^0n$, $\pi^-p \rightarrow \gamma n$, and $\pi^-p \rightarrow e^+e^-n$ have well determined branching ratios, the much rarer capture mode $\pi^-p \rightarrow \gamma\gamma n$ is unmeasured.

For capture from the 1S atomic state, the predicted mechanism for the $\pi^-p \rightarrow \gamma\gamma n$ reaction is the annihilation of the real π^- and a virtual π^+ into a photon-pair (i.e. $\pi^-\pi^+ \rightarrow \gamma\gamma$). Crossing symmetry relates the $\pi^-\pi^+ \rightarrow \gamma\gamma$ annihilation diagram to $\gamma\pi \rightarrow \gamma\pi$ Compton scattering, and offers potential sensitivity to the pion's electric polarizability. The predicted branching ratio is 0.51×10^{-5} [Beder, Nucl. Phys. **B156**, 491 (1979)].

We propose to measure the $\pi^-p \rightarrow \gamma\gamma n$ branching ratio, and its photon energy and opening angle dependence, using the RMC spectrometer. Negative pions will be stopped in a liquid hydrogen target and photon-pairs detected in the RMC spectrometer. The spectrometer comprises a Pb photon converter, cylindrical wire and drift chambers for e^-e^+ tracking, and beam and trigger scintillator arrays for pion-stop counting and photon-pair triggering. Background concerns include the near back-to-back photons from π^0 decay and random $\gamma\text{-}\gamma$ coincidences from coincident π^- stops.

We have completed two runs, a test run in June, 1997 and a production run in December, 1998. In the June, 1997 test run we tested the two-photon trigger and measured the two-photon acceptance. In the

December, 1998 production run we collected approximately 1.5×10^{10} pion stops in liquid hydrogen and expect, assuming the calculated branching ratio, several hundred $\pi^-p \rightarrow \gamma\gamma n$ events.

Undergraduate/graduate teaching beam time

(*S. Yen, TRIUMF*)

In November, a week of beam time on channel M11 was used by students of several undergraduate and graduate courses at three local universities. These included UBC undergraduates (S. Yen, instructor), UBC graduate students (M. Hasinoff, instructor), SFU graduate students (M. Vetterli, instructor), and University of Victoria graduate students (M. Roney, instructor). Students were brought into the lab in groups of 5–10 students, given a brief orientation lecture, and then asked to do one or two simple experiments using the pion beam in M11.

To keep things as simple and robust as possible, the detector consisted of a telescope of 3 thin plastic scintillators. One experiment was to measure the mass of the pion by plotting channel momentum versus the time of flight through the channel. The latter was determined by starting with the arrival of the particles and stopping with the rf timing pulse. This time could then be either simply observed on an oscilloscope, or measured with a CAMAC TDC. A second experiment was to produce ^{11}C by bombarding a polyethylene target with pions, and determining the cross section for ^{11}C production and the half-life of ^{11}C , by measuring the annihilation gamma rays with the TRIUMF Safety group's calibrated Ge(Li) detector system. The students were also given a tour of the whole lab.

A total of about 40 students at the three universities participated in this activity.

Experiment 684 **μ SR spin relaxation studies of small molecules in the gas phase***(J. Pan, D. Fleming, UBC-TRIUMF)*

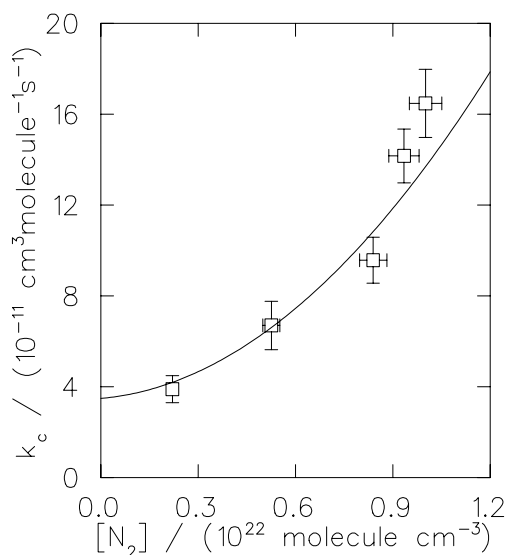
This experiment studies the muon spin relaxation in some simple gas-phase systems with the primary goal of measuring the chemical reaction rates. This year, the focus of our research is on the low temperature studies of the $\text{Mu} + \text{CO}$ and $\text{Mu} + \text{NO}$ reactions with two different moderators, He and N_2 , in both longitudinal (LF) and transverse (TF) magnetic fields.

A total of five weeks of experiments were carried out on M9 at pressures from 60 to 500 bar and temperatures from 140 K to 300 K.

 $\text{Mu} + \text{NO} + \text{N}_2$

For the reaction of $\text{Mu} + \text{NO} + \text{N}_2$, the moderator dependence is apparently different from that observed at room temperature where the bimolecular reaction rate constant is linearly proportional to total moderator concentration.

At 227 K, the $\text{Mu} + \text{NO}$ reaction rate constants were measured in LF. The results are shown in Fig. 60. The quadratic moderator dependence indicates that the dominant reaction mechanism is different than at room temperature. The spin exchange rate constant, which is moderator independent at room temperature, also strongly depends on the total pressure. The NO dimer formation could not account for the experimental results. One explanation is that the intermediate-complex forming mechanism, which is probably negligible at room temperature, becomes more important at lower temperatures because there are more Lennard

Fig. 60. $\text{Mu} + \text{NO}$ at 227 K.

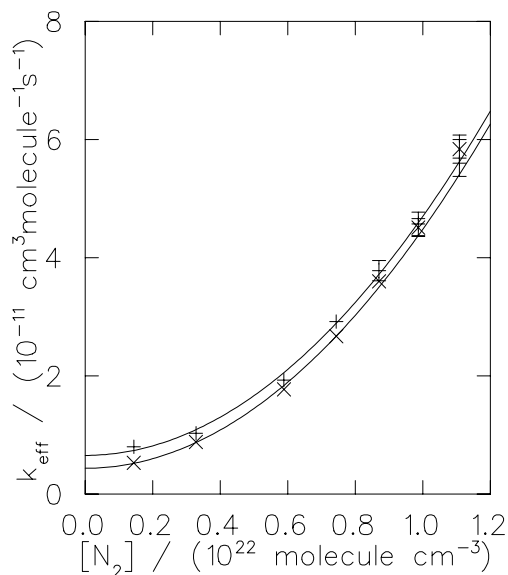
Jones molecular complexes ($\text{NO}\cdot\text{N}_2$) formed. More likely, both energy transfer mechanism and the intermediate complex mechanism contribute to the total reaction. Unfortunately, these two contributions cannot be separated under the current experimental conditions. More temperature variation studies are required to confirm the reaction mechanisms involved.

 $\text{Mu} + \text{CO}$

The $\text{Mu} + \text{CO}$ reactions were studied with both He and N_2 moderator in TF (5 and 60 G). At all temperatures, the moderator dependence of the chemical reaction rate constants are quadratic in N_2 . Figure 61 shows a typical plot of the total reaction rates which include both chemical and spin relaxation contributions.

In He, however, since the concentration range is relatively small, there is no obvious deviation from a linear dependence at pressures higher than 200 bar (Fig. 62). Experiments extending the pressure range down to a few bar are planned for the coming beam period.

Again, the intermediate-complex and energy transfer reaction channels and the coupling of both channels are expected. The results certainly ruled out a straightforward energy transfer mechanism even at room temperature. Currently, the reaction mechanism is not completely understood. Further measurements at lower pressures (0–60 bar) are under way. Theoretical investigation of the reaction mechanisms is also being actively pursued.

Fig. 61. $\text{Mu} + \text{CO} + \text{N}_2$ at 180 K. Lower curve: 5 G TF. Upper curve: 60 G.

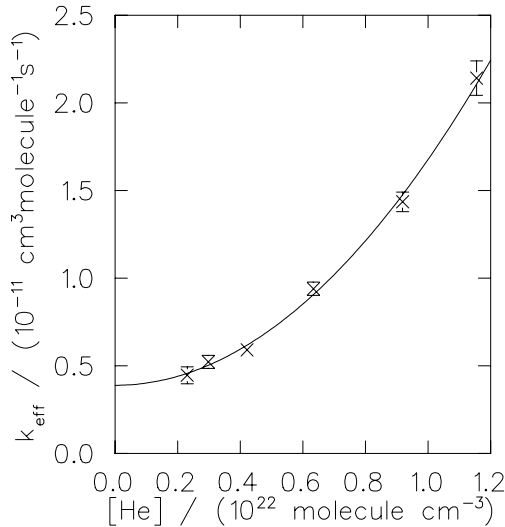


Fig. 62. $\text{Mu} + \text{CO} + \text{He}$ at 178 K. Measurements were made only at 5 G TF.

Experiment 691

The vortex cores in type-II superconductors

(*J.H. Brewer, CIAR/UBC; J.E. Sonier, CIAR/Los Alamos*)

In 1998 we continued our investigation of the vortex core size r_0 in type-II superconductors. Previous studies under Expt. 691 found a novel increase in r_0 at low magnetic fields in the conventional superconductor NbSe_2 [Phys. Rev. Lett. **79**, 1742 (1997)] and in the oxygen deficient high- T_c superconductor $\text{YBa}_2\text{Cu}_3\text{O}_{6.60}$ [Phys. Rev. Lett. **79**, 2875 (1997)]. The temperature dependence of r_0 in both of these compounds was also found to deviate from the known theoretical predictions at that time.

Much of what is known about high- T_c superconductors comes from experiments on compounds which are doped to give the maximum value of T_c . Thus, it was of great interest to check the size, temperature and magnetic field dependence of r_0 in optimally doped $\text{YBa}_2\text{Cu}_3\text{O}_{6.95}$, with a maximum T_c of 93 K. Furthermore, since the considerable progress in our μSR measurements in the high- T_c materials in recent years is due in part to the improvements in crystal growth, it was imperative that we verified the influence of extrinsic sample effects on our findings.

Our main findings from high-statistic TF- $\mu^+\text{SR}$ measurements on several twinned and detwinned crystals of $\text{YBa}_2\text{Cu}_3\text{O}_{6.95}$ are summarized in Fig. 63. The temperature dependence of r_0 is observed to be weak at low T (compared to NbSe_2) and r_0 is found to increase at lower magnetic fields, where it approaches an extraordinarily large value of about 100 Å. Furthermore, we find that the absolute value of r_0 is essentially the same in all samples studied.

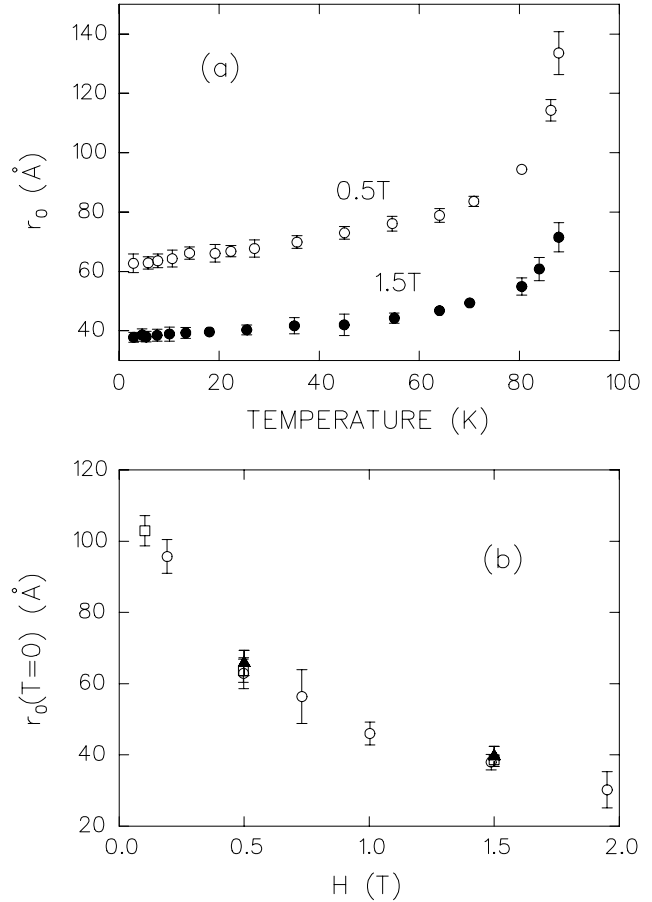


Fig. 63. (a) The temperature dependence of r_0 at $H = 0.5$ T (open circles) and 1.5 T (solid circles) in twinned $\text{YBa}_2\text{Cu}_3\text{O}_{6.95}$. (b) The magnetic field dependence of r_0 extrapolated to $T = 0$ in twinned (both open circles and squares) and detwinned (solid triangles) crystals of $\text{YBa}_2\text{Cu}_3\text{O}_{6.95}$.

In the wake of these and our previous measurements under Expt. 691, numerous theoretical studies are now aimed at redeveloping the general picture of the vortex state. In particular, considerable effort is being made to understand why the vortex cores expand at low magnetic fields. We surmise from our μSR experiments that this is a general property of all superconductors in the vortex state. Recently, the expansion of the vortex core size in NbSe_2 was used to explain the low magnetic field anomaly of the electronic specific heat observed in conventional s -wave superconductors [Sonier *et al.* (submitted to Phys. Rev. Lett.)]. Our measurements of r_0 are now being seriously considered in the interpretation of other experiments performed in the vortex state.

In 1998 we also carried out both TF and LF μSR measurements in the underdoped superconductor $\text{YBa}_2\text{Cu}_3\text{O}_{6.57}$ in an effort to find evidence for the existence of antiferromagnetic (AFM) vortex cores, as predicted in the proposed $SO(5)$ theory of high- T_c su-

perconductivity [Zhang, *Science* **275**, 1089 (1997)]. A similar experiment performed under Expt. 691 in 1997 suffered from distortions in the LF time spectra and a lack of statistics in the TF lineshapes. Despite improvements in both of these areas as well as an improvement in sample quality, no definitive conclusion could be made in the 1998 version of this experiment. Instead we determined that if there are indeed AFM moments in the vortex cores, they are fluctuating at a rate too fast or too slow to be unambiguously observed with the current sensitivity of LF- μ SR measurements. Similarly, evidence for their existence from TF- μ SR lineshapes continues to suffer from the difficulties associated with transforming the spectra into the frequency domain. Both advancements in μ SR data collection and analysis techniques are needed to further this investigation.

Present status of Expt. 691

In December the decision was made to replace Expt. 691 with several new experiments (i.e. Expts. 846, 847 and 848) to carry out a thorough and detailed investigation of important but specific topics of the vortex state in high- T_c superconductors, which are uniquely suited for μ SR.

Experiment 713 Muonium chemistry in supercritical water (P.W. Percival, SFU)

The properties of water change markedly when it is subjected to temperatures and pressures near or above the critical point (374°C, 220 atm). The ionic product falls by many orders of magnitude and the dielectric constant is reduced to values typical of organic solvents. It is even possible to sustain a flame in supercritical water, by injecting oxygen into an aqueous solution of methane. This has led to several investigations of the potential of supercritical water (SCW) oxidation as a means for hazardous waste destruction, including chemical weapons and the clean-up of nuclear processing sites.

A significant hurdle to practical development of SCW destruction facilities is the current lack of detailed knowledge of physical, chemical and transport properties of supercritical fluids at the molecular level, particularly free radical chemistry and kinetics under such conditions. Probing reactions at the molecular level clearly calls for spectroscopic methods. However, there are considerable experimental difficulties, and until recently most studies were limited to stable species in solution. In any event, optical spectroscopic methods are not suited to the study of transient free radicals. The preferred option for free radical characterization is ESR, but the severe practical problems involved have precluded the necessary development.

TRIUMF Expt. 713 was designed to explore the potential of μ SR to probe SCW chemistry, using muonium as a model for the hydrogen atom. The first stage of the project involved development of a sample cell with a window which allows penetration of muons (typically 70 MeV/c momentum), yet is strong enough to withstand pressures up to 500 atm and temperatures to 500°C. The apparatus has been used for μ SR experiments on water over a wide range of temperatures and pressures, up to 350 atm and 420°C, corresponding to water densities from below 0.1 g cm⁻³ to 1.0 g cm⁻³. We have demonstrated that muonium is long-lived over the whole range of conditions and that the muonium signal amplitude and hyperfine constant vary with density. Our first measurements of muonium kinetics in sub- and super-critical water revealed remarkable effects – the rate constant for a spin exchange reaction was found to rise with temperature at a rate much less than that predicted by simple diffusion theory, and then to go through a maximum. We suspect this signals differential location of ions and hydrophobic solutes (in this case Mu) in water clusters and voids, respectively. If so, this has important practical consequences for the performance of a SCWO reactor.

In the summer we achieved the final goal of Expt. 713 – successful detection of muonium-substituted free radicals in supercritical water. We were able to obtain transverse field μ SR spectra of cyclohexadienyl and tert-butyl in aqueous solutions of their precursors, benzene and isobutene, respectively. Examples are given in Figs. 64 and 65.

We believe this is the first direct identification of organic free radicals in sub- and super-critical water by *any* technique. It opens up a wide area of free radical chemistry to detailed study. Free radicals almost

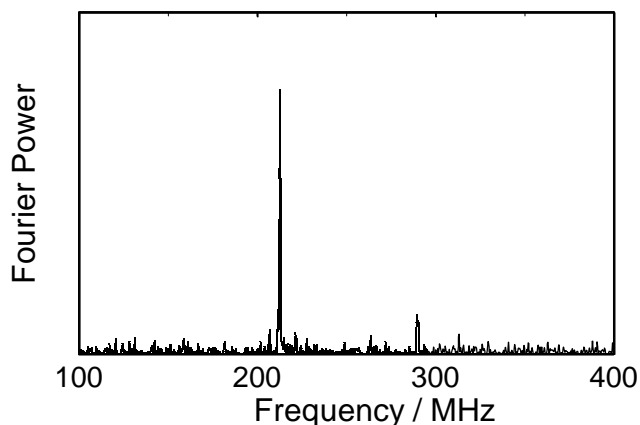


Fig. 64. Fourier power μ SR spectrum from a solution of benzene in water at 230°C, 250 atm, in a transverse field of 2.05 kG. The peaks at 210 and 290 MHz are due to the cyclohexadienyl radical C₆H₆Mu. A large diamagnetic signal is off scale.

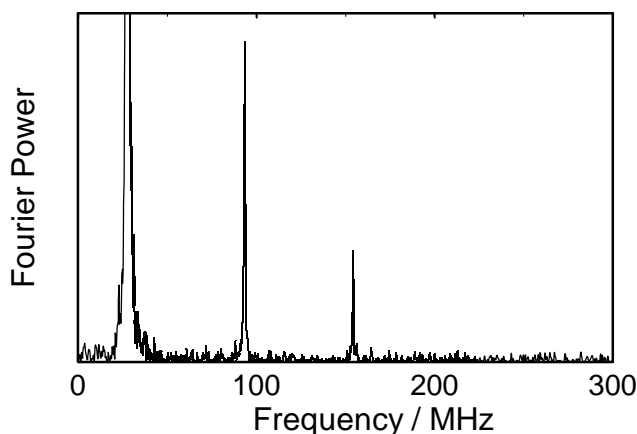


Fig. 65. Fourier power μ SR spectrum from a solution of tert-butanol in water at 385°C , 250 atm, in a transverse field of 2.05 kG. The truncated peak at 28 MHz is due to muons in a diamagnetic environment. The other two peaks arise from the tert-butyl radical $\text{MuCH}_2\text{C}(\text{CH}_3)_2$.

certainly play a major role in SCW waste destruction, but studies are typically limited to end-product analysis. Furthermore, ‘aquathermolysis’, the reactions of organic molecules in superheated water, is a growing area of organic chemistry, and the ability to detect radical intermediates will surely aid its development.

Although we detected radicals in SCW this was by transverse field (1–2 kG) μ SR, using samples of almost molar concentration. Full characterization (measurement of proton hyperfine coupling constants as well as that of the muon) and detection at low concentrations requires muon level-crossing spectroscopy (μ LCR).

The necessary spectrometer (HELIOS) exists but the sample access and detector geometry is completely different, since HELIOS is a superconducting solenoid while SFUMU, the μ SR spectrometer used for Expt. 713 is based on an open Helmholtz pair. Thus, the SCW sample cell must be completely re-engineered. All the inlets/outlets to the cell must be fitted at the rear, and the cell must be better insulated (probably water cooled) to protect a new set of custom built plastic scintillators. This project will be pursued under a new TRIUMF experiment, Expt. 842, which was approved at the December meeting of the EEC.

Experiment 717

Muonic hyperfine transition rates in light nuclei

(T.J. Stocki, D.F. Measday, UBC)

The muonic hyperfine transition rates were measured in LiF, $(\text{CF}_2)_n$, Na, NaH, Al, LiAlH_4 and for the first time in K and P. These measurements were performed by detecting neutrons via liquid scintillators. The most precise measurement of the muonic hyperfine transition rate was made on LiF. Figure 66 shows

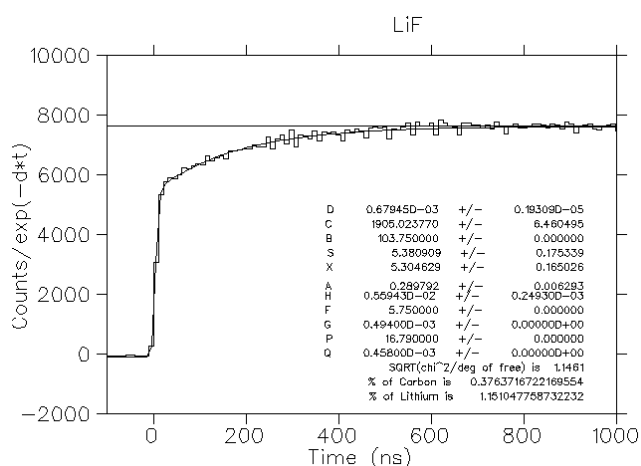


Fig. 66. Time spectrum of neutrons after muon capture on LiF with the muon lifetime in LiF divided out.

the data and the fit for the neutron time spectrum for LiF. No chemical effect was observed when comparing the transition rates in LiF and $(\text{CF}_2)_n$, Na and NaH, Al and LiAlH_4 . In the case of P and K the newly measured hyperfine transition rates are $48 \pm 5 \mu\text{s}^{-1}$ (this value is model dependent) and $25 \pm 15 \mu\text{s}^{-1}$.

Nitrogen should not have a hyperfine transition if the only hyperfine transition process is through Auger emission, because the hyperfine splitting energy is smaller than the energy needed for the Auger process. So confirmation of a previous nonzero measurement of a hyperfine effect in ^{14}N was attempted. This search for a hyperfine effect in ^{14}N was performed by detecting neutrons and γ -rays in two separate experiments. In the neutron experiment liquid scintillators were used to measure the time spectra of the electrons and neutrons. It was found that the muon lifetime obtained from the neutron time spectrum was different than the lifetime measured in the electron time spectrum. This difference may indicate a hyperfine transition in nitrogen. In the case of the γ -ray experiment, which was performed using two high purity germanium detectors, the results lacked sufficient statistics.

During this nitrogen γ -ray experiment, much new information was obtained. The yields of γ -ray produced from muon capture in ^{14}N were measured. Previously only the yield from one γ -ray had been measured. In this experiment yields from three γ -rays in ^{14}C , from three γ -rays in ^{13}C , from one γ -ray in ^{12}C , and two γ -rays in ^{10}B were measured. From these yields, the nuclear level yields were obtained. In addition, the energies of two γ -rays in ^{14}C were measured more accurately than before; these γ -rays are at energies of $7016.8 \pm 1.3 \text{ keV}$ (shown in Fig. 67) and $6730.6 \pm 1.0 \text{ keV}$.

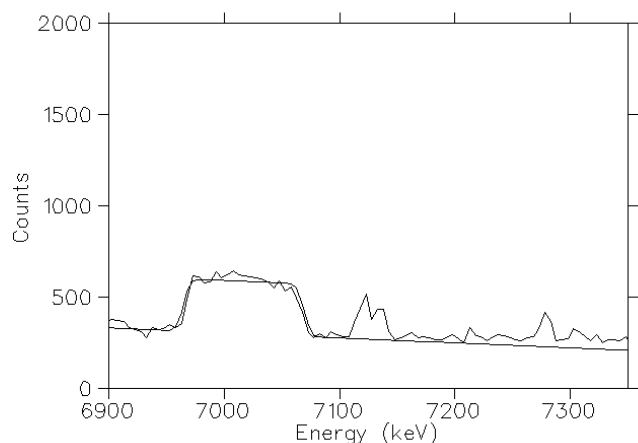


Fig. 67. The 7017 keV γ -ray and its doppler broadend fit.

Experiment 720/750

Muonium as a light isotope of hydrogen

(D.C. Walker, UBC)

Our major publication during the year was an Invited Faraday Research article [J. Chem. Soc., Faraday Trans., **94**, 1 (1998)] (including one of the figures on the journal cover). This provides an overview of our work on muonium atoms (Mu) in water. It shows the variation of reactivity of Mu with different types of

additives to the water. Mu is shown to react according to classical reaction-dynamic principles in one type, and according to quantum-mechanical principles in the other.

The hundred or so solutes discussed fall into two camps: (i) those whose reactivity towards Mu – compared to ordinary H atoms – gives a kinetic isotope effect (KIE) which can be explained, to a good approximation, by classical transition state theory (corresponding to enhanced reaction path barriers of H over Mu, but higher encounter frequencies of Mu over H), Table X; and (ii), those reactions which give contrary KIEs and which can only be explained by the dominance of quantum effects. In the latter category lie reactions in which Mu adds to an aromatic ring at the ortho-meta-para positions in the opposite sense found for H atom addition; and Mu reactions in which Mu adds to the O atom of a carbonyl group in a ketone (where H adds to the C atom), as demonstrated in Table XI.

There is another overall feature revealed in this review: Mu's reactions as a reducing agent fall directly between those of H atoms and hydrated electrons ($e_{(aq)}^-$). This in-between character is expressed in the relative reaction rates of Mu compared to H and $e_{(aq)}^-$, as in Table XII.

Table X. A sample of observed k_M values and KIEs (k_M/k_H) in water at ~ 295 K for reactions which seem to involve the same mechanism and form isotopomeric products with Mu and H.

Solute (type of Mu reaction)	$k_M/M^{-1}s^{-1}$	KIE	Origin of KIE
H ₂ C ₂ O ₄ /HC ₂ O ₄ ⁻ , pH=1 (addition)	3.4×10^8	850	tunneling
C ₂ O ₄ ²⁻ , pH=8 (addition)	5.4×10^6	>300	tunneling
OH ⁻ (acid, Mu ⁺ transfer)	1.7×10^7	0.7	none
uracil (addition to C(5) & C(6))	6×10^9	16	addition
thymine (addition to C(5) & C(6))	3×10^9	5	steric hindrance
benzene (addition to ring)	3×10^9	3	solvation
styrene (addition to side chain)	2×10^{10}	3	diffusion-limited
acrylic acid (addition to vinyl)	1.6×10^{10}	4.5	diffusion-limited
O ₂ (spin-exchange + combination)	2.4×10^{10}	1.5	diffusion-limited
Ag ⁺ (reduction to Ag ^o)	1.6×10^{10}	0.8	diffusion-limited
2-propanol (abstraction)	$1.0(\pm 0.3) \times 10^6$	0.015	ZPE effect

Table XI. A sample of k_M values and observed KIEs in water at ~ 295 K for representative solutes which react differently towards Mu and H.

Solute	k_M	KIE _(obs)	Mu reaction	H reaction
acetone	1.0×10^8	75	addition to O	abstraction of H ($\frac{2}{3}$)
butanone	1.0×10^8	4.5	addition to O	abstraction of H ($\geq 90\%$)
CH ₃ CSNH ₂	3×10^{10}	5	addition to C	addition to S?
pyridine	5.8×10^9	10	addition to C	addition to N?
pyrazine	7.7×10^9	26	addition to C	addition to N?
benzoic acid	7.5×10^9	8	addition to C	addition to C
Cr ³⁺ ions	$2-6 \times 10^{10}$	>10 ⁴	spin exchange	reduction to Cr ²⁺

Table XII. Examples of different reaction types which illustrate that Mu lies between H and e_{aq}^- in its reactivity. These rate constants refer to aqueous solutions at ~ 295 K; k_e for e_{aq}^- , k_M for Mu, and k_H for H, all in units of 10^7 $M^{-1}s^{-1}$.

Solute	k_e	k_M	k_H
chloroacetic acid	69	0.23	0.013
N ₂ O	900	6.5	0.21
2-propanol	<0.01	0.1	7.4
nitrate ions	970	150	0.14
oxalate ions (pH=8)	3.1	0.54	<0.004
acetone	650	10	0.1
Tl ⁺	2000	80	4.1
cytosine (DNA)	1300	300	9.2

Experiment 724

Effects of dilute (Cu,Zn) substitution in spin gap system SrCu₂O₃

(M.I. Larkin, G.M. Luke, Y.J. Uemura, Columbia; M. Takano, Kyoto)

Spin systems having spin gaps and a singlet ground state are of great interest due to the quantum nature of the ground state, and superconductivity obtained by charge doping in some systems. Spin-ladder systems have spins arranged in a ladder geometry. In copper-oxide spin ladder compounds, nearest neighbour spins on a ladder and a rung, in this case spin-1/2 Cu²⁺, are anti-ferromagnetically coupled via 180° Cu-O-Cu bonds with J on the order of 1,000–2,000 K. Inter-ladder coupling occurs via 90° Cu-O-Cu bonds and is geometrically frustrated, strongly reducing the effective coupling, and making the system quasi-1 dimensional. The two-leg ladder system SrCu₂O₃ has been seen in susceptibility and neutron experiments to have a spin-gapped singlet ground state with the gap energy $\Delta \approx 680$ K. Our previous μ SR experiments at TRIUMF confirmed an absence of magnetism down to 20 mK, the lowest measured temperature.

In spite of such a large value for the gap energy of the singlet state which may be naively related to the robustness of the state, a cusp in the magnetic susceptibility suggesting static magnetic freezing has been observed in the Zn-doped 2-leg ladder systems where Cu was substituted with non-magnetic Zn, even at a Zn concentration x of 1% or smaller. We recently performed μ SR measurements on ceramic samples of Sr(Cu_{1-x}Zn_x)₂O₃ for $0.003 \leq x \leq 0.07$ at beam lines M13 and M15, both in conventional gas-flow cryostats and a dilution refrigerator. In all these Zn-doped 2-leg ladder samples, the relaxation rate of the muon spin exhibits rapid increase with decreasing temperature below T_N in zero external field, with clear decoupling in longitudinal fields, indicating onset of static spin freezing.

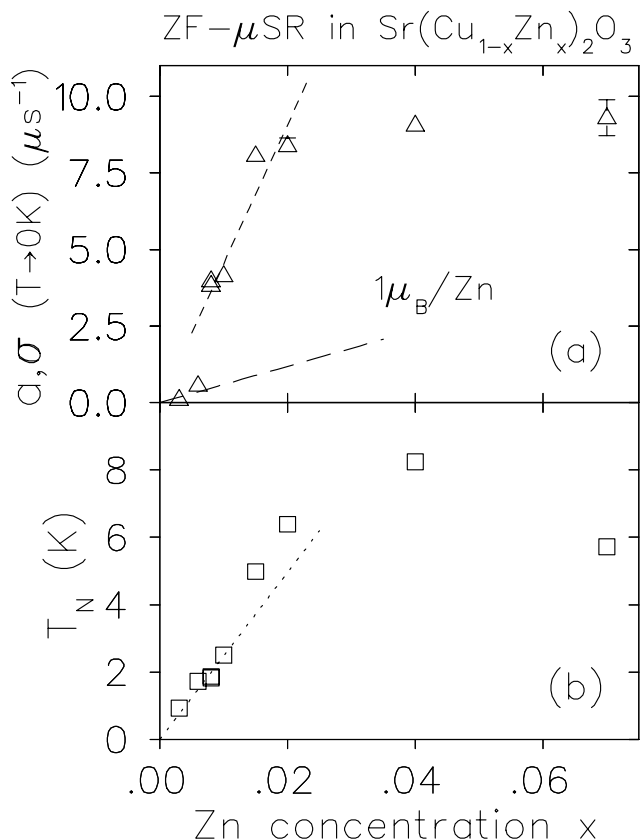


Fig. 68. (a) saturated μ SR static relaxation rate (limit as $T \rightarrow 0$ K), proportional to the saturated moment size, vs. Zn concentration x . The long-dashed line indicates the relaxation expected for $1\mu_B$ of moment liberated by each substituted Zn. Note the jump from 0.6% to 0.8%. (b) The Néel temperature T_N vs. Zn concentration x . T_N linearly increases with x for low x , as has also been seen in bulk measurements, without a pronounced jump.

In Fig. 68 we show the muon relaxation rate extrapolated to zero temperature (saturated relaxation rate), and T_N vs. Zn concentration x . We see that at low Zn concentration, the relaxation rate is consistent with $1\mu_B$ of moment liberated for each Zn atom. With increasing Zn concentration, the saturated relaxation rate increases quite sharply and non-linearly. There is an abrupt change near 0.8% Zn substitution. At higher concentration, the relaxation rate increases linearly with x until it saturates around 2%. In contrast to the relaxation rate, the Néel temperature T_N determined by μ SR does not show any anomaly and increases linearly with increasing x , as was found in other bulk measurements.

The μ SR line shapes for $x < 0.008$ are consistent with dilute, random moments, while those for $x > 0.008$ are consistent with spatially denser moments. An absence of clear precession at all x values indicates randomness in the ordered moment size and/or frozen spin orientation.

These results demonstrate that a crossover from

freezing of dilute isolated spins to freezing of the spin network extending presumably to the entire system occurs around $x = 0.008$. A rather high Néel temperature observed even for systems with $x < 0.008$ indicates that singlet spin pairs between unpaired Cu moments play a role in increasing exchange coupling. For $x > 0.008$, the saturated relaxation rate increases linearly with Zn concentration, indicating an increase of the average ordered moment size per Cu. Simulation studies are under way on line shapes and relaxation rates for selected values of spin correlation length and ordered moment size, to consider the present results in terms of characteristic length scale(s) of the 2-leg ladder system.

Experiment 746

Muonium in Si

(*B. Hitti, S.R. Kreitzman, TRIUMF*)

The structure and dynamics of muonium ($\text{Mu} = \mu^+ e^-$) in semiconductors have long been recognized as directly relevant to understanding the analogous hydrogen defect centres. To study the dynamics of transitions between the muonium states in Si we employed two muon spin resonance (μSR) spectrometers developed at TRIUMF.

The radio frequency (rf- μSR) spectrometer (10 to 200 MHz) was mainly used to measure the temperature dependence of the diamagnetic amplitude in p -type and n -type Si samples of various dopant concentrations. The rf data show a complicated set of transitions active during the muon lifetime and involving four separate muonium states. Two types of neutral muonium centres are observed in Si at low temperature, the stable configuration has the muon at or near a bond-centre site, Mu_{BC}^0 ; the second configuration is metastable and is located within the tetrahedral region, Mu_T^0 . In addition to the neutral states, charged muonium centres occur. In p -type Si, the charge centre is positive and resides near the BC site, Mu_{BC}^+ ; while the negative charge state is observed in the moderately to heavily doped n -type samples and is stable at the T site, Mu_T^- . Recent analyses have enabled us to infer parameter values describing the dynamics of muonium in silicon and in particular to determine for the first time ever the binding energy of the negative muonium ion Mu_T^- . This work is complete and has been accepted for publication in Physical Review B [Hitti *et al.* (in press)].

The microwave (μw - μSR) spectrometer (0.8 to 2 GHz) operates at higher frequency than the rf which allows high field measurements to be made for tetrahedral muonium. This avoids low field broadening that is normally present due to various interactions. We used the μw spectrometer to measure the amplitude of the neutral state Mu_T^0 at low temperature in Si and

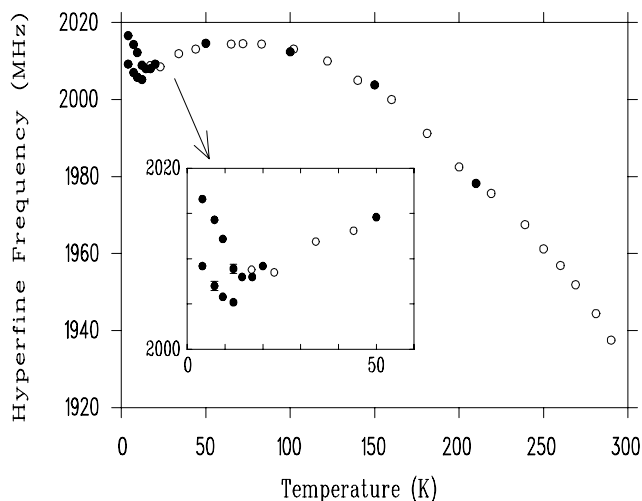


Fig. 69. The Mu_T^0 hyperfine frequency in Si as a function of temperature. The open circles are the values measured by Holzschuh [*op. cit.*], the filled circles are from our μw data.

observed unexpected structure. Below 14 K two signals corresponding to two different values of the hyperfine parameter were observed for the first time. This new result appears to be related to the anomaly in the measured hyperfine frequency of Mu_T^0 in Si below 50 K first reported by Holzschuh in 1983 [Phys. Rev. **B27**, 102 (1983)]. In Fig. 69 the values of the hyperfine frequency obtained from the μw experiment (filled circles) and those measured by Holzschuh (open circles) are plotted as a function of temperature. Holzschuh used a zero field high timing resolution apparatus and directly measured the transition between the triplet and singlet energy levels of Mu_T^0 in Si. The agreement between the two techniques is very good down to 20 K, the lowest temperature measured by Holzschuh.

A satisfactory explanation of this structure and the temperature dependence is lacking. There is indirect evidence of rapid long range tunneling of Mu_T^0 in Si which makes two distinct structures with different hyperfine values hard to understand. Experiments using the high magnetic field high timing resolution apparatus are planned and should provide additional information on whether one of the signals is related to delayed formation of Mu_T^0 and/or muons stopped close to a ^{29}Si isotope.

Experiment 749

Muonium-substituted free radicals

(*P.W. Percival, SFU*)

The purpose of Expt. 749 is to study the structure and intramolecular motion of organic free radicals. Muon hyperfine constants are measured by transverse-field muon spin rotation (μSR) and, where necessary, radio frequency muon spin resonance (rf- μSR). Other

hyperfine constants are determined by muon level-crossing resonance (μ LCR). Of recent interest are the muonium adducts of fullerenes and various polyaromatic hydrocarbons which can be viewed as fragments of fullerenes. The overall question being pursued is: How does curvature of an unsaturated carbon skeleton affect radical adduct formation?

In the summer we investigated fluoranthene (Fig. 70). The transverse field μ SR spectrum (Fig. 71) shows the presence of five radicals – note that there are two almost degenerate signals close to 60 MHz. Each radical gives rise to a pair of muon precession frequencies, but only the low frequencies' signals are visible in the range displayed in Fig. 71. The radicals are formed by Mu addition to different carbon sites in fluoranthene, which has in all 9 unique carbons: 1,2,3,7,8,11,12,15,16.

To identify the sites of Mu addition we turned to muon level-crossing spectroscopy (μ LCR). There is a rich spectrum, as evident from Fig. 72. Each resonance

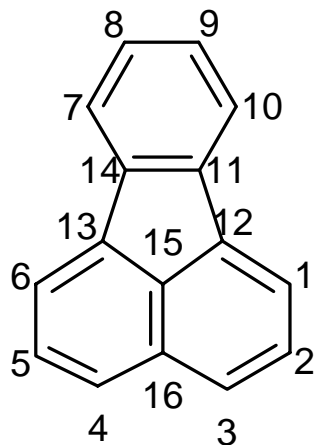


Fig. 70. Fluoranthene, a polyaromatic hydrocarbon. Not shown are the hydrogen atoms attached to carbons 1–10.

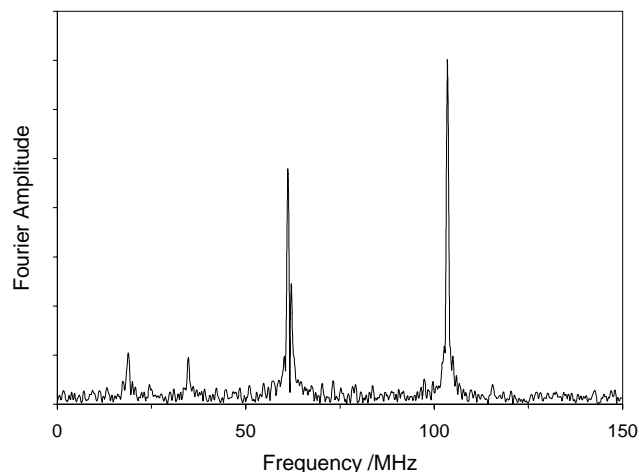


Fig. 71. Part of the Fourier μ SR spectrum from pure liquid fluoranthene at 117°C in a transverse field of 17.34 kG.

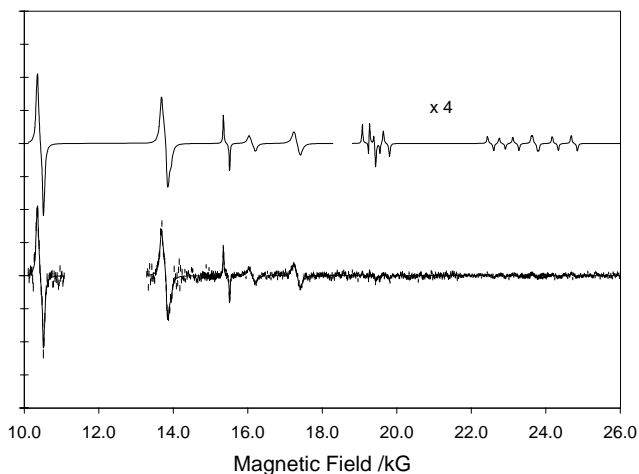


Fig. 72. μ LCR spectrum from pure liquid fluoranthene at 117°C. The solid curve represents the best fit to the data points. For clarity it is also redrawn with an offset, and with part magnified to show the weak resonances at high field.

corresponds to a particular value of a proton hyperfine constant (hfc). Some of the resonances are due to -CHMu- groups, i.e. the relevant radical is formed by addition of Mu to a carbon to which a H atom is bound. Such resonances are relatively easily identified, as the H and Mu atoms are effectively isomers, subject to the same electron spin distribution. There is a trivial isotope effect, due to the different magnetic moments of the proton and the muon, but there is also an effect which has been ascribed to zero-point vibrations of the C–Mu bond. This latter effect has been well characterized in other similar radicals (cyclohexadienyl and pyrenyls) and amounts to a factor of about 1.2 in favour of the muon hfc. Thus, the resonances at 10.43, 13.77, 13.86, 16.12 and 17.33 kG are assigned to -CHMu- structures of the five radicals detected by transverse field μ SR.

The remaining resonances are all consistent with so-called α Hs – H atoms attached to carbon sites with significant unpaired electron spin density. Their hyperfine constants are predicted to be *negative*, as opposed to the positive hfc's characteristic of the -CHMu- groups. A preliminary assignment of individual resonances with particular muon hfc's (i.e. particular radicals) gives plausible values for the corresponding proton hfc's, and the predicted narrow linewidths are also in accord with experiment. Final confirmation and assignment of the measured hyperfine constants to specific radicals awaits quantum chemical calculation of the various isomeric radical structures and spin distributions. However, it already seems clear that only five radicals are formed, and that these correspond to Mu addition at carbons 1+6, 2+5, 3+4, 7+10, and 8+9. There is no sign radicals formed by Mu addition at carbons 11–16.

Experiment 751

μ SR measurements of off-axis internal magnetic fields in anisotropic superconductors

(*W.J. Kossler, College of William and Mary*)

The major accomplishments of this experiment so far have been:

- The discovery of magnetic transparency of the ab planes to magnetic fields in the superconducting state of BSCCO.
- The observation of longitudinal field depolarization associated with vortex motion.

Transparency of the ab planes in highly anisotropic superconductors

For many anisotropic superconductors, e.g., $\text{YBa}_2\text{Cu}_3\text{O}_7$ (YBCO) the anisotropy may be represented by an effective mass tensor. Then one finds the fields from the minimization of the free energy:

$$\mathcal{F} = \frac{1}{8\pi} \int_V (b^2 + \lambda^2 m_{ij} (\nabla \times \vec{b})_i (\nabla \times \vec{b})_j) dV \quad (1)$$

The effective reduced mass tensor m_{ij} expresses the anisotropy and m_c/m_{ab} , the ratio of the mass along \mathbf{c} to mass along the \mathbf{a} or \mathbf{b} is a measure of this anisotropy. For an isotropic superconductor $m_{ij} = \delta_{ij}$ and the currents form vortices independent of crystalline axis (top of Fig. 73). For YBCO this mass ratio is about 25. The vortices that then form have currents which are not everywhere perpendicular to their axes. This is shown in the lower left portion of Fig. 73. This model produces vortices of a 3D tilted nature and has average fields parallel to the axis of this tilted vortex even for arbitrarily large masses along the \mathbf{c} axis.

For BSCCO the anisotropy is much larger than for YBCO and is of order 3000. Such extreme anisotropy had previously led Lawrence and Doniach to introduce a model in which the weak inter-planar coupling along the \mathbf{c} axis occurs via Josephson tunneling. Clem introduced the notion of ‘‘pancake’’ vortices which are confined to the CuO planes for these extremely anisotropic systems. The general picture is shown schematically in the bottom centre of Fig. 73. Clem and Artemenko and Kruglov have shown how one may calculate the magnetic fields of pancake arrays. Clem has further shown that the equilibrium arrangement in the limit of very weak coupling is like that shown in the lower right portion of Fig. 73, i.e., the pancakes of current line up on top of each other along the \mathbf{c} axis while the field in the \mathbf{ab} planes penetrates freely and unshielded.

When cosine transforms are performed on $P_{yz}(t)$ and $P_{yy}(t)$, (initial polarization along y and detection along z and y respectively), only those components

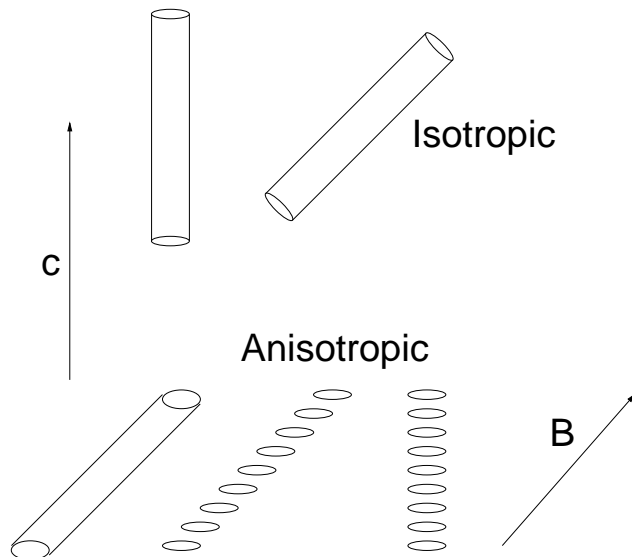


Fig. 73. For the isotropic case a vortex may be considered to be a tube like structure oriented in any direction. This is illustrated in the top portion. For the anisotropic case, one may have tube like structures with currents tipped with respect to the axis or separated pancakes of current, see the text.

with $b = \omega/\gamma\mu$ will be selected from the distribution of fields. We thus obtain the Fourier amplitudes:

$$\tilde{P}_{yz}(\omega) = \frac{dn \langle b_z b_y(\omega) \rangle}{db b^2} \quad (2)$$

and

$$\tilde{P}_{yy}(\omega) = \frac{dn \langle b_x^2(\omega) + b_z^2(\omega) \rangle}{db b^2}. \quad (3)$$

Here the terms enclosed within $\langle \dots \rangle$ refer to the average value of the expression at the given ω . Note that if the internal fields pointed everywhere in the same direction, as in isotropic superconductors, the ratio of fields factors in these cosine transforms would be dependent on the direction, but not the magnitude of the field. Then $\tilde{P}_{yz}(\omega) \propto \tilde{P}_{yy}(\omega)$ and the cosine transforms have exactly the same shape.

We have applied this technique to a BSCCO sample. A field of approximately 100 G was applied 45 degrees from the beam axis in the \mathbf{yz} plane, (y vertical, and z along the beam). The sample was field cooled to 2 K. The cosine transforms of data taken in this configuration are shown in the top portion of Fig. 74. For both detector pairs one sees a strong peak centered near the 8.5 Mrads^{-1} expected for a 100 G external field.

Immediately after taking this data the external field was turned off while maintaining the temperature at 2 K. The cosine transforms for this zero field arrangement are shown in the bottom portion of Fig. 74. There are two striking features to observe. First, the peak from the F-B data is now completely missing. The disappearance of this peak may be simply understood in

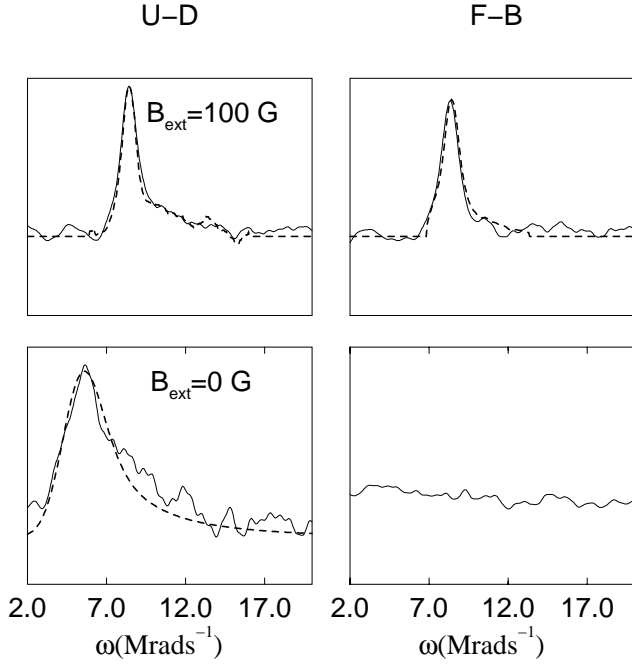


Fig. 74. Fourier transforms for the data from the U-D and F-B detector arrays for BSCCO single crystals. The top set was for field cooled and the field still applied. The bottom pair were taken immediately after $B_{ext.}$ was set to 0. All data were at 2 K. The dashed line in the upper left is our prediction from the data of the lower left, see text. The dashed line of the lower left is derived from a vortex lattice model with $\lambda_{ab} = 2000$ Å and a local field variation of 13 G.

that the muons are precessing around a field totally aligned along the \mathbf{c} axis so that the angle the spin makes with respect to this direction is constant. Second, the peak in the U-D data has shifted to about 70 G, as would be expected for precession about only the field component along the \mathbf{z} direction, i.e., $\langle b_z \rangle \approx 70$ G and $b_y = 0$.

With the external field off, the U-D cosine transform for the BSCCO remained invariant at 2 K and 10 K for time periods of at least an hour. This implies that the field along \mathbf{c} axis was pinned at these temperatures. If the vortices were truly three dimensional, as in the tilted stack structure in the lower middle of Fig. 73, and if they maintained a 3D integrity through this sample as the field was turned off, vortices at their ends would have to move a distance ≈ 0.05 mm, half the crystal thickness, in order to form their final vertical stacks. We believe such motion to be inconsistent with the observed pinning. Further, to maintain a constant magnetic flux through the sample, pancake vortices would have had to enter and leave through the sample sides as the field was reduced to zero. This too is inconsistent with the observed pinning. Thus the pancake vortices must not be arranged with tilted correlations which would lead to a trapped tilted average field, but may at most have \mathbf{c} axis aligned correlations.

With only pinned \mathbf{c} axis correlations, the magnetic field in the \mathbf{ab} planes is just the applied field component, i.e., even at 2 K the \mathbf{ab} planes are transparent to magnetic fields. This agrees with the suggestion of Clem, illustrated at the lower right of Fig. 73, that for sufficiently weak interplanar coupling, the vortices would form stacks along the \mathbf{c} axis.

To test this transparency notion we predicted the Fourier transform of the top left of Fig. 74 from the data of the lower left of Fig. 74 as follows: When an applied field is present, the local magnetic field would arise from a \mathbf{z} distribution, dn/db_z , as determined from the data of the lower left of Fig. 74, plus a fixed component in the \mathbf{y} direction. The probability of b is then:

$$\frac{dn}{db} = \frac{dn}{db_z} \frac{db_z}{db}; \quad b^2 = b_y^2 + b_z^2. \quad (4)$$

Thus from Eq. 3 we expect:

$$\tilde{P}_{yy}(\omega) \propto \frac{dn}{db_z} \frac{b_z}{b}. \quad (5)$$

The dashed curve in the top left of Fig. 74 is the result of this transformation of the data of the bottom left of that figure plus a residual background component. Further, we can predict from Eqs. 2 and 3 that

$$\tilde{P}_{yz}(\omega) = \frac{b_y}{b_z} \tilde{P}_{yy}(\omega). \quad (6)$$

The dashed line in upper right of Fig. 74 is this prediction. Thus, we see that an assumption of perfect \mathbf{ab} transparency, combined with a fixed \mathbf{c} oriented pancake correlation allows us to predict the applied field case in excellent agreement with experiment.

For comparison, we performed a similar experiment using a large single crystal of YBCO with pinning inclusions. As for BSCCO, the YBCO sample was first field cooled to 2 K in an applied field of about 100 G, 45 degrees from the \mathbf{c} axis, and at 2 K the applied field was then turned off. The cosine transforms at the lowest temperatures with field off are identical to those with the field on. This implies that the vortices are 3 dimensional and completely pinned.

Vortex motion

The muon's polarization parallel to a static local field at the muon's site remains fixed. But if the local field has fluctuating components perpendicular to its local average these will lead to a slow loss of polarization proportional to $\exp(-(\gamma_\mu b_\perp)^2 \tau t)$.

For most studies of superconductors it would be expected that local vortex density fluctuations give rise to the largest field fluctuations. These field fluctuations, for the case that the field is applied parallel to

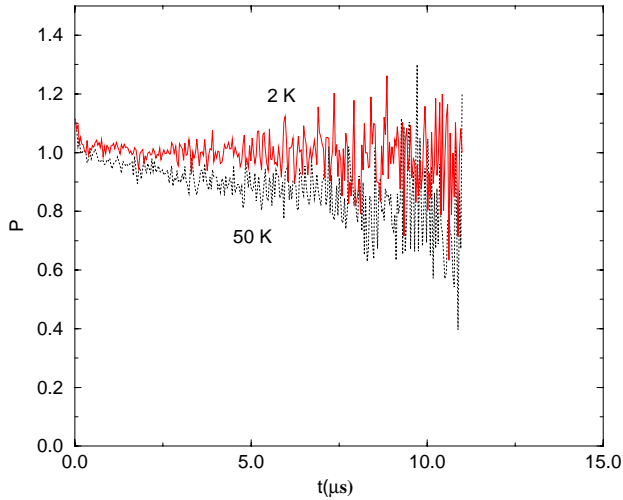


Fig. 75. The longitudinal depolarization in BSCCO for a 100 G field 45 degrees from the \mathbf{c} axis.

the one of the principal axes, are parallel to the vortices themselves and hence parallel to the average field and therefore produce no perpendicular field and no depolarization. But if the average field is tipped relative to \mathbf{c} , longitudinal depolarization experiments can be carried out.

For our study of off-axis fields in BSCCO we used a 100 G field at 45 degrees from the \mathbf{c} axis and an initial polarization roughly along the y axis. After first calibrating the detectors with a field along the x direction we obtained the polarization component parallel to the applied field seen in Fig. 75.

That we can see depolarization at 50 K is evidence for local fluctuations of the magnetic field. Note that in the case of a field 45 degrees from the \mathbf{c} axis and with currents dominantly in the \mathbf{ab} planes the field fluctuations will be along the \mathbf{c} axis and hence have components perpendicular to the average field.

We propose to carry out high statistics measurements of all the samples and for a variety of applied fields to measure the temperature and field dependence of τ .

Experiment 774

Muonium dynamics in GaAs

(*B. Hitti, S.R. Kreitzman, TRIUMF*)

The goal of this experiment is to further the understanding of hydrogen dynamics in the technologically important compound semiconductor GaAs. Direct resonance techniques are not practical and since the muon is an electronic analogue of the proton in these materials μ SR can be used to extract much of the relevant information. Experiment 774 is a long term research project in which we plan to use the various techniques of muon spin rotation/relaxation (μ SR) to obtain dynamical information similar to our highly successful results in Si.

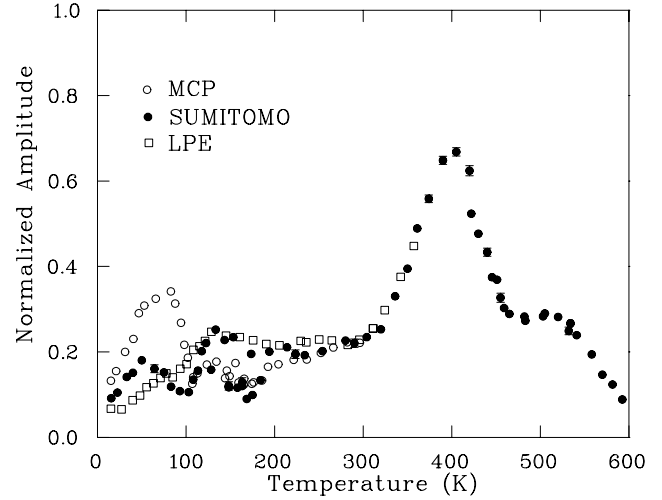


Fig. 76. The temperature dependence of the diamagnetic fraction in two commercial undoped semi-insulating GaAs samples (MCP and SUMITOMO) and in a high quality n -type ($2 \times 10^{13} \text{ cm}^{-3}$) liquid phase epitaxy (LPE) GaAs sample.

To date (c.f. Fig. 76) we have used the radio frequency (rf) μ SR technique to measure the temperature dependence of the diamagnetic fraction in two commercial semi-insulating (SI) samples and one high quality liquid phase epitaxy (LPE) n -type sample with carrier concentration of about $2 \times 10^{13} \text{ cm}^{-3}$. Several differences are apparent in the behaviour of the diamagnetic amplitude measured in the three samples. Starting at low temperature the peak near 50 K observed in the two commercial samples is not present in the LPE sample. The diamagnetic amplitude in the LPE sample increases monotonically up to 100 K similar to some of the doped Si samples where the increase was shown to result from the ionization of shallow dopant. Between 100 and 300 K, the two commercial samples show a complicated behaviour while the LPE sample is flat at about 20%. In all three GaAs samples the diamagnetic fraction does not increase at the expected ionization temperature of the neutral muonium states, about 100 K for Mu_{BC}^0 and 200 K for Mu_T^0 . The data below room temperature indicate the presence of intrinsic defects related to deviation from ideal stoichiometry and structure control the material properties of commercial SI samples and make it impossible to obtain sample independent data.

The diamagnetic amplitude measured in the SUMITOMO sample starts to increase above room temperature and peaks near 400 K. This is followed by a plateau centered around 500 K and then a second drop. Only few points are available from the LPE sample above room temperature but the presence of the EL2 defect in commercial material dictates that it is very important to gather high temperature (LPE) data before drawing any conclusions about the nature of the

400 K peak. Finally, the drop centered around 550 K is expected to result from charge exchange involving electrons thermally ionized across the bandgap.

Overall, it is clear that more easily comprehensible results will be obtained from the LPE samples (which have much lower defect concentrations than commercial SI samples) and future experiments will initially concentrate on these. Two μ SR techniques are at our disposal. The rf- μ SR experiment detects a given centre independently of whether it is formed promptly upon muon implantation or slowly by a transition from a precursor state, and thus detects *final* state amplitudes. In contrast the more standard transverse field (TF) technique is limited by the requirements of phase coherence to detect states that form only rapidly within a small fraction of the (high) frequencies associated with any precursor state. These two techniques are complementary in the information they provide, viz. the initial and final occupancy fractions of the various charge states in the material. Our plans are therefore to utilize rf- μ SR measurements (which are state selective) to complete the temperature dependence of final state diamagnetic amplitude and to obtain analogous data for the two neutral states. TF experiments (which can be obtained simultaneously for all states) will then give us the required temperature dependence amplitudes of the prompt states.

Experiment 776

Rare-earth materials with disordered spin structures

(D.R. Noakes, Virginia State)

This experiment is a muon spin relaxation (μ SR) study of RE-Mg-Zn (RE = rare earth) quasicrystals and PrP_x induced moment “spin glasses”, motivated by the common features in the results of Expt. 665 (Al-Mn-Si quasicrystals) and Expt. 640 (low carrier density Kondo-lattice CeNiSn and related materials). Results of our study of the rare earth quasicrystals, discussed in the previous Annual Report, have now appeared in Phys. Lett. A [Noakes *et al.*, Phys. Lett. **A238**, 197 (1998)].

The rare earth quasicrystals behaved magnetically like fairly standard dense-moment spin glasses, with some interesting particular details, and a further addition to the mystery of power-exponential relaxation. In contrast, our PrP_x failed to exhibit spin-glass freezing (in spite of freezing reported in the literature), and instead showed unusual paramagnetic dynamics, which require some explanation.

Normally, when magnetic moments in a sample are static, causing a static field distribution at the muon sites, this will generate faster relaxation of polarization than when the moments become dynamic. A fast

enough fluctuation rate should even decouple the moments from the muon, leaving no evidence of the moments. This behaviour is seen with the standard Gaussian distribution of local fields and simplistic strong-collision dynamics, which are completely random. This then is the representation of ordinary paramagnetic materials in μ SR. Dilute spin glasses are known to have Lorentzian field distributions in their frozen states and also show dynamic decoupling at higher temperatures, in their paramagnetic states. Strong-collision dynamics do not decouple the Lorentzian distribution, however, and in the 1980’s Uemura showed that local-environment correlations in dilute spin glasses modify the dynamics so that decoupling still occurs.

It was then a surprise to find that in PrP_x samples, zero-field (ZF) and (LF) μ SR spectra below 40 K fit best to strong-collision-dynamic Lorentzian Kubo-Toyabe relaxation functions. At first, the indications of this were weak, because while the generic features of strong-collision-dynamic Lorentzian relaxation have been known for a long time, there are no closed-form expressions for it. To fit, interpolation tables can be developed from numerical simulations, and good approximations must be used when parameters move outside the range of those tables. J.H. Brewer had developed the required tables in the 1980’s, but the equally essential approximations had not been identified, because there had been no data that needed them until now. For a Gaussian distribution with width B_{rms} and applied longitudinal field B_{LF} it is known (from NMR) that in the limit of fast fluctuations $\nu \gg \Delta$ (where $\Delta = \gamma_{\mu} B_{\text{rms}}$, the muon Larmor precession frequency in B_{rms}) the relaxation becomes exponential with rate:

$$\lambda_G \cong \frac{-2\Delta^2 t / \nu}{1 + (\omega_{LF}^2 / \nu^2)},$$

where $\omega_{LF} = \gamma_{\mu} B_{LF}$. We have found that for a Lorentzian distribution of width B_{hwhm} in the same case (applied LF, $\nu \gg a = \gamma_{\mu} B_{\text{hwhm}}$),

$$\lambda_L \cong \frac{-4at/3}{\sqrt{1 + (\omega_{LF}^2 / \nu^2)}}.$$

Incorporating this into the TRIUMF standard MSR-FIT program, we have obtained reasonable fits to all our PrP_x data.

There then is the question of how strong-collision dynamics can take place in a Lorentzian field distribution in PrP_x, when they do not occur in ordinary dilute spin glasses. Ordinary spin glasses feature stable magnetic moments. When dynamics begin as temperature is raised, individual moments change orientation without changing magnitude. This moment stability is a crucial feature in the local environment model

leading to correlated local field dynamics and fluctuation decoupling in dilute spin glasses. PrP, however, exhibits “singlet ground state” magnetic effects. The praseodymium electronic moment is generated by a $J = 4$ angular momentum state of its unpaired electrons, the individual J_z substates of which have charge-multipole moments which interact with the “crystalline electric field” at each Pr site generated by all the other charges in the lattice. This causes energy differences, between the nine J_z states, that can be from ~ 1 K to hundreds of K effective temperature. In PrP, it happens that the Pr ground is an isolated non-magnetic singlet state, with magnetic excitation states above 60 K. When measurement temperature drops below 60 K, then magnetic states become depopulated, and the magnetic response of the material weakens. Thus PrP has *unstable magnetic moments* below 60 K. The removal of a fraction of the phosphorus ions, to make PrP_{0.9}, is supposed to rearrange the J_z levels of Pr ions adjacent to vacancies, make their ground states magnetic, and so generate spin-glass freezing, but we do not see that. Instead, our Lorentzian distribution with strong collision dynamics can be explained by slow fluctuations of each Pr ion out of a non-magnetic ground into a magnetic excited state, and back to non-magnetic again. We plan to present the details of this work at the International Conference on μ SR to be held in Switzerland in the summer of 1999.

Neither the rare earth quasicrystals nor the PrP_x samples generated the shallow, static relaxation functions we had observed as the common feature of Mn quasicrystals and Ce(Ni,Cu)Sn alloys, so those still stand in some isolation. Noakes, however, has completed Monte Carlo simulations showing that our idea of “range-correlated moment magnitude variation” (RCMMV), mentioned in last year’s Annual Report, does indeed generate the shallow, static relaxation functions observed, and that the depth of the minimum is governed by the correlation length over which ion-moment magnitudes remain the same. A manuscript describing the work has been accepted for publication in *J. Phys. Cond. Matter*.

Experiment 777

Vortex state of s-wave superconductors investigated by muon spin rotation

(R.F. Kiefl, TRIUMF-UBC; G.M. Luke, McMaster; R. Kadono, KEK-IMSS)

Motivation

The goal of Expt. 777 is to elucidate the structure and behaviour of magnetic vortices in conventional superconductors using μ^+ SR to probe the magnetic field distribution near the vortex cores. Under Expt. 777, we have measured the core radius and magnetic pene-

tration depth in NbSe₂ and recently in LuNi₂B₂C.

Many recent articles about conventional superconductors followed the 1989 discovery with scanning tunneling microscopy (STM) of bound states in the vortex cores of NbSe₂. These bound states were predicted theoretically in the 1960’s, and shown in 1974 by Kramer and Pesch to give rise to a sharp shrinking in the vortex core with decreasing temperature. Recent numerical calculations have confirmed their prediction. These predictions, however, are in strong disagreement with the popular Ginzburg-Landau theory, which predicts a constant core radius at low temperature.

NbSe₂

We have previously reported measurements of the temperature dependence of the core radius in NbSe₂ at low temperature (see 1997 Annual Report, Experiment 777). A further investigation over a larger temperature range confirmed our earlier findings that the core radius does not shrink dramatically with decreasing temperature. This work is currently being written up.

LuNi₂B₂C

In November, we made a series of measurements in the borocarbide LuNi₂B₂C ($T_c = 16$ K). Initial analysis of the temperature dependence of the vortex core radius in LuNi₂B₂C seems to show a sharp shrinking of the core radius as the temperature is lowered to 2 K. Figure 77 shows the Fourier transform of the muon polarization signal in LuNi₂B₂C at 8 K ($T = T_c/2$) and at $T = 2.5$ K. Initial analysis of the muon polarization in the time domain suggests that the change in the high-field tail is due to a shrinking of the core radius.

Detailed analysis of the data is ongoing. It is not very clear why this Kramer Pesch effect may occur in a borocarbide but not in NbSe₂, both of which belong to the class of conventional superconductors. Furthermore, we expect to have characterized the field dependence of the vortex core radius in LuNi₂B₂C upon completion of the analysis.

Doped conventional superconductors

A decision to begin a collaboration with the KEK-IMSS group has now brought all current μ^+ SR research at TRIUMF on borocarbides into Expt. 777. This collaboration will also allow Expt. 777 access to more samples. Recent specific heat measurements comparing YNi_{1-x}Pt_xB₂C with pure YNi₂B₂C and Nb_{1-x}Ta_xSe₂ with pure NbSe₂ [Nohara *et al.*, (submitted to *Phys. Rev. Lett.*)] lead us to hypothesize that the introduction of dopants in the superconducting borocarbides and NbSe₂ may weaken the previously reported strong field dependence in the vortex core radius. We

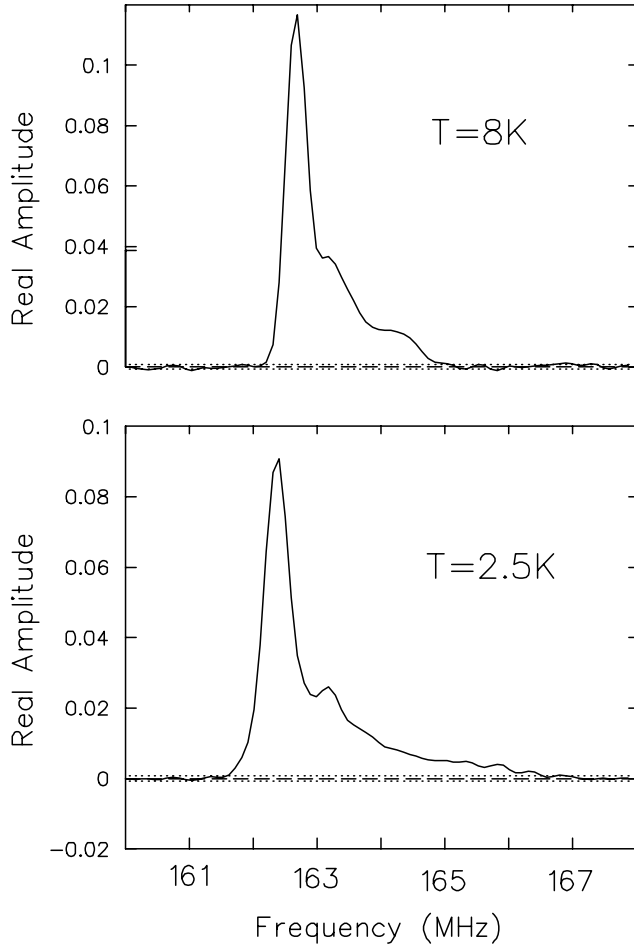


Fig. 77. Fourier transform of the muon polarization signal in $\text{LuNi}_2\text{B}_2\text{C}$ at $T = 8 \text{ K}$ and $T = 2.5 \text{ K}$, in a field of 12 kG.

hope to characterize the temperature and field dependence of the vortex cores in both $\text{Nb}_{1-x}\text{Ta}_x\text{Se}_2$ and $\text{YNi}_{1-x}\text{Pt}_x\text{B}_2\text{C}$ in July, 1999.

MULTI high flux spectrometer

Construction of a new high flux spectrometer, designed to increase the rate of acquisition of muon decay events by a factor of ten, is nearing completion. Currently, the spectrometer is undergoing off-line tests and new software for the data acquisition program is being designed and written. We hope to test MULTI in a high-rate muon beam in May, 1999.

Experiment 782

Non-fermi-liquid behaviour and other novel phenomena in heavy-fermion alloys

(D.E. MacLaughlin, California-Riverside)

Nozières [J. Low Temp. Phys. **71**, 205 (1974)] was the first to suggest that low-lying excitations in Kondo alloys can be described by Landau’s fermi-liquid theory, in which there is a one-to-one correspondence between the excitations of the correlated-electron system and those of a free-electron gas. Signatures of this

fermi-liquid behaviour are usually taken to be the well-known low temperature thermal and transport properties of a fermi liquid: the susceptibility $\chi(T)$ and Sommerfeld (T -linear) coefficient $\gamma(T) = C(T)/T$ of the specific heat both become constant as $T \rightarrow 0$, and the resistivity $\rho(T)$ varies asymptotically as T^2 . Fermi-liquid behaviour has also become the canonical description of concentrated Kondo or heavy-fermion systems, principally alloys and intermetallic compounds of lanthanide (Ce, Yb) and actinide (U) ions.

A large and growing number of heavy-fermion alloys are not described by this fermi-liquid picture. Thermal and transport properties of these so-called non-fermi-liquid (NFL) materials as $T \rightarrow 0$ seem to fall into a limited number of classes; most (but not all) exhibit a logarithmic divergence of $\gamma(T)$ and a linear departure of $\rho(T)$ from its value at $T = 0$. The susceptibility has been reported to vary either as $1 - b(T/T_K)^{1/2}$ or as $-\ln(bT/T_K)$, where T_K is the Kondo temperature and b is a dimensionless factor of order unity. Nearly all NFL heavy-fermion materials are disordered alloys, and all are found in the neighbourhood of a transition to magnetic order in a temperature-composition phase diagram. Both Ce- and U-based heavy-fermion alloys exhibit NFL behaviour, and it is found both with and without a disordered f sublattice.

A number of mechanisms for NFL behaviour have been proposed, of which two have received the most attention to date. These are (a) the multichannel Kondo effect, first associated with a two-channel quadrupolar Kondo mechanism by Cox [Phys. Rev. Lett. **59**, 1240 (1987)] and since extended to other mechanisms for two-channel Kondo screening, and (b) magnetic instability due to a quantum critical point at zero temperature, the critical behaviour of which generates NFL properties [Millis, Phys. Rev. **B48**, 9887 (1993)]. Our μSR and NMR studies of NFL systems have raised the possibility of a third possible mechanism: an inhomogeneous distribution of Kondo temperatures due to structural disorder in the alloy, referred to as “Kondo disorder”.

We have carried out TF- μSR measurements in the nominally ordered NFL compounds UCu_4Pd and CeNi_2Ge_2 , for the purpose of determining the role of structural disorder in the formation of the NFL state which characterizes these materials. The goals of our μSR studies of NFL behaviour are (a) to ascertain the applicability of disorder-driven mechanisms by measuring the consequent inhomogeneity of the magnetic susceptibility [MacLaughlin *et al.*, J. Phys. Condens. Matter **8**, 9855 (1996)], and (b) to determine whether static magnetism, which could affect bulk properties and masquerade as NFL behaviour, is present.

We have also studied ZF- μ SR in the $4f$ -electron compound PrAg_2In , which exhibits a novel nonmagnetic form of Kondo behaviour at low temperatures. Here it is the nonmagnetic character of the Kondo effect which is the primary subject of interest, although the possibility of NFL behaviour in nonmagnetic Kondo systems has been raised on theoretical grounds.

Non-fermi-liquid heavy-fermion systems

In a recent neutron scattering study on a stoichiometric sample of the NFL heavy-fermion compound UCu_4Pd [Chau *et al.*, Phys. Rev. **B58**, 139 (1998)], it was reported that the data suggest an ordered structure, thus casting doubt on the Kondo disorder mechanism for this compound. The experimental uncertainty in the degree of disorder in these measurements was, however, considerable. Our μ SR results show that the μ SR linewidth increases strongly with decreasing temperature, in quantitative agreement with our previous results [Bernal *et al.*, Phys. Rev. **B54**, 13000 (1996)] and predictions of disorder-driven theories of NFL behaviour [Miranda *et al.*, Phys. Rev. Lett. **78**, 290 (1997); Castro Neto *et al.*, Phys. Rev. Lett. **81**, 3531 (1998)] in the same sample used for the neutron scattering experiments. Figure 78 shows this agreement in a plot of the quantity $\delta K/(a^*\chi)$ vs. bulk susceptibility χ , where δK is the spread in muon frequency shifts derived from the linewidth and a^* is an effective hyperfine coupling constant. This quantity is an estimator of the relative spread $\delta\chi/\chi$ of the inhomogeneous local susceptibility. The data are compared with $\delta\chi/\chi$ from the Kondo disorder theory in Fig. 78, where it can be seen that the agreement is quite good.

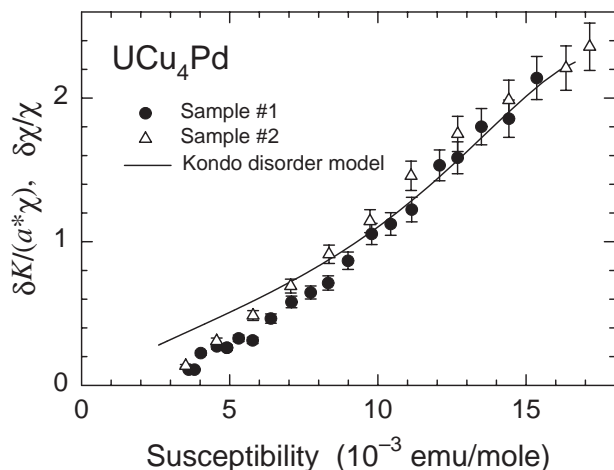


Fig. 78. Dependence of $\delta K/(a^*\chi)$ on bulk susceptibility χ , with temperature an implicit parameter, in UCu_4Pd . Symbols are defined in the text. Sample #1: previously-studied sample [Bernal *et al.*, *op. cit.*]. Sample #2: present sample, used in neutron diffraction studies [Chau *et al.*, *op. cit.*]. Curve: $\delta\chi/\chi$ from the Kondo disorder theory [e.g. MacLaughlin *et al.*, *op. cit.*].

Our results show that the neutron data cannot be taken as evidence for structural order in UCu_4Pd . We argue that the susceptibility inhomogeneity is due to residual disorder, which also dominates the NFL behaviour. The data also show that the correlation length which characterizes the susceptibility inhomogeneity is short (~ 1 lattice spacing or less), and that the low temperature U-moment relaxation rate is rapid ($\sim 10^{12} \text{ s}^{-1}$ or greater). These results constrain cluster-based models of NFL behaviour, such as that of Castro Neto *et al.* [*op. cit.*], as the clusters can be neither too large nor too slowly fluctuating at the temperatures of measurement.

These results motivated a study of structural disorder in UCu_4Pd using the x-ray-absorption-fine-structure (XAFS) technique [Booth *et al.*, Phys. Rev. Lett. **81**, 3960 (1998)], which discovered unambiguous evidence for Cu/Pd site interchange disorder of the right amount to account for the needed T_K distribution width in the Kondo disorder model.

We have also carried out TF- μ SR studies of a powder sample of nominally ordered CeNi_2Ge_2 , in which transport and thermodynamic properties exhibit NFL behaviour at low temperatures. In CeNi_2Ge_2 the linewidth, expressed as a rms spread $\delta K(T)$ of Knight shifts, is found to vary proportionally to the average (bulk) susceptibility $\bar{\chi}(T)$ as measured by the average μ^+ Knight shift $\bar{K}(T)$ (with temperature T an implicit parameter). This is in contrast to the prediction of disorder-driven theories of NFL behaviour, for which $\delta K(T)$ varies as $[\bar{\chi}(T)]^2$ or faster. Thus the quantity $\delta K(T)/\bar{K}(T)$, which is an estimator of the fractional susceptibility inhomogeneity $\delta\chi(T)/\bar{\chi}(T)$, is nearly temperature independent, in contrast to our results in UCu_4Pd (Fig. 78). The observed muon line broadening in CeNi_2Ge_2 is of the same order as the anisotropy in the magnetic susceptibility, and can therefore be attributed to anisotropy in the Knight shift rather than disorder. But the observed relative broadening $\delta K(T)/\bar{K}(T)$, after correction of $\bar{K}(T)$ for Lorentz and demagnetization fields, is large enough to obscure a significant contribution of disorder to the linewidth. We conclude that the data obtained to date are inconclusive as concerns the question of a disorder-driven mechanism in CeNi_2Ge_2 .

Nonmagnetic Kondo effect in PrInAg_2

In a seminal paper, Yatskar *et al.* [Phys. Rev. Lett. **77**, 3637 (1996)] reported evidence for unconventional heavy-fermion behaviour in the praseodymium-based intermetallic PrInAg_2 . This compound is one of only a handful of Pr-based materials which exhibit heavy-fermion or Kondo-like properties. Specific heat,

magnetic susceptibility, and neutron scattering experiments indicate a non-Kramers doublet (Γ_3) ground state due to crystalline-electric-field (CEF) splitting of the $\text{Pr}^{3+} \ ^1\text{H}_4$ term. The Γ_3 state is *nonmagnetic*, i.e., there are no matrix elements of the magnetic moment operator within its doubly degenerate manifold. A nonmagnetic ground state would make the heavy-fermion-like specific heat anomaly found below 1 K and the enormous low temperature Sommerfeld specific heat coefficient $\gamma(T) \approx 6.5 \text{ J mole}^{-1} \text{ K}^{-2}$ quite unexpected, and suggests that PrInAg_2 may be a system in which an unusual nonmagnetic path to heavy-fermion behaviour is realized. But such a scenario depends crucially on the nonmagnetic nature of the ground state.

We have obtained two results from μSR experiments in PrInAg_2 which support the conclusion of Yatskar *et al.* that the Kondo effect in PrInAg_2 is nonmagnetic in origin. First, we observe no temperature dependence of the muon relaxation rate at low temperatures, contrary to what would be expected if the specific heat anomaly involved magnetic degrees of freedom. Second, the temperature and field dependence of the muon relaxation indicates that the CEF ground state in PrInAg_2 is in fact nonmagnetic, since the low temperature muon relaxation appears to be due only to nuclear magnetism; no electronic magnetic moment is necessary to understand the observed rates. Quantitative agreement indicates strong *hyperfine enhancement* of the ^{141}Pr nuclear magnetic moment. Hyperfine enhancement is an effect of the hyperfine coupling between the nucleus and the Van Vleck susceptibility of f electrons of a non-Kramers f ion in a nonmagnetic ground state, and only occurs when the Pr^{3+} CEF ground state is in fact nonmagnetic.

Figure 79 shows the relaxation function $G(t)$ at 0.7 K in zero field and a longitudinal field of 100 Oe. The relaxation in 100 Oe (triangles) is much faster than expected if the zero-field relaxation (circles) were due to a static distribution of local fields. Dynamic Kubo-Toyabe fits yield a spread in muon local fields and a fluctuation rate which are quantitatively consistent with nuclear magnetism and only nuclear magnetism, provided that hyperfine enhancement of the ^{141}Pr nuclear moment is taken into account. This is strong evidence against a Pr^{3+} electronic magnetic moment, and correspondingly strong evidence for the nonmagnetic doublet (Γ_3) crystal field ground state required for a nonmagnetic route to heavy-electron behaviour. The data also imply the existence of an exchange interaction between neighbouring Pr^{3+} ions of the order of 0.2 K in temperature units, which should be taken into account in a complete theory of a nonmagnetic Kondo effect in PrInAg_2 .

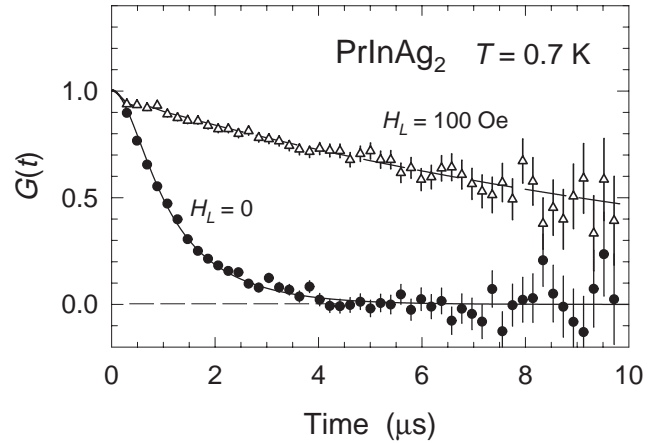


Fig. 79. Dependence of μ^+ relaxation function $G(t)$ on longitudinal applied field H_L in PrInAg_2 , $T = 0.7 \text{ K}$. Curves: fits to dynamic K-T model for $H_L = 0$ (solid curve) and $H_L = 100 \text{ Oe}$ (dashed curve).

Experiment 784

The μSR studies of spin-singlet states in oxides
(Y. Fudamoto, G.M. Luke, Y.J. Uemura, Columbia)

Static spin freezing in NaV_2O_5

NaV_2O_5 is the second inorganic compound, after CuGeO_3 , which has been considered to show a spin-Peierls transition ($T_{SP} = 35 \text{ K}$). In this report, we present muon-spin relaxation (μSR) studies of pure ($x = 1.00$) and hole-doped ($x = 0.99$ and 0.90) $\text{Na}_x\text{V}_2\text{O}_5$ systems. We have found a static magnetic freezing at $T \sim 11 \text{ K}$ in undoped NaV_2O_5 , and suppression of this freezing in Na deficient charge-doped systems. We present a possible interpretation and consider relevance to recent results of thermal conductivity.

The zero-field (ZF) μSR spectra below $\sim 11 \text{ K}$ exhibit a fast reduction of muon-spin polarization followed by a slow depolarization of about 1/3 of the total asymmetry, characteristic of relaxation due to co-existing static and dynamic random local fields. The predominant effect of static random fields at low temperatures has been confirmed by decoupling the relaxation by longitudinal fields (LF). Figure 80 shows temperature dependence of (a) the static relaxation rates Δ_i in ZF (b) the dynamic relaxation rates λ_i in ZF and LF=1 kG, and (c) the stretching power β_i above T_f in ZF. Static spin freezing at $T_f \sim 11 \text{ K}$ is indicated by (1) the sudden appearance of static field amplitude Δ below T_f , (2) a maximum of dynamic relaxation rate λ around T_f and (3) a sharp reduction of the stretching power β around T_f . The common slope of λ for $i = 1, 2$ indicates that local fields at the two different muon sites $i = 1, 2$ are subject to the same dynamic process. The high static relaxation rate $\Delta(T \rightarrow 0) \sim 35 \mu\text{s}^{-1}$ for the high-field site $i = 1$ cannot be ascribed to a freezing of dilute impurity moments. To account for the

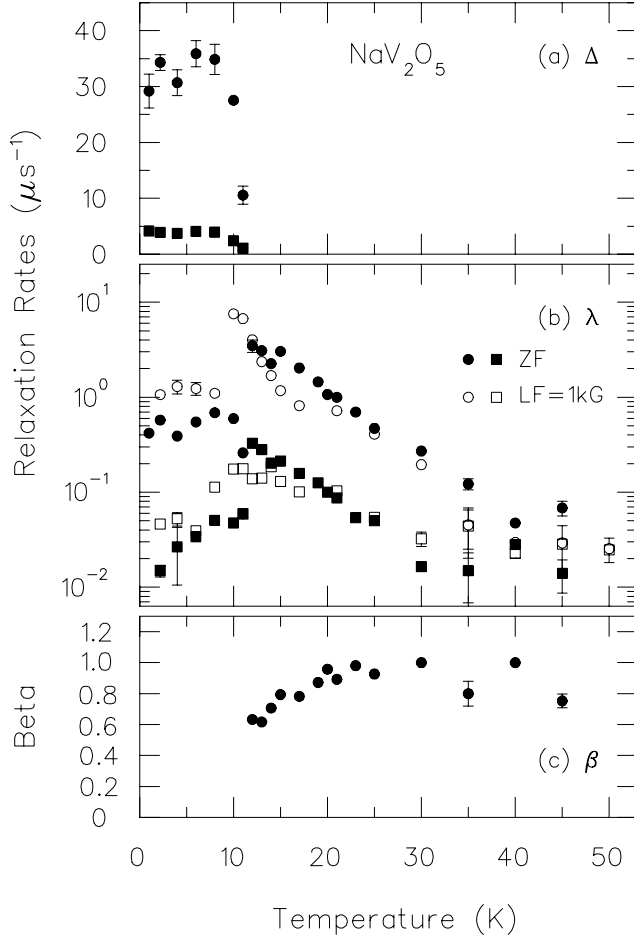


Fig. 80. Temperature dependence of (a) static relaxation rate Δ , (b) dynamic relaxation rate λ and (c) the exponent β , obtained in a (mosaic) single crystal specimen of NaV_2O_5 .

observed field amplitude, we have to assume a freezing of at least about 10% of the V^{4+} moments.

We can estimate the fluctuation rate ν of local fields by using a well known relationship $\lambda \sim 1/T_1 = 2\Delta^2/\nu$. Since stretched exponential functions with $\beta \ll 1$ have a very sharp reduction at early times, the relaxation rate resulting from stretched exponential fit with low β values tends to underestimate the average depolarization rate. To compensate for this effect, we calculated $\lambda^* = \ln(2)/[\ln(2)]^{1/\beta} \times \lambda$, and obtained an average fluctuation rate $\nu^* \equiv 2\Delta^2/\lambda^*$. Comparing with the activation behavior $\nu \propto \exp(-E_g/kT)$, we obtain a gap energy $E_g = 77$ K, which is roughly comparable to the spin-gap energy $E_g \sim 110$ K obtained in neutron measurements.

NaV_2O_5 can be doped with holes with a small Na deficiency. The spin-gap formation is suppressed with increasing Na-deficiency, and doped holes are mobile and probably move via variable range hopping. The fast static relaxation observed in pure NaV_2O_5 no longer exists in hole-doped $\text{Na}_x\text{V}_2\text{O}_5$. The dynamic re-

laxation rate also becomes smaller with increasing hole doping.

In NaV_2O_5 , we propose a picture in which a small amount of excess V^{4+} moments, as a subset spin system different from majority V^{4+} moments forming singlet pairs, undergo the spin freezing. The singlet coupling of remaining majority spins may be essential in obtaining effectively high exchange interaction between unpaired V^{4+} spins inferred from a rather high transition temperature T_f . This effective exchange coupling would be suppressed with disappearance of the spin gap, leading to disappearance of the static spin freezing. When the spin gap is suppressed, such subset unpaired spins should be subject to a fluctuation process with all other majority spins. This would reduce the dynamic muon spin relaxation rate via exchange narrowing process, similar to the situation in the paramagnetic state above T_{sp} . The activation behavior of the fluctuation rate ν of unpaired V moments below T_{sp} can be ascribed to thermal excitations of neighbouring singlet pairs to magnetically active triplet states.

Recently, Vasilev *et al.* found a giant peak of thermal conductivity κ of NaV_2O_5 around $T \sim 15$ K. The height of this peak is sharply reduced with increasing hole doping in Na deficient specimens, and the peak disappears when the spin gap is completely suppressed. Phenomenologically, this behaviour seems to be deeply related to our results, and gives another possible support for interpretation of bulk spin freezing (there is no effect of μ^+ in the κ results). The spin freezing below T_f would reduce magnetic scattering of phonons, and thus helps increasing κ . The sharp reduction of κ above T_f can be attributed to increasing spin scattering of phonons.

In summary, we found signatures of spin freezing in undoped NaV_2O_5 around $T_f \sim 11$ K. The spin freezing is suppressed when the spin gap is suppressed in charge-doped Na deficient specimens. Available information favours a picture with spin freezing of more than 10% of magnetic V moments.

This work was supported financially by NSF (DMR-95-10453, 10454, 98-02000; from USA) and NEDO (International Joint Research Grant; from Japan).

Experiment 791

Electronic structure and dynamics of charged muonium centres in semiconductors

(K.H. Chow, Lehigh; R.F. Kiefl, UBC; B. Hitti, TRIUMF)

Results of experiments on muonium in semiconductors are generally considered to be the main source of information on *isolated* hydrogen in semiconductors. Hydrogen is an important impurity which can dramatically affect the electrical and optical properties

of these technologically relevant materials. Recently, we have turned our attention to studying muonium in heavily doped p -type GaAs with the intention of addressing the issue of passivation, i.e. formation of muonium-impurity complexes. Observing and understanding this process as it happens at the microscopic level potentially available with using the μ SR technique would provide information unobtainable using other techniques used to investigate hydrogen.

A high concentration of dopants is necessary to improve the chance of passivation. At the same time, the existence of many free holes implies that all the implanted muons retain their initial positive charge. Figure 81 shows the temperature dependence of the decay (assumed to have a Gaussian functional form) of the muon polarization taken under zero-field and transverse-field conditions. The results for two samples, one doped at $2.5 \times 10^{19} \text{ cm}^{-3}$ and the other at $5 \times 10^{18} \text{ cm}^{-3}$, are shown. Both transverse-field and zero-field data are available for the $2.5 \times 10^{19} \text{ cm}^{-3}$ sample. The former is scaled by a constant factor of 1.7 so that the higher temperature (above 530 K) data for both types of experiments agree.

The results can be interpreted as follows: Initially, as the temperature is raised, there is a decrease in the

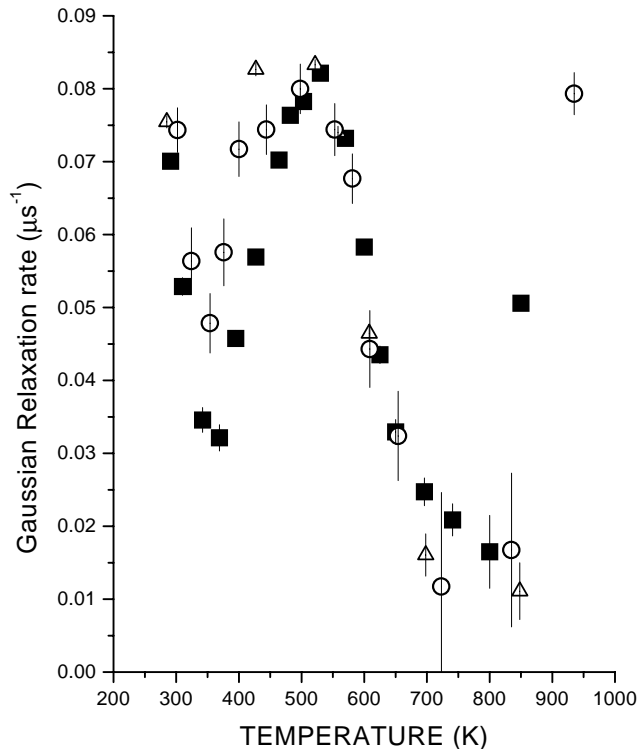


Fig. 81. Gaussian relaxation rate as a function of temperature in p -type GaAs:Zn samples. The open triangles represent the $2.5 \times 10^{19} \text{ cm}^{-3}$ and the closed squares indicate the $5 \times 10^{18} \text{ cm}^{-3}$ sample studied under zero-field conditions. In addition, the open circles show transverse-field data for the $2.5 \times 10^{19} \text{ cm}^{-3}$ sample, scaled as described in the text.

relaxation because of the increasing muon hop rate. Then, by about 530 K, the muon reaches a trap and is essentially static there. The differences between the two concentrations from 300 K to 530 K suggest that it reaches a trap site sooner in the more heavily doped sample, as would be expected. Above 530 K, breakup of the complex occurs and the muon diffuses freely through the lattice. At the highest temperatures shown ($\approx 850 \text{ K}$), charge state changing reactions occur when a sufficient number of free electrons are thermally generated. In this case, the reaction of relevance is $\text{Mu}^+ \leftrightarrow \text{Mu}^0$, probably involving alternating electron/hole capture. The differences in the two samples are due to the smaller minority electron concentration in the more heavily doped p -type material.

Clearly, more data are needed, such as zero-field measurements in the region below 530 K in the more heavily doped of the two samples. The aim of such experiments is to verify that there is indeed a dependence on the dopant concentration, as would be expected for passivation, and also to extract the relevant rate parameters. Furthermore, experiments below room temperature are also required. Future experiments on this system are likely to be interesting and are eagerly anticipated.

Experiment 792

Muonium in III-V semiconductors

(*R.L. Lichti, Texas Tech*)

The goals of Expt. 792 were to identify the muonium states in III-V compound semiconductors and to investigate the transitions among those states. Earlier data on GaAs, InP, InAs, and GaSb indicated a trapping peak in the transverse field (TF) μ SR diamagnetic signal.

Time allocated to Expt. 792 was used primarily for high field relaxation measurements in these compounds, with some additional high temperature work at low fields. Quadrupolar decoupling curves, i.e. relaxation rate vs. transverse field strength, were obtained at the trapping peaks and at low temperature. These data provided guidance in selecting the field range within which to search for QLCR spectra, which were then pursued in separate experiments. Secondly, longitudinal field depolarization studies were undertaken to investigate transition dynamics, especially for the cyclic charge state transitions present at high temperatures in most semiconductors.

Quadrupolar decoupling curves

Figure 82 shows the quadrupolar decoupling curves for an n -type sample of InP taken at 410 K on the

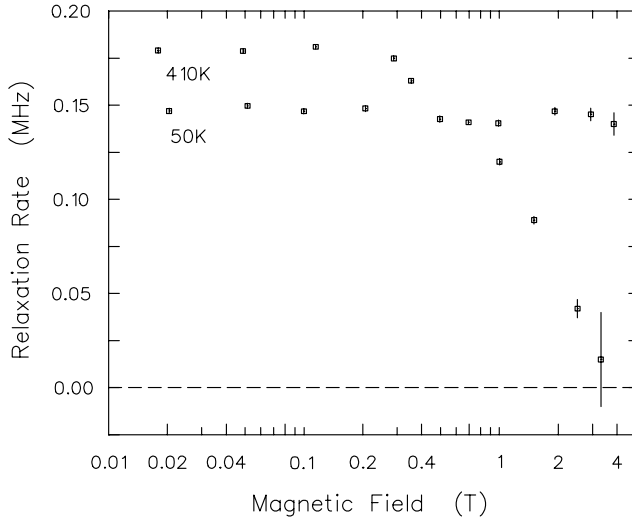


Fig. 82. Field dependence of the TF- μ SR relaxation rates at two temperatures for n -type InP. The curve for 410 K implies a site having neighbours with quadrupole moments (In) along (111) directions.

trapping peak and at 50 K where the low temperature states are still static. These curves imply that these two states have quite different local environments. Zero field relaxation data taken at these temperatures yield quite different local dipolar fields as well. Based on a combination of indirect evidence, we have assigned the state at 410 K to Mu^- . Because the state at 50 K is the same in n - and p -type InP, it has been assigned to Mu^+ .

Similar data were obtained for other III-V compounds, and in each case the conclusion is that the higher temperature trapped states are significantly different from the low temperature states. However, precisely identifying either state has proven difficult in most cases.

Transitions in semi-insulating GaAs

Figure 83 displays the diamagnetic TF- μ SR amplitude for semi-insulating GaAs indicating several transition regions, subsequently examined in longitudinal fields. The small peak in amplitude below room temperature is Mu^+ , identified by the onset of motional narrowing near 200 K as for Mu^+ in p -type GaAs rather than at 550 K which is characteristic of Mu^- [Adams *et al.*, *Phil. Mag.* **B72**, 183 (1995)]. The rise near 400 K is assigned to Mu_T^0 ionization. The additional rise above 550 K represents the effects of a high temperature charge cycle which shows up in these data as a fast relaxing diamagnetic signal. The precise nature of the transitions below room temperature is not completely clear, although they probably represent ionization of Mu_{BC}^0 in competition with a BC to T site

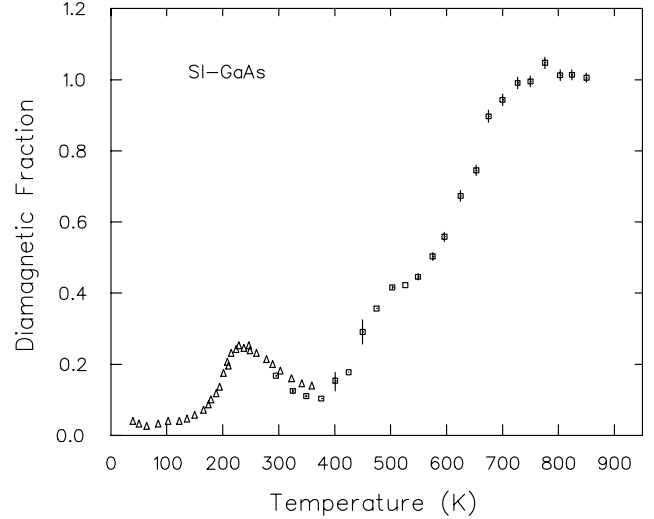


Fig. 83. Temperature dependence of the diamagnetic TF- μ SR amplitude in semi-insulating GaAs with at least four transition features. Triangles are data from ISIS to complete the curve.

change for Mu^0 , thus may provide additional evidence that the T-site is most stable for Mu^0 in GaAs.

Charge cycle characterization

The main effort in this experiment was to characterize the high temperature cyclic charge state transitions in several III-V compounds. All of the materials investigated except for InP show depolarization from charge cycles. The standard technique applied to this problem is to obtain the temperature and field dependences of relaxation rates in longitudinal field; however, when all the muons are involved in the cyclic transitions TF- μ SR relaxation rates probe the same depolarization processes.

Data for GaAs is illustrative: several n -type samples of varying concentration were studied. Above n_e of roughly 10^{17} cm^{-3} the cycles are between Mu_T^- and Mu_T^0 as previously characterized in heavily doped samples [Chow *et al.*, *Phys. Rev. Lett.* **76**, 3790 (1996)]. For semi-insulating and weakly n -type GaAs, the cycles involve Mu^+ , with results suggesting a metastable Mu_T^+ state rather than the stable Mu_{BC}^+ . There is clear evidence for two separate cycles in weakly n -type samples, with only a fraction of the muons involved below 550 K [Lichti *et al.*, *Mat. Sci. Forum* **258-263**, 849 (1997)]. Figure 84 shows the charge cycle depolarization in two samples, illustrating the difference in onset temperature of ~ 500 K for the dominant $\text{Mu}^0 \rightleftharpoons \text{Mu}^+$ cycle compared to ~ 700 K for $\text{Mu}_T^- \rightleftharpoons \text{Mu}_T^0$. Although charge cycles have been studied in other III-V materials, such as GaSb, and InAs, the data appear to be much more complicated and the exact nature of the transitions has not been determined.

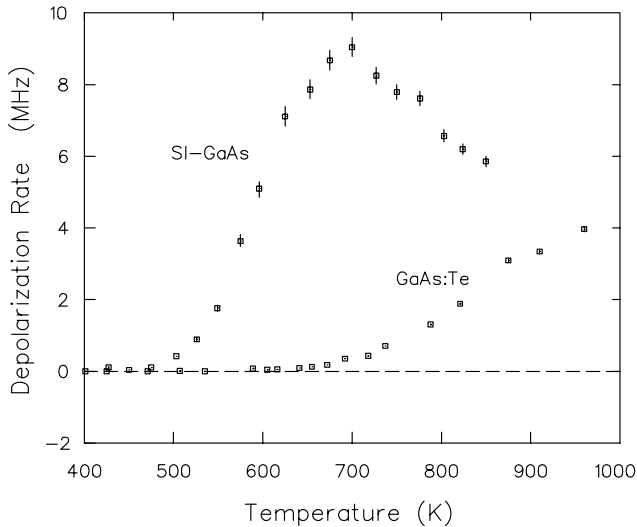


Fig. 84. Mu charge cycle depolarization rates at 10 mT in two GaAs samples: one is semi-insulating where the charged state is Mu^+ and the other is an $8 \times 10^{16} \text{ cm}^{-3}$ n -type Te-doped sample where it is Mu^- .

Experiment 804 Muonium in gallium nitride (*R.L. Lichti, Texas Tech*)

This experiment continues a long standing effort to understand the behaviour of isolated hydrogen impurities in semiconductors by investigating muonium which provides an analogous and experimentally accessible defect. The group-III nitrides are important widegap opto-electronic materials in which hydrogen plays a significant role, particularly with respect to p -type doping and electrical activity. TRIUMF Expt. 804 and associated experiments at the ISIS Facility represent the first efforts to investigate Mu in GaN.

During the past year we primarily investigated two GaN samples, both very thick (150–200 μm) c -axis oriented films. One is nominally undoped, but has an n -type concentration in the mid- 10^{16} cm^{-3} range due to an intrinsic defect. The second is doped with Si to give an n -type concentration of $\sim 10^{18} \text{ cm}^{-3}$. Very late in the year we also examined a small GaN single crystal, compensated by Mg doping.

We performed two types of μSR measurements aimed at characterizing the muonium states in GaN and studying transitions among those states. The first technique is a form of muon level-crossing resonance known as QLCR which probes the interaction of diamagnetic muonium centres with neighbouring quadrupolar nuclei. The other series of measurements provide muon spin relaxation functions under three magnetic field conditions, transverse and parallel to the initial polarization and for zero field.

QLCR spectra

Figures 85 and 86 display the QLCR spectra obtained for the more strongly n -type GaN:Si sample at 293 and 150 K, respectively. The room temperature spectrum is identical to that for the undoped film. These figures demonstrate the qualitative differences between spectra obtained above and below ~ 200 K. The two nearly identical sets of features in Fig. 85 are characteristic of interactions with Ga and are assigned to Mu^- at the two Ga anti-bonding sites (AB_{Ga}) in the GaN wurtzite structure. The single central line associated with each isotope is due to a site with the Mu–Ga bond parallel to the applied field, thus along the c -axis. The weaker doublet for each isotope is assigned to the AB_{Ga} site extending into the channel regions with the bond at roughly 70° to the c -axis. The doublets remain present at lower temperatures while the lines from the c -axis site disappear below 200 K, thereby verifying our initial assignment of the doublet to a separate site

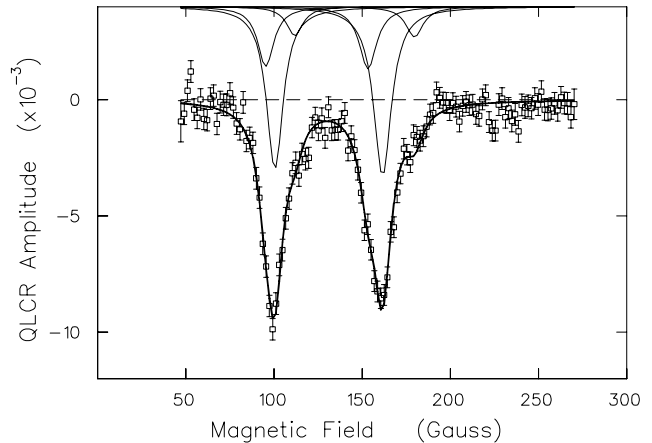


Fig. 85. Room temperature QLCR spectrum for 10^{18} cm^{-3} n -type Si-doped GaN. These features are from interaction with the two Ga isotopes and represent two Mu^- sites.

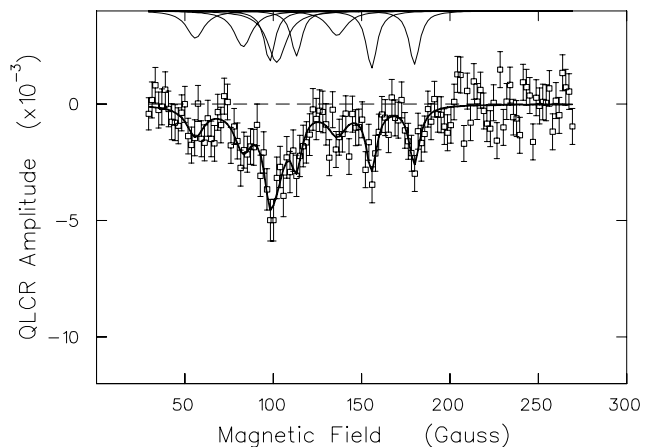


Fig. 86. The 150 K QLCR spectrum characteristic of the low temperature data. Resonance lines not present in Fig. 85 are assigned to nitrogen neighbours of Mu^+ centres.

rather than to more distant neighbours associated with a single on-axis Mu^- centre.

A different set of lines is present in the low temperature spectra as shown in Fig. 86, none of which show the characteristic Ga signature except for the doublets just discussed. The additional features are assigned to interactions of Mu^+ with N nuclei. Mu^+ is strongly attracted to nitrogen, although the specific sites differ for various theoretical approaches. Likely Mu^+ locations include nitrogen anti-bonding (AB_N) and bond-centered (BC) sites: wurtzite has two inequivalent sites of each type. A great deal of additional work remains to complete site assignments and obtain detailed structures.

Low temperature transitions

The temperature dependence of the zero-field (ZF) and weak transverse-field (TF) relaxation functions have been determined for both thick film GaN samples. ZF and TF relaxation rates were also obtained for the compensated GaN crystal in a coarse temperature scan up to 300 K. The two n -type films show similar low temperature relaxation characteristics suggesting a transition near 100 K in the TF data and a jump in the ZF static Kubo-Toyabe width, Δ_{KT} , near 200 K accompanied by growth of the KT amplitude for higher temperatures. The increase in Δ_{KT} occurs in the region where the QLCR spectrum changes; therefore, it can be correlated with occupation of the on-axis AB_{Ga} site for Mu^- . The ZF relaxation also has a weakly relaxing component over the full range and a small exponentially relaxing amplitude above 300 K and at very low temperatures. The weakly relaxing amplitude decreases below the 200 K increase in the KT amplitude and is tentatively assigned to Mu^+ states. A missing fraction in the TF diamagnetic amplitude is consistent with existence of paramagnetic Mu^0 centres. The TF- μ SR diamagnetic amplitude dips near 150 K consistent with a transition out of one charged state and at higher temperature into the second one, in general agreement. Preliminary analysis on the compensated crystal also supports these general assignments. This sample does not show the Mu^- zero-field KT signal, consistent with a lack of electrons.

Motion of Mu^-

The Kubo-Toyabe component in the zero-field data is dynamic above roughly 500 K and was fit assuming motion of Mu^- . Figure 87 shows the hop rates for the undoped GaN film. The barrier obtained for the 500 to 850 K activated region is 0.98 ± 0.03 eV. This is very close to the value from ISIS data on the GaN:Si film and for a powdered GaN sample in which only the Kubo-Toyabe component was observed. It is not clear at present which sites are involved in the Mu^- motion.

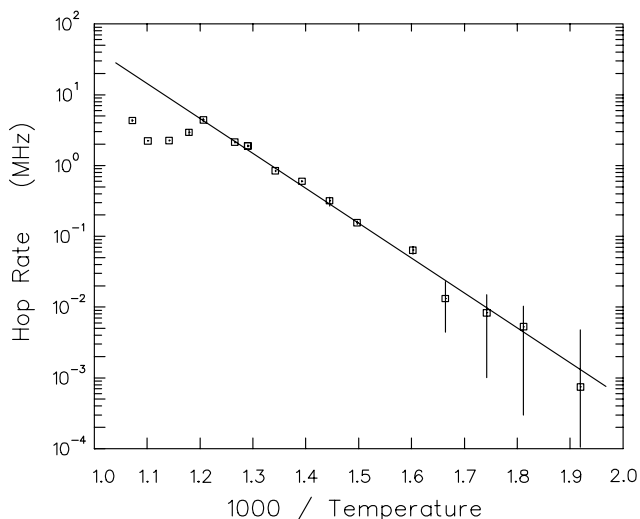


Fig. 87. Hop rates for Mu^- motion extracted from the dynamic Kubo-Toyabe zero-field component in undoped GaN.

High temperature transitions

Data on both the undoped and Si-doped films show a change in behaviour at the very highest temperatures, seen in Fig. 87 as a deviation below the activated curve for temperatures above 850 K. The ZF data for the undoped film also show a small exponential amplitude with an increasing rate in this region, generally consistent with the onset of charge cycles as implied by a TF relaxation feature associated with a small fraction of the muons. Other transitions are also apparent. The KT amplitude increases from about 40% of implanted muons below 700 K to nearly 65% by 900 K and the exponential component representing $\sim 10\%$ of the muons shows a sharp divergence in the rate constant near 600 K. These features suggest a transition from a Mu^0 state into Mu^- .

We examined the undoped film at high temperature in longitudinal fields to identify features associated with transitions, particularly high-T charge-state cycles. Hyperfine decoupling curves at room temperature and at 540 K imply that an isotropic Mu^0 state is present, while the field dependence of one relaxing component suggests possible involvement of an anisotropic Mu^0 state in charge cycles at 850 K. Figure 88 shows the relaxation rates associated with the more strongly relaxing LF component at high temperatures at two fields, 10 and 200 mT. These data are consistent with cyclic charge state transitions in GaN involving a small fraction of Mu states.

We plan to pursue questions left open by these very promising initial results and expect significant progress as thicker films and better quality GaN samples become available in the near future.

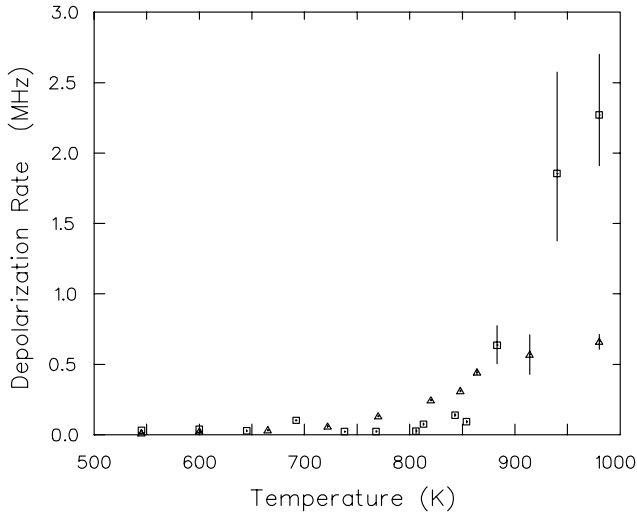


Fig. 88. Temperature dependent longitudinal relaxation rates in undoped GaN at 10 mT (squares) and 200 mT (triangles) implying cyclic Mu charge-state transitions.

Experiment 809

Muonium localization in solid methanes

(V.G. Storchak, Kurchatov Inst.; J.H. Brewer, CIAR/UBC)

Light particles such as electrons, muons, impurity atoms and isotopic defects often propagate by quantum tunneling in solids; a key question in such non-classical transport is whether the tunneling is coherent or incoherent, i.e. whether a wave-like or particle-like description is appropriate. This in turn depends on the particle's interaction with the environment. One of the possible channels for localization of a particle is through its interaction with lattice excitations (phonons, librations, magnons etc.). At low temperatures, such excitations are frozen out, in which case conventional understanding suggests that the only possible channel for particle localization is the introduction of crystal disorder, which thus may dramatically change the transport properties of a solid. A well-known example is the spatial localization of electron states near the Fermi level in a disordered metallic system, which leads to the "Anderson transition" [Anderson, Phys. Rev. **109**, 1492 (1958)] into a dielectric state: coherent tunneling of a particle is possible only between levels with the same energy (e.g. between equivalent sites in a crystalline lattice); in the case of strong randomness, states with the same energy may be too spatially separated for tunneling to be effective.

We have been exploring the quantum diffusion of the light *neutral* muonium ($\text{Mu} = \mu^+e^-$) atom in *insulating* crystals composed of molecules, in particular CH_4 and CD_4 , where *orientational ordering* causes localization of interstitial Mu by creating a source of *weak, short-range* disorder.

The transport properties of a neutral particle in a simple crystalline insulator (e.g. a monatomic or ionic crystal) depend only on the phonon modes of the lattice. For crystals composed of molecules, an additional contribution enters from the rotational degrees of freedom of the molecules. Two extremes are possible: the molecules may rotate almost freely in the crystal or the rotational motion may be severely restricted and hence transformed into torsional excitations (*librons*). Since typical rotational frequencies of molecules in crystals are still much higher than the particle bandwidth, in the first extreme the energy levels for a particle moving in different unit cells are degenerate and therefore particle dynamics remain unperturbed. In the second extreme the anisotropic interaction between molecules (which causes orientational ordering in the first place) changes the crystalline potential so that this degeneracy is lifted. As far as the particle dynamics are concerned, this splitting of the energy levels of adjacent sites acts as an effective disorder. To demonstrate this, we studied muonium dynamics (by measuring the Mu spin relaxation rate in weak transverse field) in solid methanes (CH_4 and CD_4), which undergo orientational ordering at 20.4 K and 22.1 K, respectively. (Partial orientational ordering starts in CD_4 at 27 K.)

The experiments were performed on the M13 beam line at TRIUMF and on the EMu beam line of the ISIS Pulsed Muon Facility at the Rutherford Appleton Laboratory. Atomic muonium was detected by observing the precession signal at the characteristic muonium frequency in a weak transverse magnetic field H . Relaxation of Mu is caused by modulation of its hyperfine interactions with nearby nuclei (parameterized by a NHF coupling constant δ) as the Mu atom diffuses through the crystal. The muonium relaxation rate T_2^{-1} has a simple form in two limits: if muonium "hops" from site to site at a rate $\tau_c^{-1} \gg \delta$ (*fast hopping* limit), then the transverse relaxation rate is given by $T_2^{-1} \approx \delta^2 \tau_c$. For very *slow* diffusion ($\tau_c^{-1} \lesssim \delta$) muonium spin relaxation takes place on a time scale shorter than τ_c and $T_2^{-1} \approx \delta$.

Figure 89 shows the temperature dependences of the muonium T_2^{-1} in solid CH_4 and CD_4 , extracted from the spectra by fitting single-exponential relaxation functions. The strong temperature dependence of T_2^{-1} abruptly levels off between about 45 K and 55 K in CH_4 and between about 32 K and 40 K in CD_4 . Such behaviour in the fast hopping regime indicates that the Mu hop rate stays constant in the indicated temperature ranges in both crystals. At the lowest measured temperatures (below about 20 K), T_2^{-1} again levels off in both crystals due to Mu localization, giving $\delta_1 \approx 5 \times 10^7 \text{ s}^{-1}$ for CH_4 and $\delta_2 \approx 8 \times 10^6 \text{ s}^{-1}$ for CD_4 . The ratio δ_1/δ_2 is about twice as large as the

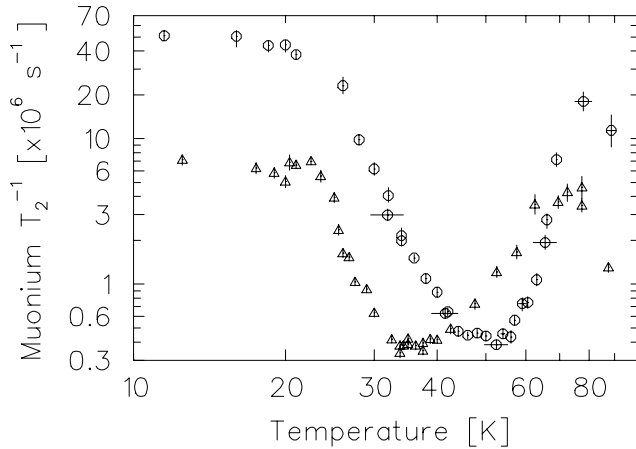


Fig. 89. Temperature dependence of muonium relaxation rate T_2^{-1} in solid methanes (circles: CH_4 ; triangles: CD_4) in a weak transverse field $H = 5$ G.

ratio of proton to deuteron magnetic moments, which is not really surprising – the NHF interaction, which governs muonium relaxation in all the substances where Mu atoms have been observed, need not scale with the magnetic moments of neighbour nuclei with different spins. Other candidates for the muonium spin relaxation mechanism, such as spin-exchange reactions with possible paramagnetic impurities (e.g. O_2) or electrons from the muon track, were ruled out by measurements in longitudinal magnetic and electric fields.

Figure 90 shows the temperature dependences of the muonium hop rate τ_c^{-1} in the solid methanes, extracted in the regime of dynamical averaging using the values of δ obtained above. At high temperatures – above 55 K for CH_4 and above 40 K for CD_4 – the hop rate in both crystals *increases* with *decreasing* temperature. This is an unambiguous manifestation of quantum diffusion which has also been recognized for muonium in KCl [Kiefl *et al.*, Phys. Rev. Lett. **62**, 792 (1989)] and solid nitrogen [Storchak *et al.*, Phys. Rev.

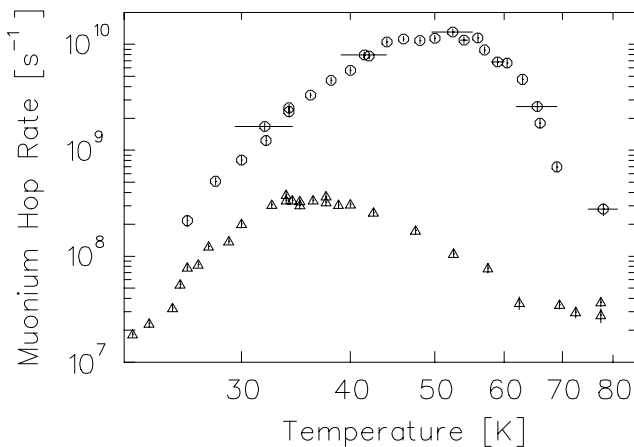


Fig. 90. Temperature dependence of muonium hop rate in solid methanes (circles: CH_4 ; triangles: CD_4).

Let. **72**, 3056 (1994)]. In the appropriate temperature ranges in both KCl and nitrogen, the muonium hop rate exhibits an empirical temperature dependence $\tau_c^{-1} \propto T^{-\alpha}$ with $\alpha \approx 3$ in KCl and $\alpha \approx 7$ in nitrogen. In solid CD_4 similar fits yield α between 5 and 6 while in CH_4 α is between 7 and 11 depending on the temperature range.

The plateaus in $\tau_c^{-1}(T)$ around 45–55 K in CH_4 and 32–40 K in CD_4 must represent the onset of muonium band motion [Kagan and Prokof'ev, *Quantum tunneling diffusion in solids*, in Quantum Tunneling in Condensed Media, eds. Leggett and Kagan (North-Holland, 1992), p.37; Storchak and Prokof'ev, Rev. Mod. Phys. **70**, 929 (1998)], which occurs if the coherence is preserved and the disorder is weak. In this case the hop rate is independent of temperature and we may estimate the muonium bandwidth to be about 3×10^{-2} K in CH_4 and about 10^{-3} K in CD_4 . These values may be compared with muonium bandwidths in KCl and solid nitrogen (0.16 K and 10^{-2} K, respectively) [Storchak and Prokof'ev, *op. cit.*].

The band motion does not extend to the lowest temperatures, however: the hop rate begins to decrease with decreasing temperature below about 45 K in CH_4 and about 30 K in CD_4 . These data indicate that interstitial muonium atoms undergo gradual localization in methanes at low temperatures where the temperature dependence of the muonium hop rate obeys the power law $\tau_c^{-1} \sim T^\alpha$ with $\alpha = 6.8(4)$ in both crystals. In this temperature range the observed power law is believed to be due to two-phonon dissipation in the regime of static destruction of the band [Kagan and Maksimov, Sov. Phys. JETP **57**, 459 (1983)].

This phenomenon can be explained in terms of the slowing down of molecular rotations in the crystal. At high temperatures, when the characteristic time of molecular reorientation $\tau_r \ll \tau_c$, the anisotropic molecular interactions are averaged out and muonium undergoes unperturbed bandlike propagation.

In conclusion, we have presented an observation of the destruction of bandlike motion of light interstitial particles in molecular crystals at low temperatures. We suggest that the particle localization is due to slowing down of molecular rotations and subsequent orientational ordering in these crystals. This study complements our knowledge of the nature of neutral particle localization due to *long-range* disorder.

Experiment 814

μ SR studies of unconventional superconductivity in Sr_2RuO_4

(G.M. Luke, McMaster)

Sr_2RuO_4 , which is isostructural to the high- T_c cuprate $\text{La}_{1.85}\text{Sr}_{0.15}\text{CuO}_4$, is to date the only known layered perovskite superconductor which does not contain copper. Although first synthesized in the 1950's, its superconductivity was only found in 1994; T_c s of early samples were roughly 0.7 K but have increased to $T_c = 1.5$ K in recent high quality single crystals.

Despite its low transition temperature, Sr_2RuO_4 is of great interest as there is growing evidence for an unconventional superconducting state. In this system, strong correlation effects enhance the effective mass seen in quantum oscillation and Pauli spin susceptibility measurements, in the same way as in ^3He . Combining this feature with Sr_2RuO_4 's expected tendency to display ferromagnetic spin fluctuations, it was argued that the pairing in Sr_2RuO_4 could be of odd parity (spin triplet) type.

One aspect of the pairing symmetry, the breaking of time reversal symmetry (TRS) can be probed directly. If the superconducting state has a degenerate representation (as is possible for some triplet superconducting states) then TRS can be broken, whereas it cannot be broken for non-degenerate representations (the case for all singlet states). For states with broken TRS, originating from either spin or orbital moments, a spontaneous internal magnetic field can appear below T_c . One can expect a finite hyperfine field at a magnetic probe for the case of spin moments, while (for both the spin and orbital cases) spontaneous supercurrents in the vicinity of inhomogeneities in the order parameter would create a magnetic field near impurities, surfaces, and/or domain walls between the two degenerate superconducting phases.

Two single crystals of Sr_2RuO_4 were grown at Kyoto University using a floating-zone method with an infrared image furnace. The superconducting T_c s were 1.478 K and 1.453 K with widths of 48 mK and 40 mK respectively, where T_c is defined as the sharp rise in the dissipative component of the ac-susceptibility and the width is its full width at half maximum. Sample A was cleaved and arranged in a mosaic so that the c -axis was normal to the sample's planar surface and parallel to the initial muon polarization while sample B was cut using a diamond saw such that the c -axis lay in the plane of the sample.

In Fig. 91 we show ZF- μ SR asymmetry spectra measured at $T = 2.1$ K and $T = 0.02$ K for sample B where $\mathcal{P}_\mu \perp c$. Spectra for sample A ($\mathcal{P}_\mu \parallel c$) are qualitatively similar. From Fig. 91 we see that the relaxation rate is quite small both above and

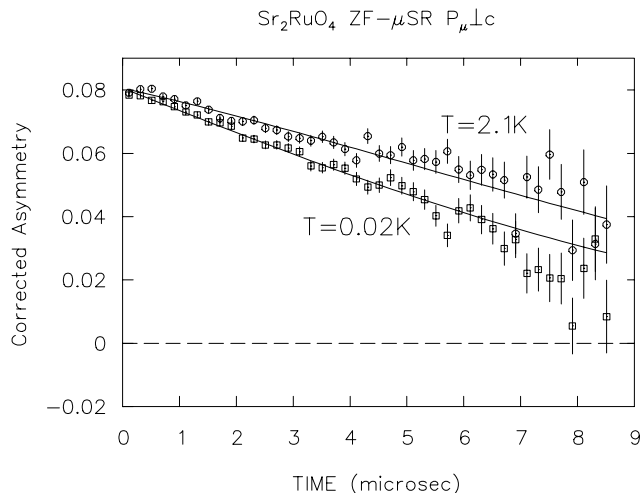


Fig. 91. Zero field μ SR spectra measured with $\mathcal{P}_\mu \perp c$ in Sr_2RuO_4 at $T = 2.1$ K (circles) and $T = 0.02$ K (squares).

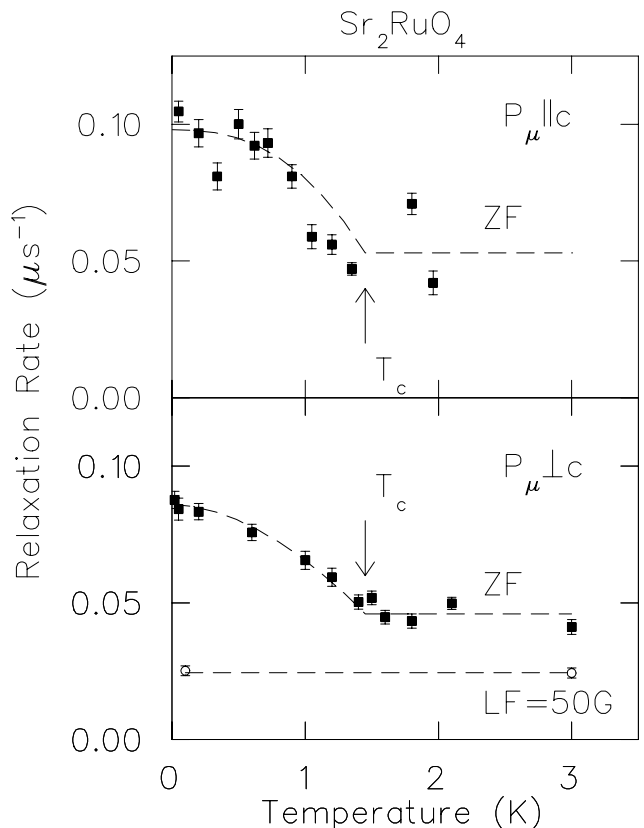


Fig. 92. Zero field relaxation rate Λ for the initial muon spin polarization $\parallel c$ (top) and $\perp c$ (bottom). T_c from ac-susceptibility indicated by arrows. Circles in bottom figure give relaxation rate in $B_{LF} = 50$ G $\perp c$. Curves are guides to the eye.

below $T_c = 1.45$ K, but that there is greater relaxation at lower temperature. This increased zero field relaxation could be caused by either (quasi-)static or fluctuating magnetic fields. We see in the lower panel of Fig. 92 that the relaxation in $B_{LF} = 50$ G is the same above and below T_c , which indicates that the zero field

relaxation must therefore be due to spontaneous fields which are static on the μs timescale.

We tried several functional forms for the additional relaxation below T_c ; fits to precessing (cosine) or Gaussian forms were essentially equivalent to each other, but were significantly worse than an exponential in fitting the data. Fitting the spectra to the product of a Kubo-Toyabe (using common values of $\Delta = 0.02, 0.06 \mu\text{s}^{-1}$ for samples A and B respectively, for all temperatures to account for the nuclear dipole fields) and an exponential $\exp(-\Lambda t)$ to characterize the additional relaxation due to the spontaneous magnetic field, we plot Λ vs. T in Fig. 92 for samples A ($\mathcal{P}_\mu \parallel c$) and B ($\mathcal{P}_\mu \perp c$). Also shown are the superconducting T_c s as determined by ac-susceptibility. We see a clear increase in Λ with an onset temperature around $T_c = 1.45$ K for both orientations indicating the presence of a spontaneous magnetic field appearing within the superconducting state. In principle, this spontaneous field could originate either from a TRS breaking superconducting state or with a purely magnetic state which coincidentally onsets near T_c . Very recently, we performed additional measurements on a third sample with a reduced $T_c = 0.9$ K and found that the spontaneous field onset at that reduced T_c . Thus, we conclude that since this field is so intimately connected with superconductivity, its existence provides direct evidence for a time reversal symmetry breaking superconducting state in Sr_2RuO_4 .

The increased relaxation in the superconducting state is exponential in character. If there were a unique field at the muon site we would observe a precession signal, while a dense collection of randomly oriented field sources results in a Kubo-Toyabe relaxation function. Both the precession and Kubo-Toyabe signals start with a Gaussian form and in the limit of weak characteristic fields are essentially indistinguishable. The exponential form which we observe in Sr_2RuO_4 indicates a broad distribution of fields arising from a dilute distribution of sources. This is consistent with the source of the internal field being supercurrents associated with variations in the superconducting order parameter around dilute impurities and domain walls. We see enhanced relaxation in both samples A and B. From this we can conclude that the local field cannot lie purely along the c -axis (this would give no relaxation from sample A). However, any orientation of the local field which has a significant component in the basal plane is consistent with our data.

The increase in the exponential relaxation below T_c is about $0.04 \mu\text{s}^{-1}$ which corresponds to a characteristic field strength $\Lambda/\gamma_\mu = 0.5$ G. This is about the same as we observed in the B phase of UPt_3 and is in line with theoretical predictions for that material. No the-

oretical estimates of the characteristic field strength in Sr_2RuO_4 are yet available; however, we would expect them to be comparable to those in UPt_3 as the fields should arise from a similar mechanism.

Several authors have considered the allowed symmetries of pairing states for the specific case of tetragonal symmetry appropriate for Sr_2RuO_4 . Spin-singlet pairing leads exclusively to non-degenerate states and the breakdown of TRS would, in general, require additional phase transitions admixing other pairing channels within the superconducting phase, for which there is no experimental indication so far. On the other hand, one can show that in the spin-triplet pairing channel, TRS breaking states appear naturally at the onset of superconductivity, consistent with our experiment. Based on these symmetry arguments we conclude that the present experiment provides strong evidence for Cooper pairing with spin-triplet (p -wave) symmetry: a superconducting analog of the A or A_1 phases of superfluid ^3He . The distinction between unitary and non-unitary states in Sr_2RuO_4 , however, cannot be done with the present results and has to wait for further studies by other means.

Experiment 831

Magnetic properties of $\text{REBa}_2\text{Cu}_3\text{O}_x$

(*M. Pinkpank, D. Andreica, F.N. Gygax, A. Schenck, ETH Zurich; B. Hitti, TRIUMF; J.H. Brewer, UBC/TRIUMF; A. Amato, PSI*)

This experiment studies the dynamic behaviour of the magnetic rare earth (RE) moments in $\text{REBa}_2\text{Cu}_3\text{O}_x$. If the Y in the $\text{YBa}_2\text{Cu}_3\text{O}_x$ system is replaced by lanthanide ions (with the exception of Ce, Pr, Tb and Pm), antiferromagnetic ordering of the lanthanide $4f$ -moments is observed at low temperatures, without any obvious adverse effect on the superconducting state. The 3D antiferromagnetic ordering in, for example, $\text{HoBa}_2\text{Cu}_3\text{O}_7$, $\text{GdBa}_2\text{Cu}_3\text{O}_x$ and $\text{ErBa}_2\text{Cu}_3\text{O}_x$ occurs, although the lanthanide ions are sandwiched by the superconducting CuO_2 -planes. Apparently the superconducting electrons are very narrowly confined to the CuO_2 -planes, as also evidenced by the extremely short coherence length along the crystallographic c -axis ($\xi_c \approx 3\text{\AA}$), and do not overlap with the local $4f$ -electrons. The absence of the conduction electrons at the rare earth sites is also implied by Mössbauer data. In view of these features, it is not very clear by what mechanism the observed magnetic order is driven.

In order to gain more insight into the coupling mechanism between the $4f$ -moments (dipolar coupling, superexchange, or others), we study the dynamic magnetic properties of $\text{REBa}_2\text{Cu}_3\text{O}_x$ (RE = Ho, Gd, Er) for samples with different oxygen content.

Earlier longitudinal field (LF) μSR measurements

on $\text{HoBa}_2\text{Cu}_3\text{O}_x$ and $\text{GdBa}_2\text{Cu}_3\text{O}_x$ at PSI show a pronounced difference in the temperature and field dependence of the LF relaxation rate.

In $\text{HoBa}_2\text{Cu}_3\text{O}_x$ the Ho^{3+} ions have a total angular momentum $J = 8$. The 17-fold degeneracy of the 5I_8 ground state multiplet is completely lifted by the crystal electric field (CEF) in the orthorhombic phase ($x \geq 6.4$). In the tetragonal phase ($x \leq 6.4$) some singlets will combine to doublets. Since the CEF ground state is a singlet, the magnetic moment has to be induced by hyperfine interaction with the nuclear moment or an overcritical exchange interaction, before any magnetic ordering can take place. The LF relaxation rate shows a strong temperature dependence with a maximum at about 5 K. The field dependence of the LF relaxation rate in the superconducting samples at 6 K can be described by a power law. Within the allocated beam time at TRIUMF we were able to show that this is no more the case for non-superconducting $\text{HoBa}_2\text{Cu}_3\text{O}_{6.2}$.

The $^8S_{7/2}$ multiplet of the Gd^{3+} ion in $\text{GdBa}_2\text{Cu}_3\text{O}_{6+x}$ is a pure spin state, and the Gd sublattice orders antiferromagnetically below 2.2 K. The dynamic relaxation rate, as function of the temperature, measured in longitudinal field (LF) μSR , is temperature independent above 20 K, and no field dependence is observed.

In order to get more insight in the different magnetic behaviour of $\text{GdBa}_2\text{Cu}_3\text{O}_x$ and $\text{HoBa}_2\text{Cu}_3\text{O}_x$, we performed LF measurements on $\text{ErBa}_2\text{Cu}_3\text{O}_7$ at TRIUMF. In this system the CEF ground state is a Kramers doublet, and the total angular momentum of the Er^{3+} ion $J = \frac{15}{2}$ is bigger than the angular momentum of Gd^{3+} , while the measured relaxation rate λ is smaller. The relaxation rate was found to be temperature independent up to ≈ 200 K, where muon diffusion sets in. As in $\text{GdBa}_2\text{Cu}_3\text{O}_x$ no field dependence of the relaxation rate was found. The analysis of the data is still in progress.

Experiment 832

Study of the non-magnetic-magnetic transition in the $\text{Yb}(\text{Cu}_{1-x}\text{Ni}_x)_2\text{Si}_2$ system

(D. Andreica, ETH Zurich)

Transverse field measurements on

$\text{Yb}(\text{Cu}_{1-x}\text{Ni}_x)_2\text{Si}_2$

Introduction

We have performed μSR transverse field (TF) measurements on $\text{Yb}(\text{Cu}_{1-x}\text{Ni}_x)_2\text{Si}_2$ samples. The aim of this investigation is to obtain information about the Kondo coupling constant J .

The chemical pressure in the $\text{Yb}(\text{Cu}_{1-x}\text{Ni}_x)_2\text{Si}_2$ series, obtained by replacing Cu by Ni, drives the system from a non-magnetic ground state in YbCu_2Si_2 to a

magnetic ground state in YbNi_2Si_2 . The main interactions which influence the transition are the screening of the Yb's magnetic moment because of the intra-site Kondo effect ($k_B T_K \propto \exp(-1/JN(E_F))$) and the intersite RKKY magnetic interaction ($k_B T_{\text{RKKY}} \propto (J^2 N(E_F))$). Both interactions depend on the same parameter J , the Kondo coupling constant between the localized and the conduction electrons. Under applied pressure, J is supposed to increase for Ce compounds and to decrease for Yb compounds [Doniach, *Physica B1*, 213 (1977)].

Theoretical background

For rare-earth compounds the corrected μ^+ -Knight shift can be written as $K = K_0 + K_f$, where K_0 and K_f correspond to the contributions of the internal fields arising from the polarization of conduction electrons and localized f -moments induced by the external field H_{ext} . At low temperatures, K_f is much larger than K_0 and contains two contributions due to the localized f -moments: the dipole-dipole interaction between the f -moments and the μ^+ , and the indirect RKKY interaction producing an additional spin polarization of the conduction electrons at the μ^+ site resulting in an increased hyperfine contact field.

For a polycrystalline sample,

$$K_{\text{iso}} = \frac{A_c}{3}(\chi_{\parallel} + 2\chi_{\perp}) + \frac{A_{\text{dip}}^{zz}}{3}(\chi_{\parallel} - \chi_{\perp}).$$

If the dipolar coupling and the anisotropy of the magnetic susceptibility are known, the value of A_c could be obtained. Since the hyperfine contact coupling constant A_c is proportional with $g = JN(E_F)$, the key parameter for the RKKY and Kondo interactions, its dependence on the Ni concentration x in the $\text{Yb}(\text{Cu}_{1-x}\text{Ni}_x)_2\text{Si}_2$ compounds will allow us to monitor the competition between these two interactions close to the non-magnetic-magnetic transition.

Results

TF temperature scans were performed at 6000 G on the $x = 0, 0.125$ and 1 samples. The samples were mounted on an iron oxide disk in order to get rid of any off-sample background signal. The μSR signal for all investigated samples contains 2 components, one of these belonging to a few percent of an impurity phase. For all investigated compounds, the low temperature Knight shift deviates from the linear scaling with the magnetic susceptibility. Some work is still to be done to compute all the contributions to the Knight shift and then the hyperfine coupling constant A_c . The preliminary fit results are plotted in Fig. 93. Only the contributions arising from the samples are displayed.

A similar work performed at PSI by Wiesinger and co-workers [*Physica B230*, 243 (1997)] on the

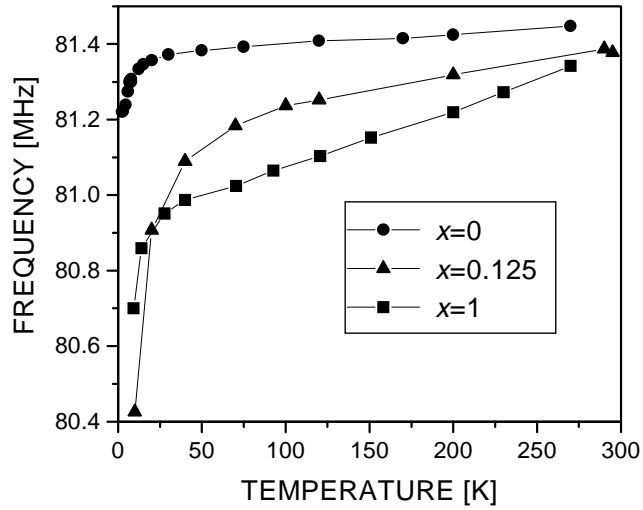


Fig. 93. Temperature dependence of the sample's signal frequency. The transverse field measurements were performed in a field of 6 kG.

effects of Cu substitutions by Al in CeCu_5 allows one to compute the A_c dependence on the Al concentration

In the Doniach model, the increase of A_c as a function of Al concentration supports the picture that for high Al concentration the Kondo interaction is dominant. We expect that for $\text{Yb}(\text{Cu}_{1-x}\text{Ni}_x)_2\text{Si}_2$ the mirror behaviour will be obtained; that means a decrease of the A_c value with increasing pressure.

LIFE SCIENCES RESEARCH

Introduction

The Life Sciences program exploits the powerful radioisotope production capabilities at TRIUMF. The four cyclotrons that provide proton beams with energy between 13 and 520 MeV having beam currents up to 500 μA makes TRIUMF the most versatile and powerful radioisotope producing facility in the world.

PET continued to be the major focus of the efforts in the Life Sciences program. The Medical Research Council of Canada awarded five major grants that make use of the PET technique as their primary research tool. Four of these projects are related to the Neurodegenerative Disorder Centre at UBC and the fifth was from the Department of Psychiatry also at UBC to study endogenous serotonin in patients diagnosed with mania.

We have developed tracers for many aspects of the dopaminergic system and the serotonin receptors labelled with ^{18}F and ^{11}C . Using these tracers we have begun a major study to follow the progression of Parkinson's disease by scanning patients who have early disease and their symptoms are asymmetric, and a group of subjects who have had the disease for an extended period. These same subjects will have repeat scans after a period of 4 years. One of the questions to answer is related to the changes in the unaffected side and how the measures change in relation to the affected side over the period between scans.

The following sections provide a brief description of the progress made during 1998 for the experiments approved by the Life Sciences Project Evaluation Committee (LSPEC).

Experiment LS0

PET facilities

(*K.R. Buckley, TRIUMF*)

The PET facilities comprise the TR13 13 MeV H^- cyclotron, the ECAT 953B/31 tomograph, and ancillary equipment such as counting and data acquisition systems.

TR13 cyclotron

The TR13 cyclotron continues to be the backbone of the PET program, conveniently and reliably supplying isotopes throughout the day for radiochemical synthesis. Usage of the cyclotron increased 57% (by delivered beam) this year over 1997, reflecting an increased demand for PET radiopharmaceuticals (LS3) and FDG (LS13, LS24), experimentation in precursor synthesis, and the irradiation of several lithium targets for the production of ^7Be nuclear physics targets.

Downtime this year was minimal and was again caused primarily by the cryopumping system and tar-

get window failures. A faulty component was found on the cryopump controller circuit board and replaced with the help of the TRIUMF Electronics group. Unusually warm weather this summer caused some difficulties with temperature interlocks but these subsided with a return to cooler weather.

The ion source filament was replaced once this year due to routine wear. In addition to this, the ion source was opened and cleaned twice following failure of the $^{18}\text{F}\text{-F}_2$ target during the Ar/ F_2 recovery run. It was found that F_2 contamination in the ion source severely affected performance. The fix is as simple as opening the ion source and cleaning the surfaces lightly with scotchbrite followed by acetone.

We performed several extraction foil changes, mostly as a result of target window failures.

Presently there are five target locations occupied of the available eight. These consist of

- one $^{18}\text{O}\text{-O}_2$ gas target
- one ^{18}O water target
- two CH_4 gas targets
- one lithium metal target

The lithium target (LS8) has a reserved location and is installed and removed for each production. A mobile shield with remote manipulator, which has been constructed by the Lithium group, can be placed in the TR13 target shield opening to remove the target and place it in a lead pig. This assembly has been tested and is now used routinely for runs exceeding 2 hours at 50 μA .

The concrete blocks for shielding the ion source/injection line area of the cyclotron were installed in the spring and have reduced ambient fields around the cyclotron and simplified access to the ion source for servicing.

A talk was given at the Canadian chapter meeting of the International Isotope Society in Toronto on the in-target production of PET precursors. A talk and a poster were presented at the Workshop on Accelerator Operations in Vancouver.

ECAT tomograph

The ECAT has had a typical year with several detector block failures. An external laser for patient alignment was mounted on the front of the camera to aid the positioning of less flexible patients.

Statistics

Table XIII. TR13 run data.

Total runs conducted	837	
Total runs lost	7	
Integrated charge delivered	485300	$\mu\text{A-mins}$
delivered to – LS3	327995	
– LS4	3610	
– LS7	637	
– LS8	99606	
– LS13	41588	
– LS24	11864	

Table XIV. ECAT run data.

Total scans conducted	488
Total scans lost	41
lost to – patient	31
– cyclotron	7
– chemistry	2
– rabbit	1

Experiment LS2

Synthesis of radiohalogenated carbohydrates

(*M.J. Adam, TRIUMF*)

The use of 2-deoxy-2- ^{18}F fluoro-D-glucose (FDG) to study glucose metabolism has seen extensive clinical applications especially in cardiology and oncology. Because of the growing importance of FDG/PET for clinical use, we have decided to study close analogs of FDG, 2,2-dihalo sugars, and see how they compare.

During this year we have synthesized 2-deoxy-2,2- ^{18}F difluoro-glucose and have carried out biodistribution studies. Briefly, this compound behaves in a similar fashion in the brain to FDG (see Fig. 94).

The details of this work have been presented at the Society of Nuclear Medicine meeting in Toronto in June. Further studies on this compound and the synthesis of other dihalo sugars are currently under investigation.

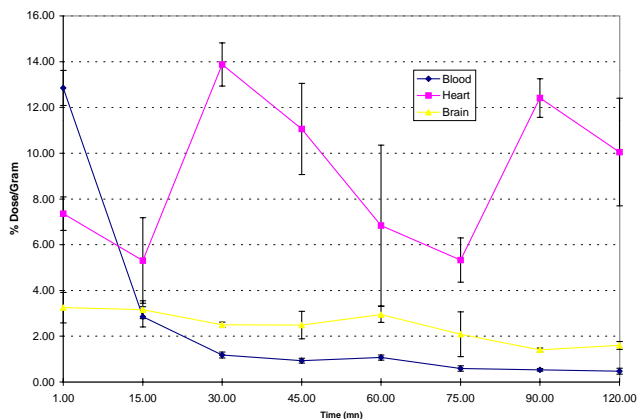


Fig. 94. Biodistribution of DFDG in mice.

Experiment LS3

PET radiopharmaceuticals

(*M.J. Adam, TRIUMF*)

PET radiopharmaceutical production deliveries continued to increase in 1998 to a total of 443 (see Fig. 95). There are a total of 7 radiopharmaceuticals used in the program: FDG, fluorodopa, raclopride, SCH23390, dihydrotetrabenazine, setoperone, and methylphenidate. In addition there were also 44 shipments of FDG to Vancouver and Lions Gate Hospitals and 54 shipments of N-13 sent to the Department of Botany in 1998. While most of the production runs are for use by the Neurodegenerative Disorders Program at UBC there is an increasing number (total of 44 FDG) of deliveries to other researchers such as Vancouver Hospital and Lions Gate Hospital.

One major project undertaken this year was to reduce the amount of precursor used in the C-11 preparations. This is important since the synthesis of precursors is very labour intensive and some of the component chemicals are difficult to obtain. This has been accomplished by the use of Al/KF as the base in some of the reactions and the development of methyl triflate to replace methyl iodide as the methylating agent.

A new PET radiopharmaceutical that is currently under development by the group is PK 11195, a peripheral benzodiazapine receptor drug that has shown promise as an anti-inflammatory drug. This new agent, when labelled with C-11, will be used as a possible imaging agent for arthritis and for the study of Parkinson's disease.

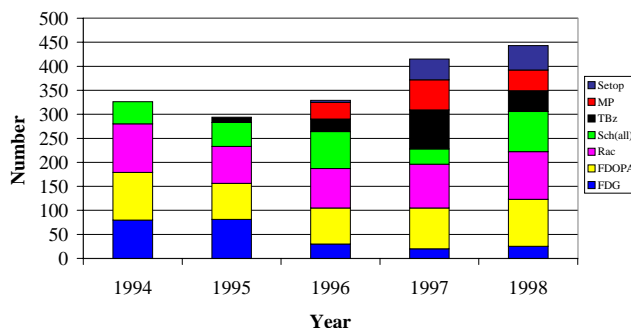


Fig. 95. PET radiopharmaceutical deliveries.

Experiment LS4

TR13 targets for PET radioisotope production

(*T.J. Ruth, TRIUMF*)

The development of targets for the production of the neutron deficient isotopes ^{18}F ($T_{1/2} = 109.8$ min), ^{11}C ($T_{1/2} = 20.4$ min), ^{13}N ($T_{1/2} = 10.0$ min) and ^{15}O ($T_{1/2} = 2.05$ min) on the TR13 has been a major task for the TRIUMF PET group during the last several years and is still in progress.

Thus far we have installed targets for the production of ^{18}F both as fluoride and fluorine (F_2) and ^{11}C targets producing CO_2 and $^{11}\text{C-CH}_4$. In order to meet the clinical research demands of the UBC Movement Disorders Program we have continued to use the prototype targets. These designs have worked well but we have determined that there are a number of improvements that can be incorporated to improve performance. Efforts in the past year have centered at increasing the yield of the $^{11}\text{CH}_4$ target. The yields from this target are substantially lower than the identical target for producing CO_2 . A number of experiments to determine the exact cause of this difference have been performed, including the determination of the quantity of ammonia formed in situ which could be a sink for the hydrogen in the target gas mixture. The ammonia production reaches equilibrium quickly and is not affected by alterations in beam current or length of bombardment. Further studies using a nickel plated target point towards the possibility that the hot atom products, namely CN, may be adhering to the walls of the target. Further studies are planned.

Both of the ^{18}F targets are performing well. We ran the water target for nearly 2 hours at $18\ \mu\text{A}$ and maintained a production rate of $115\ \text{mCi}/\mu\text{A}$ at saturation. The gas target using the double shoot method yields about $70\ \text{mCi}/\mu\text{A}$ and a follow up irradiation results in another $28\ \text{mCi}/\mu\text{A}$ at saturation.

Experiment LS8 Radiotracers for the physical and biosciences (*T.J. Ruth, TRIUMF*)

This project provides radiotracers to a number of collaborators both on the UBC campus as well as elsewhere when the half-life is sufficiently long that it can be transported. The radioisotopes are used as probes for fundamental research in other disciplines in the physical and biological sciences. Listed below are brief reports on the progress of the active experiments.

The production of ^7Be is in collaboration with the Beryl group at TRIUMF as part of their effort to measure the cross section for the $^7\text{Be}(p,\gamma)^8\text{B}$ reaction to address anomalies in the international solar neutrino measurements. Irradiations have been performed up to the $50\ \mu\text{A}$ required for full production and yields of $10\ \text{mCi}$ have also been processed. Optimization of the separation chemistry is under way.

^{13}N tracers have been used extensively at UBC to study the kinetics of nitrogen incorporation by plants. This program attempts to integrate research at the ecophysiological level, through physiology to molecular biology. During 1997/98 we have compared the absorption rates for NO_3^- and NH_4^+ by rice. There is evidence that in the superficial paddy soil, aeration by O_2

transport from leaf tissues (produced by photosynthesis) may generate localized oxidative conditions leading to NO_3^- production. Thus, roots localized in this region of the soil may be able to acquire NO_3^- as effectively as NH_4^+ . Our studies demonstrate that $^{13}\text{NO}_3^-$ uptake by these seminal roots is as large and even larger than rates of NH_4^+ uptake.

It appears that conifers from climax forests, as well as salal (a shrub species common to evergreen forests), prefer reduced N (NH_4^+ , amino acids) to NO_3^- . Tissue N and N uptake rates may be ~ 6 times greater for reduced N than nitrate. Clearcuts, fires and other disturbances result in a conversion of soil N from reduced to oxidized form so that replanting of climax species in this altered soil environment disadvantages these species, reducing replanting success. We have examined $\text{NO}_3^-/\text{NH}_4^+$ preferences of lodgepole pine, aspen and spruce in comparative experiments.

We have been examining the expression of the AMT1 gene which codes for the NH_4^+ transporter in Arabidopsis while undertaking correlated studies of NH_4^+ uptake by use of ^{13}N . It appears that the gene is only expressed when N supply is limited. At high available N a second transport system is adequate to deliver sufficient N. We have demonstrated by the use of parallel $^{13}\text{NH}_4^+$ flux studies and Northern analysis of AMT1 expression that the gene is regulated by glutamine accumulation and not by NH_4^+ itself. At the same time, it appears that accumulated NH_4^+ is capable of reducing the influx of $^{13}\text{NH}_4^+$ through the transporter.

Based on results from the nitrogen studies, the researchers in Dr. Glass' lab wish to explore the kinetics of K uptake in plants as a function of nitrogen concentration. In order to perform these experiments they will need access to ^{42}K .

One of the major uses of kinetic isotope effects (KIEs) is to help chemists model the transition states of organic reactions so they can understand how and why reactions occur. KIEs are the major tool used in these investigations because they give both qualitative and semi-quantitative information about the structure of the transition state. Dr. Westaway from Laurentian University wishes to measure KIEs for iodine. We are proposing using ^{120}I and ^{135}I as the isotopes of iodine that have half lives sufficiently long for this study.

Researchers at Children's Hospital are implementing a near infrared system for the monitoring of blood flow in infants. They are using immature pigs as the model for this development. They wish to calibrate their NIR system against blood flow as measured via PET with H_2^{15}O as tracer.

Use of the $^{122}\text{Xe}/^{122}\text{I}$ system has as its major objective the development of brain and myocardial perfusion methods using PET. Such a generator system could

alleviate the need to have an on-site accelerator for the generic clinical PET centre. Miniature NaI targets suitable for irradiation on the TRIUMF BL2C solid target facility have been constructed and preliminary irradiations have been initiated to determine production and shipping parameters. Preliminary shipments of radioxenon have been supplied to the LBL group as part of LS14.

Experiment LS6/LS21

Accelerator mass spectrometry for trace element analysis in living organisms

(R.R. Johnson, UBC)

LS6, the experiment on the resorption and release of ^{41}Ca from a single subject, is in its seventh year. Over this time period the subject has gone through pre-, peri- and menopause.

In Expt. LS21, the uptake and release of Al is being monitored by using ^{26}Al as a tracer. The data are collected over several days and indicate that aluminum is retained in the plants. There appear to be several compartments in the release process.

A Wein filter has been constructed and installed at the Weizmann Institute where some of the AMS measurements are performed.

Experiment LS10

Aptamer imaging agents

(H. Dougan, TRIUMF)

Research is progressing with radiolabeled ^{123}I short DNA molecules (aptamers), in this example with an affinity for blood clot components. The goals are to master the use of DNA radiopharmaceuticals and obtain an imaging agent for thrombus. The aptamers function readily in simple test-tube experiments but encounter pitfalls in-vivo. This year's progress attempts to master the science required to extend activity to in-vivo conditions. (1) Aptamer interaction with clots is better understood, revealing aspects which were not anticipated: One class of aptamers binds thrombin in-vitro, but access is blocked by fibrin (the major protein in clots) in-vivo. A second class of aptamers binds thrombin in-vitro and in-vivo, but unexpectedly binds also to fibrin; this complicates the in-vivo behaviour. The latter aptamers are suited for in-vivo imaging studies. (2) Destruction of aptamers in-vivo has limited the availability of the aptamer to the clot, and has limited the lifetime of aptamer bound to the clot. I have been able to extend the lifetime of the aptamer in blood to several hours by modifying the aptamer with a small molecule. Attaching a larger molecule to the aptamer allows aptamer to be transferred from the site of injection to the thrombus with improved efficiency. Dr. Can Vo worked with the project nine months developing animal assays.

Experiment LS23/LS34

Radioisotope production targets

(R.R. Johnson, UBC)

These two projects aim to produce $^{94\text{m}}\text{Tc}$ and ^{103}Pd . These are two radioisotopes that may have research or clinical utility. Principally, the technetium isotope can be used in PET to derive quantitative kinetic information which may not be available from using the standard $^{99\text{m}}\text{Tc}$ and SPECT.

Experiment LS24

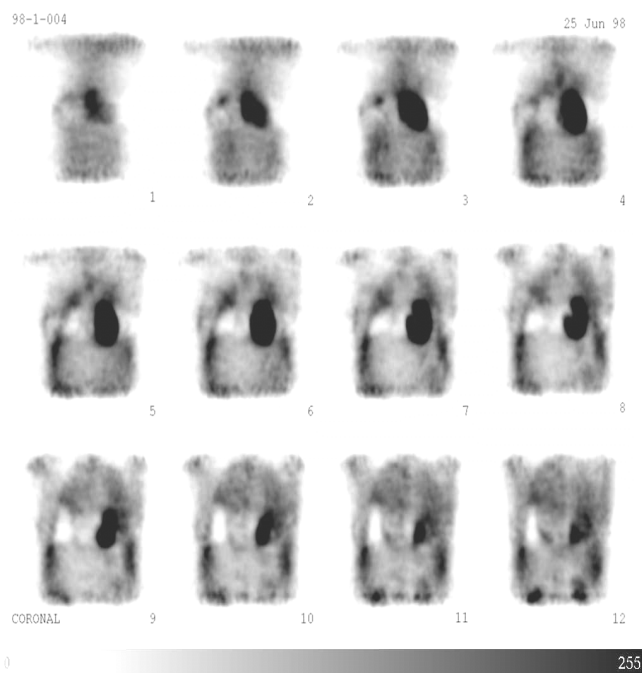
PET of breast cancer in a community hospital: a study of advanced disease using a coincidence gamma camera

(P.F. Cohen, Lions Gate Hospital)

Lions Gate Hospital is unique in having the only coincidence PET system in Canada at the moment, and one of the few sites doing clinical PET studies in oncology. This year at Lions Gate Hospital involved further characterization of our ADAC coincidence PET camera doing phantom studies. Clinical studies were begun, initially on a normal volunteer, and then followed by two patients with extensive bone metastatic breast cancer lesions previously detected on bone scan. There was a good agreement between the coincidence PET and Tc-99m MDP bone scans, but some lesions were seen on PET and not on bone scan, and vice-versa. It was felt that this might make a good initial clinical study, as the discordance between bone scan and PET scan has not been reported on very extensively. One of the clinical difficulties facing our site has been that the closest dedicated PET system capable of performing whole-body oncology studies for comparison is at the University of Washington Medical Center. It was thought that bone metastases at least could be verified in comparison with regular nuclear medicine bone scans.

Our clinical directions were changed, however, by growing awareness of our system by the Vancouver community, and growing use of our system by the Lions Gate Hospital oncologist. Two patients presented themselves to our department, one who had previously had a dedicated PET scan in Seattle, showing extensive breast cancer metastases, and another with recurrent lymphoma which could not be detected by the usual radiology modalities (CT, gallium scan, and chest x-ray). The patient with extensive breast cancer disease was confirmed on our coincidence system, with detection of most of the lesions seen at the University of Washington. The other patient with recurrent lymphoma showed multiple lesions on our system, and was sent to Seattle for confirmation (both scans are included in Fig. 96). At this point it was decided to do PET scans on patients with recurrent cancers referred by our

LGH ADAC Coincidence



UW GE ADVANCE dedicated PET

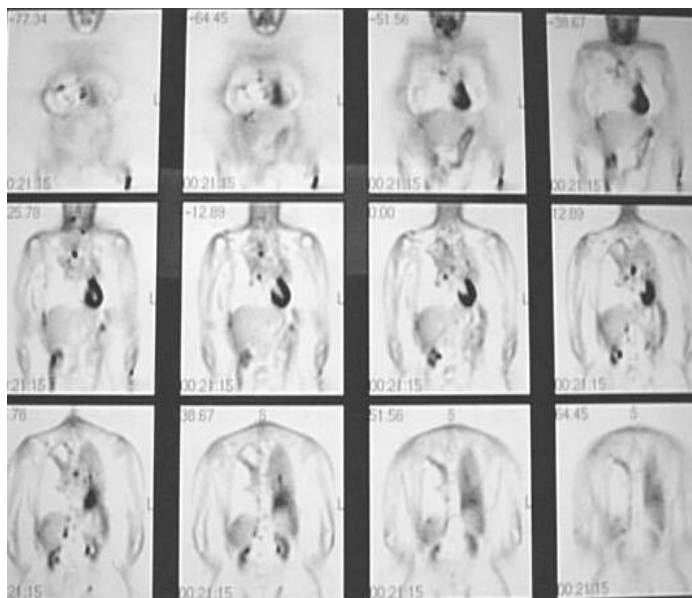


Fig. 96. Female age 41; metastatic breast cancer.

oncologist, with concentration on recurrent breast cancer and recurrent lymphomas. The rationale was that we were still attempting to do initial clinical studies with the ADAC coincidence camera, and rather than attempt to dictate to clinicians which patients should be referred for PET, we would have greater success in attempting to see if PET could answer clinical questions for our clinicians. At the same time we have been optimizing our parameters based on phantom studies for image acquisition times, methods of display, and reconstruction algorithms. It appears we are now producing images whose clinical appearance is starting to approximate images produced at other PET centres with dedicated PET systems. It appears likely there will be further improvements with the acquisition by our department of commercially available attenuation correction packages, as well as further random and scatter correction algorithms. We have now done a further five patients with breast cancers, showing lesions which were not apparent on other standard radiology tests.

Experiment LS25

3D PET in human neuroreceptor studies: quantification and reconstruction

(V. Sossi, UBC/TRIUMF)

We had previously developed the quantitative aspect of 3D PET (see 1997 Annual Report). In this

last year we solved the last outstanding problem associated with 3D PET, the reduction of the time required to reconstruct a 3D data set. Up to now we have been using the 3D FBP algorithm developed by Kinahan and Rogers [IEEE Trans. Nucl. Sci. **36**, 964 (1989)], which requires approximately 20 minutes of processing time/frame. Since we have on-going studies, a new reconstruction method had to produce identical reconstructed images to 3D FBP. We have implemented and tested the Fourier rebinning method [Kinahan and Townsend, Proc. 1995 Int. Meeting on Fully 3D Image Reconstruction in Radiology and Nuclear Medicine, p.235] to reduce 3D sinograms to 2D ones, followed by several 2D reconstruction methods. We found that FORE followed by 2DFPB produced identical images (within approximately 1%) compared to 3DFBP and the reconstruction time decreased by approximately a factor of 10. Tests were performed on phantom and human data. This study was part of a thesis project of a M.Sc. physics student who thus completed his degree. The results were presented at the 1998 IEEE/MIC conference in Toronto and submitted for refereed publication to the IEEE Trans. Nucl. Sci. This project is thus completed.

Experiment LS26

A gaseous planar positron source for routine 3D PET normalization

(*T.R. Oakes, TRIUMF*)

A plane-source containing a β^+ emitting gas was constructed which approaches the theoretical lower limit for contribution of scattered photons. The scattering properties of a gas plane-source are defined by the housing thickness, which for a β^+ emitting medium is in turn defined by the maximum energy of the β^+ ; the housing must be thick enough to stop the most energetic β^+ .

The location of a positron emission in a gaseous medium is partially decoupled from the site of the positron decay, which can reduce the effect of some non-uniformities while creating others. A plane-source containing a gaseous positron emitter can produce good uniformity over the width of the plane-source, except within 3 cm from the sides. Such a source is useful for normalization in 3D PET. By optimizing a gas plane-source so the housing is just thick enough to contain the most energetic positron for a given isotope, the lowest possible scatter fraction may be achieved. Our plane-source optimized for ^{18}F CH_3F yields a scatter fraction of 2.09%.

Experiment LS28

Evaluation of potentially viable myocardium with dobutamine myocardial SPECT imaging

(*D. Worsley, VHHSC*)

The purpose of this project is to evaluate whether combined perfusion and functional imaging with Tc-99m sestamibi (MIBI) augmented by low dose dobutamine is a useful technique for detecting viable myocardium.

In patients with chronic coronary artery disease, regional myocardial contraction dysfunction may be due to severe tissue hypoperfusion (hibernation), rather than infarcted myocardium. The differentiation between infarcted and hibernating myocardium can be clinically important. Patients with myocardium contraction dysfunction, secondary to infarction, have little recovery following successful revascularization. In contrast, patients with hibernating myocardium are likely to improve left ventricular function following revascularization. The development of a readily available, non-invasive technique that would permit an accurate pre-operative assessment of hibernating (viable) myocardium would clearly be beneficial.

Using FDG SPECT as the gold standard for defining viable myocardium, this study will compare the diagnostic accuracy of dobutamine augmented gated SPECT imaging and perfusion imaging with MIBI.

Currently we have performed and analyzed scans

and dobutamine gated SPECT plus FDG SPECT in 45 patients. Another 15 patients have been imaged but the data have not been analyzed.

Of the 405 segments evaluated, perfusion/metabolism mismatch was present in 18.8% (77 of 405 segments). The sensitivity, specificity and accuracy of perfusion imaging and dobutamine augmented gated SPECT imaging are presented in Table XV.

Table XV. Change in perfusion without and with dobutamine SPECT as compared to FDG viability.

Change in perfusion	Sensitivity	Specificity	Accuracy
<80%	100%	50%	51%
<60%	46%	67%	59%
<40%	18%	88%	75%
⋮	⋮	⋮	

Experiment LS29

Production and distribution of FDG for clinical studies

(*T.J. Ruth, TRIUMF*)

Following the Workshop on the Distribution of FDG held at the LSPEC Review of 1996/97, discussions ensued as to how best to provide FDG to the local community for clinical utility. There is no mechanism established for the real-cost reimbursement. However, there continues to be interest in access to FDG, both for research purposes and for clinical applications. While the research uses for FDG can continue to be supplied under existing protocols, we will have to find out from the Canadian Health Protection Branch (HPB) what is required for approval before FDG can be used clinically by the local user community.

The aim of this proposal is to determine the level of involvement TRIUMF is willing to have in meeting the local needs for FDG prepared for clinical applications. The primary effort will consist of contacting HPB in Ottawa and determining the scope of work of a regulatory nature. In addition, based on the outcome of our discussions with HPB we will derive a cost estimate for establishing an independent (chemistry/delivery system different from existing PET group chemistry systems) supply of FDG.

Experiment LS30

Life Sciences five year plan

(*T.J. Ruth, TRIUMF*)

A Workshop was held at TRIUMF in September, 1997 to determine the possible research directions of the Life Sciences User community during TRIUMF's next five year funding period (2000–2005). While what was presented reflected ongoing research, much of this effort has a long term component associated with it

and from the presentations it was possible to create a program which would form the basis of the future research programs in the Life Sciences into the next century.

There are two large projects that will seek major funding from new initiatives from the Canadian Federal Government. One is for the construction of a radiochemistry laboratory in existing space in the Meson Hall Annex basement. This area would have hot labs, sterile labs and shipping facilities. Funding for this project was sought from a number of sources including the Canadian Foundation for Innovation (CFI), MDS Nordion and the Provincial Government. By the end of the year we had learned that our proposal to the CFI was not successful.

The second project is the establishment of a Network of Centres of Excellence (NCE) based on PET Methodologies. There is a movement within Canada for the establishment of such a Network. In response to this initial effort a Special Interest Group on Clinical PET has been established. Funding for this project would be through the Federal Government program on NCE.

The review of the TRIUMF five year plan took place in the fall. Preliminary feedback from the review is very positive for the Life Sciences Program.

Experiment LS33

Evaluation and improvement of a dual head coincidence camera

(V. Sossi, UBC/TRIUMF)

The ADAC molecular coincidence dual head camera had been installed at Lions Gate Hospital in North Vancouver in August/September, 1997. The physics aspect of the research performed during the first year was mostly focused toward establishing an optimum scanning protocol for oncology imaging. To accomplish this we have:

- Determined the basic characteristics of the camera, such as sensitivity and scatter fraction.
- Determined the count rate performance of the camera both following NEMA guidelines and in a clinically meaningful situation.
- Determined the optimum acquisition mode and optimum count rate range.
- Determined an empirical formula for an optimum radiotracer dose to be injected to the patient, which was verified with patient studies.
- Examined contrast evaluation as a function of count rate.

- Performed a NEMA-NU2 evaluation test in collaboration with ADAC at Milpitas, CA, USA.

Results of studies 1–4 were presented at the 1998 Society of Nuclear Medicine meeting [Sossi *et al.*, J. Nucl. Med. **39**, 5 (1998)]. Particular emphasis was placed on defining and using scanning conditions that would mimic real patient scanning, such as the use of an extended phantom and clinically realistic scanning times. As a consequence of the phantom studies an empirical formula for an optimum tracer dose to be injected to the patient was determined: 1.88 MBq/kg at time of scanning. Nine patients have been scanned to date using this formula and in each case the single event rate fell in the optimum count range as defined from the noise equivalent count rate (NECR) curve. Since maximizing the scan length was found to be crucial to image quality, patients are now scanned in two bed positions covering the area of interest, 37 min/bed position as opposed to the initially recommended 20 minutes. Data are acquired in list mode and p-p and p-C images are reconstructed separately. Images obtained from p-p data have to date proven to yield sharper contrast, confirming the results of phantom studies

Results from study 5 were presented at the 1998 IEEE/MIC meeting in Toronto. In a situation where random events are not subtracted prior to reconstruction, the measured radioactivity contrast will be altered compared to the contrast actually present in the object. Since the random event fraction is a function of single event count rate it is to be expected such alteration would be count rate dependent thus potentially leading to inaccurate and artificially varying estimates of contrast. Such an effect would invalidate therapy efficacy assessment investigations. We have examined the magnitude of this effect. Results showed that it is very important to maintain similar count rate conditions when a repeat scan needs to be compared to a baseline scan. Photopeak-photopeak (p-p) only was found to be the acquisition mode that yields higher contrast compared to the photopeak-photopeak + photopeak-Compton (p-C).

Measurements at Milpitas defined the image characteristics of the camera according to a preliminary version of the NEMA-NU2 standards. The purpose of the NEMA-NU2 standards is to define the camera properties in a clinically meaningful setting in terms of count rate, concentration and scan duration. The measurements themselves were a test of the feasibility of the NEMA-NU2 protocol and as a result minor modifications to the protocol were suggested.

Experiment LS35

¹⁸F-nitroimidazole hypoxia agents

(M.J. Adam, TRIUMF)

Labelled nitroimidazoles have been used as markers for hypoxic tissue for some time. The compounds are retained in hypoxic tissue and serve as “hot spot” markers for tissue that is oxygen deficient but still viable. Knowing if a tumour is hypoxic is important to

treatment since the tumours are more likely to survive radiation and chemotherapy.

Recently, a new agent, EF5, has received clinical trial approval in the U.S. We have begun a collaboration with this group (Cameron Koch’s group at the University of Pennsylvania, Radiation Oncology) and with Kirsten Skov at the B.C. Cancer Research Centre to try to synthesize ¹⁸F labelled EF5 and its analogs.

THEORETICAL PROGRAM

Introduction

The motivation for a Theory group at TRIUMF has been to assemble a group of active people doing high quality research in areas which are relevant, in the broadest sense, to the physics program at TRIUMF and to the interests of the subatomic physics community across Canada. The Theory group provides a focus for the theoretical research at TRIUMF and support for the TRIUMF experimental program in all its many facets. Complementing the experimental program the theoretical research program also covers a wide range of topics in nuclear and particle physics. Part of this research involves working directly with the experimentalists on particular experiments; part with a more general background to the experimental program; and part with fundamental areas not currently related to the experimental program.

The Theory group has four permanent staff members: H.W. Fearing (group leader), B.K. Jennings, J.N. Ng, and R.M. Woloshyn; plus E.W. Vogt (professor emeritus, UBC). This year our research associates are: H.-W. Hammer, T. Hemmert (until February), B.D. Jones, S. Karataglidis, I. Maksymyk (until September), G.C. McLaughlin (since September) H. Müller (until September), T.S. Park (since September), T. Shoppa (until April) and P.R. Wrean (since September, shared with the DRAGON group). A graduate student, M. Nobes is being supervised by R.M. Woloshyn.

The visitors to the Theory group this year include:

K-L. Chan	J. Juge	A. Rinat
L.N. Chang	F. Khanna	S. Scherer
C. Davies	I.B. Khriplovich	R. Sinha
B. Dutta	V. Kuzmin	Z. Sullivan
A. Gal	C.S. Lam	R. Surman
J. Gasser	K.C. Leung	I. Towner
K. Goeke	H. Lipkin	E. Truhlik
J. Greben	P. Maris	C. Unkmeir
A. Halasz	G.A. Miller	D. Wilkinson
T. Hemmert	A. Misra	C. Wolfe
S.W. Hong	J. Niskanen	L. Zamick
C. Johnson	A. Ramos	

In addition to their research activities the theorists have taken an active part in the laboratory activities including: the Long Range Planning Committee, the Experiments Evaluation Committee, the TRIUMF Summer Institute and computer support.

As usual the Theory group has been very active and below we briefly describe some of the specific research projects undertaken by the group during the year.

Miscellaneous

Active-sterile neutrino transformation solution for r -process nucleosynthesis

(A.B. Balantekin, J.M. Fetter, Wisconsin; G.M. Fuller, San Diego; G.C. McLaughlin)

We study how matter-enhanced active-sterile neutrino transformation in the $\nu_e \rightleftharpoons \nu_s$ and $\bar{\nu}_e \rightleftharpoons \bar{\nu}_s$ channels could enable the production of the rapid neutron capture (r -process) nuclei in neutrino-heated supernova ejecta. In this scheme the lightest sterile neutrino would be heavier than the ν_e and split from it by a vacuum mass-squared difference of $3 \text{ eV}^2 \lesssim \delta m_{es}^2 \lesssim 70 \text{ eV}^2$ with vacuum mixing angle $\sin^2 2\theta_{es} > 10^{-4}$.

Nucleon-nucleon bremsstrahlung: an example of the impossibility of measuring off-shell amplitudes

(H.W. Fearing)

For nearly fifty years theoretical and experimental efforts in nucleon-nucleon bremsstrahlung ($NN\gamma$) have been devoted to measuring off-shell amplitudes and distinguishing among various NN potentials on the basis of their off-shell behaviour. New experiments are under way, designed specifically to attain kinematics further off shell than in the past, and thus to be more sensitive to the off-shell behaviour. We show in a recently published issue of Phys. Rev. Lett. that, contrary to these expectations, and due to the invariance of the S -matrix under transformations of the fields, the off-shell NN amplitude is *as a matter of principle* an unmeasurable quantity in $NN\gamma$.

Nuclear Structure and Reactions

GT strength in mass-6,7 and mass-56

(S. Karataglidis, G.C. McLaughlin)

The Gamow-Teller strength in ^{56}Fe is being calculated within the shell model to determine the usefulness of ^{56}Fe as a target material for a supernova neutrino detector. Such a detector would operate by observing neutrons from neutrino-induced neutron spallation reactions. Since supernovae produce high energy electron, mu and tau neutrinos and antineutrinos, the GT response is being calculated for both the neutral and charged currents. The wave functions for mass-56 have been determined within the fp model space assuming $0p-0h$ configurations with the addition of $2p-2h$ excitations in those cases where such is possible.

The GT matrix elements are also being calculated for the β -decays of ^6He and ^7Be using wave functions determined in a complete $(0 + 2 + 4)\hbar\omega$ model space. This "traditional" shell model calculation is being done to compare with the calculations using the

exact mass-6 and mass-7 wave functions obtained using the Green's functions Monte Carlo shell model by the Argonne National Laboratory.

Alternative evaluations of halos in nuclei

(*S. Karataglidis; K. Amos, P.J. Dortmans, Melbourne; C. Bennhold, George Washington Univ.*)

Data for the scattering of ${}^6\text{He}$, ${}^8\text{He}$, ${}^9\text{Li}$, and ${}^{11}\text{Li}$ from hydrogen have been analyzed within a fully microscopic folding model of proton-nucleus scattering. The model is based on the shell model and the g matrix constructed from the bare NN potential. The nuclear states were calculated in complete multi- $\hbar\omega$ spaces. Current data suggest that of these only ${}^{11}\text{Li}$ has a noticeable halo, although no definitive conclusion may be reached for ${}^6\text{He}$. For that nucleus, one may look to the alternative reaction, ${}^6\text{Li}(\gamma, \pi^+){}^6\text{He}_{gs}$, the data for which support the assertion that ${}^6\text{He}$ is not a halo system. However, more data for both the proton scattering and (γ, π^+) reaction are needed before such a conclusion may be reached.

S_{eff} and the ${}^7\text{Be}(p, \gamma){}^8\text{B}$ reaction

(*B.K. Jennings, S. Karataglidis*)

We explore approximations to the effective S factor for the ${}^7\text{Be}(p, \gamma){}^8\text{B}$ reaction using different approximation for the integral over the Gamow peak. In the temperature range of interest for solar neutrino production, S_{eff} may be determined to within 0.5% from $S(20)$ with no direct information on the derivatives of $S(E)$.

Extrapolation of the astrophysical S factor for ${}^7\text{Be}(p, \gamma){}^8\text{B}$ to solar energies

(*B.K. Jennings, S. Karataglidis, T.D. Shoppa*)

We investigate the energy dependence of the astrophysical S factor for the reaction ${}^7\text{Be}(p, \gamma){}^8\text{B}$, the primary source of high energy solar neutrinos in the solar pp chain. Using simple models we explore the model dependence in the extrapolation of the experimental data to the region of astrophysical interest near 20 keV. We find that below approximately 400 keV the energy dependence is very well understood and constrained by the data for the elastic scattering of low energy neutrons from ${}^7\text{Li}$. Above 400 keV nuclear distortion of the wave function of the incident proton introduces a significant model dependence. This is particularly important for the s -wave contribution to the S factor. The extracted value of $S(0)$ is $19.0 \pm 1.0 \pm 0.2$ eVb. The first error is experimental while the second is an estimate of the theoretical error in the extrapolation.

On the equivalence of the impulse approximation and the Gersch-Rodriguez-Smith series for structure functions

(*A.S. Rinat, Weizmann; B.K. Jennings*)

For a non-relativistic system we compare the Gersch-Rodriguez-Smith and the IA approaches to the structure function. The first of these two approaches generates a series in $1/q$, whereas the second treats the interaction between the struck and core nucleons perturbatively. Instead of the IA series we derive a DWIA representation and prove that, up to and including terms of order $\mathcal{O}(1/q^2)$, it is contained in the GRS series of the same order. This clarifies the relation between the two approaches and suggests that the two approaches, when treated exactly, produce identical structure function to arbitrary order in $1/q$.

Quark-meson coupling models for nuclear matter and finite nuclei

(*H. Müller and B.K. Jennings*)

The basic motivation of applying quark models to nuclear structure is the hope to reveal medium modifications of the internal structure of the nucleon. The idea that nucleons might undergo considerable change of their internal structure in a baryon-rich environment is supported by our understanding of asymptotic freedom in QCD. At sufficiently high densities one expects a transition to a new phase of matter with deconfined quarks and gluons. Quark-meson coupling (QMC) models are designed to explore indications of this phenomena at normal nuclear densities. However, it is important that these models which connect observed nuclear phenomena and the underlying physics of strong interactions respect established results.

In the original version of the QMC model proposed by Guichon [Phys. Lett. **B200**, 235 (1988)] nucleons arise as non-overlapping MIT bags interacting through meson mean fields. Although it provides a simple and intuitive framework to incorporate quark degrees of freedom in the study of nuclear many-body systems, the QMC model has a serious shortcoming. The predicted nucleon mass is too high and, as a consequence, the spin-orbit force is too weak to explain spin-orbit splittings in finite nuclei. The QMC model can be significantly improved by introducing the concept of a density dependent bag constant. In our work we have demonstrated that such a modified quark-meson coupling (MQMC) model can be accurately calibrated to produce the empirical saturation properties of nuclear matter and that it provides a good description of the bulk properties of finite nuclei. By analyzing binding energies, charge radii, nuclear shapes and single-particle spectra of spherical nuclei we find that the MQMC model leads to results of the same quality

as in established hadronic models. Most importantly, the accurate reproduction of the effective nucleon mass leads to a realistic description of spin-orbit splittings. Furthermore, unrealistic features of the nuclear shapes which arise in the original version of the QMC model are significantly corrected.

Effective field theory for $\Lambda - \Sigma^0$ mixing in nuclear matter

(H. Müller)

Strangeness adds another, still largely unexplored, dimension to nuclear structure. On the experimental side, physics of hypernuclei is approaching a phase in which not only ground state energies but also excitation spectra and electromagnetic properties are being measured. To explain properties of hypernuclei, detailed information on the elementary nucleon-hyperon and hyperon-hyperon interaction is needed which, at present, is scarce and incomplete.

We extend the effective field theory approach which successfully describes ordinary nuclei and nuclear matter to incorporate strangeness in nuclear structure. The central object is a chiral effective Lagrangian involving the baryon octet, the Goldstone boson octet, the vector meson octet and a light scalar singlet. According to the rules of effective field theory, we include all interaction terms (up to a given order of truncation) that are consistent with the underlying symmetries of QCD.

We develop a mean-field approximation and study nuclear matter as a simple model for multi-strange systems. A D-type Yukawa coupling between baryons and vector mesons leads to $\Lambda - \Sigma^0$ flavour mixing in the nuclear medium. The primary result is that nuclear matter is generally in a state of mixed flavour rather than in a state with distinct Λ and Σ^0 particles. As a consequence, systems which contain Λ hyperons always have a small admixture of Σ^0 hyperons. Disturbing the time independent nuclear matter ground state leads to flavour oscillations characterized by distinct frequencies. This effect is closely related to the phenomenon of neutrino oscillations.

Effective Field Theories and Chiral Perturbation Theory

The power of effective field theories in nuclei: the deuteron, NN scattering and electroweak processes

(T.-S. Park; K. Kubodera, USC; D.-P. Min, SNU; M. Rho, Saclay)

We show how *effectively* effective quantum field theories work in nuclear physics. Using the physically transparent cut-off regularization, we study the simplest nuclear systems of two nucleons for both bound and scattering states at a momentum scale much less

than the pion mass. We consider all the static properties of the deuteron, the two-nucleon scattering phase-shifts, the $n + p \rightarrow d + \gamma$ process at thermal energy and the solar proton fusion process $p + p \rightarrow d + e^+ + \nu_e$, and we demonstrate that these are all described with great accuracy in the expansion to the next-to-leading order. We explore how a “new” degree of freedom enters in an effective theory by turning on and off the role of the pion in the Lagrangian.

The solar proton burning process: revisited in chiral perturbation theory

(T.-S. Park; K. Kubodera, USC; D.-P. Min, SNU; M. Rho, Saclay)

The proton burning process $p + p \rightarrow d + e^+ + \nu_e$, important for the stellar evolution of main-sequence stars of mass equal to or less than that of the Sun, is computed in effective field theory using chiral perturbation expansion to the next-to-next-to-leading chiral order. This represents a model-independent calculation consistent with low energy effective theory of QCD comparable in accuracy to the radiative np capture at thermal energy previously calculated by first using very accurate two-nucleon wave functions backed up by an effective field theory technique with a finite cut-off. The result obtained thereby is found to support within theoretical uncertainties the previous calculation of the same process by Bahcall and his co-workers.

Effective field theory for low energy two-nucleon systems

(T.-S. Park; K. Kubodera, USC; D.-P. Min, SNU; M. Rho, Saclay)

We illustrate how effective field theories work in nuclear physics by using an effective Lagrangian in which all other degrees of freedom than the nucleonic one have been integrated out to calculate the low energy properties of two-nucleon systems, viz, the deuteron properties, the np 1S_0 scattering amplitude and the $M1$ transition amplitude entering into the radiative np capture process. Exploiting a finite cut-off regularization procedure, we find all the two-nucleon low energy properties to be *accurately* described with little cut-off dependence, in consistency with the general philosophy of effective field theories.

Effective theory for the non-relativistic three-body system

(H.-W. Hammer; P.F. Bedaque, INT; U. van Kolck, Caltech)

Following a proposal by Weinberg, there has been much interest recently in applying the successful concept of effective field theory (EFT) to nuclear physics. However, the presence of shallow bound states and the

associated unnaturally large scattering length in nuclear systems complicate the problem as the EFT resembles a condensed matter system near a phase transition. During the last year a consistent power counting scheme, the basis of an EFT, has been established for the two-body system. We have applied the EFT ideas to the three-body system and neutron-deuteron scattering in particular. While precise predictions are straightforwardly obtained for neutron-deuteron scattering in the spin-3/2 channel, additional complications due to a nonperturbative renormalization arise in the spin-1/2 channel and the bosonic system. These complications are related to the well known Thomas and Efimov instabilities. The problem can be solved by introducing a one-parameter three-body force at leading order. Although one additional parameter appears, the EFT still retains its predictive power. We have successfully applied this idea to the bosonic system of ^4He -atoms and neutron-deuteron scattering in the spin-1/2 channel and the triton.

Bianchi identities and the extension of the chiral perturbation theory meson Lagrangian to order p^6

(H.W. Fearing; S. Scherer, Mainz)

We discuss the application of Bianchi identities in the construction of the chiral perturbation theory meson Lagrangian to order p^6 . We propose a strategy to implement the constraints due to the Bianchi identities in combination with the trace and epsilon relations previously derived and explicitly identify terms of our original Lagrangian which are related by these identities and thus not independent. We find a reduction by 4 and 7 terms in the even and odd intrinsic parity sectors, respectively, resulting in 107 and 25 independent structures for SU(3).

Few-body processes in heavy baryon chiral perturbation theory

(H.W. Fearing; T. Hemmert, Julich; R. Lewis, N. Mobed, Regina; S. Scherer, C. Unkmeir, Mainz)

We have begun a series of calculations of few-body processes involving pions, photons, and a single nucleon in the framework of heavy baryon chiral perturbation theory. The approach follows that of our recently published calculation of ordinary muon capture, $\mu + p \rightarrow n + \nu$. The reactions of interest include radiative muon capture, $\mu + p \rightarrow n + \nu + \gamma$, radiative pion capture, $\pi + p \rightarrow n + \gamma$ and the associated electron processes, $\pi + p \rightarrow n + e^+ + e^-$ and $e + p \rightarrow e + n + \pi$, and doubly radiative pion capture $\pi + p \rightarrow n + \gamma + \gamma$ and its associated process $e + p \rightarrow e + n + \pi + \gamma$.

Comment on ‘Induced pseudoscalar coupling constant’ by I-T. Cheon and M.K. Cheoun

(H.W. Fearing)

In a recent preprint Cheon and Cheoun have derived from a chiral model an additional term, not usually appearing in the standard matrix element for radiative muon capture. Using that term they generate a large correction to the RMC spectrum which tends to resolve the problem caused by the too large value of g_P found in the TRIUMF RMC experiment. In this comment we observe first that their extra term leads to an amplitude which is not gauge invariant and second that such a term should be present, in a gauge invariant way, in an earlier full chiral perturbation theory calculation, which, however, found negligible differences from the standard approach.

Hadronic Structure

Spectral content of isoscalar nucleon form factors

(H.-W. Hammer; M.J. Ramsey-Musolf, Connecticut)

The low energy structure of the nucleon’s $s\bar{s}$ sea has become a topic of intense studies in the hadron physics community. In particular, the contribution of strange quarks to the spatial distribution of the nucleon’s charge and magnetic moment is interesting, since it can be measured directly in parity violating electron scattering. On the theoretical side a plethora of calculations is available, each having its particular merits and limitations. Our alternative approach is to start from a spectral decomposition of the strange vector form factors and to evaluate the obtained imaginary parts using dispersion relations and experimental data. Some previous model calculations are recovered as certain approximations in this framework. Most model calculations base on the so called “kaon cloud dominance” assumption, i.e. the strange sea in the nucleon is generated by virtual transitions of the nucleon to a kaon and a hyperon (e.g. $p \rightarrow K^+ \Lambda \rightarrow p$). Using dispersion relations, we study the lightest such contribution stemming from the $K\bar{K}$ -intermediate state. Based on an analytic continuation of experimental KN scattering amplitudes and bounds from unitarity, we evaluate the $K\bar{K}$ contribution to the electric and magnetic radii as well as the magnetic moment to all orders in the strong interaction. We also demonstrate the relationship between non-resonant and resonant $K\bar{K}$ contributions to the form factors and derive values for the vector and tensor $\phi N\bar{N}$ couplings. The $K\bar{K}$ spectral functions are used to evaluate the credibility of model calculations for the strange quark vector current form factors.

K^* mesons and nucleon strangeness

(*H.-W. Hammer; L.L. Barz, F.S. Navarra, M. Nielsen, Sao Paulo; H. Forkel, Heidelberg; M.J. Ramsey-Musolf, Connecticut*)

We study contributions to the nucleon strange quark vector current form factors from intermediate states containing K^* mesons. We show how these contributions may be comparable in magnitude to those made by K mesons, using methods complementary to those employed in quark model studies. We also analyze the degree of theoretical uncertainty associated with K^* contributions.

Parity violating excitation of the $\Delta(1232)$: hadron structure and new physics

(*H.-W. Hammer; J. Liu, N.C. Mukhopadhyay, RPI; S.J. Pollock, Colorado; M.J. Ramsey-Musolf, Connecticut*)

We consider the prospects for studying the parity violating (PV) electroweak excitation of the $\Delta(1232)$ resonance with polarized electron scattering. Given present knowledge of standard model parameters, such PV experiments could allow a determination of the $N \rightarrow \Delta$ electroweak helicity amplitudes. We discuss the experimental feasibility and theoretical interpretability of such a determination as well as the prospective implications for hadron structure theory. We also analyze the extent to which a PV $N \rightarrow \Delta$ measurement could constrain various extensions of the standard model.

Phenomenology of B_c mesons

(*M. Nobes, SFU; R.M. Woloshyn*)

The leptonic and semi-leptonic decays of B_c mesons are calculated in an extended NJL model which has been extended further for use with heavy quarks. A shortcoming of this approach is the lack of confinement which prevents the application of this model to the description of certain light vector mesons. To overcome this limitation, calculations are also being done using the quark confinement model. Lepton spectra as well as total decay rates for all semi-leptonic decay modes of B_c are being calculated and will be compared with other kinds of model calculations. Leptonic and semi-leptonic decays of D , D_s , B and B_s mesons are being studied as well to determine the parameters in the calculation.

Mesonic decay constants in lattice NRQCD

(*B.D. Jones, R.M. Woloshyn*)

Lattice NRQCD with leading finite lattice spacing errors removed is used to calculate decay constants of mesons made up of heavy quarks. Quenched simulations are done with a tadpole improved gauge action

containing plaquette and six-link rectangular terms. The tadpole factor is estimated using the Landau link. For each of the three values of the coupling constant considered, quarkonia are calculated for five masses spanning the range from charmonium through bottomonium, and one set of quark masses is tuned to the $B(c)$. “Perturbative” and non-perturbative meson masses are compared. One-loop perturbative matching of lattice NRQCD with continuum QCD for the heavy-heavy vector and axial vector currents is performed. The data are consistent with the vector meson decay constants of quarkonia being proportional to the square root of their mass and the $B(c)$ decay constant being equal to 420(13) MeV.

Valence QCD

(*K.F. Liu, S.J. Dong, T. Draper, J. Sloan, Kentucky; D.B. Leinweber, Adelaide; W. Wilcox, Baylor; R.M. Woloshyn*)

A valence QCD theory was developed to study the valence quark properties of hadrons. To keep only the valence degrees of freedom, the pair creation through the Z graphs was deleted in the connected insertions, whereas the sea quarks were eliminated in the disconnected insertions. This was achieved with a new “valence QCD” Lagrangian where the action in the time direction was modified so that the particle and antiparticle decouple.

It was shown in this valence version of QCD that the ratios of isovector to isoscalar matrix elements (e.g. F_A/D_A and F_S/D_S ratios) in the nucleon reproduce the SU(6) quark model predictions in a lattice QCD calculation.

In addition, it was found that the masses of N , Δ , ρ , π , a_1 , and a_0 all drop precipitously compared to their counterparts in the quenched QCD calculation. This was interpreted as due to the disappearance of the ‘constituent’ quark mass which is dynamically generated through tadpole diagrams. The origin of the hyper-fine splitting in the baryon was largely attributed to the Goldstone boson exchanges between the quarks. Both of these are the consequences of the lack of chiral symmetry in valence QCD.

The Standard Model and Beyond

Constraints on T-odd, P-even interactions from electric dipole moments, revisited

(*G.C. McLaughlin; M.J. Ramsey-Musolf, A. Kuriliov, Connecticut*)

One manifestation of possible physics beyond the standard model (SM) may be the existence of new low energy interactions which violate time-reversal invariance (T) but conserve parity invariance (P). On general grounds, one expects the most important low energy effects to arise from the lowest-dimension effective

operators, since their effects scale as $(\frac{p}{M_x})^{d-4}$, with p being a typical momentum associated with the low energy process of interest, d the operator dimension, and M_x being the low mass scale associated with the new physics. We work to derive the bounds on these operators from experiment. We are computing the effective T-odd P-odd dimension seven operators generated by parity violating weak radiative corrections. We are then relating this TOPO operator and the original TOPE operator to quantities such as \bar{g}_π and \bar{g}_ρ .

Invisible decays of quarkonium states

(L.N. Chang, O. Lebedev, VPISU; J. Ng)

We estimated the most important corrections to the branching ratios for the invisible decays of quarkonium states, arising from possible extensions of the standard model. Among the possibilities considered are the presence of extra Z -bosons, minimal supersymmetric extensions of the standard model with R -parity violation and decays into Goldstinos. Prospects of detecting these corrections at existing and future B -factories and τ -charm factories are discussed.

EXPERIMENTAL FACILITIES

Proton Therapy Facility

(*E.W. Blackmore, TRIUMF*)

A total of 11 patients were treated during seven available treatment weeks in 1998, bringing the total number of patients treated with protons at TRIUMF to 47. Ten of the treatments were for ocular melanoma and one for an ocular hemangioma. As for previous years about half of the patients were from British Columbia and the remaining from Alberta, Saskatchewan and Manitoba.

Results to date indicate that about 60% of these tumours could not have been treated with radioactive plaque therapy – the usual alternative to protons. Those patients would have had to receive proton treatment outside of Canada or have the eye removed. The remaining 40% are considered to be better treated with protons based on location and size of the tumour. Control of tumours (at this relatively early stage) appears excellent. Factors pre-disposing to the development of significant treatment-related complications include large tumours, and those situated close to the anterior eye structures such as the ciliary body. Overall the clinical results appear to be in line with larger series from Europe and the United States.

It now appears that about 1/3 of the patients are being treated through the eyelid requiring slightly more range than originally planned for. We have re-measured beam data for a 74 MeV extracted beam, which gives 5 mm more range than the presently used 70 MeV, and will start to use this higher energy in 1999.

No significant changes were made to the hardware or software of the treatment control system. The dedicated computer PTCS0 which provides the operator interface was upgraded from a MicroVAX 3400 to a VAX 4100, resulting in faster response for displays, in particular during dose scanning measurements. The software code for homing the patient treatment chair at start up was modified. One motor on the chair failed and had to be replaced. The three-axis scanner which was developed in 1997 was commissioned and now lateral dose scans can be made in both the horizontal and vertical directions, as well as depth dose scans. At present the scanning program allows only two motions to be used at one time and needs to be re-written to provide the full three-axis capability.

The M.Sc. student project to measure proton dose profiles using a sensitive scintillation screen viewed by an integrating CCD camera was completed and a thesis written. Effort has now switched to using the same technique for imaging the x-rays taken for patient alignment, in order to speed up this process. Mea-

surements show that the present camera is not quite sensitive enough and intensified cameras are being investigated, as well as the software for image processing.

During the August treatment week another set of cell irradiations was carried out by the biophysics group at the Cancer Research Centre to measure the relative biological effectiveness (RBE) of 70 MeV protons.

Proton Irradiation Facility

(*E.W. Blackmore, TRIUMF*)

The proton irradiation facility (PIF) is used to simulate the proton fluxes in space for testing and characterizing electronic components, materials or various types of radiation dosimeters intended for space applications. Typically a few minutes of testing in a few nanoampere proton beam from BL1B or BL2C corresponds to years of exposure in space. BL1B is used for energies from 500 MeV to 180 MeV and BL2C-1, the proton therapy line, for energies from 120 MeV down to about 20 MeV.

There was only limited PIF running during 1998 as beam time on both beam lines was difficult to schedule and a one week run at the end of October had to be cancelled due to serious problems with the cyclotron. In May a 40 MeV proton irradiation was carried out for the CAL Corporation in Ottawa on a CCD camera. A total dose of 10 kRad was used.

To make up for some of the beam time lost in October, two brief periods were scheduled at a later time. In November, a series of passive irradiations were carried out for DREO on three types of GaAs or AlGaAs devices: QWIPs (quantum well infrared photodetectors), LEDs and QWIP-LEDs. Proton energies of 30 and 63 MeV were used with fluences to 10^{12} protons/cm². In December, two days were used to test several devices for SPAR Space Systems. These included tests of proton upsets in two types of Pentium computers P-II and MMX under different operating conditions, and radiation damage studies of CCD and CMOS cameras. The computer tests were carried out at 200 MeV and 60 MeV with proton fluences to 10^{10} protons/cm². The radiation damage studies were carried out to total doses of 25 kRad.

μ SR User Facility

(*S. Kreitzman, TRIUMF*)

This year saw a somewhat attenuated activity in the basic experimental science program at TRIUMF, due principally to long shutdown periods devoted to the installation of the ISAC beam line components. Also, the fall beam period was beset by substantial problems in the cyclotron operations further reducing

(to ~ 13 weeks) the high intensity beam available from an already thinned schedule. Finally, 1998 was the last year (for the foreseeable future) in which μ SR will have any access to M13, with only 4 weeks of effective beam time attained. Thus μ SR usage in 1998, comprising approximately 30 experiments taking 37 beam weeks distributed on an average of three μ SR channels, was considerably reduced from historical norms. 1999 sees a return to the historical allocation (~ 26 weeks) of high intensity beam delivered at TRIUMF and it is hoped that this will allow the μ SR program to return to prior levels of activity.

More significantly in the longer term, the μ SR user facility was required to reapply for its MFA (Major Facility Access) Grant from its funding body in 1998. This application was a request for the salary support of five individuals (two technicians, two liaison scientists and a new position) who maintain and facilitate μ SR operations at TRIUMF. The grant application is for three years, and included the new position so that the facility could also support the condensed matter program taking shape in ISAC. The relative success of this application will determine the fundamental level of support the facility can provide its users.

On a more specific note, various initiatives that the facility undertook during 1998 are detailed in the sections below. The Infrastructure section discusses the basic changes in our standard data acquisition deployment encompassing both hardware and software issues. A section on spectrometers describes significant news regarding these experimental apparatus. Finally, a brief section on documentation lists the location of relevant information which can be found on the facility's Web site.

Infrastructure

TDC clocks: The infrastructure development work centered mainly around testing and debugging the new BNC 980 VME based TDCs which the facility is about to adopt as its standard clock. We now have five of these instruments, all operating within the design parameters at high rates of data acquisition. It has been found that the key to stable timing within 100 ps/bin is careful calibration of each individual channel at the factory. These clocks along with their service modules (a dedicated VME PowerPC based processor board) can acquire data up to 100 K event/s, comfortably exceeding the requirements for μ SR experiments. The clocks will run in all permanent μ SR channels in the spring of 1999.

Cryogenic control: The long standing need of complete remote management of a sample's cryogenic environment has also been addressed. A VME base deployment of the hardware and software needed to remotely

control needle valves (on both cryostats and transfer lines) and mass flow controllers has been integrated into the CAMP slow control system. With this new capability the need for the users to intervene in the beam area to facilitate cryogenic control will be much reduced.

Spectrometers

SFUMU: The SFUMU spectrometer rebuild has been completed. This newly versatile instrument is now capable of running either with its field along the beam momentum (the condensed matter set-up) or its field perpendicular to the beam (used in TF experiments for high momentum muons). Since SFUMU provides fields of up to 4 kG it extends the field range available from conventional spectrometers.

Belle: The 7.5 T Belle superconducting Helmholtz magnet, used in the high timing resolution spectrometer, has received a minor technical upgrade which will allow its field to be stabilized over a long period of time. This has proved necessary, since the supercurrent in persistence mode was found to degrade by 1 part in 10^5 /hour, too high for precision experimental work. The method used was to rebuild the room temperature bore of the magnet and incorporate into it a correction coil whose flux lines are mostly well within the superconducting pancakes. Thus there is little net flux within the coil on the application of a small correction field, allowing one to correct the central field without having overall superconducting current change. In conjunction with this was the commissioning of a new type of cryogenic hall probe which could be located in the central field right beside the sample, thereby allowing for real-time field stabilization for experiments utilizing the high timing resolution spectrometer.

GEANT: A further issue which was confronted for this magnet/spectrometer surrounded the fact that creating a well focused beam in a sample regime that is closely bounded by counters on all sides is extremely non-trivial. The source of complication (and resolution) is the fact that at the high fields (>4 T, such as that found in our superconducting magnets) themselves focus and defocus the muon beam as it proceeds to the sample at the centre of the field. Controlling this action coupled with the beam scattering due to a somewhat remote muon counter and cryogenic windows is a great challenge. To help understand all the parameters involved the facility has developed an expertise in the use of GEANT to model such situations. It has allowed for the optimization of collimators, muon counter thickness and beam injection focusing in this apparatus, resulting in more muons landing in the central sample region, with the attendant reduction of correlated backgrounds.

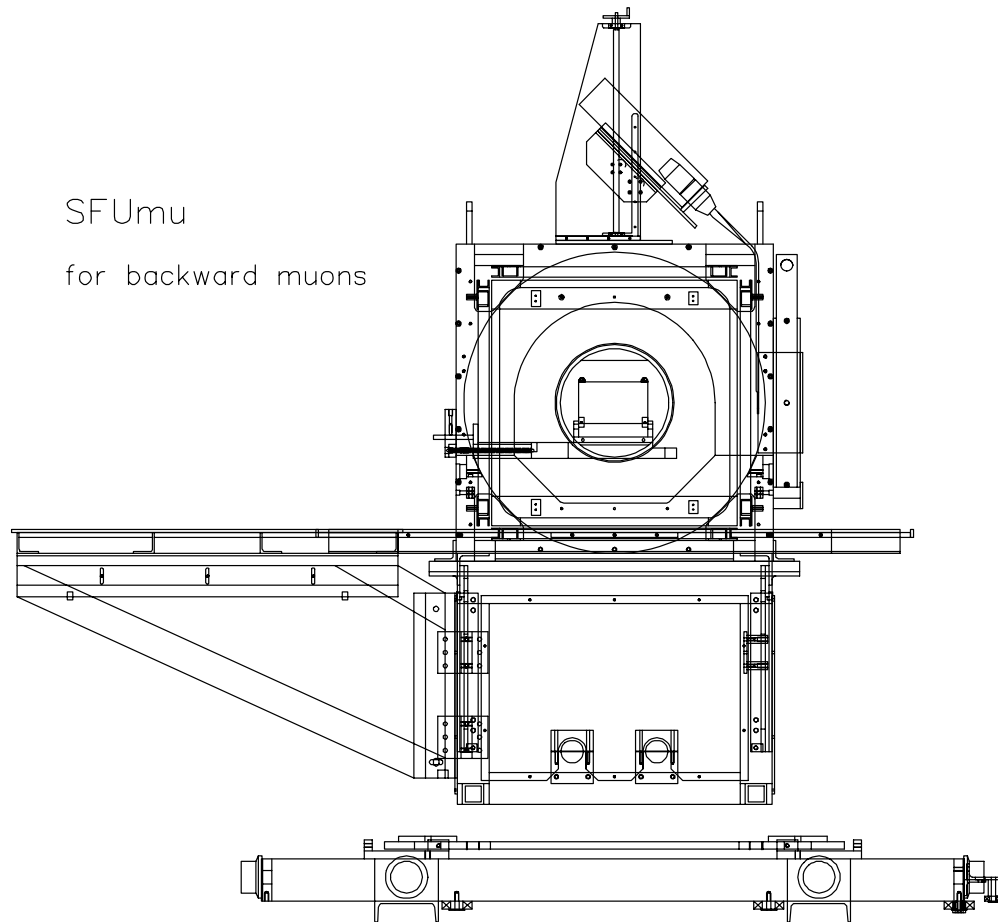
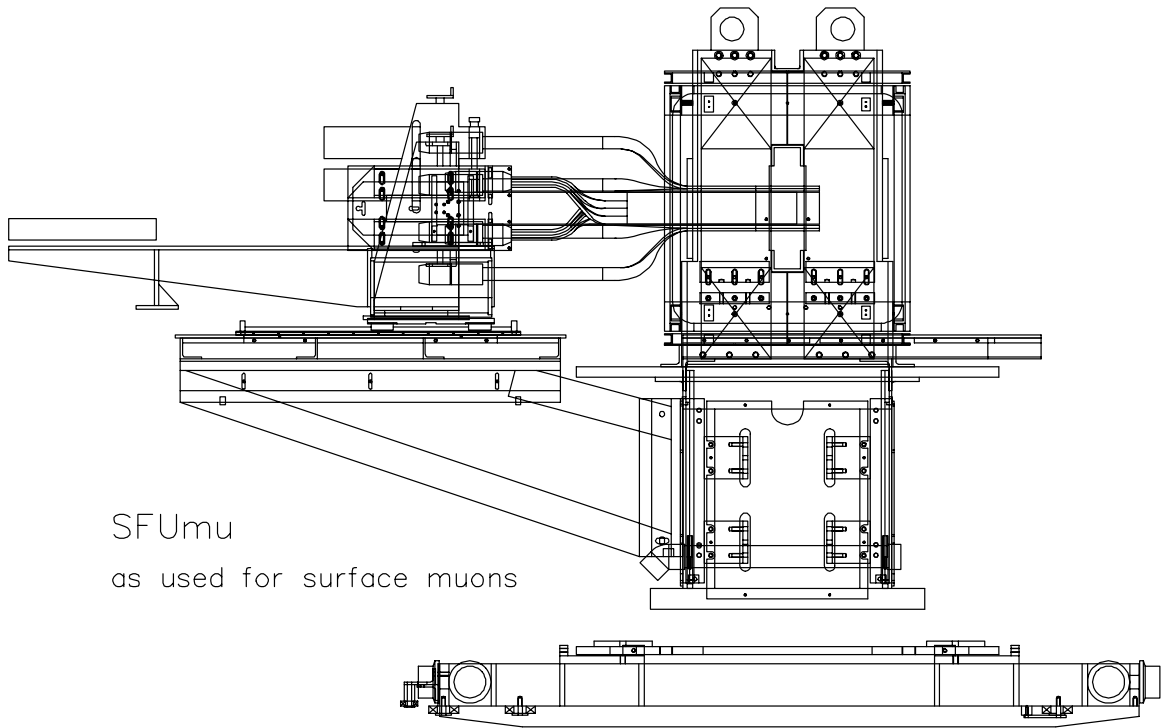


Fig. 97. The new SFUMU spectrometer.

Facility documentation and Web pages

For current or potential users of the facility, two guide documents are available. The TRIUMF μ SR Facility Users Guide details general information about the nature of μ SR experiments and how to go about preparing for them. The TRIUMF μ SR Operations Guide is mostly for on site researchers who are involved in the actual running of an experiment. It is concerned with details of the data acquisition/analysis and experimental control. These documents can be obtained on request from msrorg.triumf.ca.

Further detailed information on many aspects of the the μ SR facility is available through <http://www.triumf.ca/musrfac>. There one can find information about schedules, spectrometers, beam lines, safety, data acquisition, having an experiment approved and scheduled and other issues relevant to μ SR users.

Detector Facility

(*R. Henderson, TRIUMF*)

This year has been a very active one for the detector facility. In particular, the large BaBar chamber was finished on time and delivered to SLAC. Since then, the facility has become strongly involved with two large projects, ATLAS and Expt. 614. In addition, we are contributing significantly to the ISAC facility.

In the Scintillator Shop a variety of scintillators have been built, the biggest customer being the μ SR group. This year there were fewer scintillators required. This was fortunate since both the ATLAS and Expt. 614 projects are in pre-production stage, where the machining requirements are very significant. The Scintillator Shop is also starting work on prototype scintillators for the G0 project at CEBAF. After these are tested at CEBAF, the shop will start scintillator production for that project, which will involve about 1.5 man-years of shop time over the next two years.

The BaBar chamber was completed and shipped to SLAC at the beginning of March. This large cylindrical wire chamber was the first major sub-system to be delivered and was on schedule. Subsequently, the readout electronics have been fully installed and the chamber installed in the BaBar spectrometer. All tests indicate the chamber is working very well. This successfully concluded two years of work by the facility and the BaBar group.

The facility designed, fabricated and commissioned a large oven specifically for the ATLAS project. This oven contains the ALTAS pneumatic press for production of the many large foil laminates the project requires. This oven, and an electric winch system to lift the lid, has been installed in the upstairs clean room and the room exhaust system modified somewhat. This

major production item for the project has been in use for several months, with excellent results.

The BaBar project required considerable modification of the large clean room and installation of large custom steelwork. Since the end of that project, the CR has been prepared for the ATLAS project. The BaBar steelwork has been removed and an extensive new crane system has just been installed for assembly of the calorimeter modules. These modules weigh 3.5 tons each. The facility organized all the changes to the clean room.

The ATLAS project also requires a 'cleaning shed' to the east of the large clean room. This steelwork will be covered with plastic. Copper plates will be cleaned in ultrasonic tanks, then rolled into the clean room on an overhead beam. This shed is now being fabricated. The granite table previously in this area had been relocated at the east end of the meson hall (beam floor level). This area of the Beam Lines group had been used mostly for storage. The facility had it cleaned, painted, an aluminum structure designed and built, then covered with plastic, making a production area for components of both the ATLAS and Expt. 614 projects. The granite table/foil stretching system has been modified for the Expt. 614 requirements. The facility was responsible for all these changes.

With ATLAS expected to use most of both the facility clean rooms, another clean room was required for the Expt. 614 project. Fortunately, there was a suitable room. The Electronics Microstructure group has been considerably reduced and their clean room was available. The detector facility remodelled this room and dramatically improved its quality.

The facility is strongly involved with the Expt. 614 group. This sophisticated experiment aims to measure the Michel parameters to ten times the precision they are now known. R. Openshaw is designing the complex gas system. It will be built and tested in the facility. W. Faszer is also a member of the Expt. 614 experiment, adding his expertise. He will help oversee the chamber production. R. Henderson has joined the experiment and is doing a large part of the detector stack design and contributing to the overall experimental design.

W. Faszer has designed and tested circuits for the ISAC facility. These have ten times the sensitivity of those currently in use. This circuit has been tested very successfully. R. Henderson and R. Openshaw designed the prototype DRAGON ionization chamber. This has been successfully bench tested and will be tested in-beam. Since then, we designed a position sensitive PGAC (parallel grid avalanche chamber). If successful, this small chamber will be installed at the front end of the ionization chamber. The PGAC has been built and will be bench tested soon.

Cryogenic Targets

(*W. Kellner, TRIUMF*)

The demand for liquid hydrogen targets in experiments remained high in 1998. After the successful upgrade of cryogenic cooling on the parity (Expt. 497) target, described in the 1997 Annual Report, it ran successfully for three weeks in January and four weeks in July/August. The small LH₂ target of the CSB experiment (Expt. 704) on SASP was in operation for a total of ten weeks over the summer and autumn schedules. It too ran well, requiring only the replacement of one inner window and the addition of a small heater to prevent unwanted condensation of LH₂ in its cold gas volumes.

The protium target was re-activated in the RMC facility for use by Expt. 838. Although some parts of the mounting system had to be re-made and the control computer showed its age, the target was recommissioned and used successfully in a two-week run in December.

The new target for CHAOS was not a success – the resources allocated to this project proving insufficient to meet the challenges of this target. Those challenges included a need for an LH₂ cell with as large a diameter as possible, but inserted via a long, small-bore aperture in the CHAOS magnet. The cold-head and heat pipe used in a previous, smaller target of CHAOS did not have sufficient cooling power for the new cell. A revised version with more powerful cold-head and a new heat pipe is under construction.

Computing Services

(*C. Kost, TRIUMF*)

Overview

As predicted in the last Annual Report, the “third wave” (Pentium based machines, where the “first wave” constituted the VAX/VMS based machines of the 1980’s and the “second wave” was based on the RISC architecture which started around 1990) has nearly matched the combined computing power of all other machines in a time spanning just 2 years. As was the case last year, the powers behind this wave were machines running LINUX. The problems of dealing with this wave largely remain:

- security concerns grow as LINUX becomes the favourite hacker environment
- decreased reliability of vendor software in a rush to market products
- lack of proper vendor support as we abandon major computer companies (or they abandon us) in an effort to reduce “costs”
- increased complexity of software management.

As a result, maintaining stability of a rapidly changing computing infrastructure continues to be a key chal-

lenge as we approach the millenium.

Hardware

Figure 98 shows the state of TRIUMF’s computing facilities in December from Computing Services’ point of view. After what must be the longest streak for an operating system, the campus MTS system was closed down early 1998. As well, many of TRIUMF’s ULTRIX based DECstations were phased out. Support of this platform will dwindle over a number of years. The dual-4100 based VAX/VMS cluster remains a reliable, low maintenance work-horse for many users, although plans are to migrate the mail service from this cluster to a RAID based LINUX platform and reduce the hardware maintenance to a per-call basis.

The single ALPHA server, alph04 (an ALPHAstation 600 5/333), upgraded to 765 Mbytes of memory and having over 60 Gbytes of disk space, continues to provide the bulk of public UNIX support at TRIUMF. The public LINUX machine, a 200 MHz Dual Pentium Pro with 256 Mbytes of memory and 20 Gbytes of disk space, was replaced by a 450 MHz Dual Pentium II with 36 Gbytes of disk space. With increasing PC compatible software availability (e.g. from Corel and StarOffice) usage of LINUX should increase at an even faster pace in 1999. The Windows NT platform is still a minor, although possibly a significant, future factor.

Figure 99 shows our annual update for the growth of CPU power.

Since a cost-effective solution of an integrated X-support environment based on the Microsoft NT platform is not yet available, we continue to use the Windows-NT server, running the Wincenter product which allows up to 15 simultaneous users on Xwindow terminals to run PC software. Cost effective “thin-PCs” supporting Xwindows (so called NetPCs) did not materialize this year as expected. With the ever increasing power/lower cost of PC hardware, and despite their increased management costs, more Windows/98 based systems were purchased. Due to limited PC support that can be provided by Electronic Services and with our Computing Services group concentrating on a more “centralized” support model for PCs, much of the management of site PCs continues to be down-loaded to the end-user. This may well have a negative impact on some of our scientists and engineers.

LAN

The local area network, with its fibre-base FDDI backbone has proven to be quite stable, despite the fact that over 700 devices are connected to it. Plans are to migrate to a star-based topology at each of the 5 FDDI linked hubs using 10baseT/100BaseT. The first areas planned for rewiring are the Chemistry Annex and the

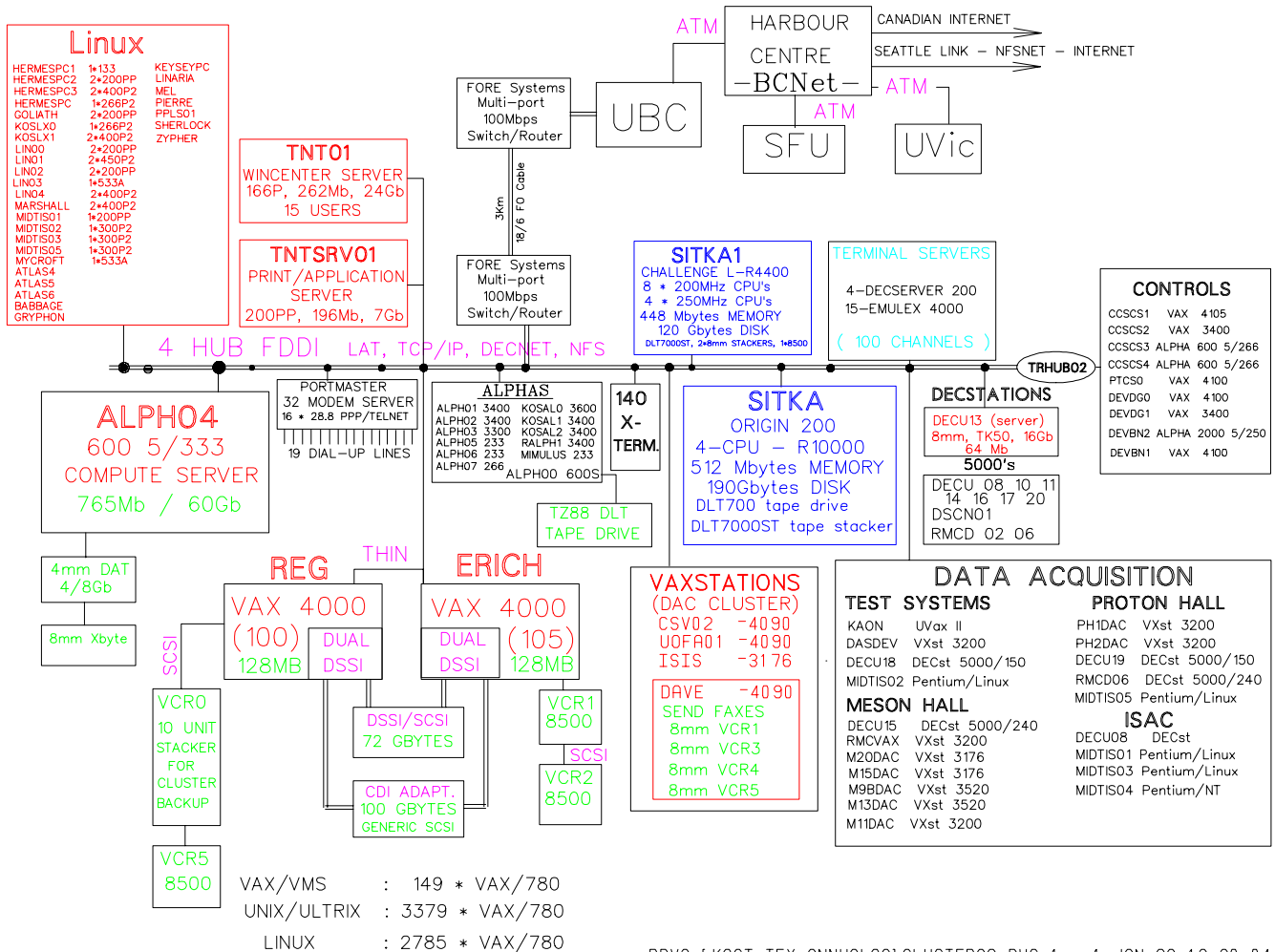


Fig. 98. TRIUMF computing facility.

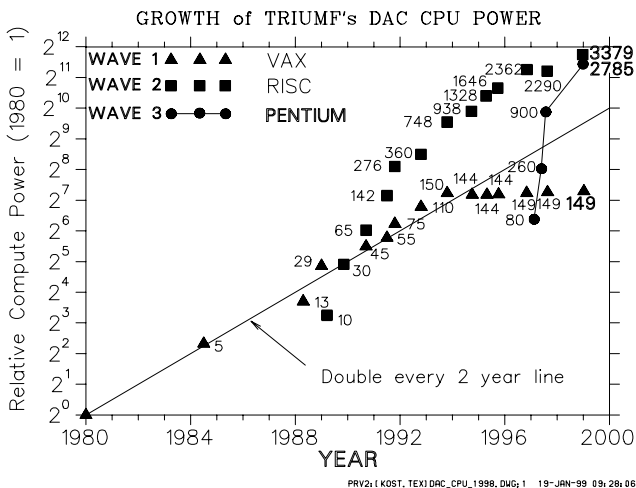


Fig. 99. DAC computing growth.

main office building. This should reduce a number of failures that have resulted when a break occurred in the currently used thin-wire loops.

Telecommuting

Offsite access to TRIUMF from home continues to grow at a modest pace as more staff acquire PCs at home. High speed network links to the home are still the exception since the costs are still high. Three 56 K modem lines will be added to the dial-up pool in early 1999.

ISAC and the Internet

The relocation of the FORE Powerhub 7000 from the main office to the ISAC building went very smoothly. The duplex 100baseT connection over the new 3 km optic fibre to UBC has proven to be very reliable.

The required cabling is now in place in the ISAC building to provide services to the ISAC controls and data acquisition areas.

Figure 100 shows the planned configuration, set for completion in the near future.

Internet and ISAC Network Diagram

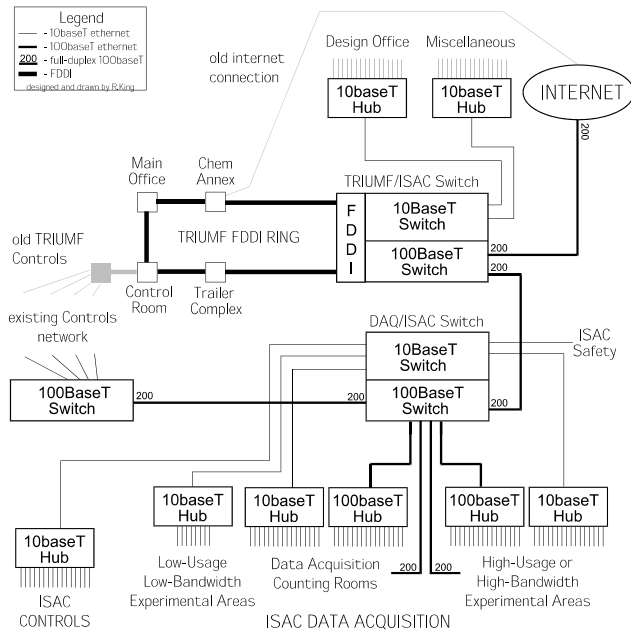


Fig. 100. Internet and ISAC network.

WAN

There were no significant changes in the performance of wide area networking over 1998 as seen from TRIUMF. The Internet is accessed via the fast Ethernet link to UBC, onto BCnet in downtown Vancouver. BCnet, as an integral part of the provincial information highway, provides direct links to the larger Canadian network, CA*net II and the BC GigaPOP, and the World Wide Internet.

Bandwidth and response time remains excellent to Canadian universities also connected to CA*net II and US institutions with a point of presence at the US STAR TAP in Chicago. For example, the University of Alberta, McGill and the University of Toronto are present on CANet II. Carlton is still on the larger Canadian network. In the US, the ESnet supported labs, Brookhaven, SLAC, Fermilab and the major research universities connected via Internet 2, are all present at STAR TAP.

Unfortunately the European and Japanese networks are not connecting in Chicago. Part of a special transatlantic link to CERN is paid by NSERC via a grant to HEP CAN to ease traffic congestion over the Atlantic. Traffic to DESY is especially bad.

Image processing station

The 133 MHz Pentium with 128 Mbytes of memory was supplemented with a 350 MHz Pentium II with twice the memory. Added to the latter was a HP PhotoSmart scanner to handle high resolution scans of 35 mm slides, negatives, and regular photographs, and a

Yamaha CRW-4260 CD-Rom burner to distribute and make legal copies in this format. A Kodak DC220 camera, taking digital images of resolution 1152*864, is now extensively used to document site projects during the assembly stage. Most of these images are subsequently catalogued in thumbnail format in pdf format and placed on a locally accessible Web page to allow users to browse and retrieve the relevant high resolution images.

This imaging station was also intensively used during the ICHEP'98 conference (URL icheck98.triumf.ca) held at TRIUMF July 23–29, to scan and place on the WWW some 7000 transparencies shown at this conference. Details on how this was done can be found via the URL www.triumf.ca/icheck_transparency_scanning.html All papers were on-line within minutes of the completion of the last conference presentation!

Software developments

GEANT4

Two members of our group continued to be very active participants in the GEANT4 international collaboration, aimed at creating a detector simulation tool kit for the next generation of HEP experiments. Their efforts were mainly directed to the development of low and medium energy hadron physics process and cross section classes. Detailed elsewhere in this Annual Report is TRIUMF's significant, and very visible contribution to this high profile, leading edge programming project. With the release of the first production version a new commitment has been recently undertaken with the signing of a 2-year Memorandum of Understanding to "define the distribution of the management, support, and future development of the GEANT4 software as from the release of the first production version".

ACCSIM

ACCSIM is a locally developed synchrotron multiparticle tracking and simulation code. This year the work was concentrated on implementing an improved model of transverse space charge, going beyond the existing "DQ" package which is able to give very efficient estimates (and simulations) of space-charge tune shifts but which is not fully self-consistent in its tracking of the macroparticle ensemble. In addition to CERN applications, the program was in active use at BNL and ORNL (for SNS accumulator ring design), KEK (JHF booster design) and LANL (PSR studies).

A survey was conducted of the common field-solution and tracking (integration) techniques. These come from the plasma physics realm and have been applied to linacs and beam lines but seldom to rings, where the ensemble must be tracked for many revolutions. Moreover, the popular FFT-based field solvers

do not lend themselves well to beams with a large and growing halo, which is of concern for intense-beam multiturn injection schemes.

A field solver was developed which is a hybrid of fast-multipole (FMM) and particle-in-cell (PIC) techniques. It can accommodate charge distributions with any number of halo particles at arbitrarily large amplitudes, and at equivalent spatial resolutions it is competitive in speed with FFTs. ACCSIM tracking in test lattices with this method produced the expected fields, single-particle tunes, and envelope tunes for K-V beams. A paper on this work was presented at the Shelter Island Workshop on Space Charge Physics in High Intensity Hadron Rings.

Other additions to the code were: generalized rf cavity element allowing arbitrary (non-integer) harmonics and phases; rf voltage plotting; interactive injection steering; and import and export of particle ensembles, allowing generation and stacking of “beamlets” at arbitrary locations.

Potpourri

- To ease centralized printing support we are upgrading all public printers, and require any future networked printers, to be able to autosense and support Postscript.
- Mathematica is now licensed for up to 6 site users on any system running Digital UNIX, and up to 8 site users on systems running LINUX on Pentiums.
- The very large LANL supplied FORTRAN codes MCNP4B and LCS (Lahet Code System), both used for shielding calculations, were installed on the public LINUX system lin01.
- The locally developed and worldwide utilized data manipulation/display program Physica now has an upgraded reference manual as well as a new user’s guide. Pdf and html versions can be accessed via WWW URL <http://www.triumf.ca/physica/html/homepage.html>. A large number of enhancements were added to Physica such as user functions implemented as a shared library for the Digital UNIX machines, MINUIT support similar to the existing FIT command, enhances to the scripting facility, and improved support for μ SR data structures.
- The interactive beam transport code INTRAN was ported to the Intel/LINUX platform, while the beam scattering/transport code REVMOC was ported to the Windows/95 platform.

WWW

Our group continued to provide software management services for TRIUMF’s main Web server, and to provide consultation and coordination with the many contributors providing content for our Web site. The growth in server content and usage continued unabated

with improved optic-fibre links (running at 100 Mb/s) to UBC and the advent of Internet-2/Canet-2 that improved connectivity to other HEP sites.

Security

Daily attacks on machines at TRIUMF continue. Despite them we have been able to maintain the open computing environment that TRIUMF has been accustomed to and finds so beneficial to the user community. A number of additional security measures have been put in place as well as the provision of user tools such as the secure shell ssh, to prevent the clear transmission of passwords over the network, and mxconns, to control access to Xwindows. Policy measures are also being adopted to ensure that all computers connected to the TRIUMF site meet minimal security standards.

The single DLT drive continues to provide excellent reliability in the daily backup of many of the site’s UNIX based machines. However, no such centralized service is as yet provided for the many PC/Windows systems.

Summary

So far the answer to last year’s question: “Will these non-integrated vendors deliver reliable hardware and software” was a resounding “NO”. Dealing with the highly fragmented software and hardware environment will prove to be the most challenging problem for the coming year.

Data Acquisition Systems

(*R. Poutissou, TRIUMF*)

Overview

During 1997, the migration from VAX host-based systems to Pentium host-based systems has accelerated.

The VAX based systems run under VMS with VDACS event by event software or μ SR MODAS software. VMS and VDACS are frozen at the present versions except for fixes of serious bugs. There are 9 active VAX legacy systems:

- 3 VMS/QBUS/CAMAC legacy systems – ph1dac, ph2dac, m11dac
- 1 VMS/CFI/FASTBUS RMC system – rmcvax
- 2 VMS/QBUS/CAMAC μ SR systems – m9bdac, m13dac
- 2 VMS/Ethernet/VME/CAMAC μ SR systems – m15dac, m20dac
- 1 test system VMS/Ethernet/VME/CAMAC or QBUS/CAMAC – dasdev

The Pentium based systems run mostly under LINUX with MIDAS software. This is the platform where software developments and improvements are active. Efforts on incorporating slow controls to the main data stream are ongoing. There are 6 new Pentium based systems:

- 2 active LINUX/Ethernet/VME-VxWorks – CHAOS, TRINAT
- 3 active LINUX/CAMAC – TISOL, GPS, DRAGON test stand
- 1 active Windows NT – LTNO

The VME front-end MVME162 68040 CPU running at 32 MHz has been replaced by a 300 MHz PowerPC CPU, MVME 2305. The VxWorks software license has been upgraded to include the PowerPC family. By changing CPU family, there is a factor 10 improvement in clock speed as well as in Ethernet with support for 100BaseT. The cost of memory is also much lower with a PowerPC than with a 68040 CPU. The new front-end systems have 16 MBytes or 32 MBytes while the older ones had only 4 MBytes.

MIDAS software

Throughout the year, the MIDAS system was used by several experiments (CHAOS, TRINAT, TISOL, DRAGON test stand). Some experiments required new acquisition hardware, which consisted of a PC running a LINUX OS with a dedicated CAMAC interface connected directly to the acquisition computer. These new systems phased out the previous acquisition system “VDACS” and users provided us feedback on how MIDAS behaved. In general the capabilities of MIDAS exceed what the users are currently requiring which makes future implementation of MIDAS in more demanding experiments possible. Programming specific to the experiment was implemented with our help and a substantial amount of our time was devoted to support and training of new users. Continuous development and improvement of the MIDAS system were the main topics of the year. Previous goals were mostly achieved and new features were implemented. The overall status of the MIDAS system can be summarized as follows: Support for direct CAMAC access through several manufacturers’ brands of CAMAC interfaces was implemented. Slow control structure has been cleaned up and EPICS device support for NT tested. Solaris OS support was added. A new MIDAS run control interface was developed for Web browser. Revision of YBOS and MIDAS utility tools was completed. Code management for MIDAS using the CVS package has been implemented and is accessible through the Web. A TRIUMF

Web site for MIDAS is currently under construction (<http://www.triumf.ca/midas>) which includes a first round of documentation in URL format and link to other MIDAS related Web pages. The current MIDAS version released is 1.6.1.

μ SR systems

The μ SR data acquisition package (MODAS running on a VAX/VMS) has been extensively modified to support a new TDC in VME (Highland V680). A customized program developed at TRIUMF was loaded into the microEngine chip to enable data rejection to be performed within the TDC module itself. The TDC is set up and read out by a MVME 162-23 PowerPC module running software under VxWorks. Valid TDC data are histogrammed in an area of memory known as the “histogram memory”. The histogram memory is read out periodically and stored by the VAX. Communication between the PowerPC and the μ SR data acquisition program is by RPC over Ethernet.

One of these new VME systems was installed in M15, and was successfully used to take data during the fall.

A driver in TCL was written to support a flux magnetometer in the CAMP slow controls system for μ SR.

Custom hardware

A. Daviel implemented a system to improve the signal/noise of UTC data for the rare kaon decay experiment E787 at BNL. The system consists of a number of complex programmable logic elements implemented in Altera FPGAs and designed to interface with commercial FASTBUS TDC units. It was deployed at BNL during the summer.

After being idle for several years, the RMC DAQ system was required again for a new experiment. The RMC DAQ computer had to be replaced, and other problems with the FASTBUS hardware had to be diagnosed and fixed.

Future development

In the coming year, development will continue to add features needed at ISAC and integration with EPICS control system elements. Special systems for the Expt. 614 FASTBUS based system and for a segmented μ SR detection system will be developed. All μ SR systems will see their dependency on the QBUS removed.

Scientific Services

(*M. Comyn, TRIUMF*)

The Scientific Services group encompasses the Information Office, Publications Office, Library and Conferences. Its activities during 1998 were mainly focused on supporting eleven past, present and future conferences and workshops.

Conferences

During 1998 support was provided for the following conferences and workshops.

- HERMES collaboration meeting, TRIUMF, February 9–13.
- 35th Western Regional Nuclear and Particle Physics Conference (WRNPPC'98), Chateau Lake Louise, Alberta, February 13–15.
- Workshop on Accelerator Operations (WAO'98), TRIUMF, May 18–22.
- XXIX International Conference on High Energy Physics (ICHEP'98), UBC, July 23–29.
This conference, with some 882 delegates from 43 countries together with 251 accompanying persons, constituted the major workload for the Scientific Services group.
- International Union of Pure and Applied Physics (IUPAP) Council meeting, TRIUMF, September 25–27.

In addition, preparations were made for the following future conferences and workshops.

- 1999 Particle Accelerator Conference (PAC'99), New York, March 29 – April 2, 1999.
- KEK/TRIUMF Workshop, Victoria, September 1999.
- Third International Conference on Isotopes (3ICI), Vancouver, September 6–10, 1999.
- 14th International Conference on Electromagnetic Isotope Separators and Techniques Related to their Applications (EMIS-14), Victoria, September, 2001.

Publications Office

This TRIUMF Annual Report Scientific Activities has been produced totally electronically, as was the 1997 report. It is available on the WWW at <http://www.triumf.ca/annrep> in both Portable Document Format and PostScript file formats. Unlike the monochrome paper version, the electronic versions allow those figures which were submitted in colour to be both viewed and printed in colour. During 1998, over 600 people accessed the 1997 Annual Report via the WWW. The Annual Report mailing list has been reduced and the trend is expected to continue as people become more accustomed to accessing the information over the WWW.

TRIUMF preprints are now produced electronically, wherever possible, and posted on the WWW at <http://www.triumf.ca/publications/home.html> to allow immediate dissemination of the publications. This has replaced the traditional distribution of paper copies by mail, resulting in significant cost savings.

Producing the PAC'97 conference proceedings constituted the major workload for the Publications Office in 1998. The 1,261 papers resulted in 4,030 pages of proceedings which were published in three formats: three paper volumes, one CD-ROM (which also included the PAC'95 proceedings), and a WWW site with mirror sites around the world.

Assistance was provided at all stages of producing the WAO'98 workshop proceedings.

Work began on producing the final camera-ready versions of the manuscripts for the ICHEP'98 proceedings.

Information Office

The TRIUMF Welcome Page, which is accessible directly at <http://www.triumf.ca/welcome> or via the TRIUMF WWW Home Page, received over 5,000 visits in each of its first two years of operation. The series of WWW pages were developed by two co-op students. They are intended to provide an overview of TRIUMF in a format understandable to the general public. The virtual tour of TRIUMF allows people to “visit” from anywhere in the world via the WWW, or to gain a good introduction before coming to TRIUMF for a real tour. The latter is particularly intended for students using TRIUMF and its science as part of school projects. The Information Office responds to any questions posed by visitors to the site.

The Information Office coordinated tours for over 1,500 people during 1998. The majority of public tours were conducted by a summer student during the May–August period when tours were offered twice a day.

The front lobby was redecorated and reconfigured during the summer months. Plans for replacing the display material and building a new ISAC model commenced during the year.

The group has operated without an Information Officer since July.

Library

Faced with declining budgets and increasing journal subscription costs, the Library had to cancel ten journal subscriptions and curtail all book purchases in 1998. The Library was fortunate to receive several book donations during the year, which ameliorated the situation a little.

The Library was able to renew all of the 1998 journal subscriptions for 1999. However, the journal sub-

scription budget and electronic access alternatives are constantly under review.

New shelving was acquired during the year and a new plan for the layout of the stacks was finalized. The new layout meets floor loading limitations and allocates empty shelf space for the active journals that will accommodate the anticipated growth of the collection over the next five years. A relatively minor addition of shelf space will allow an extension to seven years. After that, the Library will have outgrown its present location due to floor space and floor loading considerations.

Relocation of the Library collection into the new, optimized shelving layout began at the end of the year and should be completed early in 1999.

The Library operates on a self-serve basis and manages with minimal support for day-to-day operations.

GEANT4

(P. Gumplinger, TRIUMF)

The original GEANT4 was a large distributed software project, involving a world wide collaboration of about 100 scientists and software engineers from over 40 institutions and laboratories, participating in more than 10 experiments in Europe, North America, and Japan. Its objective was the production of a detector simulation program which has the functionality and flexibility necessary to meet the requirements of the next generation of subatomic physics experiments. The GEANT4 strategy was proposed to and approved by the CERN Detector Research Development Committee at the end of 1994 as the R&D project RD44. TRIUMF joined RD44 in September, 1995 with the decision to set up a three year program at the laboratory. Our efforts centered around the upgrade and porting of FORTAN code in the low energy electromagnetic and hadronic physics sector of the venerable GEANT3 package.

From 1995 to its completion in 1998, the RD44 project represented a pioneering effort in redesigning a major CERN software package for a modern object oriented (OO) environment based on C++. RD44 exploited advanced software engineering techniques and OO technology to improve the validation of physics results and to facilitate distributed software design and development, in order to profit from the expertise and contributions of scientists regardless of their geographical locations. Thirteen specialized working groups were responsible for fields as diverse as physics, geometrical modelling, visualization, event generation and user interfaces. Collaborators from TRIUMF made extensive contributions to RD44 and TRIUMF associates became prominent contributors in discussions concerning the overall architecture of the program.

RD44 has met all the required milestones. A first prototype was delivered at the end of 1995, the first alpha version was released in spring 1997, and the first beta version in mid-1998. At the end of 1998, with the release of the first full production version, which included detailed documentations, examples, and tutorials, the RD44 project had achieved its goals and ended. A Memorandum of Understanding was subsequently signed by many of the same laboratories and experiments who participated in RD44, including TRIUMF. It set up a new GEANT4 collaboration to address the management, support, and future development of the software during the production phase. TRIUMF has a seat in both the Collaboration Board and the Technical Steering Board of the new collaboration. We also have representatives in the following GEANT4 domains: Hadronic Physics, Electromagnetic Physics, Testing and Quality Assurance, Software Management, and Documentation Management.

The RD44 collaboration was unprecedented in high energy physics (HEP), both for its size and its geographical extension, and in many ways will provide a benchmark for future large-scale scientific software development. The GEANT4 (G4) detector simulation toolkit has already been selected as the main simulation platform for several major particle physics experiments in the next decade (ATLAS, BaBar, CMS, ALICE etc.) Although G4 has now gone beyond the initial R&D phase, new physics algorithms are being introduced on an ongoing basis. Many collateral benefits are anticipated from applications in a number of fields other than particle physics detectors.

During the past three years TRIUMF had a key role in RD44. Canadians were involved in low energy hadronic interactions (parameterization and cross section generalization), stopping kaons and muon physics, intra-nuclear cascade models at <20 GeV, and optical photon physics. The latter involvement consisted of code development for Čerenkov and scintillation photon generators, and the propagation of optical photons, which includes absorption, wavelength shifting, Rayleigh scattering and refraction and reflection at media boundaries.

The OO design and coding of the low and medium energy hadron physics models in G4 involved, firstly, the conversion to C++ of the well-known hadronic shower package GHEISHA. This had the obvious benefit that algorithms and physics insight contained in the original code were re-utilized. Secondly, the code was redesigned in order to better match the OO paradigm. This facilitates the ease of program maintenance, as well as provided a framework for refining and expanding the physics models, and for including new data and improved parameterization. The bulk of hadronic pro-

cesses were amalgamated into a single structure that allows for flexibility in process type, particle type and energy range. The work is now in the final phase of stepwise improving the essential hadronic physics.

This year we also implemented the hadronics portions of the test and example suites that are part of the G4 distribution. In addition to extensive testing and debugging of our own code, we appointed a member to the G4 system testing team which carried out the same activities for the entire code and established testing and problem-reporting procedures that carried us forward from beta releases to the first production version. In July we sent a representative to the Fourth Annual G4 Workshop in Niigata, Japan.

The TRIUMF GEANT4 team has started to support the construction of end-user applications by TRIUMF and affiliate-university physicists. In December one of us undertook a week long work-trip to the University of Montreal to help a graduate student launch a G4 based simulation of the ATLAS hadronic endcap calorimeter (HEC). Following the first G4 production release, we have begun to inform researchers about the use of and capabilities of G4, and provide assistance in evaluating G4 for specific user applications. We act as a resource to those who want to create the next generation analysis software, for skills in OO analysis and design, C++ programming, simulation techniques, OO data management, and other technologies required to support the GEANT4 project. Such technologies include, the concurrent version system (CVS) and various GNU code management tools, 3D graphics and visualization, and graphical user interfaces (GUI).

In summary, the GEANT4 project has brought a new level of computing expertise to our laboratory. We most recently advanced the intention of the TRIUMF/ATLAS group to reap the benefits of its significant investment in the detector, by initiating a G4 application to simulate the ATLAS HEC, so that TRIUMF can evolve into a regional ATLAS analysis centre.

The GEANT4 collaborators are: D.A. Axen, University of British Columbia; J. Chuma, L. Felawka, P. Gumplinger, F.W. Jones, C.J. Kost, A. Olin, D.H. Wright, TRIUMF; L.G. Greeniaus, University of Alberta.

Sudbury Neutrino Observatory

(R. Helmer, TRIUMF)

Most of the equipment built and/or designed at TRIUMF is now in use in the SNO detector. All of it has performed flawlessly. The whiffletrees on which the acrylic vessel is hung have been in use since early 1997. The storage device for the source umbilicals and the glove box were installed during 1998 and have been used extensively. The cards, cables and backplanes supplied by the Electronics Shop are connected into the

electronics systems and are in continuous use. The high voltage cards and front end card motherboards tested at TRIUMF last year are also now in continuous use.

The components of the device used for spooling the water sampling tube have been manufactured, and the unit will be assembled in the near future. It will not be needed in the detector for some time.

Infrastructure support for SNO was provided during the past year with a TRIUMF physicist acting as the commissioning manager for scientific components in the detector. Most of this effort was related to overseeing commissioning of the electronics and DAQ systems.

The BaBar Experiment

(C. Hearty, UBC)

Physics of BaBar

BaBar will study the violation of charge/parity (CP) symmetry in the decay of B -mesons at the PEP-II, the “B-Factory” currently being commissioned at the Stanford Linear Accelerator Center.

The origin of CP violation is one of the most important unresolved issues in particle physics, as it is an essential ingredient to our understanding of the baryon-antibaryon asymmetry in the universe. The only experimental observation of CP violation is in K_L^0 decays. The standard model describes these observations using an imaginary phase in the CKM matrix, but it is not known whether this explanation is correct.

The study of B^0 decays to CP eigenstates promises a definitive test of the standard model explanation. More generally, it will provide us with a series of unique consistency tests of the quark sector of the standard model and the best opportunity for precision determination of CKM parameters.

The large sample of identified B decays will be cleanly obtained at PEP-II, a high-luminosity asymmetric energy e^+e^- storage ring running at the $\Upsilon(4S)$. The $\Upsilon(4S)$ decays roughly 50% to B^+B^- and 50% to $B^0\bar{B}^0$. The two B mesons are almost at rest in their centre of mass with no additional particles, making this an ideal situation for complete reconstruction of rare decay modes. In addition, the B^0 and \bar{B}^0 are produced in a coherent state which remains coherent until one of the particles decays. Events in which one B^0 decays to a flavour-tagging mode and the other to a CP eigenstate can be used to reconstruct the time dependence of the CP asymmetry.

PEP-II collides 9 GeV electrons on 3.1 GeV positrons in order to produce an $\Upsilon(4S)$ system with sufficient boost that the measured separation between the two B decay vertices can be used to determine the relative time of the two decays. PEP-II is designed to

operate with a luminosity of $3 \times 10^{33} \text{ cm}^{-2}\text{s}^{-1}$, producing 3×10^7 pairs per year.

PEP-II will also provide the ability to make precise measurements of many interesting B decay channels, perform measurements of rare B decays, search for rare effects in the charm sector and make precision measurements in the tau lepton sector. Studies of charmless B decays, for example, produce additional constraints on the CKM matrix elements V_{ub} and V_{cb} that help to over-constrain the CKM unitary triangle and thereby probe new physics.

The construction of the BaBar drift chamber

The drift chamber is one of the central components of the BaBar detector, providing the first level trigger, momentum measurement of charged tracks and particle identification at low momentum. The Canadian hardware contribution to BaBar has been the construction of the drift chamber at TRIUMF, which was undertaken with substantial infrastructure support from TRIUMF.

Following the completion of stringing in November, 1997, the chamber was made gas tight and tested using a gaseous ^{133}Xe source. None of the 7,104 channels were found to be dead or noisy. The detector was shipped to SLAC, on time, in early March (Fig. 101).

The chamber has subsequently undergone cosmic ray tests by itself and integrated into the complete BaBar detector, including the superconducting solenoid. The tests indicate that the cell resolution and efficiency already meet the requirements and are likely to improve with more sophisticated calibration techniques.

BaBar will move onto the PEP-II beam line in early 1999 in preparation for the start of data-taking in May, 1999. This engineering run will last several months.



Fig. 101. The BaBar drift chamber being inspected upon delivery to SLAC in March.

Scientific personnel involved with the construction of the BaBar drift chamber at TRIUMF: C. Hearty, M. Kelsey, J. McKenna (UBC); P. Bloom, P.M. Patel, J. Trischuk (McGill); A. Hasan, J.-P. Martin, R. Seitz, P. Taras, V. Zacek (Montreal); R. Henderson (TRIUMF); A. DeSilva, R. Kowalewski, M. Roney (Victoria).

Low Temperature Nuclear Orientation Facility at ISAC

(P. Delheij, TRIUMF)

In the past year negotiations with DOE led in May to the transfer of the Low Temperature Nuclear Orientation facility from the Oak Ridge National Lab to TRIUMF-ISAC. The dilution refrigerator cryostat provides vertical access for the radioactive ion beams. The implanted nuclei can be subjected to a horizontal magnetic field of 1.5 T. An advantage of this configuration is identical detector geometries for the directions at 0 degree and at 90 degree with respect to the magnetic field. A drawback is the extensive height of the set-up which is indicated in Fig. 102. In the past this system has reached temperatures below 10 mK during on-line experiments.

After inspection of the components a service structure was designed and installed at the end of the year to provide safe access for operation of the set-up as

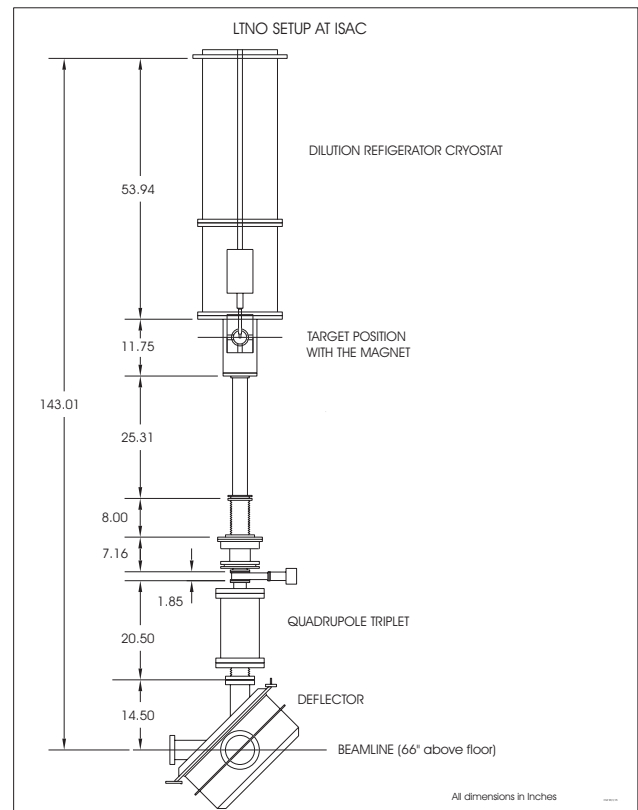


Fig. 102. Elevation view of the LTNO cryostat and vertical beam line section.

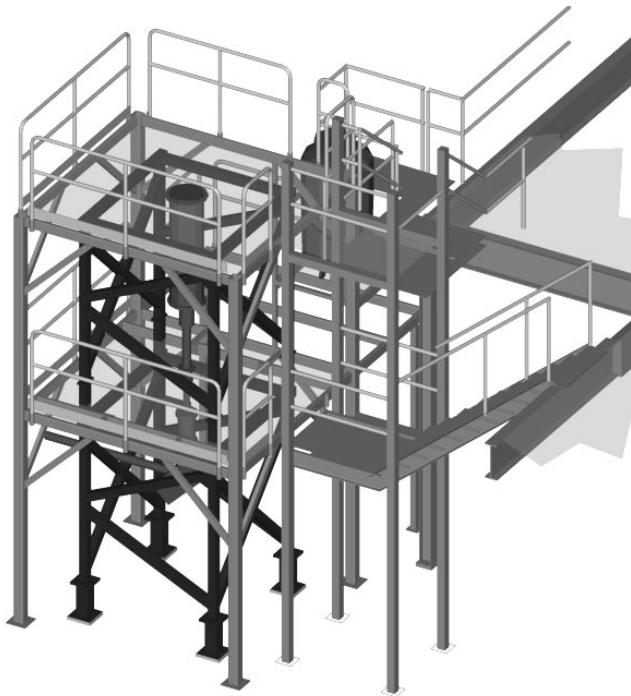


Fig. 103. The LTNO set-up integrated in the ISAC hall.

shown in Fig. 103. It was found that vibrations were transmitted through the floor at a level that is considered unacceptable. Therefore, a support system with self-leveling air pads is installed for the cryostat and all vacuum lines have been fitted with force-compensated bellows arrangements.

For experiments in the low energy area of ISAC, the PC based version of the MIDAS software was selected for data acquisition. Several germanium detectors were tested with evaluation models of the D(igital) S(ignal) P(rocessor) based integrated multichannel units from ORTEC and Canberra. A substantially improved stability was observed compared to conventional shaping amplifier-adc combinations. After these preparations the goals in the first half of 1999 are evaluation of the cryogenic performance and installation of the beam transport. In the second half of the year are planned the start of magnetic moment measurements (Expt. 828, K.S. Krane, Oregon State Univ. and P. Mantica, Michigan State Univ.) and the investigation of thin magnetic layers (Expt. 826, B. Turrell, Univ. of British Columbia).

DRAGON at ISAC: A Status Report

(J.M. D'Auria, SFU)

Overview

The TRIUMF-ISAC facility will produce and accelerate high-intensity radioactive beams of $A < 31$ to energies from 0.15 to 1.5 MeV/u. An essential part of the experimental program with such beams is to make

a $\sim 20\%$ measurement of the absolute rates of radiative capture reactions in which one of the reactants is unstable. The DRAGON facility uses inverse kinematics to measure capture rates, in which the beam is the heavy, unstable nuclide and the target is hydrogen or helium gas. Table XVI indicates some of the initial reactions that are planned for study.

Table XVI. Reactions to be studied using inverse kinematics at the DRAGON facility.

Reaction	Proposal	Interest
$^{13}\text{N}(p, \gamma)^{14}\text{O}$	E805	Hot CNO Cycle
$^{15}\text{O}(\alpha, \gamma)^{19}\text{Ne}$	E813	Hot CNO Cyc/Breakout
$^{19}\text{Ne}(p, \gamma)^{20}\text{Na}$	E813	Hot CNO Cycle/Out
$^{20}\text{Na}(p, \gamma)^{21}\text{Mg}$	-	Hot NeNa Cycle
$^{21}\text{Na}(p, \gamma)^{22}\text{Mg}$	E824	Hot NeNa Cycle
$^{22}\text{Mg}(p, \gamma)^{23}\text{Al}$	LOI	^{22}Na Production
$^{23}\text{Mg}(p, \gamma)^{24}\text{Al}$	E810	rp process
$^{23}\text{Al}(p, \gamma)^{24}\text{Si}$	LOI	^{22}Na Production

The main components of the DRAGON system are a windowless gas target; a two-stage electromagnetic mass separator, detectors of the heavy reaction products and detectors of the capture gamma rays. The expected radiative capture rates are typically of the order of 1 event/sec or lower for a beam intensity of 10^{10} sec^{-1} . The role of the DRAGON is to provide clean separation of the recoiling reaction product from the incident beam and to allow for the measurement of the rates of these essential reactions as a function of the incident beam energy.

Funding over a three-year period for the building of DRAGON and its initial operation was received from NSERC (and TRIUMF) in April, while funding for the gas target was received in 1997. A detailed conceptual design of DRAGON is displayed in Fig. 104. The location of the DRAGON in the ISAC hall is shown in the ISAC experimental hall figure that appears elsewhere in this Annual Report. A summary of the status of the various components is provided below.

The DRAGON

The gas target

All of the components of the gas target system are now available and are being assembled at the University of Alberta. Following initial testing and modifications, the system will then be moved to the ISAC hall in the summer of 1999, where a systematic testing of the completed system will be performed. Figure 105 displays a schematic oblique view of the gas target. In addition, a system is being developed to clean and recirculate hydrogen or helium target gas while the experiment is in progress.

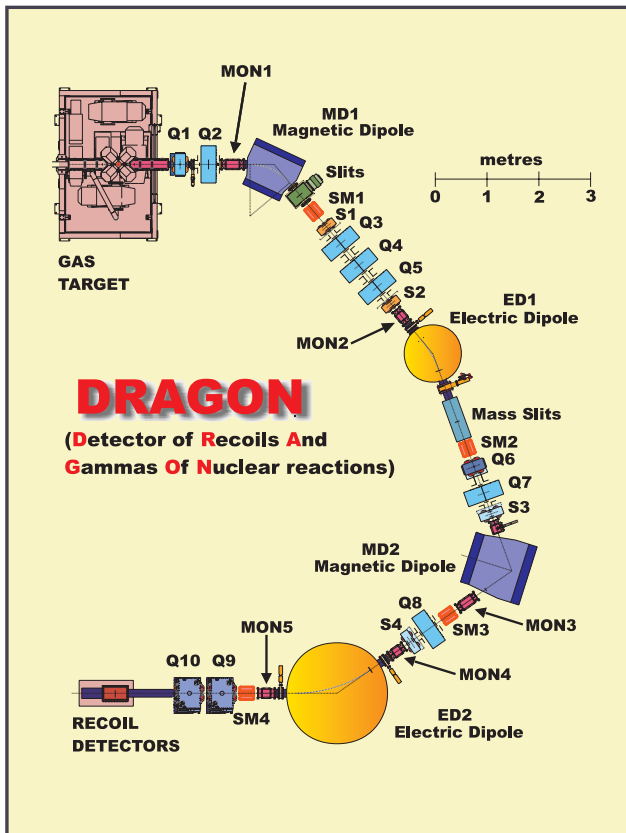


Fig. 104. Top view of the DRAGON layout showing components of interest.

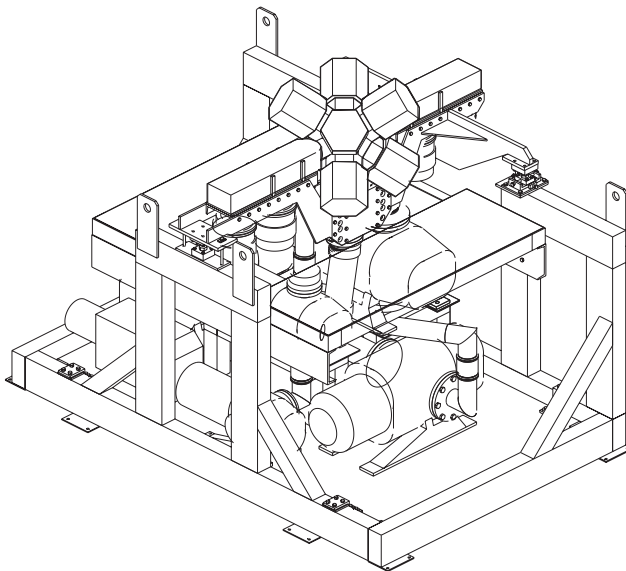


Fig. 105. Oblique view of gas target.

Recoil separator

The recoil separator uses both magnetic and electrostatic dipoles to separate recoil product from the up to 10^{16} times more intense beam of the same average momentum. In Fig. 106 a top view of the

DRAGON TRIUMF - ISAC

horizontal view of $^{15}\text{O}(\alpha,\gamma)^{19}\text{Ne}$ GIOSP tune shown

axial scale (m)
0 1 2
(transverse scale X 6)

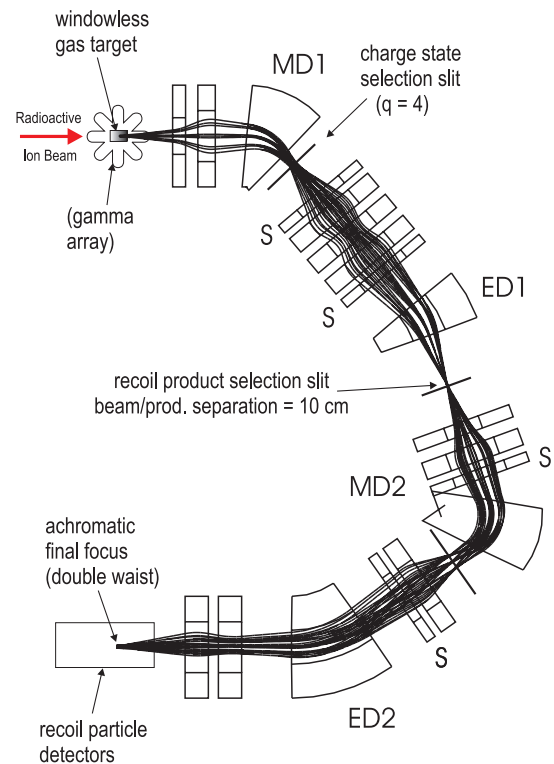


Fig. 106. DRAGON layout showing projection of ^{19}Ne trajectories onto the horizontal plane. The scale transverse to the beam axis has been expanded 6 times for clarity.

separator illustrates its mode of operation for ^{19}Ne recoils. It is a two stage device, each stage ending in an energy-achromatic, mass-dispersive focus. After selecting a single charge state of beam and product following the magnetic dipole (MD1), the electric dipole (ED1) directs the lower energy recoil product towards the mass selection slits. Mass dispersions after the first and second stages are 0.47 cm% and 1.85 cm% respectively. Each stage has 5 quadrupoles (Q) for focusing, 2 sextupoles (S) to correct aberrations, and 2 steering magnets (SM) (see Figs. 104 and 106).

Initial design and optimization was done to third order using the matrix-based program GIOS (Fig. 106 shows GIOS ^{19}Ne trajectories). Separator performance was simulated using the ion optic code RAYTRACE. A Monte Carlo simulation that included the beam emittance, the capture reaction and scattering of beam and product within the gas target was made for each reaction using GEANT. In addition, a number of simulations of different types of background to be expected from beam scattered off residual gas and surfaces were

made. None of these simulations resulted in more beam than product passing through the final slits of the DRAGON.

The last significant change in ion optics of the DRAGON separator, in the sequence of magnetic (M) and electrostatic (E) dipoles, was made early in the year. The original design had dipoles in the sequence M-E-E-M. Simulation of background due to beam collisions with residual gas molecules revealed a susceptibility to successive charge-changing collisions in the E dipoles. The revised design with sequence M-E-M-E avoids this potential problem. While the shape of the separator changed from 'S' to 'C' (see Figs. 104 and 106), the basic ion optics design is not much different from the original M-E-E-M version.

Once the optics design was frozen, a number of tests of sensitivity were undertaken. The method used was to simulate the transmission of recoil ions of the important $^{15}\text{O}(p,\gamma)^{19}\text{Ne}$ reaction to find the conditions leading to an additional 2% reduction in transmission for canonical slit settings.

- Field strengths: amongst the quadrupoles, transmission was most sensitive to the field in Q2 – 2% loss in transmission was experienced for an increase of 0.25% in the nominal field.
- Misalignments: an extensive study of possible translational or rotational misalignments was undertaken. Two aspects of the problem were studied: the extent of losses if no corrective action was taken, and the extent to which losses could be reduced with correction by steering magnets. The conclusion was that with re-steering the transmission criterion could be met for any reasonable values of errors in position or orientation of the quads.

Component design status

Detailed design has been completed for the magnetic dipoles and bid tendering has been initiated [Clark, TRIUMF Design Notes TRI-DN-98-10, TRI-DN-98-12 (1998)]. Two pairs of sextupole magnets presently installed in TRIUMF channels M13 and M15 will be available to DRAGON. Two 'SMIT' quadrupoles from CERN are being refurbished for use as Q9 and Q10. Conceptual design of the remaining eight quads is nearly complete, after considerable design effort to determine a pole shape which extends the region of uniform field gradient and to understand the contribution of end effects to aberrations.

The electrostatic dipole fields in the region of the electrode ends have been studied with both 2-D and 3-D models, determining the location of the effective field boundary for the design location of field clamps, and variation of effective length with height above the

median plane. A concept of the electrode mounting system has been worked out, including detailed design of the backing structure. Detailed designing of the Ti electrodes for the electric dipoles is completed and two concepts for their support structure are under consideration. A drawing showing some details of the electrostatic dipoles can be found in the engineering section of this Annual Report (see work of N. Khan, project engineer for the DRAGON project).

A conceptual design for the four steering magnets (labelled SM in Fig. 104) has been completed [Stinson, TRIUMF Design Note TRI-DN-98-7 (1998)].

Recoil detection systems

The prototype ionization chamber, used to $\Delta E - E$ discriminate between beam and recoil product ions (see drawing and photo in Figs. 107 and 108), has been designed, built, assembled and tested successfully with alpha sources. As part of a local time-of-flight system, a PGAC (parallel-grid avalanche chamber), which will be mounted on the front of the chamber, has been built and is ready for testing.

The gamma ray detector array

Detection of the reaction gamma rays in coincidence with the recoil ions could add orders of magnitude to the beam suppression capability of DRAGON. An array of scintillators is seen as the optimal approach but the device must deal with potentially high singles counting rates from the radioactive beam itself. A new scintillator material, LSO, has light output close to that of NaI and is relatively fast in comparison. Studies of its properties revealed new features previously unknown which are described elsewhere in this Annual Report.

Conceptual design of the gamma array has been continued using GEANT Monte Carlo simulations. The design of the pixelated detector module, including a method for 3-dimensional gamma position determination, is nearing completion. A preliminary report will appear in the proceedings of the 1997 IEEE Nuclear Science Symposium, held in Toronto [Rogers and Gumplinger, *A pixelated 3D Anger camera with light-loss compensation*, oral presentation NM1-7, IEEE Trans Nucl. Sci. (in press)]. In addition, experiments with the new LSO crystals have further elucidated the advantages and limitations of LSO as a gamma detector material. One limitation we discovered is the presence of a substantial afterglow component to the scintillation light emitted following gamma irradiation [Rogers and Batty, *Afterglow in LSO* (submitted to IEEE Trans. Nucl. Sci.)]. Although the afterglow will require pulser gain stabilization in the electronics, LSO is still considered the best scintillator choice for the DRAGON gamma array.

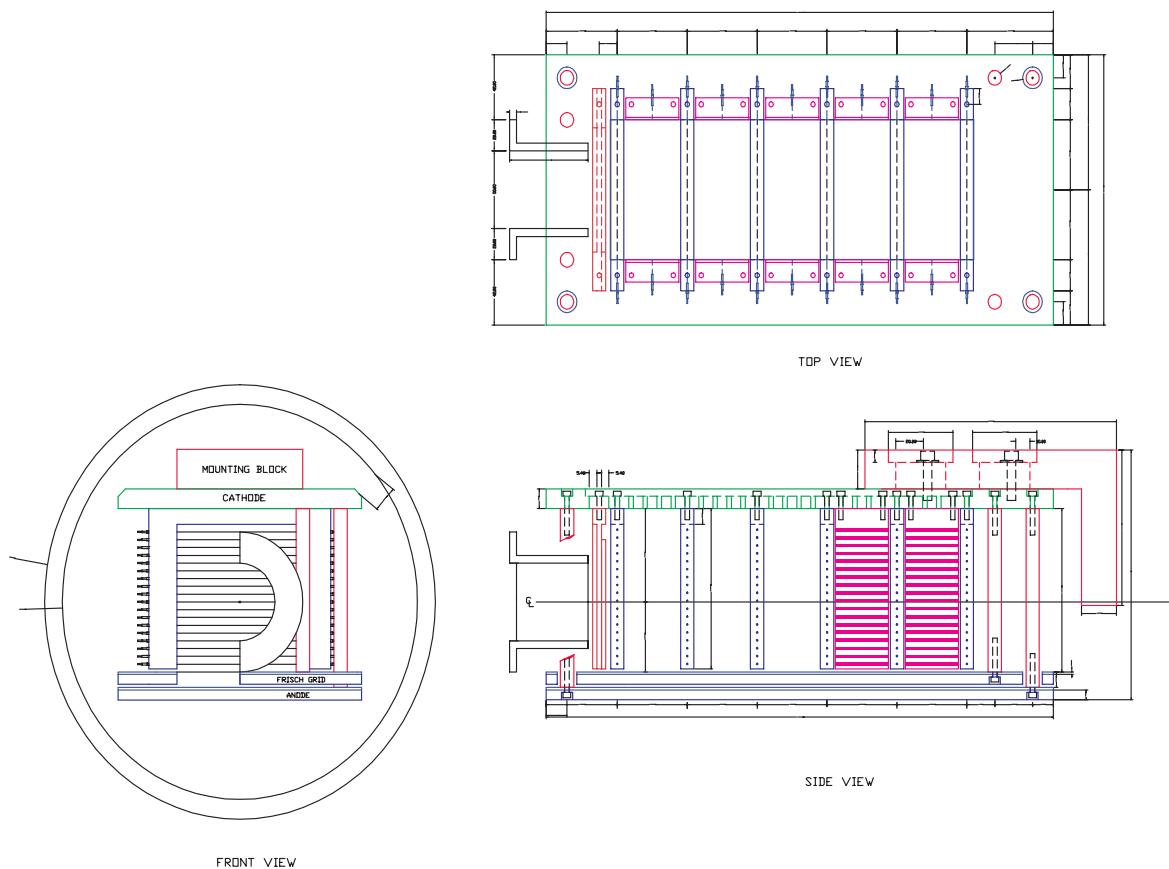


Fig. 107. Schematic representation of ionization chamber.

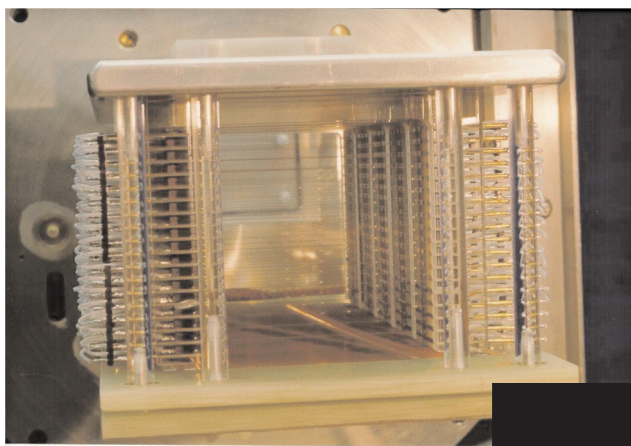


Fig. 108. Beam's eye view into ionization chamber.

The Science

Experiment 824

The first experiment planned for the ISAC-DRAGON facility is a measurement of the rate of the $^{21}\text{Na}(p, \gamma)^{22}\text{Mg}$ reaction. The rate of this reaction is influential in the production of ^{22}Na during explosive hydrogen burning in novae. The isotope ^{22}Na is interesting because its decay can be detected by gamma ray telescopes and because it is present in pre-solar

meteorites. Unfortunately the resonance energies are not well known for this reaction, so we have initiated a study to accurately measure them in Japan, using the $^{24}\text{Mg}(p, t)^{22}\text{Mg}$ reaction. Further details of this study can be found under Expt. 824 of this Annual Report.

Network calculations

In order to test theoretical models of the dynamics of novae and supernovae, network calculations can be performed which simulate the chains of nuclear reactions occurring in such explosive events. Final isotopic abundances can then be calculated which are compared with observed abundances. These network calculations require computer codes containing the experimentally-determined rates of all relevant reactions which may occur, as well as an approximation of the physical processes involved.

Such a code is being implemented at TRIUMF to explore further the key reactions important for heavy element production and pinpointing to what precision such rates must be measured for an accurate nucleosynthetic mode. The code is presently being validated and will be modified to allow simulations using temperature and density profiles as a function of time to better simulate the nova process.

Gamma-ray Detectors for DRAGON and Industrial Applications

(J.G. Rogers, TRIUMF)

As reported last year, a gamma-ray detector array is being developed for use in the ISAC-DRAGON facility. This year, the detector development has concentrated on the use of the new scintillator lutetium oxyorthosilicate (LSO) in position-sensitive detectors, both for the ISAC application and others. Several small LSO crystals were obtained from CTI, Knoxville, TN, and used in experiments to validate the ongoing GEANT computer simulations. In the simulations, the gamma-ray energy range usable in the detector was extended from the ISAC energies (i.e. 1–5 MeV) to span a wider range, 100 keV to 100 MeV, for new applications in industry, medicine, and physics.

To validate the GEANT simulations, certain basic properties of LSO, and for comparison NaI, were measured using small crystals and gamma-ray sources over the energies 16 keV to 6 MeV. The recently reported non-proportional response was confirmed at TRIUMF for energies below 100 keV, in the vicinity of the L-absorption edges. In LSO, significant afterglow was discovered to be induced by high energy gamma activation. The presence of this afterglow will require pulser stabilization for high-rate applications of LSO, such as DRAGON. Our findings were submitted to IEEE Trans. Nucl. Sci. for publication [Rogers and Batty, *Afterglow in LSO and its effect on energy resolution*, TRI-PP-98-30].

GEANT simulations were extended to a segmented-detector design which accomplishes three-dimensional gamma-ray position encoding. As reported last year, the DRAGON detector incorporates an array of long narrow LSO fingers, of length appropriate to the gamma-ray energy of interest. To this basic design was added a new feature which induces a small shift in the apparent transverse position of the gamma detection, the amount of the shift being proportional to the depth-of-interaction of the gamma ray along the length of the finger. This provides a vernier encoding the depth coordinate (Z) of the scintillation point in the array. When added to the usual transverse (X and Y) finger coordinates, this Z -encoding completes the three-dimensional read-out of each gamma-ray's position. A key feature of the detector design is its scalability with gamma-ray energy. Detection of higher energy gamma rays, useful in resonant-gamma contraband detection, and lower energies, useful in nuclear medicine cameras, are optimized by simply scaling of the dimensions of the fingers and photomultiplier tubes incorporated in the detector module. These simulation results were reported in an oral presentation at the 1997 IEEE Nuclear Science Symposium in Toronto and will

soon appear in the conference proceedings [Rogers and Gumplinger, *A pixelated 3D Anger camera with light-loss compensation* (in press)]. The same paper has also been submitted to IEEE Trans. Nucl. Sci. for publication.

Experiment 715 Off-line Laser Development Lab: Optical Pumping of ^{41}K

(P. Dubé, SFU; J.A. Behr, K.P. Jackson, TRIUMF)

Experiments with ^{37}K require that nuclear polarization of a small, confined sample of atoms, such as that produced by a magneto-optical trap (MOT), be known to an accuracy of about 0.1% [Häusser, EEC report, Dec. 1997]. Such an accuracy in the measurement of the nuclear spin of a small ensemble of atoms is not readily obtained, and we make use of the similarity between the atomic energy levels of ^{41}K with that of ^{37}K to carry out the developmental stage of this experiment with the convenience of stable isotopes.

Off-line trapping of ^{41}K

We have set up a magneto-optical trap in an off-line lab for the cooling and trapping of ^{41}K , and obtained our first trap with that system in the spring. Our all solid-state laser system consists of a 10 mW external-cavity diode laser seeding a semiconductor power amplifier that is capable of producing a 500 mW laser beam. The combination of the seed laser with the power amplifier is often referred to as a MOPA, which stands for master oscillator power amplifier. The output from the power amplifier has the same frequency properties as that of the seed laser, which in the present case is a laser linewidth estimated at <500 kHz when locked to a Doppler-free potassium line obtained by saturated absorption spectroscopy.

In a first stage we have measured various characteristics of our system as a function of parameters such as laser frequency detunings, laser power, magnetic field gradient, and background density of potassium atoms. Typical values were 2×10^7 for the maximum number of trapped ^{41}K atoms, and $2 \times 10^9/\text{cm}^3$ for the maximum density observed with a field gradient of 14 g/cm.

Trap lifetimes

We have also measured trap lifetimes of (100 ± 20) seconds for the low density regime, limited by the residual gas pressure in our vacuum system. At high trap densities, collisions between the trapped atoms accelerate the decay rate. Collisions between ground state atoms have little effect since their energies can only change by the hyperfine structure energy of 254 MHz which is insufficient to kick the atoms out of the trap. However, the internal energy available in collisions between an atom in its excited state and an atom in its ground state, or between two atoms in their excited

states, can lead to an energy transfer which releases enough kinetic energy to expel the atoms from the trap. We have modeled the decay of the atomic number density as follows:

$$\frac{dn}{dt} = -\alpha n - \beta n n^*$$

where n and n^* represent the atomic number densities of ground and excited state atoms, respectively. α is the decay rate at low density of $(0.010 \pm 0.002)/\text{s}$ mentioned above, and β is the non-linear decay rate that we found to be $(5.0 \pm 2.5) \times 10^{-10} \text{cm}^3/\text{s}$ for ^{41}K . The main contribution to the error quoted is from the estimate of the density of excited state atoms. The Gaussian number density distribution was taken into account in the present analysis. The equation above leads to a rate β that is insensitive to intensity to within 10% for intensities between 40 and 160 mW/cm^2 .

In the literature, β is rather defined by the following equation, where n^* is replaced by n in our equation above:

$$\frac{dn}{dt} = -\alpha n - \beta' n^2$$

This definition gives a value β' that depends on laser intensity. An upper limit for β' in ^{41}K is given in Williamson *et al.* [J. Opt. Soc. Am. **B12**, 1393 (1995)]: $\beta' < 9 \times 10^{-11} \text{cm}^3/\text{s}$. This value must be multiplied by the ratio n/n^* , which typically ranges from 2 to 20, before it can be compared with our result. This correction depends on the fine details of laser detunings and intensities, and a good model to extract the correction factor. Our data are thus in reasonable agreement with that upper limit. Our analysis does not rely on a model to estimate the total population, but rather on the trap fluorescence for a measurement of the excited state population.

For the β -decay experiments, using a total number of trapped atoms of 10000, and a fraction of excited atoms of 0.20, in a 0.001cm^3 trap volume, we find that this decay mechanism alone would give a trap lifetime of 1000 seconds, which far exceeds the ≈ 1 second half-life of $^{37,38}\text{mK}$.

Trap temperatures

Our present scheme for polarizing the atomic nuclei is based on optical pumping of the atoms into a single Zeeman sublevel, a ‘stretched’ state, that defines the nuclear spin as being directed along a known magnetic field axis provided externally. In order to achieve this, the atoms must first be trapped in a MOT and then released, because the unwanted magnetic fields from the coils and the random optical pumping from the trapping laser beams must be turned off. The release from the MOT allows the atoms to spread according to their temperature, and this happens at a rate of 64

cm/s for a temperature of 1.0 mK, causing the diameter of the sample to expand at twice that rate. This expansion limits the time that we can usefully carry out the measurement without deteriorating the quality of the recoils data, and thus the temperatures must be kept as low as possible.

We have carried out temperature measurements of the MOT sample with a CCD camera. The diameter of the trap was measured by recording an image of the cloud at different time intervals after release, with short laser exposures of 2–3 ms. The rate of expansion of the diameter was readily converted into a temperature by assuming a Maxwell-Boltzmann velocity distribution of the atoms. Temperatures along one axis as a function of the total laser intensity at the centre of the trap are shown in Fig. 109. As expected from the Doppler cooling theory, the temperature decreases with lower intensities. The lowest temperature we have measured so far is about 1 mK. According to the Doppler cooling limit for a two-level atom, we should be able to reach a temperature of 148 μK . The values of frequency detunings and laser powers required for optimum capture efficiency and for lowest temperatures are substantially different; this has been a limitation for the signal-to-noise ratio of measurements in low temperature regimes with the present set-up. With additional acousto-optic modulators for the rapid control of those parameters we should be able to obtain and measure temperatures close to the Doppler limit. The $^{37,41}\text{K}$ isotopes have a small hyperfine splitting in the $4P_{3/2}$ excited state manifold which prevents the usual methods of sub-Doppler cooling, routinely used for most other alkali, to be easily implemented here. However, it is believed that sub-Doppler temperatures are possible in potassium although this hasn’t been demonstrated yet [Fort *et al.*, Eur. Phys. J. **D3**, 113 (1998)].

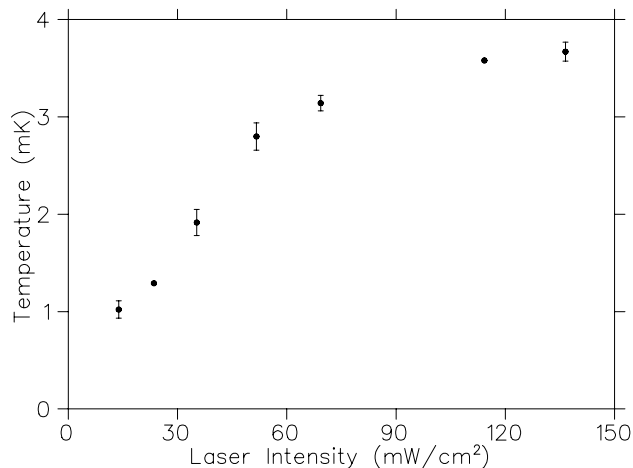


Fig. 109. MOT temperature for ^{41}K atoms as a function of total laser intensity at centre of trap, for a detuning of 1 MHz below lowest level in the $4P_{3/2}$ excited state manifold.

An Ultra-sensitive Radioactivity Monitoring Station on UBC Campus and its Relation to TRIUMF

(T.J. Stocki, D.F. Measday, UBC)

On the University of British Columbia campus, there is an atmospheric radiation monitoring station of very high sensitivity. It is one of 20 stations around the world that are prototypes for enforcement of the Comprehensive Test Ban Treaty. Along with atmospheric monitoring, there are three other methods of detecting nuclear explosions, which are also used to enforce the treaty. These other methods are seismic monitoring, infrasonic monitoring, and hydroacoustic monitoring. These three methods will not be discussed here, but details can be found at the Web site <http://www.pidc.org>.

The station monitors airborne radioactivity by blowing approximately 24000 m³ of air through a 60 × 60 cm filter paper over a 24 hour period. This is two orders of magnitude more air than previous monitors and is similar to the amount of air a human lung receives in 30 months. The purpose of the glass fibre filter is to trap radioactive aerosols. To reduce the amount of natural radioactivity from radon, the filter is changed in the late afternoon. The filter is then folded and compressed under a pressure of 11 metric tonnes, after which it is a 6 cm diameter disk. Then it is allowed to cool down for 24 hours, to reduce the background. After 24 hours, the filter is placed in front of 2 high purity germanium detectors which are 40% of the efficiency of a 3 × 3 in. NaI crystal. Thus the efficiency of each of these detectors at a γ -ray energy of 1 MeV is approximately 2×10^{-2} for the full energy peak.

One advantage of this method is that the large air-flow through the filter concentrates the activity. Another advantage is that the γ -rays retain origin information by not losing energy before detection. The high purity germanium detectors also have high resolution (approximately 2 keV) in the energy region of interest, so there are very few misidentifications. The disadvantages of the system are that gases, pure α emitters, and pure β emitters do not get detected. Gases go right through the filter paper, so the germanium detector will not see them. The filter paper can trap pure α emitters, and pure β emitters, but the germanium detector does not detect α or β particles, because of the thickness of the paper disk.

The station detection goal is to pick up γ -rays from the following isotopes: ¹⁴⁰Ba, ^{134,136,137}Cs, ^{95,97}Zr, ^{131,133}I, ⁹⁵Nb, ¹⁰³Ru, or ¹³²Te (to detect atmospheric nuclear tests or to detect reactor accidents like Chernobyl); and ¹³⁷Cs, ⁹⁵Zr (to detect nuclear weapons fabrication). There have been a few sightings of ¹³⁷Cs, but these are presumed to be false or accidental readings.

So, there has been no verified detection of atmospheric weapons tests, reactor accidents, or nuclear weapon fabrication.

The Vancouver station has seen a few anthropogenic isotopes in small amounts. These small amounts are several orders of magnitude below permissible limits. These isotopes have originated from controlled releases, from the TRIUMF site, which is approximately 1.7 km away in the southeast direction. Figure 110 shows the locations of the lab with respect to the monitoring station. The rosette on the figure also shows the annual average wind speed and the direction. The length of each arm on the rosette is proportional to the frequency of winds from each direction in percent. As one can see, SE winds are common, about 20% of the time. These winds could then bring man-made isotopes to the station from the laboratory.

One of the isotopes seen at the station is ¹²³I, which has a half-life of 13.3 hours, so it lives long enough to

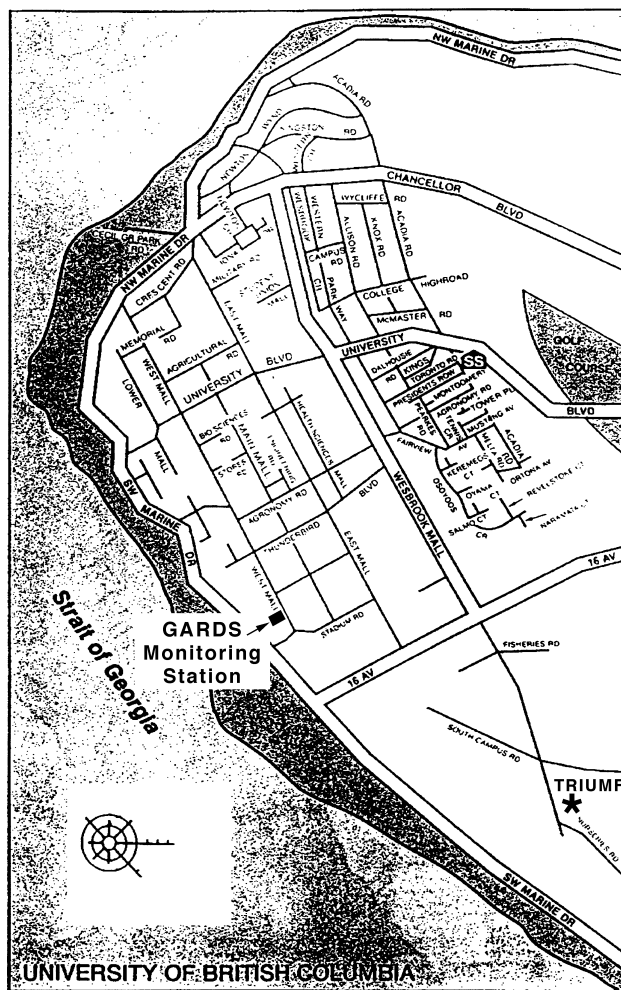


Fig. 110. The relative location of the monitoring station and subatomic physics lab (TRIUMF). The rosette shows the frequency of the wind direction, in percent, for this area.

survive the cool down period and its 159 keV γ -ray is detected. ^{123}I is produced at the medical radioisotope facility, MDS Nordion.

Another man-made isotope that has been seen at the station is ^{24}Na , by detection of its 1369 keV and 2759 keV γ -rays. ^{24}Na is a product of ^{24}Ne , which is also a noble gas. This isotope is produced whenever the laboratory's cyclotron is producing a 500 MeV, $150\mu\text{A}$ proton beam. The beam interacts with the argon in the atmosphere producing ^{24}Na directly or Ne which

decays into ^{24}Na with a 3.38 minute half-life. This activity is only just above detection threshold even for this very sensitive monitor.

In conclusion, a very sensitive air monitoring station has picked up radioactive emissions from TRIUMF, at the limit of detectability.

This paper was the winning student paper presented at the Canadian Radiation Protection Association conference in Ottawa in May and was published in the Bulletin of C.R.P.A [19, 8 (1998)].

CYCLOTRON OPERATIONS DIVISION

INTRODUCTION

The strategy reported in 1997-98 of operating the cyclotron with a low budget and minimum manpower, to make more resources available to the ISAC and CERN efforts, was continued during 1998-99. In addition, the duration of the beam time schedule was reduced to less than 4,000 hours to allow time for the construction and installation of the new 100 μA 500 MeV extraction proton beam line for ISAC. This involved a number of new elements and modifications to shielding and flanges at the cyclotron periphery, where the residual activation is high. The work proceeded in a faultless manner with relatively low dose exposure, and is reported in the Beam Lines section below and in the Beam Line 2A sections of the ISAC chapter of this Annual Report. The policy of minimum budget and minimum resources for operations, and minimum scheduled production time, however, was not conducive to highly efficient, reliable beam production, and our results in terms of reliability and beam availability were below our previous good records. A series of problems, which plagued operations mainly towards year end, are reported in detail in the report from the beam production group. We should emphasize that so far none of these problems in terms of cyclotron reliability are structural and, in fact, most of the problems have been coming from ancillary systems like failing pumps and water services, main magnet power supply, or cooled collimators, or other water cooling down beam line 1A. Beam line 1A is probably the system which deserves most attention, especially along the section including the T2

target and the high intensity beam dump. Operators and maintenance personnel should be commended for their usual high dedication to the machine and for having dealt with and solved several problems in difficult circumstances.

During 1999-00 TRIUMF's priority will be to complete the ISAC-I project and deliver low energy beam to ISAC experiments, and to honour our commitments with CERN. Low resources for cyclotron operation will continue, but it is anticipated that the budget situation will improve with the new 2000-2005 five-year plan.

BEAM PRODUCTION

This report describes beam production for the full 1998 calendar year, starting with the final two weeks of Schedule 92 and ending with the completion of Schedule 94. With more shutdown time than usual required for the construction of BL2A, and because of budgetary reasons, a total of only 3834 operational hours were scheduled of which 3147 were achieved, with a rather low availability of 82.1%. These totals include 100 hours used for development and tuning and, as shown in Fig. 111, were split roughly 3:1 between high current beam production and low intensity, polarized operation with the availability considerably better for the latter. While high intensity periods served a variety of users, polarized operation was for the most part dedicated to the parity non-conservation experiment running in beam line 4A2. As Fig. 112 shows, the total beam charge delivered to meson hall experiments

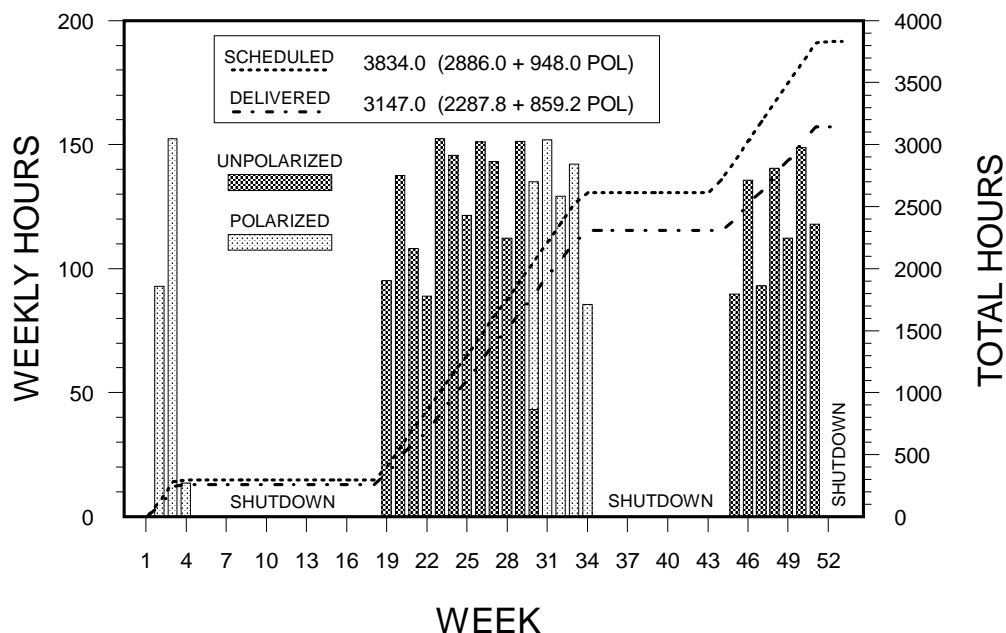


Fig. 111. Operational hours for 1998.

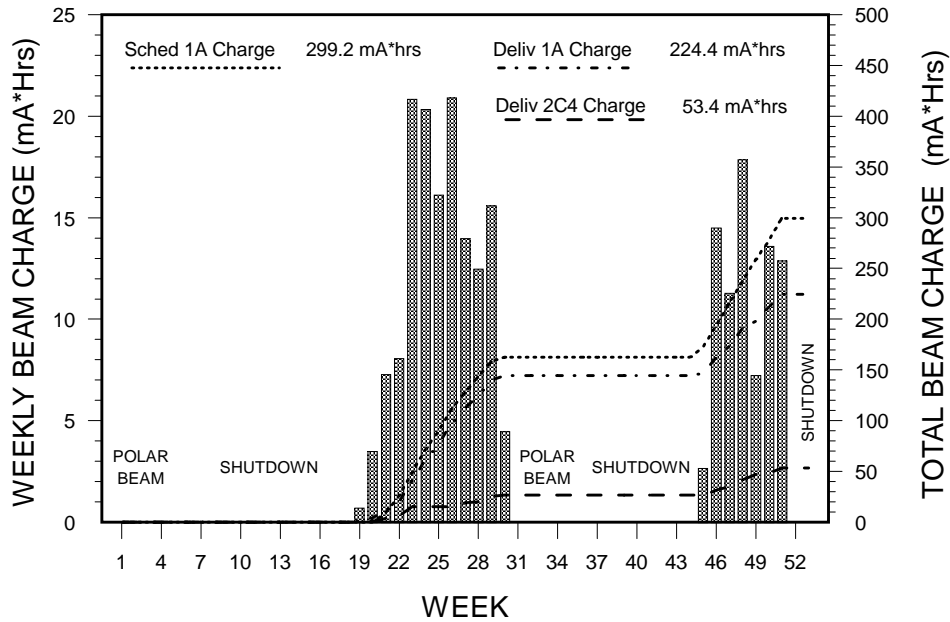


Fig. 112. Beam delivery for 1998.

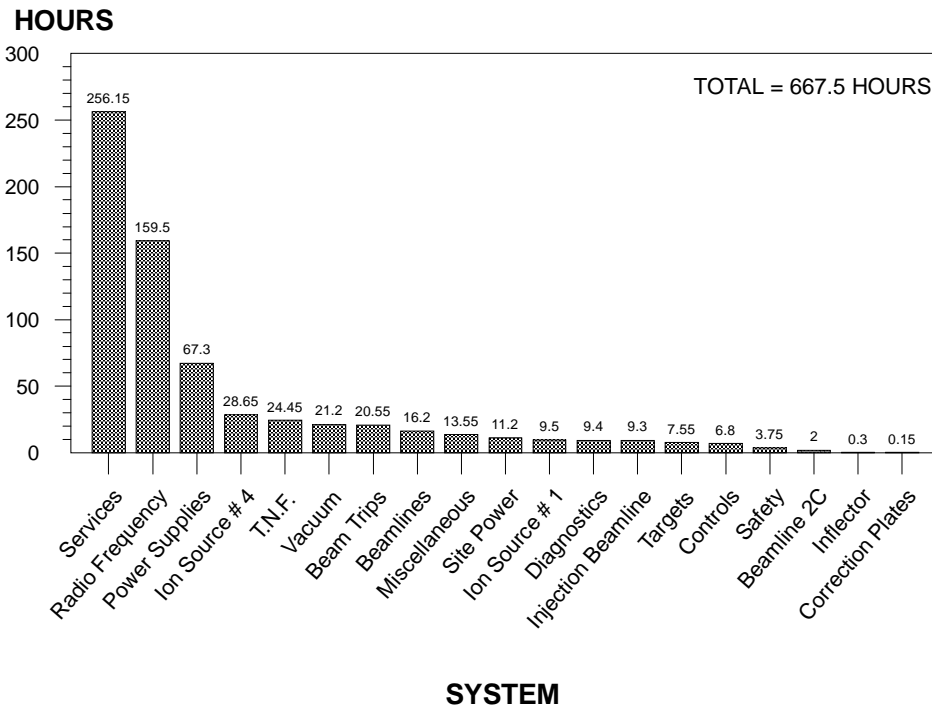


Fig. 113. Cyclotron downtime for 1998.

during high current production was 224 mAh or only 75% of that scheduled, usually at 150 μ A. This percentage is lower than the availability largely because of current restrictions at TNF through much of Schedule 94. There were also 53.4 mAh delivered at 85 MeV to the solid target facility (STF) in beam line 2C4 for the production of radiopharmaceutical generators. Eleven patients were treated for ocular melanomas during six proton therapy sessions in beam line 2C1 operated at

70 MeV. The annual downtime (Fig. 113) was 667.5 hours, the fourth highest it has been in the last ten years. Unlike most years, however, it was Plant Services (with 256 hours) rather than RF (with 159 hours) responsible for the lion's share of the downtime, largely due to the failure of the aluminum active low conductivity water (Al ALCW) pump at the start of the fall schedule. The operational record and beam to experiments for the year are given in Tables XVII and XVIII.

Table XVII. Operational record for 1998.

	Scheduled hours			Actual hours		
<u>Cyclotron off:</u>						
Maintenance	274.5			305.05		
Startup	182.0			140.40		
Shutdown	4490.5			4513.50		
Other	24.0			16.95		
Cyclotron downtime	0.0			667.50		
Overhead	99.0			113.60		
Totals	5070.0			5757.00		
<u>Cyclotron on:</u>						
Development	63.0	+	0.0 P	2.15	+	0.00 P
Cyclotron tuning	144.0	+	51.0 P	36.50	+	62.45 P
Beam to experiments	2679.0	+	897.0 P	2249.10	+	796.80 P
Totals	2886.0	+	948.0 P	2287.75	+	859.25 P
Actual/Scheduled = (2287.75 + 859.25)/(2886 + 948) = 82.1 % availability						
<u>Beam to experiments:</u>						
1A Production	2337.0	+	0.0 P	2099.95	+	0.00 P
1A Development/tuning	9.0	+	0.0 P	13.35	+	1.70 P
1A Down/open/no user	246.0	+	897.0 P	122.05	+	795.10 P
1B Production	87.0	+	0.0 P	9.95	+	0.00 P
1B Development/tuning	0.0	+	0.0 P	0.80	+	0.00 P
1B Down/open/no user	0.0	+	0.0 P	3.00	+	0.00 P
Total 1A+1B production	2424.0	+	0.0 P	2109.90	+	0.00 P
2A2 Production/tests/tuning	397.0	+	0.0 P	73.60	+	0.00 P
2C1 Production/tests/tuning	88.0	+	23.0 P	42.50	+	8.20 P
2C4 Production/tests/tuning	1538.0	+	0.0 P	1259.35	+	0.00 P
2C5 Development/tune	18.0	+	0.0 P	16.05	+	0.00 P
4A2 Production	44.5	+	888.0 P	17.60	+	695.50 P
4A2 Development/tuning	0.0	+	0.0 P	0.85	+	74.40 P
4A2 Down/open/no user	0.0	+	9.0 P	8.80	+	26.90 P
4A3 Production	1101.0	+	0.0 P	782.20	+	0.00 P
4A3 Development/tuning	0.0	+	0.0 P	8.30	+	0.00 P
4A3 Down/open/no user	2.0	+	0.0 P	120.25	+	0.00 P
4B Production	1482.5	+	0.0 P	971.40	+	0.00 P
4B Development/tuning	0.0	+	0.0 P	31.85	+	0.00 P
4B Down/open/no user	49.0	+	0.0 P	307.85	+	0.00 P
Total BL4 production	2628.0	+	888.0 P	1771.20	+	695.50 P
1A Beam charge	299236 μ Ah			224426 μ Ah		
2C4 Beam charge	70870 μ Ah			53403 μ Ah		

P = Polarized source on-line (although not necessarily polarized beam)

Table XVIII. Beam to experiments for 1998.

Experiment *	Channel	Sched.#	Scheduled			Delivered		
			h	h (pol)	μAh	h	h (pol)	μAh
497	4A2	92	0.0	273.0	0	0.00	211.05	0
497	4A2	93	44.5	615.0	0	17.60	496.70	0
614	M11	93	567.0	0	61670	446.90	0	46478
614	M11	94	271.0	0	40650	179.90	0	16116
669	M20B	94	150.0	0	22500	136.60	0	18073
684	M9B	93	589.0	0	74200	604.30	0	63234
684	M9B	94	320.5	0	36650	230.20	0	21786
687	M20B	93	150.0	0	22500	149.50	0	20658
687	M15	94	150.0	0	22500	136.60	0	18073
691	M15	93	150.0	0	15000	124.25	0	12643
691	M15	94	124.5	0	17865	113.25	0	13484
697	M15	93	145.0	0	18020	124.70	0	14840
704	4B	93	730.0	0	0	475.85	0	0
704	4B	94	626.5	0	0	413.50	0	0
713	M9B	93	293.5	0	32870	270.55	0	30622
713	M9B	94	121.0	0	18150	95.25	0	5179
715	4A3	93	627.0	0	0	497.00	0	0
724	M15	93	150.0	0	22500	149.50	0	20658
737	M15	93	52.0	0	7800	57.30	0	8400
741	4A3	94	404.0	0	0	280.70	0	0
746	M20B	93	127.0	0	19050	84.40	0	10389
749	M20B	93	127.0	0	19050	125.00	0	17651
757	M9B	94	254.0	0	38100	187.00	0	24780
758	M20B	93	150.0	0	22500	140.90	0	19038
768	M15	94	161.0	0	18740	116.95	0	8302
774	M20B	94	150.0	0	22500	84.65	0	10937
775	M20B	93	148.5	0	14850	145.85	0	15782
777	M15	93	127.0	0	19050	125.00	0	17651
777	M20B	94	196.0	0	18785	116.95	0	8302
778	M13	93	1349.5	0	162536	1196.50	0	141802
782	M15	93	69.0	0	10120	66.10	0	9265
784	M15	93	127.0	0	19050	84.40	0	10389
784	M20B	93	150.0	0	15000	133.55	0	13091
791	M20B	94	104.0	0	15600	68.85	0	8257
792	M15	93	150.0	0	22500	140.90	0	19038
793	4A3	94	70.0	0	0	4.50	0	0
794	M9B	93	81.0	0	8100	71.75	0	6665
798	M15	94	104.0	0	15600	68.85	0	8257
798	M20B	94	121.0	0	18150	95.25	0	5179
799	M9B	93	271.0	0	40420	264.30	0	36703
799	M9B	94	46.0	0	6900	34.25	0	4230
804	M20B	93	121.0	0	17920	123.40	0	17665
804	M20B	94	142.0	0	21300	139.75	0	15844
807	M15	93	148.5	0	14850	145.85	0	15782
808	M13	94	121.0	0	18150	95.25	0	5179
809	M20B	93	145.0	0	18020	124.70	0	14840

Table XVIII (cont'd.)

Experiment *	Channel	Sched.#	Scheduled			Delivered		
			h	h (pol)	μAh	h	h (pol)	μAh
809	M13	94	150.0	0	22500	136.60	0	18073
814	M15	94	150.0	0	22500	84.65	0	10937
818	M15	94	121.0	0	18150	95.25	0	5179
819	M9B	93	69.0	0	6900	61.80	0	6426
831	M20B	93	139.0	0	4446	103.00	0	6100
832	M20B	93	92.0	0	9200	75.50	0	7036
833	M15	93	150.0	0	12550	99.30	0	8891
833	M13	94	285.5	0	36605	230.20	0	21786
834	M13	94	246.0	0	36900	208.60	0	24101
837	M11	94	124.5	0	17865	113.25	0	13484
838	M9B	94	344.0	0	51600	306.45	0	35319
1UA TEST	2A	94	4.0	0	0	1.00	0	0
737/782	M13	94	150.0	0	22500	84.65	0	10937
737/782	M20B	94	124.5	0	17865	113.25	0	13484
797/798	M15	94	142.0	0	21300	139.75	0	15844
BELLE	M15	93	81.0	0	1096	79.20	0	4245
CS TEST	2C5	94	4.0	0	50	4.55	0	53
FOIL TEST	2C4	94	2.0	0	10	0.85	0	10
ISAC RIB †	2A2	94	397.0	0	0	73.60	0	0
ISOPROD	2C4	93	816.5	0	35430	695.10	0	26905
ISOPROD	2C4	94	721.5	0	35440	566.55	0	26738
P THERAPY	2C1	92	0.0	9.0	0	0.00	4.50	0
P THERAPY	2C1	93	140.0	0	0	23.30	0	0
P THERAPY	2C1	94	130.0	0	0	10.30	0	0
PIF	1B	94	87.0	0	0	9.95	0	0
PIF	2C1	94	47.0	0	0	8.35	0	0
TBA	M11	93	736.5	0	100820	708.10	0	93224
TBA	M11	94	396.0	0	59400	345.20	0	42174
TEST	2C5	93	8.0	0	80	11.25	0	205
UBC	M11	94	196.0	0	18785	116.95	0	8302

* See Appendix D for experiment title and spokesman

† total for commissioning, TRINAT/715 and GPS/823

Beam Schedule 92

Schedule 92 was completed with about two weeks of polarized operation in January just before the year's first shutdown. With the exception of a proton therapy session for a single patient, the beam was used exclusively by the Parity group which extracted 200 nA of 80% longitudinally polarized, 223 MeV beam from a cyclotron tuned to about 13% transmission (with no bunchers). Depending on the type of extraction 4 (X4) foil in use, a variety of cyclotron probe configurations had earlier been used to horizontally shadow and/or

vertically scrape the beam to clean it up before extraction to the LH2 target. Due to certain probe failures, this nominally meant vertically scraping with a short X1 foil, taking around 100 nA of 220 MeV beam down 1A, while using a light, unshadowed foil on X4. At the end of the run the HE1 probe was used to horizontally shadow a prototype bow-saw styled foil that provided encouraging results. With the exception of the failure towards the end of the run of one of the outer trim coils, which prevented beam transmission to the outside of the machine, but only marginally affected parity, the cyclotron behaved reasonably well delivering 200 hours

of adequate beam and 40 hours of tuning time during this period. There were 50 hours of downtime, much of it caused by one of the non-active copper LCW pumps failing at the beginning of the run. One last item of note was the rf booster test just prior to shutdown. The deferment of this test from earlier in the schedule was well advised because the RFB feedthrough failed again, resulting in a tank vacuum burst that heralded the beginning of the shutdown.

Spring Shutdown

The cyclotron lid remained down for the first five weeks allowing the tank to cool more than usual while extensive BL2A assembly took place in the vault (and 2A tunnel). Adjustments to the elevation system control electronics were made for a trouble-free lid-raising, and a shields-in radiation survey showed general fields to be 15% lower than the previous spring. A long list of activities other than the 2A work included: electrical and plumbing repairs to vault beam line magnets, realignment of the 4AQ4/5 quadrupole doublet, two iterations of resonator levelling adjustments, inspections of the cyclotron centre region, maintenance of tank vacuum equipment, repair of burned wiring in the trim coil 45 junction box, updating of the 1AT1 water cooling package, overhaul of the rf CuLCW system north pump and a heavy slate of cyclotron probe and beam line monitor maintenance. An upgrade of the site fire detection system was also completed with all zones, including ISAC, now protected by a uniform Cerberus system. Even though this was a very busy shutdown, all the work was done with doses managed within the sliding time guidelines with the final statistics showing a total dose of 82.6 mSv distributed among 90 workers.

Beam Schedule 93

There were roughly 11.5 weeks of high current and 4.5 of polarized operation in this schedule. Start-up was reasonably smooth and initial BL1A currents were held back to a maximum of 10 μA during BL2A beam commissioning tests to a temporary dump located at the end of 2A1. These nA tests went extremely well, with several energies tuned without difficulty and included various beam spill tests for TSG. A couple of weeks later beam was run successfully to the 2A2 dump module at the west ISAC target station. After the initial tests, currents were increased to 140 μA in BL1A and 60 μA in BL2C4 for several weeks of reasonably successful running until a Rb target in the latter beam line developed a small leak very near the end of its scheduled irradiation. ISOPROD runs were then suspended for three weeks while a target engineering and safety review was completed. After this, two remaining Rb target cassettes were used without incident. The last half of the high intensity beam production time was

characterized by lower than usual BL1A currents as the cyclotron was tuned to reduce the beam pulse width to around 2 ns FWHM as requested by the CHAOS experiment. This was largely accomplished with radial flags which reduced the cyclotron transmission from 60% to 40% and the total available accelerated beam to 140 μA with 350 μA injected. When BL2C4 was off during the safety review, the full 140 μA was available to 1A users but when STF came back on-line taking 40 μA , then BL1A was left with 100 μA . A total charge of 144 mAh or 89% of the scheduled amount was delivered to BL1A during high current operation with the cyclotron on for 1450 or 87% of the scheduled hours. Downtime was a little high at 166 hours, the chief causes being rf sparking, services UPS trouble and a 1AT1 water leak. BL2C was also used for the treatment of 3 patients with proton therapy (5 nA at 70 MeV in 2C1) and weekly tests in 2C5, where a total of 205 $\mu\text{A h}$ of 105 MeV beam was delivered to a Cs target. On the BL4 side, beam alternated between 1 μA at 500 MeV to TISOL in BL4A3 and lower currents to Expt. 704 operating in proton mode in BL4B2 at 300 MeV and in neutron mode in BL4B3 at 283 MeV.

Except for one PT session during which two patients were treated, parity was again the sole user of polarized beam. Initially there was an attempt to extract with a bow-saw foil but after two early failures a parity 'standard' foil was used and for most of the run, 200 nA of slightly lower energy beam was sent down BL1A as a short, broad X1 foil was used to vertically shadow the parity foil. The remaining beam was stopped in the machine with HE probes which were occasionally used to horizontally shadow the parity foil. Parity had their best run to date with over 250 hours of data collected from about 500 hours of delivered beam. The OPPIS ECR microwave tube failed during the run causing about 12 h of 64 h total downtime. At the end of the run there was a successful test of an improved bow-saw foil.

Fall Shutdown

There was a day of cyclotron checks before things were turned off for the fall shutdown, including a Controls Y2K test after which beam was still able to be delivered. Since no urgent faults were known to exist with the cyclotron, it was decided that the lid would not be raised for any routine maintenance; instead this would be deferred to a longer shutdown at the beginning of 1999. This saved dose and freed personnel to concentrate on preparing ISAC for its first radioactive beam. However, there was still a demand for maintenance on existing systems as performed and reported by the various support groups including: the replacement of the

old, site UPS; the installation of a water cooled beam stop in BL2C5; improvements to the vault lighting and a long list of repairs to beam line devices. Other MRO was done (RF, Vacuum, Controls) but one job, at TNF, had to be left unfinished. Tests there were unsuccessful in locating the source of a small, elusive, water leak. Diagnosis was partly masked by a pre-existing air leak and somewhat thwarted by a 1AT2 target water leak that sprung during these tests and was later repaired. The eventual proposal was to run with the vacuum vessel back-filled with helium at atmospheric pressure and steps were taken to assure that this would be a satisfactory temporary solution. The total shutdown dose was 21.2 mSv distributed among 41 workers, lower than usual because the lid had not been raised for any tank work as noted above.

Beam Schedule 94

Beam delivery was beset by one problem after another to produce one of the poorest performance records for a single beam schedule in recent history. Start-up was reasonably smooth as expected because the tank remained under vacuum the entire shutdown. Soon afterwards there was a catastrophic failure of the Al ALCW pump (that circulates cooling water through the resonators and main magnet coil) whose replacement took nearly a week out of the schedule. Two weeks later the main magnet power supply was off for 2.5 days because of a faulty pre-driver circuit for which the diagnosis was hazardous and difficult. During these first few weeks of operation, TNF water levels and air activation were closely monitored and nothing too unusual was noted. In late November, however, the water loss rate there started dramatically increasing and the TNF vacuum vessel soon filled up to the beam plane. The collimator of the 500 MeV radiation facility was then identified as the culprit, its cooling circuit was bypassed and a couple of thermocouples were inserted into the empty cooling lines, close to the collimator. Currents were slowly raised to a limit of 120 μA in order to keep temperatures less than 80°C, with some cooling achieved by circulating air. Before higher current tests could be done there, a reheat coil in the rf room HVAC ducting froze and burst, causing a major flood which brought about a slightly premature end to the beam schedule. With the above failures, only 80 mA h or 59% of the scheduled charge was delivered over 838 or 68% of the scheduled hours. Downtime was high at 378 hours, nearly half of it because of the failed pump. In spite of the difficulties there were some major milestones this period. BL2A 1 μA tests went well on November 17 preparing the way for ISAC's first RIB on November 30 when 6×10^6 ^{37}K ions/sec were transported to a Faraday cup just outside the relocated TRINAT. (First radioactive beam was delivered

to TRINAT on December 5. Unfortunately, ISAC suffered its first CaO target failure soon afterwards and although it was successfully replaced by the Remote Handling group using the interim warm cell facilities, further beam was not realized because of tank vacuum problems caused by extraction probe 2A.) New Rb targets were approved for 2C4 and strontium production there went well. In 2C1, five proton therapy patients were treated and further PT development work took place at 74 MeV. The machine transmission was generally good (around 60%) and tank spills were kept below 3 μA during high current production. The winter shutdown got under way December 20 before Christmas break.

BEAM AND CYCLOTRON DEVELOPMENT

Short Bunches from the Cyclotron

The CHAOS experiment required a beam with bunches less than 2 ns long at high intensity ($\sim 100 \mu\text{A}$). This condition was set up by operators using centre region flags. The T1 Čerenkov monitor was used to show that the requirement had been achieved and the wall current monitor gave a less precise but perfectly adequate 'live' display of conditions.

Multipactoring in the RFB Coupling Loop

The loop that couples power into the 92 MHz RFB accelerating cavity has a ceramic cylinder as vacuum feedthrough. This cylinder has been cracked several times during operation and track marks of what were assumed to be secondary electrons could be seen on the aquadag coating. It was felt necessary to measure the magnetic field in the vicinity of the feedthrough to gain a more quantitative understanding. The feedthrough is located in a region difficult to access, near a magnet pole and with a radiation field of 1.5 mSv/h. The cyclotron was under vacuum so it was not possible to measure at the location of the cylinder so a hand held gaussmeter was used to measure the field at several points around the outer housing and interpolation used to estimate the fields at the damage points. These were a horizontal component between 0.7 and 2 kG and a vertical component of ~ 1.8 kG. A simple mathematical model was fit to the data to give the field distribution in the region in order to enable electron tracking if desired. A more accurate measurement surrounding the region occupied by the ceramic cylinder would require a special jig to be built and the cyclotron to be vented.

Cyclotron Beam Dynamics

Several calculations simulating beam behaviour in the cyclotron were carried out. These included calculations of stripped beam trajectories to determine the location of copper blocks protecting the 2A exit horn

and simulations of the effect of shadowing the BL4B stripping foil with a high energy probe to improve the beam quality extracted for the parity experiment.

Stripping Foils for the Parity Violation Experiment

The polarization distribution across the extraction foil surface is a source of polarization moments, which were identified as major systematic error contributions to the parity experiment. They are affected by the betatron amplitudes and number of turns. This distribution had been measured by scanning a short (6 mm height) “hockey stick” foil across the beam. Up to 2–3% transverse polarization difference was observed across the beam. Since the polarization moments are products of polarization and beam size, extracting only the central part of the beam by the short stripping foil, or vertical “shadowing” of the long foil, helps to keep moments within a tolerable range (less than $10 \mu\text{m}$).

Three types of stripping foils were used for the parity experiment. Initially, a 32 mm long, 5.0 mg/cm^2 thick, pyrolytic graphite foil suspended at one end was tested (see Fig. 114a). The foil width was 2.5 mm and it extracted about 60–70% of the circulating beam. The vertical beam size is quite large at 220 MeV beam energy and use of a long foil helps to reduce beam current fluctuations caused by vertical beam oscillations. As discussed above, the short hockey stick foil (see Fig. 114b) was used for polarization distribution measurements. To avoid beam extraction by the holder’s thick stainless parts, one of the cyclotron diagnostics probes was used to shadow the holder and to reduce the effective foil width to about 2–3 mm. Polarized beam scattering in the carbon foil produces an asymmetry in the beam halo distribution, which can cause systematic errors in the parity detectors. The scattering effect is proportional to the foil thickness, which can be reduced significantly.

A foil 0.2 mg/cm^2 thick is sufficient to strip 98% of a 220 MeV H^- ion beam. In the tests, such a thin foil was supported along one side – the hockey stick geometry. The use of thin foil reduces significantly

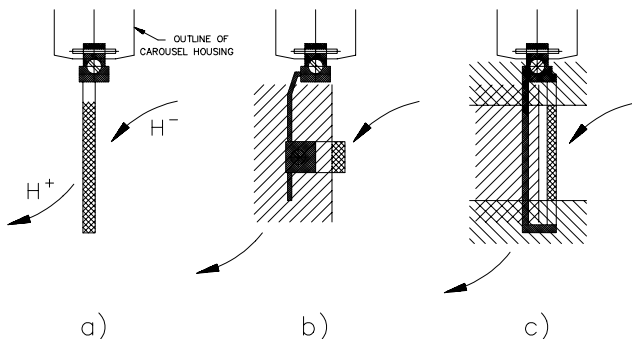


Fig. 114. Stripping foils for the parity experiment.

the extracted beam emittance due to reduction of multiple scattering and hence improves beam transport conditions. The drawback of radial shadowing is an appearance of beam profile asymmetry caused by the fuzziness of the shadowing. This asymmetry is sensitive to the cyclotron tune and produces polarization moments. The solution is the use of a 0.2 mg/cm^2 foil strip, 2.5 mm wide, attached at both ends to a C-shaped holder (see Fig. 114c). The holder shadowing doesn’t affect the beam profile in this case, due to a 5 mm gap between the foil and holder. The end parts of the holder are shadowed by a second stripping foil, which is situated at smaller radius and therefore trims beam symmetrically at top and bottom. Narrow symmetrical beam profiles were obtained with the thin foil in the C-holder and this foil will be used for the next run.

RADIO FREQUENCY SYSTEMS

RF Operations

The total cyclotron rf downtime for the year was 160 hours which represents 24% of the total machine down time. The combination of sparking, crowbars and out of driven caused 118 hours of this down time, despite efforts to adjust resonator tips to reduce rf leakage and temperatures in the beam gap.

A system for automatically switching through 32 rf signals from the amplifier system, measuring and logging them has been developed. This allows system problems to be diagnosed more quickly, and provides trend information on the amplifiers for maintenance purposes. The system uses a 32×8 rf switch matrix controlled by a PC running a Labview program and controlling the measuring instruments over a GPIB bus.

RF Support

The remaining manpower load of the RF group was dedicated to commissioning the seven-ring RFQ system with successful rf and beam tests, the assembly of the remaining 15 RFQ rings, and higher order mode dampers and filters for the CERN collaboration. The detail work on these projects is reported elsewhere.

RADIO FREQUENCY CONTROLS

A major area of activity for the RF Control group this year has been the redesign of the ISIS buncher system controls. The system currently in use employs 20 year old microprocessor technology. It has never provided adequate speed or bandwidth to ensure effective closed-loop amplitude and phase control of the pre-buncher frequency components. Recently the system had several failures. The new design takes advantage

of some of the modules developed as part of the ISAC effort, and adds a couple of others unique to the ISIS system requirements.

Like the ISAC and cyclotron rf subsystems, this system is housed in a VXI mainframe. The local system controller consists of an embedded Pentium PC. Frequencies at 4.6, 11.5, 23 and 46 MHz require control. Each is provided with both in-phase and quadrature control by a single dedicated digital signal processor. A 23 MHz signal from the cyclotron provides the reference frequency. This goes first to a master phase shifter module. This unit employs a digital phase shifter to provide overall control of the buncher phase. The phase-adjusted 23 MHz reference then goes to two frequency synthesizer modules. One of these provides the 4.6 MHz subharmonic, while the second produces the remaining three frequencies.

The design and construction of this system is essentially complete. It is currently being installed and commissioned, and is expected to be operational by the end of the shutdown in early 1999.

CYCLOTRON PROBES AND DIAGNOSTICS

Probes and Diagnostics Mechanical MRO

The major efforts throughout the year were focused on providing beam diagnostics for the ISAC west target station and the ISAC mass separator system. All other non-ISAC related work was limited to essential repairs of the cyclotron probes and beam line monitors. The Diagnostics group biweekly meeting notes are available electronically via the Operations CYCINFO information service on the site computer cluster (accessible also through the TRIUMF home page on the WWW). The cyclotron spring shutdown activities are summarized in detail in the Diagnostics group meeting notes of April 17.

Probes MRO

The high energy probe HE2 was removed in the spring shutdown for a complete overhaul. The failure that had taken it out of operation late in 1997 was found to be due to a seized bearing in the cable drum. This and several other bearings were replaced. All other bearings were cleaned and the drive cable was re-tensioned. HE1 was removed but only required minor service – bearings were cleaned and the cable was re-tensioned. The LE1 track was cleaned and realigned. The water cooled probe limit switch was adjusted in situ. The gear drive reduction ratio was increased for the vertical motion of variable PIP 3 to improve its operation. The 2C extraction probe was removed for inspection and routine service. The molybdenum shear plate appears to have alleviated the beam

heating problem. Extraction probe Ex4 was removed for routine service.

Late in the year, the 2A extraction probe radial drive ferro-fluidic feedthrough began to leak just after start up of the radioactive beam to TRINAT GPS experiments in ISAC. The problem can be solved with a minor design modification which will be done early in the new year.

Monitor MRO

All vault and standard beam line monitors were serviced during the spring shutdown. Only the vault monitors were serviced in the shortened fall shutdown. Several monitors developed leaks during beam operation in November and required an extra application of ferro-fluid. These now require semi-annual attention and should be replaced soon with a new monitor design.

VACUUM AND ENGINEERING PHYSICS

The cyclotron and beam lines vacuum systems operated well during the year with minimal downtime until the end of November. At that time a water leak in the TNF vacuum space caused the loss of several days of high current operation. An acceptable operating mode was found and beam was run at 120 μ A from December 9 until December 20, when operation ceased.

There was much accomplished on ISAC vacuum. The vacuum systems for beam line 2A, west target station, mass separator, LEBT to TRINAT and the general purpose station and the RFQ were all installed and commissioned during the year. A large part of the installation of beam lines and mass separator equipment was performed by persons from the Beam Lines and ISIS groups, with the Vacuum group providing assistance and guidance as required. The operating storage portion of the target vacuum exhaust system was installed. This allows the gases evolved during beam on target to be confined in shielded vessels until it is determined that they can be safely released. Beam had been transported through all installed sections by the end of the year.

Engineering Physics continued support for the RFQ and DTL work, as well as other tasks. A safety shield for the target high voltage conductors was designed and fabricated and the beam diagnostic station from Chalk River was completely rebuilt. There was also work on CERN rf equipment and on a tape transport system for ISAC.

ISIS AND POLISIS

ISIS

The CUSP ion source was modified with a new double half ring filament assembly. This change eliminates

the run in time required after a filament change, which previously took some 36 hours of high arc current. Additional benefits are that filament changes can be done more easily and the expected lifetime of this type of filament is fifty per cent greater than the previous type. Both the ion source and injection line continued to operate well for the past year. As last year, there were no major activities undertaken during the past year as ISIS personnel were involved in the completion of the ISAC low energy beam transport systems (LEBT).

POLISIS

Polarized H⁻

Parity violation experiment

The optically pumped polarized ion source (OPPIS) I4 provided very high quality beam to the parity experiment (Expt. 497) in January and for 5 weeks during the summer. The focus of the continuing development to minimize systematic errors in Expt. 497 shifted to beam extraction in the cyclotron. Details of the stripping foil and tunes used to minimize the transverse polarization moment of the extracted beam are given in the Beam and Cyclotron Development section of this Annual Report.

OPPIS injector for RHIC

Polarization facilities planned for RHIC will provide 70% polarized proton-proton collisions at centre of mass energies up to 500 GeV and a luminosity of $2 \times 10^{32} \text{ cm}^{-2} \text{ s}^{-1}$. The polarized injector must produce 0.5 mA H⁻ ion current during the 300 μs pulse, or current \times duration of 150 mA μs , within a normalized emittance of 2π mm mrad. This is an ideal application for the TRIUMF-type OPPIS, where a 1.64 mA dc current was obtained, albeit at 60% polarization. Pulsed operation will greatly simplify and reduce the cost of the laser system, while providing high polarization due to ample optical pumping laser power.

Polarized beam is not presently required at KEK, and the KEK OPPIS will be moved to BNL in 1999 to supply polarized H⁻ for RHIC. Meanwhile, it has been at TRIUMF since September, 1997 to be upgraded to meet RHIC's requirements. Design of the matching optics between the source and the RFQ was also begun.

The existing TRIUMF OPPIS could meet the RHIC requirements even with CW laser pumping, if 300 μs pulses were accelerated (the source itself produces continuous beam). However, 100 μs accelerated pulse durations with peak currents of 1.5 mA would be preferred, since that would improve injection efficiency. The preference for the higher current, combined with the relatively low cost of pulsed lasers, dictates the use of pulsed optical pumping.

The KEK OPPIS as delivered to TRIUMF used a pulsed 18 GHz ECR proton source and CW laser pumping. At TRIUMF the KEK OPPIS is being optimized using a dc 28 GHz ECR proton source. A preliminary result of 0.52 mA dc H⁻ current was obtained, using a 121-aperture ECR extraction electrode with an overall diameter of 13 mm. This already satisfies the minimum RHIC beam current requirement, and a 199-aperture electrode, as used in the best TRIUMF OPPIS result, would give proportionately more beam current.

In previous tests at TRIUMF, near 100% rubidium polarization was measured in a 2 cm diameter rubidium cell having a vapour thickness of 1×10^{14} atoms cm^{-2} using a pulsed (80 μs) flashlamp-pumped Ti:sapphire laser. This year development began on producing a reliable, relatively long pulse (over 100 μs duration) flashlamp-pumped solid state laser system.

A new sodium-jet, negative-ionizer target was developed, which has some advantages over the original canal-and-condensers arrangement. A jet target can be shorter and the beam apertures larger, since sodium vapour is more effectively confined. Large apertures reduce secondary electron emission caused by the intense polarized atomic hydrogen beam striking the cell, and therefore may allow biasing the sodium cell up to 32 kV. If so, a 35 keV beam from the source will be injected into an RFQ, without requiring that the whole source be placed on a high voltage platform.

INR-type pulsed OPPIS for HERA

Studies of the hadron spin structure functions in collisions of polarized electrons with polarized-³He, -hydrogen and -deuterium internal targets are in progress at DESY (HERMES experiment). The proposal to extend the kinematic range of these studies and measure the gluon contribution was recently examined. A polarized H⁻ ion current of 10–20 mA is required to provide sufficient luminosity for the above experiments. Such high currents were proven feasible this year at TRIUMF during development of the "INR-type" OPPIS.

In the INR-type OPPIS, the ECR proton source is replaced by two components – an atomic hydrogen "neutral injector" outside the magnetic field surrounding the rubidium vapour cell, and a pulsed helium gas ionizer cell inside the magnetic field. Hydrogen atoms pass unaffected through the magnetic fringe field and enter the helium cell, forming a small emittance proton beam that in turn enters the rubidium cell. The very high currents are due to the performance of the neutral injector. It consists of a plasmatron proton source that produces a small emittance, converging 8 A proton beam that is neutralized with high efficiency in a pulsed H₂ cell.

As part of the SPIN Collaboration, an INR-type source has been developed at TRIUMF that demonstrated by the end of 1998 a polarized H^- current of 15 mA in pulse durations of approximately 100 μs . This is by far the largest current ever attained by a polarized source. We believe that this current can be polarized to 70–80% polarization.

PRIMARY BEAM LINES

Beam line 1A T1 water package was upgraded to the same standard as that of T2 which was upgraded last year. The hydrogen recombiner system was replaced with a monitored expansion tank on the meson hall mezzanine to maintain improved water resistivity and to reduce the possibility of the release of active air. The new system was successfully tested in the summer and operated without problems for the balance of the year. MRO of existing installations continued as much as possible through the year limited by manpower resources which were employed in the onerous ISAC tasks. These tasks included the installation in beam line 2A of one combination magnet, four dipoles, sixteen quadrupoles, nine steering magnets, eighteen monitor boxes with stands and four turbo pumping stations. After the completion of the 2A line, the group focused on the alignment of the ISAC target station tank, the target module and target, exit modules I and II, the pre-separator, and the mass separator as well as the RFQ.

2C

Proton therapy on 2C1 continued to be regularly scheduled for 5 days each month during high current and polarized beam operation for a total of approximately 30 days.

The production of the radioisotope ^{82}Sr , which is produced in the solid target facility (STF) on 2C4, dropped significantly from the previous two years because of a reduction in the high current schedule, a decrease in demand and the failure of a rubidium target. In 1998 there were 85 days of ^{82}Sr production for a total charge of 553.2 mAh and a yield of 21.9 Ci at the end of bombardment. This compares with 123 days for a charge of 88.9 mAh and a yield of 31.3 Ci in 1997 and 121 days for a charge of 92.3 mAh and a yield of 34.7 Ci in 1996.

During irradiation of a rubidium target in June, the target developed a minor leak in the weld that attaches the stainless steel foil window to the target body. This was similar to two previous failures in approximately fifty target irradiations, so an engineering design review was held to review the target design and the irradiation procedure. The target foil weld has been modified so that the foil is held by a ring that is electron-beam welded to the target body. Procedures were put

in place for quality control during target manufacturing. A beam trip was installed that will trip if there is a sudden drop in STF cooling water resistivity which can be caused by a rubidium leak. A ballast volume has been attached to the STF to store the kryptons released during a target leak and handling procedures if there is a leak have been modified. Two of the re-designed targets have been irradiated without incident.

Commissioning of the cesium target on 2C5 for ^{127}Xe production continued. The hole in the halo monitor and collimator was enlarged to 25 mm during the spring shutdown following a number of unsuccessful attempts to reduce the beam size. A number of commissioning tests followed, with currents up to 25 μA at 105 MeV and two gas transfers of ^{127}Xe were made. 206 μA h of beam were delivered to the cesium target in this period. In the fall shutdown, the graphite beam stop was replaced by a water beam stop with water circulating through the STF cooling water package. The heat load on the Cs target containment volume exit window has been greatly reduced because the water beam stop is designed for 10°C rise at full current of 50 μA compared with over 300°C rise for the graphite beam stop. The beam stop has been tested to 28 μA with a charge of 54 μA h.

The 2C extraction probe ran smoothly despite missing a regular maintenance and foil replacement during the fall shutdown because the lid was not raised. The extraction foils had twice the nominal use with up to 29,000 μA h on one foil.

The target shineblockers continue to operate erratically. The water pressure of the vault water system that operates the shineblockers will be increased in the 1999 spring shutdown and redesign of the system is being considered.

CONTROLS

CCS Operation

The Central Control System (CCS) ran well during 1998. Downtime was 6.8 hours, compared to 16 hours for 1997, and an average of 24 hours for each of the previous 10 years. The majority of 1998's downtime was as a result of significant hardware failures. The remaining CCS downtime is a result of software related problems. Many other hardware problems occur but are not serious enough to prevent Operations from delivering beam. There are also occasions, such as unexpected power outages, where failures occur to many systems including the CCS but the control system problems do not occur first. As a result, they are not recorded as CCS downtime. As well, the CCS problems are usually more quickly fixed than other simultaneous problems, so no CCS downtime occurs afterwards.

Power outages, both planned and unexpected, have been destructive to a wide variety of CCS hardware. Much of the CCS is protected by uninterruptible power supplies (UPS) but on two occasions the UPS failed, causing some inconvenience. One of the smaller UPS units had its batteries replaced and resumed running reliably at its specifications. Another, more important development was the replacement of the old, site UPS by a new, larger facility. The present UPS configuration is a tremendous improvement and allows Operations to assess the cyclotron (pumps, vacuum, etc.) via the CCS immediately after power outages and thus helps to shorten beam downtime. In addition, much less of the CCS requires attention after these outages, saving downtime and money in hardware repairs.

Beam Line 2A

The beam line 2A (BL2A) controls component of the ISAC project was the largest area of development for Controls during 1998. Work on BL2A controls proceeded through 1997 but accelerated in 1998 to the successful completion of the beam line and beam delivery to the ISAC west target dump on May 25. This milestone was later followed by the successful delivery of beam onto a CaO target and the first production of radioactive beam on November 30. To meet the controls requirements for these milestones, a number of tasks were completed. The BL2A serial CAMAC branch was extended, including optical isolation, to the ISAC electrical room and hardware support for a variety of equipment was installed. Dedicated Xwindow terminals were established in the 500 MeV cyclotron's control room and the ISAC temporary control room. Beam line 2A software (safety displays, device scans, display pages, parameter logging, beam line save and restore, and other software components) was configured to be consistent with software for existing beam lines thus providing the same look and feel to which Operations is accustomed. To enhance safety issues, a beam line overcurrent scan and support for target interlocks was implemented.

Year 2000 Issues

There was concern about Year 2000 (Y2K) issues involving the CCS. To address this, the software components in the CCS were reviewed to determine which might fail. Only one software program was expected to have difficulty and it was not related to beam delivery but used in an off-line procedure for extracting data related to the cyclotron (and can be easily fixed to be Y2K compliant). Under controlled conditions the date on CCS computers was pushed ahead, and while the clock rolled over to January 1, 2000, personnel watched how the control system performed. No problems were detected and subsequently beam was

injected and accelerated without problems. TRIUMF does not run beam over the New Years period but this testing indicates that the CCS should run smoothly in the new year. Some similar work has been done on the proton therapy facility and no Y2K problems have been detected but more investigation and testing will be done during 1999.

Other Systems

The proton therapy computer was upgraded from a VAX 3400 to a VAX 4100. In addition, the operating system was updated to OpenVMS version 7.1 to be in line with the CCS.

Although the beam line 2C (BL2C) computer seriously needs to be replaced, only the memory was improved during 1998. BL2C control system hardware received attention to help improve reliability and in diagnosing errors. The BL2C control system software, from Vista Control Systems, was upgraded to version 2.7.

Support for the parity experiment and ion source 4 continued on items such as the rotary stage and Wien filter. More work is anticipated during the 1999 running period.

CCS Facilities

There were a number of CCS hardware developments other than those already mentioned. In the on-going process of slowly phasing out old VAXes, one used ALPHA was purchased and two very old VAXes were removed. The remaining two production cluster VAXes should be phased out next year. To handle increasing CCS requirements, CPU memory and disk space were expanded. Together, these changes precipitated a reconfiguration of the production and development clusters' hardware. One of the benefits was the significant improvement in the ability to run diagnostic programs on the CCS. The policy of replacing old CAMAC equipment has dramatically improved reliability. In 1998 two more old CAMAC crates were replaced. To support new requirements, an additional crate was set up in the computer room. One area of concern was the aging Xwindow terminals of which approximately 50 are supported by the Controls group. An increased frequency of failures has been noted.

Software associated with the CCS infrastructure received a number of improvements. The operating system on both clusters and on the proton therapy VAX was upgraded to OpenVMS version 7.1. DECMesageQ, an interprocessor/interprocess messaging product, was upgraded to version 3.2. ORACLE was moved to a production cluster ALPHA and upgraded to version 7.3 and SQLnet support was expanded to an Ops

PC. CAMAC interrupt (LAM) handling has been developed and support provided on the production cluster ALPHAs.

The task of relocating existing processes from the VAXes to ALPHAs has proceeded smoothly. In addition, there were several enhancements to the control system software functionality. In one development, a beta version of an Xwindow based program to display logged cyclotron parameters (Xstrip) was released. A new software utility called Xsoftwatch was written to monitor computers, key processes, batches, and queues. It starts the primary CCS processes when computers boot, sends messages to the Operator log when problems occur, and tries to restart processes if they are stopped. Xsoftwatch has an Xwindow interface which provides both a convenient summary and a detailed breakdown. A similar software utility (Xhardwatch) to watch hardware components is under development and already in use. Requests from the Operations group led to control of the rf voltage from the main console and several improvements in the main magnet run-up procedure. Colleagues at Fermilab have kindly provided an electronic log software package that is being evaluated with the anticipation of Controls group use in the next year.

A development that has received both hardware and software effort was the expansion of PC functionality. The successful CCS configuration of having separate production and development facilities is being followed for PCs. A simple NT server has been set up for each of the production and development activities. A SCSI tape drive from the control system computers was relocated for backups. Unfortunately, the PC hardware was not initially very reliable although after a number of failures were fixed these servers have run smoothly.

Miscellaneous

A project to provide hardware and software support for a PCI to CAMAC executive crate interface proceeded well. The initial implementations were completed by the end of the year and they are expected to be in service during the first quarter of the new year.

The second international Workshop on Accelerator Operations (WAO'98) was hosted by TRIUMF with some Web and database support provided by the Controls group.

OPERATIONAL SERVICES

Remote Handling

ISAC

By year end virtually all of Remote Handling personnel were committed to various ISAC construction

jobs with responsibilities for target hall shielding, module services, TIS/RIB beam optics component assembly and alignment, remote handleable beam line sections and pre-separator services as well as an interim shielded low level handling facility for removal of the first irradiated CaO target assembly.

Design of the new ISAC target handling hot cell is near completion. Work will begin on construction immediately following wrap-up work on the completed ISAC jobs. The target hall crane is now manually operable by wireless remote, although not fully commissioned.

Cyclotron servicing

During the single shutdown for the year a routine operation of personnel shadow shielding was installed and the 2C extraction probe removed for servicing.

Cyclotron elevating system

Routine maintenance was performed on the elevating jacks and gear reducers during the shutdown.

Beam lines servicing

During the winter shutdown assistance was given with removal of the neutrals mask probe and valve on exit horn #4. A remote handling indium vacuum blank-off was installed at this location.

A leaking monitor drive feed-thru required replacement of the 4VSM2/4VB1 indium seal.

A new water cooled window was designed, built and installed in the 2A proton beam line. This and other remote handling equipment were developed for use in the ISAC radioactive ion beam line and for handling of the ISAC pre-separator magnet.

Hot cells and targets

During the year the 1AT2 Mk-II target twice required replacement of a lower C-seal in two separate incidents. The 1AT1 Mk-I also required a lower C-seal replacement. The T2 Mk-I target required a rebuild of the target positioning gear box drive. The M9 beam blocker also experienced an air leak and required replacement of the vertical drive seal.

The T1 target cooling package was upgraded this year for improved operation, and a new design of expansion tank installed on both T1 and T2 packages.

Support was given to beam line 2C operation by replacement of the de-ionizer resin, repair of resin can, and repair to the 2C target handling shielding flask door.

In the lab a series of heat/strength testing was performed on MYKROY insulator material and a new vacuum brazing oven was set up and used for carbon target development.

Magnet Power Supplies

1998 saw the installation and commissioning of the remaining power supplies which were required for beam transport through the mass separator of ISAC. This included 2 bender power supplies which were acquired from Chalk River.

Routine maintenance and experimental support was carried out with leaking pass banks still being a major activity.

Coming out of the fall shutdown, difficulties were experienced with the main magnet power supply which was no longer regulating, and delivering only about 90% of normal current. A solution was found which was the independent powering of the master/slave amplifier boards as opposed to the previous connection which was to the raw dc supply for the driver stage. Due to the high gain of the system, eliminating the noise present on the raw dc supply for the pre-driver and amplifier resulted in much more stable operation of the supply which is now almost an order of magnitude more stable than previously with the precision feedback loop provided by trim coil 54 disabled. As well, during turn on, there is now a smooth transition from ramp up, to regulated current. This can be seen by monitoring the collector emitter voltage of the pass transistors which goes smoothly from near saturation during the ramp up to normal regulating voltage of roughly 7 V. Previously one had always seen a transition from near saturation to roughly 14 V as the current set point was reached and then after a minute or so the Vce would settle down to the normal 7 V.

Difficulties were experienced on the BL1A supplies which caused a number of beam trips. The problem was traced to the 1AQ10 supply which was repaired. Primary beam line supplies will be examined and recalibrated during the spring shutdown.

Electrical Systems

The major effort of the electrical department was the support of the ISAC project, which is described in the ISAC chapter of this Annual Report. Other responsibilities included the CERN project, cyclotron operation, maintenance of the site electrical services, power delivery and engineering support to TRIUMF users. Additional activities started and/or completed during the year are listed below.

- Installation and commissioning of the final stage of the fire alarm upgrade (cyclotron vault, service annex, proton annex and extension), including a fully supervised style 7 communication with the fire department.

- Replacement of half section of cyclotron vault lighting. The other half will be installed in the 1999 winter shutdown.

- Improvement of the outdoor site lighting.
- Replacement of the obsolete main power distribution centre in the radiochemistry laboratory. Given the importance of production losses, a careful plan was drafted and the system was re-energized in a record 7 days.

- Modifications to the services in the clean room 112 required by Nordion for new radioprocessing equipment.

- The trouble-plagued Elgar 37.5 kVA UPS system installed in the service annex was finally phased out and replaced with a modern MGS 50 kVA system. This new unit will provide much needed power to the electronic loads located in the accelerator building. Another locally dedicated 10 kVA UPS unit was added to the cyclotron data acquisition computer system.

Routine maintenance included lighting, power distribution centres, motors and transformers. An investigation of the non-active low conductivity water pumping system, which tripped a few times, revealed that the change of pump impeller increased the power requirements. Temporary modifications were introduced to continue operation to the winter shutdown when higher HP motors will be installed.

Power delivery

A transmission line bridge was installed by BC Hydro and UBC between lines 60L56 to UBC and 60L57 to Discovery Park. The new link is not a fully redundant feeder, but it offers greater continuity of service should a fault occur on the BC Hydro side of the transmission line. In case of loss of line 60L57 (from Camosun substation to Paprican), TRIUMF will no longer be subject to the 1.5 MW power restriction and may continue regular operation, after a brief shutdown for switching over.

Power management continued as routine work. The start-up of the ISAC facility is evident in the increased power demand and electricity consumption. To make possible the construction of the ISAC facility, the cyclotron was shutdown for a longer period of time. This is reflected in the large decrease both in the average peak power demand, -21% from 7391 kVA to 5856 kVA (Fig. 115) and the electricity consumption, -23% from 54.67 GWh to 42.11 GWh (Fig. 116). The average monthly electricity consumption was 3509 MWh. However, both kVA and kWh increased during the operating months as the ISAC systems started operation. The annual average load factor decreased 6.2% to 81.4%, primarily due to increased problems with cyclotron cooling services and the main magnet. The annual average power factor (PF) edged up 0.5% to 97.1% (Fig. 117) thanks to the larger number of shutdown months, which have a much higher PF value. The average PF for an operating month decreased

about 0.8% to 95.4%. Additional capacitors will have to be installed during next year to limit the peak power demand at current values. A 1% power factor decrease corresponds to an additional power bill of about \$8000/year at 8000 kW demand, assuming 8 months of beam production.

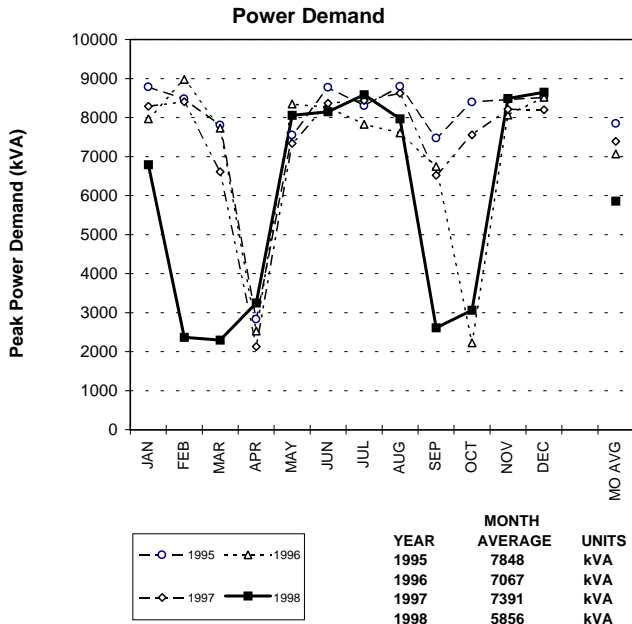


Fig. 115. Electrical system power demand – four year comparison.

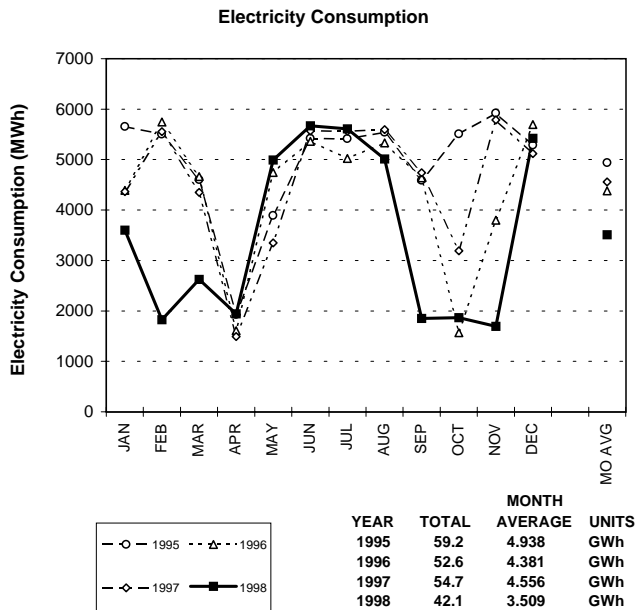


Fig. 116. Electrical system energy consumption – four year comparison.

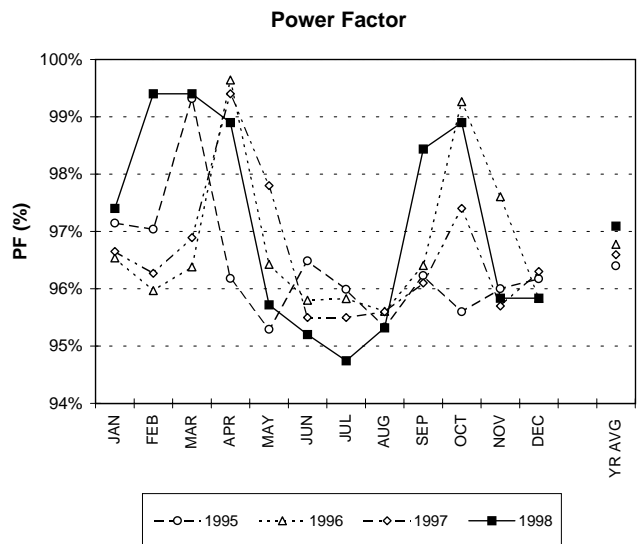


Fig. 117. Electrical system power factor – four year comparison.

Mechanical Systems

Activity was divided between ISAC work and the remainder of the site. ISAC work consumed almost 90% of the time.

The TRIUMF-related work included: machine shop exhaust system upgrades in three areas, the replacement of the Al ALCW pump with a temporary pump while awaiting delivery of a new one, new air conditioning for the telephone exchange room, new exhaust system for the carpenter's shop, repair of the GERBER room air conditioner, check calculation and certification of hoist beam in MESA basement, tie-in of the new ISAC air compressor to the TRIUMF air system, and studies for new uses of the medical annex and MESA.

ISAC PROJECT

INTRODUCTION

TRIUMF has again this year heavily invested resources into the ISAC project. The results and milestones, described in the following pages, are evidence that the investment has provided many observable successes. In fact, a major milestone, namely the achievement of radioactive ion beam to the low energy experimental area, was achieved approximately one month ahead of schedule. This milestone required a completed BL2A, a full set of target modules, completed radiation shielding and safety system, mass separation system, low energy beam transport to TRINAT, controls, TRINAT and an AECB operating licence. Although this part of the project received priority, progress continued with the accelerators and beam lines required for the astrophysics program. The RFQ accelerated beam from the off-line ion source up to 54 keV/amu, displaying an acceptance similar to that projected.

The first ring buncher required by the DTL was tested successfully at full power. At year end the first tank of the DTL was ready for power tests. Many of the magnetic components required for the MEBT and HEBT were acquired from the TASC facility. Consequently, it appears that ISAC should be able to begin the high energy physics program by the end of 2000. In anticipation of the next five year plan, a concept design has been prepared which would allow the beams to be taken up to 6.5 MeV/amu for masses as high as 150.

SCHEDULE AND PLANNING

The Planning group was actively involved in planning, scheduling, coordinating and expediting several sub-projects for ISAC. Various plans and PERTs were prepared, manpower estimated and analyzed and PERTs were updated regularly. Priorities were evaluated and the highest priority was assigned to produce the first radioactive ion beam (RIB) from ISAC by the end of November. This required the completion of beam line 2A, target areas with five modules and shielding, separator system (pre-separator, mass separator and LEPT to TRINAT). The resource levelling was done, activities were expedited and this goal was achieved on schedule with the first RIB with ISAC on November 30 and RIB delivered to TRINAT on December 5. Other intermediate milestones which were planned and achieved in 1998 include:

- February: 11 MHz, saw-tooth buncher test;
- April 29: proton beam to temporary dump;
- May 25: proton beam to the dump module at west target station;

- June 6: first accelerator beam out of RFQ with ^{14}N ;
- July 13: full voltage on RFQ electrodes;
- September 24: first stable beam out of exit module at Faraday cup;
- September: accelerated beam out of RFQ at full power;
- October 23: first stable beam through pre-separator;
- October: DTL rebuncher tested to full power;
- November 3: first high resolution beam at separator image slit.

Approximately 89% of the total available Design Office effort and 83% of the total available Machine Shop effort were invested in ISAC. In addition, significant design and assembly support was provided by the University of Victoria and other groups at TRIUMF (Beam Lines, RF, Targets) to meet various challenging schedules. The PERTs of ISAC sub-projects which required substantial manpower from various groups included: completion of beam line 2A; target hall (target stations, five modules, shielding and remote handling); separator system (pre-separator, mass separator plus LEPT with associated diagnostics, controls and services); RFQ task force (off-line source, LEPT, RFQ with seven rings plus optics and diagnostics), TRINAT (move from proton hall to ISAC and new LEPT), GPS (tape drive system and LEPT), DTL (tank 1 and rebuncher); and MEBT (prototype buncher).

Progress on PERTed projects is described elsewhere in this report under the respective principal group. The following is a summary of projects along with major milestones planned and achieved, which required a substantial part of the Planning group's effort in planning, scheduling and expediting various activities.

Beam Line 2A

Major emphasis was to complete the installation and commissioning of the vault and tunnel sections. Beam line 2A was commissioned with proton beam to a temporary dump (in the tunnel) on April 29, and to the dump module at the west target station on May 25.

Target Areas

Work primarily included fabrication, assembly, installation and alignment of 2 vacuum tanks; fabrication and assembly of 5 target modules for the west target station (entrance, dump, target and 2 exit modules); target hall crane; guard rails, walkways and refinishing of target hall concrete walls by surface paring and painting; shielding (up to 525 tons of concrete poured in several steps and 1,000 tons of steel shielding); high voltage system (cage, interlocks and HV lines); services (electrical, water, air); vacuum system; target station (module access area, services, cabling); machine protect system (interlocks, thermocouples, etc.).

Several problems were encountered in the fabrication and assembly of two vacuum tanks and many target module components due to poor copper plating, design and manufacturing errors compounded by the lack of quality control and proper timely inspections of fabricated components. Consequently, more manpower was required to correct technical problems and the milestone of extracting stable beam out of the exit module at the Faraday cup was achieved approximately two months later on September 24.

RFQ

Along with installation and alignment of the platens, seven rings and rf shroud in an 8 m long RFQ tank; the rf short, LEBT from OLIS to RFQ, optics and diagnostics were also installed with the associated vacuum system, services and controls to test RFQ with seven rings up to 60 keV/u. After systematic bead pull measurements and rf tests (signal and power level), full voltage on RFQ electrodes was achieved on July 13. First accelerated beam with ^{14}N was extracted through the RFQ in June and with ^{28}N at full power in September. More beam tests will continue until January, 1999. All 19 rings were designed, fabricated and assembled by December, with an aim to send out for EDM in February, 1999, completion of installation of all rings by July, 1999 and signal level and power level rf tests by October, 1999.

Separator System

The pre-separator was received and field mapped in June and installed by September. A maze to separate the pre-separator section and the mass separator pit was designed and built during the summer. The mass separator, high voltage platform, diagnostics, vacuum system, controls and LEBT (from DB11 to TRINAT) were installed and tested by October. The commissioning sequence involved getting the first stable beam through the pre-separator on October 23, the first high resolution beam at the separator image slit on November 3, followed by a stable beam to TRINAT on November 19, and RIB with ISAC on November 30.

Drift Tube Linac (DTL)

The overall progress on the DTL project was slow due to a relatively higher priority (in terms of manpower and other resources) placed on getting the RIB to TRINAT by the end of November.

After prototyping and a few design iterations, the first tank (including stems, ridges and end plates) was fabricated and copper plated by September. However, due to problems associated with copper plating of the tank and DTL components, the installation and alignment were delayed until January, 1999 and will be followed by rf tests by May, 1999. The DTL buncher was designed and fabricated at INR, Troitsk. It was received at TRIUMF in August and tested to full voltage by October. The plan is to order the other two bunchers (after evaluating the tests) by February, 1999. The DTL triplet was specified and design was started. It needs higher priority so that it can be reviewed and ordered by April, 1999 or earlier, and then field mapped and installed by November, 1999.

DRAGON

A work breakdown structure (WBS) was developed and a detailed PERT was prepared and updated regularly. The progress and major milestones included: gas target designed and fabricated at the University of Alberta with an aim to test at TRIUMF in May, 1999; two magnetic dipoles (MD1, MD2) designed and will be ordered in January, 1999; design of two electrostatic dipoles (including electrodes, HV power supplies, support and alignment structure) started.

Manpower

Manpower estimates for all ISAC sub-projects were completed showing heavy manpower requirements in 1998 and 1999. Priorities were evaluated and work on the DTL and RFQ 19 rings was given a lower priority compared to activities required to produce the first RIB to ISAC by the end of November.

In addition to the above sub-projects, the Planning group was actively involved in planning, scheduling and expediting the activities for the GPS experiment, the TRINAT move to the ISAC building, LEBT (to TRINAT and GPS), yield station, MEBT layout, LNTO (for beam in July, 1999) and β -NMR (for beam in November, 1999).

CONTRACT ADMINISTRATION

In the past year, five contracts were awarded. Holaco Construction Ltd. (B.C.) built miscellaneous concrete shielding blocks for the target hall. Sunrise Engineering Ltd. (B.C.) was awarded two contracts; the pre-separator magnet and the first drift tube linac tank

DTL1. Talvan Machine Shop (B.C.) built the 45 degree dipole magnets for the MEBT. The coils were sub-contracted by Talvan to Stangenese Industries Inc. of California. Brandt Industries Ltd. of Saskatchewan built nine target station shield plugs which were used to cover the module shield plugs in the target tanks.

Personnel Resources

In 1998 the personnel effort for ISAC increased steadily to average 79.97 full time equivalent (FTE) people per month, compared to an average 63.6 FTE people per month for 1997 and 39.6 FTE people per month in 1996 (see Fig. 118).

In 1998 the average personnel effort per system (see Fig. 119) was as follows:

Table XIX. Personnel effort per system.

System	Monthly FTE
Project management & administration	4.06
Beam line 2A	6.55
Target station	12.13
LEBT	9.69
Accelerator	13.22
Science facilities (TRIUMF personnel)	10.06
Infrastructure	9.33
Integration	12.95
Science facilities (non-TRIUMF personnel)	1.98
Total ave. FTE monthly personnel	79.97

The total personnel effort since the project began is shown in Fig. 120. The graph illustrates the total FTE years per project section. The combined effort totals 183.62 years of work, based on a FTE month of 150 hours.

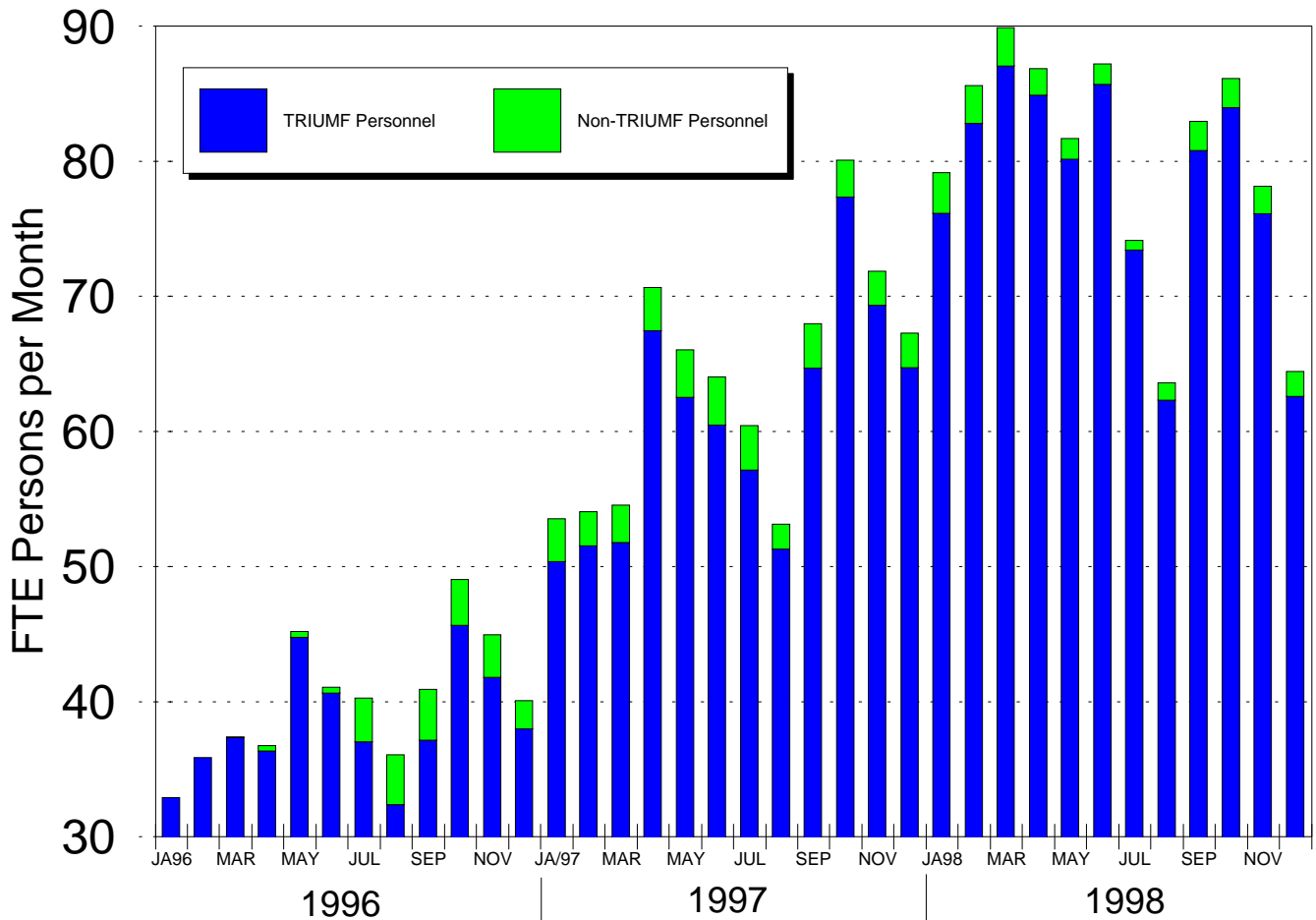


Fig. 118. ISAC project personnel, January 1, 1996 to December 31, 1998.

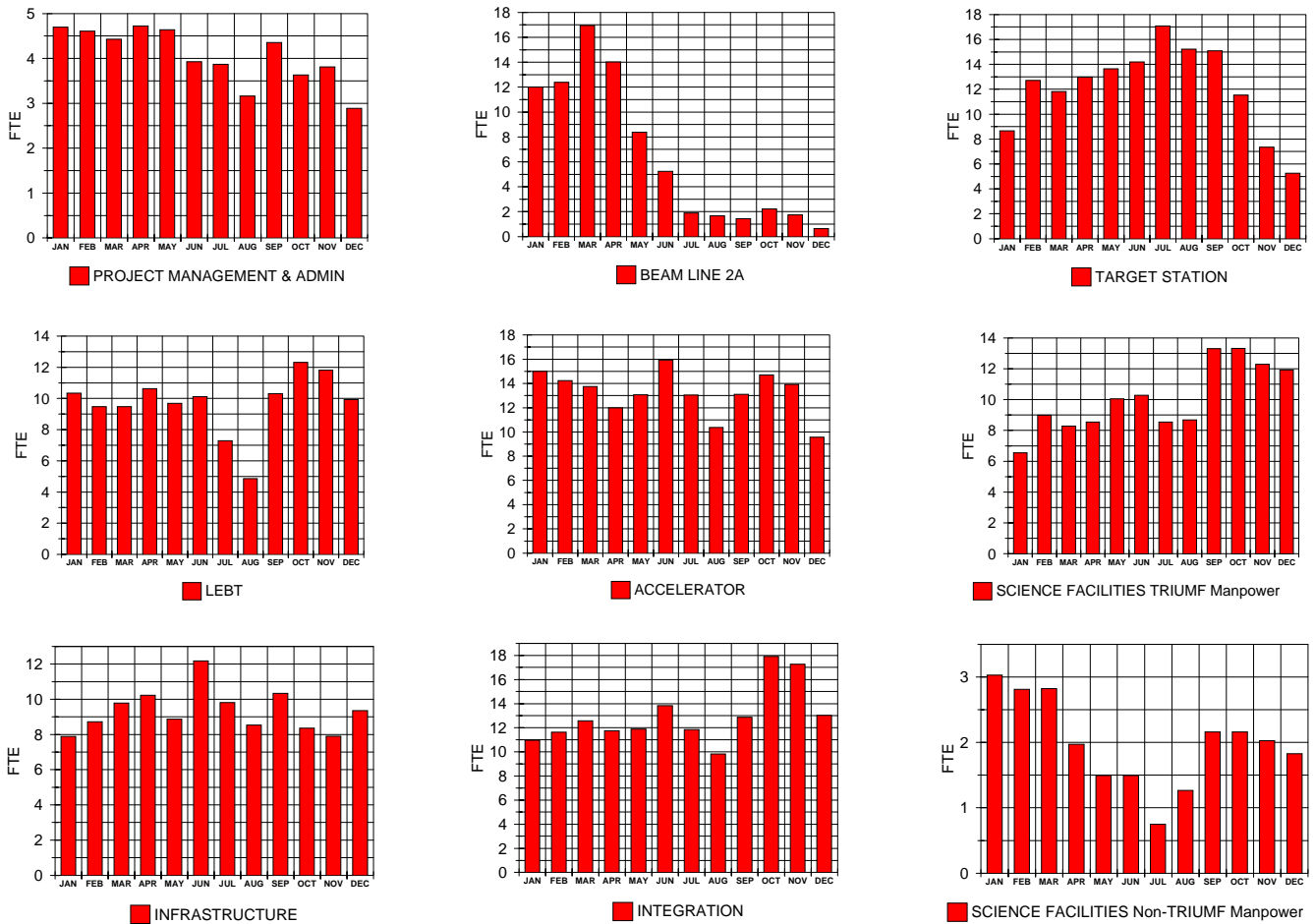


Fig. 119. ISAC personnel. Monthly FTE people for 1998 (by system).

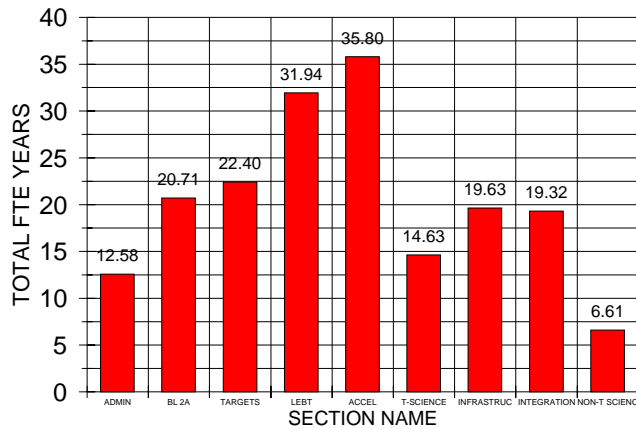


Fig. 120. ISAC project personnel, January 1, 1996 to December 31, 1998.

CONVENTIONAL FACILITIES AND INFRASTRUCTURES

1998 was the year in which the formal occupancy of the ISAC building was obtained. Two of the major contracts remaining, namely electrical and mechanical, were formally completed early this year. With their

completion the UMA group project management team reduced its presence and left the site in February. TRIUMF ISAC technical facilities assumed direct responsibility for the completion of the conventional facilities while UMA helped manage the transition. Many other contracts were brought to completion during the year, including the upgrade to the fire alarm system to satisfy the new requirements of the fire department. We also supervised the warranty repair work carried out by various contractors. The extra claims by Swagger Construction Ltd. were successfully settled during the summer with mutual satisfaction. NORELCO continued to work at solving the target hall crane radio controls problems. After many ideas were tested in the field with partial success it was decided to re-engineer the whole controller design. The upgrade will be commissioned in 1999. The last phase of the target hall shielding was installed in the spring along with a masonry block maze to the pre-separator. After concerns were raised that potential radiation contamination may accumulate in the large holes in the walls, the target hall walls were surface parged and painted. The construc-

tion of the TRINAT clean room was completed in the summer along with the preparation of the area to house the LEBT vertical section. Covers for the experimental hall mezzanine were gradually installed during the fall. Once the major construction activities were completed a systematic cleaning program was started in the fall to make the ISAC facility a fully operational laboratory. Continuing support was provided to the Science Division for development of the arrangement of the experimental facilities and integration with the rest of the accelerator systems and building services. In the late summer we finally managed to re-do the landscaping of the boulevard along the road to TRIUMF.

Data and Ethernet Communication

The data communication system for ISAC was a major project this year. All conduit were traced, confirmed and mapped to AutoCAD drawings after it was discovered that the contractor as-built drawings were not accurate. February to June were dedicated to pulling twisted 100 base-T cables, making terminations, jumpers and commissioning. TRIUMF personnel pulled the fibre optics cables, but the terminations and testing were contracted out. During the remainder of the year we continued to add to the system as required for the ISAC controls and TRINAT. Some of this work involved installing fibre optics isolated systems due to the special grounding requirements of the target systems and the mass separator. In November ISAC was formally connected to the rest of the TRIUMF site and the Internet. Altogether 124 twisted cables and 3 sections of fibre optics cables ranging from 200 ft to 550 ft were installed. There are 212 data connections available, with a fibre optics backbone that connects to the rest of the site network and the Internet.

Electrical Services

Another extremely busy year was dedicated to the design and installation of the services to the systems required for the first ISAC experiment in the TRINAT experimental set-up. Since TRIUMF was not staffed to carry the workload with its internal resources, an arrangement with outside contractors was made to retain flexibility during construction while keeping costs under control. TRIUMF supplied all design and engineering, procured all material, and coordinated the work of the outside labour force. The task was particularly challenging but in the end proved to be successful. The arrangement allowed the necessary flexibility to proceed with the installation of services to systems that were not fully specified in detail and to retain control of the installation of especially critical systems like the mass separator grounding. A good example of the above is given by the pre-separator services and

controls relocated to the electrical room after the decision to move the TRINAT lab in the mass separator support room.

Major tasks completed during the year included the installation of cable tray systems and ac power services for the following systems/areas:

- Beam line 2A tunnel side and associated auxiliaries
- Electrical room and target ion source Faraday cage
- Target hall and west target station and associated cooling and vacuum packages
- Mass separator, pre-separator, and low energy beam transport to the experimental hall
- TRINAT clean room
- GPS and LEBT in the experimental hall
- RFQ and auxiliaries, including vacuum pumps, cooling systems and bake-out, and controls for the blanket electrical heaters
- Extensive conduit runs for the radiation safety monitoring systems and area safety units
- Mass separator isolated grounding.

The commissioning of the RFQ amplifier revealed that the specified tripping speed of the line breaker was not adequate to protect the rf tube in case of an internal short circuit. To reduce the breaker tripping speed from 55 ms to 20 ms required the coordinated effort of the supplier as well as TRIUMF engineers and a series of tests to determine the optimum voltage to apply to the tripping coil.

The rf grounding was engineered to force the return of rf leakage currents back to the source through the rf transmission line. All the remainder of the structures were isolated except for a safety ground wire which offered a high impedance path to the rf signal.

The design of the grounding system for the target ion source–target station–pre-separator–mass separator systems required a particular effort. This grounding must provide a voltage stability of ± 1 V/60,000 V between the ion source terminal room and the exit slit of the mass separator located about 60 linear feet away for power frequencies up to the 50 harmonics (3,000 Hz) in order to provide the required signal reference stability to achieve the desired mass resolution in the spectrometer. The initial design of a single-point signal ground plane embedded in the concrete floor had to be changed once it was found out that the large surface available around the target station and the limited electrical resistance (k Ω) offered by the concrete

would prevent maintaining a good ground isolation all the way from the ion source to the mass separator exit slit. The new design incorporated a signal ground plane made of a 12 in. copper strip, completely isolated from the building structures and the target station frame, run from the ion source terminal room ground plane to the mass separator ground plane. The ion source itself was isolated from the rest of the target module metal frame and connected back to the terminal room via isolated ground wire. The grounding of the two ac power distributions to the ion source terminal room and the mass separator beam line had to be engineered to accommodate the above requirements. The installation of the public address system was postponed to the next fiscal year and the required manpower was busy in other priority tasks. The OLIS safety interlocks were completed and the system declared fully commissioned. Some rf noise problems emanating from the source were addressed and corrected.

Mechanical Services

The ISAC activity may be divided into two classifications: the contractual project and the post-contractual projects. The contractual project was carried out under the management of UMA Projects, the project manager for the construction of the conventional facilities. The post-contractual projects were managed by TRIUMF and included the connection of the beam lines, targetry and experimental facilities to the backbone systems built under the contractual project.

The contractual project saw the completion of the construction, the start-up and commissioning of the building mechanical systems. This work was managed by UMA Projects with the coordination of TRIUMF and the supervision of Keen Engineering, the mechanical consultant responsible for the design. The installation was carried out by the main contractor, Lockerbie and Hole, the controls were by the subcontractor, Modern Systems Management, while KD Engineering performed the commissioning of the water, compressed air, ventilation and sump systems. Wherever possible, systems were 100% complete, for example: building HVAC, washroom facilities, storm drainage. However, some systems were left in a "roughed-in" condition for completion in a post-contractual project as beam lines, target modules and experimental systems were completed. Examples of these are the cooling water distribution to beam line components and the radiation exhaust ducting into target areas. Work on the contractual project was essentially complete by spring.

The post-contractual projects occupied the majority of effort in 1998 and covered all phases from design, procurement, contracted installation supervision, and commissioning. A series of milestones was reached on

time and under budget. These projects can be classified as supply of cooling water, compressed air and vacuum pumps exhaust connection to the radiation exhaust system, and air handling systems.

Air, cooling and vacuum exhaust installations completed during the year in rough order of magnitude included:

- the high active low conductivity water cooling system (HALCW) for the target stations and services in the target hall,
- the RFQ and associated PA-dummy load bake-out systems,
- plumbing for the mass separator-pre-separator-maze-LEBT, TRINAT clean room, electrical room and target ion source terminal room in non-conductive material,
- 2A vault and 2A tunnel beam lines and relative power supplies,
- LTNO and GPS services,
- nitrogen capping and resistivity sensors for the low active and non-active LCW systems.

The air handling and ventilation jobs included:

- the TRINAT clean room air conditioning;
- the extension of the radiation exhaust system to the target area;
- HVAC extension into the Faraday room with grounding isolation;
- the installation of HEPA filters and monitoring instrumentation into the target area, mass separator area, 2A tunnel and mechanical penthouse;
- the connection of the TSG monitoring system exhaust to the radiation exhaust system.

In addition, the experimental hall crane north-south drive controls were revised to obtain a finer motion control.

Voice and Telephone Communication

Telephone services were initially provided with temporary cabling as installation and commissioning personnel moved into new areas of the building during the ongoing beam line construction stage. Permanent cabling was completed by BC Tel in early May. Telephone installation and programming were carried out by the TRIUMF telephone group and to date 28 locals serve a large portion of the ISAC facility. The ISAC telephone system is fully integrated with the rest of

the TRIUMF system. The TRIUMF system has a limited capacity for additional locals to ISAC. The telephone management group is reviewing the situation to determine whether to expand the existing hardware or recover locals from elsewhere on site.

ISAC-I EXPERIMENTAL FACILITIES

Having defined the initial ISAC scientific program with the help of the ISAC Scientific Advisory Panel, users met biweekly during the year to organize the experimental hall and define the required experimental facilities. The experimental space available has been subdivided between a low energy area where beams of up to 60 keV produced from ISAC are used and a high energy area which will make use of the accelerated beams (up to 1.5 MeV/amu) in the year 2000.

Figure 121 gives the current agreed upon layout for the beam delivery system. One experimental area is not shown on this diagram because it is occupying the mezzanine directly above the separator room. Because of the shielding and strict environmental requirements, the TRIUMF neutral atom trap has been located on the mezzanine. It is described on page 45 of this Annual Report.

The low energy area is shared between two main beam lines; one feeds the general purpose tape station (see Expt. 823, page 60), and the low temperature nuclear orientation set-up (see LTNO, page 118). It will accommodate other stations along the main backbone

beam line in the future. The second beam line will feed initially a polarizer section to produce polarized ion beams for a condensed matter program. The first such beam will be ^8Li which is being developed on the ISAC test stand (see page 154). This same beam line will have a Paul trap to bunch the ions which could feed a Penning trap system as well.

In the high energy area, two beam lines are anticipated initially: one feeding the DRAGON recoil spectrometer system (see DRAGON report, page 119), the other a general purpose scattering facility to be developed in collaboration with the University of Edinburgh. During the past year, considerable engineering studies helped freeze the final configuration for DRAGON which occupies a large piece of real estate in the hall.

As reported in this document, two experimental stations, TRINAT and GPS, were commissioned in time to accept the very first potassium beams from ISAC. The LTNO fridge was moved from Oak Ridge and is being recommissioned in the ISAC hall. Designs of the ^8Li beam system and of a β -NMR spectrometer were finalized. Designs of the DRAGON spectrometer elements were also finalized, and tendering and procurement are being carried out.

The successes of the ISAC construction teams are now coming to the attention of the physics community and new groups are considering moving some of their experimental programs to ISAC.

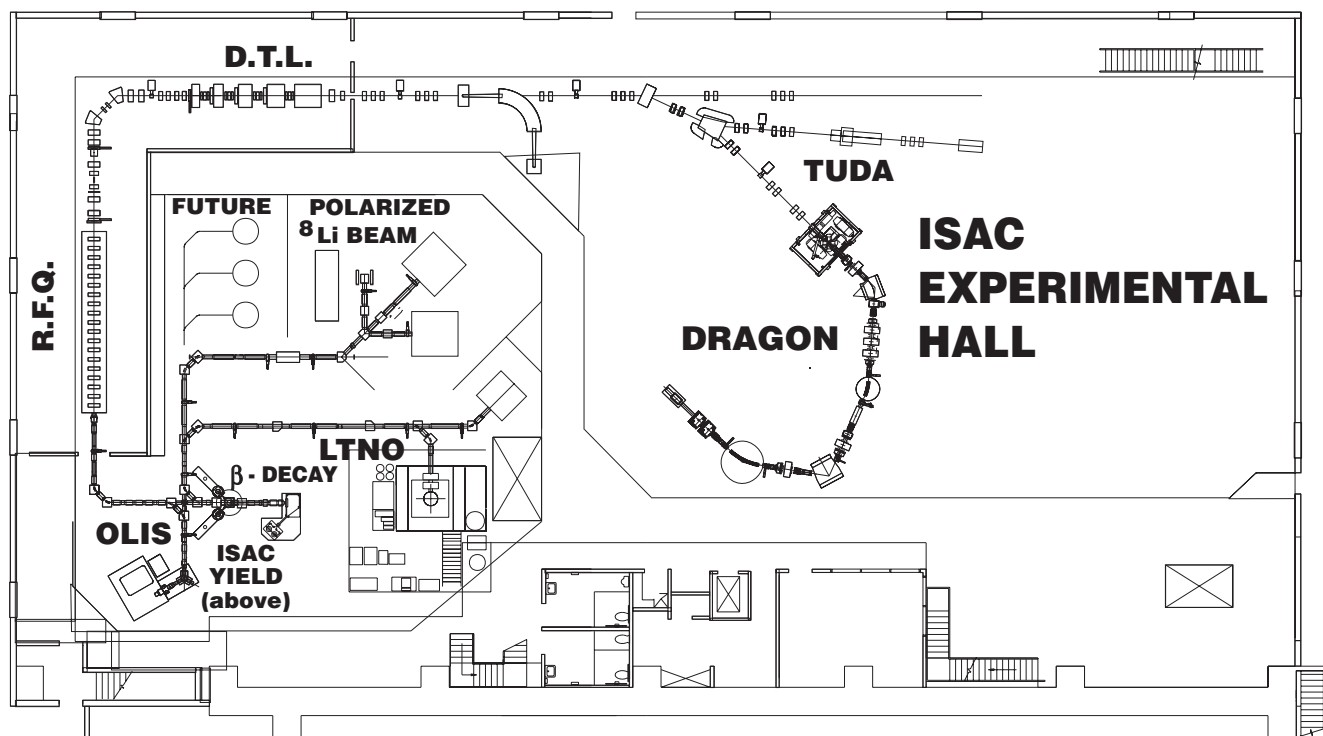


Fig. 121. ISAC experimental facilities and beam delivery systems.

TARGET HALL

The function of this hall (from west to east) is to contain two target stations and most services, a storage pit, two hot cells, an entry hatch and several landing areas. The hall itself acts as a radiation shield during operation and target module transport to the hot cells. The hall is 137 ft long (E-W), 18 ft wide and 45 ft high, with the lowest level at 264 ft at the bottom of the storage pit. The entire area is serviced by a special 20 ton crane which ultimately will be remotely controlled from the remote handling control room.

At the end of 1997 work had just begun to construct the two target stations and the service zone at the west end of the hall. This was the major undertaking of 1998 and involved seven steps requiring framing and concrete pours, several steps requiring 10 ton steel block placements as well as electrical and ventilation chases and numerous service ducts, conduits and penetrations. This work had to be done accurately to satisfy the requirements of the placement of the two

target tanks and minimize surrounding air gaps to reduce radiation activation. Many gaps were packed with scrap steel to augment shielding. The final result is a chevron-shaped pit that surrounds the two target vacuum tanks and the pre-separator magnet at its apex (see Fig. 122). The tanks sit on three alignment pins that are part of a prealigned alignment frame buried in the concrete. Construction was so precise that very little final adjustment was required. In the end, the seven steps involved 525 tons of concrete poured and 1000 tons of steel placed. Work then began to prepare the west target station – installing and aligning the vacuum tank, installing the high voltage conductors in the chase, installation of services, etc. In September, the five modules were installed and aligned and stable beam was produced and transported to the Faraday cup in exit module 2 and through the pre-separator magnet shortly thereafter. Radioactive beam was produced in early November and transported to the yield station in the experimental hall later that month.

TARGET HALL WEST

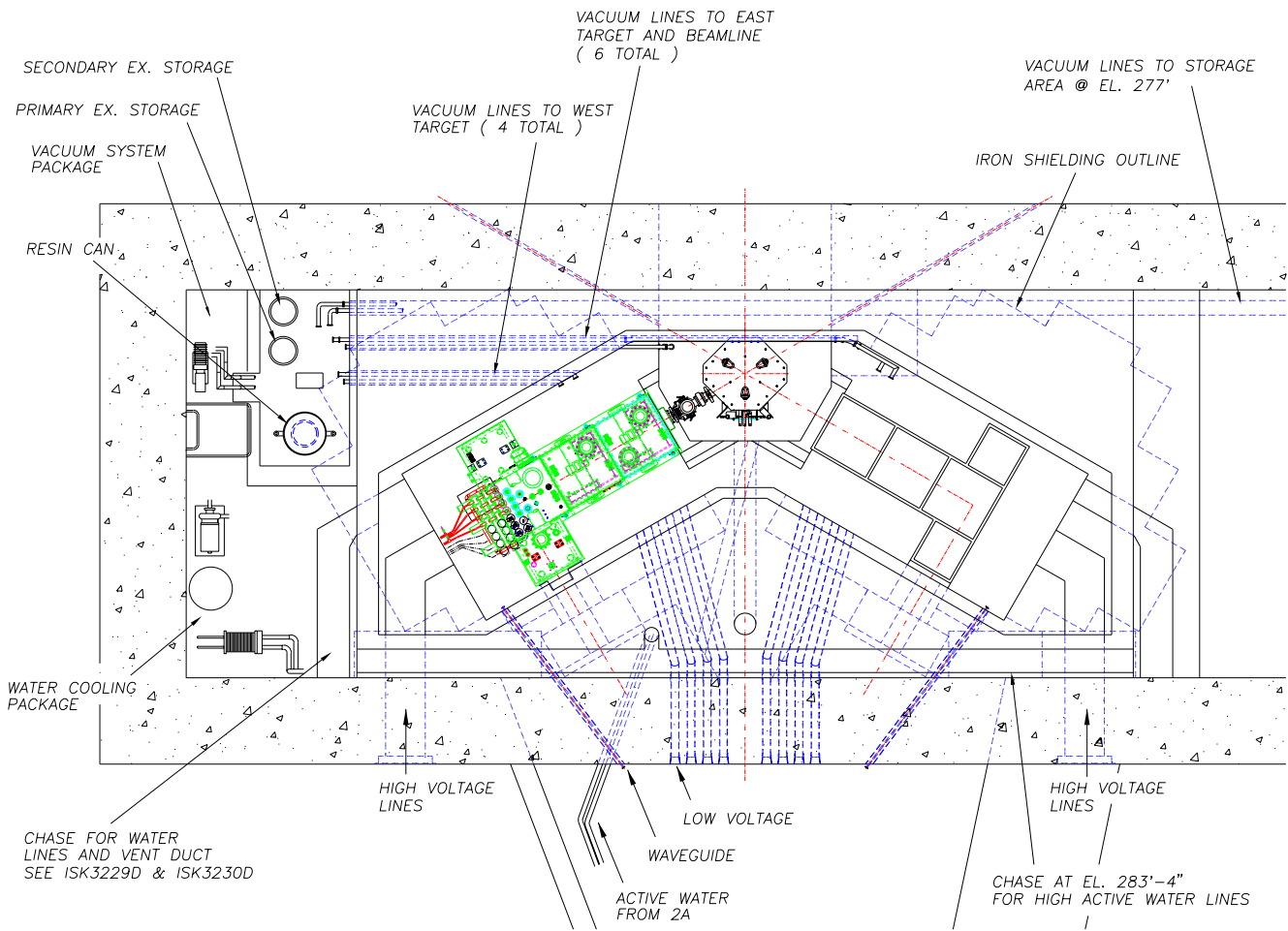


Fig. 122. Arrangement of target stations within the target hall.

Elsewhere in the target hall and in parallel with the aforementioned work, the crane was installed and, after many initial problems, was eventually commissioned. Some problems have persisted and are still being evaluated.

The storage pit was utilized as a work area once the module alignment frame was installed. Completion of the storage pit and hot cells will commence in 1999.

Other activities in the target hall involved the installation of walkways and guard rails, steps into the storage pit and a total refinishing of all concrete surfaces within the hall by surface parging and painting.

Shielding

The target hall design stems from its primary function which is to shield adjacent work areas from radiation during operation and module transport. This has already been described in the previous section insofar as the target stations are concerned. The design concept is based on an extensive investigation into projected radiation levels in the adjacent work areas. The steel and concrete surrounding the target stations, combined with the 4 ft walls, ensure that radiation levels are below $10 \mu\text{Sv/hr}$ in these areas. To complete the picture, special removable, triangular shield blocks cover the pre-separator magnet leaving two rectangular volumes above both target stations. Each of these volumes is covered by five steel/concrete shield blocks that also are removable. Thus, the operating station is covered while the other station is not and radiation levels are such that workers can be at the non-operating station. All this special shielding required special form work and the introduction of steel pallets as the concrete was poured to achieve the optimum shielding protection. These blocks were manufactured as steel boxes off-site and filled at TRIUMF. The other specially shaped shield blocks were formed and poured on-site. All were built during the latter half of the year.

During 1999, more shield blocks will be produced to provide shielding in the service zone for the high active water package and the vacuum storage tanks. There will also be a requirement for special shielding in the storage pit and for shielded storage silos for modules.

Target Station Modules

All five of the modules for the west target station were built, leak checked, aligned, installed and operated in 1998. The entrance module and dump module were completed first since they are smaller and simpler and the others followed until completion in early fall. Figure 123 shows the target module.

Assembly of the modules took place in the east end of the ISAC experimental hall where an assembly area was created. This involved the construction of a large U-shaped assembly frame to support all five

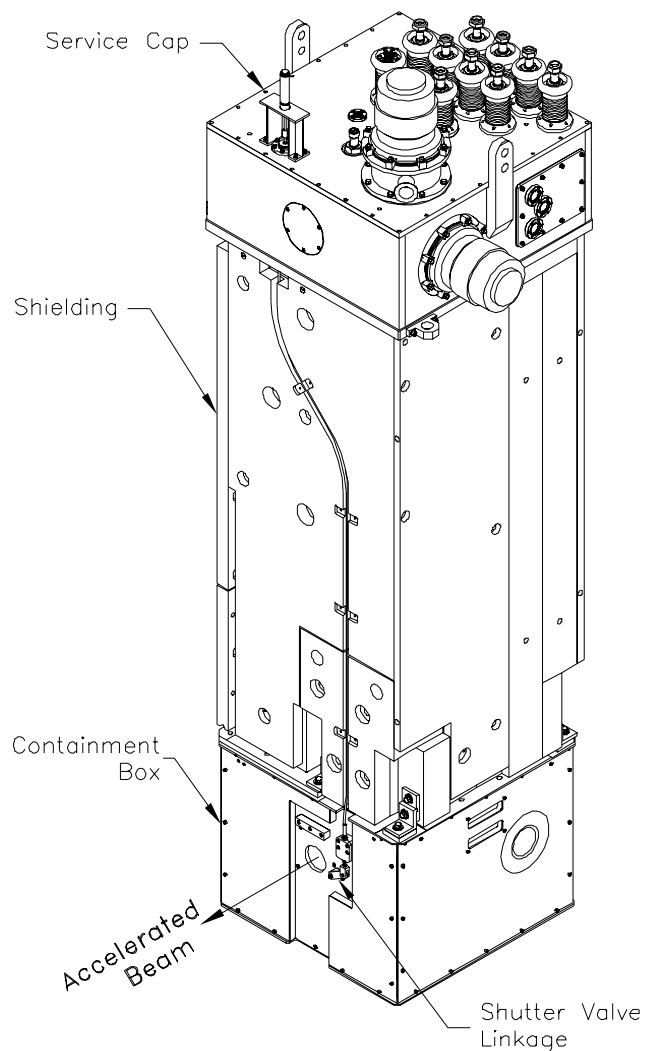


Fig. 123. Target station module.

of the modules during assembly (approximately 56 tons). There were several problems associated with the assembly, mainly due to manufacturing errors arising from the very tight schedule. For example, one unexpected problem was with the copper plating. All the shield plugs of the five modules are mild steel, copper-plated for corrosion protection. A large number of the pieces began to blister after delivery and had to be re-plated. This was a result of poor preparation prior to plating. There were also certain aspects of the design that were found to be impractical and required changes such as the containment box used at the bottom of the target and exit modules. The design was altered and the piece parts modified accordingly.

Once the modules were in a semi-complete state they were placed in the east target vacuum tank (not yet installed) for leak checking. This proved to be a very tedious task due to the sheer number of welded joints and O-ring joints. Eventually this was overcome

and after the tank was installed and aligned the modules were installed and installation of the services could then be completed. The target module required several iterations of modifications subsequent to this due to high voltage sparking in the service duct. This involved altering insulator supports and redesigning corners and adding smooth sheet metal at the entrance and exit of the duct.

Another very important step in the assembly of the modules was alignment. This is reported in the Remote Handling section of this Annual Report. Each individual component in the target and exit module containment boxes had to be aligned to each other and then aligned relative to the module alignment pins at the top flange. A series of jigs and fixtures were built to achieve this. Although very difficult to check once the modules are installed, there is confidence that errors are <0.010 in relative to true position.

The goal of all of this work was to achieve stable beam to TRIUMF in October and radioactive beam to TRIUMF in November. This goal was achieved.

ISAC Diagnostics

The west target station entrance module diagnostics, associated drive mechanics and controls were built and installed in time for the 2A commissioning beam tests in May. The pneumatically driven retractable beam position monitor 2A2M19 design is based on the standard 32 by 32 multiwire monitor package with a two inch aperture. The design incorporates remote handling connectors and a replaceable monitor head. A multiwire monitor head was chosen to facilitate the beam commissioning and initial operation up to $1 \mu\text{A}$; but as with the beam line 2A profile monitors a scanning wire head can be installed for use at higher beam currents. The last elements in the entrance module just upstream of the target are the stationary protect monitor and water cooled copper collimator. The protect monitor which is mounted directly to the collimator consists of a set of transverse aperture plates and a halo plate. To minimize scattering, there is no total current foil. The collimator and protect monitor present a 0.75 in. diameter aperture.

The exit module diagnostics and their associated drives and controls were designed, built and installed in time for beam commissioning in the fall. Exit module 1 contains a multiwire profile monitor ITW-harp3 and a three position collimator ITW-col3. Exit module 2 contains a multiwire profile monitor ITW-harp5A, a three position collimator ITW-col5 and a Faraday cup ITW-FC5. These are all pneumatically driven and designed with remote handling connections.

Multiwire monitor ITW-harp5B and the diagnostics stations IMS-DB0 and IMS-DB10A were built in the fall and installed in time for the stable beam tests

in October. Harp 5B is based on the 2A monitor design. DB0 has a set of scanning slits, a harp monitor and a Faraday cup; DB10A has a set of scanning slits and a Faraday cup, but no harp. A vertical scanning wire will be installed in DB10A.

Assistance was also given to the IMS-DB11 diagnostics station and the RFQ in-tank diagnostics. The Diagnostics Electronics Support group provided electronics modules, cabling and system integration for all of the beam line 2A and ISAC diagnostics.

Finally, a capacitive pickup was installed at 2AM14 and a toroid was installed at 2AM12 to provide redundant non-intercepting beam intensity measurements for the proton beam in beam line 2A.

SAFETY AND RADIATION CONTROL

Licensing

Early in 1998 a submission was made to the Atomic Energy Control Board (AECB) of Canada for a licence to operate ISAC. TRIUMF again made personal representation at the meeting of the Board where the application was initially considered. A licence valid for four years was subsequently granted effective March 31, 1998 in time to allow the initial extraction of proton beam into beam line 2C.

This licence contained a number of conditions and required the written approval of the AECB for the production of radioactive ion beam. Some further documentation concerning handling of irradiated targets and a site visit by AECB staff were required before approval was finally granted November 12, 1998.

Access Control and Radiation Monitoring

The control of the access for those areas affected by the radiation fields due to the proton beam was incorporated in the existing 500 MeV cyclotron Access Control System. The same design principles were used for what is essentially an extension to the present system. A few minor changes were made in the hardware such as, for example, replacing the traditional 'break-out' bolts on the access doors by a new chain and pin mechanism which should require less maintenance.

The Radiation Monitoring System (RMS) for the 500 MeV facility was extended to ISAC. Five beam-spill monitors, seven air monitors, two neutron monitors and one residual radiation monitor were installed before the start of commissioning. The existing RMS does not have sufficient capacity for the large number of monitors which will be required to monitor the radioactive ion beam losses in the ISAC experimental hall. Work was begun on a new system based on VME hardware and EPICS software. By year-end the work had progressed to the point where several monitors had been built and the system was able to read and write to some of the VME modules.

Commissioning

The commissioning of ISAC started in late April, with the extraction of a proton beam of a few nanoamperes intensity into beam line 2C. The proton beam was stopped in a temporary graphite beam dump in the beam line 2C tunnel. This allowed measurements to be made to verify the estimates of radiation fields above the shielding due to proton beam losses in this tunnel. Figure 124 shows a comparison of some measurements above the shielding with calculations made using the Monte Carlo shielding code FLUKA. The agreement is better than it appears because the monitor used does not measure the high energy neutron component which is included in the calculation.

Commissioning continued in mid-November with radioactive ion beam production from a CaO target bombarded by approximately $1 \mu\text{A}$ of proton beam. No surprises were found and from the radiological viewpoint the commissioning went very smoothly. A target failure during commissioning required that the irradiated target be replaced with a spare target/ion source assembly using the temporary target maintenance station. There was no detectable contamination on the outside of the target module and the dose to personnel was lower than expected.

REMOTE HANDLING

The entire TRIUMF Remote Handling group was committed to various ISAC construction jobs during the year. With responsibilities for target hall shielding fabrication, module services, module assembly, TIS/RIB beam optics component assembly and alignment, as well as conventional ISAC remote handling tasks.

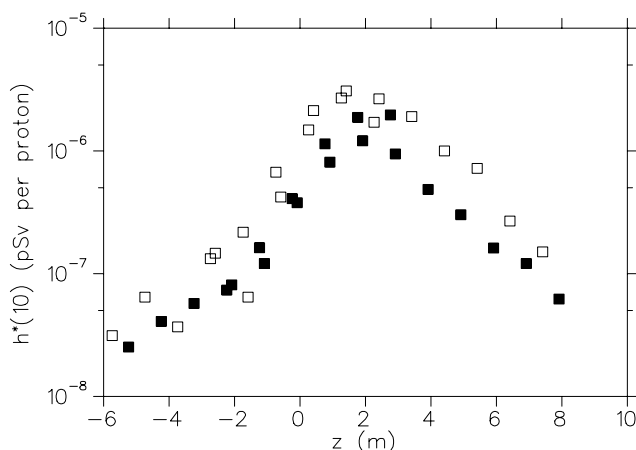


Fig. 124. Comparison of the ambient dose equivalent measured by a moderated BF_3 neutron monitor (solid squares) and that calculated using the Monte Carlo code FLUKA (open squares). $z = 0$ corresponds to the front face of the beam dump.

Service Shielding

Both fixed and moveable radiation shielding for the target hall was designed and fabricated by contractors. Five independent, 18 ton steel/concrete composite shielding blocks, required to shield the operational target station, were constructed, installed and commissioned. When both east and west ISAC target stations are completed these blocks will be shuttled between the operational station and that station under service.

Beam Lines Servicing

A new design of peripheral-edge water cooled window was developed for, and installed in, the 2A proton beam line. Both 0.010 in. thick stainless steel test windows and a 0.004 in. thick aluminum beam operation window were designed and utilized.

The beam line section between the west vacuum tank and the pre-separator magnet was designed, built and installed. This incorporates a rad-hard vacuum gate valve, turbo-molecular vacuum pump and beam diagnostics monitor stack, all remotely handleable for future servicing.

The power and cooling services connections for the ISAC RIB pre-separator magnet were designed, installed, and commissioned.

Hot Cell Facility

An interim, shielded low-level radiation handling facility was constructed for use until completion of the fully qualified hot cell. This temporary facility provided the operator with 4 in. of steel radiation shielding, moveable Pb glass shielding window ports, and an air exhaust ducting system. The facility was used for removal of the first irradiated CaO target assembly.

Design of the new ISAC target handling hot cell is near completion. Work will begin on construction immediately following wrap-up work on the completed ISAC jobs.

Remote Crane Handling System

The target hall crane was supplied and installed by the contractor and is now manually operable by wireless remote. Design of a remote operable control system is under way and will be phased in to operation during 1999.

Alignment

The philosophy for the physical alignment of potentially radioactive target station components was developed and assembly took place during 1998. Using a transfer alignment jig, the true position of the target station module locations w.r.t. the defined proton and radioactive ion beam centre lines can be transferred to a more accessible alignment frame or to the target servicing hot cell. Optical alignment telescopes

at either location, with an indexed master reference alignment jig, confirm the positioning of the appropriate module base mounting table. All module target/ion source, beam diagnostics and RIB optics components are then jig-aligned on their base mounting trays during initial assembly to agree with the master alignment jig dimensioning. The concept allows the construction of new interchangeable target station components as well as assuring and conforming to the alignment of component assemblies to be installed in the ISAC hot cells facility.

BEAM LINE 2A

For reference purposes, Fig. 125 shows the configuration of the final version of beam line 2A. As noted in last year's Annual Report, only the west target will be operated during the first years of operation.

At the end of 1997 the extraction probe, the combination magnet and the first two quadrupoles in the cyclotron vault had been installed and commissioned. Beam had been extracted over an energy range from 472 MeV to 510 MeV to a temporary beam dump that was installed downstream of the second quadrupole. In addition, the 36 ft long vacuum pipe linking the vault section of the beam line to its tunnel section and all quadrupoles and steering magnets upstream of the first 15° dipole in the tunnel had also been installed. During the spring shutdown the remaining elements were installed. The two 15° dipoles and following quadrupole doublet were first installed so as to complete the tunnel portion of the beam line. Emphasis then shifted to the installation of the remaining

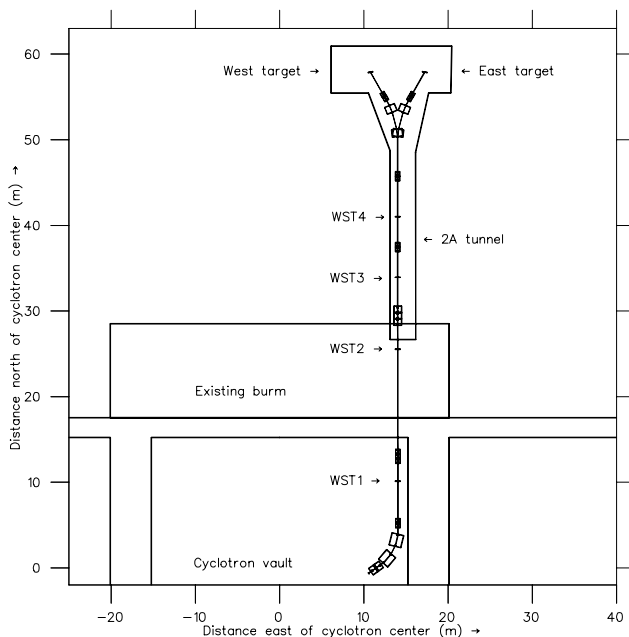


Fig. 125. The configuration of beam line 2A.

vault components – the two 27.5° dipoles, a quadrupole doublet and quadrupole triplet, steering magnets, vacuum system, and all related cabling and services. By May, when beam production resumed, all elements of the beam line were operational. However, the beam dump of the target vessel was not yet ready. Consequently, beam was extracted to a (temporary) beam dump positioned at the straight-through port of the first 15° dipole in the tunnel. With this configuration, optics of the beam line – at least to the entrance of this dipole – were verified over an energy range from 480 MeV to 500 MeV. Shortly after this the beam dump was installed in the target module and the remainder of the beam line was commissioned. Figure 126 shows the observed beam profiles at a monitor positioned approximately 1 m upstream of the target position.

The above commissioning runs were undertaken at beam currents of ≤ 10 nA. In November, commissioning runs with beam currents of the order of $1 \mu\text{A}$ were performed. Subsequently, the west target assembly was installed and beam intensities of this magnitude were delivered to it. Radioactive beams were extracted from the target and delivered through the mass separator for the first experiments in each of the TRINAT and GPS facilities.

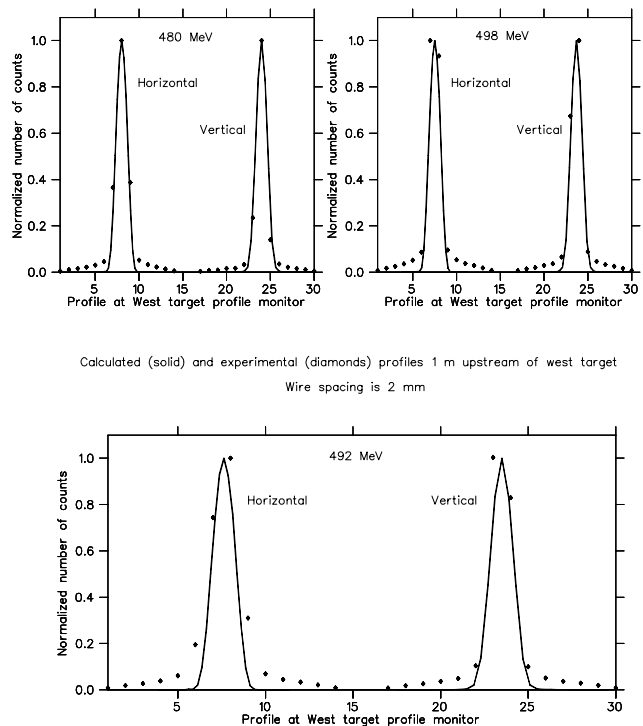


Fig. 126. Observed beam profiles approximately 1 m upstream of the west target.

ION SOURCE TEST STAND

The ISAC ion source test stand was used to determine the thermal and mechanical stability of the surface ionization source prior to its installation in the ISAC target module. Towards the end of 1998, a new version of a TRIUMF ECR source was installed in the ion source test stand to evaluate plasma and beam characteristics in preparation for its future use in the ISAC facilities. The test stand will also be used as a ${}^7\text{Li}^+$ source to test components for the polarized ${}^8\text{Li}^+$ beam line to be built in the low energy area of ISAC.

Surface Ionization Source

A prototype target/surface ionization source, support structure and extraction column were tested on the ISAC test stand. The prototype was designed to mimic the geometry in the containment box of the ISAC target module and was an initial iteration of the final design. The prototype target/ion source was heated in the test stand vacuum chamber to a temperature of 2200°C . Target oven temperature was monitored by thermocouples placed in contact with the oven wall and inside the target oven. The target, ionizer and conductor temperatures were also monitored using a 2 colour optical pyrometer through view ports in the vacuum chamber. During heating, the position of the ionizer aperture was monitored using an optical alignment instrument on the ion beam axis. A series of heating cycles showed that the ionizer exit aperture did not move off axis due to thermal stress. The copper conductor and heat shield cooling was shown to be adequate, however, one of the tantalum ionizer leads was found to be much hotter than originally anticipated. The thickness of this component was increased for subsequent designs.

Electron Cyclotron Resonance Source

A microwave-driven electron cyclotron resonance ion source was installed on the ISAC ion source test stand during the last quarter of 1998. The source is equipped with a 2.45 GHz, 1.2 kW microwave generator operating in cw mode and up to 20 kHz in pulsed mode. The microwave power is fed radially into the resonance cavity of the source with the beam extracted in the axial direction. A flat ECR magnetic mirror region with a non-symmetric low mirror ratio is used to confine the plasma. The unique feature of this source is that the plasma region is much smaller than the physical size of the resonance cavity in order to maximize the efficiency and minimize the ions' transient time. The source is intended to produce short and intermediate half-life radioactive ion beams of volatile elements for low and high energy experiments.

Polarized ${}^8\text{Li}$ Beam

The polarized ${}^8\text{Li}^+$ beam planned for the ISAC low energy area will be used to supply beam to condensed matter β -NMR experiments. The beam will be polarized in the following way. The incoming unpolarized ${}^8\text{Li}^+$ beam is neutralized with high efficiency in a sodium-vapour target to create a neutral ${}^8\text{Li}$ beam. The neutral atoms are accessible to optical pumping by circularly polarized laser light tuned near the Li D_1 resonance at 671 nm (deep red). The optical pumping light is collinear with the fast atomic beam, providing about $2\ \mu\text{s}$ pumping time over a 1.5 m length. The polarized atoms then enter a helium gas reionizer cell, where they are reionized to ${}^8\text{Li}^+$ and are deflected to the experimental station. The sodium and helium cells have been designed and are being fabricated. They will be placed on the end of the test stand, allowing their performance to be measured and optimized using a ${}^7\text{Li}$ test beam, before being transferred later in 1999 to the ISAC floor. The helium reionizer is novel, and it is important to measure the ion yield and emittance growth of the beam as functions of helium thickness (atoms cm^{-2}) and beam energy. The sodium cell is a jet-type target designed at TRIUMF, similar to one built for the KEK OPPIS upgrade (see POLISIS section), and it will be initially tested on the KEK OPPIS with a H^+ beam. Neutralization cross sections of H^+ in sodium are well known, providing a way to calibrate the thickness of the sodium vapour as a function of temperature in the cell.

Target/Ion Source

During 1998, the design for the ISAC target and surface ionization source was finalized and the design concepts tested on a prototype in the ISAC test stand. After modifications and refinements to the design, a commissioning version of the target/ion source was used to produce beams of stable alkali elements for commissioning of ISAC. For on-line use, two targets containing pressed CaO pellets were used for providing radioactive potassium beams to two initial ISAC experiments.

On-line Targets

Final construction and assembly of the on-line target/ion source design was completed by July. In August, the target/ion source and extraction column were installed and aligned on the ISAC target module. The initial commissioning target consisted of $35\ \text{g}/\text{cm}^2$ of pressed graphite containing alkali salts for stable beam production. The first stable ion beam at ISAC was successfully extracted to a Faraday cup in the second exit module on September 24. The graphite target continued to be used for beam tuning and mass separator

commissioning until November 22, at which time it was replaced with the first experimental target.

The first experimental target consisted of 36 g/cm² of CaO as pressed pellets on the order of 1 mm thick. ISAC commissioning continued using a stable potassium beam from this target until November 30. At that time, proton beam was put on the target and the first radioactive ISAC beams were measured at a Faraday cup located just short of the TRINAT experimental station. Mass separated beams of ³⁶K, ³⁷K and ³⁸K were observed. The target/ion source operated successfully for a period of 12 days until the surface ionizer failed; the cause of the ionizer failure has not yet been determined.

Table XX. Maximum potassium yields observed from the first CaO target.

³⁶ K	$3.6 \times 10^4/s/\mu A p^+$
³⁷ K	$6.6 \times 10^6/s/\mu A p^+$
^{38g} K	$9.8 \times 10^8/s/\mu A p^+$

The second on-line target was prepared consisting of 31 g CaO/cm² in pressed pellets 2–4 mm thick. After outgassing in situ, the target provided a ³⁷K beam to the β -decay experimental station in the ISAC experimental hall. Although further on-line operation of this target was prevented by loss of proton beam due to cyclotron problems, this target remains functional.

ISAC MASS SEPARATOR

The mass separator was installed and operated for experiment at the end of 1998. ^{37,38}K were produced on-line and mass analyzed to form the first radioactive ion beam for the new ISAC facility.

The quality of a mass separator is not only the resolving power, but also the enhancement factor. The enhancement factor is a measure of how well the separator succeeds in delivering the desired mass to the focal plane, uncontaminated by unwanted nuclei. It has two parts: the efficiency of delivering the required nucleus, and the efficiency of rejecting the unwanted species. If I_{iw} and I_{fw} are the initial and final concentrations of the desired nucleus, and I_{iu} and I_{fu} are the initial and final concentration of the unwanted contaminants, the enhancement factor is then, $E = I_{fw}/I_{iw} * I_{iu}/I_{fu}$. The real figure of merit of a separator is its enhancement factor E . It is mainly determined by the tails of the beams. Clearly much effort should be spent on the reduction of long tails. The tail formation is mainly dominated by collision with the residual gas at various places along the mass separator. These give rise to ions with the wrong energy and the wrong momentum that are scattered through the slit, or ions of wrong mass and correct momentum which pass the slit because they have not been fully accelerated. Even

the best ion source will not provide a pure ion beam. Ions of neighbouring isobars must be attenuated using an electromagnetic separator. Even if the separation of different masses by a sector magnet is very effective, there is some limit as to how well ions of a different mass $m + dm$ can be separated from the desired ion of mass m . We propose to suppress this type of contamination by adding a second separator stage at different voltage. The contaminants that pass the first sector magnet will have a different magnetic rigidity after acceleration and will not pass through the slits of the second sector magnet. The potential elevation can be as low as 10 kV and does not need to be higher than 60 kV. In our case the main separation stage will be preceded by two quadrupole doublets that allow adjustments to the size of the beam in the x and y planes. Furthermore, the position of the x -image can be adjusted to be exactly at the position of the entrance slit by changing the strengths of the quadrupoles. The y -image at the separator slit is magnified 10 times, reducing, by the same way, the vertical dispersion thus keeping the magnet gap as small as possible. The image aberrations can be corrected easily. The largest image aberration for a mass separator is usually the aperture aberration, which is proportional to the square of the divergence. Since horizontal divergence is much larger than the vertical divergence, we need to correct only for the horizontal part of the aberration. This can be accomplished with a single curved field boundary. The main mass separation stage is composed of a magnet having a bending radius of 1 m, a bending angle of 135° and a field index equal to 0.5. The resolving power is obtained with this type of mass separator by having a very large dispersion in the x -plane while the beam is kept small in the vertical plane.

The ISAC mass separator consists of two mass analysis stages. The first stage is used as a combining magnet for the two stations. It is also used as a pre-separator allowing the rejection of most unwanted ions coming from the on-line ion source. The second stage has a much larger resolving power, $\sim 10,000$, is installed on a high voltage platform, and combined with the first magnet is very efficient in removing cross contamination coming from low energy tails.

Target Station and Matching Section

The target and the two exit modules were installed in September. The two exit modules contain the matching optics to the pre-separator magnet. They also housed the diagnostics, which are used to adapt the beam to the pre-separator magnet. On September 24, the first stable beams were produced and the beam optics were tested.

Pre-separator Stage

The pre-separator magnet was delivered in June. This magnet can accept RIB from either one of the two target stations. The measured mass dispersion of the magnet is in good agreement with the predicted value.

Mass Separator Stage

The main mass separator was built for the Chalk River facility in the 1970s. The measured resolving power was around 6000. Beam transmission was between 90% and 95% between the pre-separator focal plane and the Faraday cup located just in front of the experimental station. The tune was stable and not sensitive to quadrupole strength variation. The remaining beam dynamics will be measured during commissioning in 1999.

Diagnostics

Several types of beam diagnostics are used for the mass separator. In the first matching section located in the exit modules where the beam is wide, harp monitors are well suited. Apertures located in front of the harp monitors are used to define the axis of the beam and they come in two sizes, 5 and 10 mm. A Faraday cup measures the beam current extracted from the ion source.

In the other matching sections, because the beam sizes are small, the harp monitors are replaced by scanning wires. The diagnostics at the focal plane of the pre-separator and mass separator include a harp monitor, slits and a Faraday cup. The slit and the Faraday cup are mounted on a platform, which moves across the beam. This feature gives a precise horizontal beam profile. The whole mass separator vacuum is divided in eight sections. The pressure achieved in all sections is lower than 1×10^{-6} mbar. The target station was installed during the summer and the first stable beam was extracted September 24. This first test allowed us to find a problem with the high voltage. The problem came from the insulator used as a neutron absorber. We will select another material for the neutron absorber in order to reduce the out-gassing that was creating the high pressure in the vicinity of the high voltage. The beam commissioning of the mass separator started October 23 and the first radioactive isotopes were produced November 30. The proton beam intensity was $1 \mu\text{AP}$ on target.

BEAM COMMISSIONING

The low energy beam transport system (LEBT, see Fig. 127) has been commissioned from the off-line ion source (OLIS) to the RFQ. Using scanning wires and steering elements, the effective lengths of the quadrupoles were determined to within 1%. These

results, along with measured distributions in phase space, were then used to adjust the theoretical tunes. When implemented, these gave profiles which were in good agreement with the theoretical ones. As well, the achromaticity of the bend section tunes was verified.

The LEBT acceptance was inferred by varying the steerer correctors and noting the strength required for a 10% loss in beam. The section measured was 5 m long and included 20 electrostatic quadrupoles and 4 45° spherical-electrode electrostatic bends (Fig. 127). The result is shown in a phase space plot, Fig. 128. The blue ellipses are for the horizontal (bend) direction, and the red is vertical. Estimated areas of the encapsulating ellipses are $109 \pi\text{mm-mrad}$ in the bend plane and $81 \pi\text{mm-mrad}$ in non-bend plane. These are consistent with design. The design acceptance is $200 \pi\text{mm-mrad}$ dynamically, but with 1 in. dia. apertures limiting to $100 \pi\text{mm-mrad}$. The philosophy has been to provide sufficient acceptance that the design maximum emittance of $50 \pi\text{mm-mrad}$ is easily accommodated.

Initially, the acceptance of the section which matches the beam to the RFQ was only $40 \pi\text{mm-mrad}$. Although this allowed easy on-line monitoring of the beam halo in this section, it did not allow exploration of the RFQ's full acceptance. For this reason, the apertures in this region were opened from 25.4 mm dia. to 31 mm, and the final 'halo' monitor was opened up from 8 mm to 14 mm. The RFQ acceptance figure ($90 \pi\text{mm-mrad}$) is shown in Fig. 129, along with the matching section apertures transported to the location of the beam waist at the RFQ entrance.

RF SYSTEMS

LEBT Pre-buncher

Instead of a bunching section in the RFQ, the beam is pre-bunched by an external pre-buncher ~ 5 m upstream of the RFQ. The pre-buncher was designed and built to operate at a frequency of 11.66 MHz plus three harmonics to produce a saw-tooth like waveform across a single gap. The pre-buncher frequency was selected at the request of experimenters to give a longer bunch spacing of 86 ns. Because of a reduction in gain at the higher frequencies, the initial testing was done with only two harmonics. The pre-buncher system was installed and commissioned in the LEBT and operated at full power very reliably for the first beam tests with the RFQ.

RFQ system

The ISAC RFQ is an 8 m long, 4-rod split-ring structure operating at 35 MHz in cw mode. The rods are vane-shaped and are supported by 19 rings spaced 40 cm apart. An initial 2.8 m section of the accelerator (7 of 19 rings) was installed and aligned in the 8 m

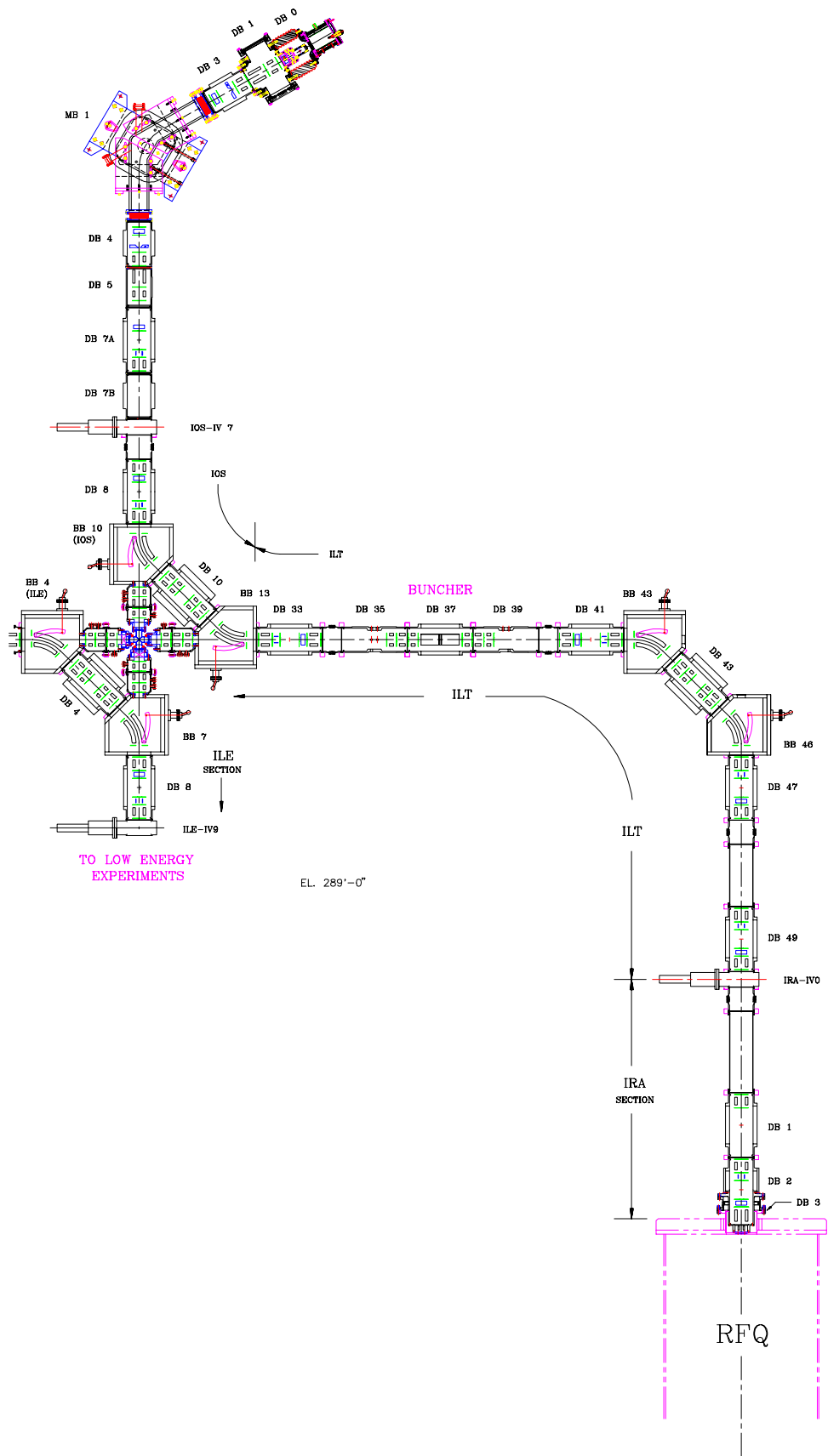


Fig. 127. Layout of LEBT — OLIS to RFQ.

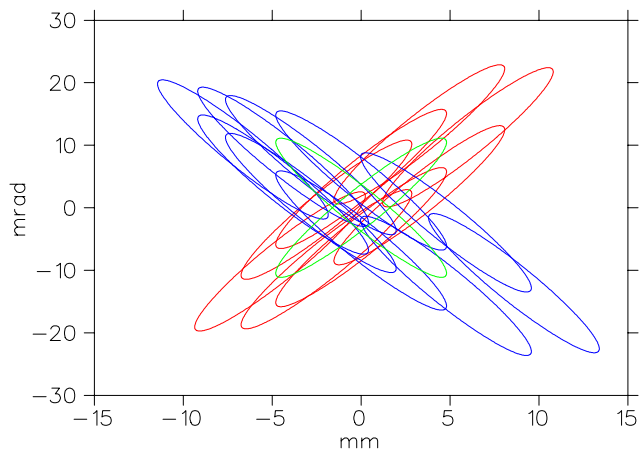


Fig. 128. Measured acceptance of LEBT.

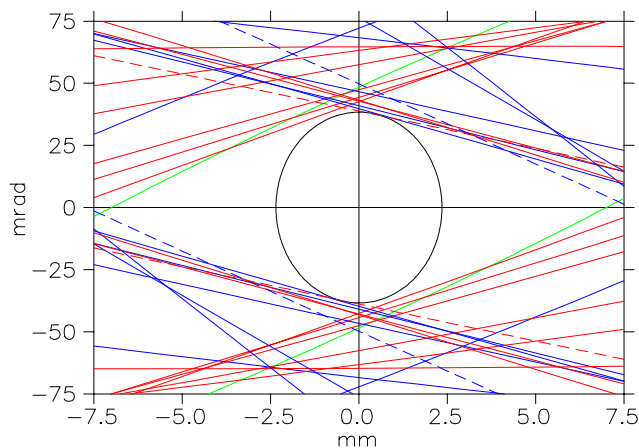


Fig. 129. Apertures in the RFQ matching section of LEBT, along with the theoretical acceptance figure for a $90 \mu\text{m}$ emittance.

long, square cross section, vacuum tank (Fig. 130) last year to allow rf and beam tests to be carried out.

The stringent, ± 0.08 mm, quadrature positioning tolerance of the four rod electrodes was achieved and a relative field variation along the 2.8 m of the RFQ was measured to be $\pm 1\%$, using the standard bead pull method. The results of the signal level measurements are compared to MAFIA simulations in Table XXI.

Table XXI. Comparison of measured values to calculated MAFIA values.

Parameter	MAFIA	Measured
Frequency (MHz)	34.7	35.7
Q	15175	8700
R_{shunt} (k Ω)	174.9	104.4
R_{shunt} (k Ωm)	489.9	292.3
R/Q	11.53	12.0

Because of the size of the mesh used in the MAFIA simulations one would expect the MAFIA simulations to give a lower frequency. Following a three day bake-out at 60°C a base pressure of 1.4×10^{-7} was achieved



Fig. 130. Seven rings assembled, installed and aligned in the bottom section of the vacuum tank

and 76 kV (2 kV above design value) was achieved on the electrodes within four hours at the anticipated power level of 30 kW with an increase in pressure to 4.0×10^{-7} torr. We were able to maintain this condition for two hours before our first major amplifier overload occurred. Subsequently, we were never able to achieve the above voltage for the same power. The rf power increased by as much as 40% for the same voltage level of 76 kV. Initially it was thought that this was due to multipactoring in a 7 cm gap between the rf shroud and the tank lid front wall. The problem was eventually traced down to dark currents associated with field emission along the electrodes. The dark currents were essentially eliminated by one hour of high power pulse conditioning. The pulses were $128 \mu\text{s}$ long at a rate of 500 Hz at a peak amplitude of ~ 100 kV peak. The RFQ operated continuously for 15 hours at nominal voltage plus various runs for 5 and 10 hours before being interrupted by amplifier trips. These amplifier trips were later found to be caused by a failing component in the grid bias power supply. The initial 2.8 meters of the RFQ operated reliably at full power for the beam tests.

The remaining 15 rings (including 3 spares) were assembled using the same cautious procedure as the initial seven rings and are ready for the final high precision EDM (electrical discharge machining) operation on the electrode mounting faces.

MEBT Rebuncher

The spiral resonator was chosen as the design option for the MEBT rebuncher. The MEBT rebuncher will be operated cw at 35 MHz with a gap voltage of 30 kV. Two designs for the 35 MHz rebuncher, a folded $\lambda/4$ and the spiral were evaluated on the basis of cost, size, rf and mechanical properties. A full-scale prototype of the spiral with water-cooling was constructed to measure the mechanical vibrations as well as rf parameters. The tests reveal that the vibrations are much

lower than the allowable limits. MAFIA simulations have been done on the spiral to check the validity of the rf measurements of the prototype. From the computed and measured values of shunt impedance, it is estimated that 1 kW of rf power will be adequate to establish a 30 kV gap voltage in the spiral resonator. Fabrication options are being considered for manufacturing the spiral.

DTL Triple Gap Buncher

The first DTL buncher, shown in Fig. 131, was developed at INR (Russia) and tested at TRIUMF. It is a triple gap split-ring rf structure operating at 105 MHz. At signal level, 72% of Q-value and frequency within 0.6% of MAFIA simulations were achieved.

The accelerating field distribution measured by the standard bead pull method is compared to MAFIA calculations in Fig. 132. The correlation is within 2.5%.

With cooling water flow of 20 l/min the mechanical vibrations were measured to be in the order of 1 μm . Following two weeks of fighting vacuum leaks, full power/voltage was achieved on the buncher drift tubes. RF conditioning started with a base pressure of 2×10^{-7} torr. It took ~ 7 hours to pass through the multipactoring level and another 6 hours to increase the rf power from ~ 100 W to the nominal level of 8 kW. Although the design parameters are 60 kV gap voltage and 8 kW nominal power, we eventually achieved 85 kV and 16 kW respectively with stable operation limited only by the allowable x-ray production in the test facility area. The longest continuous run at nominal voltage lasted for 80 hours. Taking into account a number of various runs from 5 to 20 hours duration, the buncher operated stable for ~ 250 hours in total.

Movement of the drift tubes due to the rf thermal load of the ring was measured using a telescope on targets installed in the drift tubes. With a cooling water flow of 17 l/min per arm of spiral, the centres of



Fig. 131. First DTL Buncher.

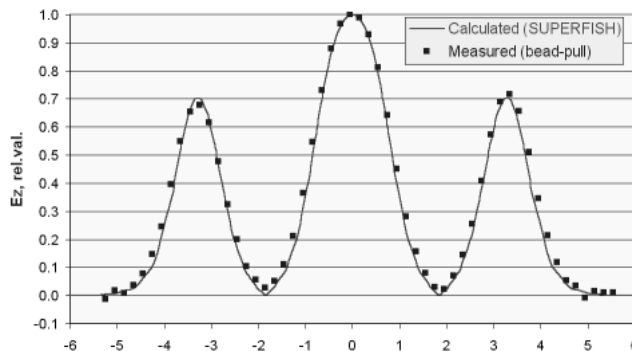


Fig. 132. Field distribution in the accelerating field.

the drift tubes were displaced by 0.25 mm when full rf power was applied. By reversing the water flow to cool the hottest ring area first, the displacement was reduced to 0.125 mm.

A charged particle current produced and accelerated in the buncher was observed in the diagnostics box, which is attached to the buncher. A field emission (design surface electric field is 13.2 MV/m) is considered to be the nature of this current. Observed current is bunched at the fundamental frequency with an intensity of tens of μA for the nominal buncher setting.

RF Amplifiers

Testing of the RFQ power amplifier at medium (80 kW) power levels was successful. Following the installation of the transmission line and the variable line trombone, rf power was successfully fed into the RFQ. The first of 9 rf power amplifiers for the DTL bunchers and cavities was completed and successfully tested into a resistive load at a power level of 22 kW. The amplifier was used to test the first INR buncher. The remaining power amplifiers for the DTL are in the process of being assembled.

RF Controls

The RF Controls group has been concentrating its effort on the ISAC project. The feedback control system for the ISAC pre-buncher has been commissioned successfully in the first quarter of 1998. The system regulates an 11 MHz signal and up to its fourth harmonic in both amplitude and phase to synthesize a special waveform for beam bunching. Each harmonic is regulated by its in-phase and quadrature phase components using a single DSP. These harmonics are combined together and the resultant signal is used to drive a 1 kW wide band rf amplifier. The output of the amplifier is used to power the pre-bunching cavity, which consists of a set of parallel plates in parallel with a broad band load. Remote controlled operation of the control system is via Ethernet connection using UDP/IP to query status information and TCP/IP for command requests. The RFQ rf control system was

commissioned in the second quarter of 1998. A phase locked loop frequency source generates a 35 MHz signal and also uses in-phase and quadrature phase for amplitude and phase regulations. The rf control system has a self-excited mode of operation which uses the RFQ cavity itself as the frequency tuning element and allows the RFQ cavity to run without tuning control. Short period perturbation to the frequency such as minor sparking is ignored by the relatively long time constant of the phase locked loop. The other electrical parameters of the phase locked loop source are chosen for spectral purity as well as enabling smooth transition between self-excited mode and driven mode. The RFQ and the pre-buncher, as well as additional rf cavities in the future, while operating at different harmonics, have to be phase locked together. A frequency distribution unit performs the task of generating these different harmonics with different phase shifts between them. The pre-buncher and RFQ portion of the frequency distribution unit was commissioned in the third quarter of 1998 enabling the pre-buncher and the RFQ to operate coherently.

Other Developments

Bead pull development

New software was written for the bead pull method for measuring the parameters of rf cavities. LabVIEW software was used to develop the program, which enables an on-line view of the bead pull measurement. The program uses a GPIB to communicate with a HP Network Analyzer and at the same time control the bead pull motor via an American Precision Instrument Power/Driver Indexer. A Pentium PC has been dedicated for this purpose and a user manual has been written.

Coupling loops

A new coupling loop was developed for the 105 MHz DTL buncher. A Jennings ceramic was chosen as the rf window and the window assembly was adapted to a 3 1/8 in. standard rigid transmission line section. The electric field around the ceramic was optimized using SUPERFISH to provide uniform power loss inside the ceramic. The ceramic window support was water cooled but the coupling loop itself was not water cooled. The coupling loop was installed in the DTL buncher and was tested up to a maximum rf power of 16 kW. The coupling loop was free of multipactor and performed without any failure. A second coupling loop, identical to the above, will be used for the DTL1 tank. Both rf windows were manufactured at TRIUMF. The coupling loop assembly for the buncher was manufactured at INR while the one for tank 1 was manufactured at TRIUMF.

Tuners

A frequency tuner driven by a stepping motor was developed for the 105 MHz DTL buncher. Stainless steel bellows provided vacuum to air interface and are shielded from rf. The tuner was tested with rf power of 16 kW in the DTL buncher cavity. A linear frequency tuning range of ± 500 kHz could be easily obtained; the nominal required tuning range of the DTL buncher is ± 100 kHz. A similar tuner will be used in the DTL1 tank with minor modification of the tuner rod and tuner plate. Both tuners were designed at TRIUMF. The tuner for the buncher was manufactured at INR and the one for tank 1 at TRIUMF.

RFQ TASK FORCE

The RFQ task force was established in 1996 with the following goals:

- design, build and commission the off-line ion source (OLIS), low energy beam transport (LEBT) and pre-buncher to provide an injector of stable beams for the RFQ
- design and build a shortened version of the RFQ for rf and beam tests, in particular to establish the operating frequency, test operation at full power, and measure the acceptance and matching conditions well in advance of the final commissioning schedule
- design and build a diagnostic station downstream of the RFQ to analyze the accelerator performance.

OLIS, LEBT and Pre-buncher Commissioning

The off-line ion source (OLIS) is required to commission the LEBT and accelerators as well as supply *analogue* beams to tune the accelerator complex prior to injection with radioactive ions. In addition, stable beams from OLIS will be used for both low and high energy experiments. In 1998 OLIS was routinely used to commission both the LEBT and the 7 ring section of the RFQ. Beams of both N^+ and N_2^+ have been selected for commissioning due to their ease of production and their masses which give beam experience under both low and high power conditions. The LEBT proves to be easy to tune and matches well the theoretical tune values.

The RFQ design is unique in that the bunching section is replaced by an external buncher in the LEBT, 5.7 m upstream of the RFQ. Up to four harmonics will be used to construct a pseudo-saw-tooth velocity modulation on the beam in a single gap. The fundamental buncher frequency was chosen as 11.7 MHz instead of 35 MHz given that the resultant 86 ns gap between pulses will be important for certain experiments.

The pre-buncher consists of two circular electrodes spaced 8 mm apart forming a single gap with a beam aperture of 7 mm radius. The fundamental frequency of 11.7 MHz and the first three harmonics are individually phase and amplitude controlled and combined at signal level. The signal is amplified by an 800 W broadband amplifier that drives the two plates in push-pull mode with a peak voltage of about 200 V (400 V between plates). Optimization of amplitude and phase of each harmonic results in an almost saw-tooth modulation on the beam velocity. The variation in the gap-crossing efficiency for each harmonic means that the driving voltage is far from a saw-tooth, being dominated by the higher, less efficient harmonics. In fact the present amplifier band width rolls off after 35 MHz and so initial testing was done with only three harmonics. We expect 76% of the beam to be accelerated in the 11.7 MHz bunches at nominal RFQ voltage with $\sim 4\%$ accelerated in the two neighbouring 35 MHz buckets, and 20% of the beam unaccelerated. Adding the fourth harmonic should increase the acceptance by 5%.

The time structure of the bunched beam as measured on a 50 Ω co-axial fast Faraday cup for one, two and three harmonic bunching is shown in Fig. 133.

The buncher is tuned on-line with beam using RFQ transmission as the diagnostic. The phase of each harmonic is set individually then the voltages are adjusted to previously calculated values followed by empirical optimization. The tuning is straightforward and the performance matches the predictions of simulation studies.

The RFQ Interim Beam Test

The final RFQ electrodes will span 7.6 m with 19 modules each consisting of one ring and 40 cm of electrodes. In 1998 an interim beam test was completed with the first 7 ring section (2.8 m), accelerating beams to 55 keV/u. A schematic of the test set-up is shown in Fig. 134. An rf short is placed after the seventh module to confine the rf fields. Eight electrostatic quadrupoles are used to transport the beam to a diagnostic

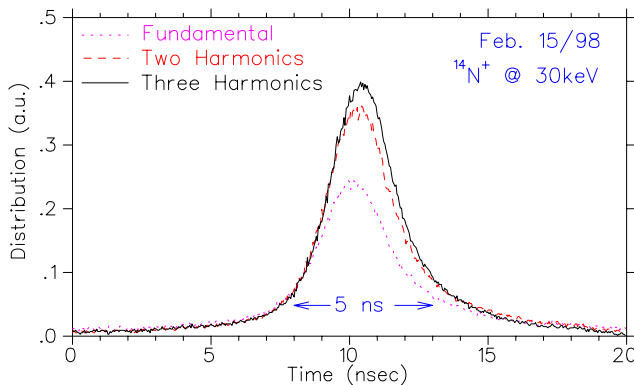


Fig. 133. Beam bunches measured on the fast Faraday cup in LEBT for one, two or three harmonic bunching.

station downstream of the RFQ tank. A Faraday cup and profile monitor assembly are placed just after the RFQ short and again in the middle of the electrostatic transport after the fourth quadrupole. The diagnostic station shown in Fig. 134 includes a Faraday cup, a transverse emittance rig and a spectrometer consisting of an object and image slit and a 90° bending magnet.

The beam from the RFQ is brought to a double waist after the first four quadrupoles and again at the exit of the RFQ. The quadrupoles are each 30 cm long with a 2.5 cm half aperture and require maximum voltages of just under 10 kV for $A = 30$. For mechanical reasons the RFQ vanes are orientated at 45° to the horizontal. As a consequence the first four electrostatic quadrupoles are also at 45°. The transverse reference frame is rotated to the normal after the first double waist where the beam is round. The quadrupoles when tuned act as an energy filter; the unaccelerated beam is lost in the first few quads. Therefore the transmission difference between the first Faraday cup and the second marks the capture efficiency of the RFQ.

The diagnostic station is designed around a $\rho = 1.5$ m analyzing magnet with a dispersion of 3 cm/%. (The magnet was generously donated by the Nuclear Physics Institute in Rez, Czech Republic.) The magnet is placed symmetrically between horizontally defining object and image slits 1.5 m upstream and downstream of the magnet respectively. A Faraday cup just downstream of the image slit records the transmitted beam and the energy and energy spread are derived from the magnetic field. A slit and harp transverse emittance rig is positioned upstream of the magnet. An Allison type emittance rig is located in the LEBT to record transverse emittances before acceleration.

Both rf and beam tests have been successfully completed. The RFQ was operated in cw mode for all beam tests. The operation of the RFQ at peak voltage (74 kV) is stable. A summary of the RFQ rf tests is given on page 156. Beams of both N^+ and N_2^+ have

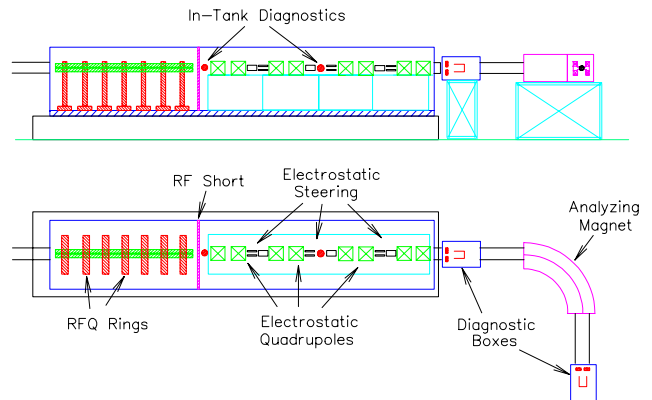


Fig. 134. Schematic diagram of the set-up for RFQ task force beam test.

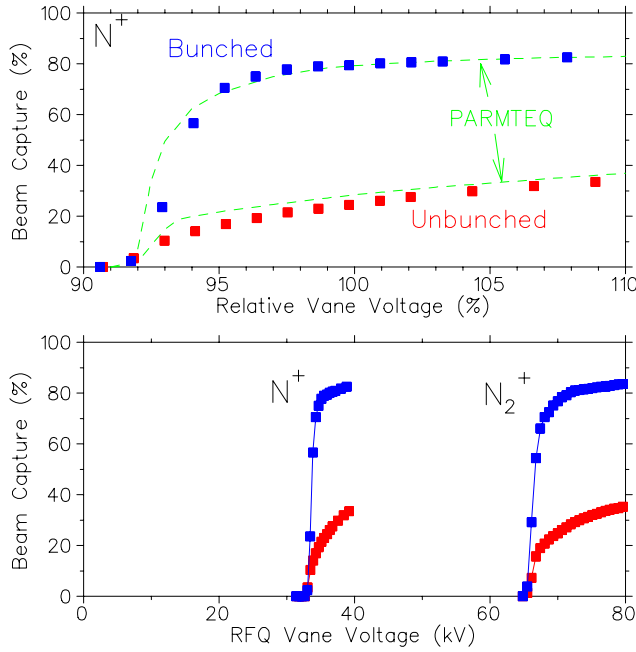


Fig. 135. Top: RFQ beam test results showing capture efficiency for beams of N^+ as a function of relative vane voltage. The beam capture for both bunched and unbunched initial beams is recorded (squares) and compared with PARMTEQ calculations (dashed lines). Bottom: the results for both N^+ and N_2^+ are plotted with respect to absolute vane voltage.

been accelerated to test the RFQ at both low and high power operation.

Beam capture as a function of RFQ vane voltage measurements has been completed for each ion and for both unbunched and bunched input beams. The results are given in Fig. 135 (squares) along with predicted efficiencies based on PARMTEQ calculations (dashed lines). The RFQ capture efficiency at the nominal voltage is 80% in the bunched case (three harmonics) and 25% for the unbunched case in reasonable agreement with predictions. The capture for one harmonic and two harmonic pre-bunching is 63% and 74% respectively.

The energy of the beam as measured with the analyzing magnet is 55 keV/u. The energy spread for the bunched and unbunched cases was measured at $\pm 0.4\%$ and $\pm 0.7\%$ respectively and compares well with PARMTEQ predictions (Fig. 136).

Transverse emittances were measured before and after the RFQ. The results show that when the matching is optimized the emittance growth in both planes is consistent with zero for an initial beam of $15 \pi \text{ mm-mrad}$. A summary of the results for N^+ is presented in Fig. 137. Space charge forces limited the longitudinal acceptance for currents above $\sim 1 \mu\text{A}$ but did not impact the transverse emittance.

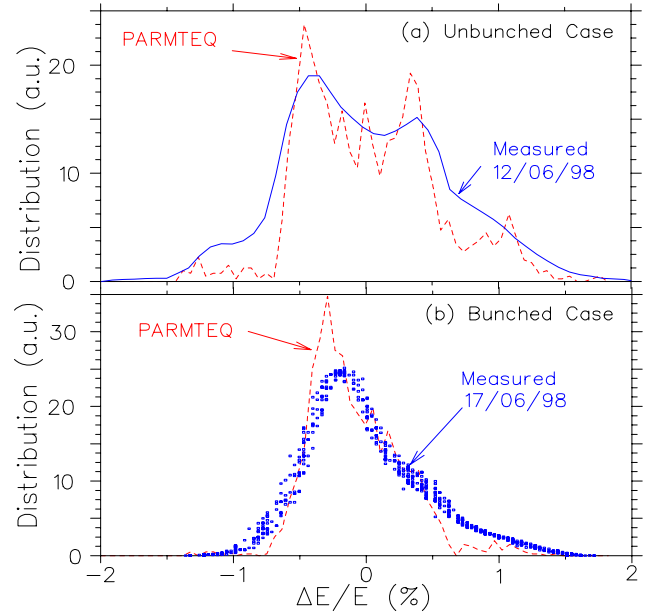


Fig. 136. Results of energy spread measurements of accelerated N^+ beams for both (a) unbunched and (b) bunched cases. PARMTEQ simulation results are plotted for comparison.

The transverse and longitudinal acceptances were explored with a so-called ‘pencil beam’ defined by two circular apertures of 2 mm each separated by 0.7 m placed in the RFQ injection line. One steering plate was available downstream of the collimators to steer the pencil beam around the RFQ aperture.

The test shows an interesting feature of an RFQ with no bunching section. The well known two term potential function gives the fields near the axis of an RFQ. From this potential function the spatial component of the accelerating field is given by

$$E_z = \frac{kAV}{2} I_0(kr) \text{sinc} kz$$

where $k = 2\pi/\beta\lambda$ and β is the relative particle velocity. The formula shows that off-axis particles experience stronger fields than on-axis particles, particularly at injection where β is small. In the ISAC RFQ the design synchronous phase is fixed at -25° at the nominal voltage but for off-axis particles the synchronous phase opens up and the acceptance grows as a result. A typical measure of the synchronous phase is the cut-off voltage, that voltage below which no acceleration can occur. Beam transmission as a function of RFQ voltage was measured for various steering plate voltages. Results for a centered beam and two off-centered cases are plotted in Fig. 138. The two off-centered cases correspond to coherent amplitudes measured at the RFQ exit of $A_c = 1.7 \text{ mm}$ and $A_c = 2.7 \text{ mm}$. The results show clearly the reduction in the cut-off voltage for increasing amounts of off-centering. It is also clear that

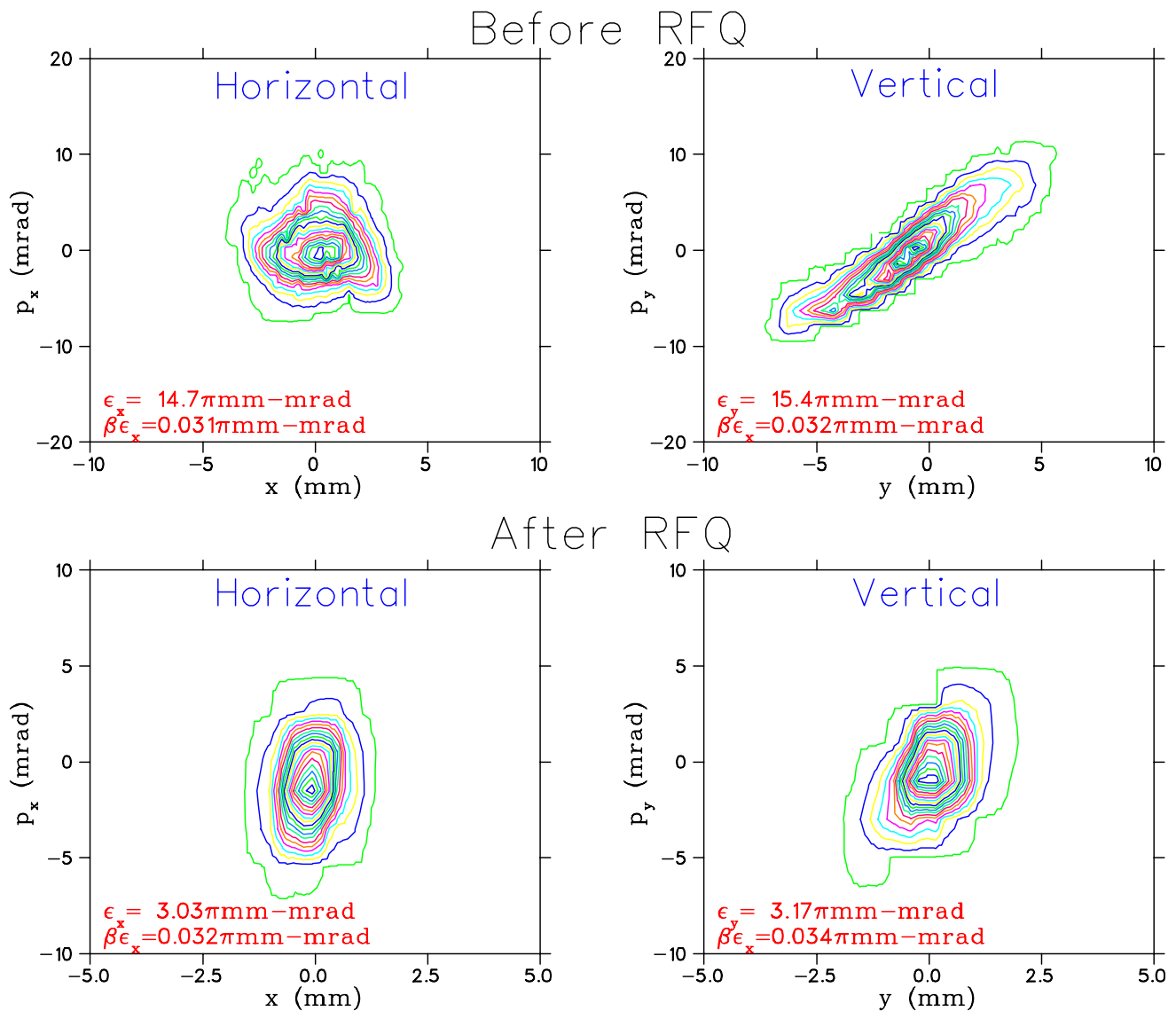


Fig. 137. Transverse emittance measurements (4RMS values) for N^+ before and after the RFQ. The normalized emittance values are also displayed.

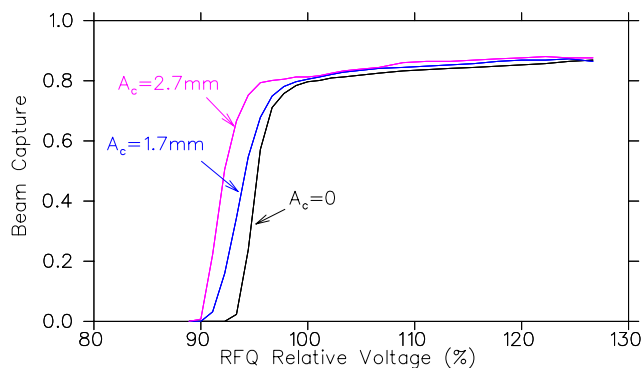


Fig. 138. Transmission of pencil beam as a function of RFQ voltage for a centered beam and two cases of off-centered beam with vertical centering errors at RFQ exit of 1.7 and 2.7 mm.

as the voltage nears cut-off the acceptance difference between on-axis and off-axis particles is enhanced.

In conducting the transverse acceptance studies we have determined a method to measure the magnitude of the centering error in the RFQ. The off-center small emittance beam passes through the RFQ making coherent oscillations about the RFQ axis. The transverse phase advance per unit length is dependent on the RFQ voltage. The centering error can be determined by scanning the RFQ voltage through a span equivalent to a change in transverse phase advance of 2π and recording the final beam position. The rate of phase change with RFQ voltage is also a useful diagnostic. It can be used to determine if the centering error was present at injection or was developed during acceleration with a dipole error.

The pencil beam was injected into the RFQ and the transmission and centering error recorded for various steering plate settings. Beam position as a function of RFQ voltage is given in Fig. 139 for three different steering plate settings 0, 400 V and 600 V. The two deflected cases correspond to the transmission data plotted in Fig. 138. Based on the steering/transmission data the transverse acceptance was estimated to be $\geq 140 \pi \text{mm-mrad}$.

The longitudinal acceptance was measured for both a centered and an off-centered beam ($A_c = 2.7 \text{ mm}$) at the nominal RFQ voltage using the pencil beam. The energy of the injected beam was varied at the source. For each energy step the phase of the bunched beam was varied with respect to the RFQ phase and the capture efficiency was recorded for each step. The settings where the acceptance dropped to 50% of the peak value were used to define the longitudinal acceptance contour. The acceptance of the centered beam was estimated to be $180 \pi\text{-deg}$ at 35 MHz or $0.3 \pi \text{keV/u-ns}$. The acceptance opens up for off-centered beams with values of $400 \pi\text{-deg}$ at 35 MHz or $0.7 \pi \text{keV/u-ns}$. The expected longitudinal acceptance based on PARMTEQ simulations is $0.5 \pi \text{keV/u-ns}$. Beam transmission contours for both the centered and off-centered cases are presented in Fig. 140. The tail in the acceptance plot seen in the upper right corner of the stable region is typical of linear accelerators.

The increase in accelerating field strength for off-axis particles provides a large stable saddle point in the longitudinal motion. One problem with having stronger off-axis fields, however, is that the transmission improves (at the expense of beam quality) as the beam moves off-centre making tuning difficult. An optimization procedure was developed where the LEBT is tuned at high RFQ voltage for maximum transmission then the last steering plates and matching quads are re-tuned at an RFQ voltage near cut-off to achieve a local minimum in the transmission. The procedure

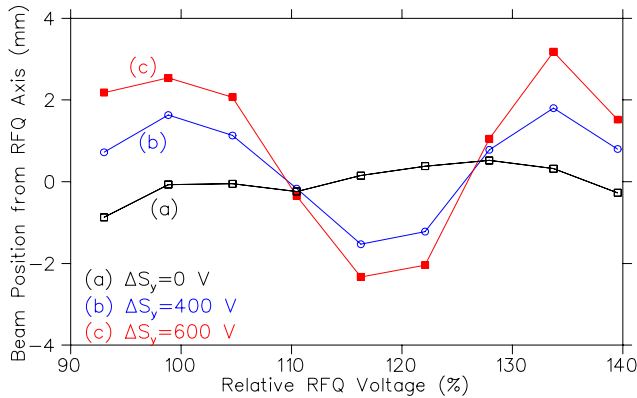


Fig. 139. Beam position at RFQ exit as a function of RFQ voltage for three different steering plate strengths – 0, 400 V and 600 V.

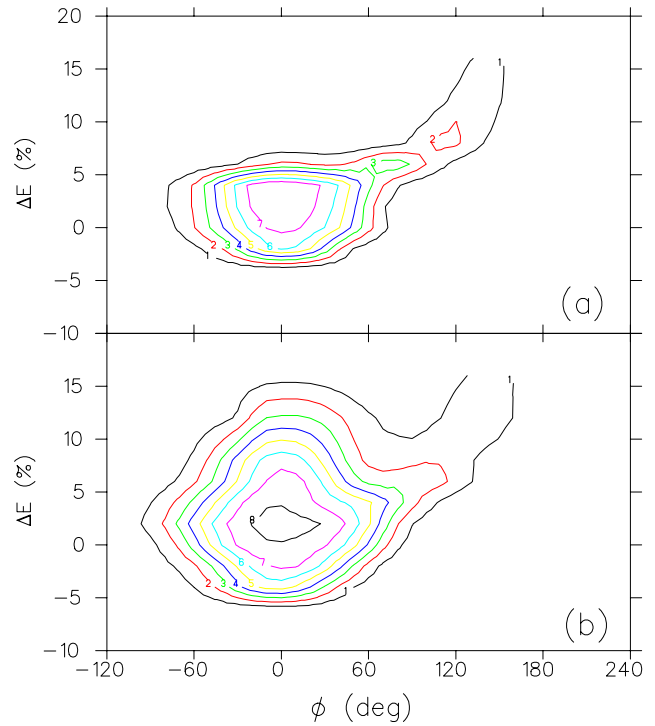


Fig. 140. Measured longitudinal acceptance of the RFQ for a centered beam and an off-centered beam ($A_c = 2.7 \text{ mm}$).

results in not only a centered beam but also a matched beam since a matched beam will see lower accelerating fields on average.

The matching is effective in reducing the final transverse emittance. Larger unmatched beams are subject to a spread in the radial tune due to the radial variation in the field strength and associated emittance growth. An example is shown in Fig. 141 where the last matching quadrupole is varied and the final emittance out of the RFQ is measured. The minimum in emittance corresponds to the saddle point in the transmission associated with a centered beam.

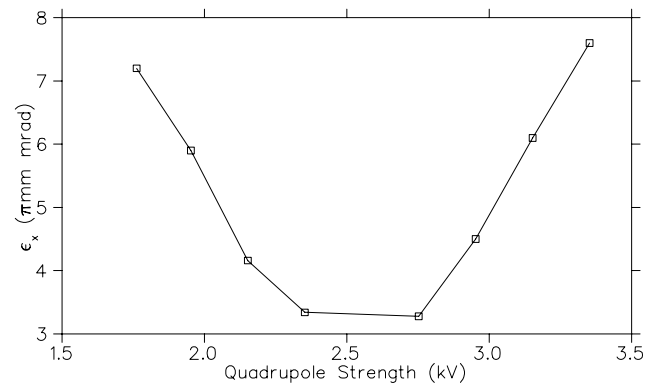


Fig. 141. Final horizontal emittance as a function of the strength of the last matching quadrupole.

In general the beam test results demonstrate a strong confirmation of both the beam dynamics design and the engineering concept and realization and give us full confidence in proceeding with the installation of the remaining twelve split rings.

MEDIUM ENERGY BEAM TRANSPORT

Further optimizations of the medium energy beam transport (MEBT) have evolved to meet various design issues. In particular, steering magnets and beam-pipe flanges and bellows have been added to the section forcing quadrupoles to shift as required. As well, it has been decided to use Chalk River 18 cm quadrupoles throughout the MEBT replacing the few TRIUMF designed ‘bunny’ quadrupoles that were initially specified. Finally, shielding is being incorporated around the collimators after the RFQ, the chopper slits and the charge selection slits.

Combined horizontal/vertical steering magnets procured from Chalk River will be used in the initial MEBT section to the stripping foil. Shorter TRIUMF designed vertical steering magnets will be used in the charge selection section. Longitudinal space is very tight in the matching section before the DTL. For this reason a short $x-y$ steerer will be placed just after the rebuncher and the two middle quadrupoles will be equipped with separate steering coils.

An engineering layout has been completed and is displayed in Fig. 142.

DTL QUADRUPOLE TRIPLET

Quadrupole triplets are positioned between IH tanks to provide transverse focusing. In particular, the

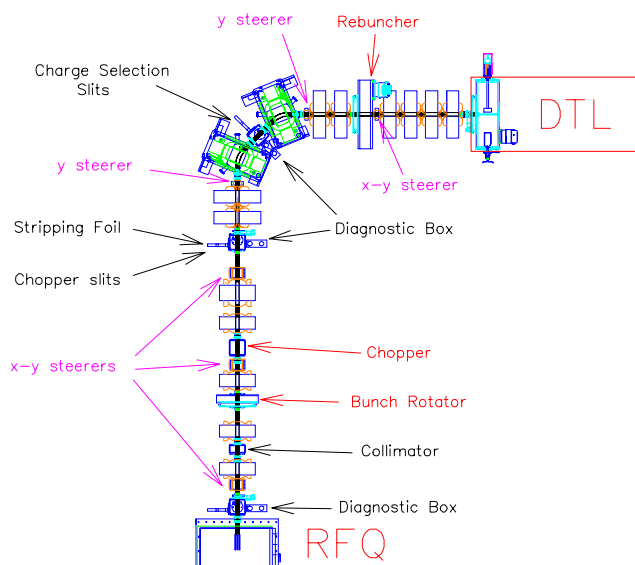


Fig. 142. Engineering layout of the medium energy beam transport.

triplets are used to refocus the diverging beam at the end of an accelerating section in such a way that the beam stays circular throughout the acceleration with a waist occurring approximately mid-way along an accelerating section. In order to maximize longitudinal acceptance it is desirable to minimize the triplet length. The challenge is to build strong gradient triplets and position and support them in the minimum longitudinal space. The strength, length and alignment tolerances of the quadrupole triplets have been specified. The engineering design of the quadrupoles is well under way and the intertank connections and triplet support have been detailed.

Even though the initial DTL design was based on ions with mass to charge ratios varying from $3 \leq A/q \leq 6$, recent discussions on a future expansion of the ISAC facility (ISAC-II) suggest that future operation of the DTL at $A/q = 7$ would be desirable. It is thought that the required accelerating gradients could be made available, at least in pulsed mode, as long as the quadrupole triplets are sufficiently robust. To this end a capability of focusing this heavier beam was included in the quadrupole specification. The length and strength values for the quadrupole are based on a gap between quadrupoles (between magnetic edges) of 50 mm. Triplet specifications are as follows: quadrupole lengths of 65, 95 and 65 mm and strengths of 65, 75 and 65 T/m.

The resultant beam envelopes through the DTL are shown in Fig. 143 assuming a transverse emittance of 0.15π mm mrad. Based on these results a quadrupole bore aperture of 24 mm was chosen. The focusing gradient in each quadrupole should be uniform to $\pm 1\%$ over ± 8 mm of this aperture.

A sketch of the inter-tank region is shown in Fig. 144. The quadrupole assembly will be at air with a stainless steel jacket surrounding the end caps joined at one end to the beam tube and ending with a flange and bellows section to form a vacuum connection with the upstream tank and the downstream buncher. In this way the quadrupole triplet can be removed for

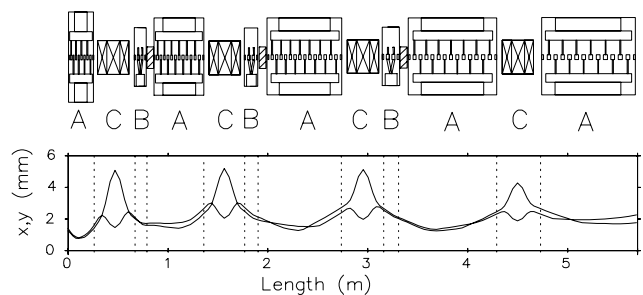


Fig. 143. Transverse beam size in the ISAC DTL assuming a transverse emittance of 0.15π mm mrad.

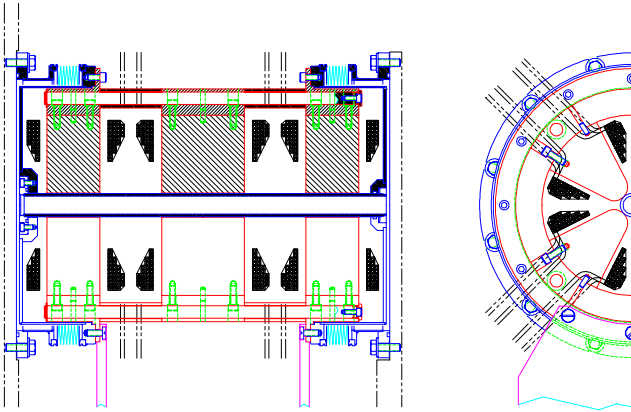


Fig. 144. Assembly drawing of the ISAC-DTL quadrupole triplet.

servicing while still occupying the minimum longitudinal space. The buncher and diagnostic box are made as a single piece. The diagnostic box is connected to the upstream box by a large O-ring flange.

The steering requirements for the DTL were investigated. Due to space restrictions, independent dipole windings will be added on the centre quadrupole of each triplet to steer the beam. Studies indicate that the imperfect steering fields lead to a small yet acceptable transverse emittance growth.

Alignment tolerances are set by demanding that the beam displacements from misalignments are small compared to the beam size or at least small compared to the acceptance. Practically speaking the quads should be aligned to better than 0.1 mm accuracy with a pole placement better than 0.1 mm.

HIGH ENERGY BEAM TRANSPORT

The design of the high energy beam transport (HEBT) has seen minor alterations in the last year mostly due to changes in the DRAGON footprint. We have moved the take-off angle from 30° back to the original 22.5° . A second 22.5° feeds the beam to the DRAGON target. The length of this achromatic section has been shortened. The second dipole in the achromat is defined as a switching magnet to allow a reverse achromatic bend of 18° to feed a second experimental area. Provision has also been made to allow the installation of a post-accelerator after the DRAGON take-off for the ISAC-II expansion.

In order to reduce HEBT costs, an 11.7 MHz rebuncher is under development. The idea is to use an 11.7 MHz rebuncher for low β particles and a MEBT style 35 MHz rebuncher for high β particles. Each buncher would be placed after the periodic/diagnostic section ~ 12 m downstream from the DTL and would remove the requirement of multiple 35 MHz rebunchers spaced throughout the HEBT.

Further changes in design will occur as the plans by experimental users solidify.

BEAM DIAGNOSTICS

The most evident progress in 1998 was the provision and installation of cables, electronic modules and racks to service 80 new diagnostic devices installed in the separators and LEBT, between the production target and the TRINAT and Yield experiments. The assembly of mechanical hardware was shared between the ISIS and Probes groups; the latter concentrating on specialty items such as equipment in the exit modules and in diagnostic boxes at the origin and image of separators.

Several electronic modules were either designed and prototypes tested or taken from the prototype stage to a properly engineered version using custom printed circuit boards and design programs such as PROTEL. These modules include:

- QSX/W, a higher, 1 kHz, bandwidth version of the popular QSX multi-range quad amplifier suitable for scanning monitors with moving beam sensors.
- Module 0926 which sets the timing of start, sample and stop pulses for scanning monitors. A potentiometer interface card 0924 for the standard ISAC rotary scanning profile monitors; this interface card reduces the noise on the position signal. Module 0927 is an isolated 6 channel 10 V precision reference power supply suitable for the potentiometers and any other floating or biased electronics attached to beam sensors. Module 0933 is an opto-isolator unit to enable the signal from MWIC or harp monitors to bridge between integrator (0518) units in one rack and digitization or display units in other racks at a different potential.
- Four small preamplifiers and associated power supplies with a output of 10 mV/pA; (the most sensitive range of the rack mounted QSX is 1 mV/pA). The preamplifiers may be located close to the beam sensing element, even placed in vacuum, and may be floated with respect to ground potential. The bandwidth, 3 db, is 12 Hz for one pair and 70 Hz for the other. They have been used on the ion source test stand and on ISOL. We will judge their operation with low RIB currents in ISAC next year before going into production.

Several tests were performed on new monitor designs or on components which may be incorporated into beam diagnostic instruments. Some of these tests utilized ion beams. The tests included:

- Measurements of the scan to scan reproducibility in position of scanning profile monitors. The actual position was determined by the beam sensing element intercepting the light beam from a fixed laser diode. A number of passes were made for each condition of operation and the standard deviation of the values obtained from the position readback calculated. The jitter results were:

Oscillating scanner with rotary drive: $\sigma=120\mu\text{m}$
 Linear scanner with pneumatic drive: $\sigma=70\mu\text{m}$
 Linear scanner with stepping motor and tensioned belt: $\sigma=8\mu\text{m}$

- A fast Faraday cup was used in the commissioning of the test 7-section RFQ to measure the longitudinal distributions of the beam at entrance and exit. The output was amplified by a gain of 20 using a Philips 774 amplifier with 2 GHz bandwidth and observed by a TDS 820 oscilloscope. Signal averaging permitted clean data to be obtained at peak currents of 50 μA with 1 μA noise. The width of the beam bunch at exit was 3 ns, the value expected for that location. There was no reason to suppose that the frequency response of the cup did not exceed that of the amplifier. Both the charge collecting electrode and a slit upstream of the cup could be biased. It was determined that there was a bunch of electrons emanating from the slit jaws and the most accurate operation was obtained with the collector at 0 V and the slit at +50 V. This cup was donated by Dr. Poggi of LNL, Italy. A new FFC has been designed for MEBT; the design permits the entrance grid that localizes the beam field to be biased if desired.
- A full size, full power, prototype has been constructed of the bunchers to be installed between tanks of the drift tube linac. Electrons had been observed on the axis of this buncher and there was some concern that they may introduce spurious signals on beam diagnostic equipment nearby. The 105 MHz buncher has been designed to produce a sinusoidal electric field of amplitude 13.2 MV/m. We measured electron currents from 2 to 20 μA dc at this field level, the current falling as the buncher was conditioned and as the vacuum improved. The electrons were in bunches about 1 ns wide with an energy $\gg 1$ keV. The current was a very steep function of buncher field and its behaviour was consistent with the assumption of field emission as the source; however, our measurements were not precise enough to make a definite statement. We also saw ev-

idence of positively charged particles and copious low energy electrons. Fortunately it should be possible to commission and operate the DTL while turning off the buncher and tank closest to the diagnostic box. If this should not be possible then measures will have to be taken to deflect or suppress these stray charges since their current may exceed that of the weak ion beams.

Some theoretical calculations have been performed; these include:

- Range vs. energy graphs have been produced for ions of interest to ISAC. Ranges in a few materials from water to lead were calculated for ions from helium to xenon over energies between 10^{-5} and 10^2 MeV/u. The data in the present TRIUMF Handbook [Greeniaus, 1987] are for lighter ions and energies above 1 MeV/u, i.e. a region where only electronic or ionization stopping need be considered and nuclear stopping may be neglected.
- Secondary electrons are produced when ions hit a wire. A monitor has been designed to measure the distribution in time of the beam by accelerating a portion of these electrons into a microchannel plate. Trajectories of both electrons and ions have been calculated in the field of the monitor and the calculations show that the broadening of resolution due to variations in path length is less than 50 ps from each source except for low energy ions in LEBT where the contribution to resolution may be 300 ps. This monitor should give time information at very low currents; it has not yet been constructed since the FFC is adequate at present.
- A pair of linear profile monitors operated successfully in the RFQ tank downstream from a shield terminating the field of the 7 section test RFQ. The carriage of each bore 3 wires at 45° to each other. A pseudo-tomography program was written to show an approximation to the beam density distribution in the X-Y plane in addition to the usual projections on the X and Y axes.
- Beam power limits were calculated for some fixed and moving beam sensors.
- Parameters, including space charge, that determine the bias voltage required on monitors, such as Faraday cups, were considered. It was concluded that the standard TRIUMF dc power supply should provide 300 V.

ISAC CONTROLS

Detailed design and implementation of the ISAC control system proceeded fairly smoothly all during the year targeting and achieving the following milestones:

- Beam line 2A vacuum system control, beam monitor control and power supply on/off control in May
- RFQ vacuum system, in-tank optics and in-tank diagnostics in June
- MEBT vacuum system and diagnostic station in July
- Target station vacuum, optics and diagnostics control in September
- Pre-separator and mass separator vacuum, optics and diagnostics control in October
- Vacuum, optics and diagnostics control for low energy beam transport from mass separator to TRINAT and GPS experiment in November/December.

As of end of the year, the ISAC control system (not counting beam line 2A) contains approximately 2500 digital and 1600 analog control channels.

Hardware

Three more VME crates were installed to house the IOCs for targets, mass separator and LEBT, a fourth VME crate is used for beam line 2A. For beam diagnostics, we started using TRIUMF designed VME modules, which are described in more detail in the Electronics Development section of this Annual Report. The VQSX, an 8-channel variable gain beam current amplifier with 100 kHz transient digitizing capability, proved very successful in measuring beam profiles with harps and wire scanners at sub-nA currents. It is also used to digitize harp readouts. Stepper motor control for pre-separator and mass separator diagnostics devices was implemented using commercial controllers (OMS58). This work is described in more detail in the Electronics Services section.

For beam line optics, 170 more device controllers were mounted on high voltage power supplies and added to the CAN-bus network. Special versions were developed to control the pre-separator and mass separator supplies, which were acquired from Chalk River National Laboratories. Both on the targets and the RFQ, sparking problems were encountered which still have to be further investigated.

The vacuum sub-system controls for RFQ and MEBT were added to the off-line ion source PLC. A second Modicon Quantum Series PLC was installed for the vacuum sub-systems for targets, mass separator and LEBT. Six more PLC breakout cabinets were pre-wired and tested in Trailer Gg and installed in the electrical services room, on the mass separator platform, in the TRINAT ante-room and on the experimental hall mezzanine.

For beam line 2A a third Modicon PLC was in-

stalled for control of the vacuum system, motion control of beam monitors and power supply on/off controls. The PLC system is used to adapt the beam line devices to the control model of the TRIUMF central control system and to provide interlock functions in a similar way as relay based hardware is used on the older beam lines. PLC data and commands are exchanged with the central control system via a VME based SDLC link. One PLC breakout cabinet each was installed for devices located in the vault and beam line 2A tunnel respectively.

At the beginning of the year we encountered random IOC crashes, which were eventually traced to the VME based Modicon PLCs. The PLC CPUs contained a design flaw in their interface to the VME bus which made them unusable in our environment. A temporary work-around was found and an exchange was negotiated with the supplier. Three of the four VME PLCs were exchanged with Ethernet based models by the end of the year. The final exchange will take place in January, 1999. The new models communicate via TCP/IP instead of through the VME back-plane, which results in an increase of overall system robustness.

For commissioning ISAC, the ion source control room next to the electrical services room was set up with a temporary control console. It consisted of two PCs with three monitors each using X-terminal software. Two SUN workstations were set up as production servers in the ISAC control room. A 24-port Ethernet switch dedicated for ISAC controls was set up in the communications room. Initially this was fed via the temporary thin-wire connection to the ISAC building. Later during the year the final site connection was installed and the remaining thin-wire connections are being phased out.

An overview of the control system hardware configuration at the end of the year is given in Fig. 145.

Software

During this year we were able to benefit fully from the high productivity of the EPICS system, both during development and especially during testing and commissioning where several scheduled weeks were collapsed into a few days.

On the operator interface level a large number of overview screens and detailed device control panels were produced following the conventions developed during the previous year. Associated configuration scripts and backup/restore scripts for all sub-systems were written. Efforts were made to automate some of the more clerical aspects of EPICS user interface production. 2D plots for pre-separator and mass separator scans were implemented and the EPICS strip-chart tool was installed and used. Parameter logging was

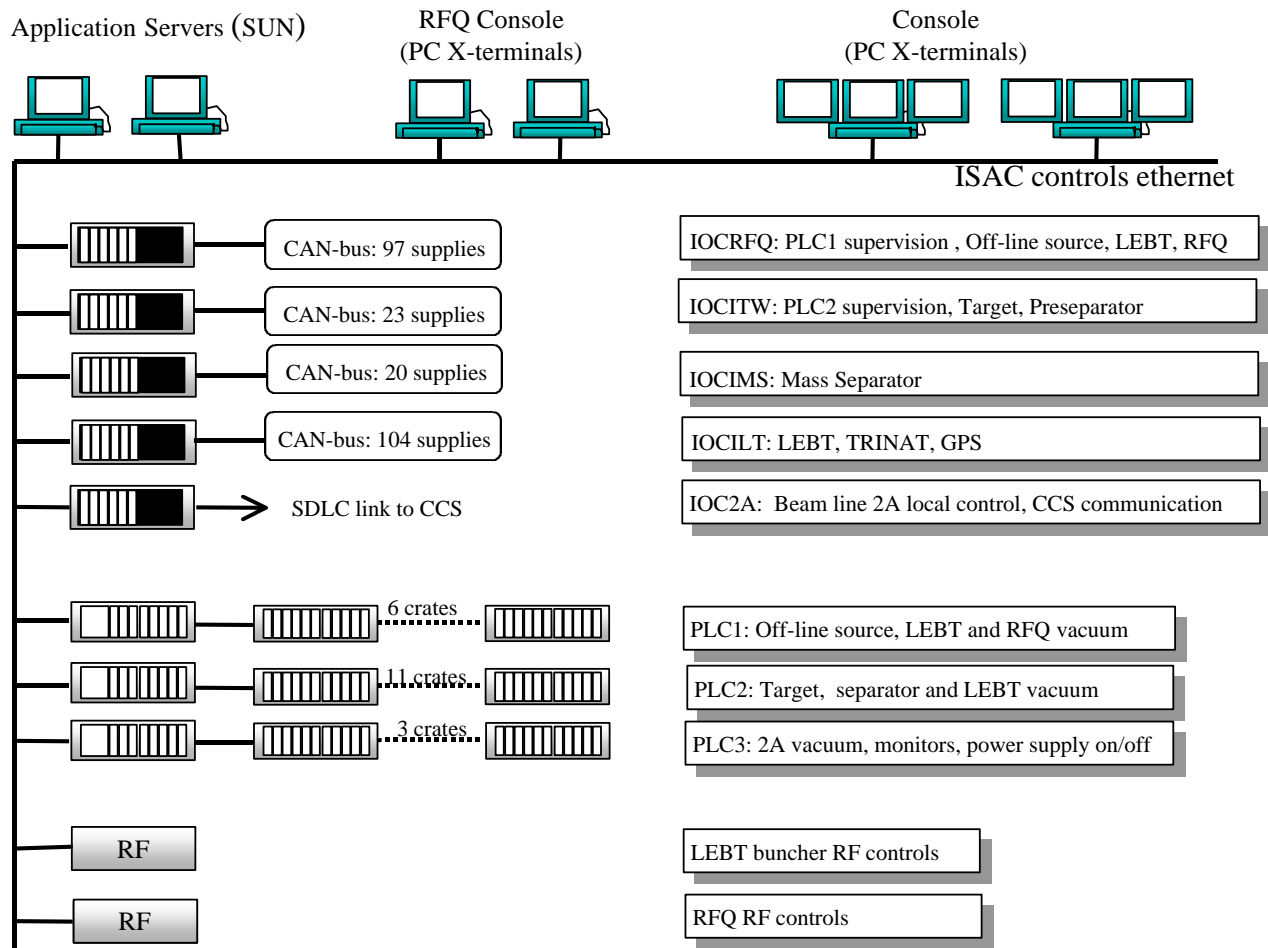


Fig. 145. ISAC control system hardware overview.

tested with the standard EPICS tool (not too satisfactory on data retrieval) and a beta version of the promising new channel archiver.

A Web-based electronic log-book program from Fermilab was installed and used during ISAC commissioning. An “alpha” version of Web-based fault reporting was implemented and connected to a PC-based database application for fault tracking.

On the level of the EPICS function block data base, CAPFAST schematics were produced for all new sub-systems. In addition, new device and component schematics were developed for the Chalk River power supplies, stepper motor driven diagnostic devices and the supervisory control of the rf systems. Component schematics were adapted to support the new TRIUMF built VME modules.

EPICS device and driver support level was written for:

- the TRIUMF designed VQ SX beam current amplifier
- the TRIUMF designed 32-channel digital I/O module
- supervising the rf control systems of low energy

buncher and RFQ using a combination of TCP/IP and UDP/IP protocols as required by the RF Controls group

- the TCP/IP based communication with the new Modicon PLCs.

Subroutine records were developed for:

- the high energy emittance rig at the RFQ which uses a rotating slit/harp combination
- digitizing the pulse train of the 0518 harp modules
- calibrating stepper motor driven devices.

In terms of EPICS infrastructure, the system was converted to use the latest EPICS release 3.13.0 beta10. All IOCs were upgraded to VxWorks version 5.3 which allowed the use of the Tornado virtual console.

The ladder logic PLC programs were extended to support all new vacuum systems and the surface ionization source.

Maintenance work was done on the ISAC device data base applications which generate specification and test documents.

ISAC-II

We have been making plans for the next stage of ISAC. As presently designed, ISAC will provide radioactive ion beams up to mass 30 and energy 1.5 MeV per amu. Two workshops have been held to poll the user community, and the result is a specification of 6.5 MeV/u with mass up to 150.

With a charge-state booster (CSB), it will be possible to raise the mass to 150 while retaining the existing RFQ. However, the equilibrium charge state for stripping at the RFQ final energy of 150 keV/u is not high enough for the heavier species: for example, for mass of 100, there will be very little beam in charge states larger than 15. Since the ISAC-I DTL requires a charge-to-mass ratio of at least 1/6, this DTL cannot be used for ISAC-II.

The solution is to increase the energy after the RFQ, but before stripping. One can minimize the linac length, and therefore overall cost, by optimizing strip-

ping energy. This is because a too-low stripping energy does not strip to a high enough charge state, while a too-high stripping energy makes the pre-stripper linac too long. The optimum stripping energy for mass up to 150 is 400 keV/u, and the median charge state is such that the lowest q/A is 1/7.

A cost effective configuration to reach 400 keV/u is to continue the acceleration straight north of the RFQ MEBT line (Fig. 146). This would require an addition to the present building to widen it northward. The energy gain of 0.25 MeV/u requires a total rf voltage of $(0.25 \times 30 =) 7.5$ MV. A DTL very similar to the ISAC-I DTL IH linac would be about 5 m long assuming an average gradient of 1.5 MV/m and could be placed downstream of the first MEBT bender after a short matching section. After the new DTL, the beam would go through a beam transport system consisting of a short matching section, stripping foil, a 90° bend for charge selection and a matching section to the post-stripper linac.

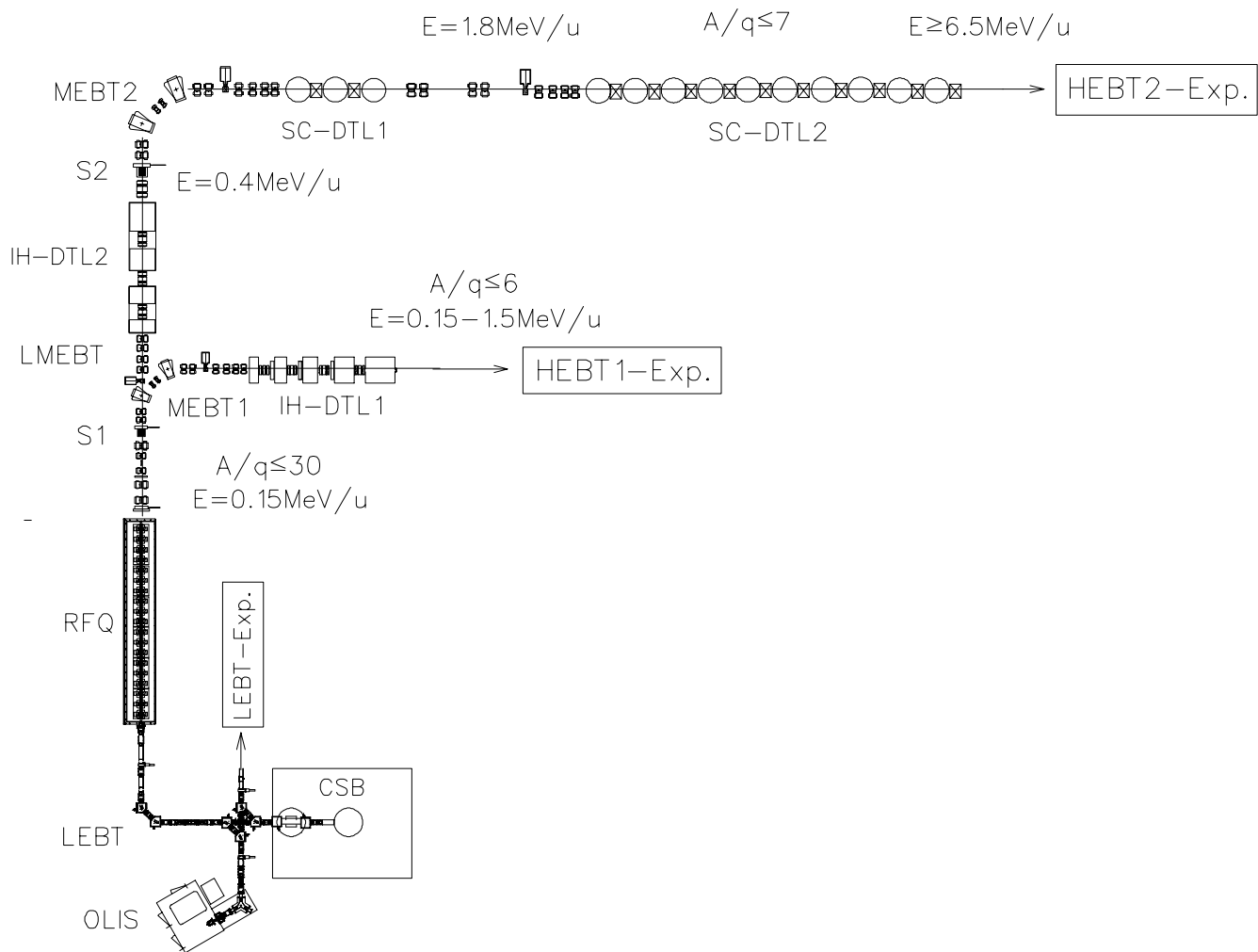


Fig. 146. ISAC-II layout.

To reach 6.5 MeV/u from 0.4 MeV/u with $A/q = 7$ requires a total voltage gain of 42.7 MV. A room temperature linac should be composed of long, many-gap modules (like the ISAC-I IH DTL), else the rf power supply and running costs become prohibitively large. Such a structure running cw would have a gradient of 2.2 MV/m and including the required focusing quadrupoles between tanks would therefore be at least 28 m in length. Higher electrical gradients are possible in principle, but in cw operation rf power dissipation in the drift tubes becomes a limiting factor. These problems disappear if we instead use superconducting cavities. In that case, an accelerating gradient of 3 MV/m is conservative (5 MV/m has been achieved).

We propose to build the linac of many short (2 to 4 cell) cavities. Short modules have the advantage that the ions do not have to rigorously follow a fixed velocity profile to stay in phase with the rf, since the modules are independently phased. This allows pushing the energy of particles with $q/A > 1/7$: for example, ~ 15 MeV/u can be attained for particles with $q/A = 1/3$. (Stripping at 400 keV/u can efficiently produce ions with $q/A = 1/3$ for $A \lesssim 30$.) Even for the

highest masses, higher energies would be possible at a cost in intensity with the addition of an intermediate stripping station (see Fig. 147).

The superconducting linac would be similar to those running at other heavy ion labs, in particular Argonne and Legnaro, Italy.

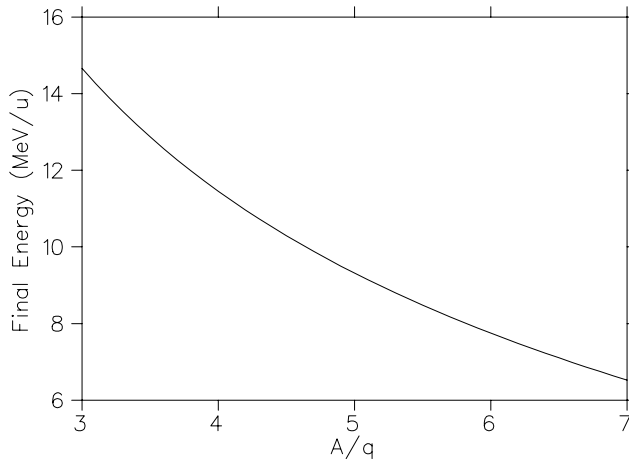


Fig. 147. Energy achievable in ISAC-II with a superconducting final stage.

ACCELERATOR TECHNOLOGY DIVISION

INTRODUCTION

As for the past two years, the ISAC project continued to be the largest user of engineering, design and fabrication effort during 1998. This is reflected in the REAs (requests for engineering assistance) submitted during the year, with 48 for ISAC-related projects and 15 for other activities. The main activities for ISAC involved completion of beam line 2A, the target stations and modules, the mass separator system and low energy beam transport (LEBT), the RFQ accelerator, and the first tank of the DTL. An increasing amount of ISAC work is now moving on to the experimental program, with engineering effort put into the TRINAT experiment relocation, DRAGON spectrometer, and the first experiments using low energy radioactive ion beams.

Design work for the CERN-LHC collaboration included the cabinet for the 66 kV resonant charging power supply, the fast blade scanner and a start on the fast wire scanner. The ATLAS collaboration received some engineering assistance in thermal calculations for the forward calorimeter, and the University of Victoria group produced final designs for series production of the hadronic endcap calorimeter and concepts for the wheel assembly. Work was also carried out on the signal feedthrough project.

Assistance was also provided to the internal program, particularly Expt. 614 where an engineer assisted in testing and shipping of the 2 T superconducting solenoid, the μ SR program where some detector stands were modified, and the CHAOS experiment, where an improved cryogenic target was designed.

The Design Office and Machine Shop were heavily loaded and outside assistance was used to cope with the demand. The Building department carried out a number of tasks related to completion of the ISAC building and target areas, the largest being the design and contracting of concrete shields for the top of the ISAC target area and separator areas. Design work has started on the completion of the second floor of the ISAC annex to house the occupants of trailer S (Design Office trailer).

The Electronics Service group was fully occupied in producing control and interlock modules for ISAC, cabling manufacture and installation of the data communications cabling. The Electronics Development group provided working ISAC controls as systems came along, and developed VME and other modules for the system. The groups found some time to support the CERN-LHC work in three instrumentation projects and the resonant charging supply project. Some other activities, notably BNL Expt. 787, μ SR, and the CDS

power supply also received help.

MAGNETS

The magnet work carried out as part of the CERN collaboration is reported in the CERN Collaboration section. The main project was production of the prototype twin aperture quadrupole magnet and subsequent developments towards series production.

The ISAC pre-separator magnet, built by Sunrise Engineering (BC), arrived on site in June, was field mapped and installed in location in September.

Figure 148 shows a photograph of the lower half of this magnet with the vacuum chamber installed. Radioactive ion beams from either of the two target stations are bent into a common exit beam line using this magnet.

The design of the ISAC MEBT 45° dipoles was documented in "Concept design of the ISAC MEBT 45° dipole magnet" [TRI-DN-98-03]. The contract was awarded to Talvan Machine Shop (BC), to make two of these small dipoles. Delivery is expected in April, 1999. The design of two dipoles for the ISAC DRAGON separator was documented in "Concept design of the DRAGON separator MD1 dipole magnet" [TRI-DN-98-12], and "Concept design of the DRAGON separator MD2 dipole magnet" [TRI-DN-98-10]. TRIUMF



Fig. 148. Photograph of the lower half of the pre-separator magnet with the vacuum chamber in place.

went to tender for these two magnets in December, and a contract is expected to be let in January, 1999.

The design of one of the types of quadrupoles for the ISAC DRAGON separator was documented in "Smit-Elma quads for the DRAGON separator" [TRIDN-98-17]. This magnet uses a steel core recycled from the CERN PS transfer line and the coil design made by TRIUMF for the CERN BT quads. The Beam Lines group started to assemble two of these quadrupoles in December.

A large superconducting solenoid is required for TRIUMF Expt. 614. A TRIUMF engineer supervised the pre-purchase testing of a used MRI magnet at Cryomag Services (New Jersey), and a decision was made to purchase this magnet. Tests were performed at 2 T at the site and the magnet was field mapped when it arrived at TRIUMF at 0.2 T to check that it survived the trip. The magnet requires a steel shield to contain the return flux and a cost estimate was made for various possible shield arrangements, resulting in a decision to proceed with the design of a rectangular shield.

Magnet Measurements

A total of 10 magnets listed in Table XXII were field mapped during the year. The Chalk River separator dipole, which is a curved magnet with 135° bending angle, was surveyed from both ends, at 4 different current levels and with 4 different combinations of trim coils settings. The ISAC pre-separator magnet was surveyed from the exit and two entrances, at three different current levels.

Two commercial Gaussmeter systems were calibrated and installed in the separator and pre-separator magnets.

Table XXII. Details of surveyed magnets.

Quantity	Project	Description
1	ISAC	Chalk River separator dipole
1	ISAC	Chalk River double steering magnet
1	ISAC	Pre-separator dipole
6	ISAC	4Q8.5/8.5 quadrupoles
1	E614	Superconducting solenoid

MECHANICAL ENGINEERING

ISAC

A considerable amount of engineering effort was expended in support of the ISAC project by all members of the group in various capacities; from project management to specific project engineering participation. Highlights of this work are briefly described below. As well, detail designing and checking continued

well into the year necessitating design reviews and engineering participation. This centered around components required for completion of the target hall, pre-separator, mass separator, beam transport, diagnostics and accelerators.

Beam line 2A

The majority of work on beam line 2A and on the vault upgrade was accomplished in the previous year. However, the completion of the vault upgrade could not be achieved until the February shutdown when the remaining magnets, diagnostics and transport elements were installed. The 2A beam line in the tunnel was also completed at that time and beam was successfully run into a temporary dump at the end of the tunnel in late April. This left the remaining beam line from the large bender magnet to the west target station to be completed and this was done later in the year once the west target vacuum tank was installed.

Target hall

The majority of engineering work was completed in the previous year. During 1998, the actual construction of the 2 target stations required a great deal of consultation and supervision due to the complexity of these stations. The creation of each target station involved the placement of 10 ton steel shield blocks in an accurate pre-arranged pattern based on shielding calculations. These were then encased in concrete along with the required penetrations for services such as electrical conduit, vacuum exhaust piping, high voltage chases, etc. This was accomplished in 7 steps starting at level 264 ft. up to the completion level of 284 ft. and involved 525 tons of concrete and 1000 tons of steel. Accurate forming was required in order to minimize gaps around the vacuum tanks and to ensure that covering shield blocks fit properly. The west tank was installed into its cavity in May, and the quality of work was such that its placement was within 0.050 in. requiring only a minor adjustment.

In-parallel work continued on the 5 modules that were to be installed in the west target station (see Fig. 149). These were being assembled in the east end of the experimental hall and involved consultation and supervision from the engineering group along with considerable assistance from the Remote Handling group.

A major effort during this report period was the design manufacture and assembly of all components contained at the bottom of the modules, i.e., target/ion source extraction elements, electrostatic quads, steerers and diagnostics. These elements had to be mounted in such a way as to be remotely handleable in future and their alignment with respect to each other can be adjusted and easily checked. This was achieved by

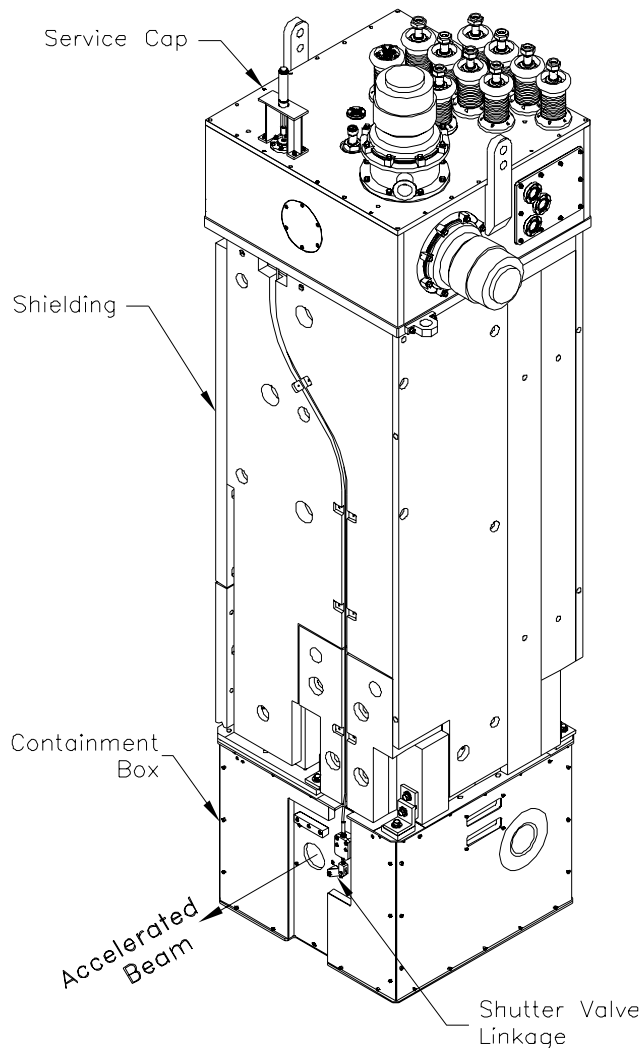


Fig. 149. The ISAC target station module which houses the target/ion source in the containment box. All services enter at the top of the module which is shielded from the target below.

mounting all the elements, in each module, on a removable tray. A special alignment tray is then used to allow adjustment with respect to the module and once this is set the component tray can be placed in situ accurately and repeatedly. Similarly, a master fixture was built to accept any of the modules and this along with a transfer fixture allowed accurate alignment of the modules with respect to the vacuum tank.

As a result of this work all the modules were installed into the west target tank (see Fig. 150) and stable beam was extracted in October, followed by radioactive beam extraction to the mass separator in November, and to TRINAT in December.

TRINAT

This facility has been successfully operating on TISOL in the proton hall extension and was moved to

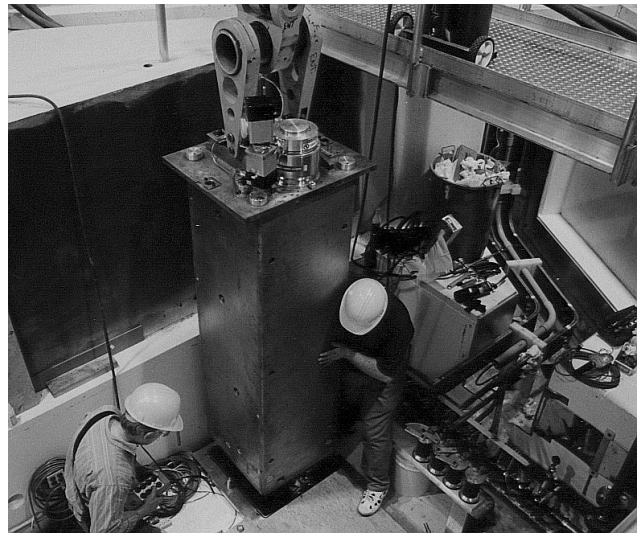


Fig. 150. Photograph of one of the 5 modules, the beam entrance module, being lowered into the west target station.

a new location on the floor above the mass separator in the ISAC building. This required a considerable amount of engineering support in the form of design layout, component design, supervision and scheduling in order to be available by late November, to meet the schedule for radioactive beam delivery. This work was accomplished successfully. At the same time the TISOL facility had to be supported since its operational schedule to other experiments was not interrupted.

Accelerators

Work continued on the installation of the 7 rings into the RFQ vacuum tank. Once the platens had been aligned via a digital theodolite interception procedure, the vanes were installed and services hooked up resulting in the commencement of rf signal level testing in the spring. All this work involved engineering support on a day-to-day basis. Subsequent RFQ tests using the off-line source have indicated operational characteristics exactly as predicted, which also indicate that the design and alignment philosophy and implementation were successful. Work paralleled the above in completing the remaining 12 rings plus 3 spares that will require completion and installation in 1999.

At the same time design work was nearing completion of the drift tube linac (DTL). The detailed drawings were released and components for tank #1 were manufactured during this report period. In order to achieve a high quality rf surface on the inside of the tank, it was plated with copper by the acid bath process which was a procedure new to TRIUMF. This process produced a beautiful surface finish, even filling in machine marks, but did cause some problems due to build up on edges and corners requiring post machining. Assembly of the DTL tank #1 began late in the

year and will be completed and rf tests begin early in 1999.

DRAGON

Project engineering assistance has been started on the DRAGON project. The main focus is on the design of 2 electrostatic dipoles (ED's). These ED's will be similar to those installed at the ATLAS facility at Argonne National Laboratory. A great deal of time and effort has been spent to understand these systems. The mean bend radius of ED1 is 2 meters with the bend angle of 20° , while the bend radius for ED2 is 2.5 meters with the bend angle of 35° . The electrodes are held at ± 200 kV with a 10 cm separation. The electrodes for both the ED's have been designed and detailed drawings are in progress. Design of the support and alignment system for electrodes is progressing. It is desired to maintain these titanium anodes and cathodes parallel to each other within $100 \mu\text{m}$ under electrostatic forces in vacuum. The surface of the Ti anodes and cathodes opposing each other must have a mirror finish.

The design and assembly issues of the compact 300 kV Cockcroft-Walton high voltage multiplier stacks are being looked into. It is proposed to buy a 10 kV power supply from Glassman and build a 30 stage full wave Cockcroft-Walton multiplier stack in-house with assistance from ANL.

Progress is under way to design different diagnostics components including charge and mass slits. Support stands and vacuum vessels for the DRAGON beam line are also being designed.

Some engineering and design assistance was given to the windowless gas target project for DRAGON which is being carried out at the University of Alberta.

Analysis

Engineering of ISAC structures and components has involved the need for structural analysis in many cases. An example is the design of a module which involves 12 tons of steel and must be supported not only in the vacuum tank but in the various assembly jigs and alignment fixtures during assembly. All this equipment required analysis to ensure structural integrity. This involves actual recognition of the requirement during a design review, the analysis accompanied by a brief report, and a signature on the drawing by the analyzer. Complex analyses may require the use of finite element analysis which is available at TRIUMF in the 2 codes ANSYS and ALGOR. These codes are also used for other complex forms of analysis (see ATLAS section in this report).

ISAC – University of Victoria

Construction of the water-cooled, copper plate, beam dump was completed. A static pressure test at

1.5 times the maximum operating pressure was carried out, and water flow versus pressure drop measurements made. The dump is now in service. The design has been documented and distributed as a Victoria Physics Note [VPN-98-1]. Technical support was provided to assist with commissioning the beam dump, assembly of the exit modules and installation of exit module, beam optic elements.

Engineering – Other

ATLAS – TRIUMF

Heat transfer studies continued for the forward liquid argon calorimeter (FCAL). The study considered the heat transport from the FCAL module to the outer support tube through the liquid argon (LARG) gap. A computational fluid dynamics (CFD) model was created using a CFD program FLOTTRAN within ANSYS. Due to symmetry in the problem, a 2D model of half of the FCAL support tube and half of the outer support tube was created.

This analysis predicted convective loops in the top section of the LARG gap which promote heat transfer to the outer tube, hence increasing heat transfer and reducing the temperature rise in the LARG gap.

ATLAS – University of Victoria

Hadronic endcap (HEC)

Final drawings for the HEC module series production and subsequent detector wheel assembly were completed. The design was presented before a production readiness review committee at CERN and was approved for manufacture by the collaborating institutes; Dubna, Protvino, Lebedev, MPI-Munich, and TRIUMF. The complete drawing series was converted to CERN compatible files and transferred via interactive Web pages to the CERN drawing directory. Conceptual design work commenced for the HEC detector wheel assembly table, wheel rotation device, and cryostat interface tooling (see Fig. 151). Module support frames and shipping containers were manufactured for transportation of test beam pre-production modules to CERN. In addition, an overhead crane to facilitate module assembly was designed for installation within the existing clean-room facility at TRIUMF.

Signal feedthrough project

Laboratory space for assembly and testing of the ATLAS detector signal feedthroughs has been prepared and the various, vacuum, leak checking, welding and electrical test equipment has been installed. Preliminary tests are under way and suitability of the two technologies available to construct the signal pin carriers is expected to be confirmed in time for the production readiness review scheduled for January, 1999.

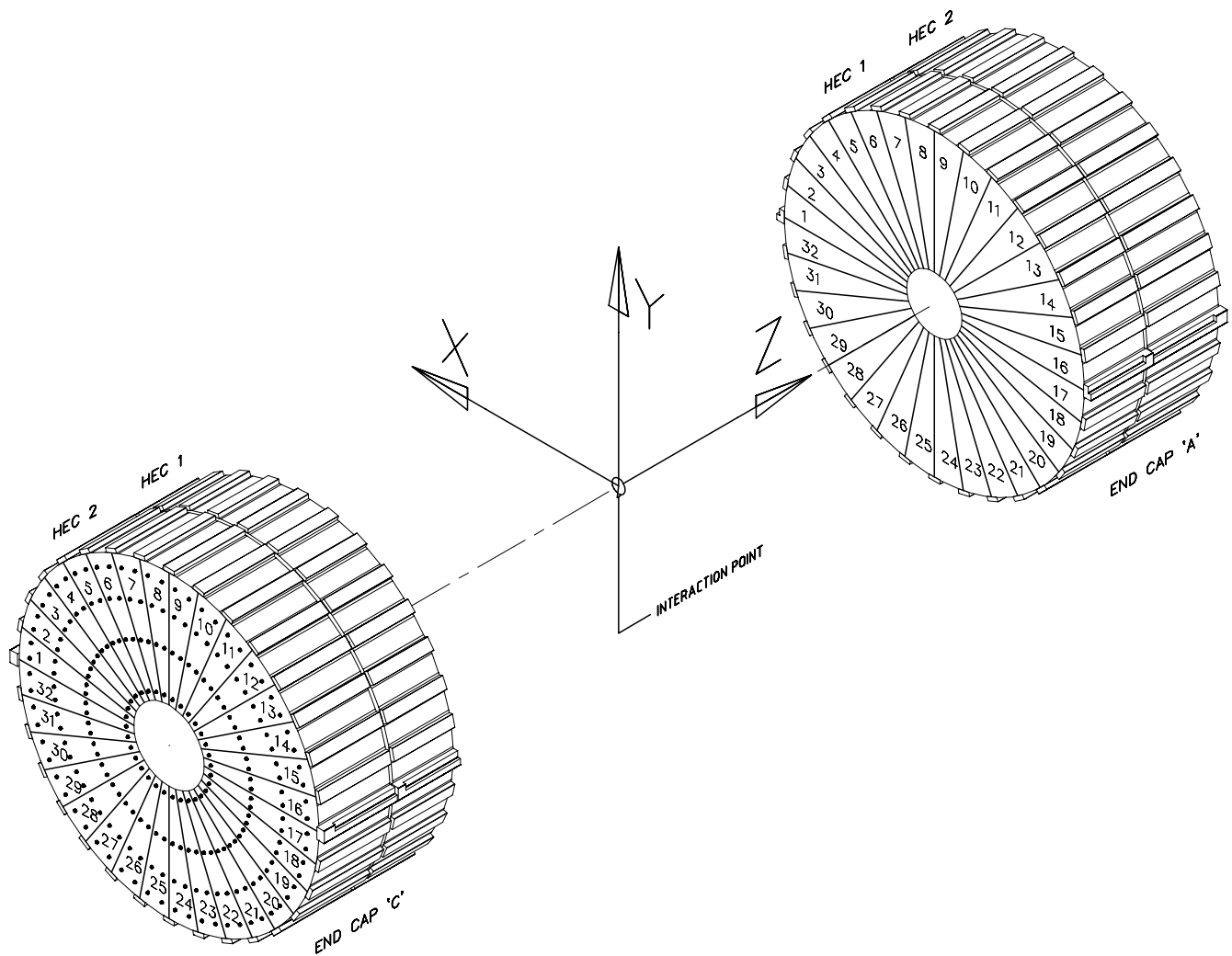


Fig. 151. Thirty two of the ATLAS HEC modules, each weighing 3000 kg, will be assembled as shown into a wheel which is 4 m in diameter, and installed in a cryostat.

Welding tests, with post-weld metallographic examinations, have been done to prepare for the weld and welder qualification processes demanded for these devices under the pressure vessel code.

PLANNING

This year the Planning group was involved in planning, scheduling, coordinating and expediting several sub-projects for ISAC; planning and coordinating activities for two scheduled shutdowns (January 20–May 6, and August 22–November 4); and planning some of the CERN collaboration projects (fast blade scanner, resonant charging power supplies and pulse forming networks).

Various plans and PERTs were prepared, manpower estimated and analyzed and updated regularly. ISAC priorities were evaluated and the highest priority was assigned to produce the first radioactive ion beam

(RIB) by the end of November. The resource leveling was done, activities were expedited, and the above goal was achieved on November 30.

The progress on PERTed projects is described elsewhere in this report under the respective principal group. However, following is a summary of projects along with the major milestones achieved:

Beam line 2A

Components were installed in the vault and tunnel in the January shutdown. 2A was commissioned with proton beam to temporary dump (in the tunnel) on April 29, and to the dump module at the west target station on May 25.

Target areas

This work included fabrication, assembly, installation, and alignment of 2 vacuum tanks; fabrication and

assembly of 5 target modules for the west target station (entrance, dump, target and 2 exit modules); target hall crane; guard rails, walkways and refinishing of target hall concrete walls by surface paring and painting; shielding (up to 525 tons of concrete poured in several steps and 1000 tons of steel shielding); high voltage system (cage, interlocks and HV lines); services (electrical, water, air); vacuum system, target station (module access area, services, cabling); machine protect system (interlocks, thermocouples, etc.).

Several problems were encountered in the fabrication and assembly of the vacuum tanks and many target module components due to poor copper plating, design and manufacturing errors. The milestone of commissioning stable beam out of the target ion source was achieved on September 24.

RFQ

After signal and power level tests, full voltage on the 7-ring RFQ electrodes was achieved on July 13. First accelerated beam was extracted through the RFQ at full power in September. The remaining 12 rings were designed, fabricated and assembled by December, with the aim to complete installation of all rings by July, 1999.

Separator system

The mass separator, high voltage platform, diagnostics, vacuum system, controls and LEBT (from DB11 to TRINAT) were installed and tested by October. The commissioning sequence involved getting first stable beam through the pre-separator on October 23, first high resolution beam at the separator image slit on November 3, followed by a stable beam to TRINAT on November 19, and RIB on November 30.

Drift tube linac (DTL)

Overall progress on the DTL project was slow due to a relatively higher priority placed (in terms of manpower and other resources) on getting the RIB to TRINAT by the end of November.

The first tank (including stems, ridges and end plates) was fabricated and copper plated by September. The DTL buncher was designed and fabricated at INR-Troisk, received at TRIUMF in August, and tested to full voltage by October. Also, the DTL quadrupole triplet was specified and design started with an aim to order the triplets by April, 1999.

Other

A work breakdown structure (WBS) for the DRAGON project was developed and a detailed PERT was prepared. Major milestones include gas target designed and fabricated at University of Alberta with an aim to test at TRIUMF in May, 1999; 2 magnetic

dipoles (MD1, MD2) designed and will be ordered in January, 1999; design of 2 electrostatic dipoles (including electrodes, HV power supplies, support and alignment structure) started.

Also, the Planning group was actively involved in planning, scheduling and expediting activities for the GPS experiment, TRINAT move to ISAC building, LEBT (to TRINAT and GPS), yield station, MEBT layout, LTNO (for beam in July, 1999), and β -NMR (for beam in November, 1999).

In addition to ISAC, the Planning group was involved in planning and scheduling the activities for CERN work; fast blade scanner, fast wire scanner, five 66 kV resonant charging power supplies (RCPS), and nine pulse forming networks (PFN's).

Shutdown Activities

The main purpose of the first shutdown (January 20–May 6) was to complete beam line 2A and all related activities in the vault and tunnel. The cyclotron lid stayed down for the first 5 weeks and then the lid came up for 4–5 weeks. Major jobs completed in this shutdown include: 2A (finish installation in the vault and tunnel), cyclotron probe MRO, vacuum (MRO, rebuilding of cryo pumps 3 and 5), rf (MRO, resonator leveling adjustments), MRO on beam line monitors, tank inflector inspection, correction plate tests, repair trim coil junction box, adjustments to the elevating system controls electronics, CM1 and 1VQ3 (worn hoses) water leak repairs, 1VQ1 damaged cable, T-1 water package, stand modifications to resolve alignment problems of 4AQ4/5 and other beam lines MRO work in the vault, meson and proton areas. The total man dose incurred in this shutdown was 82.6 mSv distributed among 90 workers.

The main purpose of the fall (August 22–November 4) shutdown was to work on beam line 2C and complete ISAC activities to deliver beam to TRINAT. Since the cyclotron lid was not raised, most of the work was done only in the vault and experimental areas. The major jobs completed in this shutdown include: 2C work (solid target facility, cesium target, shine blockers and rubidium target), repair both B20's, replace UPS, rf (MRO and wasterload #3), investigate and repair water and vacuum leaks at T2 and TNF, M13 (triplet and short separator), 4BQ7 magnet coil repair and MRO work in the vault, meson hall and proton hall. The man dose incurred in this shutdown was 21.2 mSv distributed among 41 workers. Beam line 2A was tested at approximately 1 μ A on November 16 and 17. Many start-up problems were encountered which caused a significant downtime and those included – aluminum ALCW pump (October 26–November 2), TNF vacuum leak (decided to run with helium), main magnet power supply pre-driver (November 18–20), and

TNF water leak. The main magnet was turned off on December 20 (instead of December 22) due to water in the rf room as the reheating coil burst.

DESIGN OFFICE

The ISAC project received 89% of available hours during the year. This has kept 10 designers, often in teams of two or three, very busy preparing detailed designs for different aspects of the project, specifically and in order of weight: pre- and mass separator sections; target and exit modules; DRAGON experiment including the gas target design; remote handling hot cell, particularly the roof structure containing the elevator turntable device for servicing the target modules; MEBT beam line; low energy experimental yield station, lifetime and β -NMR experiments; RFQ diagnostic station for the 7-ring test and the drift tube linac tank #1.

The CERN contribution accounted for 9.2% of available hours with most effort concerned with the 66 kV resonant power supply and the fast blade profile monitor. Because of the concentration of effort required for ISAC, the only other significant TRIUMF project undertaken was the CHAOS LH2 target design. Continued assistance from the University of Victoria, TRIUMF remote handling personnel, and from students, joining us as part of their mechanical technology program at Camosun College in Victoria, has helped us cope with the heavy workload.

The demand for graphic art services continues to increase in support of seminars, conferences and publications. The addition of digital photography and the increasing use of Web sites for communication has enhanced these services.

MACHINE SHOP

The TRIUMF Machine Shop produced approximately \$133,000 worth of fabricated and machined components for the various on-site groups each month. During the year we sub-contracted work from the TRIUMF Machine Shop to local industry worth over \$536,000, all in small packages and none above \$25,000.

As shown in Table XXIII, ISAC was by far the major user of our services again this year manufacturing

Table XXIII. Machine Shop utilization.

ISAC	8.3%
Science	6.9%
CERN	5.8%
Cyclotron	2.2%
Affiliated institutions	1.5%
NSERC	0.5%
Accelerator	0.1%

the last 15 RFQ ring assemblies and associated components, vacuum chambers, beam lines, tantalum targets and DTL components.

A new fume and dust extraction system was installed in the welding and grinding areas which is proving to be a huge improvement in the air quality.

BUILDING PROGRAM

The Building department was presented with a variety of challenges, foremost being the upkeep of the TRIUMF site and buildings. Contracts were let for a wide range of maintenance and repair work such as blacktop repair, parking lot restoration after the departure of the ISAC contractors, repairs to buildings and reroofing of office trailer complexes as well as interior and exterior repainting of various facilities.

With the primary ISAC structure completed, the Building department was called upon to attend to second stage finishing work and also to identify and monitor the correction of architectural and structural deficiencies by outside consultants engaged in the ISAC project.

A major effort was required for the design and contracting of approximately 12 ft. high, cast in place, concrete shielding with channels for the target vacuum tanks, and modular steel shielding blocks in the ISAC target hall. Other work in the target hall was the design and casting of several large movable reinforced concrete shielding blocks to be located over the pre-separator magnet. Further, the construction of a set of steel stairs into the 14 ft. deep target module storage pit, as well as contracting cement parging and subsequent painting of the very roughly cast concrete walls and roof of the target hall.

An 11 ft. high and 3 ft. wide angular shielding wall consisting of stacked masonry blocks was designed and built in the mass separator room.

Other projects were the design and contracting of the TRINAT clean room on floor level 278.0 ft. below the experimental hall, and the building of the high voltage room in the ISAC service annex.

ELECTRONICS SERVICES

Overview

This year was a definite challenge to the Electronics Services group. The demands of fast-tracked ISAC installations as well as supporting the cyclotron program put personnel in high pressure situations at times. The group showed great dedication and abilities by inter-actively supporting areas that required assistance both inside our own group and for numerous groups on site.

Technical Support

Technical support had a large number of projects covering all facets of electronics this year. Support for ISAC included a major circuit design to allow remote control of the Power Ten power supplies used in the new beam line. Also for ISAC, the TRIMAC based ISAC west target protect system was designed, programmed and commissioned. When the Electronics Shop was overloaded, technical support assisted in the assembly of bias supplies, QSX modules, and numerous cables. For BNL Expt. 787 a schematic and PCB layout for the UTC system was worked on. Ongoing software maintenance was carried out for the BL2C safety and TRIM TRIMAC systems. CERN work included a control system and packaging of the fast blade scanner. Background work included continuing work on the CAMAC power and diagnostic module for the Controls group.

Experimental and Target Support

The major effort of experimental and target support was directed towards ISAC. These jobs include: installing cables for the high active cooling system and wiring them into the west target PLC control system; installing all the signal cables for the west target cooling manifold, and design of the west target/dump protect system. A prototype motor control box was built to support the mass spectrometer and help was also given in wiring up the Faraday cup. Ongoing maintenance of the existing systems included 1AT1, 1AT2 and the parity twisters. Experimental support was also involved with the building and wiring of the CERN 66 kV control system.

Electronics Shop

This was a most productive year, with 80% of shop time spent on ISAC requests for cables and modules: QSX, flow-switch, bias supplies, fiducial units and digi modules. Due to many last minute requests for ISAC cables, the shop was severely overloaded on a number of occasions. Shop personnel handled the demand very well with additional help from other members of the Electronics Services group. For CERN, a prototype 200 MHz calibrator filter 0917/1 module was assembled and all requisitions for parts for 250 more of these modules were processed and tracked.

Electronics Repair Shop

This was a busy year for the Electronics Repair Shop, with infrastructure support for the TRIUMF cyclotron and experimental program requiring most of the repair effort. Towards that end, a total of 253 items of electronic equipment were serviced, including: 18 terminals, 59 colour and monochrome monitors, 26 SCSI and LAN devices such as tape drives and

hard disks, 60 power supplies for NIM, CAMAC, high-voltage and miscellaneous units, 17 Nucleonics NIM or CAMAC devices, 22 items of test equipment such as oscilloscopes, and 51 other electronic devices mostly related to controlling or measuring the vacuum systems. In addition, 19 detector electronics devices were repaired in support of Expt. 787 at Brookhaven.

Microprocessor Support

The majority of the effort spent related to learning and working on ISAC control system software, specifically EPICS. The RFQ vacuum control system was the first live installation, followed by beam optics for all sections of the mass separator (IMT), and low energy beam transport (ILT), and beam optics to experimental areas ILZ and ILG. UNIX scripting languages were used to create automated systems for creation of EPICS display manager screens, and EPICS databases.

Ongoing consulting services to TRIUMF staff were provided as usual, in areas such as networking, PC support, and miscellaneous software support issues. Programming services provided include low-level drivers written for the Controls Hardware group's development of PCI to CAMAC interface hardware.

High level software support

During the year work was done on several ISAC components. Principally motor drives and controls were built, tested and installed for the diagnostics in the ISAC beam lines. A large shipment of defective rad-hard limit switches was identified in stores and procedures were created to disassemble, clean and reassemble the switches. Changes to the BL2A extraction probe control system were started. Work for CERN involved porting a signal analysis program from BASIC to C++.

Infrastructure work included changes to the CAMP (control and monitoring of peripherals) slow controls software for the Data Acquisition group for μ SR experiments. Changes were made to several TRIMAC based control systems. These included addition of a level sensor unit in the TNF target monitor system, and ongoing changes to the thermocouple monitoring program for the CCS.

A new Sun workstation was purchased and some of the software development for VxWorks real-time applications currently run on an obsolete DECStation was transferred to this computer.

PC support

Many tasks were completed throughout the year by PC support such as: distribution of Norton Anti-Virus about site, building new Pentium II PCs, refurbishing old 486s and providing them for users of older systems,

and upgrading most of the Design Office workstation hardware and operating systems. This year saw the demand for PC storage and memory capacity increase as applications continue to grow and images play a larger role in computer communications. This has led to many requests for hard disk installations and memory upgrades. There are a large variety of PC problems due to many variations in hardware, operating systems and installed applications. Much effort is being dedicated to reducing these problems by maintaining the site PC standard and detailing it on the PC support Web site. Support of the site's 400+ PC based computers logged 600+ repair calls.

Site communications

The data communications cabling for ISAC was a major project this year. In January, as the as-built drawings were not accurate, all conduits were traced, confirmed and mapped to AutoCAD drawings. February to June involved the twisted cable pulling, terminations, jumpers and commissioning. This was followed by fibre optics cable pulls, plus coordinating an external contractor for terminations and testing. Some of the ISAC work involved isolated systems due to the special grounding requirements in ISAC. Altogether, 124 twisted cables, and 3 pieces of fibre optics cables were installed. There are 212 data connections available, with a fibre optics backbone that connects to the site and the Internet. A Web page was set up and some 40 updated drawings for Ethernet cabling were published in the PDF format for easy access on site. Planning and estimating commenced for upgrading to 100base-T for both the chemistry annex and the main office building.

ELECTRONICS DEVELOPMENT

This year, the majority of the group's effort went to support of the ISAC control system design and installation. In addition, the CERN and CDS projects continued.

ISAC Support

The CAN-bus power supply controllers received minor upgrades and bug-fixes based on the initial operating experience. Especially, the power-up surge current was reduced. By November, 250 of these controllers were tested, installed and commissioned on the ISAC beam lines. Production of 100 additional units was organized towards the end of the year.

The Chalk River Danfysik current supplies were modified to be controllable via CAN-bus. New controller and adapter cards with modified embedded software were developed. These supplies are used to power

the ISAC pre-separator and mass separator dipole magnets.

For the ISAC control system several VME modules were developed:

- An 8-channel, variable gain beam current amplifier with transient digitizing capability was designed as a replacement for the TRIUMF 4-channel NIM QSX module. By combining the functionality of a current amplifier, an ADC and a transient digitizer into a single-width 6U VME module, significant savings were obtained in overall module cost, rack space requirements as well as installation and documentation effort. The module has eight gain ranges between 1 nA and 1 mA. For transient digitizing, storage is provided for 4 k samples per channel. Digitizing frequency is programmable up to 100 kHz. Binary output signals for driving 0518 harp monitor readout modules are provided. All module functions are programmable through VME registers. A first batch of 8 modules was produced, tested, and commissioned for ISAC.
- A 32-channel optically isolated digital I/O module was developed. Four groups of 8 channels each can be configured as input or output. 7 modules were produced, tested, and commissioned for ISAC.
- Design work was started for an 8-channel VME-based bias supply for beam current monitors which is programmable for 100 to 300 V output.
- For the ISAC ^8Li polarizer, design work on fibre-optics signal transmitters was started.
- A new version of a VME-based SDLC memory link was developed for connecting the TRIUMF central control system to the beam line 2A PLC. It was implemented in software using a Motorola MV162 CPU with an SDLC capable industry pack.

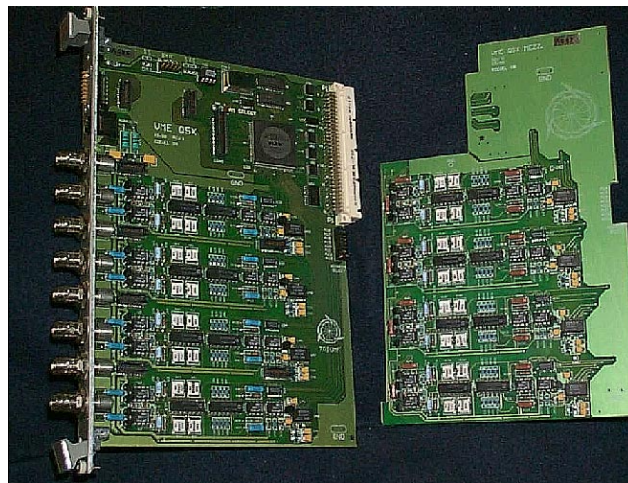


Fig. 152. The VQSX module, an 8-channel VME based beam current amplifier and transient digitizer.

CERN Support

Early in the year, 5 more timing surveillance VME modules (TSM) were built, tested and shipped to CERN. The empty events problem, which was reported in the previous year, was investigated and found to be caused by distortion of the external clock in some VME crates at CERN. Circuitry enhancements to overcome this problem were designed and tested. Another batch of 8 TSMs was built in November.

Support was given to the fast blade scanner project. Software was written under the VxWorks real-time operating system for several VME devices. This included basic driver support and a program file loader for the Galil 1380 motor controller, control and data acquisition drivers for the CERN DPM memory module, and control and data acquisition drivers for the INCAA VD71 transient digitizer. In order to simplify the development work on the blade scanner, a graphical user interface was developed by interfacing these drivers to EPICS.

Support of the Kicker group continued with modifications to the control unit and assembly of the 66 kV

resonant charging power supply. Before shipment to CERN all changes were consolidated and a couple of PCBs were redesigned.

CDS

The controllers for the 30 kHz low voltage and 100 kHz high voltage power supply inverters were tested. The high voltage transformer was driven and the stack voltage profile measured to verify that the compensation design was acceptable. The transformer was tested in SF6 to 860 kV output but suffered from sparking at higher voltages.

Work continued on the 100 kHz inverter to improve its operation and power handling capability. The low voltage core was tested to 3 kW into a resistive load.

Nordion TR30

Minor improvements and repairs were carried out on the TR30 rf controller as part of maintenance work on the rf system. After the maintenance work was completed data were collected on the new operating conditions in order to better understand the operation and to provide reference data for the future.

CERN COLLABORATION

INTRODUCTION

By the end of 1997 a large amount of equipment had been delivered to CERN in time for the 4 month shut-down at CERN for the PS (Proton Synchrotron) Conversion and the PSB (Booster) energy upgrade. This equipment included: 36 transfer line power supplies and 8 high voltage supplies produced by Inverpower Controls; several smaller supplies and control boards produced by other firms; 5 large rectifier transformers for the Booster main magnet supply made by Ferranti-Packard; a 20 MVar static var compensator assembled by GEC-Alsthom in the UK with some components made in Canada; 7 water-cooled BT quadrupoles, 5 DVT steering dipoles and 3 larger BVT bending magnets for the PSB to PS transfer line assembled and field mapped at TRIUMF; and ferrite rings for the PSB cavities and several designs of higher order mode dampers for the PS cavities.

This equipment was installed and commissioned at CERN and the collaborators at both TRIUMF and CERN were pleased to find that the equipment worked reliably at start-up in March, and has given little trouble during beam operations in 1998. There are still a few active tasks related to the PS Conversion project. A second order of 100 kW and 250 kW transfer line power supplies was placed in October. These supplies will be designed and built by an alliance of three firms in Ontario, I.E. Power, Inverpower Controls and DPS. Delivery of the first 100 kW unit is scheduled for April, 1999. Two other tasks are the design and fabrication of a prototype fast blade scanner and 4 sets of X and Y fast wire scanners for the PS Booster. The fast blade scanner has been built and is being tested at TRIUMF. Tuning of the servo motor and blade mechanism is proceeding, but achieving the fast response with smooth motion of the blade is proving difficult. The design of the fast wire scanners is based on a CERN design for the PS and this work has started.

The production run for the front-end electronics for the SPS beam position monitors was completed during the year. First, a run of 40 of the 200 MHz modules was completed and these were tested on the SPS during the summer. Then the remaining 245 modules, with some minor improvements, were assembled by a local firm and sent to CERN before the end of the year. A problem with the TSM (timing surveillance modules) produced by TRIUMF was resolved and two batches of these modules were built and sent to CERN during the year.

The prototype twin aperture quadrupole manufactured by ALSTOM Canada (previously GEC-Alsthom) in Quebec was completed and shipped to

CERN for testing. Magnetic field measurements show that the harmonic content is larger than desired and is correlated to the physical measurements of the pole gaps. Even tighter assembly tolerances than originally specified will be required. A number of improvements have been proposed by CERN, TRIUMF and ALSTOM engineers for the series production. The production of a second set of prototype coils with fewer splices is under way and a contract for new punching dies for the improved lamination shape will be let in January, 1999.

The fabrication of the prototype 60 kV resonant charging supply for the LHC injection kickers was completed at TRIUMF and the supply sent to CERN for testing with a prototype pulse forming network (PFN) built at CERN. High voltage measurements carried out in August confirmed the design predictions from PSpice, and the group has now moved to the series production. Five power supplies, 9 PFNs and 20 thyatron switches are to be manufactured by TRIUMF over the next few years.

The collaboration with the PS radio frequency group is essentially complete. All of the required higher order mode dampers and filters for the 40 and 80 MHz cavities were delivered to CERN. One of the prototype high voltage supplies was returned to Inverpower for retrofitting to the later design.

In the beam dynamics area work has continued on studies of dual harmonic acceleration in the PS Booster, with participation in machine development runs at CERN. Space charge was added to the ACCSIM code along with several other improvements. The task to study impedances of the LHC components continued with calculations and measurements on kickers, and calculations of the effect of beam screens and pumping port shields.

The optics of the LHC cleaning insertions to provide efficient momentum and betatron collimation have been settled. The new solution replaces some of the warm quadrupoles with cold quadrupoles, and to arrange for one of the warm quadrupoles in each of the four central sets to be powered for symmetric focusing. This reduces the number of twin aperture quadrupoles to 48 plus spares. The task of generating a computer model to simulate beam behaviour in the SPS and LHC for tune control has made good progress and beam measurements on the SPS and HERA at DESY have been used to validate the code.

The first meeting of the LHC Board was held at CERN at the end of March. This Board has representatives from non-member states who are contributing

to the LHC (Canada, India, Japan, the Russian Federation and the USA), along with representatives from France and Switzerland who are making special contributions as host countries.

A second contribution to the LHC is included in the request for TRIUMF funding for the next five-year plan (2000–2005). This request would allow completion of the series production of twin aperture quadrupoles, the LHC kicker work and power supplies for the warm magnets in the cleaning insertions.

BEAM DYNAMICS

Second Harmonic in PSB

Dual harmonic acceleration

The PS booster has two rf systems. The fundamental rf is synchronized to the beam fundamental, while the second harmonic may be locked either to: (a) the beam or (b) the fundamental rf. In 1997, operating with harmonics 5 and 10, the longitudinal instability occurring when type (b) control is used was diagnosed as a sextupole mode (see Fig. 153), with growth rate almost independent of beam current. The dual-harmonic confining potential causes bunches that exceed a critical length to lose Landau damping of their within-bunch oscillation modes, thus making them susceptible to being driven by the low-level rf system. The relative amplitude and phasing of the two rf systems varies widely during the acceleration cycle, and a computer program BTF-FAST2 was written to compute the corresponding beam transfer functions (BTFs) for amplitude and phase modulations. In fact, there are two BTFs – one from fundamental rf to beam (B_{11}) and another from second harmonic to beam (B_{12}).

Measurements during the year showed that the instability survived the migration from harmonics 5 and 10 to harmonics 1 and 2, and from analogue to digital

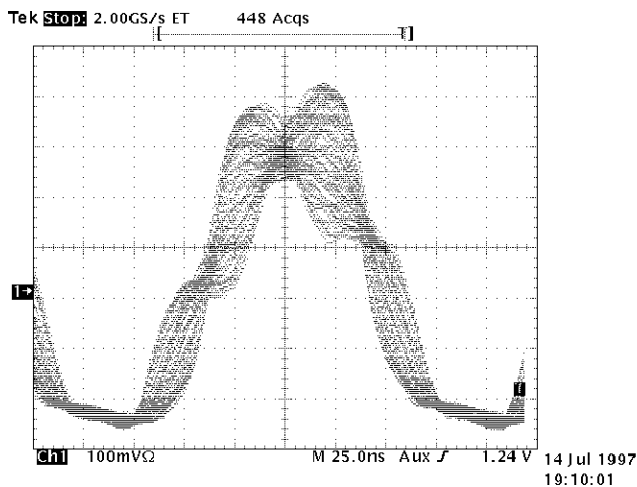


Fig. 153. Overlays of sextupole oscillation time series.

control and the 5 times smaller delay-induced phase lags; they also confirmed that switching to type (a) control is still sufficient to avoid the instability. Based on a mixture of numerical modelling of the beam and analytic modelling of the low-level rf systems, it was realized that the stabilization mechanism arises from a quirk in the control topology. As is well known, a feedback system with large gain and 180° phase lag is unstable. With type (b) control the beam response is $B_{11} + B_{12}$, whereas with type (a) the beam response is roughly $B_{11}/(1 - B_{12})$. In this latter case, the B_{12} BTF acts as a phase-advance network where the gain of the composite transfer function is large, thus avoiding the 180° lag condition.

Acceleration of hollow bunches

The peak transverse space-charge tune-shift can be reduced if the longitudinal charge density is reduced. One means to achieve this is dual-harmonic rf; an alternative or complementary procedure is to create bunches with a hollow distribution in longitudinal phase space. If high-harmonic empty buckets are decelerated into the core of an unbunched coasting beam, and this is subsequently captured into a normal rf bucket, then the result will be a hollow beam. Preliminary tests, performed in the early summer with low current beams, indicated the procedure to be feasible as demonstrated in Fig. 154.

Space-charge forces complicate the procedure: transverse forces limit the dwell time and longitudinal forces modify both the high-harmonic empty buckets and the fundamental-frequency full ones. Numerous computer simulations of the beam dynamics with an improved space-charge algorithm but no rf control loops indicated that the hollow structure could be maintained, provided the beam current is not too great. These simulations also showed that fine-tuning

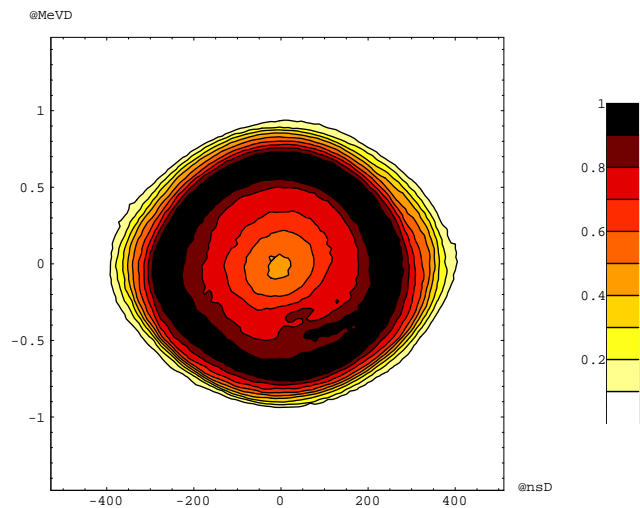


Fig. 154. Tomographic reconstruction of phase space.

of the empty bucket deposition becomes difficult at high current.

Experimental studies in the fall confirmed these predictions and also indicated a further problem: an instability occurs when hollow bunches are accelerated in dual-harmonic buckets. The dominant oscillation mode seems to vary with time, and the oscillation can be tamed temporarily by running the second harmonic rf open loop.

Measurements later in the year concentrated on using the beam transfer function measurement (BTfM) to carefully specify the initial beam conditions and precisely target the central momentum of the empty high-harmonic buckets compared with that of the beam. A procedure was devised that allows $h = 15$ bucket deposition followed by either a fast BTfM or capture into $h = 1$ buckets during a 12 ms flat-bottom. Despite these improvements, repeatable and reliable capture and acceleration of a high-intensity beam was still elusive. A large amount of experimental data was acquired and awaits quantitative analysis.

Injection and Collimation in the PSB

This task involves the development and support of the ACCSIM multi-particle tracking and simulation code. This year efforts were concentrated on implementing an improved model of transverse space-charge, going beyond the existing DQ package, which is able to give very efficient estimates (and simulations) of space-charge tune-shifts, but which is not fully self-consistent in its tracking of the macroparticles ensemble.

A survey was conducted of the common field-solution and tracking (integration) techniques. These come from the plasma physics realm and have been applied to linacs and beam lines but seldom to rings, where the ensemble must be tracked for many revolutions. Moreover, the popular FFT-based field solvers do not lend themselves well to beams with a large and growing halo, a feature of concern for intense-beam multi-turn injection schemes.

A field solver was developed which is a hybrid of fast-multipole (FMM) and particle-in-cell (PIC) techniques. It can accommodate charge distributions with any number of halo particles at arbitrarily large amplitudes, and at equivalent spatial resolutions it is competitive in speed with FFTs. ACCSIM tracking of K-V beams in test lattices with this method produced the expected fields, single-particle tunes, and envelope tunes. A paper on this work was presented at the Shelter Island Workshop on Space-Charge Physics in High Intensity Hadron Rings.

Other additions to the code were: a generalized rf cavity element allowing arbitrary (non-integer) harmonics and phases; rf voltage plotting; interactive injection steering; and import and export of particle en-

sembles, allowing generation and stacking of “beam-lets” at arbitrary locations.

Beam Stability

LHC abort kicker

The broadband impedance of the abort kickers has been investigated using coaxial wire measurements and numerical simulations, especially the screening effect of a thin metallized layer on a ceramic pipe around the beam. The purpose of the metallic layer is to reduce the impedance by shielding the beam from the kicker components, and also to reduce the heat load on the ferrite; at the same time the layer must be thin enough to be transparent at low frequencies so that the magnetic pulse from the kicker can penetrate it.

The measurements showed that a $0.1\ \mu\text{m}$ -thick layer of copper (or $0.4\ \mu\text{m}$ -thick layer of chromium) with a sheet resistivity of $0.1\ \Omega/\text{square}$ can effectively shield the kicker environment from electromagnetic fields generated by the LHC bunches at frequencies from 0.5 MHz to 1 GHz (the most dangerous range), even though the skin depth of copper at 1 GHz is $2\ \mu\text{m}$ and some theories predict that a layer that thin should be transparent in this frequency range. It has been found that, provided there is good electrical contact between the beam pipe and the conducting layer, the image current from the beam pipe will almost entirely pass through the layer. The total impedance of the kicker is therefore determined by the impedance of the conducting layer, which normally is very small (less than $1\ \Omega$) and is virtually unaffected by the kicker elements such as magnet coils, cables, etc., located outside the pipe.

Theoretical and experimental work related to the screening effect of a thin metallic film were discussed at a special mini-workshop held at CERN in November. The measurement results led to rejection of a theoretical model for the screening efficiency of a metallized ceramic pipe which has been widely used in kicker designs for more than a decade. A new theoretical model has now been developed which explains both the experimental results and the failure of the old model.

LHC injection kicker

The longitudinal impedance of the LHC injection kicker has been measured using the coaxial wire method and analysed using MAFIA 3D simulations. The measurements focused on the properties of ferrite specimens, which then were used to calculate power losses in the kicker.

LHC beam screen

The new “ribbed” design for the LHC beam screen, intended to better absorb synchrotron radiation and

avoid promoting electron cloud instability, has been found to make a relatively small (but not negligible) contribution to the total LHC broadband impedance budget.

SPS pumping ports

3D MAFIA impedance calculations of the proposed shields for the roughly 800 SPS pumping ports (thought to be the major contributors to SPS impedance) have been made in an attempt to optimize their designs.

Beam Optics and Collimation

This year has seen the successful determination of optics which will allow efficient momentum and betatron collimation in the LHC cleaning insertions (IR3 and IR7 respectively).

The optics solutions available in early 1998 required too much strength from the warm quadrupoles in the straights (for which the field quality was rather uncertain at maximum excitation) and from the trim quadrupoles in the dispersion suppressors, especially after a 1997 redesign introduced special cold quadrupoles longer than the standard ones in the arcs, and shortened the trims from 1.7 m to less than 1.3 m. Moreover, the maximum achievable normalized dispersion $D_{xn} \equiv D_x/\sqrt{\beta_x}$ at the primary collimator in IR3 was 0.16, just marginal for protecting the arcs from off-momentum halo protons. These optics were somewhat constrained by the focusing-defocusing quadrupole antisymmetry about the midpoint of the insertion (Fig. 155, top) imposed by the use of twin aperture quadrupoles wired so that if one beam were focused the other would be defocused.

The basic feature of the new solutions is to relax this constraint, increasing the optical asymmetry and giving improved performance with reduced overall focusing strength. To achieve this, we suggested converting some of the 3 m long modules making up each warm quadrupole so that they focused both beams (realized in practice by changing the coil connections).

The current arrangement, adopted for LHC version 6 (Fig. 155, bottom), has one of the new “symmetric” focusing modules (black) in each of the four central

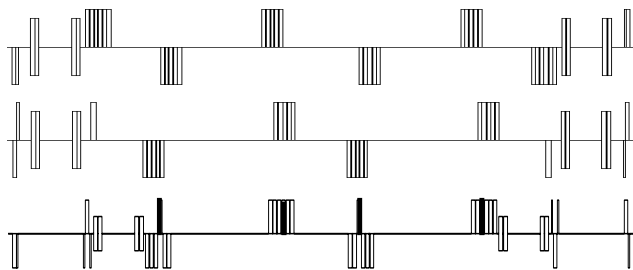


Fig. 155. Evolution (from top to bottom) of the IR3 straight section.

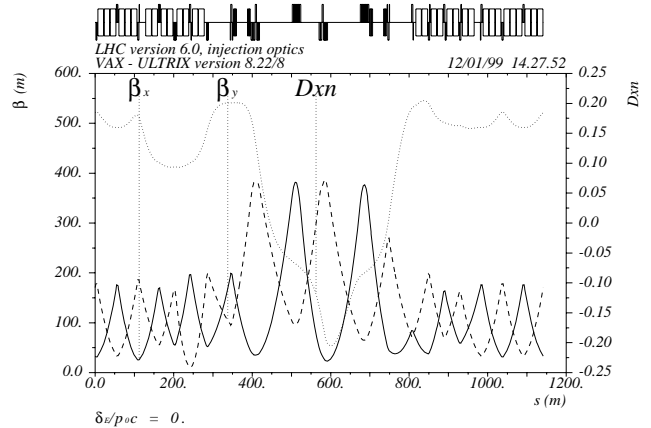


Fig. 156. Lattice functions for IR3 in LHC version 6 (straight section and both dispersion suppressors).

quadrupoles. With such a set-up, a peak normalized dispersion 0.2–0.24 (depending on the LHC working point) can be achieved (Fig. 156), and no modules need work near their top field.

It may also be noted that the dispersion suppressor quadrupoles have reverted to standard length, with 1.15 m long trims, and that the outermost warm quadrupole has been replaced by a standard cold one (to save space), requiring the dogleg magnets to be shifted to its midpoint side to make the cryogenic connections easier. The quadrupole hardware needed for the two straights is $2 \times 4 \times 6 = 48$ warm modules (of which $2 \times 4 = 8$ are symmetric), and $2 \times 2 = 4$ cold (trim+quadrupole+trim) groups replacing 24 warm modules.

Other tasks completed include: implementation of the new IR3 and IR7 lattices into the LHC database; tuning for different LHC working points; and development of the code “Distribution of Jaws” with the aim of studying how collimation is affected by misalignments of the collimator jaws and quadrupoles and by orbit errors left after simulated correction by DIMAD.

Simulation Tool for LHC/SPS Tune Control

An important issue for LHC operation will be the continuous monitoring and correction of the betatron-tunes and chromaticities in the presence of time-varying magnet non-linearities. In collaborating with CERN’s efforts to develop a system to do this, TRIUMF is generating a computer model to simulate the proton beam’s behaviour, while CERN looks after the control side. The FASTMAP suite of tools has therefore been written to facilitate high-speed tracking using COSY-generated maps, and to customize the maps to at least 12 tuning parameters (“knobs”) in addition to the six kinematic variables. FASTMAP has also been interfaced with a Measurement front end capable of simulating measurements of tune, chromaticity and

coupling by a variety of techniques. Using FASTMAP involves the following steps:

1. TWISS2COSY converts SPS and LHC lattices from MAD8/9 file format into a FOX file executable in COSY.

2. COSY is used to obtain a set of parameterized maps. As memory and performance limitations in COSY make it difficult to work with more than 2 or 3 free parameters for a 6th order map, the requirement for at least 12 free parameters means that several maps have to be produced.

3. MAPMERGE combines all the parameterized maps into one table (a map-like object that depends on all the parameters). Note that the output file is not a “map” in the strictest mathematical sense unless all cross-coefficients are supplied.

4. The FMLIB objects are used to read the MAPMERGE output, evaluate parameters in the map, collect coefficients, and perform the particle tracking.

An important feature of the TWISS2COSY converter is its ability to identify repetitive parts of the lattice and factor these out to produce the shortest possible representation. The maps for repetitive sequences can then be pre-computed and used repeatedly in the final stage of calculating the map for the whole ring, with a considerable saving in computer time.

The advantage of tracking with FASTMAP rather than COSY arises from a reduction procedure in which, prior to tracking, numerical values are substituted for symbolic parameters, allowing coefficients of like-order kinematic monomials and polynomials to be collected, so that potentially very large maps collapse to 6th order in the six kinematic variables.

In order to validate FASTMAP the following sets of measurements were completed at the SPS:

1. Emittance growth. These measurements were performed with 26 GeV lead ions from the main SPS cycle. The beam was displaced from the closed-orbit by a kicker, resulting in filamentation due to the amplitude dependence of the betatron-tune, and eventually an increase in the rms emittance.

2. Betatron-tune. The tune was measured as a function of the main quadrupole strength, using the 26 GeV proton beam of the Machine Development cycle.

3. Chromaticity. The SPS lepton cycle was used to study the effect of chromaticity changes on the betatron-tune spectrum, by varying the sextupole strength and observing the change in amplitude of the synchrotron sidebands with respect to the main peak. Lepton maps were computed for this case.

For all three measurements the experimental data were in good agreement with the FASTMAP simulations, so we have concluded that the model correctly describes these features. As the quadrupole and

sextupole strengths are parameterized quantities in FASTMAP, their measurement provides an important test of FASTMAP’s use of parameterized maps and the correct representation of the lattice by them. The results also allowed us to calibrate the kicker, quadrupole and sextupole strengths in terms of their parameterized values.

FASTMAP has also been used in support of experiments on HERA at DESY to test a procedure for measuring LHC chromaticity by analyzing a beam’s head-tail motion. The measurements confirmed FASTMAP predictions and made it possible to test new hardware and algorithms. In particular, it was shown possible to excite the beam sufficiently with a chirped pulse.

CONTROLS AND INSTRUMENTATION

Fast Blade Profile Monitor

The fast blade scanner (FBS) is intended for destructive diagnosis of the betatron amplitude distribution of charged particles in the CERN PS Booster by measuring circulating beam current versus blade position. The device accelerates from rest to 5 m/s and decelerates to a stop in 50 ms (moving a distance of 25 cm) while recording its position with 0.1 mm accuracy. The FBS will complement measurements made with wire scanners.

The two Y-shape arms carrying the blade mounting are actuated through a pivot-bellows mechanism which in turn is driven by a bell-crank double linkage. The principal mechanical items (servo motor, driver amplifier and motion controller) arrived in 1997 and were bench tested with a simple dummy load. Assembly of the blade mechanism was delayed until the summer, pending arrival of several sets of precision bearings. During the fall fabrication of the vacuum box and stand progressed swiftly, but e-beam welding of the beam-pipe bellows proved difficult and parts had to be delivered from CERN. Testing and tuning of the blade mechanism and controller progressed in parallel, but very slowly. The blade assembly appears to have a mechanical resonance and tuning of the system for fast response is not compatible with damping of that resonance.

During December, it was realized that the proprietary controls and acquisition hard/software were inadequate for the stringent timing accuracy demanded by the position-acquisition specification. In response, it was determined to separate control from acquisition and build a VME-based system around digitizing and memory components borrowed from CERN. In addition supervision of the motor controller was moved from a PC to a VME host.

Software was written under the VXworks real-time operating system for several VME devices. This in-

cluded basic driver support and a program file loader for the Galil 1380 motor controller, control and data acquisition drivers for the CERN DPM memory module, and control and data acquisition drivers for the INCAA VD71 transient digitizer. In order to simplify the development work on the blade scanner, a graphical user interface was developed by interfacing these drivers to EPICS.

In parallel, work on building remotely controllable breakers for the power supply, installing safety interrupts and fail-safe break progressed swiftly. It is anticipated to test the VME-based control in February, 1999, and complete tuning of the FBS assembly in March, 1999.

Fast Wire Scanner

The fast wire scanner provides a non-destructive measurement of horizontal or vertical beam profiles by rapidly moving a wire across the beam and using downstream scintillators to measure the beam scattered by the wire. A design exists for the PS and this design must be modified for operation in the four rings of the PS Booster. A TRIUMF designer visited CERN in July to learn about the new requirements and design work was started towards the end of the year. The plan is to build a first prototype by March, 1999, and after approval from CERN, produce 9 more scanners, 4 horizontal, 4 vertical and a spare, for installation during the winter 2000 shutdown.

Upgrading SPS Orbit Observation System

The 240 front-end electronics for beam position measurement in the SPS are to be replaced with new compact, modern modules designed at TRIUMF during 1997. The modules consist of a variable phase-shifter, 200 MHz band pass filters and a calibration unit. In May, 1997, CERN asked for the delivery of an initial batch of 40 by February, 1998 and a further 240 modules by November, 1998 with delivery starting in September. These large production runs, with their very demanding tolerances for phase matching and low insertion loss, were a significant achievement and the outcome of many incremental improvements in the components, the manufacturing/assembly process and the quality assurance procedures.

Initial batch 0917/1 modules

Most parts for the run of 40 modules arrived by January and were forwarded to Link Technologies for assembly. However, the filters from the Microwave Filter Company were delayed due to a problem with silver plating. In February, most of the module construction, including automated parts placement, soldering and assembly was satisfactorily completed by Link Technologies. The modules were finished at TRIUMF by

attaching the rf hybrids, phase shift capacitors, filters and precision-length internal cables. Two testing programs were written for the HP8753D network analyzer which plays back pre-recorded sequences of steps to set up tests and make measurements. Some electronics were constructed to allow the analyzer to control the mode and phase shift of the module being tested. In this way, the time to test and document a module's performance was reduced from hours to minutes. A CERN engineer visited TRIUMF in February to help with quality assurance, and the TRIUMF engineer responsible for this task visited CERN in July to work on calibration of the new MOPOS with the 40 modules installed in the SPS (see Fig. 157).

Much was learned from the first production run of 40 modules and several changes were made to the design. M/A-Com quadrature hybrids were found to be more consistent in their SWR than the Olektron hybrids, and were substituted throughout. The filters used for the 40 modules were not as precisely matched as desired; and 11 filter pairs were rejected. Two manufacturers were asked to build a similar filter but using a precision-machined aluminum casing in place of a folded brass sheet. Lorch responded with greatly improved filters costing twice that of the original, and Microwave Filter failed to meet the May deadline for producing a prototype. The anticipated savings in time, in not having to adjust the substitute filters, and their impeccable performance were deemed sufficient reasons to place the order with Lorch. Link Technologies proved themselves capable and resourceful and it was decided to have them attach all the components, make the phase matching cables and run the module test program.

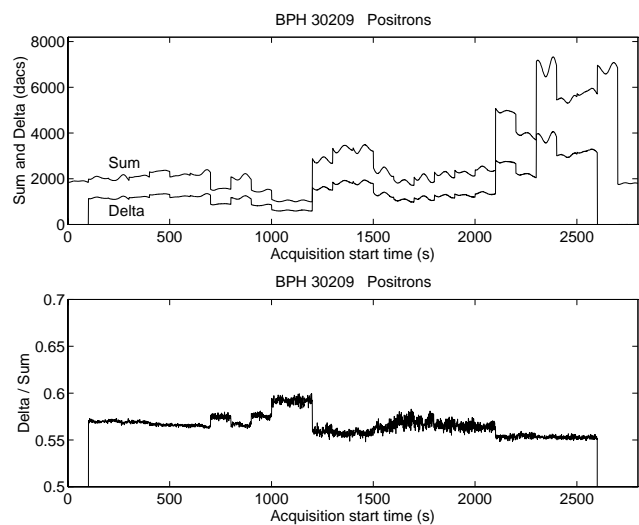


Fig. 157. Closed-orbit (at one location) versus turns in SPS; upper figure is sum & difference; lower figure is difference/sum.

Series production 0917/2 modules

Most of the parts for the further 245 modules were delivered by June ready for sorting into kits. However, delivery of two critical components had to be carefully staged. The customized quadrature hybrids arrived in allotments spanning July to September. The 245 filter pairs in machined aluminum cases arrived in allotments during August and September. The printed circuit cards were ordered last, and the small rf shields and front panels were machined locally. The first pair of improved filters was delivered to CERN in August and tested on-line with proton and lepton signals. Results were favourable and the order for 245 filter pairs was increased to 285. During the summer Link Technologies was bought by US-based Aimtronics.

The automatic test set-up, demonstrated at CERN in August, was later modified at TRIUMF to suit the network analyzer's available memory. Tune up sequences were added to allow the Aimtronics technicians to cut the internal cables to length for phase matching and to adjust the variable capacitors to centre the phase adjustment range. The tests consist of filter performance, the two tuning procedures and a final test of the complete module, with thorough documentation at all stages.

By September the first 100 modules were assembled and the internal tuning and matching of the first 5 finished modules were tested at TRIUMF and found to be excellent. The production run then moved into full swing: by November, 151, and by December, a total of 242 of the 0917/2 calibrator modules had been shipped to CERN. In December it was decided to move the forty 0917/1 series modules to a beam transfer line and substitute them in the SPS with forty more 0917/2 modules. Orders for additional parts were placed in January, 1999.

Design and Production of VME TSM

Early in the year, 5 more timing surveillance VME modules (TSM) were built, tested and shipped to CERN. The empty events problem, which was reported in the previous year, was investigated and found to be caused by distortion of the external clock in some VME crates at CERN. Circuitry enhancements to overcome this problem were designed and tested. Another batch of 8 TSMs was built in November.

POWER SUPPLIES

Booster Transfer Line Power Supplies

All Inverpower Controls power supplies and ancillary equipment were delivered, with installation and commissioning completed by the end of February. The supplies have proven to be reliable and have now been

in service for a period of about 8 months. The topology used for the batch 1 supplies was selected as the basis for the design for the dipole supplies which were required for batch 2.

After some delay, due to other commitments of the PS/PO group, specifications for the batch 2 supplies were generated and sent out to tender in the summer. Approval for purchase of the batch 2 supplies was received in October, with delivery aimed for installation during the spring 2000 shutdown at CERN. The contract was awarded to the alliance of I.E. Power, Inverpower Controls and DPS. Design reports for the 100 kW and 250 kW supplies have been forwarded to CERN, with construction of the first 100 kW unit scheduled for the beginning of 1999.

Booster Magnet Power Supply Transformers

The 5 new Ferranti Packard transformers for the booster main magnet power supply were installed and commissioned successfully in January. Figure 158 shows one of the transformers in location.

Reactive Power Compensator

The new static VAR compensator supplied by GEC Alstom was installed and successfully commissioned in March (Fig. 159).

MAGNET DEVELOPMENT

Transfer Line Magnets

Quadrupole and dipole magnets of four different designs, designed and manufactured by TRIUMF and described in last year's Annual Report, have been installed in the PSB to PS transfer line, except for one BV2 dipole which will be installed in 1999. These magnets have laminated yokes and higher current capability than the solid pole magnets they replace. Two CERN reports, SL-Note-98-052 and SL-Note-98-063, were written jointly by the CERN and TRIUMF

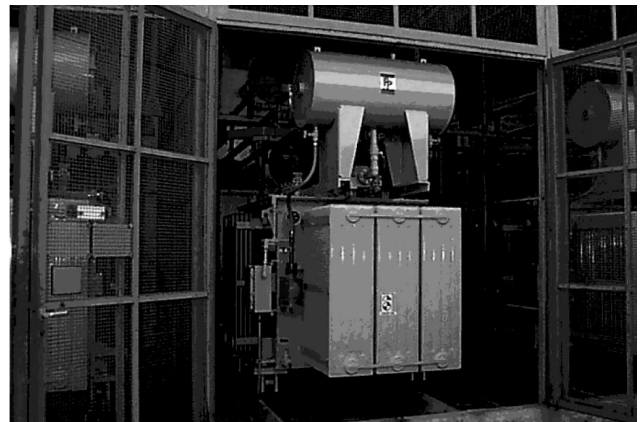


Fig. 158. One of the five large rectifier transformers for the PSB main supply made by Ferranti Packard.



Fig. 159. Static VAR compensator for transient suppression made by GEC Alsthom, UK (40% Canadian content).

collaborators describing the design and parameters of these magnets and the results of the magnetic field measurements.

Cleaning Insertion Magnets

The prototype twin aperture quadrupole manufactured by ALSTOM Canada Inc., arrived at CERN May 7 (see Fig. 160). Magnetic measurements were started in September and discussed at an October

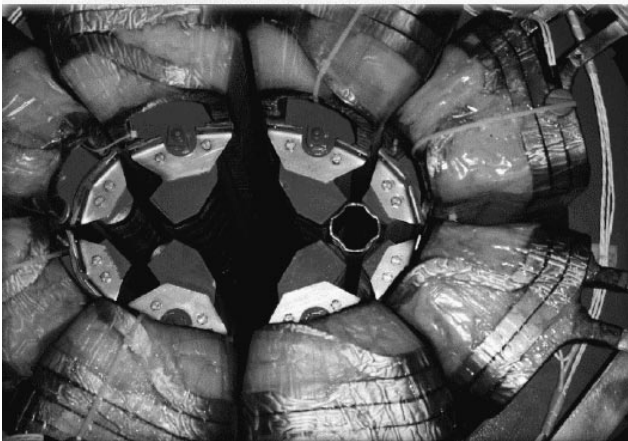
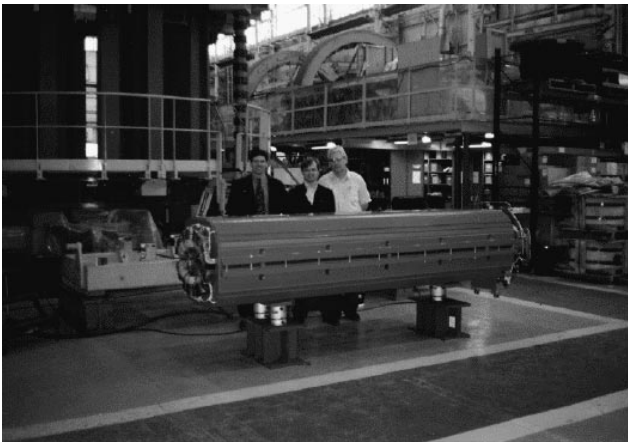


Fig. 160. The 3 m long twin aperture quadrupole made by ALSTOM Canada Inc.

meeting between CERN, TRIUMF and ALSTOM. At a low current of 41 A (LHC injection) the low order multipole components are about a factor of 5 too high. The dipole, quadrupole, sextupole and octupole components are respectively 150, 10000, 20 and 20 LHC units. At high current (710 A) they are a bit lower but still very large: 70, 10000, 15 and 15 units.

The field errors do correlate with the dimensions of the pole gaps as measured at CERN with a “Grabnermeter” device. It has now been determined that the production magnets must be assembled with much higher tolerances than originally envisaged. Thirteen methods of improving the design magnetically were identified. The shape of the laminations was fixed in early December. A contract for new punching dies is presently being considered.

A contract was awarded to ALSTOM Canada in July to make new prototype coils with at most 4 splices per coil. These prototype coils are expected to be finished in late February, 1999. Before the series production of the magnets can start CERN must specify more completely the changes they wish to make to the design. CERN is working on purchasing the steel and conductor needed. TRIUMF expects to award the series production contract for the first 25 magnets during the summer of 1999.

KICKER MAGNETS

LHC Injection Power Supply and PFN

A prototype resonant charging power supply (RCPS) was designed and assembled at TRIUMF (Fig. 161). The RCPS has a 2.6 mF storage capacitor bank charged to 3 kV. A gate turn-off thyristor (GTO) is used to switch the energy on the capacitor bank onto the primary of a 1:23 step-up transformer of low leakage inductance. The output of the secondary is being transferred to two 5 Ω pulse forming networks (PFNs) through two coaxial cables, two diode stacks and two 70 Ω resistors. The RCPS is designed so that the PFNs can be charged up to 66 kV at a repetition rate of 0.2 Hz. An LHC injection system will consist of a RCPS, which has two parallel outputs, to charge two 5 Ω PFNs. The PFN has thyratrons at both ends. The main switch (MS) thyatron will be connected to a 5 Ω transmission line kicker magnet, via 10 parallel 50 Ω coaxial cables, and the kicker magnet output is connected to a 5 Ω resistive terminator. The dump switch (DS) thyatron will also be connected to a 5 Ω resistive terminator. The DS thyatron is used to control field flat-top duration to be either 4.25 μ s or 6.6 μ s. The prototype PFN was built at CERN (Fig. 162).

During March acceptance tests were carried out on the prototype RCPS in the presence of CERN collaborators. Tests with an open circuit and a short-circuit

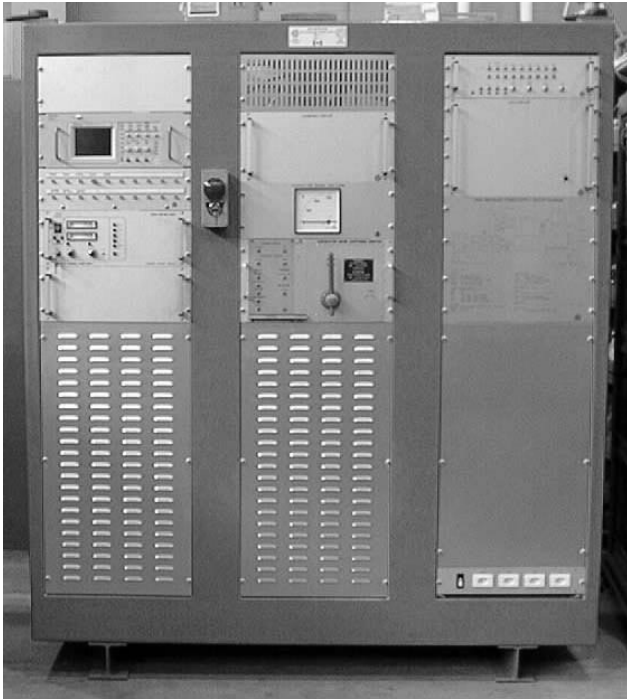


Fig. 161. Prototype RCPS.



Fig. 162. Prototype PFN with capacitors and coil installed.

secondary were carried out. The RCPS was also tested at frequencies up to 0.2 Hz and voltages, on 2 dummy PFN loads, of 66 kV. The measured charge time of less than 840 μs and effective charge time of less than 1300 μs both improved upon the specified maximum values of 1 ms and 2 ms, respectively.

A stability test was carried out on the RCPS for 46 hours of continuous operation. The RCPS was operated at 55 kV and 0.1 Hz and the voltage on one of the dummy loads was measured periodically. The maximum spread in voltages was $\pm 0.085\%$ over two days, whereas the maximum permitted spread is $\pm 1\%$. At the end of the test, voltages were measured every

10 s and the maximum voltage spread was $\pm 0.03\%$ for 30 pulses (the maximum permitted spread is $\pm 0.1\%$ over 12 consecutive pulses for LHC injection). Measurements taken from a cold start had a maximum voltage spread of $\pm 0.016\%$ for 14 pulses. The RCPS passed all tests.

Low voltage measurements (up to 10 kV) were carried out on the prototype PFN during May. Analysis of measurements indicated that the inductance of each cell of the PFN is approximately 4% greater than predicted. This is now attributed to the coil inductance being high due to the coil tubing being distorted during winding, resulting in an increased mean radius of the coil.

The RCPS was shipped to CERN in June and set up to prepare for high voltage testing of the prototype PFN. High voltage measurements (up to 66 kV) were carried out starting in August. The test circuit did not include a kicker magnet. In addition the second output of the RCPS was connected to a dummy load, which was designed and built at TRIUMF.

A FET-based pulse generator, designed and built at TRIUMF, was used to generate a “known” voltage pulse for calibration purposes.

It is not possible to use the available adjustments in the probe compensation box to meaningfully measure flat-top ripple and post pulse ripple in the $\pm 0.1\%$ region. Thus a procedure was developed to calibrate the high voltage probe and oscilloscope amplifier:

- Use the FET-based pulse generator to generate a “known” waveform. Compensate the probe and store this reference waveform digitally. The compensation at this stage is only approximate;
- Comparison of the reference and “known” waveforms gives the calibration curve (for a given waveform shape), as a function of time, for the probe and oscilloscope amplifier (for a given gain).

Figure 163 shows predicted field for a 33 cell transmission line type kicker magnet. The prediction is obtained by using PSpice to stimulate the equivalent circuit of the kicker magnet using the voltage waveform measured across the MS terminator, for a PFN voltage of 55 kV.

Detailed measurement and analysis of pulse shapes show:

- a) the top of the measured voltage pulse was flat to within $\pm 0.3\%$ for the “as designed” PFN, i.e., without any adjustments to the PFN component values.

- b) Mismatching the DS terminator resistor by approximately 10%, and measuring the MS terminator voltage, confirms that, for a PFN voltage of 55 kV, the MS thyatron (CX2003) blocked the reverse voltage.
- c) The 0.2% to 99.8% kicker magnet field rise time is 834 ns (shown between arrows on Fig. 163), and is within specification (900 ns).
- d) The 99.8% to 0.2% kicker magnet field fall time is 2.94 μ s (shown between arrows on Fig. 163), and is within specification (3 μ s).
- e) The kicker magnet field is within $\pm 0.2\%$ during a 4.69 μ s flat-top (shown between arrows on Fig. 163).

The LHC injection design requires that the flat-top and post pulse field are flat to within $\pm 0.5\%$.

In order to fully test the RCPS, a series of tests were carried out where the MS and DS thyatrons were deliberately turned on at times which are known to test the integrity of various RCPS and high voltage components. If the thyatron turns on just after current zero in the GTO the rapid collapse of voltage across the transformer secondary results in a forward dV/dt of approximately 110 V/ μ s across the GTO. As expected, the GTO was not damaged by this forward dV/dt immediately following current zero. In addition, the GTO had previously been subjected to more severe tests of 160 V/ μ s.

In subsequent tests the PFN was pulsed at 0.1 Hz for 130,000 cycles. One of the transformer primary connections failed, and the transformer has been rebuilt with mechanical design changes to prevent such an occurrence again.

The combined stability of the RCPS, PFN and MS terminating resistor is such that the maximum excursion of the flat-top of the MS terminator voltage is $\pm 0.035\%$ with the PFN pre-charged to 60 kV.

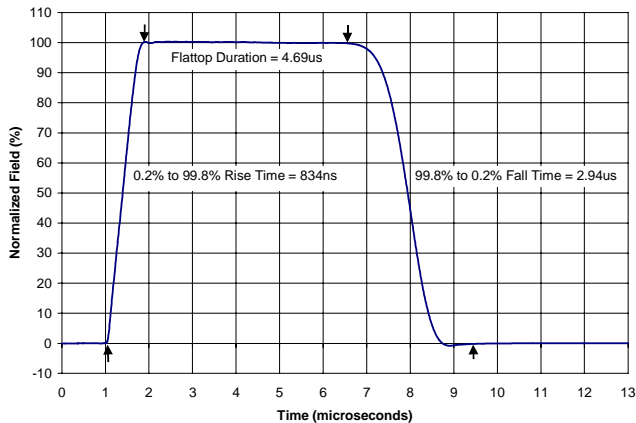


Fig. 163. Predicted field in kicker magnet, derived from measured PFN voltage of 55 kV.

The prototype RCPS and PFN passed their tests. Hence the TRIUMF Kicker group are starting on the series production of 5 RCPS, 9 PFNs and 20 thyatron switch units. Orders for many of the main components, including 3 kV power supplies, storage capacitors, low leakage inductance step-up transformers, filter capacitors, high voltage diodes, and high voltage receptacles have been placed. In addition quotations for 550 PFN capacitors have been received, and 10 sample capacitors have been ordered from the two low bidders. A circuit for testing the sample capacitors has been designed, and is presently being assembled.

RADIO FREQUENCY SYSTEMS

Coordination/Project Planning

Two 40 MHz and three 80 MHz cavities have been built at CERN as part of the preparation of the improvement program of the PS as an injector for the LHC. The 40 MHz cavities provide bunch spacing, while the nominal small bunch length is provided by the 80 MHz cavities. Higher order mode dampers for these cavities have been provided by TRIUMF. Both the second 40 MHz and the third 80 MHz cavities equipped with higher order mode dampers are ready to be installed in the PS. The dampers installed in the first 40 MHz and the first and the second 80 MHz cavities have already been tested with beam in the PS. The dampers have performed as designed and have withstood the full operating voltage of the cavities without any multipactoring, breakdown or heating problems.

40 MHz Cavity Structure

Higher order mode dampers at 260 MHz and 504 MHz were needed for the second 40 MHz cavity at CERN. These dampers were similar to the dampers, which were designed and fabricated at TRIUMF for the first 40 MHz cavity. Two of each kind of dampers were fabricated at TRIUMF and a signal level test was performed at CERN on the second 40 MHz cavity. The design goal of damped shunt impedance of less than 1 kW for the monopole modes was achieved with a damping of about 5% of the fundamental mode. This 40 MHz cavity has successfully undergone rf power tests with these higher order mode dampers installed where a cavity gap voltage more than 400 kV was reached.

80 MHz Structure and HOMs

Four kinds of higher order mode dampers and three high pass filters were required for the third 80 MHz cavity at CERN. A total quantity of seven dampers and three filters were manufactured and assembled at TRIUMF and were shipped to CERN. These dampers were the same as the previous dampers made for the first two 80 MHz cavities (see Fig. 164).

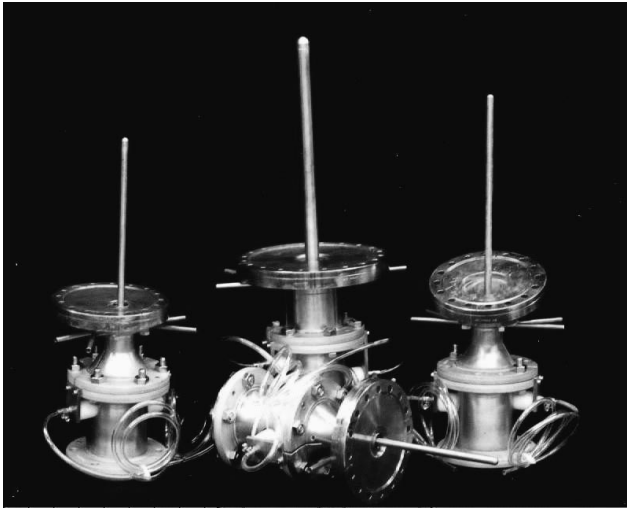


Fig. 164. Higher order mode dampers for the 80 MHz cavities.

High Voltage Power Supplies

Shipment of all power supplies was achieved as scheduled from Inverpower, I.E. Power and Xantrex. Difficulties with the high voltage transformer in the 22 kV prototype resulted in a redesign of the high voltage output stage for these units, with the prototype being returned to Inverpower for retrofit to the latest design. Condensation problems experienced in the summer resulted in supplies being cooled by warmer demineralized water. This subsequently resulted in thermal trips which were solved at CERN by the use of an improved heat sink for the inverter section.

TECHNOLOGY TRANSFER DIVISION

INTRODUCTION

Technology Transfer is the TRIUMF division responsible for the commercial interactions of the laboratory. It is comprised of a small group dedicated to ongoing technology transfer, plus the Applied Technology group that is responsible for the operations of the on-site commercial cyclotrons on behalf of MDS Nordion.

TECHNOLOGY TRANSFER

The mandate of the Division is the pursuit of all financially and technically viable opportunities for commercializing the technologies evolving from research at TRIUMF, in any appropriate manner that will enhance the Canadian economy.

The current Contribution Agreement between the National Research Council (NRC) and TRIUMF includes the requirement for TRIUMF to enhance its impact on the economies of western Canada. Specifically, there is an emphasis on providing benefits to small and medium-sized businesses in the western provinces, both through the TRIUMF purchasing practices, and through the transfer of technical knowledge and skills. The NRC has commissioned both Western Economic Diversification (WED) and the Industrial Research Assistance Program (IRAP) to provide assistance in this effort.

As the arm of TRIUMF responsible for this activity, the objectives of the Division are:

1. To transfer TRIUMF technical knowledge and skills to the Canadian economy, in particular the western Canadian economy; and
2. To generate income for TRIUMF, for further research and development.

The crucial first step to commercializing new or innovative technologies from a research laboratory is to generate disclosures of such innovations. To this end, 18 potentially commercial disclosures have been documented this past year, and 5 of those have been funded by TRIUMF for further development.

In keeping with the focus on western Canadian small to medium-sized businesses, TRIUMF has, with the help of WED, organized 4 industry supplier shows in each of the western provinces this past year. The purpose of these shows was to acquaint industry representatives with TRIUMF's activities, to present procurement opportunities, and to establish contacts.

Our contract administrator is also ensuring that there is a conscious effort made to attract bids from as

many eligible western Canadian companies as is reasonably possible. To date, the results of this effort have shown a steadily increasing success.

TRIUMF's strength lies in the unique aspects of the facilities, combined with the scientific excellence of the staff and the research conducted here. The Division has established a network of contacts with many commercialization offices and facilities throughout North America and the world, and constantly utilizes those contacts in its own activities. The Division is also responsible for patent protection at TRIUMF, but it must be noted that although it can be important in identifying a novel technology, at this level of scientific discovery, merely patenting cannot be relied on as a long-term shield from competitive alternatives.

New technology such as that emanating from TRIUMF is, by definition, a high-risk venture. Although projects may appear to have promising potential, from experience it can be predicted that not all of them will actually fulfil expectations. The Division always takes a conservative approach in projecting current opportunities into future commercial activities.

APPLIED TECHNOLOGY GROUP

500 MeV Isotope Production Facility

During this year the 500 MeV irradiation facility received 119 mAh. Eight Mo targets were irradiated to produce $^{82}\text{Sr}/^{82}\text{Rb}$ for MDS Nordion. In collaboration with LAMPF, we also irradiated a KCl target to produce ^{32}Si . This target was shipped to LAMPF for chemical processing.

CP42 Facility

The total beam delivery for this year was 0.61 Ah. The weekly beam delivery graph is shown in Fig. 165, the (quarterly) time evolution of the beam delivery is displayed in Fig. 166, and the downtime and maintenance statistics are analyzed in Fig. 167 and compared with the TR30.

The main power transformer of the rf anode power supply shorted out and had to be repaired. Several other high voltage components were also broken as a consequence of a major spark that went through the system. As a result, the CP42 was down for 3 weeks in August/September.

Work is proceeding on the upgrade to the CP42 control system and replacement of the power supplies. The new main magnet and ion source supplies had arrived on-site by year end. Installation will proceed in early 1999.

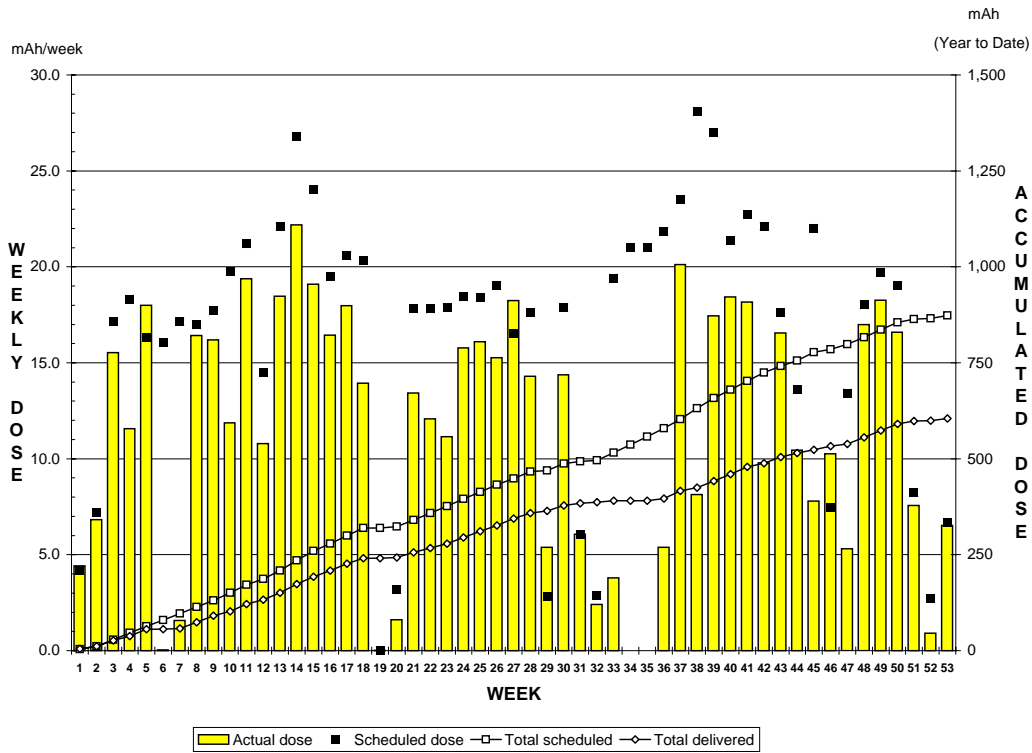


Fig. 165. Weekly beam delivery for the CP42.

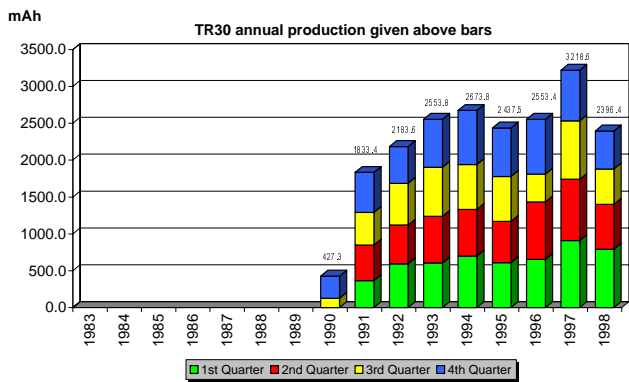
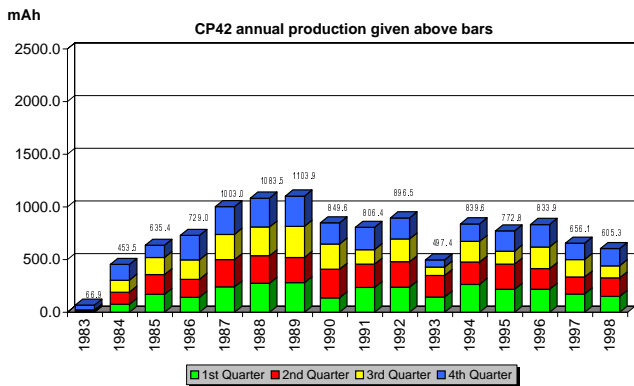


Fig. 166. Quarterly time evolution of the beam delivery for the CP42 (top) and TR30 (bottom).

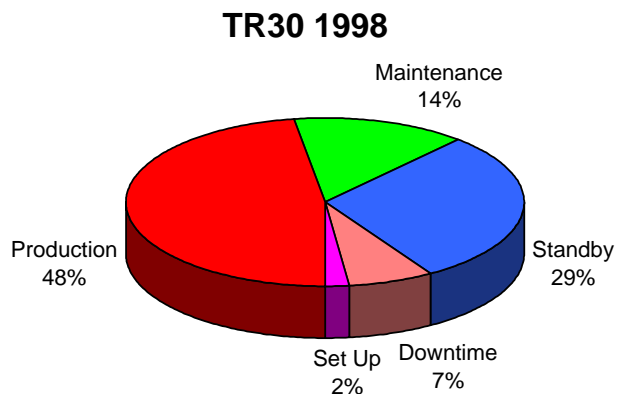
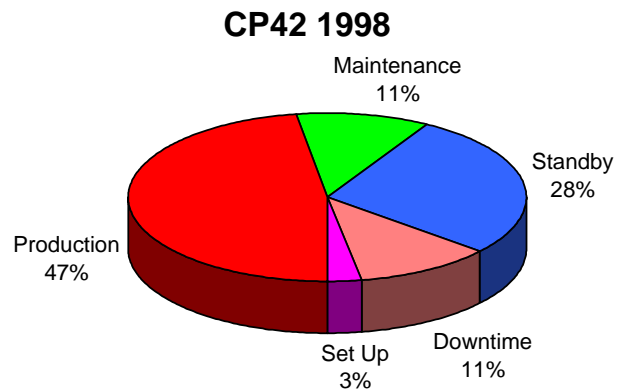


Fig. 167. Breakdown of downtime and maintenance for the CP42 (top) and TR30 (bottom) during operational hours.

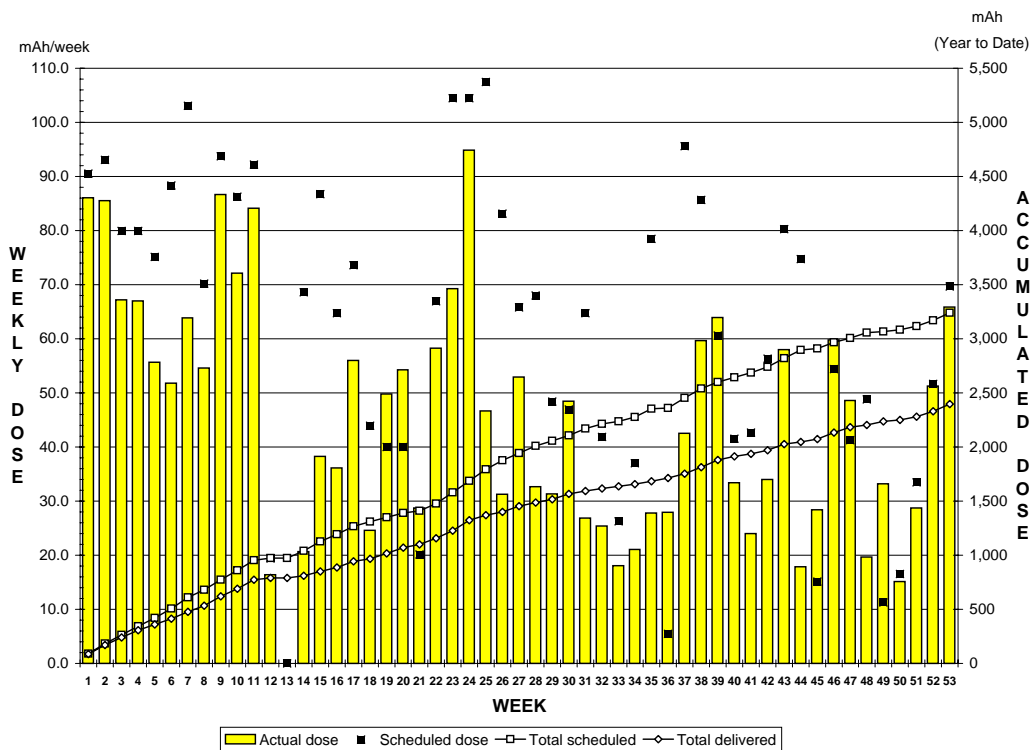


Fig. 168. Weekly beam delivery for the TR30.

TR30 Facility

The total beam delivery for this year was 2.40 Ah. The weekly beam delivery graph is shown in Fig. 168, the (quarterly) time evolution of the beam delivery is displayed in Fig. 166, and the downtime and maintenance statistics are analyzed in Fig. 167 and compared with the CP42.

The TR30 cooling tower was replaced with a compressor-based chiller system. This has improved the beam stability (which is water temperature dependent) and the ability of the TR30 to run at full power even on very hot days.

ATG Research Projects

During 1998 ATG members were actively involved with organizing workshops and conferences. These activities included organizing the Second Workshop on Accelerator Operations (WAO98) at UBC. This workshop attracted over 140 operations personnel from research and commercial accelerators all over the world. ATG personnel presented two oral papers and a poster paper in addition to chairing the workshop. ATG personnel also organized the Sixth Canadian Isotope Symposium at the University of Ottawa.

The ATG made extensive improvements to the design of the solid target systems that includes a dynamic braking system, magnetic orientation of the targets,

and a positive locking mechanism for holding the targets in the shuttles during transportation within the pneumatic system. Another project involved evaluating potential improvements to the TR30 ion source and injection system by experimenting on the centre region cyclotron. These two major projects each employed a co-op student resulting in useful technical reports.

RADIOISOTOPE PROCESSING (MDS NORDION)

During 1998, MDS Nordion shipped large quantities of short-lived medical isotopes produced using the TR30 and CP42 cyclotrons. The main contributors to sales were iodine-123 and thallium-201, used around the world for nuclear medicine studies.

The TRIUMF cyclotron was used to produce large-scale batches of strontium-82 whose daughter product, rubidium-82, is used in PET studies. As well, work continued on the development of new isotopes and applications in cooperation with TRIUMF.

A TRIUMF-led project to upgrade Nordion's CP42 cyclotron was approved and work started during the year. The Atomic Energy Control Board approved a licence amendment to allow sustained high current irradiations. The TR30 remains the most powerful isotope production cyclotron in the world.

ADMINISTRATION DIVISION

INTRODUCTION

In 1998 TRIUMF discontinued the use of the TRIUMF Safety Advisory Committee for providing advice, formally to the Director, on all personnel, public and environmental safety policies and procedures. A regime of divisional safety committees or panels, appointed for specific issues, has been implemented. The division head will chair the advisory committee or panel, make the final decisions on recommendations to the Director on the policies, procedures and facility designs to obtain safe operations in their division, and ensure their implementation.

All of the computer programs operated on the IBM AS/400 administration computing system are now Y2K compliant. Some PCs used in the word processing systems will require special action in January, 2000 if they have not been replaced before then. The only system still requiring program upgrading for the Y2K problems is our telephone system. This will be done when its ongoing viability is determined, before the end of 1999.

Long distance charges are now being billed directly by Fonorola at substantial savings in toll charges and billing administration costs.

OPERATIONAL SAFETY

Safety Organization

The long-standing TRIUMF Safety Advisory Committee was officially dismantled and replaced with a system of divisional safety committees. Each division head is now responsible for convening meetings of standing safety committees or temporary panels to review the personnel and public safety of operations within their division. Recommendations and decisions will be recorded in meeting minutes and filed with TRIUMF Safety group for archiving and auditing purposes.

AECB Licensing

The AECB has changed how it regulates activities at TRIUMF. An AECB Project Officer is now assigned to TRIUMF on a full-time basis, being assisted in his evaluation by other AECB groups with specific areas of expertise. TRIUMF and TSG now allocate more time to licence management and compliance documentation.

A TR13 shielding upgrade was completed in the spring allowing lithium targets to be irradiated at currents up to 50 μ A. The TR13 operating console was moved to the far corner of the fenced-in area later in the year, further reducing the dose-rate at the operator's table by more than a factor of two.

The AECB issued an amended Operating Licence approving both the lithium irradiations at the TR13 and the irradiation of a new target material at the TR30. The TR30 is now licensed for currents up to 650 μ A on the new target material.

The AECB reviewed documents pertaining to the Derived Release Limits for TRIUMF and ISAC. The documents were subsequently revised and reissued as TRIUMF Safety Note 2.4.3, Revision 2.

Site Security

Site security is still a concern although there were no major break-ins or significant material thefts during 1998. Cromwell Security Inc. continue to patrol the site daily.

Several lighting improvements were completed, including the installation of a new lamp standard on the road leading from the main office building to the upper parking lot.

WCB and Site Environmental

New Workers' Compensation Board Occupational Health and Safety Regulations are being put into effect. Some of these new WCB regulations are also concerned with ionizing radiation. Most of the new WCB requirements, such as the need for regularly scheduled monitoring and personnel dose management programs, are already covered by existing AECB licence requirements.

All industrial safety programs were expanded to include the new ISAC building. A new first aid room was commissioned, an approved fire safety plan was drawn up, and workplace hazardous materials information system (WHMIS) stations were established. The ISAC building was approved for occupancy late in the year.

A 10,000 kg shipment of low specific activity radioactive waste was shipped to Chalk River Laboratory for disposal in mid-December.

Interlocks and Monitoring

The 500 MeV Central Safety System was modified to include the access control and machine protect functions for beam line 2A and its associated exclusion areas. The documentation of access control functions and system requirements was further refined and several changes were made to the software to bring the program in line with the newly specified requirements.

All changes were formally tested and signed-off as part of a new system Quality Assurance program.

Six new air monitors, two new neutron monitors and five new beam spill monitors were commissioned

and connected to previously unused channels in the 500 MeV facility's radiation monitoring system. All monitors were associated with beam line 2A and the ISAC facility.

Safety-critical software and hardware were examined for year-2000 compliance. All radiation monitoring and access control data acquisition and display systems were found to be compliant. Some work will be required to ensure that the VAX-based data logging and PC-based gamma spectroscopy systems become Y2K certified before the end of 1999.

Personnel Dosimetry

The 1998 TRIUMF collective dose as measured by the TSG direct reading dosimeter service was 258 mSv, the lowest level in some years. The primary reason for the low dose is the involvement of many 500 MeV facility operational support groups in the construction and commissioning of the new ISAC facility. The facility was a non-radioactive area for most of the year.

The 1998 Applied Technology group personnel collective dose was approximately the same as in 1997. Applied Technology staff were not involved with the new ISAC facility, hence the group dose represents a higher percentage of the total site dose than in previous years.

Table XXIV. Collective DRD dose.

Group	Dose (mSv)	Fraction of Total (%)	Median (mSv)
Applied Technology	78.5	30.4	4.5
Beam Lines/Probes	9.0	3.5	1.3
Experimenters	4.0	1.6	0.1
500 MeV Operations	25.3	9.8	1.2
Life Sciences	28.6	11.1	0.4
Mech. Engineering	4.8	1.9	0.4
Outside Contractors	10.4	4.0	0.8
Plant Group	5.4	2.1	0.2
RF Group	6.4	2.5	0.6
Remote Handling	12.9	5.0	1.0
Safety Group	13.5	5.2	0.4
Tech Support	17.3	6.7	1.6
Vacuum	12.4	4.8	1.9
Others	29.9	11.6	—
Total	258.4	100	0.3

ADMINISTRATION COMPUTING

Data Processing

There were incremental changes to the IBM AS/400 computer system that is used for administration data processing. The operating system was upgraded to a Version 4 Release 2, and memory and disk storage were increased, which resulted in additional performance improvements and improved system utilities.

There was additional development of Web-based utilities. In support of the ICHEP'98 conference, a second, secure, Web-server was set up to process conference payments from attendees around the world. This was done in coordination with the main ICHEP data base system. On the original server, a number of new utilities such as an interactive, searchable and printable Stores catalogue were made available.

A prototype "paperless" system was implemented to report telephone long-distance usage. With this system, telephone billing information is transferred electronically into our data base. Account holders are automatically notified by email of the total cost of calls per authorization code, and account holders and callers can review the call-logs using a Web browser. It is expected that this will become the model for report distribution for any new applications on the administration system.

The year-2000 compliance project was completed this year. While all hardware and operating system software was already certified year-2000 compliant, all custom software (either developed in-house or purchased and modified) needed to be reviewed to ensure Y2K compliance, and many software modifications were required. The central data base also needed review and modification.

Word Processing

The word processing systems saw only incremental changes in 1998. All client PCs were refreshed with current versions of software to ensure that they all conformed to a single standardized configuration. All PCs were tested for year-2000 compatibility. PCs requiring special action in January, 2000, and those requiring replacement, were identified.

Telephones and Telecommunications

The major change to the site telephone system in 1998 was the implementation of an "automated switchboard", based on the existing voice mail system. Prior to this change, the switchboard operator was frequently overloaded with calls, causing many incoming calls to be queued for unacceptably long times. With the change in effect, only calls requiring a live attendant were transferred to the switchboard operator. The majority of calls, where the caller already knew the correct telephone local, could now be dialed directly by the caller. As expected, fewer calls had to wait in queues, and queue-waits were shortened.

Unfortunately, the automated switchboard placed significant additional load and dependence on the voice mail system. Over the past few years, the voice mail system had become less reliable, but failures had little impact. In 1998 failures not only became more frequent, but also lasted longer, and caused considerable

operational problems. In some cases, voice mail failures brought down the whole site telephone system. In another case, the voice mail component did not function for nearly a week.

It has proved impossible to be sure of the exact cause of the failures, however, it is clear that various environmental factors were likely culprits. At the start of the year, the room air conditioner occasionally leaked water on to the telephone processors. For much of the remainder of the year the faulty air conditioner was shut off, but installation of a new one was delayed. It was also determined that neither the site

power nor the telephone system UPS was providing an appropriate level of service.

Due to the age of the hardware, there were often significant delays in obtaining replacements, which were no longer being manufactured.

At the end of 1998, a new air conditioner was installed and power problems were being addressed. All hardware components of the voice mail system had been tested and suspect components were replaced. Since this was done, no additional failures have occurred.

CONFERENCES, WORKSHOPS AND MEETINGS

1998 WESTERN REGIONAL NUCLEAR AND PARTICLE PHYSICS CONFERENCE

The Western Regional Nuclear and Particle Physics Conference was held February 13–15 at the traditional location of Lake Louise, Alberta. This year the conference was organized by the University of Manitoba and TRIUMF. The organizing committee consisted of Des Ramsay (chair), Larry Lee, Kumar Sharma, and Elly Driessen (coordinator). Normally the conference is able to obtain funding from both TUEC and TRIUMF, but this year no money was available from either of these sources. We were very grateful to obtain some University of Manitoba funding from the Department of Subatomic Physics, the Dean of Science, and the Office of Research and Administration. Together with the registration fees, the conference was able to meet expenses, but we were unable to offer a graduate student subsidy this year.

Attendance was low this year with only 19 participants. While we would have liked to see more participants, particularly graduate students, the small size of the group fostered interesting and lively discussion.

The eclectic program included a wide variety of topics. The invited talks were:

- “Exploring the Strangeness Content of the Nucleon via Parity Violation at Jefferson Lab”, Lawrence Lee, University of Manitoba
- “Pion-Nucleon Physics and the Chiral Symmetry of Low Energy QCD”, Marcello Pavan, MIT
- “Nuclear Pion Absorption Studies with the CHAOS Detector and TRIUMF”, Roman Tacik, University of Regina/TRIUMF
- “Application of Low Energy Spin Polarized Radioactive Beams at ISAC to Condensed Matter Physics”, Rob Kiefl, UBC/TRIUMF
- “Progress at the CPT and the Radioactive Beam Facility at Argonne”, Guy Savard, Argonne National Laboratory
- “Studies of Explosive Nucleosynthesis using the DRAGON at ISAC”, John M. D’Auria, Simon Fraser University

- “Supersymmetry and its Consequences”, John Ng, TRIUMF
- “Recent Results from the HERMES Experiment”, Jinsong Ouyang, TRIUMF

The calibre of the excellent student papers was such that the judges declared a three-way tie for first place. The prize was shared by

- Araz Hamian, University of Manitoba, “The TRIUMF Parity Violation Experiment”.
- Michael Landry, University of Manitoba, “Search for Ξ - Hypernuclei”.
- Richard Lange, Simon Fraser University, “Preparation of a Radioactive ^{44}Ti Target”.

As usual, sessions were held in the mornings and evenings, leaving the afternoons free. Fortunately, we were blessed with excellent sunny weather for the delegates to enjoy ice-climbing, hiking, downhill and cross-country skiing, and skating.

At the end of the conference a meeting was held to discuss the future of the Western Regional. Most people agreed that the scope should be kept broad, not only because this is intrinsically interesting, but because the number of graduate students in ‘straight’ nuclear physics is declining. A variety of reasons for declining participation were identified, primarily lack of money, conflicting meetings and experimental runs, and reduced numbers of graduate students, and not aggressive enough pre-conference promotion. To address this last point the 1999 organizers plan to appoint a local representative at each institution who will be responsible for maximizing the participation of his or her immediate colleagues. TUEC will also try to obtain money to support graduate students.

Thanks to all the participants in the 1998 conference and we hope to see you all again in 1999, each with several graduate students in tow!

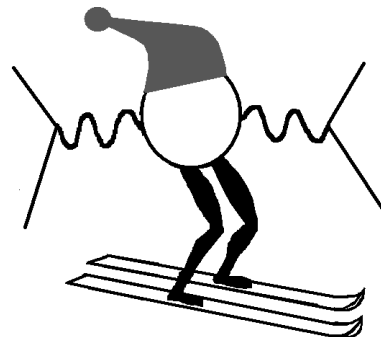


Fig. 169. The 1998 WRNPPC logo.

WORKSHOP ON ACCELERATOR OPERATIONS

The second Workshop on Accelerator Operations (WAO'98) was held May 18–22 at the University of British Columbia in Vancouver, Canada. Ronald Lauz conceived the workshop series and organized the first one at the Thomas Jefferson National Accelerator Facility, Virginia, USA in 1996. The WAO workshops are concerned with the practical day to day issues of running accelerators. Example topics include staffing, training, documentation, commissioning, safety and maintenance.

The first workshop focused on “How We Do Business”; the second Program Committee used “Maintenance” and “Training” as major themes for two full days of presentations. Other sessions covered the topics of “Control Room Layout” and “Scheduling”. Poster sessions focusing on each of the above topics were held. A “How We Do Business” poster session was also included. The issues of “Problems at Small Labs” were discussed. Two evening sessions were added to cover “The DOE Accelerator Order” and “Web Based Logbooks and Other Web Tools”.

Three invited speakers from outside of the accelerator community gave presentations. Ian Graham gave a talk on “How the BC Transit Skytrain Control Centre Does Business”, Lynn Duncan presented “Eight Myths of Team Building” and Cary Meyers spoke about the “Nav Canada Training Program for Air Traffic Controllers”.

An opening reception was held on Monday evening before the Workshop began. On Wednesday afternoon we toured the TRIUMF site. Highlights included the brand new ISAC radioactive beams building and the MDS Nordion facility. Later that evening cable cars carried us up to an evening banquet on top of Grouse Mountain. The restaurant's large windows presented a magnificent view of downtown Vancouver as the sun sank into the ocean. Thanks to El Nino, exceptionally good weather prevailed during the workshop.

The industrial displays highlighted technologies particularly relevant to the operations environment.

With about 150 registrants, WAO'98 more than doubled the attendance of the first workshop. The success of the event is due mainly to the shared energy and contributions of the participants. Corporate sponsorship was generously provided by MDS Nordion, Ebco Technologies, Dehnel Consulting, Philtek Electronics and Accelsoft Inc. Program Committee support was provided by CERN, LANL, SLAC, TJNAF, and TRIUMF.

The idea to host WAO'98 sprang from a badge room discussion between Fred Bach and Rick Bloemhard. Gerardo Dutto, Philip Gardner, Dave

Pearce and Nigel Stevenson provided crucial early support. Unfortunately there is not enough room to mention all of the TRIUMF staff members and their contributions. Major responsibilities taken on by the organizers include:

Fred Bach – workshop secretary, Web site, communications, on-line registrations

Rick Bloemhard – program committee, poster, Web site, proceedings editor

Elly Driessen – workshop coordinator, registration, transportation, banquet, TRIUMF tour

Shirley Reeve – treasurer, budget

Dave Pearce – program committee, workshop office equipment

Jane Richards – registration database

Nigel Stevenson – program committee, budget

Jana Thomson – presenters submissions, publishing

A soft cover book of the proceedings is being published. CERN will host the next WAO workshop in January, 2001 (tentatively).

INTERNATIONAL CONFERENCE ON HIGH ENERGY PHYSICS

The twenty-ninth International Conference on High Energy Physics was held in Vancouver from July 23 to July 29. Some 882 delegates from 43 countries attended the conference together with 251 accompanying persons. The conference followed the traditional format of three days of parallel sessions, organized at various locations on the campus of the University of British Columbia. These were followed by three days of plenary talks, which took place in the Chan Centre for the Performing Arts on the UBC campus. Dr. Martha Piper, President of UBC, formally opened the conference.

The meeting was organized by the TRIUMF laboratory, and this was the first occasion that the “Rochester Conference” had taken place in Canada. The laboratory followed the recent tradition of making extensive use of the World Wide Web for communication.

The conference was held under the aegis of the International Union of Pure and Applied Physics, C11 commission and we are grateful for their sponsorship. We also received financial support from the British Columbia Information, Science and Technology Agency, the University of British Columbia, ALSTOM, MDS Nordion, Sun Rise Engineering, Talvan Machine Shop and UMA.

The social program included a buffet dinner at TRIUMF with a tour of the facility. Saturday saw a salmon barbecue and fireworks with options to attend Shakespeare's *As You Like It* at the Bard on the Beach, or

a visit to the Pacific Space Centre. The vigour and vitality of the delegates were very much in evidence by the oversubscribed hikes on Sunday. There was a slight break from the classical tradition, with the staging of a jazz concert by the Michael Kaeshammer Trio in the Chan Centre. Dr. Rocky Kolb provided an entertaining and very educational public lecture entitled *The Earliest Moments of the Big Bang* in which he endeavoured to extol the benefits of “Primordial Soup”.

TRIUMF SUMMER INSTITUTE

The tenth annual TRIUMF Summer Institute was held at TRIUMF August 10 to 21. This year’s Institute focused on three related topics roughly defining an important new area of science: trapping techniques and the impact of these techniques on fundamental symmetries and on nuclear physics. Special emphasis was placed on the use of radioactive or exotic ion beams and related non-accelerator experiments involving complementary symmetry tests. Very new and elegant experimental techniques are involved. The symmetry issues are crucial for tests of the standard model of quarks, leptons and the unified forces. The aim of this Institute was to provide a detailed overview of this whole new field.

The lecturers in 1998 were:

- N. Fortson, University of Washington, *Atomic PNC and EDM Experiments*
- S. Freedman, Berkeley, *Tests of Fundamental Symmetries*
- J. Behr, SFU/TRIUMF, *TRIUMF’s Neutral Atom Trapping Project*
- M. Kasevich, Yale University, *Precision Measurements with Laser Cooled Atoms*
- L.A. Orozco, SUNY at Stony Brook, *Studies of trapped radioactive atoms*
- I.S. Towner, Queen’s University, *The Weak Interaction*
- G. Savard, Argonne National Laboratory, *Ion Traps*

The organizers of the Summer Institute were B.K. Jennings, K.P. Jackson and E.W. Vogt.

TRIUMF USERS’ GROUP ANNUAL GENERAL MEETING

Following a poll of the TRIUMF users, the TRIUMF Users’ Group AGM was moved from December to June to coincide with the only subatomic EEC held in 1998. The AGM was held on June 30 in the TRIUMF Auditorium.

L. Buchmann	Introduction
J.-M. Poutissou	TRIUMF Director’s Report and the Next 5 Year Plan
P. Kitching	The LRPC 5 Year Plan Report
	Open Discussion on the 5 Year Plan
M. Vetterli	NSERC Report
P. Schmor	ISAC Update
L. Buchmann	Open Issues Regarding the TRIUMF Users’ Group
	Otto Häusser Memorial Session
K.P. Jackson	Opening Thoughts
G. Cates	Physics with ^3He :
(Princeton U.)	from Muons to MRI
A. McDonald	Status of SNO
(Queen’s U.)	
M. Vetterli	Otto Häusser’s Years at TRIUMF

The morning session began with J.-M. Poutissou presenting the Director’s report and outlining the next five year plan in the absence of A. Astbury, who was in Ottawa attending an Agency Committee on TRIUMF meeting. P. Kitching discussed the LRPC 5 Year Plan Report which had been published in June following an LRPC meeting in May. Prior to the LRPC meeting, TUEC had sponsored a series of seminars by proponents of new facilities for consideration in the formulation of the 2000–2005 five year plan. An open discussion followed in which the users raised various issues contained in the LRPC report and the draft five year plan. M. Vetterli gave a report on the NSERC subatomic physics grant selection committee which covered the reallocation exercise, the funding envelope, the committee membership, and the upcoming competition. P. Schmor gave an overview of the present status of ISAC. L. Buchmann led a discussion, prompted by comments from TRIUMF Management, concerning the role of the TRIUMF Users’ Group and its self image. The recent efforts of TUEC on behalf of the TRIUMF Users’ Group were outlined. TUEC proposed to use the new reconfirmation of membership every three years as a method of maintaining a group which is truly interested in TRIUMF. In addition, a survey of members’ interests will enable TUEC to direct relevant information to sub groups rather than always to the complete membership. In that way the TRIUMF Users’ Group would be more relevant to the diverse groups that use TRIUMF, and therefore it should attract more active participants.

The afternoon was dedicated to a memorial session for the late Otto Häusser. K.P. Jackson and M. Vetterli, TRIUMF/SFU physicists who had worked with

Otto at TRIUMF, were joined by G. Cates of Princeton University and A. McDonald of Queen's University to describe Otto's influence on their careers and his contributions to physics.

The AGM ended with a reception in the hot sunshine in the TRIUMF courtyard.

TUEC membership for 1998

L. Buchmann	TRIUMF	<i>Chair</i>
J.M. D'Auria	SFU	<i>Chair-elect</i>
M.D. Hasinoff	UBC	<i>Past-chair</i>
S.R. Kreitzman	TRIUMF	1997/98
S. Yen	TRIUMF	1997/98
A. Konaka	TRIUMF	1998/99
N. Rodning	U. Alberta	1998/99
M. La Brooy	TRIUMF	<i>Liaison Officer</i>

ORGANIZATION

Board of Management

The Board of Management of TRIUMF manages the business of the facility and has equal representation from each of the four founding universities. At the end of 1998 the Board comprised:

University of Alberta	Dr. P. Kitching Dr. W.J. McDonald Dr. A. Noujaim	
Simon Fraser University	Dr. B.P. Clayman Dean C.H.W. Jones Dr. R.G. Korteling	Chairman
University of Victoria	Ms. G. Gabel Dr. T. Gough Dr. M. Taylor	
University of British Columbia	Dr. B. Bressler Dr. C. Eaves Dr. D.F. Measday	
Non-voting members:	Ms. J. Verrett Dr. D.G. Stairs Dr. A. Astbury Dr. J.-M. Poutissou Mr. J. Hanlon	National Research Council McGill University Director, TRIUMF Associate Director, TRIUMF TRIUMF Recording Secretary

Towards the end of 1987, Board membership was expanded in anticipation of a broadening of the TRIUMF joint venture to include a more national representation of Canadian universities long associated with the TRIUMF experimental program. The University of Manitoba and Université de Montréal became associate members, and the University of Toronto joined as an observer. At the end of 1988, University of Toronto status changed from that of observer to associate member. In March, 1989 the University of Regina became an associate member. In December, 1998 Carleton University and Queen's University became associate members. Associate membership at year-end:

Associate members:	Dr. J. Keselman M.A. Caillé Dr. P. Sinervo Dr. K. Denford Dr. P.J.S. Watson D.A. McDonald	University of Manitoba Université de Montréal University of Toronto University of Regina Carleton University Queen's University
--------------------	--	--

The following changes occurred in Board membership in 1998: Drs. W.J. McDonald and A. Noujaim replaced Drs. E.W. Brooker and B. Kratochvil as University of Alberta members; Dr. D. Rowlatt replaced Dr. A. McAuley as University of Victoria member until June; Dr. M. Taylor then replaced Dr. D. Rowlatt; Ms. J. Verrett replaced Dr. N. Sherman as National Research Council member; Mr. J. Hanlon replaced Mr. M. La Brooy as recording secretary. The board met 5 times during the year.

Administration

Under the directorship of Dr. A. Astbury, TRIUMF personnel were grouped into divisions, with division heads as follows:

Division Head, Science Division	J.-M. Poutissou
Division Head, Accelerator Technology Division	E.W. Blackmore
Division Head, Cyclotron Operations Division	G.G. Dutto
Division Head, Technology Transfer Division	P.L. Gardner
Division Head, Administration Division	I.M. Thorson
ISAC Project Leader	P.W. Schmor

Operating Committee

The Operating Committee of TRIUMF is responsible for the operation of the facility. It reports to the Board of Management through its chairman, the Director, Dr. A. Astbury. The Operating Committee consists of one voting member from each of the four universities, two voting members representing the interests of external users and one representing TRIUMF staff. The Associate Director is a non-voting member. Members of the committee (alternate members in parentheses) at the end of 1998 were:

Dr. A. Astbury	Chairman	Director	
Dr. J.-M. Poutissou	(<i>ex officio</i>)	Associate Director	
Dr. N. Rodning		University of Alberta	(Dr. L.G. Greeniaus)
Dr. P. Percival		Simon Fraser University	(Dr. K.P. Jackson)
Dr. M. Lefebvre		University of Victoria	(Dr. M. Roney)
Dr. M.D. Hasinoff		University of British Columbia	(Dr. C. Hearty)
Dr. W.T.H. van Oers		Users	(Dr. E. Mathie)
Dr. J. Rogers		Users	(Dr. J. Vincent)
Mr. J. Yandon		TRIUMF	(Dr. T.J. Ruth)
Mr. J. Hanlon	Recording Secretary	TRIUMF	
Ms. J. Verrett	(<i>ex officio</i>)	National Research Council	

Changes in 1998: Dr. P. Percival replaced Dr. M. Vetterli as the Simon Fraser University member with Dr. K.P. Jackson as alternate; Dr. M. Lefebvre replaced Dr. R. Keeler as the University of Victoria member with Dr. M. Roney as alternate; Ms. J. Verrett replaced Dr. N. Sherman as the National Research Council member. The Operating Committee met 11 times in 1998.

NRC Advisory Committee on TRIUMF

Dr. D.G. Stairs	Chairman	McGill University
Dr. D. Santry	Secretary	National Research Council
Dr. P.-G. Hansen		Michigan State University
Dr. J.C. Hardy		Atomic Energy of Canada Ltd.
Dr. J.G. Martel		National Research Council
Dr. D. Perkins		Oxford University
Dr. B. Peters		unaffiliated
Prof. V. Soergel		Werner-Heisenberg Inst.
Dr. R. Taylor		SLAC
Prof. R. Carnegie	(<i>ex officio</i>)	Carleton University
Dr. C.H.W. Jones	(<i>ex officio</i>)	Simon Fraser University
Dr. P. Kalyniak	(<i>ex officio</i>)	Carleton University

Changes in 1998: Dr. D. Santry replaced Dr. N. Sherman as secretary; Prof. M. Stott stepped down; Dr. P. Kalyniak replaced Dr. P. Sinervo as an *ex officio* member.

Agency Committee on TRIUMF

Dr. A.J. Carty	Chairman	President, National Research Council
Dr. T. Brzustowski		President, Natural Sciences and Engineering Research Council
Mr. K. Lynch		Deputy Minister, Industry Canada
Mr. J. McLure		Deputy Minister, Western Economic Diversification
Ms. J. Verrett	Secretary	National Research Council

Changes in 1998: Ms. J. Verrett replaced Dr. N. Sherman as secretary.

TRIUMF Safety-Management Committee

Dr. A. Astbury	Director, TRIUMF
Dr. E.W. Blackmore	Head, Accelerator Technology Division
Dr. G.G. Dutto	Head, Cyclotron Operations Division
Mr. P.L. Gardner	Head, Technology Transfer Division
Dr. J.-M. Poutissou	Associate Director/Head, Science Division
Mr. I.M. Thorson	Head, Administration Division
Dr. P.W. Schmor	ISAC Project Leader
Mr. J. Drozdoff	Head, TRIUMF Safety Group
Mr. M. Stenning	Head, Operations Group
Dr. M. Adam	TAPC Chairman
Mr. G. Wood	Industrial Safety Officer
Mr. J. Hanlon	Manager, Human Resources & Administrative Services
Dr. N. Stevenson	Head, Applied Technology Group
Mrs. K. Gildert	Recording Secretary

Experiments Evaluation Committee

Subatomic Committee:

Dr. K. Langanke	Chairman	Aarhus University
Dr. J.-M. Poutissou	Associate Director / (<i>ex officio</i>)	TRIUMF
Dr. H. Fearing	Secretary	TRIUMF
Dr. C. Batty		Rutherford Appleton Laboratory
Dr. P.-G. Hansen		NSCL – Michigan State University
Dr. L. Buchmann		TUEC/TRIUMF
Dr. W.C. Haxton		University of Washington
Dr. B.R. Holstein		University of Massachusetts
Dr. A. Richter		Technische Universität Darmstadt
Dr. M.D. Hasinoff		TUEC Past Chair/University of British Columbia
Dr. I.S. Towner		Queen's University
Dr. M.C.T. Wiescher		University of Notre Dame

μ SR Committee:

Dr. M. Thewalt	Chairman	Simon Fraser University
Dr. J.-M. Poutissou	Associate Director / (<i>ex officio</i>)	TRIUMF
Dr. P.W. Percival	Secretary / (<i>ex officio</i>)	TRIUMF
Dr. I.K. Affleck		University of British Columbia
Dr. D.K. Bohme		York University
Dr. R.E. Wasylshen		Dalhousie University
Dr. S. Roorda		Université de Montréal

In July, 1994 the Experiments Evaluation Committee was formally split into two committees representing subatomic physics and μ SR physics. Changes in membership during the year were: Dr. L. Buchmann joined as TUEC chairman, and Dr. M. Hasinoff replaced Dr. G. Roy as TUEC past chairman (Subatomic); Dr. L. Taillefer completed his term (μ SR). The committee welcomed Dr. S. Roorda (μ SR).

Life Sciences Project Evaluation Committee

Dr. T. Lewellen	Chairman	University of Washington
Dr. J.-M. Poutissou	Associate Director	TRIUMF
Dr. L.P. Robertson	Secretary	University of Victoria
Dr. D.A. Axen		University of British Columbia
Dr. T. Budinger		Lawrence Berkeley National Laboratory
Dr. R. Finn		Memorial Sloan-Kettering Cancer Center
Dr. R. Flocchini		Crocker Laboratory, University of California
Dr. J. Fowler		Brookhaven National Laboratory

Biomedical Experiments Evaluation Committee

Dr. L.D. Skarsgard	Chairman	British Columbia Cancer Research Centre
Dr. J.M. Cameron		EEC/IUCF
Dr. D.A. Axen		EEC/University of British Columbia
Dr. M.J. Ashwood-Smith		University of Victoria
Dr. A. Astbury		TRIUMF
Dr. R.R. Johnson		University of British Columbia
Dr. T.R. Overton		University of Alberta
Dr. D.C. Walker		University of British Columbia
Dr. G.F. Whitmore		University of Toronto

PUBLICATIONS

This appendix lists publications describing work performed at TRIUMF and also work conducted elsewhere by TRIUMF personnel and TRIUMF users.

Journal Publications

Particle, Nuclear and Atomic Physics

E.G. Adelberger, L. Buchmann, T.D. Shoppa *et al.*, *Solar fusion cross sections*, Rev. Mod. Phys. **70**, 1265 (1998).

S.L. Stephenson, L.Y. Lowie, G.E. Mitchell, J.D. Bowman, C.M. Frankle, J.N. Knudson, S.I. Penttilae, S.J. Seestrom, Y. Yen, V.W. Yuan, B.E. Crawford, N.R. Roberson, P.P. Delheij, M. Iinuma, A. MASAike, Y. Matsuda, H. Postma and E.I. Sharapov, *Parity nonconservation in neutron resonances in ^{232}Th* , Phys. Rev. **C58**, 1236 (1998).

B.E. Crawford, N.R. Roberson, J.D. Bowman, G.M. Frankle, J.N. Knudson, S.I. Penttilae, S.J. Seestrom, Y. Yen, V.W. Yuan, P.P. Delheij, M. Iinuma, A. MASAike, Y. Matsuda, L.Y. Lowie, G.E. Mitchell, S.L. Stephenson, H. Postma and E.I. Sharapov, *Parity nonconservation in neutron resonances in ^{238}U* , Phys. Rev. **C58**, 1225 (1998).

B.E. Crawford, N.R. Roberson, J.D. Bowman, J.N. Knudson, S.I. Penttilae, S.J. Seestrom, V.W. Yuan, P.P. Delheij, T. Haseyama, A. MASAike, Y. Matsuda, L.Y. Lowie, G.E. Mitchell, S.L. Stephenson, H. Postma and E.I. Sharapov, *Neutron resonance spectroscopy of ^{106}Pd and ^{108}Pd from 20 to 2000 eV*, Phys. Rev. **C58**, 729 (1998).

G. White, N.J. Stone, J. Copnell, J. Rikovska, I.S. Towner, A.M. Oros, K. Heyde, B. Fogelberg, L. Jacobsson and F. Gustavsson, *Magnetic dipole moments near ^{132}Sn : measurement on isomeric $11/2^-$ states in odd- A ^{131}Te and ^{133}Te by NMR/ON*, Nucl. Phys. **A640**, 322 (1998).

C. Bochna *et al.* (E89-012 collaboration), *Measurements of deuteron photodisintegration up to 4.0 GeV*, Phys. Rev. Lett. **81**, 4576 (1998) [NPL-98-1].

E. Vogt, *The glorious history of nuclear physics at Chalk River*, Phys. in Canada, Jan/Feb (1998) [TRI-PP-98-6].

K. Ackerstaff *et al.* (HERMES collaboration), *Determination of the deep inelastic contribution to the generalised Gerasimov-Drell-Hearn integral for the proton and the neutron*, Phys. Lett. **B444**, 531 (1998) [DESY-98-122].

HERMES collaboration, *Measurement of the proton spin structure function g_1^p with a pure hydrogen target*, Phys. Lett. **B442**, 484 (1998) [hep-ex/9807015].

HERMES collaboration, *Flavor asymmetry of the light quark sea from semi-inclusive deep inelastic scattering*, Phys. Rev. Lett. **81**, 5519 (1998) [hep-ex/9807013].

HERMES collaboration, *The HERMES spectrometer*, Nucl. Instrum. Methods **A417**, 230 (1998) [hep-ex/9806008].

F. Balestra *et al.* (DISTO collaboration), *Production of ϕ and ω mesons in near-threshold pp reactions*, Phys. Rev. Lett. **81**, 4572 (1998).

T.M. Ito, R.S. Hayano, S.N. Nakamura, T.P. Terada, M. Iwasaki, D.R. Gill, L. Lee, A. Olin, M. Salomon, S. Yen, K. Bartlett, G.A. Beer, G. Mason, G. Trayling, H. Outa, T. Taniguchi, Y. Yamashita and R. Seki, *Observation of kaonic hydrogen atom x rays*, Phys. Rev. **C58**, 2366 (1998).

S.N. Nakamura, M. Iwasaki, K. Bartlett, G.A. Beer, D.R. Gill, R.S. Hayano, T.M. Ito, M. Kuwata, L. Lee, G. Mason, H. Ohkubo, A. Olin, H. Outa, M. Salomon, R. Seki, K. Shibuya, T. Taniguchi, T.P. Terada, G. Trayling, T. Watanabe, Y. Yamashita and S. Yen, *A new approach to measure kaonic hydrogen x-rays*, Nucl. Instrum. Methods **A408**, 438 (1998).

G. Suft, P. Amaudruz, E. Boschitz, B. van den Brandt, B. Brinkmoller, A. Glombik, J. Goetz, W. Gruebler, P. Hautle, J.A. Konter, W. Kretschmer, M. Lauterbach, S. Mango, R. Meier, C. Riedel, R. Tacik and R. Weidmann, *Polarization transfer observables in πd elastic scattering*, Phys. Lett. **B425**, 19 (1998).

D.H. Wright, S. Ahmad, D.S. Armstrong, G. Azuelos, W. Bertl, M. Blecher, C.Q. Chen, P. Depommier, B.C. Doyle, T. von Egidy, T.P. Gorringer, P. Gumplinger, M.D. Hasinoff, D. Healey, G. Jonkmans, A.J. Larabee, J.A. Macdonald, S.C. McDonald, M. Munro, J.M. Poutissou, R. Poutissou, B.C. Robertson, D.G. Sample, E. Saettler, C.N. Sigler, G.N. Taylor and N.S. Zhang, *Measurement of the induced pseudoscalar coupling using radiative muon capture on hydrogen*, Phys. Rev. **C57**, 373 (1998).

R. Tacik, F. Farzanpay, E.L. Mathie, P. Amaudruz, J.T. Brack, L. Felawka, R. Meier, D. Ottewell, G.R. Smith, G. Hofman, M. Kermani, S. McFarland, K. Raywood, M. Sevier, F. Bonutti, P. Camerini, N. Grion, R. Rui and E.F. Gibson, *Pion absorption in ^{12}C* , Phys. Rev. **C57**, 1295 (1998).

J.B. Lange, F. Duncan, A. Feltham, G. Hofman, R.R. Johnson, G. Jones, M. Pavan, K.J. Raywood, D. Vetterli, J.T. Brack, D. Ottewell, G.R. Smith and M.E. Sevier, *Determination of the $\pi^\pm p \rightarrow \pi^\pm \pi^+ n$ cross section near threshold*, Phys. Rev. Lett. **80**, 1597 (1998).

M. Kermani, O. Patarakin, G.R. Smith, P.A. Amaudruz, F. Bonutti, J.T. Brack, P. Camerini, L. Felawka, E. Fraga-como, E.F. Gibson, N. Grion, G.J. Hofman, E.L. Mathie, S. McFarland, R. Meier, D. Ottewell, K. Raywood, R. Rui, M.E. Sevier, R. Tacik, V. Mayorov and V. Tikhonov, *$\pi\pi \rightarrow \pi\pi$ cross sections near threshold*, Phys. Rev. **C58**, 3431 (1998).

- M. Kermani, P.A. Amaudruz, F. Bonutti, J.T. Brack, P. Camerini, L. Felawka, E. Fragiaco, E.F. Gibson, N. Grion, G.J. Hofman, R.R. Johnson, E.L. Mathie, S. McFarland, R. Meier, D. Ottewell, K. Raywood, R. Rui, M.E. Seviar, G.R. Smith and R. Tacik, *Exclusive measurements of $\pi^\pm p \rightarrow \pi^\pm \pi^\pm n$ near threshold*, Phys. Rev. **C58**, 3419 (1998).
- G.J. Hofman, G.R. Smith, T. Ambardar, F. Bonutti, J.T. Brack, P. Camerini, J. Clark, P. Delheij, F. Farzanpay, L. Felawka, E. Fragiaco, E.F. Gibson, J. Graeter, N. Grion, M. Kermani, E.L. Mathie, R. Meier, D. Ottewell, R.J. Peterson, R.A. Ristinen, R. Rui, M.E. Seviar, H. Staudenmaier, R. Tacik and G. Wagner, *Analyzing powers for $\pi^\pm \bar{p}$ elastic scattering between 87 and 263 MeV*, Phys. Rev. **C58**, 3484 (1998).
- F. Bonutti, P. Camerini, E. Fragiaco, N. Grion, R. Rui, J.T. Brack, L. Felawka, E.F. Gibson, G.J. Hofman, M. Kermani, E.L. Mathie, S. McFarland, R. Meier, D. Ottewell, K. Raywood, M.E. Seviar, G.R. Smith, R. Tacik and M. Vicente-Vacas, $\pi^+ \rightarrow \pi^+ \pi^\pm$ on deuterium at $T_{\pi^+} = 283$ MeV, Nucl. Phys. **A638**, 729 (1998).
- J. Gräter, R. Bilger, H. Clement, R. Meier, G.J. Wagner, E. Friedman, M. Schepkin, P.A. Amaudruz, L. Felawka, D. Ottewell, G.R. Smith, A. Ambardar, G.J. Hofman, M. Kermani, G. Tagliente, F. Bonutti, P. Camerini, N. Grion, R. Rui, P. Hong, E.L. Mathie, R. Tacik, J. Clark, M.E. Seviar and O. Patarakin, *The ${}^4\text{He}(\pi^+, \pi^-)$ reaction at low energies*, Phys. Lett. **B420**, 37 (1998).
- J. Gräter, R. Bilger, H. Clement, R. Meier, G.J. Wagner, E. Friedman, M. Schepkin, P.A. Amaudruz, L. Felawka, D. Ottewell, G.R. Smith, A. Ambardar, G.J. Hofman, M. Kermani, G. Tagliente, F. Bonutti, P. Camerini, N. Grion, R. Rui, P. Hong, E.L. Mathie, R. Tacik, J. Clark, M.E. Seviar and O. Patarakin, *Energy dependence of the ${}^4\text{He}(\pi^+, \pi^-)$ total cross section*, Phys. Rev. **C58**, 1576 (1998).
- J.C. Chow, A.C. Morton, R.E. Azuma, N. Bateman, R.N. Boyd, L. Buchmann, J.M. D'Auria, T. Davinson, M. Domb-sky, W. Galster, E. Gete, U. Giesen, C. Iliadis, K.P. Jackson, J.D. King, G. Roy, T. Shoppa and A. Shotter, *Three-particle breakup of the isobaric analog state in ${}^{17}\text{F}$* , Phys. Rev. **C57**, R475 (1998).
- T.A. Swanson, J.A. Behr, A. Gorelov, D. Melconian, D. Asgeirsson, *Efficient transfer in a double magneto-optical trap system*, J. Optical Soc. of America **B** (1998).
- J. Goerres, J. Meissner, H. Schatz, E. Stech, P. Tischauser, M. Wiescher, D. Bazin, R. Harkewicz, M. Hellstroem, B. Sherrill, M. Steiner, R.N. Boyd, L. Buchmann, D.H. Hartmann and J.D. Hinnefeld, *Half-life of ${}^{44}\text{Ti}$ as a probe for supernova models*, Phys. Rev. Lett. **80**, 2554 (1998).
- S. Adler *et al.* (E787 collaboration), *Upper limit on the decay $K^+ \rightarrow e^+ \nu \mu^+ \mu^-$* , Phys. Rev. **D58**, 012003 (1998) [TRI-PP-98-1].
- N.C. Mukhopadhyay, Liu-Jun, M.J. Ramsey-Musolf, C.T. Storrs, S.J. Pollock and H.-W. Hammer, *Parity-violating excitation of the $\Delta(1232)$: hadron structure and new physics*, Nucl. Phys. **A633**, 481 (1998).
- F. Duncan, H. Hahn, C. Aclander, D. Ashery, E.G. Auld, D.R. Gill, D.A. Hutcheon, G. Jones, E. Korkmaz, S. Maytal-Beck, M.A. Moinester, J.A. Niskanen, D. Ottewell, A. Rahav, S. Ram, M. Seviar, P.L. Walden and R. Weiss, *Differential cross section of the $pn \rightarrow pp({}^1S_0)\pi^-$ reaction extracted from $pd \rightarrow \pi^- ppp$* , Phys. Rev. Lett. **80**, 4390 (1998) [TRI-PP-97-72].
- K. Ackerstaff *et al.* (OPAL collaboration), *Search for chargino and neutralino production at $\sqrt{s} = 170$ GeV and 172 GeV at LEP*, Eur. Phys. J. **C2**, 213 (1998) [CERN-PPE-97-083].
- K. Ackerstaff *et al.* (OPAL collaboration), *Measurement of the quark to photon fragmentation function through the inclusive production of prompt photons in hadronic Z^0 decays*, Eur. Phys. J. **C2**, 39 (1998) [CERN-PPE-97-086].
- K. Ackerstaff *et al.* (OPAL collaboration), *Measurement of $f(c \rightarrow D^{*+} X)$, $f(b \rightarrow D^{*+} X)$ and $\Gamma_{c\bar{c}}/\Gamma_{had}$, using $D^{*\pm}$ mesons*, Eur. Phys. J. **C1**, 439 (1998) [CERN-PPE-97-093].
- K. Ackerstaff *et al.* (OPAL collaboration), *A measurement of the B_s^0 lifetime using reconstructed D_s^- mesons*, Eur. Phys. J. **C2**, 407 (1998) [CERN-PPE-97-095].
- K. Ackerstaff *et al.* (OPAL collaboration), *Tests of the standard model and constraints on new physics from measurements of fermion pair production at 130 GeV to 172 GeV at LEP*, Eur. Phys. J. **C2**, 441 (1998) [CERN-PPE-97-101].
- K. Ackerstaff *et al.* (OPAL collaboration), *Polarization and forward-backward asymmetry of lambda baryons in hadronic Z^0 decays*, Eur. Phys. J. **C2**, 49 (1998) [CERN-PPE-97-104].
- K. Ackerstaff *et al.* (OPAL collaboration), *Multiplicity distributions of gluon and quark jets and tests of QCD analytic predictions*, Eur. Phys. J. **C1**, 479 (1998) [CERN-PPE-97-105].
- K. Ackerstaff *et al.* (OPAL collaboration), *Multiphoton final states in e^+e^- collisions at $\sqrt{s} = 130$ GeV – 172 GeV*, Eur. Phys. J. **C1**, 21 (1998) [CERN-PPE-97-109].
- K. Ackerstaff *et al.* (OPAL collaboration), *Search for the standard model Higgs boson in e^+e^- collisions at $\sqrt{s} = 161$ GeV – 172 GeV*, Eur. Phys. J. **C1**, 425 (1998) [CERN-PPE-97-115].
- K. Ackerstaff *et al.* (OPAL collaboration), *Measurement of the W boson mass and W^+W^- production and decay properties in e^+e^- collisions at $\sqrt{s} = 172$ GeV*, Eur. Phys. J. **C1**, 395 (1998) [CERN-PPE-97-116].
- K. Ackerstaff *et al.* (OPAL collaboration), *Search for a massive di-photon resonance at $\sqrt{s} = 91$ GeV – 172 GeV*, Eur. Phys. J. **C1**, 31 (1998) [CERN-PPE-97-121].
- K. Ackerstaff *et al.* (OPAL collaboration), *Search for unstable heavy and excited leptons in e^+e^- collisions at $\sqrt{s} =$*

- 170 GeV – 172 GeV, Eur. Phys. J. **C1**, 45 (1998) [CERN-PPE-97-123].
- K. Ackerstaff *et al.* (OPAL collaboration), *Search for anomalous production of dilepton events with missing transverse momentum in e^+e^- collisions at $\sqrt{s} = 161$ GeV and 172 GeV*, Eur. Phys. J. **C4**, 47 (1998) [CERN-PPE-97-124].
- K. Ackerstaff *et al.* (OPAL collaboration), *Measurement of triple gauge boson couplings from W^+W^- production at $\sqrt{s} = 172$ GeV*, Eur. Phys. J. **C2**, 597 (1998) [CERN-PPE-97-125].
- K. Ackerstaff *et al.* (OPAL collaboration), *Search for anomalous production of photonic events with missing energy in e^+e^- collisions at $\sqrt{s} = 130$ GeV to 172 GeV*, Eur. Phys. J. **C2**, 607 (1998) [CERN-PPE-97-132].
- K. Ackerstaff *et al.* (OPAL collaboration), *Search for the B/C meson in hadronic Z^0 decays*, Phys. Lett. **B420**, 157 (1998) [CERN-PPE-97-137].
- K. Ackerstaff *et al.* (OPAL collaboration), *Measurement of the one prong hadronic tau branching ratios at LEP*, Eur. Phys. J. **C4**, 193 (1998) [CERN-PPE-97-152].
- K. Ackerstaff *et al.* (OPAL collaboration), *Search for an excess in the production of four jet events from e^+e^- collisions at $S(1/2) = 130$ GeV – 184 GeV*, Phys. Lett. **B429**, 399 (1998) [CERN-EP-98-013].
- K. Ackerstaff *et al.* (OPAL collaboration), *A search for neutral Higgs bosons in the MSSM and models with two scalar field doublets*, Eur. Phys. J. **C5**, 19 (1998) [CERN-EP-98-029].
- K. Ackerstaff *et al.* (OPAL collaboration), *An upper limit on the anomalous magnetic moment of the τ lepton*, Phys. Lett. **B421**, 188 (1998) [CERN-EP-98-033].
- K. Ackerstaff *et al.* (OPAL collaboration), *Search for stable and longlived massive charged particles in e^+e^- collisions at $\sqrt{s} = 130$ GeV – 183 GeV*, Phys. Lett. **B433**, 195 (1998) [CERN-EP-98-039].
- K. Ackerstaff *et al.* (OPAL collaboration), *An upper limit for the τ neutrino mass from $\tau \rightarrow 5\pi^\pm\nu_\tau$ decays*, Eur. Phys. J. **C5**, 229 (1998) [CERN-EP-98-055].
- K. Ackerstaff *et al.* (OPAL collaboration), *Bose-Einstein correlations of three charged pions in hadronic Z^0 decays*, Eur. Phys. J. **C5**, 239 (1998) [CERN-EP-98-068].
- K. Ackerstaff *et al.* (OPAL collaboration), *Multiphoton production in e^+e^- collisions at $\sqrt{s} = 183$ GeV*, Phys. Lett. **B438**, 379 (1998) [CERN-EP-98-092].
- K. Ackerstaff *et al.* (OPAL collaboration), *Search for Higgs bosons and new particles decaying into two photons at $\sqrt{s} = 183$ GeV*, Phys. Lett. **B437**, 218 (1998) [CERN-EP-98-093].
- K. Ackerstaff *et al.* (OPAL collaboration), *Production of χ_{c2} mesons in photon-photon collisions at LEP*, Phys. Lett. **B439**, 197 (1998) [CERN-EP-98-106].
- G. Abbiendi *et al.* (OPAL collaboration), *Measurement of the average polarization of B baryons in hadronic Z^0 decays*, Phys. Lett. **B444**, 539 (1998) [CERN-EP-98-119].
- G. Abbiendi *et al.* (OPAL collaboration), *First measurement of Z/γ^* production in Compton scattering of quasi-real photons*, Phys. Lett. **B438**, 391 (1998) [CERN-EP-98-120].
- G. Abbiendi *et al.* (OPAL collaboration), *Measurement of the longitudinal cross-section using the direction of the thrust axis in hadronic events at LEP*, Phys. Lett. **B440**, 393 (1998) [CERN-EP-98-124].

Instrumentation/Accelerator Physics/Computing Sciences

O. Biebel, S. Braibant, S.J. deJong, R. Hammarstrom, R. Hilgers, A.K. Honma, P. Jovanovic, J.A. Lauber and H.A. Neal, *Radiation monitoring and beam dump system of the OPAL silicon microvertex detector*, Nucl. Instrum. Methods **A402**, 351 (1998) [CERN-PPE-97-091].

E.W. Blackmore, D.A. Bryman, Y. Kuno, C. Lim, T. Numao, P. Padley, G. Redlinger, R. Soluk and R.A. McPherson, *Central tracking chamber with inflated cathode-strip foils*, Nucl. Instrum. Methods **A404**, 295 (1998) [TRI-PP-96-39].

T.A. Shibata, Y. Sakemi, H. Kobayashi, S. Yoneyama, T. Harano, K. Shibatani, M. Kurisuno, H. Ogami and C.A. Miller, *A high precision laser alignment monitoring system for HERMES tracking detectors*, Nucl. Instrum. Methods **A411**, 75 (1998).

J.G. Rogers, C. Moisan, I.M. Thorson and M.S. Andreaco, *A 7–9 MeV isotopic gamma ray source for detector testing*, Nucl. Instrum. Methods **A413**, 249 (1998) [TRI-PP-96-7].

G. Sciolla *et al.*, *The BaBar drift chamber*, Nucl. Instrum. Methods **A419**, 310 (1998).

W.Z. Gelbart *et al.*, *In situ thickness measurements in molecular beam epitaxy using alpha particle energy loss*, Surface Coatings and Tech. **94–95**, 374 (1998).

W.Z. Gelbart *et al.*, *Film thickness and composition monitoring during growth by molecular beam epitaxy using alpha particle energy loss*, App. Phys. Lett. **72**, 3288 (1998).

Chemistry and Solid-State Physics

D.C. Walker, *Kinetic isotope effects in solution: Reactions of muonium atoms as H isotopes*, J. Chem. Soc., Faraday Trans. **94**, 1 (1998).

G.M. Luke, Y. Fudamoto, K.M. Kojima, M.I. Larkin, J. Merin, B. Nachumi, Y.J. Uemura, Y. Maeno, Z.Q. Mao, Y. Mori, H. Nakamura and M. Sigrist, *Time reversal symmetry breaking superconductivity in Sr_2RuO_4* , Nature **394**, 558 (1998).

V. Storchak and N.V. Prokof'ev, *Muon/muonium quantum diffusion – review article*, Rev. Mod. Phys. **70**, 929 (1998).

V. Storchak, J.H. Brewer and S.F.J. Cox, *Quantum diffusion in cryocrystals studied by muon spin relaxation*, J. Low Temp. Phys. **111**, 303 (1998).

D.E. MacLaughlin, R.H. Heffner, G.J. Nieuwenhuys, G.M. Luke, Y. Fudamoto, Y.J. Uemura, R. Chau, M.B. Maple and B. Andraka, *Susceptibility inhomogeneity and non-Fermi-liquid behaviour in nominally ordered UCu_4Pd* , Phys. Rev. **B58** (Rapid Comm.), R11849 (1998).

D.R. Noakes, G.M. Kalvius, R. Wäppling, C.E. Stronach, M.F. White, H. Saito and K. Fukamichi, *Spin dynamics and freezing in magnetic rare-earth quasicrystals*, Phys. Lett. **A238**, 197 (1998).

W.J. Kossler, Y.X. Dai, K.G. Petzinger, A.J. Greer, D.Ll. Williams, E. Koster, D.R. Harshman and D. Mitzi, *Transparency of the ab planes of $Bi_2Sr_2CaCu_2O_{8+\delta}$ to magnetic fields*, Phys. Rev. Lett. **80**, 592, (1998).

Life Sciences

G.L-Y. Chan, J.E. Holden, J. Stoessl, D.J. Doudet, T. Dobko, K.S. Morrison, C.L. English, J.M. Huser, B. Legg, M. Schulzer and T.J. Ruth, *Reproducibility of [^{11}C]Sch23390 distribution, a dopamine D1 receptor tracer in normal human subjects*, J. Nucl. Med. **39**, 792 (1998).

D.J. Doudet, G.L.Y. Chan, J.E. Holden, E. McGeer, T.A. Aigner, R.J. Wyatt and T.J. Ruth, *6-Fluoro-L-Dopa PET studies of the turnover of dopamine in MPTP-induced Parkinsonism in monkeys*, Synapse **29**, 225 (1998).

N.M. Crawford and A.D.M. Glass, *Molecular and physiological aspects of nitrate uptake in plants*, Trends in Plant Science **3**, 381 (1998).

H.J. Kronzucker, R.D. Guy, K. Kirk, M.Y. Siddiqi and A.D.M. Glass, *Effects of hypoxia on $^{13}NH_4^+$ uptake in rice roots: kinetics and compartmental analysis*, Plant Physiol. **116**, 581 (1998).

Y. Wang, J.E. Holden, G.L-Y. Chan, T. Dobko, E. Mak, M. Schulzer, J.M. Huser, B.J. Snow, T.J. Ruth, D.B. Calne and A.J. Stoessl, *Age-dependent decline of dopamine D1 receptors in human brain: a PET study*, Synapse **30**, 56 (1998).

Setyawati, K.H. Thompson, Y. Sun, D.M. Lyster, C. Vo, V.G. Yuen, J.H. McNeill, T.J. Ruth, S. Zeisler and C. Orvig, *Vanadium uptake, distribution and excretion of ^{48}V -labeled compounds in rat. Comparison of bis(malto)oxovanadium(IV) (BMOV) and vanadyl sulfate trihydrate (VS) by conventional and compartmental analyses*, J. App. Physiol. **84**, 569 (1998).

T.R. Oakes, V. Sossi and T.J. Ruth, *Normalization for 3D PET with a low-scatter planar source and measured geometric factors*, Phys. Med. Biol. **43**, 961 (1998).

V. Sossi, T.R. Oakes and T.J. Ruth, *A comprehensive evaluation of quantitation for 3D PET brain imaging using phantom studies*, Physics Med. Biol. **43**, 2615 (1998).

A. Kishore, T.G. Nygaard, R. de la Fuente-Fernandez, A.B. Naini, M. Schulzer, E. Mak, T.J. Ruth, A.J. Stoessl, D.B. Calne and B.J. Snow, *Striatal D2 receptors in symptomatic and asymptomatic carriers of dopa-responsive dystonia measured with [^{11}C]raclopride and positron emission tomography*, Neurology **50**, 1028 (1998).

Theoretical Program

H.W. Fearing and S. Scherer, *Virtual Compton scattering off spin zero particles at low energies*, Few Body Systems **23**, 111 (1998) [TRI-PP-96-28].

H.W. Fearing, *Nucleon nucleon bremsstrahlung: an example of the impossibility of measuring off-shell amplitudes*, Phys. Rev. Lett. **81**, 758 (1998).

C.P. Burgess, A. de la Macorra, I. Maksymyk and F. Quevedo, *Supersymmetric models with product groups and field dependent gauge couplings*, JHEP **9809**, 007 (1998).

L.L. Barz, H. Forkel, H.-W. Hammer, F.S. Navarra, M. Nielsen and M.J. Ramsey-Musolf, *K^* mesons and nucleon strangeness*, Nucl. Phys. **A640**, 259 (1998) [DOE-ER-40561-345].

P.F. Bedaque, H.-W. Hammer and U. van Kolck, *Effective theory for neutron deuteron scattering: energy dependence*, Phys. Rev. **C58**, R641 (1998) [TRI-PP-98-2, DOE-ER-40561-356, KRL MAP-219].

R. Lewis and R.M. Woloshyn, *$\mathcal{O}(1/M^3)$ effects for heavy-light mesons in lattice NRQCD*, Phys. Rev. **D58**, 074506 (1998) [TRI-PP-98-3, JLAB-THY-98-05, hep-lat/9803004].

B.K. Jennings and S. Karataglidis, *$S_{\text{eff}}(E)$ and the $^7\text{Be}(p, \gamma)^8\text{B}$ reaction*, Phys. Rev. **C58**, 3002 (1998).

B.K. Jennings, S. Karataglidis and T.D. Shoppa, *Extrapolation of the astrophysical S factor for $^7\text{Be}(p, \gamma)^8\text{B}$ to solar energies*, Phys. Rev. **C58**, 3711 (1998).

B.K. Jennings, S. Karataglidis and T.D. Shoppa, *Direct capture astrophysical S factors at low energy*, Phys. Rev. **C58**, 579 (1998).

H. Müller and B.K. Jennings, *Critical analysis of quark-meson coupling models for nuclear matter and finite nuclei*, Nucl. Phys. **A640**, 55 (1998).

H. Müller, *Properties of finite nuclei in the modified quark-meson coupling model*, Phys. Rev. **C57**, 1974 (1998).

V.E. Shapiro, *The gyro force of high frequency fields lost by the concept of effective potential*, Phys. Lett. **A238**, 147 (1998) [TRI-PP-97-70].

A.M. Rakhimov, F.C. Khanna, U.T. Yakhshev and M.M. Musakhanov, *Density dependence of meson nucleon vertices in nuclear matter*, Nucl. Phys. **A643**, 383 (1998).

A. Rakhimov, M.M. Musakhanov, F.C. Khanna and U. Yakhshev, *Medium modification of nucleon properties in*

Skyrme model, Phys. Rev. **C58**, 1738 (1998) [NUCLTH-9609049].

A.E. Santana, F.C. Khanna and Y. Takahashi, *Galilei covariance and (4, 1) de Sitter space*, Prog. Theor. Phys. **99**, 327 (1998).

T.R. Hemmert, B.R. Holstein, J. Kambor and G. Knochlein, *Compton scattering and the spin structure of the nucleon at low-energies*, Phys. Rev. **D57**, 5746 (1998) [TRI-PP-97-20, ZU-TH-18/97, MKPH-T-97-21].

V. Bernard, H.W. Fearing, T.R. Hemmert and U.-G. Meissner, *The form factors of the nucleon at small momentum transfer*, Nucl. Phys. **A635**, 121 (1998); Nucl. Phys. **A642**, 563 (1998) [KFA-IKP(TH)-1998-01, LPT-98-01, TRI-PP-97-73].

D.H. Wilkinson *Phase space for neutron beta-decay: an update*, Nucl. Instrum. Methods **A404**, 305 (1998).

D.H. Wilkinson, *Evaluation of beta-decay. Pt. VII. The Z-independent outer radiative correction for unique-forbidden decay*, Nucl. Instrum. Methods **A406**, 89 (1998).

D.H. Wilkinson, *The rate of semi-leptonic hyperon decay in recoil order*, Nucl. Instrum. Methods **A413**, 457 (1998).

V.G.J. Stoks, *Can the magnetic moment contribution explain the A(Y) puzzle?*, Phys. Rev. **C57**, 445 (1998) [NUCLTH-9710068].

C. Alexandrou, R. Rosenfelder and A.W. Schreiber, *Variational field theoretical approach to relativistic scattering*, Nucl. Phys. **A628**, 427 (1998) [UCY-PHY-96-7].

Journal Publications In Press or Submitted

Particle, Nuclear and Atomic Physics

B.A. Mofteh, E. Gete, D.F. Measday, D.S. Armstrong, J. Bauer, T.P. Gorringe, B.L. Johnson, B. Siebels and S. Stanislaus, *Muon capture in ^{28}Si and g_p/g_a* (Phys. Lett. B, in press) [TRI-PP-97-3].

G.M. Marshall, T.A. Porcelli, A. Adamczak, J.M. Bailey, G.A. Beer, M.P. Faifman, M.C. Fujiwara, T.M. Huber, R. Jacot-Guillarmod, P. Kammel, S.K. Kim, P.E. Knowles, A.R. Kunselman, M. Maier, V.E. Markushin, G.R. Mason, F. Mulhauser, A. Olin, C. Petitjean and J. Zmeskal, *Resonant formation measurements of $d\tau$ via time of flight*, (Hyp. Int., in press).

T.M. Huber, A. Adamczak, J.M. Bailey, G.A. Beer, J.L. Beveridge, B.P. Ellerbusch, M.C. Fujiwara, R. Jacot-Guillarmod, P. Kammel, S.K. Kim, P.E. Knowles, A.R. Kunselman, G.J. Lindquist, M. Maier, V.E. Markushin, G.M. Marshall, C.J. Martoff, G.R. Mason, F. Mulhauser, A. Olin, C. Petitjean, T.A. Porcelli, J. Woźniak and J. Zmeskal, *Time-of-flight studies of emission of $\mu\tau$ from frozen hydrogen films*, (Hyp. Int., in press).

M.C. Fujiwara, A. Adamczak, J.M. Bailey, G.A. Beer, J.L. Beveridge, M.P. Faifman, T.M. Huber, R. Jacot-

Guillarmod, P. Kammel, S.K. Kim, P.E. Knowles, A.R. Kunselman, M. Maier, V.E. Markushin, G.M. Marshall, C.J. Martoff, G.R. Mason, F. Mulhauser, A. Olin, C. Petitjean, T.A. Porcelli, J. Woźniak and J. Zmeskal, *Time-of-flight spectroscopy of muonic tritium*, (Hyp. Int., in press).

HERMES collaboration, *Beam induced nuclear depolarization in a gaseous polarized hydrogen target* (Phys. Rev. Lett., in press) [DESY-98-058, hep-ex/9896006].

J. Graeter, P.A. Amaudruz, R. Bilger, P. Camerini, J. Clark, H. Clement, E. Friedman, L. Felawka, S.N. Filippov, E. Fragiaco, Yu. K. Gavrilov, E. Gibson, N. Grion, G.J. Hofman, B. Jamieson, T.L. Karavicheva, M. Kermani, E.L. Mathie, R. Meier, G. Maloney, D. Ottewell, J. Paetzold, O. Patarakin, K. Raywood, R. Rui, M. Schepkin, M.E. Sevir, G.R. Smith, H. Staudenmaier, R. Tacik, G. Tagliente, G.J. Wagner and M. Yoemans, *Search for a bound trineutron with the $^3\text{He}(\pi^-, \pi^+)nnn$ reaction* (Eur. Phys. J. A, in press).

A.J.T. Jull, S. Cloudt, D.J. Donahue, J.M. Sisterson, R.C. Reedy and J. Masarik, *^{14}C depth profiles in Apollo 15 and 17 cores and lunar rock 68815* (Geochim. et Cosmochim. Acta., in press).

R. Tacik, E.L. Mathie, P. Amaudruz, J.T. Brack, L. Felawka, R. Meier, D. Ottewell, G.R. Smith, G. Hofman, M. Kermani, S. McFarland, K. Raywood, M. Sevir, F. Bonutti, P. Camerini, N. Grion, R. Rui and E.F. Gibson, *Simultaneous study of the $^{12}\text{C}(\pi^+, pd)$ and $^{12}\text{C}(\pi^+, ppd)$ reactions* (submitted to Phys. Rev. C).

J. Zhao, R. Abegg, A.R. Berdoz, J. Birchall, J.R. Campbell, C.A. Davis, P.P.J. Delheij, L. Gan, P.W. Green, L.G. Greeniaus, D.C. Healey, R. Helmer, N. Kolb, E. Korkmaz, L. Lee, C.D.P. Levy, J. Li, C.A. Miller, A.K. Opper, S.A. Page, H. Postma, W.D. Ramsay, J. Soukup, G.M. Stinson, W.T.H. van Oers and A.N. Zelenski, *Precision measurement of charge symmetry breaking in np elastic scattering at 347 MeV* (submitted to Phys. Rev. C) [TRI-PP-97-4].

M. Benjamintz, W.R. Falk, J.R. Campbell, A. Green, P.G. Roos, P.L. Walden, S. Yen, A.G. Ling, E.G. Auld, E. Korkmaz and M.A. Punyasena, *Investigation of the $^{12}\text{C}(\bar{p}, d\pi^+)^{11}\text{B}$ reaction in the quasifree region* (submitted to Phys. Rev. C).

K. Ackerstaff *et al.* (OPAL collaboration), *Production of K_S^0 and Λ in quark and gluon jets from Z^0 decay* (submitted to Eur. Phys. J.) [CERN-EP-98-058].

K. Ackerstaff *et al.* (OPAL collaboration), *Measurements of flavor dependent fragmentation functions in $Z^0 \rightarrow q\bar{q}$ events* (submitted to Eur. Phys. J.) [CERN-EP-98-089].

K. Ackerstaff *et al.* (OPAL collaboration), *Measurement of τ branching ratios to five charged hadrons* (submitted to Eur. Phys. J.) [CERN-EP-98-090].

K. Ackerstaff *et al.* (OPAL collaboration), *Inclusive production of charged hadrons and K_S^0 mesons in photon-photon collisions* (Eur. Phys. J., in press) [CERN-EP-98-091].

K. Ackerstaff *et al.* (OPAL collaboration), *Measurement of the strong coupling constant α_s and the vector and axial vector spectral functions in hadronic tau decays* (submitted to Eur. Phys. J.) [CERN-EP-98-102].

K. Ackerstaff *et al.* (OPAL collaboration), *Measurement of the Michel parameters in leptonic tau decays* (submitted to Eur. Phys. J.) [CERN-EP-98-104].

K. Ackerstaff *et al.* (OPAL collaboration), *Search for scalar top and scalar bottom quarks at $\sqrt{s} = 183$ GeV at LEP* (submitted to Eur. Phys. J.) [CERN-EP-98-107].

G. Abbiendi *et al.* (OPAL collaboration), *Tests of the standard model and constraints on new physics from measurements of fermion pair production at 183 GeV at LEP* (submitted to Eur. Phys. J.) [CERN-EP-98-108].

G. Abbiendi *et al.* (OPAL collaboration), *Dijet production in photon-photon collisions at $\sqrt{s}_{ee} = 161$ GeV and 172 GeV* (submitted to Eur. Phys. J.) [CERN-EP-98-113].

G. Abbiendi *et al.* (OPAL collaboration), *A study of parton fragmentation in hadronic Z^0 decays using $\Lambda\bar{\Lambda}$ correlations* (submitted to Phys. Lett. B) [CERN-EP-98-114].

G. Abbiendi *et al.* (OPAL collaboration), *Search for acoplanar lepton pair events in e^+e^- collisions at $\sqrt{s} = 161$ GeV, 172 GeV and 183 GeV* (submitted to Eur. Phys. J.) [CERN-EP-98-122].

G. Abbiendi *et al.* (OPAL collaboration), *A measurement of R_b using a double tagging method* (submitted to Eur. Phys. J.) [CERN-EP-98-137].

G. Abbiendi *et al.* (OPAL collaboration), *Search for chargino and neutralino production at $\sqrt{s} = 181$ GeV – 184 GeV at LEP* (submitted to Eur. Phys. J.) [CERN-EP-98-136].

G. Abbiendi *et al.* (OPAL collaboration), *Search for anomalous photonic events with missing energy in e^+e^- collisions at $\sqrt{s} = 130$ GeV, 136 GeV and 183 GeV* (submitted to Eur. Phys. J.) [CERN-EP-98-139, CERN-EP-98-143].

G. Abbiendi *et al.* (OPAL collaboration), *Measurement of the semileptonic branching ratio of charm hadrons produced in $Z^0 \rightarrow c\bar{c}$ decays* (submitted to Eur. Phys. J.) [CERN-EP-98-146].

G. Abbiendi *et al.* (OPAL collaboration), *W^+W^- production and triple gauge boson couplings at LEP energies up to 183 GeV* (submitted to Eur. Phys. J.) [CERN-EP-98-167].

G. Abbiendi *et al.* (OPAL collaboration), *Bose-Einstein correlations in $e^+e^- \rightarrow W^+W^-$ at 172 GeV and 183 GeV* (submitted to Eur. Phys. J.) [CERN-EP-98-174].

G. Abbiendi *et al.* (OPAL collaboration), *A measurement of the $\tau \rightarrow e^-\bar{\nu}_e\nu_\tau$ branching ratio* (submitted to Phys. Lett. B) [CERN-EP-98-175].

G. Abbiendi *et al.* (OPAL collaboration), *A measurement*

of the product branching ratio $f(b \rightarrow \Lambda_b) \cdot BR(\Lambda_b \rightarrow \Lambda X)$ in Z^0 decays (submitted to Eur. Phys. J.) [CERN-EP-98-186].

G. Abbiendi *et al.* (OPAL collaboration), *Search for baryon and lepton number violating Z^0 decays* (submitted to Phys. Lett. B) [CERN-EP-98-194].

G. Abbiendi *et al.* (OPAL collaboration), *Measurement of the B^+ and B^0 lifetimes and search for $CP(T)$ violation using reconstructed secondary vertices* (submitted to Eur. Phys. J.) [CERN-EP-98-195].

G. Abbiendi *et al.* (OPAL collaboration), *Color reconnection studies in $e^+e^- \rightarrow W^+W^-$ at $\sqrt{s} = 183$ GeV* (submitted to J. Phys. B) [CERN-PPE-98-196].

G. Abbiendi *et al.* (OPAL collaboration), *Measurement of the W mass and width in e^+e^- collisions at 183 GeV* (submitted to Phys. Lett. B) [CERN-EP-98-197].

G. Abbiendi *et al.* (OPAL collaboration), *Searches for R parity violating decays of gauginos at 183 GeV at LEP* (submitted to Eur. Phys. J.) [CERN-EP-98-203].

K. Ackerstaff *et al.* (HERMES collaboration), *Observation of a coherence length effect in exclusive ρ^0 electroproduction* (submitted to Phys. Rev. Lett.) [DESY-98-178].

Instrumentation/Accelerator Physics/Computing Sciences

M. Landry, J. Birchall, C.A. Davis, W. Faszer, L. Gan, L. Lee, S.A. Page, W.D. Ramsay, M. Salomon and W.T.H. van Oers, *Performance of micro strip gas chambers in BNL-E885: a search for $\Lambda\Lambda$ -hypernuclei* (Nucl. Instrum. Methods A, in press) [TRI-PP-98-4].

P. Botton *et al.*, *Mass discrimination using double-sided silicon microstrip detectors for pions and protons at intermediate energies* (Nucl. Instrum. Methods A, in press).

R. Lange, J.S. Vincent, J.M. D’Auria, U. Geisen and T.J. Ruth, *Production of ^{44}Ti for astrophysical studies* (submitted to Nucl. Instrum. Methods B).

R. Helmer, *The Sudbury Neutrino Observatory* (submitted to IEEE Trans. Nucl. Sci.).

S. Koscielniak, *Longitudinal single bunch coherent instability theory with narrow-band impedances part 1: harmonic oscillator* (submitted to Part. Accel.).

S. Koscielniak, *Longitudinal single bunch coherent instability theory with narrow-band impedances part 2: pendulum oscillator* (submitted to Part. Accel.).

ATLAS collaboration, *ATLAS first-level trigger: technical design report* [CERN-LHCC-98-14].

ATLAS collaboration, *ATLAS trigger performance: status report* [CERN-LHCC-98-15].

ATLAS collaboration, *ATLAS DAQ, EF, LVL2 and DCS: technical progress report* [CERN-LHCC-98-16].

Chemistry and Solid-State Physics

D.R. Noakes, *A correlation length measured by zero-field muon spin relaxation in disordered magnets* (J. Phys. Cond. Matter, in press).

X. Wan, W.J. Kossler, C.E. Stronach and D.R. Noakes, *Cauchy magnetic field component and magnitude distributions studied by the zero-field muon spin relaxation technique* (Hyp. Int., in press).

P.W. Percival, B. Addison-Jones, J.C. Brodovitch, K. Ghandi and J. Schüth, *Free radicals formed by H(Mu) addition to pyrene* (Can. J. Chem., in press).

J.E. Sonier, R.F. Kiefl, J.H. Brewer, D.A. Bonn, S.R. Dunsiger, W.N. Hardy, R. Liang, R.I. Miller, D.R. Noakes and C.E. Stronach, *Expansion of the vortex cores in $YBa_2Cu_3O_{6.95}$ at low magnetic fields* (Phys. Rev. B, in press).

B. Hitti, S.R. Kreitzman, T.L. Estle, E.S. Bates, M.R. Dawdy, T.L. Head and R.L. Lichti, *Dynamics of negative muonium in n-type silicon* (Phys. Rev. B, in press).

V. Storchak, J.H. Brewer, G.D. Morris, D.J. Arseneau and M. Senba, *Muonium formation via electron transport in solid nitrogen* (submitted to Phys. Rev. B).

V. Storchak, J.H. Brewer, D.G. Eshchenko, S.P. Cottrell and S.F.J. Cox, *Destruction of bandlike propagation in orientationally ordered crystals* (submitted to Phys. Rev. Lett.).

Y. Fudamoto, K.M. Kojima, M.I. Larkin, G.M. Luke, J. Merrin, B. Nachumi, Y.J. Uemura, Y. Ueda and M. Isobe, *Static spin freezing in NaV_2O_5 detected by muon spin relaxation* (submitted to Phys. Rev. Lett.).

D.E. MacLaughlin, R.H. Heffner, G.J. Nieuwenhuys, P.C. Canfield, A. Amato, C. Baines, A. Schenck, G.M. Luke, Y. Fudamoto and Y.J. Uemura, *Muon spin relaxation and nonmagnetic Kondo state in $PrInAg_2$* (submitted to Phys. Rev. B).

J.S. Gardner, S.R. Dunsiger, B.D. Gaulin, M.J.P. Gingras, J.E. Greedan, R.F. Kiefl, M.D. Lumsden, W.A. MacFarlane, N.P. Raju, J.E. Sonier, I. Swainson and Z. Tun, *Cooperative paramagnetism in the geometrically frustrated pyrochlore antiferromagnet $Tb_2Ti_2O_7$* (submitted to Phys. Rev. Lett.).

Life Sciences

X. Min, M.Y. Siddiqi, R.D. Guy, A.D.M. Glass and H.J. Kronzucker, *Induction of nitrate uptake and nitrate reductase in trembling aspen and lodgepole pine* (Plant Cell and Environ., in press).

A.D.M. Glass *et al.*, *Inorganic nitrogen absorption by plant roots* (Plant & Soil, in press).

H.J. Kronzucker, A.D.M. Glass and M.Y. Siddiqi, *Inhibition of nitrate uptake by ammonium in barley: analysis of*

component fluxes (Plant Physiol., in press).

X. Min, M.Y. Siddiqi, R.D. Guy, A.D.M. Glass and H.J. Kronzucker, *A comparative study of fluxes and compartmentation of nitrate and ammonium in early successional tree species* (Plant Cell and Environ., in press).

D. Zhou *et al.*, *Differential expression of two putative high affinity NO_3^- transporter genes (Nrt) in arabidopsis* (Plant Journal, in press).

D.J. Doudet, J. Holden, G.L.Y. Chan, S. Jivan, O. DeJesus, T.A. Aigner and T. Ruth, *Investigation of the DA presynaptic function by PET $6-^{18}F$ fluoro-L-dopa vs. $6-^{18}F$ fluoro-L-m-tyrosine* (J. Cereb. Blood Flow Metab., in press).

G.L-Y. Chan, J.E. Holden, A.J. Stoessl, A. Samii, D.J. Doudet, T. Dobko, K.S. Morrison, M.J. Adam, M. Schulzer, D.B. Calne and T. Ruth, *Reproducibility studies with a monoamine vesicular transporter inhibitor in normal human subjects* (J. Nucl. Med., in press).

G.L-Y. Chan, J.E. Holden, J. Stoessl, A. Sammi, D.J. Doudet, T. Dobko, K.S. Morrison, M.J. Adam, M. Schulzer and T.J. Ruth, *Reproducibility of [^{11}C]dihydrotrabenazine positron emission tomography in normal human subjects* (J. Nuc. Med. **39**, in press).

A.J. Stoessl and T.J. Ruth, *Neuroreceptor imaging* (Current Opinion in Neurology, in press).

R. de la Fuente-Fernandez, A. Kishore, B.J. Snow, M. Schulzer, C.S. Lee, T.J. Ruth, A.J. Stoessl and D.B. Calne, *Effect of aging on the dopaminergic function of caudate nuclei in idiopathic Parkinsonism* (Parkinson's and Related Disorders, in press).

V. Sossi, T.R. Oakes, G.L-Y. Chan and T.J. Ruth, *Quantitative comparison of 3D and 2D PET with human brain studies* (J. Nucl. Med., in press).

H. Dougan, J. Hobbs, D.M. Lyster and J.I. Weitz, *High specific activity radiolabeling of organotin DNA* (J. Lab. Cmpds. and Radiopharmaceuticals, in press).

G.L-Y. Chan, J.E. Holden, H-T. Chan, A.J. Stoessl, Y. Wang, D.J. Doudet, T. Dobko, K.S. Morrison, M.J. Adam, M. Schulzer and T.J. Ruth, *Reproducibility of [^{11}C]d-threo-methylphenidate by positron emission tomography and the effect of normal aging on the dopamine transporter availability in normal human subjects* (submitted to J. Cereb. Blood Flow and Anal.).

G.L-Y. Chan, D.J. Doudet, J.E. Holden, C.L. English, J.M. Huser and T.J. Ruth, *Comparison of binding of [^{11}C]SCH 23390 and [^{11}C]SCH 39166 to dopamine D1 receptors using PET in non-human primates* (submitted to J. Cereb. Blood Flow and Anal.).

V. Sossi, T.R. Oakes and T.J. Ruth, *A phantom study evaluating the quantitative aspect of 3D PET imaging of the brain* (submitted to Phys. Med. Biol.).

R. de la Fuente-Fernandez, F.J.G. Vingerhoets, A. Kishore, M. Schulzer, E.K. Mak, T.J. Ruth, B.J. Snow, A.J. Stoessl and D.B. Calne, *Motor fluctuations in idiopathic Parkinsonism are not directly related to the dopaminergic deficit* (submitted to Brain).

L.N. Yatham, P.F. Liddle, J. Dennie, I-S. Shiah, M.J. Adam, C.J. Lane, R.W. Lam and T.J. Ruth, *Effects of desipramine treatment on brain 5-HT₂ receptors in patients with major depression: a positron emission tomography study with [¹⁸F]-setoperone* (submitted to Archives of General Psychiatry).

Theoretical Program

H. Müller, *Effective field theory for $\Lambda - \Sigma^0$ mixing in nuclear matter* (Phys. Rev. C, in press).

A. Plastino, A.R. Plastino, H.G. Miller and F.C. Khanna, *A lower bound for Fisher's information theory* (Phys. Lett. A, in press).

F.X. Lee and D.B. Leinweber, *Light hadron spectroscopy on coarse lattices with $\mathcal{O}(\alpha^2)$ mean field improved actions* (Phys. Rev. D, in press) [CU-NPL-1154].

K.F. Liu, S.J. Dong, T. Draper, D. Leinweber, J. Sloan, W. Wilcox and R.M. Woloshyn, *Valence QCD: connecting QCD to the quark model* (Phys. Rev. D, in press) [UK-98-03].

B.D. Jones and R.M. Woloshyn, *Mesonic decay constants in lattice NRQCD* (Phys. Rev. D, in press) [TRI-PP-98-39].

L.N. Chang, O. Lebedev and J.N. Ng, *On the invisible decays of the Υ and J/Ψ resonances* (submitted to Phys. Rev.) [TRI-PP-98-08].

P.F. Bedaque, H.-W. Hammer and U. van Kolck, *Renormalization of the three-body system with short-range interactions* (submitted to Phys. Rev. Lett.) [TRI-PP-98-17, DOE/ER/40561-28-INT98, KRL MAP-235, NTUW-98-24].

H.-W. Hammer and M.J. Ramsey-Musolf, *Spectral content of isoscalar nucleon form factors* (submitted to Nucl. Phys. A) [DOE/ER/40561-18-INT98, TRI-PP-98-26].

P.F. Bedaque, H.-W. Hammer and U. van Kolck, *The three-boson system with short-range interactions* (submitted to Nucl. Phys. A) [TRI-PP-98-27].

A.S. Rinat and B.K. Jennings, *On the equivalence of the impulse approximation and the Gersch-Rodriguez-Smith series for structure functions* (submitted to Phys. Rev. C) [TRI-PP-98-29, WIS-98/28 Oct-DPP].

H.W. Fearing, *Comment on 'Induced pseudoscalar coupling constant' by Il-Tong Cheon and Myung Ki Cheoun (nucl-th/9811009)* (submitted to Phys. Rev.) [TRI-PP-98-37].

H.-W. Hammer and M.J. Ramsey-Musolf, *$K\bar{K}$ -continuum and isoscalar nucleon form factors* (submitted to Phys. Lett. B) [TRI-PP-98-41].

M. Welsh and H.W. Fearing, *Reply to the comment on 'Validity of certain soft photon amplitudes'* (submitted to Phys. Rev. C) [TRI-PP-98-42].

A.E. Santana, A. Matos Neto, J.D.M. Vianna and F.C. Khanna, *W^* -algebra, Poincare group and the quantum kinetic theory*, (Int. J. Math Phys., in press).

J. Smejkal, E. Truhlik and F.C. Khanna, *Chiral Lagrangians and the transition amplitude for radiative muon capture* (submitted to Few Body Syst.).

H.W. Fearing, *Off-shell effects in nucleon-nucleon bremsstrahlung* (submitted to Phys. Rev. Lett.) [TRI-PP-97-31].

D.H. Wilkinson, *Analysis of super-allowed Fermi beta-decay* (submitted to Nucl. Phys. A) [TRI-PP-97-74].

S. Karataglidis, P.J. Dortmans, K. Amos and C. Bennhold, *Alternative evaluations of halos in nuclei* (submitted to Phys. Rev. Lett.).

Conference Presentations

Particle, Nuclear and Atomic Physics

G.M. Marshall, J.M. Bailey, G.A. Beer, J.L. Beveridge, M.C. Fujiwara, T.M. Huber, R. Jacot-Guillarmod, P. Kammel, S.K. Kim, P.E. Knowles, A.R. Kunselman, M. Maier, G.R. Mason, F. Mulhauser, A. Olin, C. Petitjean, T.A. Porcelli, L.A. Schaller and J. Zmeskal, *Muonic processes in solid hydrogen*, Proc. **Workshop on Physics at the First Muon Collider and at the Front End of the Muon Collider**, eds. S.H. Geer, R. Raja (AIP Conf. Proc. **432**, Woodbury, NY, 1998).

A. Olin, A. Adamczak, G.A. Beer, V.M. Bystritsky, M. Filipowicz, M.C. Fujiwara, T.M. Huber, R. Jacot-Guillarmod, P. Kammel, S.K. Kim, P.E. Knowles, A.R. Kunselman, M. Maier, V.E. Markushin, G.M. Marshall, F. Mulhauser, C. Petitjean, T.A. Porcelli, V.A. Stolupin, J. Woźniak and J. Zmeskal, *Study of μ -catalyzed fusion in H-D mixtures*, Proc. **EXAT'98, Ascona, Switzerland** (Hyp. Int., in press).

F. Mulhauser, A. Adamczak, G.A. Beer, V.M. Bystritsky, M. Filipowicz, M.C. Fujiwara, T.M. Huber, R. Jacot-Guillarmod, P. Kammel, S.K. Kim, P.E. Knowles, A.R. Kunselman, V.E. Markushin, G.M. Marshall, A. Olin, C. Petitjean, T.A. Porcelli, V.A. Stolupin, J. Woźniak and J. Zmeskal, *Scattering of muonic hydrogen atoms, *ibid.**

J. Woźniak, A. Adamczak, G.A. Beer, V.M. Bystritsky, M. Filipowicz, M.C. Fujiwara, T.M. Huber, R. Jacot-Guillarmod, P. Kammel, S.K. Kim, P.E. Knowles, A.R. Kunselman, V.E. Markushin, G.M. Marshall, F. Mulhauser, A. Olin, C. Petitjean, T.A. Porcelli, V.A. Stolupin and J. Zmeskal, *New effects in the low energy scattering of μp atoms, *ibid.**

- S.D. Reitzner, A.K. Opper, R.W. Finlay, K. Hicks, E. Korkmaz, G.V. O’Rielly, D.A. Hutcheon, R. Abegg, P.W. Green, L.G. Greeniaus, D.V. Jordan, P.L. Walden, C.A. Davis, S. Yen, R. Churchman and J.A. Niskanen, *A study of systematic effects in a $np \rightarrow d\pi^0$ charge symmetry breaking experiment*, Proc. **American Physical Society Meeting, Columbus**.
- J. D’Auria *et al.* (DRAGON collaboration), *Studies of the rates of nuclear reactions using the DRAGON separator at the radioactive beam facility, ISAC*, Proc. **5th Nuclei in the Cosmos Conf., Volos, Greece**.
- J. Goerres, J. Meissner, H. Schatz, E. Stech, P. Tischhauser, M. Wiescher, D. Bazin, R. Harkewicz, M. Hellstroem, B. Sherrill, M. Steiner, R.N. Boyd, L. Buchmann, D.H. Hartmann and J.D. Hinnefeld, *Lifetime of ^{44}Ti as a probe for supernova models*, Proc. **Int. Workshop XXVI on Gross Properties of Nuclei and Nuclear Excitations, Hirschegg, Austria, Jan 11-17** (Darmstadt, 1998) p.182.
- A. Astbury, B.A. Campbell, F.C. Khanna, J.L. Pinfold and M.C. Vetterli, eds. Proc. **1998 Lake Louise Winter Institute, February 15–21** (World Scientific, Singapore, in press).
- R.A. Ritchie, F.C. Khanna and H.G. Miller, *Nuclear matter and Landau Ginzberg theory*, *ibid.*
- M.C. Vetterli, *The spin structure of the nucleon*, *ibid.*
- M.G. Vincter, *Flavor asymmetry of the light quark sea from semi-inclusive deep inelastic scattering*, *ibid.*
- R. Kiefl, *Spin polarized radioactive beams for condensed matter physics*, Proc. **Int. Workshop on JHF Science, JHF’98, Tsukuba, March 3–7**, ed. J. Chiba *et al.* (KEK 98-5, 1998) vol. I, 118.
- J.-M. Poutissou, *The status of TRIUMF*, *ibid.*, vol. I, 131.
- K.P. Jackson, *Summary: fundamental and nuclear physics at the JHF E-arena*, *ibid.*, vol. I, 224.
- J. Doornbos, *DC and rf separated kaon beams*, *ibid.*, vol. II, 33.
- P. Schmor, *ISAC project facility status*, *ibid.*, vol. II, 229.
- J.M. D’Auria, *The DRAGON facility at ISAC — a progress report*, *ibid.*, vol. II, 288.
- N. Bateman, *Nuclear spectroscopy needs for astrophysics experiments with radioactive beams*, *ibid.*, vol. II, 304.
- J. Behr, *Neutral atom traps for fundamental studies of beta decays*, *ibid.*, vol. II, 325.
- G.C. Ball, *Gamma-ray spectroscopy with radioactive beams*, *ibid.*, vol. II, 350.
- R.E. Laxdal, *Status of the ISAC post accelerator*, *ibid.*, vol. II, 415.
- M. Dombisky, *High power RIB target issues*, *ibid.*, vol. II, 419.
- P. Bricault, *Design of the target/ion source system at ISAC-TRIUMF*, *ibid.*, vol. II, 422.
- J.E. Sonier, *Measuring the characteristic length scales of superconductivity with μSR* , *ibid.*, vol. III, 294.
- D. Bryman, *Rare decays of kaons and muons*, Proc. **Lepton-Baryon’98, Trento, April 20–25** [TRI-PP-98-32].
- D. Bryman, *Rare and exotic decays*, Proc. **NATO Advanced Study Inst., St. Croix, April 20–25** [TRI-PP-98-33].
- T.J. Stocki and D.F. Measday, *Protecting the world from nuclear fallout through detection*, Proc. **Canadian Radiation Protection Assn. Conf., Ottawa, May** (Bulletin of CRPA **19**, 1998) p.8.
- L. Moritz and J.R. Johnson, *Bioassay requirements for the TRIUMF ISAC facility*, *ibid.*
- R. Bilger *et al.* (LEPS, CHAOS, WASA/PROMICE collaboration), *Hunting the dibaryon $D'(2065)$* , Proc. **Workshop on the Structure of Mesons, Baryons, and Nuclei, Cracow, May 26–30** (Acta Phys. Polon. **B29**, 1998) p.2415.
- D. Bryman, *Rare decays of kaons and muons*, Proc. **Fifth Int. Symp. on Physics Beyond the Standard Model, WEIN’98, Los Alamos, June 14–19**, eds. C. Hoffman, P. Herczeg (World Scientific, Singapore, in press) [TRI-PP-98-31].
- A. Astbury, D. Axen and J. Robinson, eds. Proc. **XXIX Int. Conf. on High Energy Physics, ICHEP’98, Vancouver, July 23–29** (World Scientific, Singapore, in press).
- C.A. Miller, *Polarized quark distributions from deep inelastic scattering*, *ibid.*
- M. Vincter, *Determination of the flavor asymmetry of the light quark sea from unpolarized deep-inelastic scattering at HERMES*, *ibid.*
- D. Bryman, *CP violation, rare decays and lepton flavour violation*, *ibid.* [TRI-PP-98-34].
- A.N. Zelenski, *High-intensity optically pumped polarized H^- ion source development for RHIC and HERA*, Proc. **13th Int. Symp. on High-Energy Spin Physics, SPIN’98, Protvino, September 8–12** [TRI-PP-98-35].
- A.N. Zelenski, N.A. Titov, Y. Kuznetsov, J. Birchall, J.B. Bland, A.A. Hamian, L. Lee, S.A. Page, W.D. Ramsay, W.T.H. van Oers, R.J. Woo, C.A. Davis, R. Laxdal, C.D.P. Levy, P.W. Green, G. Roy, G.M. Stinson, J.D. Bowman and R.E. Mischke, *The TRIUMF parity violation experiment in $p-p$ scattering at 221 MeV*, *ibid.* [TRI-PP-98-36].
- A. Konaka *et al.* (E926 collaboration), *$K_L \rightarrow \pi^0 \nu \bar{\nu}$ at the AGS (E926)*, Proc. **Int. Workshop on CP Violation in K, Tokyo, December 18–19**.

R.L. Poirier, P. Bricault, G. Dutto, K. Fong, R. Laxdal, A.K. Mitra and B. Uzat, *RF tests on the initial 2.8 m section of the 8 m long ISAC RFQ at TRIUMF*, Proc. **Linear Accelerator Conf.**, Chicago.

F.W. Jones, *A hybrid fast-multipole technique for space-charge tracking with halos*, Proc. **Workshop on Space Charge Physics in High Intensity Hadron Rings**, Shelter Island, NY, May 4–7 (AIP Conf. Proc. 448) [TRI-PP-98-21].

N.R. Stevenson, *A new encapsulated target system for isotope production*, Proc. **6th Canadian Symp. on Isotope Production and Applications**, Ottawa, May.

K.R. Buckley, E.T. Hurtado and T.J. Ruth, *TR-13 cyclotron/PET programme*, **2nd Workshop on Accelerator Operations**, WAO'98, Vancouver, May 18–22.

R. van den Elzen, *Challenges facing TRIUMF-ATG operations*, *ibid.*

J. Orzechowski, *Application of the industrial PM to the cyclotron operation*, *ibid.*

P. Bloemhard, *How the TRIUMF-ATG does business*, *ibid.*

W.Z. Gelbart, N.R. Stevenson *et al.*, *Solid target systems: a brief history*, Proc. **XV Int. Conf. on Cyclotrons and their Applications**, Cyclotrons'98, Caen, France, June 14–19 (in press).

G. Dutto, R. Baartman, E. Blackmore, P. Bricault, A. Hurst, T. Kuo, R. Laxdal, B. Milton, R. Poirier, G. Mackenzie, K. Reiniger, P. Schmor, G. Stanford, G. Stinson, J. Welz, L. Root and F. Mammarella, *Recent progress at TRIUMF*, *ibid.* [TRI-PP-98-10].

B.F. Milton, R.J. Dawson, M.P. Dehnel, T. Kuo, R. Ruegg and R. Risler, *Design of an axial injection system for the Seattle MC50 cyclotron*, *ibid.* [TRI-PP-98-14].

M.K. Craddock, *Critical beam-intensity issues in cyclotrons – overview of the Santa Fe workshop*, *ibid.* [TRI-PP-98-18].

M.K. Craddock and D.J. Clark, *John Reginald Richardson*, *ibid.* [TRI-PP-98-19].

T. Kuo, W.Z. Gelbart, N.R. Stevenson *et al.*, *Injection study for high current H^- cyclotrons*, *ibid.* [TRI-PP-98-22].

M.V. Lachinov and B.F. Milton, *Optimized bunching in the spiral inflector of the CYCLONE-44 injection system*, *ibid.* [TRI-PP-98-25].

L. Moritz, *Radiation protection considerations in the design of accelerated radioactive beam facilities*, *ibid.*

A.N. Zelenski, G. Dutto, A.A. Hamian, R. Laxdal, C.D.P. Levy, G.H. Mackenzie, D.W. Ramsay, P. Schmor, N.A. Titov and W.T.H. van Oers, *A high quality polarized cyclotron beam for the TRIUMF parity violation experiment*, *ibid.*

M.J. Barnes, M. Jheeta, G.D. Wait, L. Ducimetière, G.H. Schroeder and E.B. Vossenberg, *Kick sensitivity analysis for the LHC inflectors*, Proc. **22nd Int. Power Modulator Symp.**, Rancho Mirage, CA, June 22–25 [TRI-PP-98-12].

G. Dutto, C.D.P. Levy, G.W. Wight, A.N. Zelenski, V. Klenov, V.I. Davydenko, J. Alessi, M. Okamura, Y. Mori and T. Takeuchi, *Development of high-current polarized H^- ion sources at TRIUMF*, Proc. **6th European Particle Accelerator Conf. (EPAC'98)**, Stockholm, June 22–26, eds. S. Myers, L. Liljeby, Ch. Petit-Jean-Genaz, J. Poole, K.-G. Rensfelt (IOP Publishing, Bristol, 1998) p.290 [TRI-PP-98-09].

D. Kaltchev, M.K. Craddock, R. Servranckx and T. Riselada, *Momentum cleaning in the CERN LHC*, *ibid.* 353 [TRI-PP-98-20].

R. Laxdal, R. Baartman, P. Bricault, G. Dutto, K. Fong, K. Jayamanna, M. McDonald, A. Mitra, R. Poirier, W. Rawnsley, L. Root, P. Schmor, B. Uzat and J. Welz, *Testing the ISAC LEBT and 35 MHz RFQ in an intermediate configuration*, *ibid.* 737 [TRI-PP-98-15].

S. Koscielniak, A. Blas, F. Pedersen, *Explanation of sextupole instability in CERN PS booster*, *ibid.* 969.

A. Boudzko, S. Koscielniak, L. Jensen, R. Jones and H. Schmickler, *SPS and LHC tune control studies using the 'fast map' tool*, *ibid.* 1168.

D. Grier, E. Jensen, R. Losito and A.K. Mitra, *The PS 80 MHz cavities*, *ibid.* 1773.

J. Corlett, D. Li and A. Mitra, *35 MHz re-buncher rf cavity for ISAC at TRIUMF*, *ibid.* 1790.

M.J. Barnes, G.D. Wait, E. Carlier, L. Ducimetière, G.H. Schröder and E.B. Vossenberg, *Measurements on a fast 66 kV resonant charging power supply for the LHC inflectors*, *ibid.* 2278 [TRI-PP-98-11].

P. Schmor, R. Baartman, P. Bricault, M. Dombisky, G. Dutto, R. Laxdal, F. Mammarella, M. McDonald, G. Mackenzie, L. Moritz, R. Poirier, J.-M. Poutissou, G. Stanford, G. Stinson, I. Thorson and J. Welz, *The high intensity radioactive beam facility at TRIUMF*, *ibid.* 2386 [TRI-PP-98-16].

P.L. Gardner and F. Douglass, *A technology transfer framework for global sustainable development*, Proc. **2nd Int. Conf. on Technology Policy and Innovation**, Lisbon, August 3–5 [TRI-PP-98-13].

T.J. Ruth, *TRIPL: TRIUMF radioisotope production laboratory*, **15th Int. Conf. on the Application of Accelerators in Research and Industry**, Denton, TX, November.

D.A. Hutcheon (DRAGON collaboration), *A program in nuclear astrophysics using DRAGON at ISAC*, *ibid.* [TRI-PP-98-43].

R.L. Helmer, *The Sudbury Neutrino Observatory*, Proc. **Nuclear Science Symp. and Medical Imaging Conf., NSS/MIC'98, Toronto, November 8–14** (IEEE Trans. Nucl. Sci., in press).

J.G. Rogers and C.J. Batty, *Afterglow in LSO and its effect on energy resolution*, *ibid.* [TRI-PP-98-30].

Chemistry and Solid-State Physics

Y. Fudamoto, K.M. Kojima, M. Larkin, G.M. Luke, J. Mermin, B. Nachumi, Y.J. Uemura, Y. Ueda and M. Isobe, *μ SR study of the spin-peierls compound $Na_x V_2 O_5$* , Proc. **APS March Meeting (O33 2)**.

Life Sciences

D.J. Doudet, G.L.Y. Chan, T.J. Ruth and A.P. Zis, *In vivo positron emission tomography studies of the effects of ECT on the dopamine receptors*, **Society of Biological Psychiatry**.

A.P. Zis, G.L.Y. Chan, T.J. Ruth and D.J. Doudet, *Effects of ECT on dopamine receptors: An in vivo PET study*, **1998 ACT Scientific Program**.

C.S. Lee, A. Sammi, M. Schulzer, V. Sossi, T.J. Dobko, G.L.Y. Chan, J. Huser, J.-M. Lu, T.J. Ruth, D.B. Calne and A.J. Stoessl, *Heterogeneous severity of lesions in the striatum of patients with Parkinson's disease: in vivo PET studies using dihydrotetrabenazine, methylphenidate and F-DOPA*, **American Academy of Neurology**.

A.J. Stoessl, P. Pal, V. Sossi, J. Wudel, T. Dobko, C.S. Lee, S. Jivan, T.J. Ruth and D.B. Calne, *Dopamine agonist therapy affects uptake of ^{18}F -6-fluorodopa as measured by PET*, *ibid.*

V. Sossi, A.J. Stoessl, A. Samii, C.S. Lee, J.-M. Lu and T.J. Ruth, *Comparison between the B_{max}/K_d plasma-input and tissue-input derived estimates of in DTBZ studies of Parkinson's*, **Neuroimage 7**.

T.J. Ruth, D.J. Doudet, A.J. Stoessl and J.E. Holden, *Monitoring the manipulation of the dopaminergic system through the measurement of the effective turnover with fluorodopa*, **American Chemical Society, Dallas, March**.

T.J. Ruth, *Accelerator production of high specific activity therapeutic radionuclides*, *ibid.*

T.J. Ruth, *Opening remarks*, **Workshop on Medical Imaging with Positron Emitting Isotopes, Pacific Northwest Chapter, Society of Nuclear Medicine, Vancouver, March**.

K.R. Buckley and T.J. Ruth, *In-target chemistry: A review of the production of precursors for PET radiopharmaceuticals*, **Int. Isotope Society, Ottawa, May**.

V. Sossi, M. Krzywinski, P. Cohen, K. Knitzek, K. Hudkins, J. DeRosario, K.S. Morrison, S. Jivan, R.R. Johnson and

T.J. Ruth, *Performance of the ADAC MCD dual head coincidence camera*, **Society of Nuclear Medicine, Toronto, June** (J. Nucl. Med. **39**, 1998) p.173P.

M.J. Adam, *Synthesis of F-18 labelled 2,2-difluoroglucose as a potential imaging agent for PET*, *ibid.*, 231P.

T.R. Oakes, T. Hurtado, S. Jivan and T.J. Ruth, *A positron plane source which approaches the limit of "low scatter"*, *ibid.*

D.J. Doudet, J. Holden, J. Huser, S. Jivan, C. English, G. Chan and T. Ruth, *Density and affinity of D1 and D2-dopamine receptors in monkey: in vivo PET studies with [^{11}C]Sch23390 and [^{11}C]raclopride*, **Neuroreceptor Mapping '98, Ann Arbor, MI, June**.

D.J. Doudet, G.L.Y. Chan, T. Ruth and A. Zis *Studies of the effects of ECT on the dopamine receptors*, **4th Int. Conf. on Functional Mapping of the Human Brain, Montreal, June**.

V. Sossi, M. Krzywinski, P. Cohen, D.A. Mankoff, J. DeRosario and T.J. Ruth, *Effect of count rate on contrast in the ADAC MCD camera*, Proc. **Nuclear Science Symp. and Medical Imaging Conf., NSS/MIC'98, Toronto, November 8–14** (IEEE Trans. Nucl. Sci., in press).

M. Krzywinski, V. Sossi and T.J. Ruth, *Comparison of 3DFBP and FORE, 2DFBP, OSEM, and SAGE with phantom and dynamic human scans in PET*, *ibid.*

Y.N. Yatham, J. Dennie, I-S. Shian, C. Lane, R. Lam, T.J. Ruth and P.F. Liddle, *A positron emission tomography study of the effects of desipramine on brain 5-HT₂ receptors*, **48th Annual Meeting, Canadian Psychiatric Assoc., Halifax, September**.

D.J. Doudet, G. Chan, J. Huser, S. Jivan, C. English and T. Ruth, *In vivo PET studies of the density and affinity of dopamine D1 and D2 receptors in the striatum of normal and MPTP-treated monkeys*, **Int. Basal Ganglia Society, Brewster, MA, October**.

A.J. Stoessl, C.S. Lee, V. Sossi and D.B. Calne, *Imaging studies of the dopamine system in Parkinson's disease*, **iN-ABis'98, December**.

Theoretical Program

S.J. Pollock, N.C. Mukhopadhyay, M. Ramsey-Musolf, H.-W. Hammer and J. Liu, *Parity violating $\Delta(1232)$ electroweak production: axial structure and new physics*, Proc. **Joint ECT*/TJNAF Workshop on N* Physics and Non-perturbative QCD, Trento, Italy, May 18–29**.

R. Lewis and R.M. Woloshyn, *S-wave charmed mesons in lattice NRQCD*, Proc. **16th Int. Symp. on Lattice Field Theory, Lattice'98, Boulder, July 13–18** (North Holland, in press) [TRI-PP-98-23, JLAB-THY-98-34].

B.D. Jones and R.M. Woloshyn, *Vector decay constants in quarkonia*, *ibid.* [TRI-PP-98-24].

H.-W. Hammer, *Effective theory for the non-relativistic three-body system*, Proc. **8th Int. Conf. on the Structure of Baryons, Baryons'98, Bonn, September 22–26** (World Scientific, Singapore, in press) [TRI-PP-98-28].

Past Conference Papers Published In 1998

Particle, Nuclear and Atomic Physics

M. Agnello, P.A. Amaudruz, G. Beer *et al.*, *Hypernuclear physics with stopped K^- at DAΦNE*, Proc. **5th Int. Conf. on Advanced Technology and Particle Physics, Como, Italy, October 7–11, 1996** (Nucl. Phys. B Proc. Suppl. **61B**, 1998), p.601.

D. Axen, H.P. Wellisch and A. Cellers, *Use of application software in the intermediate energy regime at TRIUMF – medical applications*, *ibid.* 678.

M.G. Vincter *et al.* (HERMES collaboration), *HERMES measurement of the spin structure of the nucleon*, Proc. **Conf. on Perspectives in Hadronic Physics, Trieste, 1997** (World Scientific, Singapore, 1998) p.27.

C. Hearty, *CP violation physics with BaBar*, Proc. **1997 Lake Louise Winter Institute: Particles and the Universe (LLWI'97), February 12–16, 1997**, eds. A. Astbury *et al.* (World Scientific, Singapore, 1998) p.305.

A.R. Berdoz, J. Birchall, J.D. Bowman, J.R. Campbell, C.A. Davis, A.A. Green, P.W. Green, A.A. Hamian, D.C. Healey, R. Helmer, S. Kadantsev, Y. Kuznetsov, R. Laxdal, L. Lee, C.D.P. Levy, R.E. Mischke, S.A. Page, W.D. Ramsay, S.D. Reitzner, G. Roy, P. Schmor, A.M. Sekulovich, J. Soukup, G.M. Stinson, T.J. Stocki, V. Sum, N. Titov, W.T.H. van Oers, R.J. Woo and A. Zelenski, *Parity violation in proton-proton scattering*, Proc. **Int. Conf. on Quark Lepton Nuclear Physics: Nonperturbative QCD Hadron Physics and Electroweak Nuclear Processes (QULEN'97), Osaka, May 20–23, 1997**, eds. H. Ejiri, T. Kishimoto, Y. Mizuno, T. Nakano, H. Toki (Nucl. Phys. **A629**, 1998) p.433c [TRI-PP-97-22].

V.G.J. Stoks, *Meson-baryon coupling constants and baryon-baryon interactions*, *ibid.* 205c.

J.D. King, J.C. Chow, A.C. Morton, R.E. Azuma, N. Bateman, R.N. Boyd, L. Buchmann, J.M. D'Auria, T. Davinson, M. Dombisky, W. Galster, E. Gete, U. Giesen, C. Iliadis, K.P. Jackson, G. Roy, T. Shoppa and A. Shotter, *Information about the $^{12}\text{C}(\alpha, \gamma)^{16}\text{O}$ reaction from the β -delayed proton decay of ^{17}F* , Proc. **Tours Symp. on Nuclear Physics III, Tours, September 2–5, 1997** (AIP Conf. Proc. 425, Woodbury, N.Y. 1998).

K. Yamamoto, D. Alburger, B. Bassalleck, A.R. Berdoz, T. Burger, M. Burger, D. Carman, R.E. Chrien, C.A. Davis, H. Fischer, G.B. Franklin, J. Franz, L. Gan, A. Ichikawa, T. Iijima, K. Imai, P. Khaustov, P. Koran, Y. Kondo, M. Landry, L. Lee, J. Lowe, R. Magahiz, M. May, R. McCrady, F. Merrill, C.A. Meyer, S.A. Page, K. Paschke, P.H. Pile, B.P. Quinn, W.D. Ramsay, A. Rusek, R. Sawafta,

R.A. Schumacher, H. Schumit, R.W. Stotzer, R. Sutter, F. Takeuchi, W.T.H. van Oers, M. Yosoi and V. Zeps, *H-dibaryon search via the (K^-, K^+) reaction using a diamond target*, Proc. **6th Int. Conf. on Hypernuclear and Strange Particle Physics, HYP'97, Upton, NY, October 13–18, 1997** (Nucl. Phys. **A639**, 1998) p.371.

M. Iwasaki, K. Bartlett, G.A. Beer, D.R. Gill, R.S. Hayano, T.M. Ito, L. Lee, G. Mason, S.N. Nakamura, A. Olin, H. Outa, M. Salomon, R. Seki, T. Taniguchi, T.P. Terada, G. Trayling, Y. Yamashita and S. Yen, *Discovery of the repulsive energy shift of the kaonic hydrogen 1S state*, *ibid.* 501.

M. Agnello *et al.* (FINUDA collaboration), *FINUDA, the physics program*, *ibid.* 537.

J. Macdonald, *Future stopped $K^+ \rightarrow \pi^+\nu\bar{\nu}$ experiment*, Proc. **Int. KEK Workshop on Kaon, Muon, Neutrino Physics and Future, Tsukuba, October 31–November 1, 1997**, eds. Y. Kuno, T. Shinkawa (KEK Proc. 97-24, JHF-97-8, Tsukuba, 1998) p.93 [TRI-PP-97-71].

D. Bryman, *KEK workshop on kaon, muon and neutrino physics: summary*, *ibid.* 329.

Instrumentation/Accelerator Physics/Computing Sciences

A.N. Zelenski, V.I. Davydenko, V. Klenov, I.I. Morozov, G. Dutto, C.D. Levy, P.W. Schmor, G.W. Wight, A.A. Hamian and W.T. van Oers, *OPPIIS development for precision experiments and high energy colliders*, Proc. **7th Int. Workshop on Polarized Gas Targets and Polarized Beams, Urbana, 1997** (AIP Conf. Proc. **421**, 1998) p.372.

A.N. Zelenski, C.D.P. Levy, P.W. Schmor, W.T.H. van Oers, G.W. Wight and G. Dutto, *OPPIIS development at TRIUMF*, Proc. **7th RCNP Int. Workshop on Polarized ^3He Beams and Gas Targets and Their Application (HELION'97), Kobe, 1997**, ed. M. Tanaka (Nucl. Instrum. Methods **A402**, 1998), p.185.

T. Sakae, T. Yamamoto, A.N. Zelenski and C.D.P. Levy, *Optical pumping of thick alkali vapor for high-intensity polarized ion source*, *ibid.*, 191.

M. Comyn, M.K. Craddock, M. Reiser and J. Thomson, eds. Proc. **1997 Particle Accelerator Conference (PAC'97), Vancouver, May 12–16, 1997** (IEEE, Piscataway, NJ, 1998).

B.F. Milton, *A high current tandem accelerator for gamma-resonance contraband detection*, *ibid.* 3775 [TRI-PP-97-34].

P.G. Bricault, *Review of radioactive ion beam accelerators*, *ibid.* 925 [TRI-PP-97-35].

F.W. Jones, *Development of the ACCSIM tracking and simulation code*, *ibid.* 2597 [TRI-PP-97-36].

F.W. Jones, *A graphical user interface for RELAX3D*, *ibid.* 2600 [TRI-PP-97-37].

- A.K. Mitra, R.L. Poirier and E. Jensen, *Coarse and fine tuners for the CERN PS 40 MHz bunching cavity*, *ibid.* 3060 [TRI-PP-97-38].
- A.K. Mitra, R.L. Poirier and R. Losito, *Measurements at TRIUMF on an 80 MHz cavity model for the CERN PS upgrade for LHC*, *ibid.* 3063 [TRI-PP-97-39].
- M. D'yachkov and F. Ruggiero, *Broad-band impedance of LHC shielded bellows*, *ibid.* 2648 [TRI-PP-97-40].
- S. Bakhtiari, W.Z. Gelbart, W. Ho and N.R. Stevenson, *Encapsulated target for isotope production cyclotrons*, *ibid.* 3842 [TRI-PP-97-41].
- W. Ho, S. Bakhtiari, W.Z. Gelbart and N.R. Stevenson, *High current encapsulated target system for radioisotope production*, *ibid.* 3845 [TRI-PP-97-42].
- W.R. Rawnsley, K. Fong, S. Fang and J.-P. Papis, *An rf signal processing module for the SPS orbit observation system upgrade*, *ibid.* 2049 [TRI-PP-97-43].
- V.E. Shapiro, *Method of strong focusing*, *ibid.* 1368 [TRI-PP-97-44].
- P.W. Schmor, R. Baartman, P. Bricault, M. Dombisky, G. Dutto, S. Koscielniak, R.E. Laxdal, F. Mammarella, G.H. Mackenzie, R. Poirier, L. Root, G. Stanford, G. Stinson, I. Thorson and J. Welz, *Status of the TRIUMF-ISAC facility for accelerating radioactive beams*, *ibid.* 956 [TRI-PP-97-45].
- G.S. Clark, A.J. Otter and P. Reeve, *Magnets for the CERN PS booster transfer line*, *ibid.* 3336 [TRI-PP-97-46].
- S. Koscielniak, *Robinson-type criteria for beam and rf cavity with delayed, voltage-proportional feedback*, *ibid.* 2389 [TRI-PP-97-47].
- H.J. Tran and S.R. Koscielniak, *Landau damping of the weak head-tail instability for beams with quadratic amplitude-dependent betatron tunes and binomial amplitude distributions*, *ibid.* 1647 [TRI-PP-97-48].
- R. Baartman and J. Welz, *60 keV beam transport line and switch-yard for ISAC*, *ibid.* 2778 [TRI-PP-97-49].
- R. Baartman, *Intrinsic third order aberrations in electrostatic and magnetic quadrupoles*, *ibid.* 1415 [TRI-PP-97-50].
- T. Kuo, D. Yuan, K. Jayamanna, M. McDonald, R. Baartman, G. Mackenzie, P. Bricault, M. Dombisky, P. Schmor, K.-N. Leung, D. Williams and R. Gough, *Initial test results from a multicusp source for TRIUMF's radioactive beams facility*, *ibid.* 2675 [TRI-PP-97-51].
- D.I. Kaltchev, M.K. Craddock, R.V. Servranckx and J.B. Jeanneret, *Numerical optimization of collimator jaw orientations and locations in the LHC*, *ibid.* 153 [TRI-PP-97-52].
- R.E. Laxdal, P.G. Bricault, T. Ries and D.V. Gorelov, *A separated function drift-tube linac for the ISAC project at TRIUMF*, *ibid.* 1194 [TRI-PP-97-53].
- E.W. Blackmore, B. Evans, M. Mouat, C. Duzenli, R. Ma, T. Pickles and K. Paton, *Operation of the TRIUMF proton therapy facility*, *ibid.* 3831 [TRI-PP-97-54].
- R.L. Poirier, P. Bricault, G. Dutto, K. Fong, K. Jensen, R. Laxdal, A.K. Mitra and G. Stanford, *Construction criteria and prototyping for the ISAC RFQ accelerator at TRIUMF*, *ibid.* 1105 [TRI-PP-97-55].
- S. Koscielniak, R.E. Laxdal, R. Lee and L. Root, *Beam dynamics studies on the ISAC RFQ at TRIUMF*, *ibid.* 1102 [TRI-PP-97-56].
- K. Fong, M. Laverty, S. Fang and W. Uzat, *Sawtooth wave generation for pre-buncher cavity in ISAC*, *ibid.* 3057 [TRI-PP-97-57].
- M.J. Barnes, G.D. Wait, K. Metzmacher and L. Sermeus, *The application of saturating inductors for improving the performance of the CERN PS kicker systems*, *ibid.* 1328 [TRI-PP-97-58].
- A.N. Zelenski, C.D.P. Levy, P.W. Schmor, W.T.H. van Oers, G.W. Wight and G. Dutto, *OPPIS development at TRIUMF*, *ibid.* 2781 [TRI-PP-97-59].
- M.J. Barnes, G.D. Wait, L. Ducimetière, U. Jansson, G.H. Schröder and E.B. Vossenberg, *A fast 60 kV resonant charging power supply for the LHC deflectors*, *ibid.* 1325 [TRI-PP-97-60].
- F. Ruggiero, J.S. Berg, O. Brüning, F. Caspers, M. Morvillo and M. D'yachkov, *Summary of the single beam collective effects in the LHC*, *ibid.* 107.
- J.W. Glenn, M. Brennan, L. Littenberg, J. Rose, C. Woody, A. Zoltzman, P. Bergbusch and D. Mjka, *Micro-bunching the AGS slow external beam*, *ibid.* 967.
- Y. Bylinsky, V. Kukhtiev, P.N. Ostroumov, V. Paramonov and R.E. Laxdal, *A triple gap resonator design for the separated function DTL at TRIUMF*, *ibid.* 1135.
- F. Caspers, M. Chanel, H. Schönauer, L. Soby and M. D'yachkov, *Longitudinal coupled-bunch instability around 1 GHz at the CERN PS booster*, *ibid.* 1587.
- A.U. Luccio, J. Beebe-Wang, D. Maletic and F.W. Jones, *Proton injection and rf capture in the National Spallation Neutron Source*, *ibid.* 1882.
- D.V. Gorelov, P.N. Ostroumov and R.E. Laxdal, *Use of the LANA code for the design of a heavy ion linac*, *ibid.* 2621.
- R. Garoby, D. Grier, E. Jensen, A. Mitra and R.L. Poirier, *The PS 40 MHz bunching cavity*, *ibid.* 2953.
- G. Cojocar, D. Martin, M. Dragusin, R. Moraru, M. Radou, C. Oproiu, S. Marghitu, I. Indreias, V. Bestea, R. Camariuc and A. Margaritescu, *Electron beam applications in chemical processing*, *ibid.* 3854.
- A. Boucham *et al.*, *The BaBar drift chamber project*, Proc. 7th Pisa Meeting on Advanced Detectors: Frontier Detectors for Frontier Physics, La Biodola, Isola d'Elba,

Italy, May 25–31, 1997 (Nucl. Instrum. Methods **A409**, 1998) p.46.

M.J. Barnes, G.D. Wait, E. Carlier, L. Ducimetière, U. Jansson, G.H. Schroder and E.B. Vossenber, *Operation modes of the fast 60 kV resonant charging power supply for the LHC deflectors*, Proc. **11th IEEE Int. Pulsed Power Conf., Baltimore, June 29–July 2** (IEEE, 1998) p.1309.

C.D.P. Levy and A.N. Zelenski, *Polarized ion sources for high-energy accelerators*, Proc. **7th Int. Conf. on Ion Sources, ICIS'97, Taormina, Italy, September 7–13, 1997** (Rev. Sci. Instrum. **69**, 1998) p.732.

K. Jayamanna, G. Cojocar, M. Dombisky, T. Kuo, R. Laxdal, M. McDonald, P. Schmor, D. Yuan and A. Zyuzin, *A microwave driven off-line ion source for ISAC at TRIUMF*, *ibid.* 753.

K. Jayamanna, A. Zyuzin, L. Buchmann, G. Cojocar, M. Dombisky, T. Kuo, M. McDonald, P. Schmor and D. Yuan, *An electron cyclotron resonance source for radioactive beryllium ion beam production*, *ibid.* 756.

T. Kuo, D. Yuan, K. Jayamanna, M. McDonald, R. Baartman, G. Mackenzie, P. Bricault, M. Dombisky, P. Schmor, G. Dutto, Y. Lee, K-N. Leung, D. Williams and R. Gough, *Beam characteristics using stable a multicusp source for the TRIUMF ISAC facility*, *ibid.* 767.

T. Kuo, D. Yuan, K. Jayamanna, M. McDonald, R. Baartman, W.Z. Gelbart, N. Stevenson, P. Schmor and G. Dutto, *Further development for the TRIUMF H^-/D^- multicusp source*, *ibid.* 959.

M. Dombisky, R. Baartman, P. Bricault, J. Doornbos, K. Jayamanna, T. Kuo, G. Mackenzie, M. McDonald, P. Schmor and D. Yuan, *Evaluation of a prototype isotope separator accelerator surface ionization source*, *ibid.*, 1170.

D. Yuan, T. Kuo, G. Cojocar, K. Jayamanna, M. McDonald, P. Schmor and Y. Yin, *Design of a parallel-plate energy spread analyzer*, *ibid.* 1194.

M.M. Mouat, B. Davison, S.G. Kadantsev, E. Klassen, K.S. Lee, J.E. Richards, T.M. Tateyama, P.W. Wilmshurst and P.J. Yogendran, *Status report on the TRIUMF central control system*, Proc. **Int. Conf. on Accelerator and Large Experimental Physics Control Systems, ICALEPCS'97, Beijing, November 3–7, 1997**, eds. J. Zhao, A. Daneels (IHEP, Beijing, 1998) p.43.

B. Davison, S.G. Kadantsev, E. Klassen, K.S. Lee, M.M. Mouat, J.E. Richards, T.M. Tateyama, P.W. Wilmshurst and P.J. Yogendran, *Event handling in TRIUMF's central control system*, *ibid.* 92.

K.S. Lee, S.G. Kadantsev, E. Klassen, M.M. Mouat and P.W. Wilmshurst, *Handling CAMAC interrupts in Alpha OpenVMS/PCI*, *ibid.* 237.

D.B. Morris and K.S. Lee, *The control system for a new proton extraction probe at TRIUMF*, *ibid.* 253.

M. Lavery, K. Fong and S. Fang, *A DSP-based control system for the ISAC pre-buncher*, *ibid.* 263.

D. Bishop, D. Dale, H. Hui, J. Lam and R. Keitel, *Distributed power supply control using CAN-bus*, *ibid.* 315.

R. Keitel, M. Leross and G. Waters, *Control system prototype for the ISAC radioactive beam facility*, *ibid.* 372.

J. Lam, G. Waters and R. Keitel, *Conversion of the TISOL control system to EPICS*, *ibid.* 593.

D. Dale, D. Bishop, H. Hui, B. Milton and B. Roberts, *The control system for a 2 MeV tandem accelerator used for contraband detection*, *ibid.* 626.

Theoretical Program

J.N. Ng, *T-odd effects in supersymmetric theories*, Proc. **Int. Workshop on Non-Accelerator New Physics, NANP'97, Dubna, July 7–11, 1997** (Phys. Atom. Nucl. **61**, 1178 (1998); Yad. Fiz. **61**, 1278 (1998)) [TRI-PP-97-29].

V.G.J. Stoks and T.A. Rijken, *NN potential from chiral $SU(3)$ Lagrangian*, Proc. **XVth Int. Conf. on Few-Body Problems in Physics (ICFBP'97), Groningen, July 22–26, 1997**, eds. J.C.S. Bacelar, A.E.L. Dieperink, R.A. Malfliet, L.P. Kok (Nucl. Phys. **A631**, 1998) p.452c [MKPH-T-97-26].

W. Kretschmer, A. Glombik, G. Suft, R. Weidmann, E. Boschitz, B. Brinkmoeller, R. Meier, B. van den Brandt, P. Hautle, J.A. Konter, S. Mango, R. Tacik, P. Amaudruz, C. Riedel and W. Grueebler, *Polarization transfer observables in πd elastic scattering*, *ibid.* 524c.

T.R. Hemmert, B.R. Holstein, G. Knochlein and S. Scherer, *Generalized polarizabilities and the chiral structure of the nucleon*, *ibid.* 607c.

H.W. Fearing, R. Lewis, N. Mobed and S. Scherer, *Radiative and non radiative muon capture on the proton in heavy baryon chiral perturbation theory*, *ibid.* 735c [TRI-PP-97-30].

H.R. Fiebig, H. Markum, A. Mihaly, K. Rabitsch and R.M. Woloshyn, *Two-body spectra of pseudoscalar mesons with an $\mathcal{O}(\alpha^2)$ improved lattice action using Wilson fermions*, Proc. **Lattice'97: 15th Int. Symp. on Lattice Field Theory, Edinburgh, July 22–26, 1997** (Nucl. Phys. **B63**, 1998), p.188 [HEPLAT-9709152].

M.M. Musakhanov, A. Rakhimov, U. Yakhshiev and F.C. Khanna, *Nucleon-Skyrmion properties in a baryon-rich environment*, Proc. **Physics and Astrophysics of Quark-Gluon Plasma, August, 1997**, eds. B.C. Sinha, D.K. Srivastava and Y.P. Viyogi (Narosa, New Delhi, 1998) p.417.

Books

J.A. Behr, A. Gorelov, D. Melconian, M. Trinczek, P. Dubé, O. Häusser, U. Giesen, K.P. Jackson, T. Swanson, J.M. D'Auria, M. Dombisky, G. Ball, L. Buchmann, B. Jennings, J. Dilling, J. Schmid, J. Deutsch, W.P. Alford, D. Asgeirsson and W. Wong, *Search for scalar contributions to the ^{38m}K beta-neutrino correlation in a magneto optic trap*, in Trapped Charged Particles and Fundamental Physics, ed. D.H.E. Dubin (AIP, 1998).

K.H. Chow, B. Hitti and R.F. Kiefl, *μSR on muonium in semiconductors and its relation to hydrogen*, chapter 4 in Semiconductors and Semimetals, vol. **51A** "Identification of defects in semiconductors" (1998) p.137 .

F. Seitz, E. Vogt and A.M. Weinberg, *Eugene Paul Wigner 1902–1995, A biographical memoir*, vol. **74** of Biographical Memoirs (National Academy Press, Washington, 1998) [TRI-PP-98-5].

V. Sossi, K.S. Morrison, T.R. Oakes and T.J. Ruth, *Emission-transmission realignment using a simultaneous emission-transmission post-injection scan*, in Quantitative Functional Brain Imaging With Positron Emission Tomography (Academic, in press).

V.K. Verma, *Managing the project team*, vol. **3** of Human Aspects of Project Management (PMI, Upper Darby, PA, 1998).

V.K. Verma, *Conflict management*, chapter 22 in Project Management Institute Handbook, ed. J.K. Pinto (Jossey-Bass, San Francisco, 1998) p.353.

Theses

P. Bhargava, *The ^{12}C pion absorption cross sections* (M.Sc., Physics, Regina).

P. Botton, *Studio e sviluppo di un rivelatore di silicio a microstrip a doppia faccia per FINUDA* (M.Sc., Trieste).

F. De Mori, *Analisi delle caratteristiche funzionali di un rivelatore a microstrip di silicio per l'esperimento FINUDA* (M.Sc., Trieste).

A. Fumagalli, *Progettazione e test di un Telescopio per la discriminazione in massa fra pioni e muoni* (Laurea (M.Sc.), Trieste).

M. Kryzwinski, *Evaluation of new iterative and rebinning reconstruction algorithms in fully three-dimensional positron emission tomography* (M.Sc., Physics, UBC).

S. Ryneveld, *Measurement of proton beam dose profiles using a sensitive scintillation screen observed with a CCD camera* (M.Sc., Physics, UBC).

J. Schmid, *Aufbau einer magnetooptischen Falle für neutrale Kaliumatome* (Diplomarbeit, Physics and Astronomy, Heidelberg).

L. Gan, *A study of the sensitivity of the H dibaryon search experiment E813 at BNL through $(\Sigma^-, p)_{atom} \rightarrow \Lambda + n$* (Ph.D., Physics and Astronomy, Manitoba).

J. Gräter, *Inclusive pionic double charge exchange reactions on ^3He and ^4He* (Ph.D., Physics, Tübingen).

A.A. Hamian, *The measurement of parity violation in proton-proton scattering and 221 MeV* (Ph.D., Physics, Manitoba).

G.D. Morris, *Muonium formation and diffusion in cryocrystals* (Ph.D., Physics and Astronomy, UBC).

J.E. Sonier, *The magnetic penetration depth and vortex core radius in type-II superconductors* (Ph.D., Physics and Astronomy, UBC).

T.J. Stocki, *Measurement of muonic hyperfine transition rates and muon capture yields in light nuclei* (Ph.D., Physics, UBC).

J. Stone, *Capturing the rare decay $K^+ \rightarrow \pi^+ \nu \bar{\nu}$* (Ph.D., Physics, Princeton).

T.K. Yokoi, *Search for T -violating muon polarization in $K^+ \rightarrow \pi^0 \mu^+ \nu_\mu$ decay* (Ph.D., Physics, Tokyo).

SEMINARS*

The following seminars were presented at TRIUMF this year.

- 12/01 *More Penguin Sightings? Rare B Decays at CLEO*, Jean Roy, U. Colorado.
- 13/01 *What is the Difference Between Low-Energy Pion-Nucleus Inelastic and High-Energy Quark-Quark Two-Body Scattering?*, Harry C.S. Lam, McGill U.
- 16/01 *Orthopositronium Decay Puzzle*, I.B. Khriplovich, Budker Institute for Nuclear Physics.
- 20/01 *$\pi - \pi$ Scattering at Low Energies*, Jurg Gasser, U. Berne.
- 22/01 *Neutrino Interactions and Heavy Element Synthesis*, Gail McLaughlin, U. Washington.
- 03/02 *The Role of Freezeout and Neutrinos in r-Process Nucleosynthesis*, Rebecca Surman, U. North Carolina.
- 05/02 *Muon Catalyzed Fusion in Solid Hydrogen*, Glen Marshall, TRIUMF.
- 09/02 *Gluonic Excitations in the Presence of a Static $q - \bar{q}$ Pair*, Jimmy Juge, U. California, San Diego.
- 17/02 *Isospin Breaking in Chiral Perturbation Theory — Selected Applications*, Carl Wolfe, York U.
- 19/02 *Pseudoscalar Mesons at Zero and Finite Temperature*, Pieter Maris, ANL.
- 23/02 *W Boson Physics with the OPAL Experiment at LEP*, Carla Sabarra, UBC.
- 24/02 *Prospects for the Observation of Supersymmetry at the Tevatron and the LHC*, Kwok-Lung Chan, Northeastern U.
- 25/02 *Selective Laser Ion Sources at ISOLDE*, V.I. Mishin, Inst. of Spectroscopy, Russian Academy of Sciences.
- 26/02 *Direct Capture Astrophysical S Factors at Low Energy*, Byron Jennings, TRIUMF.
- 02/03 *Polarizabilities of Pions and Nucleons*, Stefan Scherer, Johannes Gutenberg U., Mainz.
- 05/03 *Light Front Nuclear Physics*, Jerry Miller, U. Washington.
- 06/03 *Applications of Random Matrix Theory in QCD*, Adam Halasz, SUNY at Stony Brook.
- 13/03 *Constraints on a Parity Conserving/Time-Reversal-Invariance Breaking Interaction and N-N Scattering*, Willem T.H. van Oers, U. Manitoba.
- 20/03 *Strange Baryon Production in e^+e^- Collisions at LEP*, Andre Joly, U. Montréal.
- 23/03 *$K^+ \rightarrow \pi^+\pi^0$ Decay on and off the Lattice*, Ka Chun Leung, Washington U. in St. Louis.
- 25/03 *Progress in Heavy Quark Physics on the Lattice*, Christine Davies, Glasgow U. and U. California, Santa Barbara.
- 26/03 *Positron Production by Laser Light*, Kirk Macdonald, Princeton U.
- 27/03 *The Muon Collider: Physics Opportunities and Technology Challenges*, Kirk Macdonald, Princeton U.
- 02/04 *The Status of the BaBar Experiment*, Chris Hearty, UBC.
- 08/04 *Status of the SNO Experiment*, Rich Helmer, TRIUMF.
- 09/04 *Fusion Enhancement with Neutron-Rich Radioactive Beams*, Kristiana Zyromski, Oregon State U.
- 14/04 *Super-Kamioka*, Jeff George, U. Washington.
- 16/04 *Pion Production Mechanism in Nucleon-Nucleon Collisions*, Keisuke Tamura, RCNP, Osaka U.
- 17/04 *Single Top-Quark Production at Hadron Colliders*, Z. Sullivan, U. Illinois.
- 23/04 *HyperCP: Finding CP Violation in Hyperon Decays*, Kam-Biu Luk, LBNL.
- 29/04 *Simultaneous Solution to Baryogenesis and Dark Matter Problem*, B. Khriplovich, INR, RAS, Moscow.
- 30/04 *Nuclear Astrophysics*, Nicholas Bateman, TRIUMF.
- 07/05 *Recent Results from HERMES*, Mike Vetterli, TRIUMF.
- 14/05 *Hyperfine Anomalies, a Handle on the Radial Neutron Distribution in Francium*, Gene Spruce, SUNY at Stony Brook.
- 19/05 *Bound-State Methodology in QCD and a Proof of Confinement*, Jan Greben, CISR, South Africa.
- 21/05 *Canada and the ATLAS Experiment*, Michel Lefebvre, U. Victoria.
- 28/05 *Decommissioning of Nuclear Power Reactors in Germany*, Martin Kueckes, TUEV Rheinland/Berlin-Brandenburg.
- 08/06 *The ${}^9\text{Be}({}^9\text{Be}, {}^8\text{B}){}^{10}\text{Li}$ Reaction with the S800 Spectrograph at Michigan State University*, Jac Caggiano, NSCL, Michigan State U.
- 02/07 *Measuring ξ'' in Polarized Muon Decay*, Paul Knowles, Fribourg U.
- 03/07 *Acceleration of Radioactive Ions at REX-ISOLDE*, Friedhelm Ames, CERN.
- 09/07 *The Physics Program at LEAR (1983–1996)*, Chris Batty, RAL.
- 16/07 *Pion Nucleon Scattering and QCD: Recent Results and Future Prospects*, Marcello Pavan, MIT.
- 04/08 *Search for Neutron EDM Using Crystal Techniques and Interference Experiments for Cold Neutrons*, Yoshie Otake, Coherent X-Ray Optics Lab, RIKEN, and C. Zeyen, ILL.
- 13/08 *Photon Correlations in Cavity QED*, Luis A. Orozco, SUNY at Stony Brook.
- 07/09 *Description of Deep Inelastic Electron Scattering on Nuclei*, Avraham Rinat, Weizmann Institute of Science.
- 17/09 *Real Physics at TISOL and ISAC*, Lothar Buchmann, TRIUMF.
- 23/09 *Revisit of Gamow-Teller Quenching Problem via the ${}^{90}\text{Zr}(\bar{p}, \bar{n})$ Measurements at 300 MeV*, Hide Sakai, U. Tokyo.

- 05/10 *New Directions in Strangeness -2 Physics*, Avraham Gal, Hebrew U.
 21/10 *Physics of ISAC-2*, Rick Casten, Yale U.
 23/10 *$\bar{K}N$ Interaction in Free Space and in the Medium*, Angels Ramos, U. Barcelona.
 03/11 *$^{22}\text{Ne}(p, \gamma)$ and Na-O Anti-Correlations in Globular Cluster Red Giants*, Steven Hale, U. North Carolina.
 12/11 *Magnetic Dipole Moment Measurements of Beta-Unstable Nuclei*, Paul Mantica, NSCL, Michigan State U.
 19/11 *Setting up an Outreach Program at the UBC Physics Department*, Chris Waltham, UBC.
 26/11 *Where We Go with LSO*, Joel Rogers, TRIUMF.
 02/12 *Update on the Production of PET Radionuclides on the He-3 RFQ at Fermilab*, Jeanne Link, U. Washington.
 09/12 *Gauge Mediated SUSY Breaking Models and Signatures*, M. Dutta, Texas A&M U.
 09/12 *GT Strength in Odd-A Nuclei: New Results from (\vec{p}, \vec{n})* , John Watson, Kent State U.
 14/12 *Search for Relic Galactic Halo Axions*, Dennis M. Moltz, LBNL.

* All matters concerning TRIUMF seminars should be referred via E-mail to SEMINAR (seminar@triumf.ca).

You can see the latest listing of TRIUMF seminars by the following methods.

On the TRIUMF VAX cluster:	Type SEMinars (SEM is sufficient)
Via DECNET:	COPY LIB1:[PUBLIC.ANONYMOUS.SEMINAR]SEMINARS.TXT
Via Anonymous FTP to FTP.TRIUMF.CA:	GET the file SEMINARS.TXT in the directory SEMINAR
On the WWW:	See TRIUMF Seminars Schedule under the section General on the TRIUMF – Around the Laboratory page
	Document URL: http://www.triumf.ca/seminars.txt

USERS GROUPS

TRIUMF USERS' GROUP

From the TRIUMF Users' Group Charter:

The TRIUMF Users' Group is an organization of scientists and engineers with special interest in the use of the TRIUMF facility. Its purpose is:

- (a) to provide a formal means for exchange of information relating to the development and use of the facility;
- (b) to advise members of the entire TRIUMF organization of projects and facilities available;
- (c) to provide an entity responsive to the representations of its members for offering advice and counsel to the TRIUMF management on operating policy and facilities.

Membership of the TRIUMF Users' Group is open to all scientists and engineers interested in the TRIUMF program. In 1998, following a reconfirmation of membership exercise, the TRIUMF Users' Group had 355 members from 37 countries.

Full details can be obtained via the WWW by going directly to <http://www.triumf.ca/triusers/users.html> or from the TRIUMF Home Page see the TRIUMF Users Group link under the Around the Laboratory section.

TRIUMF Users' Group Executive Committee (TUEC) 1998

L. Buchmann	TRIUMF	<i>Chair</i>
J.M. D'Auria	SFU	<i>Chair-elect</i>
M.D. Hasinoff	UBC	<i>Past-chair</i>
S.R. Kreitzman	TRIUMF	1997/98
S. Yen	TRIUMF	1997/98
A. Konaka	TRIUMF	1998/99
N. Rodning	U. Alberta	1998/99
M. La Brooy	TRIUMF	<i>Liaison Officer</i>

J. Brewer (UBC) was elected as chair elect for 1999.

G. Marshall (TRIUMF) and B. Turrell (UBC) were elected as members for 1999/2000.

μ SR USERS GROUP

Full details regarding the μ SR Users Group can be obtained via the WWW by going directly to http://www.triumf.ca/msr/musr/musr_home.html or from the TRIUMF Home Page see TRIUMF muSR under the section Experiments and Collaborations on the TRIUMF – Around the Laboratory page.

EXPERIMENT PROPOSALS

The following lists experiment proposals received up to the end of 1998 (missing numbers cover proposals that have been withdrawn or replaced by later versions or rejected or combined with another proposal). Page numbers are given for those experiments which are included in this Annual Report.

Page

1. Low-energy π scattering [completed], R.R. Johnson (*TRIUMF-UBC*), K.L. Erdman (*Univ. of British Columbia*), T. Masterson (*Univ. of Colorado*), P. Walden (*TRIUMF*)
3. The study of fragments emitted in nuclear reactions [completed], R.E.L. Green, R.G. Korteling (*Simon Fraser Univ.*), K.P. Jackson (*TRIUMF*), L. Church (*Reed College*)
6. Studies of the proton- and pion-induced fission of light to medium mass nuclides [completed], B.D. Pate (*Univ. of British Columbia*), H. Blok (*Novatrack*), H. Dautet, F.M. Kiely (*Simon Fraser Univ.*), Z. Fraenkel (*Weizmann Inst.*)
9. A study of the reaction $\pi^- + p \rightarrow \gamma + n$ at pion kinetic energies from 20–200 MeV [completed], K. Aniol (*California State Univ.*), A. Bagheri, M.D. Hasinoff, D.F. Measday (*Univ. of British Columbia*), J.-M. Poutissou, M. Salomon (*TRIUMF*), R. Poutissou (*Univ. de Montréal*), B.C. Robertson (*Queen's Univ.*)
10. Positive pion production in proton-proton and proton-nucleus reactions [completed], E.G. Auld, G. Jones (*Univ. of British Columbia*), R.R. Johnson (*TRIUMF-UBC*), T. Masterson (*Univ. of Colorado*), P. Walden (*TRIUMF*)
11. Nuclear spectroscopic studies of short-lived radioactive products of high energy reactions [completed], J.M. D'Auria, H. Dautet (*Simon Fraser Univ.*), K.P. Jackson (*TRIUMF*)
14. The interaction of protons with very light nuclei in the energy range 200–500 MeV [completed], J.M. Cameron, G.S. Moss, G. Roy (*Univ. of Alberta*), L.G. Greeniaus, D.A. Hutcheon, C.A. Miller, J.G. Rogers (*TRIUMF*), M. de Jong, W.T.H. van Oers (*Univ. of Manitoba*), C. Goulding (*Los Alamos National Lab*), A.W. Stetz (*Oregon State Univ.*), J. Källne (*JET Joint Undertaking*)
15. A proposal to study quasi-free scattering in nuclei [completed], J.M. Cameron, W.K. Dawson, W.J. McDonald, G.C. Neilson, W.C. Olsen, G.M. Stinson (*Univ. of Alberta*), P. Kitching (*TRIUMF-Univ. of Alberta*), E.D. Earle (*Chalk River Nuclear Labs*), D.A. Hutcheon, C.A. Miller (*TRIUMF*), J.T. Sample (*Research Secretariat of B.C.*), A.W. Stetz (*Oregon State Univ.*), A.N. James (*Univ. of Liverpool*)
21. Optical activity induced by polarized elementary particles [completed], L.D. Hayward, D.C. Walker (*Univ. of British Columbia*)
22. Negative pion capture and absorption on carbon, nitrogen and oxygen [passed to Biomedical Experiments Evaluation Committee], H.B. Knowles (*Washington State Univ.*)
23. Study of decay modes a) $\pi^0 \rightarrow 3\gamma$, b) $\pi^+ \rightarrow e^+\nu_e\gamma$, c) $\pi^+ \rightarrow \pi^0 e^+\nu_e$ [completed], P. Depommier, J.P. Martin, R. Poutissou (*Univ. de Montréal*), D. Bryman (*TRIUMF-Univ. of Victoria*), J.A. Macdonald, J.-M. Poutissou, M. Salomon (*TRIUMF*), M. Dixit (*National Research Council*), M.D. Hasinoff, D.F. Measday (*Univ. of British Columbia*)
24. Elastic scattering of polarized protons on ^{12}C [completed], G.A. Moss, G. Roy, D.M. Sheppard,* H. Sherif (*Univ. of Alberta*), L.G. Greeniaus, D.A. Hutcheon, C.A. Miller (*TRIUMF*)
26. Measurement of the differential cross section for free neutron-proton scattering and for the reaction $D(n, p)2n$ [completed], L.P. Robertson (*Univ. of Victoria*), C. Amsler (*CERN*), E.G. Auld, D.A. Axen (*Univ. of British Columbia*), D.V. Bugg, J.A. Edgington (*Univ. of London, QMC*), A.S. Clough (*Univ. of Surrey*), J.R. Richardson* (*UCLA*), N.M. Stewart (*Univ. of London, Bedford College*), J. Va'vra (*SLAC*)
27. Measurement of the polarization in free neutron-proton scattering [completed], D.A. Axen, E.G. Auld (*Univ. of British Columbia*), C. Amsler, (*CERN*), D.V. Bugg, J.A. Edgington (*Univ. of London, QMC*), A.S. Clough (*Univ. of Surrey*), J.R. Richardson* (*UCLA*), L.P. Robertson (*Univ. of Victoria*), G. Roy (*Univ. of Alberta*), N.M. Stewart (*Univ. of London, Bedford College*), J. Va'vra (*SLAC*)
35. A study of positive muon depolarization phenomena in chemical systems [completed], J.H. Brewer, D.G. Fleming, D.C. Walker, J.B. Warren* (*Univ. of British Columbia*), Y.C. Jean (*Univ. of Missouri, KC*), K.M. Crowe (*Lawrence Berkeley Lab*)
40. A proposal for neutron experiments at TRIUMF [completed], D.A. Axen, M.K. Craddock (*Univ. of British Columbia*), I.M. Blair (*AERE Harwell*), D.V. Bugg, J.A. Edgington (*Univ. of London, QMC*), A.S. Clough (*Univ. of Surrey*), N.M. Stewart (*Univ. of London, Bedford College*), J. Va'vra (*SLAC*)

41. a) Radiative capture of pions in light nuclei [completed], b) Charge exchange of stopped negative pions [completed], J.-M. Poutissou, M. Salomon (*TRIUMF*), D. Berghofer, M.K. Craddock, M.D. Hasinoff, R. MacDonald (*Univ. of British Columbia*)
42. π^- - ^3He : a) Strong interaction shift, b) Neutron-neutron scattering length [completed], G.A. Beer, S.K. Kim, G.R. Mason, R.M. Pearce,* C.E. Picciotto, L.P. Robertson, C.S. Wu (*Univ. of Victoria*), D. Bryman, A. Olin (*TRIUMF-Univ. of Victoria*), J.A. Macdonald, J.S. Vincent (*TRIUMF*), M. Dixit (*National Research Council*), M. Krell (*Univ. de Sherbrooke*)
46. Hyperfine splitting in polarized muonic ^{209}Bi atoms [completed], G.T. Ewan, H.B. Mak, B.C. Robertson (*Queen's Univ.*), G.A. Beer, G.R. Mason, R.M. Pearce* (*Univ. of Victoria*), A. Olin (*TRIUMF-Univ. of Victoria*), D.G. Fleming (*Univ. of British Columbia*), K. Nagamine, T. Yamazaki (*Univ. of Tokyo*)
47. Photon asymmetry in radiative muon capture [completed], J.H. Brewer, M.D. Hasinoff, R. MacDonald (*Univ. of British Columbia*), K. Krane (*Oregon State Univ.*), J.-M. Poutissou (*TRIUMF*)
48. Fertile-to-fissile conversion in electrical breeding (spallation) targets [completed], I.M. Thorson, F.M. Kiely (*Simon Fraser Univ.*), B.D. Pate (*Univ. of British Columbia*)
52. Measurement of the $\pi \rightarrow e\nu$ branching ratio [completed], D. Bryman, A. Olin (*TRIUMF-Univ. of Victoria*), G.R. Mason (*Univ. of Victoria*), D. Berghofer (*Univ. of British Columbia*), M. Dixit (*National Research Council*)
53. Emission of heavy fragments in pion absorption [completed], D.R. Gill, M. Salomon, E.W. Vogt (*TRIUMF*), P.W. Martin, G. Jones (*Univ. of British Columbia*)
54. π^\pm reaction cross-section measurements on isotopes of calcium [completed], R.R. Johnson (*TRIUMF-UBC*), K.L. Erdman (*Univ. of British Columbia*), J.L. Beveridge (*TRIUMF*)
55. μ^- capture in deuterium and the two-neutron interaction [completed], J.M. Cameron, W.J. McDonald, G.C. Neilson (*Univ. of Alberta*), H.W. Fearing (*TRIUMF*)
56. A study of the decay of the muon [completed], M.D. Hasinoff, R. MacDonald (*Univ. of British Columbia*), P. Depommier (*Univ. de Montréal*), J.-M. Poutissou, M. Salomon (*TRIUMF*)
57. Search for $\mu^+ \rightarrow e^+ + \gamma$ decay mode [completed], P. Depommier, J.P. Martin, R. Poutissou (*Univ. de Montréal*), J.-M. Poutissou (*TRIUMF*)
58. Polarization effects of the spin-orbit coupling of nuclear protons [completed], W.K. Dawson, P. Kitching (*TRIUMF-Univ. of Alberta*), J.M. Cameron, W.J. McDonald, G.A. Moss, G.C. Neilson, W.C. Olsen, G. Roy, D.M. Sheppard,* H. Sherif, G.M. Stinson (*Univ. of Alberta*), D.A. Hutcheon, C.A. Miller (*TRIUMF*), J.T. Sample (*Research Secretariat of B.C.*)
59. Investigation of the ($p, 2p$) reactions on ^3He , ^3H and ^4He [completed], D.K. Hasell, W.T.H. van Oers (*Univ. of Manitoba*), J.M. Cameron, G.A. Moss (*Univ. of Alberta*), R. Abegg*, L.G. Greeniaus, J.G. Rogers (*TRIUMF*), M.B. Epstein, D.J. Margaziotis (*California State Univ. LA*), A.W. Stetz (*Oregon State Univ.*)
60. Study of muonium formation in MgO and related insulators and its diffusion into a vacuum [completed], J.H. Brewer, D.G. Fleming, G. Jones, J.B. Warren* (*Univ. of British Columbia*)
61. Pre-clinical research on the π^- beam at TRIUMF [completed], J. Brosing, C.J. Eaves, R.W. Harrison, M. Korbelik, G.K.Y. Lam, B. Palcic, K.R. Shortt, L.D. Skarsgard (*B.C. Cancer Foundation*), B.G. Douglas, R.O. Kornelsen, M.E.J. Young (*B.C. Cancer Control Agency*), R.M. Henkelman (*Univ. of Toronto*)
65. Radiosensitivities of tumours *in situ* to π -meson irradiation [completed], S. Okada, K. Sakamoto, N. Suzuki (*Univ. of Tokyo*), T. Ono (*Univ. of Alberta*)
66. Survey of p - p bremsstrahlung far off the energy shell [completed], J.G. Rogers, H.W. Fearing (*TRIUMF*), J.M. Cameron, A.N. Kamal (*Univ. of Alberta*), J.V. Jovanovich (*Univ. of Manitoba*), J.R. Richardson* (*UCLA*), A.W. Stetz (*Oregon State Univ.*), A. Szyjewicz (*Univ. of Saskatchewan*)
71. Muon spin rotation project [completed], J.H. Brewer, A. Duncan, D.G. Fleming, D.Ll. Williams (*Univ. of British Columbia*), M. Doyama, R. Hayano, K. Nagamine, T. Yamazaki (*Univ. of Tokyo*), B.D. Patterson (*Univ. Zürich*)
72. Solid state studies by muonic x-ray polarization [completed], H. Hayano, K. Nagamine, N. Nishida, T. Yamazaki (*Univ. of Tokyo*), R.M. Pearce* (*Univ. of Victoria*)
73. Artificial muon polarization [completed], R. Hayano, K. Nagamine, N. Nishida, T. Yamazaki (*Univ. of Tokyo*), J.H. Brewer, D.G. Fleming, M.D. Hasinoff (*Univ. of British Columbia*), H.B. Mak (*Queen's Univ.*)

74. Proposal to measure D , R and R' in pp scattering, 200 to 500 MeV [completed], D.V. Bugg, J.A. Edgington, K. Shakarchi (*Univ. of London, QMC*), D.A. Axen (*Univ. of British Columbia*), A.S. Clough (*Univ. of Surrey*), S. Jaccard (*Univ. de Neuchâtel*), N.M. Stewart (*Univ. of London, Bedford College*), G. Ludgate, C. Oram (*TRIUMF*), J. Va'vra (*SLAC*)
75. The $d(p, \pi^+)t$ pion production reaction for high momentum transfer [completed], W.C. Olsen (*Univ. of Alberta*), P. Kitching (*TRIUMF-Univ. of Alberta*), E.G. Auld, G. Jones (*Univ. of British Columbia*), H.W. Fearing, D.A. Hutcheon, P. Walden (*TRIUMF*), T. Masterson (*Univ. of Colorado*), C.F. Perdrisat (*College of William and Mary*)
77. Evaporation-cooled metallic cesium target assembly for production of ^{123}I [completed], J.W. Blue (*NASA*), T.A. Hodges (*Univ. of Victoria*), D. Lyster, R.T. Morrison (*Vancouver General Hospital*), J.S. Vincent (*TRIUMF*), J.B. Warren* (*Univ. of British Columbia*), W. Wieseahn (*Simon Fraser Univ.*)
78. Importance of defects in μ^+ SR in metals [completed], T. Yamazaki, K. Nagamine (*Univ. of Tokyo*), B. Bergersen, J.H. Brewer, D.G. Fleming, L.C. Vaz (*Univ. of British Columbia*), A.T. Stewart (*Queen's Univ.*)
79. (Experiment 'X') Low energy π production as a function of energy at 500 MeV and below [completed], G.A. Beer, G.R. Mason, R.M. Pearce,* L.P. Robertson (*Univ. of Victoria*), D.A. Bryman, A. Olin (*TRIUMF-Univ. of Victoria*), J.-M. Poutissou, J.S. Vincent (*TRIUMF*), R.R. Johnson (*TRIUMF-UBC*), J.B. Warren* (*Univ. of British Columbia*), P.W. James (*Atomic Energy of Canada*)
80. Measurement of pionic x-ray energies, widths and intensities [completed], G.A. Beer, G.R. Mason, R.M. Pearce,* L.P. Robertson, (*Univ. of Victoria*), D.A. Bryman, A. Olin (*TRIUMF-Univ. of Victoria*), J.A. Macdonald (*TRIUMF*), M. Dixit (*National Research Council*), W.C. Sperry (*Central Washington Univ.*)
83. Bound muon decay in nuclei [completed], J.H. Brewer, M.D. Hasinoff, T. Suzuki (*Univ. of British Columbia*), J. Alster (*Tel-Aviv Univ.*), K. Nagamine (*Univ. of Tokyo*), J.-M. Poutissou (*TRIUMF*)
84. The (π^\pm, d) reaction on light nuclei [deferred], R.R. Johnson (*TRIUMF-UBC*), K.L. Erdman, H.R. Johnston (*Univ. of British Columbia*), T. Masterson (*Univ. of Colorado*), V.G. Lind, R.E. McAdams, O.H. Otteson (*Utah State Univ.*), J.S. Vincent (*TRIUMF*)
86. Elastic and inelastic scattering of polarized protons from calcium and lead [completed], D.A. Hutcheon, C.A. Miller (*TRIUMF*), P. Kitching (*TRIUMF-Univ. of Alberta*), R. Liljestr and, W.J. McDonald, G.C. Neilson, H. Sherif, G.M. Stinson (*Univ. of Alberta*), J.S. Blair (*Univ. of Washington*), D.K. McDaniels (*Univ. of Oregon*)
87. Proton radiography studies at TRIUMF [completed], E.W. Blackmore, G.H. Mackenzie (*TRIUMF*), D.A. Bryman (*TRIUMF-Univ. of Victoria*)
88. Systematic studies of total muon capture rates [completed], R. Hayano, K. Nagamine, T. Yamazaki (*Univ. of Tokyo*), J.H. Brewer, F. Entezami, D.F. Measday, S. Stanislaus (*Univ. of British Columbia*), D. Garner, (*TRIUMF*)
89. μ fission [completed], S.N. Kaplan (*Lawrence Berkeley Lab*), S. Ahmad, G.A. Beer, G.R. Mason, R.M. Pearce,* (*Univ. of Victoria*), A. Olin (*TRIUMF-Univ. of Victoria*), O. H usser* (*TRIUMF-SFU*), J.A. Macdonald (*TRIUMF*), A. Mireshghi (*Univ. of California*)
91. Muonium in semiconductors [completed], J.H. Brewer, D.G. Fleming (*Univ. of British Columbia*), K.M. Crowe, S.S. Rosenblum (*Lawrence Berkeley Lab*), K. Nagamine (*Univ. of Tokyo*)
93. Production of radioisotopes at medium energies for pure and applied research [completed], L. Moritz, J.S. Vincent (*TRIUMF*), B.D. Pate, L. Patrick (*Univ. of British Columbia*), C.H.W. Jones (*Simon Fraser Univ.*), D. Lyster, W. Rowe (*Vancouver General Hospital*)
97. Rare electromagnetic decays of pionic atoms [completed], M.D. Hasinoff, E. Mazzucato, D.F. Measday (*Univ. of British Columbia*), J.-M. Poutissou, M. Salomon (*TRIUMF*), P. Depommier, R. Poutissou (*Univ. de Montr al*), B. Bassalleck (*Univ. of New Mexico*), T. Marks (*Los Alamos National Lab*)
99. Studies of (p, d) reactions in nuclei [completed], A.N. Anderson, J.M. Cameron, W.J. McDonald, G.C. Neilson, W.C. Olsen, G. Roy (*Univ. of Alberta*), W.K. Dawson, P. Kitching (*TRIUMF-Univ. of Alberta*), D.A. Hutcheon, C.A. Miller, J.G. Rogers (*TRIUMF*), J. K allne (*JET Joint Undertaking*), B.K.S. Koene, W.T.H. van Oers (*Univ. of Manitoba*), J.J. Kraushaar, E. Rost, J.R. Shepard (*Univ. of Colorado*), D.K. McDaniels (*Univ. of Oregon*), B.T. Murdoch (*Schlumberger Well Systems*), A. Olin (*TRIUMF-Univ. of Victoria*), A.W. Stetz, L.W. Swenson (*Univ. of Oregon*)
101. Investigation of $(\pi, 2\pi)$ reaction [letter of intent], E.G. Auld, G. Jones (*Univ. of British Columbia*), R.R. Johnson (*TRIUMF-UBC*), P. Walden (*TRIUMF*)
102. Absolute cross sections of $^{12}\text{C}(\pi^\pm, \pi, N)^{11}\text{C}$ reactions at low energy [completed], R.G. Korteling (*Simon Fraser Univ.*), G.E. Butler, B.J. Dropesky, R.E.L. Green, C.J. Orth, R.A. Williams (*Los Alamos National Lab*), R.M. Henkelman (*Univ. of Toronto*)

103. Search for target spin dependence in proton elastic scattering [completed], D.P. Gurd, G.A. Moss, G. Roy, H. Sherif, G.M. Stinson (*Univ. of Alberta*)
104. The time projection chamber – A new facility for the study of decays of muons and pions [completed], D.A. Bryman (*TRIUMF–Univ. of Victoria*), M. Dixit, C.K. Hargrove, R. McKee, H. Mes (*National Research Council*), G. Azuelos, A. Bennett, J.A. Macdonald, T. Numa, J.-M. Poutissou, J.E. Spuller (*TRIUMF*), L.P. Robertson, (*Univ. of Victoria*), M.D. Hasinoff (*Univ. of British Columbia*), P. Depommier, J.P. Martin, R. Poutissou, Y. Sirois (*Univ. de Montréal*), H.L. Anderson* (*Los Alamos National Lab*), A.L. Carter, C. Irwin, D. Kessler, J. Stapeldon (*Carleton Univ.*), C.S. Wright (*Univ. of Chicago*)
105. Backward inclusive scattering [completed], G. Roy, G.A. Moss (*Univ. of Alberta*), J.L. Beveridge, D.A. Hutcheon, R.M. Woloshyn (*TRIUMF*)
108. Meson cascade studies [deferred], G.A. Beer, G.R. Mason (*Univ. of Victoria*), A. Olin (*TRIUMF–Univ. of Victoria*), M. Dixit (*National Research Council*), S.N. Kaplan, C. Wiegand (*Lawrence Berkeley Lab*), J.A. Macdonald (*TRIUMF*), W.C. Sperry (*Central Washington Univ.*)
110. Microdosimetry of π^- beam at TRIUMF [completed], A. Ito, H. Koyama (*Univ. of Tokyo*)
111. Study of the absorption of π^- at rest in ^4He , ^9Be , ^{12}C , ^{14}N and ^{16}O [completed], C. Cernigoi, N. Grion, G. Pauli, R. Rui (*Univ. di Trieste and INFN*), R. Cherubini (*Lab Nazionali di Legnaro INFN and Univ. di Padova*), D. Gill (*TRIUMF*), W. Gyles (*Univ. of British Columbia*)
113. A proposal for $^3\text{He}(p,p)^3\text{He}$ at backward angles [completed], J.M. Cameron, G.A. Moss (*Univ. of Alberta*), B.S. Bhakar, B.K.S. Koene, W.T.H. van Oers (*Univ. of Manitoba*), M.B. Epstein, D.J. Margaziotis (*California State Univ. LA*), R. Aberg*, L.G. Greeniaus, D.A. Hutcheon, C.A. Miller (*TRIUMF*), J. Källne (*JET Joint Undertaking*), B.T. Murdoch (*Schlumberger Well Systems*), A.W. Stetz (*Oregon State Univ.*)
114. The $(p, 2p)$ reaction on ^4He and ^3He [completed], B.K.S. Koene, W.T.H. van Oers (*Univ. of Manitoba*), M.B. Epstein, D.J. Margaziotis (*California State Univ.*), G.A. Moss (*Univ. of Alberta*), L.G. Greeniaus, J.G. Rogers (*TRIUMF*), B.T. Murdoch (*Schlumberger Well Systems*)
115. Neutral pion production from ^{208}Bi at intermediate proton energies [completed], J.M. D’Auria, D.H. Boal (*Simon Fraser Univ.*), T. Ward (*Indiana Univ.*), A. Yavin (*Tel-Aviv Univ.*)
117. Single particle inclusive spectra of light fragments over their entire energy range [completed], R.G. Korteling (*Simon Fraser Univ.*), R.E.L. Green (*Los Alamos National Lab*), K.P. Jackson (*TRIUMF*)
119. Small angle scattering of thermal neutrons for the study of magnetism and liquid crystals [completed], A.S. Arrott, J.F. Cochran, S.D. Hanham, B. Heinrich, M.J. Press (*Simon Fraser Univ.*), B.D. Patterson (*Univ. Zürich*)
120. A study of the production and decay of ^{11}Be with intermediate-energy protons [completed], K.P. Jackson (*TRIUMF-SFU*), J.M. D’Auria, W.J. Wieseahn (*Simon Fraser Univ.*)
121. Test of charge symmetry in n - p scattering [completed], G.R. Plattner (*Basel Univ.*), J. Birchall, N.E. Davison, W.T.H. van Oers (*Univ. of Manitoba*), D.A. Axen (*Univ. of British Columbia*), J.L. Beveridge, C.A. Miller, J.G. Rogers (*TRIUMF*), W.J. McDonald, G.A. Moss, G. Roy, G.M. Stinson (*Univ. of Alberta*), L.P. Robertson (*Univ. of Victoria*), H.E. Conzett (*Lawrence Berkeley Lab*), S. Mango (*SIN*)
122. A μSR investigation of dipolar fields in cobalt [completed], A.S. Arrott (*Simon Fraser Univ.*), B.D. Patterson (*Univ. Zürich*)
123. Observation of e^+ channeling from stopped μ^+ in a crystalline host [completed], A.S. Arrott (*Simon Fraser Univ.*), B.D. Patterson (*Univ. Zürich*)
124. Excitation of giant multipole resonances by intermediate-energy protons [completed], F.E. Bertrand, E. Gross, D.J. Horen, T. Sjoreen (*Oak Ridge National Lab*), L. Lisantti, D.K. McDaniels, J. Tinsley (*Univ. of Oregon*), L.W. Swenson (*Oregon State Univ.*)
126. Measurement of the line shape of pionic x-rays [deferred], A. Olin (*TRIUMF–Univ. of Victoria*), G.A. Beer, G.R. Mason, R.M. Pearce* (*Univ. of Victoria*), M. Dixit (*National Research Council*), J.A. Macdonald (*TRIUMF*)
127. Measurement of the strong interaction shift in pionic deuterium [completed], G.A. Beer, G.R. Mason, R.M. Pearce* (*Univ. of Victoria*), A. Olin (*TRIUMF–Univ. of Victoria*), M. Dixit (*National Research Council*), E. Klempt (*Univ. Mainz*), J.A. Macdonald (*TRIUMF*), C. Wiegand (*Lawrence Berkeley Lab*), A.W. Thomas (*Univ. of Adelaide*)
128. Variation of muonic x-ray intensities with atomic number [completed], G.A. Beer, G.R. Mason (*Univ. of Victoria*), A. Olin (*TRIUMF–Univ. of Victoria*), M. Dixit (*National Research Council*), J.A. Macdonald (*TRIUMF*), W.C. Sperry (*Central Washington Univ.*), C. Wiegand (*Lawrence Berkeley Lab*)

129. Quasielastic pion scattering at resonance energies for light $T=0$ nuclei [deferred], R.R. Johnson (*TRIUMF-UBC*), B. Barnett, K.L. Erdman, B. Gyles (*Univ. of British Columbia*), G. Azuelos, D. Gill, E.W. Vogt, P. Walden (*TRIUMF*), D. Ashery, A. Errell, A. Yavin (*Tel-Aviv Univ.*), B. Bassalleck (*Univ. of New Mexico*), T. Masterson (*Univ. of Colorado*), A.W. Thomas (*Univ. of Adelaide*)
130. The energy dependence of the polarization parameter in proton-proton scattering [completed], D.A. Axen, E.G. Auld (*Univ. of British Columbia*), D.V. Bugg, J.A. Edgington, W.R. Gibson (*Univ. of London, QMC*), A.S. Clough (*Univ. of Surrey*), N.M. Stewart (*Univ. of London, Bedford College*), M. Comyn, G. Ludgate (*TRIUMF*), J.R. Richardson* (*UCLA*), L.P. Robertson (*Univ. of Victoria*)
131. A study of (\bar{p}, γ) reactions on ${}^3\text{H}$ and ${}^6\text{Li}$ at intermediate energies [completed], J.M. Cameron, W.J. McDonald, G.M. Stinson, I.J. Van Heerden (*Univ. of Alberta*), P. Kitching (*TRIUMF-Univ. of Alberta*), A.W. Stetz, L.W. Swenson (*Oregon State Univ.*), D.A. Hutcheon, C.A. Miller, H.W. Fearing (*TRIUMF*)
132. Differential cross section of the reaction $pp \rightarrow d\pi^+$ between lab proton energies of 325 to 500 MeV [completed], P.L. Walden (*TRIUMF*), E.G. Auld, G. Jones (*Univ. of British Columbia*), R.R. Johnson (*TRIUMF-UBC*)
134. Measurement of the eta parameter in muon decay [completed], J.A. Bistirlich, K.M. Crowe, C.J. Martoff, J.M. Miller, W.A. Zajc (*Lawrence Berkeley Lab*), C.M. Clawson (*Univ. of California, Berkeley*), J.H. Brewer (*Univ. of British Columbia*)
137. Lifetime of the positive muon [completed], W. Dey, M. Eckhause, K. Giovanetti, R.D. Hart, R. Hartmann, D.W. Hertzog, J.R. Kane, W.A. Orance, W.C. Phillips, R.T. Siegel, W.F. Vulcan, R.E. Welsh, R.G. Winter (*College of William and Mary*)
138. Surface muon studies of germanium [completed], K.M. Crowe, S.S. Rosenblum (*Lawrence Berkeley Lab*), C.M. Clawson (*Univ. of California, Berkeley*), J.H. Brewer (*Univ. of British Columbia*)
139. Macroscopic diffusion of positive muons in aluminum [completed], K.M. Crowe, S.S. Rosenblum (*Lawrence Berkeley Lab*), C.M. Clawson (*Univ. of California, Berkeley*), J.H. Brewer (*Univ. of British Columbia*)
140. Transfer effects for stopping π^- in $\text{H}_2\text{-D}_2$ mixtures [completed], M.D. Hasinoff, D.F. Measday (*Univ. of British Columbia*), J.-M. Poutissou, M. Salomon (*TRIUMF*), V. Highland (*Temple Univ.*)
141. Muonic hydrogen at STP – A feasibility study [deferred], J.H. Brewer (*Univ. of British Columbia*), C. Oram (*TRIUMF*)
142. A study of the single scattering mechanism for non-evaporative fragment emission [completed], D.H. Boal, R.G. Korteling (*Simon Fraser Univ.*), K.P. Jackson (*TRIUMF*), R.E.L. Green (*Los Alamos National Lab*)
143. A study by recoil detection of proton-induced reaction on ${}^9\text{Be}$ [completed], K.P. Jackson (*TRIUMF*), D.H. Boal, J.M. D'Auria, R.G. Korteling (*Simon Fraser Univ.*), R.E.L. Green (*Los Alamos National Lab*)
144. Studies of (\bar{p}, d) reaction in nuclei [completed], J.M. Cameron, R. Liljestr and, W.J. McDonald, G.C. Neilson, W.C. Olsen, D.M. Sheppard,* G.M. Stinson (*Univ. of Alberta*), P. Kitching (*TRIUMF-Univ. of Alberta*), J.J. Kraushaar, J.R. Shepard (*Univ. of Colorado*), D.A. Hutcheon, C.A. Miller, J.G. Rogers (*TRIUMF*), C. Stronach (*Virginia State Univ.*), D.K. McDaniels, J. Tinsley (*Univ. of Oregon*)
145. The neutron and gamma-ray correlation in the negative pion capture in ${}^{165}\text{Ho}$ and ${}^{181}\text{Ta}$ [completed], Y.K. Lee, R. Levin, L. Madansky (*Johns Hopkins Univ.*)
147. The formation and reactivity of muonium in the gas phase [completed], J.H. Brewer, D.G. Fleming, R.J. Mikula, D.P. Spencer, J.B. Warren* (*Univ. of British Columbia*), D.M. Garner, R. Kiefl (*TRIUMF*)
149. μSR studies of phase transition [completed], M. Doyama, R. Nakai, R. Yamamoto, T. Yamazaki (*Univ. of Tokyo*), J.H. Brewer, H. Schilling, D.Ll. Williams (*Univ. of British Columbia*)
150. Utilization of backward muons to study muonium reaction intermediates [completed], J.A. Bartlett, J.C. Brodovitch, S.K. Leung, K.E. Newman, P.W. Percival (*Simon Fraser Univ.*), D.G. Fleming, D.C. Walker (*Univ. of British Columbia*)
151. Interaction of muons with fissile nuclides II [completed], A. Olin (*TRIUMF-Univ. of Victoria*), S. Ahmad, G.A. Beer, R.M. Pearce* (*Univ. of Victoria*), J.C. Brown (*Lawrence Livermore National Lab*), S.N. Kaplan (*Lawrence Berkeley Lab*), O. H usser* (*TRIUMF-SFU*), J.A. Macdonald (*TRIUMF*)
152. Measurement of the spin rotation parameter R in $p\text{-}{}^4\text{He}$ elastic scattering [completed], G.A. Moss, G. Roy, J. Uegaki (*Univ. of Alberta*), R. Abegg*, L.G. Greeniaus, D.A. Hutcheon, C.A. Miller (*TRIUMF*), C.A. Davis, W.T.H. van Oers (*Univ. of Manitoba*), J.M. Greben (*CSIR/NRMIS, Pretoria*)
153. Elastic scattering of protons from ${}^3\text{He}$ [completed], W.T.H. van Oers, D.K. Hasell (*Univ. of Manitoba*), J.M. Cameron, G.A. Moss (*Univ. of Alberta*), R. Abegg*, L.G. Greeniaus, C.A. Miller (*TRIUMF*), M.B. Epstein, D.J. Margaziotis (*California State Univ. LA*), H. Postma (*Technical Univ. Delft*), A.W. Stetz (*Oregon State Univ.*)

154. Muonium in solids [completed], J.H. Brewer, D.G. Fleming, H. Schilling, D.P. Spencer, D.Ll. Williams (*Univ. of British Columbia*), K.M. Crowe, S.S. Rosenblum (*Lawrence Berkeley Lab*), C.M. Clawson (*Univ. of California, Berkeley*), T. Yamazaki (*Univ. of Tokyo*), R. Kiefl (*TRIUMF*), Y.J. Uemura (*Columbia Univ.*)
155. Study of deep hole states in ^{40}Ca with $(\bar{p}, 2p)$ reaction [completed], P. Kitching (*TRIUMF–Univ. of Alberta*), P.W. Green, W.J. McDonald, K. Michaelian, W.C. Olsen, D.M. Sheppard,* J. Soukup, G.M. Stinson, I.J. van Heerden (*Univ. of Alberta*), D.A. Hutcheon, C.A. Miller (*TRIUMF*), A.N. James (*Univ. of Liverpool*)
156. Deuteron production in proton-nucleus collisions [completed], J.M. Cameron, R. Liljestr and, W.J. McDonald, W.C. Olsen, (*Univ. of Alberta*), P. Kitching (*TRIUMF–Univ. of Alberta*), J. K allne (*JET Joint Undertaking*), C.F. Perdrisat (*College of William and Mary*)
157. The chemistry of muonium atoms in condensed media [completed], J.H. Brewer, D.G. Fleming, R. Rist, D.C. Walker (*Univ. of British Columbia*), D. Garner (*TRIUMF*), Y.C. Jean (*Univ. of Missouri–Kansas City*), Y. Ito (*Univ. of Tokyo*), P.W. Percival (*Simon Fraser Univ.*)
158. Study of the reactions $p^2\text{H} \rightarrow d\pi^+n$ and $p^3\text{He} \rightarrow t\pi^+p$ [completed], J.M. Cameron, W.J. McDonald, W.C. Olsen, H. Wilson (*Univ. of Alberta*), I. van Heerden (*Univ. of Alberta and Sumi*), P. Kitching (*TRIUMF–Univ. of Alberta*), C.F. Perdrisat (*College of William and Mary*), H.W. Fearing, C.A. Miller (*TRIUMF*), J. K allne (*JET Joint Undertaking*)
159. $\bar{p}p$ and $\bar{p}d$ interactions at threshold [completed], E.G. Auld, D.A. Axen, K.L. Erdman, J.B. Warren,* B.L. White (*Univ. of British Columbia*), M. Comyn (*TRIUMF*), G.A. Beer (*Univ. of Victoria*), W. Dahme (*Univ. Munich*), U. Gastaldi, G. Graff, H. Kalinowsky, E. Kayser, E. Klempt, R. Landau, R. Schulze, R.W. Wodrich, (*Univ. Mainz*), C.J. Martoff (*Lawrence Berkeley Lab*), C. Sabev (*Univ. of Geneva*), P. Truol (*Univ. Z urich*)
160. Studies of some ternary magnetic superconductors with muons [completed], C.Y. Huang (*Los Alamos National Lab*), J.H. Brewer, H. Schilling (*Univ. of British Columbia*), C.W. Clawson (*Univ. of California, Berkeley*), K.M. Crowe, S.E. Kohn, S.S. Rosenblum (*Lawrence Berkeley Lab*), A. Schenck (*SIN*)
161. Studies of spin dynamics of some amorphous spin glasses with muons [completed], C.Y. Huang (*Los Alamos National Lab*), J.H. Brewer, H. Schilling (*Univ. of British Columbia*), C.W. Clawson (*Univ. of California Berkeley*), K.M. Crowe, S.E. Kohn, S.S. Rosenblum (*Lawrence Berkeley Lab*), A. Schenck (*SIN*)
162. Survey of x-ray production of high-energy protons [completed], D.C. Gregory, B.M. Johnson, K.W. Jones (*Brookhaven National Lab*), G.J. Basbas (*Physical Review Letters*), J.T. Sample (*Research Secretariat of B.C.*)
164. Measurement of the $1/E$ dependence in $^7\text{Li}(p, n)^7\text{Be}$ reactions [completed], J.M. D’Auria, M. Dombisky (*Simon Fraser Univ.*), T.W. Ward (*Indiana Univ.*), T. Ruth (*TRIUMF*)
165. Cross sections and analysing power measurements of giant resonances for incident 200–500 MeV [completed], J. Lisannti, D.K. McDaniels, J. Tinsley (*Univ. of Oregon*), F.E. Bertrand, E.E. Gross, T. Sjoreen (*Oak Ridge National Lab*), D. Drake (*Los Alamos National Lab*), L.W. Swenson (*Oregon State Univ.*), I. Bergqvist (*Univ. of Lund*)
166. Neutron-nuclear structure with pion [completed], R.R. Johnson (*TRIUMF–UBC*), B. Barnett, K.L. Erdman, W. Gyles (*Univ. of British Columbia*), E.W. Blackmore, D.R. Gill (*TRIUMF*), E.L. Mathie (*Univ. of Regina*), D. Ashery (*Tel-Aviv Univ.*), N. Gri on (*INFN and Univ. di Trieste*), J.J. Kraushaar, T. Masterson (*Univ. of Colorado*), C.A. Wiedner (*Max Planck Institut*), S.A. Martin (*KfA J ulich*)
168. 2S muonium production from thin foils [completed], R. Kiefl, C.J. Oram (*TRIUMF*), J.H. Brewer, A. Fry, J.B. Warren,* (*Univ. of British Columbia*), G.M. Marshall (*Univ. of Victoria*)
169. Proton elastic scattering from ^{16}O [completed], D.A. Hutcheon, C.A. Miller (*TRIUMF*), P. Kitching (*TRIUMF–Univ. of Alberta*), J.M. Cameron, R. Liljestr and, G.C. Neilson, W.C. Olsen, D.M. Sheppard,* H. Sherif, G.M. Stinson, H. Wilson (*Univ. of Alberta*), P. Schwandt (*Indiana Univ.*), D.K. McDaniels, J. Tinsley (*Univ. of Oregon*), W.T.H. van Oers (*Univ. of Manitoba*)
170. Fission-evaporation competition in heavy nuclei at intermediate energies [completed], P. Kitching (*TRIUMF–Univ. of Alberta*), H. Fielding, S.T. Lam, G.C. Neilson, W.C. Olsen, J. Uegaki (*Univ. of Alberta*), A. Breskin, Z. Fraenkel (*Weizmann Institute*), R. Abegg*, D.A. Hutcheon (*TRIUMF*)
171. Test of T -invariance in pp scattering [completed], R. Abegg*, L.G. Greeniaus, D.A. Hutcheon, C.A. Miller (*TRIUMF*), J.M. Cameron, D.P. Gurd, R. Liljestr and, G.A. Moss, G. Roy, H. Wilson (*Univ. of Alberta*)
173. Measurement of pionic 4–3 x-ray transitions in heavy nuclei [completed], A. Olin (*TRIUMF–Univ. of Victoria*), G.A. Beer, G.R. Mason (*Univ. of Victoria*), P.R. Poffenberger (*Univ. of Manitoba*), J.A. Macdonald, T. Numao (*TRIUMF*), B. Olaniyi (*Univ. of Ife*)

174. Spin dependence of the $pp \rightarrow pn\pi^+$ reaction [completed], D.A. Axen, C. Waltham (*Univ. of British Columbia*), D.V. Bugg, J.A. Edgington (*Univ. of London, QMC*), N.M. Stewart (*Univ. of London, Bedford College*), M. Comyn, G. Ludgate (*TRIUMF*), J.R. Richardson* (*UCLA*), L.P. Robertson (*Univ. of Victoria*), R. Dubois (*SLAC*)
175. An investigation of inclusive one-pion production in proton nucleus collisions [completed], K.D. Bol, M.R. Clover, R.M. DeVries, N.J. Digiacomo, J. Kapustinsky, J.C. Peng, W.E. Sondheim, J.W. Sunier (*Los Alamos National Lab*)
177. Proton radius determinations for C, N and O [completed], R.R. Johnson (*TRIUMF-UBC*), B. Barnett, K.L. Erdman, W. Gyles (*Univ. of British Columbia*), E.W. Blackmore, D.R. Gill (*TRIUMF*), G. Lolos (*Univ. of Regina*), J. Alster (*Tel-Aviv Univ.*), N. Grion (*INFN and Univ. di Trieste*), J.J. Kraushaar, T. Masterson (*Univ. of Colorado*)
178. Nuclear radius studies in the Ca region [completed], R.R. Johnson (*TRIUMF-UBC*), B. Barnett, K.L. Erdman, W. Gyles, (*Univ. of British Columbia*), E.W. Blackmore, D.R. Gill (*TRIUMF*), G. Lolos (*Univ. of Regina*), N. Grion (*INFN and Univ. di Trieste*), J.J. Kraushaar, T. Masterson (*Univ. of Colorado*), S. Martin (*KfA Jülich*), C. Weidner (*Max-Planck Institut*)
182. Measurement of the n - p spin correlation parameter A_{nn} [completed], J. Birchall, C.A. Davis, N.E. Davison, W.P. Lee, W.T.H. van Oers (*Univ. of Manitoba*), P.W. Green, W.J. McDonald, G.A. Moss, G. Roy, G.M. Stinson (*Univ. of Alberta*), R. Abegg*, L.G. Greeniaus, C.A. Miller (*TRIUMF*)
184. Investigation of the $\bar{p}^+ + {}^2\text{H} \rightarrow {}^3\text{H} + \pi^+$ reaction from 275 to 450 MeV using polarized protons [completed], E.G. Auld, G. Giles, G. Jones, W. Ziegler (*Univ. of British Columbia*), P. Walden (*TRIUMF*)
185. Precise measurement of the polarization parameter ξ : A search for the effects of a right-handed gauge boson in μ^+ decay [completed], J. Carr, G. Gidal, A. Jodidio, K. Shinsky, H.M. Steiner, D. Stoker, M. Strovink, R.D. Tripp (*Univ. of California-LBL*), C. Oram (*TRIUMF*), B. Gobbi (*Northwestern Univ.*)
186. Measurement of collision-induced de-excitation rates of the 2S state of muonic helium [completed], M. Eckhause, K. Giovanetti, D. Hertzog, D. Joyce, J. Kane, W. Phillips, R. Siegel, W. Vulcan, R. Welsh, R. Whyley, R.G. Winter (*College of William and Mary*)
187. Pion production from ${}^{10}\text{B}$ and ${}^{16}\text{O}$ bombarded with polarized protons [completed], E.G. Auld, G. Giles, G. Jones, B. McParland, W. Ziegler, (*Univ. of British Columbia*), G. Lolos (*Univ. of Regina*), W. Falk (*Univ. of Manitoba*), P. Walden (*TRIUMF*)
189. Radiochemical study of $\sigma_T(E)$ for ${}^{209}\text{Bi}(p, \pi^- xn){}^{210-x}\text{At}$ reactions from threshold to ~ 0.8 GeV [completed], J.M. D'Auria, M. Dombisky (*Simon Fraser Univ.*), J. Clark (*LAMPF*), T. Ward (*Indiana Univ.*), A. Yavin (*Tel-Aviv Univ.*)
190. Radiative polarized neutron capture on protons [completed], J.M. Cameron, W.J. McDonald, J. Soukup, J. Uegaki (*Univ. of Alberta*), P. Kitching (*TRIUMF-Univ. of Alberta*), R. Abegg*, D.A. Hutcheon, C.A. Miller (*TRIUMF*), I.J. Van Heerden (*Southern Nuclear Inst.*), A.W. Stetz (*Oregon State Univ.*), Y.M. Shin (*Univ. of Saskatchewan*)
191. Muons and muonium on surfaces [completed], J.H. Brewer, D. Harshman, J.B. Warren* (*Univ. of British Columbia*), C.J. Oram (*TRIUMF*), K.M. Crowe (*Lawrence Berkeley Lab*), G. Dash (*Univ. of Washington*), W.S. Glausinger, R.F. Marzke (*Arizona State Univ.*)
192. Measurement of the pion production asymmetries from the reaction $\bar{p}p \rightarrow d\pi^+$ with a polarized proton beam between energies of 400 and 520 MeV [completed], D. Ottewell, P. Walden (*TRIUMF*), W. Falk (*Univ. of Manitoba*), G. Giles, G. Jones, W. Ziegler (*Univ. of British Columbia*), G. Lolos (*Univ. of Regina*)
194. The $pd \rightarrow t\pi^+$ reaction at 330, 470 and 500 MeV [completed], R. Abegg*, L.G. Greeniaus, D.A. Hutcheon, C.A. Miller (*TRIUMF*), J.M. Cameron, W.J. McDonald, G.A. Moss, W.C. Olsen, G. Roy, J. Uegaki (*Univ. of Alberta*), C.A. Davis (*Univ. of Manitoba*)
195. ${}^{24}\text{Mg}(p, p'){}^{24}\text{Mg}^* \rightarrow {}^{12}\text{C} + {}^{12}\text{C}$ [completed], R. Abegg*, L.G. Greeniaus, D.A. Hutcheon, C.A. Miller (*TRIUMF*), J.M. Cameron, W.K. Dawson, C.A. Moss, G. Roy, H. Sherif, J. Uegaki, H. Wilson (*Univ. of Alberta*), C.A. Davis (*Univ. of Manitoba*)
196. Measurement of pionic x-rays in ${}^{23}\text{Na}$, ${}^{24}\text{Mg}$ and ${}^{27}\text{Al}$ [completed], A. Olin (*TRIUMF-Univ. of Victoria*), J.A. Macdonald, T. Numao (*TRIUMF*), G.A. Beer, G.R. Mason (*Univ. of Victoria*), B. Olaniyi (*Univ. of Ife*), P.R. Poffenberger (*Univ. of Manitoba*)
197. A precise measurement of the Lamb shift in muonium in the 2S state [letter of intent], J.H. Brewer, A. Fry, J.B. Warren* (*Univ. of British Columbia*), R. Kiefl, C. Oram (*TRIUMF*)

198. n - p total cross section in pure spin states [letter of intent], D.A. Axen, F. Entezami, C. Waltham (*Univ. of British Columbia*), J.A. Edgington (*Univ. of London, QMC*), M. Comyn, G. Ludgate (*TRIUMF*), L.P. Robertson (*Univ. of Victoria*)
199. A study of low energy pion absorption in ^3He [completed], J. Alster, A. Altman, D. Ashery, L. Lichtenstadt, M.A. Moinester (*Tel-Aviv Univ.*), R.R. Johnson (*TRIUMF-UBC*), B. Barnett, W. Gyles, H. Roser, R. Tacik (*Univ. of British Columbia*), D.A. Gill, J.S. Vincent (*TRIUMF*), K. Aniol (*California State Univ. LA*), S. Levenson (*Northwestern Univ.*)
202. Nuclear radii measurements in the $A \sim 20$ region [completed], T.E. Drake, R. Sobie (*Univ. of Toronto*), A. Altman, M.A. Moinester (*Tel-Aviv Univ.*), B. Barnett, J. Coopersmith, K.L. Erdman, W. Gyles, R. Tacik (*Univ. of British Columbia*), R.R. Johnson (*TRIUMF-UBC*), G.A. Beer (*Univ. of Victoria*), E.W. Blackmore, D. Gill (*TRIUMF*), A. Olin (*TRIUMF-Univ. of Victoria*), S. Martin (*KfA Jülich*), C. Wiedner (*Max Planck Institut*)
203. Inelastic pion scattering on neon isotopes [completed], T.E. Drake, R. Sobie (*Univ. of Toronto*), A. Altman, M.A. Moinester (*Tel-Aviv Univ.*), B. Barnett, J. Coopersmith, K.L. Erdman, W. Gyles, R. Tacik (*Univ. of British Columbia*), R.R. Johnson (*TRIUMF-UBC*). E.W. Blackmore, D. Gill (*TRIUMF*), S. Martin (*KfA Jülich*), C. Wiedner (*Max-Planck-Institut*), B.H. Wildenthal (*Michigan State Univ.*)
204. Strong interaction shift and width in pionic ^{22}Ne atoms [completed], G.A. Beer, G.R. Mason (*Univ. of Victoria*), A. Olin (*TRIUMF-Univ. of Victoria*), T.E. Drake, R. Sobie, (*Univ. of Toronto*), B. Olaniyi (*Univ. of Ife*)
205. Tensor analysing power in pion deuterium scattering [complete], L. Dallin, K. Itoh, Y.M. Shin (*Univ. of Saskatchewan*), B. Barnett, K.L. Erdman, W. Gyles, R. Tacik (*Univ. of British Columbia*), R.R. Johnson (*TRIUMF-UBC*), E.W. Blackmore, D.R. Gill, G.D. Wait (*TRIUMF*), G. Lolos (*Univ. of Regina*), K. Aniol (*California State Univ. LA*), T.E. Drake (*Univ. of Toronto*), S. Martin (*KfA Jülich*)
206. A study of (p, n) and related reactions [completed], D.H. Boal, J.M. D'Auria, R.G. Korteling (*Simon Fraser Univ.*), K.P. Jackson (*TRIUMF*), R. Helmer (*Univ. of Western Ontario*), R.E.L. Green (*Los Alamos National Lab*)
207. $^{48}\text{Ca}(\bar{p}, p')^{48}\text{Ca}(1^+)$ [completed], R. Abegg*, D.R. Gill, C.A. Miller (*TRIUMF*), J.M. Cameron (*Univ. of Alberta*), P. Kitching (*TRIUMF-Univ. of Alberta*), C.A. Davis (*Univ. of Manitoba*), J. Coopersmith, (*Univ. of British Columbia*), R.R. Johnson (*TRIUMF-UBC*), G. Berg, S. Martin (*KfA Jülich*), J. Lisantti (*Univ. of Oregon*), M.A. Moinester (*Tel-Aviv Univ.*), R. Santo (*Münster Univ.*)
208. Proton-proton bremsstrahlung [completed], P. Kitching (*TRIUMF-Univ. of Alberta*), P.W. Green, M. Hugi, M. Michaelian, G.C. Neilson, W.C. Olsen, D.M. Sheppard,* J. Soukup, J. Uegaki, J. Wesick (*Univ. of Alberta*), R. Abegg*, H.W. Fearing, L.G. Greeniaus, D.A. Hutcheon, C.A. Miller (*TRIUMF*), N. Stevenson (*Univ. of Saskatchewan*)
211. The neutron and gamma-ray correlation in the π^- and μ^- captures in medium-heavy nuclei [completed], T.J. Hallman, Y.K. Lee, R. Levin, L. Madansky, E. McIntyre (*Johns Hopkins Univ.*), G.R. Mason (*Univ. of Victoria*), K.S. Kang (*Neung Univ.*), B. Olaniyi (*Univ. of Ife*)
212. In search of a tredecabaryon resonance [completed], R. Abegg*, K.P. Jackson, C.A. Miller (*TRIUMF*), D.H. Boal, J.M. D'Auria, R.G. Korteling (*Simon Fraser Univ.*), R.E.L. Green (*Los Alamos National Lab*), R. Helmer (*Univ. of Western Ontario*)
213. Absorption at rest of π^- in ^4He and ^6Li [completed], C. Cernigoi, N. Grion, G. Pauli, R. Rui (*INFN and Univ. di Trieste*), R. Cherubini (*National Lab of Legnaro-Univ. di Padova*), D.R. Gill (*TRIUMF*), W. Gyles (*Univ. of British Columbia*)
215. Inclusive (p, p) spectra [completed data taking], R.E. Segel, A. Hassan, S.M. Levenson (*Northwestern Univ.*), P. Gumplinger, A.W. Stetz, L.W. Swenson (*Oregon State Univ.*), K.P. Jackson (*TRIUMF*), P.P. Singh (*Indiana Univ.*), J. Tinsley (*Univ. of Oregon*)
216. Investigation of spin-flip resonances and energy dependencies of components of the Love-Franey interaction [completed], F.E. Bertrand, E.E. Gross, D.J. Horen, T.P. Sjoreen (*Oak Ridge National Lab*), J. Lisantti, D.K. McDaniels, J. Tinsley (*Univ. of Oregon*), L.W. Swenson (*Oregon State Univ.*)
217. Low-energy, electromagnetic pion form factors [completed], J.-M. Poutissou (*TRIUMF*), P. Gumplinger, D. Ila, A.W. Stetz (*Oregon State Univ.*), M.D. Hasinoff (*Univ. of British Columbia*), T. Mulera, V. Perez-Mendez, A. Sagle (*Lawrence Berkeley Lab*)
218. Pion production from ^{12}C and ^{10}B with polarized protons of 350 MeV [completed], G. Lolos (*Univ. of Regina*), R.R. Johnson (*TRIUMF-UBC*), G. Giles, G. Jones, B. McParland (*Univ. of British Columbia*), D. Ottewell, P. Walden (*TRIUMF*), R.D. Bent (*IUCF*), W. Falk (*Univ. of Manitoba*)

219. The chemistry of pionic hydrogen atoms [completed], D. Horváth (*Central Research Inst. for Physics, Budapest*), D.F. Measday, S. Stanislaus (*Univ. of British Columbia*), M. Salomon (*TRIUMF*), K. Aniol (*California State Univ. LA*)
220. Temperature dependence of the spin exchange cross sections between muonium and alkali metal [completed], D.J. Arseneau, D.G. Fleming, M. Senba (*Univ. of British Columbia*), D.M. Garner (*TRIUMF*)
221. Search for evidence of a delta-nucleus intermediate state in proton elastic scattering [completed data taking], C.A. Davis, W.P. Lee, W.T.H. van Oers (*Univ. of Manitoba*), H.O. Meyer (*IUCF*), P. Schwandt (*Indiana Univ.*), K.P. Jackson (*TRIUMF*), H.W. Roser (*Univ. of British Columbia*)
223. The ${}^2\text{H}(p, 2p)$ reaction and momentum distributions of the deuteron [completed], H.P. Gubler, W.P. Lee, W.T.H. van Oers (*Univ. of Manitoba*), C.F. Perdrisat (*College of William and Mary*), J.M. Cameron (*IUCF*), M.B. Epstein, D.J. Margaziotis (*California State Univ.*), H. Postma (*Technical Univ. Delft*), A.W. Stetz (*Oregon State Univ.*), R. Abegg* (*TRIUMF*)
224. Inclusive pion scattering from light nuclei [completed], K.G.R. Doss, I. Halpern, M. Khandaker, D.W. Storm (*Univ. of Washington*), J.F. Amann (*Los Alamos National Lab*)
225. Search for isovector properties of IBA nuclei [deferred], J. Alster, J. Lichtenstadt, M. Moinester (*Tel-Aviv Univ.*), G. Azuelos, D.R. Gill (*TRIUMF*), R.R. Johnson (*TRIUMF-UBC*), B.M. Barnett, W. Gyles, H. Roser, R. Tacik (*Univ. of British Columbia*), S. Martin (*KfA Jülich*), R. Sobie (*Univ. of Toronto*), K. Aniol (*California State Univ. LA*)
226. Study of neutron-proton transition amplitudes in ${}^{14}\text{C}$ using 50 MeV pions [completed], R.R. Johnson (*TRIUMF-UBC*), H. Roser, R. Tacik (*Univ. of British Columbia*), K. Aniol (*California State Univ. LA*), J. Alster, J. Lichtenstadt, M.A. Moinester (*Tel-Aviv Univ.*), G. Azuelos, D.R. Gill (*TRIUMF*), S. Martin (*KfA Jülich*), R. Sobie (*Univ. of Toronto*), H.W. Baer (*LAMPF*)
227. Elastic and inelastic scattering of polarized protons from ${}^{10}\text{B}$ [completed], P.R. Andrews, S.M. Banks, P. Lewis, V.C. Officer, G.G. Shute, B.M. Spicer (*Univ. of Melbourne*), C.W. Glover (*IUCF*)
229. Pion double charge exchange at low energy in the TPC [completed], D.A. Bryman, M.J. Leitch, I. Navon, A. Olin, P. Schlatter (*TRIUMF-Univ. of Victoria*), A. Burnham,* M. Hasinoff (*Univ. of British Columbia*), G. Azuelos, J.A. Macdonald, T. Numao, J.-M. Poutissou, J. Spuller (*TRIUMF*), P. Depommier, R. Poutissou (*Univ. de Montréal*), M. Blecher, K. Gotow (*VPI and State Univ.*), M. Dixit, C.K. Hargrove, H. Mes (*National Research Council*), M.A. Moinester (*Tel-Aviv Univ.*), H. Baer, M. Cooper (*LAMPF*)
230. Muonic molecule formation rates in HD gas [completed], K. Aniol (*California State Univ. LA*), F. Entezami, D.F. Measday, C. Virtue (*Univ. of British Columbia*), D. Horváth (*Central Research Inst. for Physics, Budapest*), M. Salomon (*TRIUMF*), J. Smith (*Univ. of Surrey*), S.E. Jones (*Idaho National Engineering Lab*), B.C. Robertson (*Queen's Univ.*)
231. Studies of light pionic atoms [completed], G.A. Beer, G.R. Mason, G.M. Marshall (*Univ. of Victoria*), A. Olin (*TRIUMF-Univ. of Victoria*), J.A. Macdonald (*TRIUMF*), E. Klempt (*Johannes Gutenberg Univ., Mainz*), C. Wiegand (*Lawrence Berkeley Lab*), K. Wetzel (*Univ. of Portland*), W.C. Sperry (*Central Washington Univ.*), B.H. Olaniyi (*Univ. of Ife*)
232. Muon Knight shifts in metals [completed], J.H. Brewer, E. Koster, D.Ll. Williams (*Univ. of British Columbia*)
233. Vector analysing power and spin transfer parameters for the $\pi^+d \rightarrow \bar{p}p$ reaction [completed], E.G. Auld, P. Couvert, G. Jones, B. McParland (*Univ. of British Columbia*), R.R. Johnson (*TRIUMF-UBC*), D. Ottewell, P. Walden (*TRIUMF*), G. Lolos (*Univ. of Regina*), W. Falk (*Univ. of Manitoba*)
234. Study of simple features of the $A(p, \pi^-)A + 1$ reaction in the (3,3) resonance region [completed], R.D. Bent (*IUCF*), G.J. Lolos (*Univ. of Regina*), G.E. Walker (*Indiana Univ.*), P. Couvert, G. Giles, G. Jones, B. McParland, W. Ziegler (*Univ. of British Columbia*), J. Iqbal, P. Walden (*TRIUMF*), W.R. Falk (*Univ. of Manitoba*)
236. (p, p') reactions in nuclei [completed], R.E. Azuma, T.E. Drake, J.D. King, S.S.M. Wong, X. Zhu (*Univ. of Toronto*), K.P. Jackson, S. Yen (*TRIUMF*), A. Zaringhalan (*Bell Laboratories*)
237. Proton-nucleus interaction [completed], R.E. Azuma, T.E. Drake, J.D. King, S.S.M. Wong, X. Zhu (*Univ. of Toronto*), S. Yen (*TRIUMF*)
238. Inelastic proton excitation of low-lying nuclear states for $E_p = 200\text{--}500$ MeV [completed], R.L. Auble, R.E. Bertrand, E.E. Gross, D.J. Horen, G.R. Satchler, T.P. Sjoreen (*Oak Ridge National Lab*), D.K. McDaniels, J. Tinsley, J. Lisantti (*Univ. of Oregon*), L.W. Swenson (*Oregon State Univ.*)
239. Muon spin relaxation studies of spin glasses and random spin systems [completed], Y.J. Uemura (*Columbia Univ.*), J.H. Brewer (*Univ. of British Columbia*), K.M. Crowe (*Lawrence Berkeley Lab*), T. Yamazaki (*Univ. of Tokyo*), Y. Miyako, K. Katsumata (*Univ. of Hokkaido*), S. Chikazawa (*Muroran Inst. of Technology*)

241. Temperature dependence of reaction rate constants for muonium addition reactions in liquid phases [completed], K.L. Cheng, R.L. Ganti, Y.C. Jean (*Univ. of Missouri-Kansas City*), D.C. Walker (*Univ. of British Columbia*), J.M. Stadlbauer* (*Hood College*), B.W. Ng (*Winona State Univ.*)
242. Radiochemical study of the (p, π^+) reaction on bismuth [completed data taking], J. D'Auria, M. Dombisky (*Simon Fraser Univ.*), T. Ruth (*TRIUMF*), T. Ward (*IUCF*), A. Yavin (*Tel-Aviv Univ.*)
243. Energy and angle dependence of the ${}^6\text{Li}(\pi^+, {}^3\text{He}){}^3\text{He}$ reaction [completed], G. Huber, G.J. Lolos, S.I.H. Naqvi, Z. Papandreou (*Univ. of Regina*), E.G. Auld, P. Couvert, G. Jones, B.J. McParland (*Univ. of British Columbia*), R.R. Johnson (*TRIUMF-UBC*), D. Ottewell, P.L. Walden (*TRIUMF*)
244. μ^+ spin relaxation in Y_9Co_7 and ternary magnetic superconductors [completed], E.J. Ansaldo (*Univ. of Saskatchewan*), C.Y. Huang (*Los Alamos National Lab*), J.H. Brewer, M. Senba (*Univ. of British Columbia*), K. Crowe (*Univ. of California, Berkeley*), S.S. Rosenblum (*Lawrence Berkeley Lab*), D.R. Harshman (*AT&T Laboratories*)
245. Muon spin rotation studies of unsupported and supported platinum catalysts [completed], W.S. Glausinger, R.F. Marzke (*Arizona State Univ.*), E. Ansaldo (*Univ. of Saskatchewan*), J.H. Brewer, S. Kreitzman, D. Noakes, M. Senba (*Univ. of British Columbia*), R. Keitel (*TRIUMF*), D.R. Harshman (*AT&T Laboratories*)
246. The double charge exchange reaction at $T = 50$ MeV on ${}^{18}\text{O}$ using the QQD spectrometer [completed], E.W. Blackmore, D.R. Gill (*TRIUMF*), R.R. Johnson (*TRIUMF-UBC*), K.L. Erdman, H. Roser, R. Tacik (*Univ. of British Columbia*), A. Altman, M.A. Moinester (*Tel-Aviv Univ.*), S. Martin (*KfA, Jülich*), C.A. Wiedner (*MPI, Heidelberg*), T. Drake, R. Sobie (*Univ. of Toronto*), T.G. Masterson (*Univ. of Colorado*)
247. Precise measurement of muon decay asymmetry parameter δ [completed], J. Carr, G. Gidal (*Lawrence Berkeley Lab*), A. Jodidio, K.A. Shinsky, H.M. Steiner, D. Stoker, M. Strovink, R.D. Tripp (*Univ. of California, Berkeley-LBL*), B. Gobbi (*Northwestern Univ.*), C.J. Oram (*TRIUMF*)
248. A study of the $\pi^+ \rightarrow e^+ \nu_e$ decay [completed], J.A. Macdonald, T. Numao, J.-M. Poutissou (*TRIUMF*), D.A. Bryman, A. Olin (*TRIUMF-Univ. of Victoria*), M.S. Dixit (*National Research Council*)
249. Radiative muon capture on hydrogen with the TPC [succeeded by 452], G. Azuelos, J.A. Macdonald, T. Numao, J.-M. Poutissou, J. Spuller (*TRIUMF*), G. Bavaria, P. Depommier, H. Jeremie, L. Lessard, J.P. Martin, R. Poutissou (*Univ. de Montréal*), D.A. Bryman (*TRIUMF-Univ. of Victoria*), M. Leitch, I. Navon, P. Schlatter (*Univ. of Victoria*), A. Burnham,* M.D. Hasinoff (*Univ. of British Columbia*), M. Blecher, K. Gotow (*VPI & State Univ.*), M. Dixit, C.K. Hargrove, H. Mes (*National Research Council*), J. Bailey (*Yale Univ.*)
250. Charge-exchange coincident with X/gamma-rays in pionic phosphorus [completed data taking], J.M. Bailey (*Yale Univ.*), G.A. Beer, G.R. Mason (*Univ. of Victoria*), D.F. Measday (*Univ. of British Columbia*), A. Olin (*TRIUMF-Univ. of Victoria*), M. Salomon (*TRIUMF*), P.R. Poffenberger (*Univ. of Manitoba*)
251. Coincident optical and x-ray transitions in muonic helium [deferred], J.M. Bailey (*Yale Univ.*), C.J. Oram (*TRIUMF*), G.M. Marshall (*Univ. of Victoria*), J.D. Silver, D.N. Stacey (*Oxford Univ.*)
252. Excitation of giant multipole resonances in sd -shell nuclei via medium energy proton inelastic scattering [completed], F.E. Bertrand, C.B. Fulmer, E.E. Gross, D.J. Horen, T.P. Sjoreen (*Oak Ridge National Lab*), J. Lisantti, D.K. McDaniels, J.R. Tinsley (*Univ. of Oregon*), L.W. Swenson (*Oregon State Univ.*), T.A. Carey, K. Jones, J.B. McClelland, S. Seestrom-Morris (*Los Alamos National Lab*)
254. Total reaction cross sections on nuclei in the 50–80 MeV range [completed], E. Friedman (*Hebrew Univ. Jerusalem*), D. Gill (*TRIUMF*), R.R. Johnson (*TRIUMF-UBC*), M. Rozon (*Univ. of British Columbia*), J. Lapointe (*Univ. de Laval*), A. Altman (*Tel-Aviv Univ.*)
255. A study of pion absorption on two nucleons, each from a different shell, through the ${}^{18}\text{O}(\pi^+, 2p){}^{16}\text{N}$ reaction [replaced by 328], A. Altman, D. Ashery (*Tel-Aviv Univ.*), R.R. Johnson (*TRIUMF-UBC*), H. Roser, R. Tacik (*Univ. of British Columbia*), D.R. Gill, U. Wienands (*TRIUMF*), K. Aniol (*California State Univ. LA*), C.A. Wiedner (*MPI, Heidelberg*), T. Drake, R. Sobie (*Univ. of Toronto*), N. Grión (*INFN Trieste*)
257. Pion radiative capture in ${}^3\text{He}$ and ${}^{15}\text{N}$ [deferred], D.F. Measday, F. Entezami, M.D. Hasinoff, S. Stanislaus (*Univ. of British Columbia*), M. Salomon, J. Vincent (*TRIUMF*)
258. Radiative decay of the Δ resonance [replaced by 537], D.F. Measday, F. Entezami, S. Stanislaus (*Univ. of British Columbia*), M. Salomon (*TRIUMF*)
260. The reaction of muonium with hydrogen peroxide in water [completed], J.A. Bartlett, J.-C. Brodovitch, S.-K. Leung, K.E. Newman, P.W. Percival (*Simon Fraser Univ.*)
261. Muon spin rotation of paramagnetic solutions [completed], J.A. Bartlett, J.-C. Brodovitch, S.-K. Leung, K.E. Newman, P.W. Percival (*Simon Fraser Univ.*)

262. Muonium-radical formation mechanism [completed], D.C. Walker (*Univ. of British Columbia*), Y. Miyake (*TRIUMF*), R. Ganti, Y.C. Jean (*Univ. of Missouri-Kansas City*), J.M. Stadlbauer* (*Hood College*), Y. Katsumura (*Univ. of Tokyo*), D. Livesey (*Univ. of New Brunswick*), R. Catterall (*Univ. of Salford*), B.W. Ng (*Winona State Univ.*)
263. The pion-nucleus interaction [completed], T.E. Drake, R. Schubank, R.J. Sobie (*Univ. of Toronto*), R.R. Johnson (*TRIUMF-UBC*), D. Gill (*TRIUMF*)
264. The proton-nucleus interaction [completed], R.E. Azuma, L. Buchmann, T.E. Drake, J.D. King, L. Lee, S.S.M. Wong, X. Zhu (*Univ. of Toronto*), C.A. Miller, S. Yen (*TRIUMF*)
265. The (p, n) reaction as a probe of isovector effective interactions at TRIUMF energies [completed], W.P. Alford, R.L. Helmer (*Univ. of Western Ontario*), R.E. Azuma, D. Frekers (*Univ. of Toronto*), J. D'Auria (*Simon Fraser Univ.*), O. Häusser* (*TRIUMF-SFU*), K.P. Jackson, S. Yen (*TRIUMF*)
266. Initial studies of the (n, p) reaction on light nuclei [completed], K.P. Jackson, S. Yen (*TRIUMF*), W.P. Alford, R.L. Helmer (*Univ. of Western Ontario*), J.M. D'Auria (*Simon Fraser Univ.*), O. Häusser* (*TRIUMF-SFU*)
267. Isovector T_{\geq} transitions in (fp) shell nuclei studies by the (n, p) reaction [deferred], O. Häusser* (*TRIUMF-SFU*), J. D'Auria (*Simon Fraser Univ.*), K.P. Jackson, C.A. Miller, S. Yen (*TRIUMF*), A. Altman (*Tel-Aviv Univ.*), W.P. Alford, R.L. Helmer (*Univ. of Western Ontario*), I.S. Towner (*Chalk River Nuclear Labs*)
268. Enhancement of 1^+ states in ^{208}Pb (n, p) : A search for the Δ [completed], K.P. Jackson, C.A. Miller, S. Yen (*TRIUMF*), O. Häusser* (*TRIUMF-SFU*), W.P. Alford, R.L. Helmer (*Univ. of Western Ontario*)
269. Inelastic pion scattering from ^{30}Si at $T_{\pi} = 50$ MeV [deferred], C.A. Wiedner (*MPI, Heidelberg*), K. Erdman, B. Forster*, R. Tacik (*Univ. of British Columbia*), A. Altman (*Tel-Aviv Univ.*), D.A. Gill, U. Wienands (*TRIUMF*), T. Drake, R. Sobie (*Univ. of Toronto*)
270. Test of charge symmetry by a comparison of $\pi^-d \rightarrow nn$ with $\pi^+d \rightarrow pp$ [completed data taking], A.D. Eichon, J. Engelage, G.J. Kim, A.A. Mokhtari, B.M.K. Nefkens, J.A. Wightman, H.J. Ziocck (*UCLA*), R.R. Johnson (*TRIUMF-UBC*), G. Jones (*Univ. of British Columbia*), A. Altman (*Tel-Aviv Univ.*), W.J. Briscoe, C.J. Seftor, M.F. Taragin (*George Washington Univ.*), T.E. Drake (*Univ. of Toronto*), D.R. Gill (*TRIUMF*), J.R. Richardson* (*TRIUMF-UCLA*), P. Truöl (*Univ. Zürich*), K. Aniol (*California State Univ. LA*)
271. Study of isovector giant resonances via the (n, p) reaction at 200 and 500 MeV [deferred], P.R. Andrews, S.M. Banks, P.B. Foot, B. Lay, P. Lewis, V.C. Officer, G.G. Shute, B.M. Spicer (*Univ. of Melbourne*)
272. Transverse spin flip probabilities in $^{24}\text{Mg}(\vec{p}, \vec{p}')$ and $^{48}\text{Ca}(\vec{p}, \vec{p}')$ [completed], O. Häusser* (*TRIUMF-SFU*), R. Abegg*, K.P. Jackson (*TRIUMF*), W.P. Alford (*Univ. of Western Ontario*), C.A. Wiedner (*MPI, Heidelberg*), T.E. Drake (*Univ. of Toronto*), J. Lisantti, D. McDaniels, J. Tinsley (*Univ. of Oregon*)
273. Triplet μ^-p absorption in H_2 gas [letter of intent], J. Bailey (*Yale Univ.*), G. Azuelos, C. Oram (*TRIUMF*), J. Brewer, K. Erdman (*Univ. of British Columbia*), K. Crowe (*Univ. of California, Berkeley*)
274. Singlet final state interaction in the $pp \rightarrow pn\pi^+$ reaction [completed], E.G. Auld, P. Couvert, G. Jones, W. Ziegler (*Univ. of British Columbia*), W. Falk (*Univ. of Manitoba*), P. Walden (*TRIUMF*), G. Lolos (*Univ. of Regina*)
275. Muons in, and muonium from, vanadium [completed], J. Bailey (*Yale Univ.*), J. Brewer, J.B. Warren* (*Univ. of British Columbia*), G. Marshall (*Univ. of Victoria*), D. Garner, R. Kiefl, C. Oram (*TRIUMF*), A. Olin (*TRIUMF-Univ. of Victoria*), D. Harshman (*AT&T Laboratories*)
276. Diluted magnetic semiconductors [completed], E.J. Ansaldo (*Univ. of Saskatchewan*), J. Bailey (*Yale Univ.*), J.H. Brewer, S. Kreitzman, D. Noakes, M. Senba (*Univ. of British Columbia*), R. Keitel (*TRIUMF*), K.M. Crowe (*Univ. of California, Berkeley*), J. Furdyna (*Purdue Univ.*), Y.J. Uemura (*Brookhaven National Lab*), T.L. Estle (*Rice Univ.*), D. Harshman (*AT&T Laboratories*)
277. The branching ratio of the rare decay $\pi^0 \rightarrow e^+e^-$ [completed], M.D. Hasinoff, C. Waltham (*Univ. of British Columbia*), D.A. Bryman (*TRIUMF-Univ. of Victoria*), E. Clifford (*Univ. of Victoria*), G. Azuelos, T. Numao, J.-M. Poutissou (*TRIUMF*), P. Depommier, H. Jeremie, R. Poutissou (*Univ. de Montréal*), C.K. Hargrove, H. Mes (*National Research Council*), B. Robertson (*Queen's Univ.*), T.A. Mulera, V. Perez-Mendez (*Lawrence Berkeley Lab*), M. Blecher (*Virginia Polytechnic Inst. & State Univ.*), A.W. Stetz (*Oregon State Univ.*)
278. Inelastic scattering of 30 and 50 MeV π^+ projectiles from the 0_2^+ state in ^{12}C [completed], L. Buchmann, T.E. Drake, L. Lee, R.J. Sobie (*Univ. of Toronto*), D.R. Gill, B. Jennings (*TRIUMF*), R.R. Johnson (*TRIUMF-UBC*), N. de Takacsy (*McGill Univ.*)
279. Non-analog pion single charge exchange total cross section on ^7Li at low energies [completed], B.J. Dropesky, G.C. Giesler, R.E.L. Green, M.J. Leitch, Y. Ohkubo, C.J. Orth (*LAMPF*), A. Olin (*TRIUMF-Univ. of Victoria*), R.G. Korteling (*Simon Fraser Univ.*)

280. Study of giant isovector spin resonances via the (p, n) and (n, p) reactions at 350 MeV [deferred], A. Altman, J. Alster, N. Auerbach, M.A. Moinester, S. Wood, A.I. Yavin (*Tel-Aviv Univ.*), O. Häusser* (*TRIUMF-SFU*), A. Moalem (*Ben-Gurion Univ.*), W.P. Alford (*Univ. of Western Ontario*), A. Klein (*Univ. of Georgia*)
281. Investigations of pion absorption reactions ${}^6\text{Li}, {}^{12}\text{C}(\pi^\pm, X_1)X_2$ [completed], G. Huber, G.J. Lolos, S.I.H. Naqvi, V. Pafilis, Z. Papandreou (*Univ. of Regina*), D. Gill, D. Ottewell, P.L. Walden (*TRIUMF*), E.G. Auld, G. Jones (*Univ. of British Columbia*), R.R. Johnson (*TRIUMF-UBC*), X. Aslanoglou (*Florida State Univ.*)
282. Exchange effects in $0^+ \rightarrow 0^-$ inelastic scattering [completed], R.E. Azuma, L. Buchmann, T.E. Drake, D. Frekers, J.D. King, S.S.M. Wong, X. Zhu (*Univ. of Toronto*)
283. (Combined with 295)
284. A study of the decays $\pi^+ \rightarrow e^+e^-e^+\nu$ and $\pi^+ \rightarrow e^+\nu\gamma$ [deferred], M. Blecher (*Virginia Polytechnic Inst. & State Univ.*), D.A. Bryman (*TRIUMF-Univ. of Victoria*), E. Clifford, P. Schlatter (*Univ. of Victoria*), M. Dixit, C.K. Hargrove, H. Mes (*National Research Council*), G. Azuelos, T. Numao, J.-M. Poutissou (*TRIUMF*), P. Depommier (*Univ. de Montréal*), A. Burnham,* M.D. Hasinoff, C. Waltham (*Univ. of British Columbia*), T. Mulura, V. Perez-Mendez (*Lawrence Berkeley Lab*)
285. Elastic scattering of pions by ${}^3,4\text{He}$ for pion energies between 20 and 50 MeV [completed], K.M. Crowe, C.A. Meyer (*Univ. of California, Berkeley*), D.R. Gill, D. Healey, U. Wienands (*TRIUMF*), R.R. Johnson (*TRIUMF-UBC*), A. Altman (*Tel-Aviv Univ.*), N. Grión (*INFN Trieste*)
286. Quantum diffusion of muons and muonium [completed], K.M. Crowe (*Univ. of California, Berkeley*), J.H. Brewer, S.R. Kreitzman, M. Senba, D.L. Williams (*Univ. of British Columbia*), R. Keitel (*TRIUMF*), E.J. Ansaldò (*Univ. of Saskatchewan*), J. Bailey (*Yale Univ.*), K. Nagamine (*Univ. of Tokyo*), D. Harshman (*AT&T Laboratories*), D.P. Spencer (*Univ. of Chicago Medical Center*)
288. Muonium reaction rates on surfaces [completed], R. Keitel (*TRIUMF*), J.H. Brewer, D.N. Noakes, M. Senba (*Columbia*), K. Nagamine (*Univ. of Tokyo*), E.J. Ansaldò (*Univ. of Saskatchewan*), D.R. Harshman (*AT&T Laboratories*)
289. Studies of positive muon states in alkali halides and other insulators by advanced μSR methods [completed], K. Ishida, Y. Kuno, T. Matsuzaki, Y. Morozumi, K. Nagamine, K. Nishiyama, T. Yamazaki (*Univ. of Tokyo*), J.H. Brewer (*Univ. of British Columbia*)
290. Positive muon probing soliton in polyacetylene [completed], K. Ishida, Y. Kuno, T. Matsuzaki, K. Nagamine, H. Shirakawa, T. Yamazaki (*Univ. of Tokyo*), J.H. Brewer (*Univ. of British Columbia*)
291. μSR studies on spin dynamics in mixed antiferromagnets with competing anisotropies [completed], I. Ito, E. Torikai (*Ochanomizu Univ.*), K. Ishida, Y. Kuno, T. Matsuzaki, K. Nagamine, T. Yamazaki (*Univ. of Tokyo*), J.H. Brewer (*Univ. of British Columbia*)
292. $\mu^\pm\text{SR}$ of graphite intercalation compounds [active], K. Ishida, T. Kondow, Y. Kuno, T. Matsuzaki, K. Nagamine, T. Yamazaki (*Univ. of Tokyo*), J.H. Brewer (*Univ. of British Columbia*)
294. Spin observables for elastic and inelastic proton scattering from ${}^{28}\text{Si}$ and ${}^{208}\text{Pb}$ at 300 MeV [completed], R.L. Auble, F.E. Bertrand, B.L. Burks, C.W. Glover, E.E. Gross, D.J. Horen, R.O. Sayer (*Oak Ridge National Lab*), O. Häusser* (*TRIUMF-SFU*), K. Hicks, U. Wienands (*TRIUMF*), A. Moalem (*Ben Gurion Univ.*), J. Lisantti, D.K. McDaniels, J. Tinsley (*Univ. of Oregon*), I. Bergqvist (*Univ. of Lund*), E. Rost, J.R. Shepard (*Univ. of Colorado*)
295. Large angle polarization tests – Test of density-dependent and relativistic theories [completed], V. Penumetcha, A. Scott (*Univ. of Georgia*), R. Abegg*, K.P. Jackson, C.A. Miller, S. Yen (*TRIUMF*), R. Azuma, L. Buchmann, T.E. Drake, D. Frekers, J.D. King, L. Lee, S.S.M. Wong (*Univ. of Toronto*), M.L. Whiten (*Armstrong College, Georgia*), R. Dymarz, U. Kuehner (*McMaster Univ.*), H.V. von Geramb (*Univ. Hamburg*)
296. Kinetics of gas phase muonium addition reactions [completed], D.M. Garner (*TRIUMF*), D.J. Arseneau, D.G. Fleming, I.D. Reid, M. Senba (*Univ. of British Columbia*)
297. Energetic neutron spectra from μ^- -capture in deuteron [completed], T.J. Hallman, Y.K. Lee, L. Madansky, E.K. McIntyre, Jr. (*Johns Hopkins Univ.*), G.R. Mason (*Univ. of Victoria*)
298. Resonant structure in $\text{Cu}(p, \pi^+)X$: A possible dibaryon signal [completed], R. Abegg*, K. Hicks, K.P. Jackson, C.A. Miller, D. Ottewell, P. Walden, S. Yen (*TRIUMF*), G. Gaillard (*Univ. of Alberta*), E.G. Auld, P. Trelle (*Univ. of British Columbia*), R. Schubank (*Univ. of Saskatchewan*), R. Henderson (*TRIUMF-Univ. of Melbourne*)
299. A measurement of the inclusive pion production from ${}^{16}\text{O}$ and the associated particles in coincidence with the pions [inactive], E.G. Auld (*Univ. of British Columbia*), P. Walden, S. Yen (*TRIUMF*), G. Lolos (*Univ. of Regina*), W. Falk (*Univ. of Manitoba*)

300. Spin transfer K_{ss} in the reaction $pp \rightarrow d\pi$ [completed data-taking], R. Abegg*, L.G. Greeniaus, D.A. Hutcheon, G.R. Smith (*TRIUMF*), L. Antonuk, J. Collot, G. Gaillard, G.A. Moss, W.C. Olsen, G. Roy, R. Sawafta, D.M. Sheppard* (*Univ. of Alberta*), B. Blankleider, J.M. Cameron (*IUCF*)
301. The reaction $pp\pi^0$ near threshold [completed], F. Entezami, D.F. Measday, S. Stanislaus (*Univ. of British Columbia*), D. Horváth (*Central Research Inst. for Physics, Budapest*)
302. Proton scattering to natural parity states in ^{90}Zr [completed data-taking], R.E. Azuma, T.E. Drake, H. Fidahic, D. Frekers, J.D. King, L. Lee, S.S.M. Wong (*Univ. of Toronto*), R. Abegg*, C.A. Miller, S. Yen (*TRIUMF*), R. Schubank (*Univ. of Saskatchewan*)
304. Muonium-antimuonium conversion [completed], A. Olin (*TRIUMF-Univ. of Victoria*), G.A. Beer, A.C. Janssen, G.R. Mason (*Univ. of Victoria*), Z. Gelbart, G.M. Marshall (*TRIUMF*), J.B. Warren* (*Univ. of British Columbia*), B. Heinrich, K. Myrtle (*Simon Fraser Univ.*), T. Bowen, P.G. Halverson, K.R. Kendall (*Univ. of Arizona*), C.A. Fry (*Univ. of Rochester*), T.M. Huber, A.R. Kunselman (*Univ. of Wyoming*)
306. Pion transfer in gaseous mixtures [completed], K.A. Aniol, M.B. Epstein, D.J. Margaziotis (*California State Univ. LA*), M. Salomon (*TRIUMF*), F. Entezami, D.F. Measday, A.J. Noble, S. Stanislaus, C.J. Virtue (*Univ. of British Columbia*), D. Horváth (*Central Research Inst. for Physics, Budapest*)
307. The effects of large oscillating fields in low frequency double electron muon resonance [completed], S.A. Dodds, T.L. Estle, S.L. Rudaz, Q. Zhu (*Rice Univ.*), J.H. Brewer, S.R. Kreitzman, D. Noakes (*Univ. of British Columbia*), R. Keitel (*TRIUMF*), E.J. Ansaldo (*Univ. of Saskatchewan*), R.H. Heffner (*LAMPF*), D. Harshman (*AT&T Laboratories*), D.P. Spencer (*Univ. of Chicago Medical Center*)
309. Transfer reaction studies with radioactive targets [deferred], E. Hagberg, J.C. Hardy, H. Schmeing (*Atomic Energy of Canada Ltd.*), G. Audi (*Lab René Bernas, Orsay*)
310. Production of a $^{211}\text{Rn}/^{211}\text{At}$ generator for radiochemical experiments [deferred], M. Adam, J. Grierson, T.J. Ruth (*TRIUMF*), K. Krohn (*Univ. of Washington*)
311. Nuclear reactions of astrophysical interest with accelerated radioactive beams [deferred], R. Azuma, L. Buchmann, J. King (*Univ. of Toronto*), J. D'Auria (*Simon Fraser Univ.*), C. Rolfs (*Univ. Münster*), M. Wiescher (*Univ. Mainz*), M. Arnould (*Univ. Libre de Bruxelles*), T. Ward (*IUCF*), C. Barnes (*California Inst. of Technology*), R. Boyd (*Ohio State Univ.*)
312. Low energy ion scattering using ISOL [deferred], S.R. Morrison, W. Sears (*Simon Fraser Univ.*)
313. Delayed neutron studies at TRIUMF-ISOL [deferred], P.L. Reeder, R.A. Warner (*Pacific Northwest Lab*)
314. Production of radioactive targets for nuclear structure studies [deferred], C. Bourgeois, P. Kilcher, G. Rotbard, B. Roussière, J. Sauvage-Letessier, M. Vergnes (*IPN, Orsay*), H. Dautet (*McGill Univ.*)
315. Development of a laser-based ion source [inactive], D. Audet, F. Buchinger, R. Corriveau, J.E. Crawford, H. Dautet, J.K.P. Lee, S.K. Mark, R.B. Moore, L. Nikkinen, D. Oxorn, G. Savard (*McGill Univ.*), J. D'Auria (*Simon Fraser Univ.*)
316. Collinear laser spectroscopy of radioactive beams [deferred], F. Buchinger and FRL Research Team (*McGill Univ.*)
317. Spectroscopic studies of nuclear properties [deferred], L.R. Kilius, A.E. Litherland (*Univ. of Toronto*), FRL Research Team (*McGill Univ.*), M. Pearson (*Univ. de Montréal*)
318. Installation of an on-line isotope separator at TRIUMF [completed], F. Buchinger, J.E. Crawford, H. Dautet, J.K.P. Lee, S.K. Mark, R.B. Moore, L. Nikkinen, K. Oxorn, V. Raut (*McGill Univ.*), J. D'Auria (*Simon Fraser Univ.*), E. Hagberg, J. Hardy, H. Schmeing (*Chalk River Nuclear Labs*)
319. Analysing powers for the inelastic continuum in ^{60}Ni and ^{208}Pb [inactive], K. Lin, J. Lisantti, D.K. McDaniels (*Univ. of Oregon*), I. Bergqvist, A. Brockstedt, B. Jakobsson (*Univ. of Lund*), O. Häusser* (*TRIUMF-SFU*), F. Bertrand, B. Burks, E. Gross, C. Glover, D. Horen, R. Sayre (*Oak Ridge National Lab*), L. Swenson (*Oregon State Univ.*)
321. Muonium spin rotations in condensed phases methane [deferred], R.L. Ganti, Y.C. Jean (*Univ. of Missouri-Kansas City*), Y. Miyake, K. Venkateswaran, D.C. Walker (*Univ. of British Columbia*), J.M. Stadlbauer* (*Hood College*)
322. Measurement of $\pi^\pm p$ differential cross sections at $T_\pi = 90$ MeV [completed], J. Brack, J.J. Kraushaar, R.J. Peterson, R.A. Ristinen, J.L. Ullmann (*Univ. of Colorado*), D.R. Gill, K. Hicks, G. Smith (*TRIUMF*), R.R. Johnson (*TRIUMF-UBC*)
323. Giant resonance study with 75 MeV π^\pm [completed data taking], D.R. Gill, G.R. Smith, U. Wienands (*TRIUMF*), K.L. Erdman, N. Hessey, D. Mills, M. Rozon (*Univ. of British Columbia*), R.R. Johnson (*TRIUMF-UBC*), A. Altman (*Tel-Aviv Univ.*), T.E. Drake (*Univ. of Toronto*)

324. Polarization-analysing power differences for inelastic proton scattering from ^{12}C at 400 MeV [completed data-taking], K.H. Hicks, K.P. Jackson, C.A. Miller, G. Smith, S. Yen (*TRIUMF*), O. Häusser* (*TRIUMF-SFU*), A. Celler (*Simon Fraser Univ.*), J.R. Shepard (*Univ. of Colorado*), R. Sawafta (*Univ. of Alberta*), A. Moalem (*Ben Gurion Univ.*), T.E. Drake, D. Frekers (*Univ. of Toronto*), R. Schubank (*Univ. of Saskatchewan*), R. Henderson (*TRIUMF-Univ. of Melbourne*), W.P. Alford (*Univ. of Western Ontario*)
325. Ultra-low energy muon production (μSOL) [completed], W.S. Crane, D.R. Harshman, A.P. Mills, Jr. (*AT&T Laboratories*), J.B. Warren* (*Univ. of British Columbia*), J.L. Beveridge, K.R. Kendall, R.F. Kiefl, C.J. Oram (*TRIUMF*), A.S. Rupaal, J.H. Turner* (*Western Washington Univ.*)
326. Determination of muon-neutrino mass [inactive], C.Y. Kim (*Univ. of Calgary*), D. Garner, R. Keitel (*TRIUMF*), Y.M. Shin (*Univ. of Saskatchewan*)
327. Study of the $(\pi^+, \pi^+\pi^-)$ reaction on ^{16}O , ^{28}Si and ^{40}Ca at $T_\pi = 240$ and 280 MeV [inactive], N. Grion (*INFN Trieste*), R. Rui (*Univ. di Trieste*), N. Hessey, M. Rozon, P. Trelle (*Univ. of British Columbia*), R.R. Johnson (*TRIUMF-UBC*), D. Gill, G. Smith, U. Wienands (*TRIUMF*), A. Altman (*Tel-Aviv Univ.*)
328. Multi-nucleon modes of pion absorption in flight on ^3He and ^4He [inactive], J. McAlister, R. Olszewski, M. Rozon, M. Sevier, P. Trelle (*Univ. of British Columbia*), R.R. Johnson (*TRIUMF-UBC*), D.R. Gill, G. Smith (*TRIUMF*), J. Alster, D. Ashery, M. Moinester (*Tel-Aviv Univ.*), N. Grion (*INFN Trieste*), R. Rui (*Univ. di Trieste*), G.J. Lolos, Z. Papandreou (*Univ. of Regina*), K. Aniol (*California State Univ. LA*), R. Tacik (*Univ. Karlsruhe*)
329. The $^4\text{He}(\pi, \pi')^4\text{He}$ reaction and the EELL effect [completed data-taking], K. Itoh, Y.M. Shin, N. Stevenson, D. Tokaryk (*Univ. of Saskatchewan*), D. Gill, B. Jennings, D. Ottewell, G. Wait (*TRIUMF*), R.R. Johnson (*TRIUMF-UBC*), A. Altman (*Tel-Aviv Univ.*), T. Drake, D. Frekers (*Univ. of Toronto*), R. Schubank (*Univ. of Saskatchewan*), N. de Takacsy (*McGill Univ.*)
330. Spin observables for inelastic proton scattering from ^{16}O at 300 MeV [completed], R.L. Auble, F.E. Bertrand, B.L. Burke, C.W. Glover, E.E. Gross, D.J. Horen, R.O. Sayer, (*Oak Ridge National Lab*), O. Häusser* (*TRIUMF-SFU*), A. Celler (*Simon Fraser Univ.*), K. Hicks, S. Yen (*TRIUMF*), A. Moalem (*Ben-Gurion Univ.*), R. Sawafta (*Univ. of Alberta*), D. Frekers (*Univ. of Toronto*), R. Henderson (*TRIUMF-Univ. of Melbourne*)
331. Spin transfer in the $\pi\vec{d} \rightarrow \vec{p}p$ reaction [completed], A. Feltham, G. Jones, R. Olszewski, M. Pavan, M. Sevier, V. Sossi, R.P. Trelle, D. Vetterli, P. Weber (*Univ. of British Columbia*), D.R. Gill, D. Healey, D. Ottewell, G. Smith, G. Wait, P. Walden (*TRIUMF*), G. Lolos, E. Mathie, Z. Papandreou, M. Yeomans (*Univ. of Regina*), R. Rui (*INFN Trieste*), M. Moinester (*Tel-Aviv Univ.*)
332. Measurement of D_t/R_t in n - p scattering [completed], J. Birchall, C.A. Davis, N.E. Davison, P.R. Poffenberger, D. Ramsey, W.T.H. van Oers (*Univ. of Manitoba*), G.A. Moss, G. Roy (*Univ. of Alberta*), L.G. Greeniaus (*TRIUMF*)
333. A search for the high frequency parts of the giant resonances [inactive], A. Moalem (*Ben-Gurion Univ.*), O. Häusser* (*TRIUMF-SFU*), A. Celler (*Simon Fraser Univ.*), K. Hicks, K.P. Jackson, C.A. Miller, S. Yen (*TRIUMF*), K. Lin, J. Lisantti, D. McDaniels (*Univ. of Oregon*), R. Sawafta (*Univ. of Alberta*), W.P. Alford (*Univ. of Western Ontario*), R. Henderson (*TRIUMF-Univ. of Melbourne*), M. Moinester (*Tel-Aviv Univ.*), I. Bergqvist (*Univ. of Lund*)
335. Energy dependence of isoscalar and isovector 1^+ excitations in $^{28}\text{Si}(\vec{p}, p')$ [completed], O. Häusser* (*TRIUMF-SFU*), A. Celler (*Simon Fraser Univ.*), K. Hicks, K.P. Jackson, C.A. Miller, S. Yen (*TRIUMF*), A. Moalem (*Ben-Gurion Univ.*), R. Sawafta (*Univ. of Alberta*), W.P. Alford, R. Helmer (*Univ. of Western Ontario*), R. Henderson (*TRIUMF-Univ. of Melbourne*), C. Günther (*Univ. Bonn*), R. Dymarz (*McMaster Univ.*)
337. Measurement of tensor observables in the $\pi^+\vec{d}$ elastic scattering reaction [completed], P. Delheij, D.R. Gill, D. Healey, D. Ottewell, G.R. Smith, G. Wait, P. Walden, U. Wienands, S. Yen (*TRIUMF*), A. Altman (*Tel-Aviv Univ.*), M. Haden, G. Jones, F. Tervisidis, R.P. Trelle (*Univ. of British Columbia*), R.R. Johnson (*TRIUMF-UBC*), G. Lolos, E.L. Mathie (*Univ. of Regina*)
338. Proton scattering from ^{208}Pb and ^{90}Zr at large momentum transfer [active], R. Azuma, L. Buchmann, T.E. Drake, R. Dymarz, D. Frekers, J.D. King, L. Lee, S. Wong (*Univ. of Toronto*), R. Abegg*, K.P. Jackson, C.A. Miller (*TRIUMF*), A. Scott (*Univ. of Georgia*), M. Whiten (*Armstrong College*), H. von Geramb (*Univ. Hamburg*)
339. Kinetic isotope effects in the $\text{Mu} + \text{H}_2$ and $\text{Mu} + \text{D}_2$ reactions [completed], D. Arseneau, D. Fleming, L.Y. Lee, I.D. Reid, M. Senba (*Univ. of British Columbia*), D. Garner, W.X. Kuang (*TRIUMF*)
340. μ^+ molecular ions and ion molecule reactions in gases [completed], D. Arseneau, D.G. Fleming, L.Y. Lee, I.D. Reid, M. Senba (*Univ. of British Columbia*), D. Garner, W.X. Kuang (*TRIUMF*)

341. Excited state production in proton-induced nuclear reactions [active], W. Benenson, C. Bloch, E. Kashy, D. Morrissey (*Michigan State Univ.*), D. Boal, J. D'Auria, R.G. Korteling (*Simon Fraser Univ.*), R. Helmer (*Univ. of Western Ontario*)
342. Dynamics of muon-produced soliton in polyacetylene [active], Y. Kuno, T. Matsuzaki, K. Nagamine, K. Nishiyama, T. Yamazaki (*Univ. of Tokyo*), K. Ishida (*Inst. of Phys. and Chem. Research*), H. Shirakawa (*Univ. of Tsukuba*), J. Brewer (*Univ. of British Columbia*), R. Kiefl (*TRIUMF*)
343. Negative pion inelastic scattering from ^2H , ^3He and ^4He at 100 MeV [deferred], I. Halpern, M. Khandaker, T. Murakami, D. Rosenzweig, D. Storm, D. Tieger (*Univ. of Washington*)
344. Excitation of "stretched" particle-hole states in charge-exchange reactions [active], B. Anderson, R. Madey, R. McCarthy, M. Plumley, J. Watson (*Kent State Univ.*), W. Alford (*Univ. of Western Ontario*), O. Häusser* (*TRIUMF-SFU*), K.P. Jackson, C.A. Miller (*TRIUMF*)
345. Muon spin relaxation studies of uranium-based heavy fermions [active], G. Aeppli, D. Abernathy (*AT&T Bell Laboratories*), Y.J. Uemura (*Brookhaven National Lab*), J. Brewer, D. Noakes (*Univ. of British Columbia*), E. Ansaldo (*Univ. of Saskatchewan*), E. Bucher (*Univ. Konstanz*), J. Kossler (*College of William and Mary*)
346. Muon spin rotation and relaxation in heavy fermion cerium compounds [active], Y.J. Uemura (*Brookhaven National Lab*), G. Aeppli, D. Abernathy, B. Batlogg, D. Harshman, J. Remeika (*AT&T Bell Laboratories*), J.H. Brewer, S. Kreitzman, D.R. Noakes, M. Senba (*Univ. of British Columbia*), B. Hitti, J. Kempton, W.J. Kossler (*College of William and Mary*), R. Keitel, R. Kiefl (*TRIUMF*), E.J. Ansaldo (*Univ. of Saskatchewan*), Y. Oonuki, T. Komatsubara (*Tsukuba Univ.*), E. Bucher (*Univ. Konstanz*)
347. Spin dynamics in amorphous rare earth intermetallics [inactive], L. Asch, G.M. Kalvius, F.J. Litterst (*Tech. Univ. Munich*), J.H. Brewer, D.R. Noakes (*Univ. of British Columbia*), B. Boucher (*CEN Saclay*), J. Chappert, A. Yaouanc (*CEN Grenoble*), O. Hartmann, R. Wäppling (*Univ. of Uppsala*), K. Nagamine, K. Nishiyama, T. Yamazaki (*Univ. of Tokyo*), E.J. Ansaldo (*Univ. of Saskatchewan*), R. Keitel (*TRIUMF*)
349. The diamagnetic μ^+ state in alkali halide and related metal halide crystals [completed], E.J. Ansaldo (*Univ. of Saskatchewan*), J. Brewer, B. Forster*, S. Kreitzman, G. Luke, D. Noakes, M. Senba, D.L. Williams (*Univ. of British Columbia*), R. Keitel, R. Kiefl (*TRIUMF*), K. Nagamine (*Univ. of Tokyo*), D. Harshman (*AT&T Laboratories*)
350. Study of the energy dependence of the $^{18}\text{O}(\pi^+, \pi^-)^{17}\text{Ne}$ reaction at the low-energy region [completed data-taking], A. Altman, E. Piasezky (*Tel-Aviv Univ.*), N. Hessey, F.M. Rozon, M. Seviator, R.P. Trelle (*Univ. of British Columbia*), R.R. Johnson (*TRIUMF-UBC*), D.R. Gill, G.R. Smith, U. Wienands (*TRIUMF*), N. Grion, R. Rui (*INFN Trieste*), T. Anderl (*KfA Jülich*), M. Leitch (*Los Alamos National Lab*)
351. Study of the (π^+, π^-) DIAS reaction on ^{34}S and ^{56}Fe at 50 MeV [active], A. Altman, E. Piasezky (*Tel-Aviv Univ.*), N. Hessey, M. Seviator, F.M. Rozon, R.P. Trelle (*Univ. of British Columbia*), R.R. Johnson (*TRIUMF-UBC*), D.R. Gill, G.R. Smith, U. Wienands (*TRIUMF*), N. Grion, R. Rui (*INFN Trieste*), T. Anderl (*KfA Jülich*), M. Leitch (*Los Alamos National Lab*)
352. Zero degree radiative capture of neutrons [active], G.W.R. Edwards, J. Collot, H. Fielding, G. Gaillard, J. Wesick (*Univ. of Alberta*), R. Abegg*, G. Greeniaus, D.A. Hutcheon, C.A. Miller (*TRIUMF*), J.M. Cameron (*IUCF*), N.E. Davison (*Univ. of Manitoba*)
354. Study of nuclear structure and density dependence of the effective interaction for the $N = 50$ isotones [active], R.E. Azuma, L. Buchmann, T. Drake, D. Frekers, A. Galino, L. Lee, S. Wong (*Univ. of Toronto*), R. Abegg*, K.P. Jackson, C.A. Miller, S. Yen (*TRIUMF*), R. Schubank (*Univ. of Saskatchewan*)
355. Exchange effects in $0^+ \rightarrow 0^-$ inelastic scattering [completed], R.E. Azuma, L. Buchmann, T.E. Drake, D. Frekers, A. Galindo, J.D. King, R. Lee, S.S.M. Wong, X. Zhu (*Univ. of Toronto*), R. Schubank (*Univ. of Saskatchewan*)
356. Y-scaling in inclusive proton scattering from ^9Be and ^{12}C at 300 MeV [active], A. Moalem (*Ben-Gurion Univ.*), O. Häusser* (*SFU-TRIUMF*), R. Abegg*, K. Hicks, K.P. Jackson, C.A. Miller, S. Yen (*TRIUMF*), R. Sawafra (*Univ. of Alberta*), R. Henderson (*TRIUMF-Univ. of Melbourne*), W.P. Alford (*Univ. of Western Ontario*), A. Altman (*Tel-Aviv Univ.*), S. Gurvitz (*Weizmann Inst. of Science*), D. Frekers (*Univ. of Toronto*)
357. Measurement of B^+ (GT) for ^{26}Mg [completed data-taking], W.P. Alford, A. Celler (*Univ. of Western Ontario*), R.L. Helmer, R. Henderson, M. Vetterli, S. Yen (*TRIUMF*), O. Häusser* (*TRIUMF-SFU*), A. Krumins (*Univ. of Toronto*), D. Miller (*IUCF*), B. Spicer (*Univ. of Melbourne*), A. Yavin (*Tel Aviv Univ.*)
358. Resolved nuclear hyperfine structure of muonium-substituted free radicals using level crossing spectroscopy [completed], R.F. Kiefl, R. Keitel (*TRIUMF*), J.H. Brewer, S. Kreitzman, G. Luke, D.R. Noakes, M. Senba (*Univ. of British Columbia*), E.J. Ansaldo (*Univ. of Saskatchewan*), A. Ito, Y. Morozumi, K. Nagamine, K. Nishiyama (*Univ. of Tokyo*), P.W. Percival (*Simon Fraser Univ.*), D. Harshman (*AT&T Laboratories*)

359. The spin response of (fp) shell nuclei [inactive], C. Glashausser (*Rutgers Univ.*), O. Häusser* (*TRIUMF-SFU*), S.K. Nanda (*Univ. of Minnesota*), K.W. Jones (*Los Alamos National Lab*), A. Moalem (*Ben-Gurion Univ.*), M. Vetterli (*Simon Fraser Univ.*), R. Abegg*, K. Hicks, K.P. Jackson, C.A. Miller (*TRIUMF*), W.P. Alford (*Univ. of Western Ontario*), R. Henderson (*TRIUMF-Univ. of Melbourne*), J. Lisantti (*Univ. of Oregon*)
360. Polarization transfer in πd elastic scattering [active], K. Itoh, R. Schubank, Y.M. Shin, N. Stevenson (*Univ. of Saskatchewan*), P. Delheij, D. Gill, D. Healey, D. Ottewell, G. Wait (*TRIUMF*), T. Drake, D. Frekers (*Univ. of Toronto*)
361. Muonium in water [completed], J. Bartlett, J.-C. Brodovitch, M. Harston, S.-K. Leung, P.W. Percival (*Simon Fraser Univ.*), K. Newman (*Univ. de Sherbrooke*)
362. High pressure muon spin resonance in liquids [completed], J. Bartlett, J.-C. Brodovitch, M. Harston, S.-K. Leung, P.W. Percival (*Simon Fraser Univ.*), K. Newman (*Univ. de Sherbrooke*)
364. Photon asymmetry measurements in radiative muon capture in heavy nuclei [completed data-taking], T. Gorrington, M. Hasinoff, A. Pouladdej, C. Virtue, C. Waltham (*Univ. of British Columbia*), G. Azuelos (*TRIUMF*), B. Robertson (*Queen's Univ.*), D. Horváth (*Central Research Inst. for Physics, Budapest*)
365. Search for tetra-neutrons using the ${}^4\text{He}(\pi^-, \pi^+){}^4n$ reaction [completed], D. Armstrong, T. Gorrington, M. Hasinoff, C. Waltham, J.B. Warren* (*Univ. of British Columbia*), G. Azuelos, J.A. Macdonald, T. Numao, J.-M. Poutissou (*TRIUMF*), D. Bryman (*TRIUMF-Univ. of Victoria*), R. Poutissou (*Univ. de Montréal*)
366. Measurement of $d\sigma/d\Omega$ and A_{NO} to exclusive states of ${}^{16}\text{O}(p, \pi^+){}^{17}\text{O}$ between 250 and 450 MeV [active], K. Hicks, M.J. Iqbal, P. Walden, S. Yen (*TRIUMF*), E.G. Auld (*Univ. of British Columbia*), R. Bent (*IUCF*), W.R. Falk (*Univ. of Manitoba*), G. Lolos (*Univ. of Regina*)
367. Resolved nuclear hyperfine structure of anomalous muonium in semiconductors [completed], R.F. Kiefl, R. Keitel (*TRIUMF*), E.J. Ansaldo (*Univ. of Saskatchewan*), J.H. Brewer, S. Kreitzman, G. Luke, D.R. Noakes (*Univ. of British Columbia*), T.L. Estle (*Rice Univ.*), D.P. Spencer (*Univ. of Chicago Medical Center*), T. Matsuzaki, K. Nishiyama (*Univ. of Tokyo*)
368. Charge symmetry breaking in $n(p, d)\pi^0$ at 477 MeV [inactive], R. Abegg*, L.G. Greeniaus, D.A. Hutcheon, C.A. Miller (*TRIUMF*), P.W. Green, C. Lapointe, G.A. Moss, G.M. Stinson (*Univ. of Alberta*), C.A. Davis, W.T.H. van Oers (*Univ. of Manitoba*), J.M. Cameron (*IUCF*)
369. Measurement of charge symmetry breaking in np elastic scattering at 350 MeV [completed data-taking], L.G. Greeniaus, N. Kolb, J. Li, A.K. Opper, J. Soukup, G.M. Stinson (*Univ. of Alberta*), R. Abegg*, P.P.J. Delheij, P.W. Green, D.C. Healey, R. Helmer, C.D.P. Levy, C.A. Miller, A. Zelenski (*TRIUMF*), A.R. Berdoz, J. Birchall, J.R. Campbell, L. Gann L. Lee, S.A. Page, W.D. Ramsay, W.T.H. van Oers, J. Zhao (*Univ. of Manitoba*), C.A. Davis (*TRIUMF-Univ. of Manitoba*) E. Korkmaz (*Univ. of Alberta*)
370. On the applicability of the macroscopic DWBA formalism for ${}^{59}\text{Ni}$ at 200 and 400 MeV [inactive], J. Lisantti, D.K. McDaniels (*Univ. of Oregon*), C. Glover, L.W. Swenson, Y. Xiao (*Oregon State Univ.*), F. Bertrand, B. Burks, D. Horen (*Oak Ridge National Lab*), I. Bergqvist (*Univ. of Lund*), K. Hicks (*TRIUMF*)
371. Muonium in micelles [completed], K. Venkateswaren, D.C. Walker (*Univ. of British Columbia*), J.M. Stadlbauer* (*Hood College*), B.W. Ng (*Winona State Univ.*), R. Ganti, Y.C. Jean (*Univ. of Missouri-Kansas City*), Wu Zhenna (*USTC, Hefei*)
372. Single pion production in np scattering [completed data-taking], A. Amer, A.R. Berdoz, J. Birchall, J.R. Campbell, N.E. Davison, W.R. Falk, S.A. Page, W.D. Ramsay, A.M. Sekulovitch, W.T.H. van Oers (*Univ. of Manitoba*), D.A. Hutcheon, C.A. Miller (*TRIUMF*), D.L. Adams, G.S. Mutchler (*Rice Univ.*), M.G. Bachman, P.J. Riley (*Univ. of Texas, Austin*), C.A. Davis (*Univ. of Manitoba-TRIUMF*), M.B. Epstein, D.J. Margaziotis (*California State Univ., Los Angeles*), P.W. Green, E. Korkmaz (*Univ. of Alberta*), B.W. Mayes, L. Pinsky, Y. Tzamouranis (*Univ. of Houston*)
373. Low energy pion scattering and pionic atom anomaly [inactive], D.R. Gill, G.R. Smith, U. Wienands (*TRIUMF*), A. Olin (*TRIUMF-Univ. of Victoria*), R.M. Rozon, M. Seviar, R.P. Trelle (*Univ. of British Columbia*), R.R. Johnson (*TRIUMF-UBC*), A. Altman (*Tel-Aviv Univ.*), T. Anderl (*KfA Jülich*), N. Grion (*INFN Trieste*), R. Rui (*Univ. di Trieste*)
374. Non-analog DCX, the ${}^{16}\text{O}(\pi^+, \pi^-){}^{16}\text{Ne}$ reaction [active], D.R. Gill, G.R. Smith, U. Wienands (*TRIUMF*), F.M. Rozon, M. Seviar, R.P. Trelle (*Univ. of British Columbia*), R.R. Johnson (*TRIUMF-UBC*), A. Altman (*Tel-Aviv Univ.*), T. Anderl (*KfA Jülich*), N. Grion (*INFN Trieste*), R. Rui (*Univ. di Trieste*)
375. Few-body physics via the pion deuteron breakup reaction [completed data-taking], G.M. Huber, G.J. Lolos, E.L. Mathie, S.I.H. Naqvi, V. Pafilis, D.M. Yeomans (*Univ. of Regina*), D. Healey, D. Ottewell, G.R. Smith, G. Wait (*TRIUMF*), G. Jones, M. Seviar, R.P. Trelle, P. Weber (*Univ. of British Columbia*), D. Humphrey (*Western Kentucky Univ.*), H. Garcilazo (*Univ. Hannover*)

376. S_{β^+} strength in $^{90}\text{Zr}(n,p)$ [active], D. Frekers, R. Helmer, K.P. Jackson, C.A. Miller, S. Yen (*TRIUMF*), B. Spicer (*Univ. of Melbourne*), R. Henderson (*TRIUMF-Univ. of Melbourne*), M. Moinester, A.I. Yavin (*Tel-Aviv Univ.*), W.P. Alford, A. Celler (*Univ. of Western Ontario*), O. Häusser* (*TRIUMF-Simon Fraser Univ.*), T.E. Drake, J.D. King (*Univ. of Toronto*), K. Hicks (*Ohio Univ.*)
377. Test of charge symmetry in πd elastic scattering [completed], D. Gill, D.F. Ottewell, G.R. Smith, P.L. Walden (*TRIUMF*), G. Jones, F. Tervisidis, P. Trelle (*Univ. of British Columbia*), R.R. Johnson (*TRIUMF-UBC*) A. Altman (*Tel-Aviv Univ.*), J.J. Kraushaar, R.J. Peterson, R.A. Ristinen, J.L. Ullmann (*Univ. of Colorado*)
378. Study of $^{48}\text{Ti}(n,p)$ as a test of lifetime calculations for the double beta decay of ^{48}Ca [active], W.P. Alford, A. Celler (*Univ. of Western Ontario*), D. Frekers, R. Helmer, K.P. Jackson, C.A. Miller, S. Yen (*TRIUMF*), O. Häusser* (*TRIUMF-SFU*), K. Hicks (*Ohio Univ.*), B.A. Brown (*Michigan State Univ.*), C.D. Zafiratos (*Univ. of Colorado*)
379. Investigation of the relation between Gamow-Teller strength and (p,n) cross sections at small momentum transfer [active], W.P. Alford, A. Celler (*Univ. of Western Ontario*), J. Watson (*Kent State Univ.*), C.D. Zafiratos (*Univ. of Colorado*), D. Frekers, R. Helmer, K.P. Jackson, C.A. Miller, S. Yen (*TRIUMF*), O. Häusser* (*TRIUMF-SFU*), K. Hicks (*Ohio Univ.*), B.A. Brown (*Michigan State Univ.*), R. Henderson (*TRIUMF-Univ. of Melbourne*)
381. Measurement of spin observables using the $(p,p'\gamma)$ reaction [completed], K. Hicks (*Ohio Univ.*), R. Abegg*, K.P. Jackson, C.A. Miller, S. Yen (*TRIUMF*), O. Häusser* (*TRIUMF-SFU*), M. Vetterli (*Simon Fraser Univ.*), A. Celler (*Univ. of Western Ontario*), R. Ristinen, J. Shepard, J. Ullmann (*Univ. of Colorado*), C. Glover, N. Hill (*Oak Ridge National Lab*), G. Igo (*UCLA*), R. Jeppesen, N. King, G. Morgan (*Los Alamos National Lab*), M. Kovash (*Univ. of Kentucky*), R. Henderson (*TRIUMF-Univ. of Melbourne*)
382. Measurements of the spin rotation parameter Q at 200 MeV as a test of Pauli blocking in elastic proton-nucleus scattering [active], O. Häusser* (*TRIUMF-SFU*), M. Ji, K. Lin, M. Vetterli (*Simon Fraser Univ.*), R. Abegg*, K.P. Jackson, C.A. Miller (*TRIUMF*), R.S. Henderson (*TRIUMF-Univ. of Melbourne*), R. Sawafra (*Univ. of Alberta*), W.P. Alford, A. Celler (*Univ. of Western Ontario*), K. Hicks (*Ohio Univ.*), C. Glover, J. Lisantti (*Oak Ridge National Lab*), D.K. McDaniels (*Univ. of Oregon*), L.W. Swenson (*Oregon State Univ.*)
383. A test of the Gamow-Teller sum rule from measurements of the $^{54}\text{Fe}(n,p)$ and (p,n) reactions at 290 MeV [active], O. Häusser* (*TRIUMF-SFU*), Ma Ji, K. Lin, M. Vetterli (*Simon Fraser Univ.*), D. Frekers, R. Helmer, K.P. Jackson, S. Yen (*TRIUMF*), W.P. Alford, A. Celler (*Univ. of Western Ontario*), R. Henderson (*TRIUMF-Univ. of Melbourne*), K. Hicks (*Ohio Univ.*), F. Osterfeld (*KfA Jülich*)
384. Abysmal astrophysics: the (n,p) reaction on ^{56}Fe and ^{58}Ni [completed], D. Frekers, R. Helmer, K.P. Jackson (*TRIUMF*), W.P. Alford, A. Celler (*Univ. of Western Ontario*), R.E. Azuma, L. Buchmann, C. Campbell (*Univ. of Toronto*), O. Häusser* (*TRIUMF-SFU*), M. Vetterli (*Simon Fraser Univ.*), B. Spicer (*Univ. of Melbourne*), R. Henderson (*TRIUMF-Univ. of Melbourne*)
385. Muon spin depolarization in Xe up to 5 atm [completed], D. Arseneau, D. Fleming, L.Y. Lee, I. Reid, M. Senba, R.E. Turner (*Univ. of British Columbia*), D. Garner (*TRIUMF*)
386. Electron-muon drag in conductors [completed], K.M. Crowe, A.M. Portis (*Univ. of California, Berkeley*), E.J. Ansaldo (*Univ. of Saskatchewan*), J.H. Brewer, S.R. Kreitzman (*Univ. of British Columbia*), R. Keitel (*TRIUMF*)
387. Measure of Birks factor in TMP [completed], A. Astbury (*TRIUMF-Univ. of Victoria*), M. Fincke-Keeler, R. Keeler, G.R. Mason, L. Robertson (*Univ. of Victoria*), D. Schinzel (*CERN*), A. Gonidec (*LAPP, Annecy*), C. Oram (*TRIUMF*)
388. Muon spin rotation of paramagnetic solution [completed], K. Newman (*Univ. de Sherbrooke*), J. Bartlett, J.-C. Brodovitch, M. Harston, S.-K. Leung, P. Percival (*Simon Fraser Univ.*)
389. Total cross-section measurements [completed], T.E. Drake, A. Galindo-Uribarri, S. Juniper (*Univ. of Toronto*), D. Frekers (*TRIUMF*), R. Schubank (*Univ. of Saskatchewan*)
390. The relativistic N - N interaction in nuclear matter and quasifree proton scattering [active], R.E. Azuma, C. Chan, T.E. Drake, J.D. King, L. Lee (*Univ. of Toronto*), R. Abegg*, D. Frekers, D.A. Hutcheon, J. Iqbal, C.A. Miller, S. Yen (*TRIUMF*), C.J. Horowitz (*Indiana Univ.*)
391. Muon spin rotation studies of supported metal catalysts [completed], R.F. Marzke (*Arizona State Univ.*), J.H. Brewer, D. Noakes (*Univ. of British Columbia*), E. Ansaldo (*Univ. of Saskatchewan*), D. Harshman (*AT&T Laboratories*)
392. Spin-flip isovector transition by pion single-charge exchange reaction [active], K. Itoh, R. Schubank, Y. Shin, N. Stevenson (*Univ. of Saskatchewan*), D. Frekers, D. Gill, D. Ottewell, G. Wait (*TRIUMF*), T.E. Drake (*Univ. of Toronto*)

394. Measurement of $\pi^\pm p$ differential cross sections at $T_\pi = 20$ to 60 MeV [inactive], J.T. Brack, J.J. Kraushaar, R.A. Loveman, R.J. Peterson, R.A. Ristinen (*Univ. of Colorado*), D.R. Gill, G.R. Smith (*TRIUMF*), R.R. Johnson (*TRIUMF-UBC*), R. Olszewski, M. Seviar, R.P. Trelle (*Univ. of British Columbia*), E.L. Mathie (*Univ. of Regina*)
395. Search for a dibaryon in the reaction $d(\pi^-, \pi^+)X$ [deferred], R. Olszewski, M. Seviar, R.P. Trelle (*Univ. of British Columbia*), R.R. Johnson (*TRIUMF-UBC*), D.R. Gill, G.R. Smith (*TRIUMF*), D. Ashery, E. Piassetzky (*Tel-Aviv Univ.*), N. Grion (*INFN Trieste*), R. Rui (*Univ. di Trieste*), J. Ernst (*Univ. Bonn*), T. Anderl (*KfA Jülich*)
396. Muonium chemical reactivities – Viscosity dependence [completed], R.L. Ganti, Y.C. Jean (*Univ. of Missouri-Kansas City*), K. Venkateswaran, D.C. Walker (*Univ. of British Columbia*)
397. Quasielastic scattering from ^{12}C and ^4He [inactive], C. Chan, T.E. Drake (*Univ. of Toronto*), R. Abegg*, D. Frekers, D.A. Hutcheon, M.J. Iqbal (*TRIUMF*), O. Häusser* (*TRIUMF-SFU*), C.J. Horowitz, E. Stephenson (*Indiana Univ.*), K. Hicks (*Ohio Univ.*)
398. MuLRC spectroscopy of free radicals [completed], J.A. Bartlett, J.-C. Brodovitch, S.K. Leung, P.W. Percival, S. Sun-Mack, D. Yu (*Simon Fraser Univ.*), D.M. Garner, R.F. Kiefl (*TRIUMF*), G.M. Luke, K. Venkateswaran (*Univ. of British Columbia*), S.F. Cox (*Rutherford Appleton Lab*)
399. Measurement of $\pi^\pm d$ elastic scattering cross sections and charge asymmetries at 30, 50 and 65 MeV [completed data-taking], M.D. Kohler, J.J. Kraushaar, R.A. Loveman, R.J. Peterson, R.A. Ristinen (*Univ. of Colorado*), D.R. Gill, G.R. Smith (*TRIUMF*), R.R. Johnson (*TRIUMF-UBC*), J.T. Brack, R. Olszewski, M. Seviar, R.P. Trelle (*Univ. of British Columbia*), E.L. Mathie (*Univ. of Regina*)
400. The Lamb shift and hyperfine structure splitting in muonic atoms [completed data-taking], G.W.F. Drake, E.E. Habib, A. Wijngaarden (*Univ. of Windsor*), C.D.P. Levy, P. Schmor (*TRIUMF*), J.A. Cameron (*McMaster Univ.*), R. Schubank (*Univ. of Saskatchewan*)
401. Measure of the neutron efficiency of organic scintillators in the energy range 50–350 MeV [completed data-taking], N. Grion (*INFN Trieste*), N. Colonna, G. d’Erasmus, M. Fiore (*Univ. di Bari*), L. Fiore, G. Guarino, A. Pantaleo, V. Paticchio (*INFN-Bari*), A. Bracco (*Univ. di Milano*), R. Rui (*Univ. di Trieste*)
402. Hyperfine structure of muon and muonium defect centres in magnetically ordered fluorides [inactive], R.F. Kiefl (*TRIUMF*), Y.J. Uemura (*Columbia Univ.*), J.H. Brewer, S. Kreitzman, G.M. Luke, D.R. Noakes (*Univ. of British Columbia*), E.J. Ansaldo (*Univ. of Saskatchewan*), A. Portis (*Univ. of California, Berkeley*)
403. Investigation of pion absorption reactions ^6Li , $^{12}\text{C}(\pi^+, X_1 X_2)A$ [completed data-taking], G.J. Lolos, E.L. Mathie, S.I.H. Naqvi, V. Pafilis, Z. Papandreou (*Univ. of Regina*), G. Jones (*Univ. of British Columbia*), D. Ottewell, P.L. Walden (*TRIUMF*), X. Aslanoglou (*Ohio Univ.*), G. Huber (*Indiana Univ.*)
404. Elastic pion scattering at 50 and 65 MeV [inactive], E. Friedman (*Hebrew Univ., Jerusalem*), D. Gill (*TRIUMF*), R.R. Johnson (*TRIUMF-UBC*), M. Hanna, O. Meirav, C. Ponting (*Univ. of British Columbia*)
405. Nuclear wobble [inactive], R.E. Azuma, T.E. Drake, J. King (*Univ. of Toronto*), R.S. Schubank (*Univ. of Saskatchewan*), R. Abegg*, D. Frekers, K.P. Jackson, C.A. Miller, S. Yen (*TRIUMF*), A. Celler (*Univ. of Western Ontario*), D. Bohle, A. Richter (*Univ. Darmstadt*), G. Gaul (*Univ. Muenster*)
407. An initial study of the $^{16}\text{O}(p, n\pi^+)$ reaction at 350 MeV [inactive], K. Hicks (*Ohio Univ.*), D. Frekers, B. Jennings, C.A. Miller, G.R. Smith, P. Walden, S. Yen (*TRIUMF*), O. Häusser* (*TRIUMF-SFU*), M. Vetterli (*Simon Fraser Univ.*), E.D. Cooper (*McGill Univ.*), J. Shepard, C. Zafaratos (*Univ. of Colorado*), W.P. Alford (*Univ. of Western Ontario*), W.R. Falk (*Univ. of Manitoba*), R. Jeppesen, N. King (*Los Alamos National Lab*)
409. Quasielastic scattering of 1s state nucleons in light nuclei [inactive], R. Abegg*, L.G. Greeniaus, D.A. Hutcheon, C.A. Miller (*TRIUMF*), P. Kitching (*TRIUMF-Univ. of Alberta*), M. Ahmad, W.J. McDonald, W.C. Olsen (*Univ. of Alberta*), J.W. Watson (*Kent State Univ.*), K. Hicks (*Ohio Univ.*)
411. The spin-isospin response of ^{48}Ca and ^9Be from the (n, p) reaction at 200 MeV [inactive], O. Häusser* (*TRIUMF-SFU*), Ma Ji, M.C. Vetterli (*Simon Fraser Univ.*), R. Abegg*, D. Frekers, R. Helmer, K.P. Jackson, C.A. Miller, S. Yen (*TRIUMF*), R.G. Jeppesen (*Los Alamos National Lab*), K. Hicks (*Ohio Univ.*), B. Spicer (*Univ. of Melbourne*), R. Henderson (*TRIUMF-Univ. of Melbourne*), W.P. Alford, A. Celler (*Univ. of Western Ontario*), F. Osterfeld (*KfA Jülich*)
412. Role of the Δ -isobar in the (p, π^+) and (p, π^-) reactions [completed data-taking], R.D. Bent (*Indiana Univ.*), M.J. Iqbal, P.L. Walden, S. Yen (*TRIUMF*), E.G. Auld, F. Duncan (*Univ. of British Columbia*), G.J. Lolos, E.L. Mathie, S.I.H. Naqvi (*Univ. of Regina*), W.R. Falk (*Univ. of Manitoba*), K. Hicks (*Ohio Univ.*), G. Huber (*Indiana Univ.*)

413. Cross sections and analyzing powers for the ${}^3\text{He}(\bar{p}, \pi^+){}^4\text{He}$ reaction in the energy range from 250 to 515 MeV [completed], J.R. Campbell, W.R. Falk, K.M. Furutani, H. Guan (*Univ. of Manitoba*), P. Walden, S. Yen (*TRIUMF*), E.G. Auld, F.A. Duncan (*Univ. of British Columbia*), G.J. Lolos (*Univ. of Regina*), R.D. Bent (*IUCF*), G.M. Huber (*IUCF-Univ. of Regina*), E. Korkmaz (*Univ. of Alberta*), A. Trudel (*Simon Fraser Univ.*), A. Celler (*Univ. of Western Ontario*)
414. Measurement of the $H(\pi^-, \pi^+\pi^-)n$ cross section very near threshold [completed], R.R. Johnson (*TRIUMF-UBC*), M. Hanna, J. McAlister, R. Olszewski, C. Ponting, M. Rozon, M. Sevier, V. Sossi, P. Trelle (*Univ. of British Columbia*), D.R. Gill, D.F. Ottewell, G.R. Smith (*TRIUMF*), Z. Wu (*IHEP Acad. Sinica Beijing*), J. Ernst (*Univ. Bonn*), N. Grion (*INFN Trieste*), R. Rui (*Univ. di Trieste*)
415. The (p, Δ^{++}) reaction on ${}^6\text{Li}$ and ${}^{28}\text{Si}$ [deferred], D. Frekers, K.P. Jackson, C.A. Miller S. Yen, P. Walden (*TRIUMF*), E.G. Auld (*Univ. of British Columbia*), K. Hicks (*Ohio Univ.*)
416. Neutron knockout with SASP [inactive], R. Abegg*, C.A. Miller (*TRIUMF*), P. Kitching (*TRIUMF-Univ. of Alberta*), M. Ahmad, W.J. McDonald (*Univ. of Alberta*), J.W. Watson (*Kent State Univ.*)
417. A survey of the (p, π^+) reaction in the Δ resonance region, $200 \text{ MeV} < T_p < 500 \text{ MeV}$, using the SASP spectrometer [completed], M.J. Iqbal, P.L. Walden, S. Yen (*TRIUMF*), E.G. Auld, F. Duncan (*Univ. of British Columbia*), W.R. Falk (*Univ. of Manitoba*), G.J. Lolos, E.L. Mathie, S.I.H. Naqvi (*Univ. of Regina*), R.D. Bent, G. Huber (*Indiana Univ.*), K. Hicks (*Ohio Univ.*)
418. A measurement of the Δ -isobar contribution to pion production from proton-nuclear interactions [deferred], E.G. Auld, F. Duncan (*Univ. of British Columbia*), P. Walden, S. Yen (*TRIUMF*), W.R. Falk (*Univ. of Manitoba*), G.J. Lolos, E.L. Mathie (*Univ. of Regina*), R.D. Bent (*Indiana Univ.*)
419. Nucleon effective polarization in Ca, Zr and Pb [inactive], W.J. McDonald, W.C. Olsen, D.M. Sheppard* (*Univ. of Alberta*), P. Kitching (*TRIUMF-Univ. of Alberta*), R. Abegg*, L.G. Greeniaus, D.A. Hutcheon, C.A. Miller (*TRIUMF*)
420. Kinetic isotope effects in gas phase reactions of muonium with diatomic halogens [completed], D.J. Arseneau, D.G. Fleming, A. Gonzalez, I. Reid, M. Senba (*Univ. of British Columbia*), D.M. Garner (*TRIUMF*)
421. Research and development studies with TISOL [active], J.M. D'Auria, M. Domsbky (*Simon Fraser Univ.*), R. Azuma, L. Buchmann, J. King (*Univ. of Toronto*), J. Crawford, J.K.P. Lee, R.B. Moore (*McGill Univ.*), J.S. Vincent (*TRIUMF*), P. Reeder (*PNL, Batelle*)
422. Calibration of SALAD [completed], J.M. Cameron (*IUCF*), E.B. Cairns, H.W. Fielding, C. Lapointe, W.J. McDonald, G.C. Neilson, W.C. Olsen, D.M. Sheppard*, J. Soukup, Y. Ye, W. Ziegler (*Univ. of Alberta*), L.G. Greeniaus, D.M. Hutcheon (*TRIUMF*), R. Pywell, D. Skopik (*Saskatchewan Accelerator Lab*)
423. A survey of the ${}^{40}\text{Ca}(p, \pi^+){}^{41}\text{Ca}$ reaction in the Δ resonance region, $200 \text{ MeV} < T_p < 500 \text{ MeV}$, using the MRS spectrometer [deferred], M.J. Iqbal, P.L. Walden, S. Yen (*TRIUMF*), E.G. Auld, F. Duncan (*Univ. of British Columbia*), W.R. Falk (*Univ. of Manitoba*), G.J. Lolos, E.L. Mathie, S.I.H. Naqvi (*Univ. of Regina*), R.D. Bent, G. Huber (*Indiana Univ.*), K. Hicks (*Ohio Univ.*)
425. An initial study of the $(p, n\pi^+)$ reaction [completed], K. Hicks (*Ohio Univ.*), D. Frekers, P. Green, B. Jennings, P. Walden, S. Yen (*TRIUMF*), O. Häusser* (*TRIUMF-SFU*), A. Trudel, M. Vetterli (*Simon Fraser Univ.*), W.P. Alford (*Univ. of Western Ontario*), M. Moinester (*Tel-Aviv Univ.*), W.R. Falk (*Univ. of Manitoba*), C. Zafaratos (*Univ. of Colorado*), R. Jeppesen, N. King (*Los Alamos National Lab*), E. Cooper (*McGill Univ.*)
428. Nuclear wobble (part II) [inactive], R.E. Azuma, C. Chan, T.E. Drake, J. King (*Univ. of Toronto*), R. Abegg*, D. Frekers, K.P. Jackson, C.A. Miller, S. Yen (*TRIUMF*), A. Celler (*Univ. of Western Ontario*), D. Bohle, A. Richter (*Univ. Darmstadt*), G. Gaul (*Univ. Münster*)
430. Spin excitations in ${}^{208}\text{Pb}$ [completed data-taking], R. Abegg*, C.A. Miller, S. Yen (*TRIUMF*), R.W. Ferguson, C. Glashausser, A. Green (*Rutgers Univ.*), O. Häusser* (*TRIUMF-SFU*), M. Vetterli (*Simon Fraser Univ.*), R. Henderson (*TRIUMF-Univ. of Melbourne*), K. Hicks (*Ohio Univ.*), F.T. Baker (*Univ. of Georgia*), R. Jeppesen, K.W. Jones (*Los Alamos National Lab*), J. Lisantti (*Oak Ridge National Lab*)
431. Quasielastic spin response for ${}^{54}\text{Fe}(\bar{p}, \bar{p}')$ at 290 MeV [completed], O. Häusser* (*TRIUMF-SFU*), K. Lin, M.C. Vetterli (*Simon Fraser Univ.*), R. Abegg*, R. Helmer, K.P. Jackson, C.A. Miller, S. Yen (*TRIUMF*), R. Henderson (*TRIUMF-Univ. of Melbourne*), K. Hicks (*Ohio Univ.*), R.G. Jeppesen (*Los Alamos National Lab*), J. Lisantti (*Oak Ridge National Lab*), R. Ferguson, G. Glashausser (*Rutgers Univ.*), W.P. Alford, A. Celler (*Univ. of Western Ontario*), A. Yavin (*Tel-Aviv Univ.*), J. Watson (*Kent State Univ.*)
432. Polarization transfer in inelastic proton scattering from ${}^{16}\text{O}$ [completed], O. Häusser* (*TRIUMF-SFU*), B. Larson, J. Mildemberger, M. Vetterli (*Simon Fraser Univ.*), R. Abegg*, D. Frekers, R.L. Helmer, K.P. Jackson, C.A. Miller, S. Yen (*TRIUMF*), R. Jeppesen (*LANL*), R. Schubank (*Univ. of Saskatchewan*), K. Hicks (*Ohio Univ.*) R. Henderson (*TRIUMF-Univ. of Melbourne*), C. Olmer, E.G. Stephenson (*IUCF*), W.P. Alford, A. Celler (*Univ. of Western Ontario*)

433. Neutron-proton charge exchange amplitudes [completed], R. Abegg*, P.W. Green, L.G. Greeniaus, K.P. Jackson, C.A. Miller (*TRIUMF*), G.C. Neilson, Y. Ye (*Univ. of Alberta*), W.P. Alford (*Univ. of Western Ontario*), J.M. Cameron (*IUCF*), I. van Heerden (*Univ. of Western Cape, S.A.*), J.W. Watson (*Kent State Univ.*), G.A. Moss (*Science World*)
434. Spin isovector monopole search with the $^{120}\text{Sn}(n, p)$ reaction [completed], M.A. Moinester, A.I. Yavin (*Tel-Aviv Univ.*), S. Long, B. Spicer (*Univ. of Melbourne*), R. Henderson (*TRIUMF-Univ. of Melbourne*), D. Frekers, R. Helmer, K.P. Jackson, S. Yen (*TRIUMF*), O. Häusser* (*TRIUMF-SFU*), M. Vetterli (*Simon Fraser Univ.*), W.P. Alford, A. Celler (*Univ. of Western Ontario*), R. Pourang, J. Watson (*Kent State Univ.*), R. Jeppesen, N. King (*Los Alamos National Lab*)
435. Measurement of spin flip probabilities with the (\bar{p}, \bar{n}) reaction [inactive], R. Abegg*, D. Frekers, R. Helmer, K.P. Jackson, C.A. Miller, S. Yen (*TRIUMF*), O. Häusser* (*SFU-TRIUMF*), M. Vetterli (*Simon Fraser Univ.*), W.P. Alford, A. Celler (*Univ. of Western Ontario*), R. Jeppesen (*Los Alamos National Lab*), W.C. Olsen (*Univ. of Alberta*), R. Henderson (*Univ. of Melbourne-TRIUMF*), J. Watson (*Kent State Univ.*)
436. Isovector spin-dipole giant resonance in (*sd*) shell nuclei [completed data-taking], W.P. Alford, A. Celler (*Univ. of Western Ontario*), R. Abegg*, D. Frekers, R. Helmer, K.P. Jackson, C.A. Miller, S. Yen (*TRIUMF*), O. Häusser* (*TRIUMF-SFU*), M. Vetterli (*Simon Fraser Univ.*), R. Henderson (*TRIUMF-Univ. of Melbourne*), M. Moinester, A. Yavin (*Tel-Aviv Univ.*), K. Hicks (*Ohio Univ.*), R. Jeppesen (*Los Alamos National Lab*), J. Watson (*Kent State Univ.*)
437. Measurement of absolute cross section for $^{14}\text{C}(p, n)^{14}\text{N}$ (2.31+3.95 MeV) [completed data-taking], W.P. Alford, A. Celler (*Univ. of Western Ontario*), R. Helmer, R. Abegg*, D. Frekers, K.P. Jackson, C.A. Miller, S. Yen (*TRIUMF*), O. Häusser* (*TRIUMF-SFU*), M. Vetterli (*Simon Fraser Univ.*), R. Henderson (*TRIUMF-Univ. of Melbourne*), M. Moinester, A. Yavin (*Tel-Aviv Univ.*), K. Hicks (*Ohio Univ.*), J. Watson (*Kent State Univ.*), R. Jeppesen (*Los Alamos National Lab*)
438. $^{70,72,74}\text{Ge}(n, p)^{70,72,74}\text{Ga}$: Shell model blocking effects on Gamow-Teller strength in the *fp* shell [completed data-taking], A. Trudel, M. Vetterli (*Simon Fraser Univ.*), D. Frekers, K.P. Jackson, S. Yen (*TRIUMF*), O. Häusser* (*TRIUMF-SFU*), A. Celler (*Univ. of Western Ontario*), R. Jeppesen (*Los Alamos National Lab*), G. Fuller (*Lawrence Livermore National Lab*), K. Hicks (*Ohio Univ.*)
439. The (n, p) , (p, p') and (p, n) reactions on ^{14}N [completed data-taking], D. Frekers, R. Helmer, K.P. Jackson (*TRIUMF*), W.P. Alford, A. Celler (*Univ. of Western Ontario*), A.I. Yavin (*Tel-Aviv Univ.*), O. Häusser* (*SFU-TRIUMF*), A. Trudel, M. Vetterli (*Simon Fraser Univ.*), R.E. Azuma (*Univ. of Toronto*), R. Henderson (*Univ. of Melbourne-TRIUMF*)
440. Muon catalyzed fusion in HD and H_2+D_2 gaseous mixtures [completed data-taking], K.A. Aniol, M.B. Epstein, D.J. Margaziotis (*California State Univ. LA*), D.F. Measday, A.J. Noble, S. Stanislaus (*Univ. of British Columbia*), B. Robertson (*Queen's Univ.*), D. Horváth (*Central Research Inst. for Physics, Budapest*), S.E. Jones (*Brigham Young Univ.*), A. Anderson (*Idaho Research Software and Idaho State Univ.*)
441. Amplitude determination of the pion-nucleon elastic scattering reaction. Part I: Analysing power [completed], D.R. Gill, D. Healey, D. Ottewell, G.R. Smith, G.D. Wait (*TRIUMF*), J.T. Brack, J.J. Kraushaar, R.J. Peterson, R.A. Ristinen (*Univ. of Colorado*), R.R. Johnson (*TRIUMF-UBC*), G. Jones, R. Olszewski, M.E. Seviar, R.P. Trelle (*Univ. of British Columbia*), E.L. Mathie (*Univ. of Regina*)
442. A dependence of the $(\pi, 2\pi)$ process through the study of $^{208}\text{Pb}(\pi^+, \pi^- X)$ with $X = \pi^+$ and p reaction at $T_\pi = 240$ and 280 MeV [completed data-taking], N. Grion, R. Rui (*INFN-Trieste & Univ. di Trieste*), D.R. Gill, G. Sheffer, G.R. Smith (*TRIUMF*), R.R. Johnson (*TRIUMF-UBC*), M. Hanna, J. McAlister, R. Olszewski, C. Ponting, M. Rozon, M. Seviar, V. Sossi (*Univ. of British Columbia*), E. Oset, M.J. Vicente-Vacas (*Univ. de Valencia*)
443. Study of the $\pi^+ + d \rightarrow \pi^- + \pi^+ + p + p$ reaction at $T_\pi = 250, 280$ MeV [inactive], N. Grion, R. Rui (*INFN Trieste & Univ. di Trieste*), D.R. Gill, G. Sheffer, G. Smith (*TRIUMF*), R.R. Johnson (*TRIUMF-UBC*), M. Hanna, J. McAlister, R. Olszewski, C. Ponting, F.M. Rozon, M. Seviar, V. Sossi (*Univ. of British Columbia*), E. Oset, M.J. Vicente-Vacas (*Univ. de Valencia*)
444. Double charge exchange reaction studies on helium above the resonance [inactive], R.R. Johnson (*TRIUMF-UBC*), K.L. Erdman, M. Hanna, R. Olszewski, F.M. Rozon, M. Seviar, V. Sossi, P. Trelle (*Univ. of British Columbia*), D.R. Gill, G. Smith (*TRIUMF*), N. Grion (*INFN Trieste*), R. Rui (*Univ. di Trieste*), C.A. Wiedner (*MPI, Heidelberg*), Z. Wu (*UBC/IHEP*)
445. Polarization measurement in the $^3\text{He}(\pi^+, \bar{p}p)$ reaction [completed data-taking], H. Aclander, A. Altman, D. Ashery, M.A. Moinester, S. May-Tal Beck, S. Ram, D. Trumer (*Tel-Aviv Univ.*), G. Jones, M. Pavan, A. Feltham (*Univ. of British Columbia*), A. Rahav (*Simon Fraser Univ.*), J. Niskanen (*Univ. of Helsinki*)

446. Pion-proton bremsstrahlung [completed data-taking], F. Farzanpay, P. Fuchs, A.W. Stetz, L.W. Swenson (*Oregon State Univ.*), P. Kitching (*Univ. of Alberta-TRIUMF*), D. Mack, W.C. Olsen (*Univ. of Alberta*), D. Otte-well, G.R. Smith, Zhang Nai-sen (*TRIUMF*), N. Stevenson (*Univ. of Saskatchewan*), R. Henderson (*Univ. of Melbourne-TRIUMF*)
447. LCR of Mu-radicals in micelles [completed], M.V. Barnabas, K. Venkateswaran, D.C. Walker (*Univ. of British Columbia*), J.M. Stadlbauer* (*Hood College*), B.W. Ng (*Winona State Univ.*), Wu Zhennan (*USTC, Hefei*)
448. Muon spin relaxation experiments on site-diluted random antiferromagnet (MnZn)F₂ [completed], G.M. Luke, Y.J. Uemura (*Columbia Univ.*), R. Keitel, R.F. Kiefl (*TRIUMF*), J.H. Brewer, S.R. Kreitzman, D.R. Noakes (*Univ. of British Columbia*), E.J. Ansaldo (*Univ. of Saskatchewan*), K.M. Crowe, A.M. Portis (*Univ. of California, Berkeley*), V. Jaccarino (*Univ. of California, Santa Barbara*)
449. Nuclear hyperfine parameters of Mu and Mu* states via radio-frequency resonance [completed data-taking], J.H. Brewer, S. Kreitzman, G. Luke, D.L. Williams (*Univ. of British Columbia*), E. Ansaldo (*Univ. of Saskatchewan*), T. Estle (*Rice Univ.*), R. Kiefl (*TRIUMF*)
450. μ SR studies of sub- and supercritical fluids [completed], K.E. Newman (*Univ. de Sherbrooke*), D.J. Arseneau, D.G. Fleming, A.C. Gonzalez, J.R. Kempton, J. Pan, I.D. Reid, M. Senba (*Univ. of British Columbia*), J.C. Brodovitch, P.W. Percival (*Simon Fraser Univ.*)
452. Radiative muon capture on hydrogen [completed data-taking], G. Azuelos (*Montréal-TRIUMF*), R. Henderson, J. Macdonald, J.-M. Poutissou, D.H. Wright (*TRIUMF*), P. Gumplinger, M. Hasinoff, W. Schott (*Univ. of British Columbia*), P. Depommier, B. Doyle, G. Jonkmans, R. Poutissou (*Univ. de Montréal*), D.S. Armstrong, M. Blecher (*Virginia Polytechnic Inst. & SU*), B. Robertson (*Queen's Univ.*), W. Bertl (*PSI*), C-Q. Chen (*IHEP, Beijing*), T. von Egidy (*Tech. Univ. Munich*), S.C. McDonald, M. Munro, G.N. Taylor (*Univ. of Melbourne*), T. Gorringer (*Univ. of Kentucky*), A. Larabee (*Buena Vista College*)
453. Muonic hydrogen in vacuum [completed], J. Beveridge, J.A. Macdonald, G.M. Marshall, M. Senba (*TRIUMF*), G.A. Beer, P.E. Knowles, G.R. Mason, A. Olin, M. Szczodrak (*Univ. of Victoria*), J.H. Brewer, B.M. Forster*, R. Jacot-Guillarmod, W. Hardy (*Univ. of British Columbia*), J.M. Bailey (*Univ. of Liverpool*), T.M. Huber (*Gustavus Adolphus College*), A.R. Kunselman (*Univ. of Wyoming*)
454. Investigations of hidden processes in muon catalyzed (dt μ) fusion with photon measurements [completed data-taking], R. Kadona, Y. Miyake, K. Nagamine, K. Nishiyama, Y. Watanabe (*Univ. of Tokyo*), K. Ishida, T. Matsuzaki (*RIKEN*), Y. Kuno (*Univ. of British Columbia*), S.E. Jones (*Brigham Young Univ.*), H.R. Maltrud (*Los Alamos National Lab*)
455. Search for wake riding electron states induced by negative muons in solids [deferred], Y. Yamazaki (*Tokyo Inst. of Technology*), F. Fujimoto, K. Komaki, T. Matsuzaki, K. Nagamine, K. Nishiyama, A. Otuka (*Univ. of Tokyo*)
456. μ^- SR studies on relaxation and chemical reactions of muonic rare gas atoms [deferred], R. Kadono, T. Kondow, K. Kuchitsu, K. Nagamine, T. Nagata, K. Nishiyama, T. Yamazaki (*Univ. of Tokyo*)
457. Studies of chemical effects on atomic negative muon capture in various chemical systems using slow negative muon beam [deferred], M.K. Kubo, K. Nagamine, T. Tominaga, Y. Sakai (*Univ. of Tokyo*)
458. Hyperfine phenomena probed by μ^- SR [deferred], R. Kadono, Y. Miyake, K. Nagamine, K. Nishiyama (*Univ. of Tokyo*), M. Motokawa (*Kobe Univ.*)
459. Exchange effects in $0^+ \rightarrow 0^-$ inelastic scattering III [completed], R.E. Azuma, C. Chan, T.E. Drake, J.D. King, L. Lee, R. Schubank, S.S.M. Wong, X. Zhu (*Univ. of Toronto*), R. Abegg*, L. Buchmann, D. Frekers, R. Helmer, K.P. Jackson, C.A. Miller, S. Yen (*TRIUMF*), E. Rost (*Univ. of Colorado*), R. Sawafta (*IUCF*)
460. A measurement of the cross section and analysing power of the $pn \rightarrow pp(^1S_0)\pi^-$ reaction at TRIUMF energies [completed data-taking], D. Gill, D. Hutcheon, P.L. Walden (*TRIUMF*), D. Ashery, M.A. Moinester, A.I. Yavin (*Tel-Aviv Univ.*), R.R. Johnson (*TRIUMF-UBC*), F. Duncan, R. Olszewski, C. Ponting, M. Seviar, P. Trelle (*Univ. of British Columbia*), B. Mayer (*DPhN/ME Saclay*)
461. μ SR studies of dioxygen and ethylene physisorbed on pure silica powder [completed data-taking], R.F. Marzke (*Arizona State Univ.*), D.G. Fleming, (*Univ. of British Columbia*), M. Senba (*TRIUMF-UBC*), J.C. Brodovitch, P.W. Percival (*Simon Fraser Univ.*)
462. Quasi-elastic scattering from ^{16}O , ^{12}C and ^4He [completed data-taking], C. Chan, T. Drake, L. Lee (*Univ. of Toronto*), R. Abegg*, D. Frekers, D. Hutcheon, J. Iqbal, C.A. Miller, S. Yen (*TRIUMF*), O. Häusser* (*TRIUMF-SFU*), K. Hicks (*Ohio Univ.*), C. Horowitz (*MIT*)

463. Muon-nuclear-spin double relaxation measurements of itinerant magnets in the critical temperature region [completed data-taking], R. Kadono (*RIKEN*), T. Yamazaki (*INS, Univ. of Tokyo*), J.H. Brewer, K. Chow, S.R. Kreitzman, T.M. Riseman (*Univ. of British Columbia*), J.W. Schneider (*TRIUMF*), C. Niedermayer (*UBC-Univ. Konstanz*)
464. Low frequency excitations in disordered magnets [inactive], S.A. Dodds (*Rice Univ.*), J.H. Brewer (*Univ. of British Columbia*), E.J. Ansaldo (*Univ. of Saskatchewan*), D. Noakes (*Chalk River Nuclear Labs*)
466. Measurement of $np \rightarrow d\pi^0$ cross sections near threshold [completed], R. Abegg*, L.G. Greeniaus, D.A. Hutcheon, C.A. Miller (*TRIUMF*), G.W.R. Edwards, W.C. Olsen, Ye Yan-lin (*Univ. of Alberta*), G.A. Moss (*Science World*), I.J. van Heerden (*Univ. of West Cape*)
467. Radiobiology of high-energy neutrons [inactive], G. Lam (*Cancer Control Agency of B.C.*), H. Dougan, J. Vincent (*TRIUMF*), D. Chaplin, R. Durand, L. Skarsgard (*B.C. Cancer Research Centre*)
468. Isovector $1^+ \rightarrow 0^+$ transitions in the $A=6$ system [completed data-taking], O. Häusser* (*SFU-TRIUMF*), B. Larson, B. Pointon, A. Trudel, M. Vetterli (*Simon Fraser Univ.*), R. Abegg*, D. Frekers, R. Helmer, K.P. Jackson (*TRIUMF*), W.P. Alford, A. Celler (*Univ. of Western Ontario*), B. Spicer (*Univ. of Melbourne*), R. Henderson (*TRIUMF-Univ. of Melbourne*), K. Hicks (*Ohio Univ.*), R. Jeppesen (*Los Alamos National Lab*)
469. μ SR study of high-temperature superconductors [completed], J.H. Brewer, A.C. Chaklader, R. Cline, W.N. Hardy, S.R. Kreitzman, G.M. Luke, T. Riseman (*Univ. of British Columbia*), R. Kiefl (*TRIUMF*), G. Aepli, B. Batlogg, D.R. Harshman (*AT&T Bell Labs*), E.J. Ansaldo (*Univ. of Saskatchewan*), S. Dodds (*Rice Univ.*), C.Y. Huang (*Lockheed*), W.J. Kossler (*College of William & Mary*), T. Yamazaki (*Univ. of Tokyo*), N. Nishida (*Tokyo Inst. Technology*), H. Yasuoka (*ISSP, Tokyo*), A.M. Portis (*Univ. of California, Berkeley*), Y.J. Uemura (*Columbia Univ.*), M. Celio (*ETH Zürich*)
470. Stretched states excited in (n, p) reactions on ^{14}C , ^{26}Mg and ^{30}Si [completed data-taking], B.D. Anderson, R. Madey, D.M. Manley, J. Watson (*Kent State Univ.*), R. Helmer, K.P. Jackson, C.A. Miller, S. Yen (*TRIUMF*), O. Häusser* (*SFU-TRIUMF*), A. Trudel (*Simon Fraser Univ.*), W.P. Alford, A. Celler (*Univ. of Western Ontario*), R. Henderson (*TRIUMF-Univ. of Melbourne*)
471. Differential cross sections for $\pi^\pm p$ elastic scattering at 87 to 143 MeV [completed data-taking], S. Høibråten, M.D. Kohler, J.J. Kraushaar, B.J. Kriss, R.A. Ristinen (*Univ. of Colorado*), P.A. Amaudruz, J.T. Brack, D.F. Ottewell, G.R. Smith (*TRIUMF*), M. Kermani, M. Pavan, D. Vetterli (*Univ. of British Columbia*), E. Gibson (*California State Univ., Sacramento*), J. Jaki, M. Metzler (*Univ. Karlsruhe*)
472. Measurement of $B^+(\text{GT})$ for ^{76}Se using the (n, p) reaction [completed data-taking], R. Abegg*, D. Frekers, R. Helmer, K.P. Jackson, C.A. Miller, S. Yen (*TRIUMF*), O. Häusser* (*SFU-TRIUMF*), A. Trudel, M. Vetterli (*Simon Fraser Univ.*), W.P. Alford, A. Celler (*Univ. of Western Ontario*), W.C. Olsen (*Univ. of Alberta*), R. Henderson (*TRIUMF-Univ. of Melbourne*), R. Jeppesen (*Los Alamos National Lab*)
473. Quasi-elastic scattering of $1s$ state nucleons in light nuclei [completed data-taking], R. Abegg*, D. Frekers, L.G. Greeniaus, D.A. Hutcheon, C.A. Miller (*TRIUMF*), P. Kitching (*TRIUMF-Univ. of Alberta*), M. Ahmad, W.J. McDonald, Y. Ye (*Univ. of Alberta*), R. Schubank (*Univ. of Saskatchewan*), J.W. Watson (*Kent State Univ.*), K. Hicks (*Ohio Univ.*), N. Chant (*Univ. of Maryland*)
474. Orbital-spin interference from GT-M1 comparisons in (sd) shell nuclei [completed data-taking], O. Häusser* (*TRIUMF-SFU*), R. Henderson (*TRIUMF-Univ. of Melbourne*), R. Helmer, K.P. Jackson (*TRIUMF*), B. Larsen, B. Pointon, A. Trudel, M. Vetterli (*Simon Fraser Univ.*), W.P. Alford (*Univ. of Western Ontario*), K. Hicks (*Ohio Univ.*), R. Jeppesen (*Los Alamos National Lab*), A. Richter (*T.H. Darmstadt*)
475. Quasielastic analyzing powers using the (p, n) reaction [completed], K. Hicks (*Ohio Univ.*), D. Frekers, R. Helmer, J. Iqbal, K.P. Jackson, S. Yen (*TRIUMF*), O. Häusser* (*TRIUMF-SFU*), A. Trudel, M. Vetterli (*Simon Fraser Univ.*), W.P. Alford, A. Celler (*Univ. of Western Ontario*), R. Henderson (*TRIUMF-Univ. of Melbourne*), R. Jeppesen (*Los Alamos National Lab*)
476. Nuclear spin response using the $(\bar{p}, p'\gamma)$ reaction [completed data-taking], K. Hicks (*Ohio Univ.*), L. Armendariz, M. Kovash, M.A. Pickar (*Univ. of Kentucky*), A. Trudel, M. Vetterli (*Simon Fraser Univ.*), R. Henderson (*TRIUMF-Univ. of Melbourne*), N.S.P. King (*Los Alamos National Lab*), N.W. Hill (*Oak Ridge National Lab*), J. Shepard (*Univ. of Colorado*), R. Abegg*, A. Celler, K.P. Jackson, S. Yen (*TRIUMF*)
477. The electronic structure of muonium in the cuprous halides [completed data-taking], R.F. Kiefl (*TRIUMF-UBC*), S.A. Dodds, T.L. Estle (*Rice Univ.*), E.J. Ansaldo (*Univ. of Saskatchewan*), K. Chow, T. Riseman (*Univ. of British Columbia*), R.C. DuVarney (*Emory Univ.*), R. Kadono (*KEK*), S. Kreitzman, J.W. Schneider, C. Zhang (*TRIUMF*), R.L. Lichti (*Texas Tech. Univ.*), C. Schwab (*Univ. Louis Pasteur*)
478. Proton-induced πNN resonances [completed data-taking], R. Abegg*, D. Frekers, P.W. Green, D.A. Hutcheon, C.A. Miller, S. Yen (*TRIUMF*), C. Chan (*Univ. of Toronto*), R. Schubank (*Univ. of Saskatchewan*), P. Trelle (*Univ. of Colorado*)

479. Study of relativistic medium effects through $A_y(\theta)$ measurements for quasielastic scattering in ^{58}Ni [inactive], D.K. McDaniels, Z. Tang, Z. Xu (*Univ. of Oregon*), X.Y. Chen, F. Farzanpay, L.W. Swenson (*Oregon State Univ.*), K. Hicks (*Ohio Univ.*), O. Häusser* (*TRIUMF-SFU*), M. Vetterli (*Simon Fraser Univ.*), F. Bertrand, D. Horen, J. Lisantti (*Oak Ridge National Lab*)
480. The spectral function of $p+n$ in ^6Li from the $^6\text{Li}(p, p\alpha)pn$ reaction [completed], R.E. Warner (*Oberlin College and Univ. of Notre Dame*), S.E. Darden, J.J. Kolata (*Univ. of Notre Dame*), R. Helmer (*TRIUMF*), C.A. Davis (*Univ. of Manitoba*), P. Schwandt (*Indiana Univ.*), A. Galonsky, L. Heilbronn, D. Krofcheck (*Michigan State Univ.*), F.D. Becchetti (*Univ. of Michigan*), C.F. Perdrisat, V. Punjabi (*College of William and Mary*)
482. Measurements of spin transfer coefficients in pd elastic scattering [completed data-taking], R. Abegg*, R. Helmer, D.A. Hutcheon (*TRIUMF-Univ. of Alberta*), O. Häusser*, N. Stevenson, S. Yen (*TRIUMF*), N. Kolb, E. Korkmaz, W.C. Olsen (*Univ. of Alberta*), C.A. Davis (*TRIUMF-Univ. of Manitoba*), D. Mack (*CEBAF*), C.A. Gossett (*Univ. of Washington*)
483. An initial look at the (p, π^+d) reaction as a nuclear probe [active], D. Frekers, M.J. Iqbal, P.L. Walden, S. Yen (*TRIUMF*), E.G. Auld, F. Duncan (*Univ. of British Columbia*), R.D. Bent (*Indiana Univ.*), W.R. Falk, K. Furutani (*Univ. of Manitoba*), G.J. Lolos (*Univ. of Regina*), K. Hicks (*Ohio Univ.*)
484. Measurement of the spin dipole resonance with $^{40}\text{Ca}(n, p)^{40}\text{K}$ at 300 MeV [completed], 92 AR - per Trudel R. Abegg*, R. Helmer, K.P. Jackson, S. Yen (*TRIUMF*), J. Mildenerger, A. Trudel, M. Vetterli (*Simon Fraser Univ.*), O. Häusser* (*TRIUMF-SFU*), W.P. Alford, A. Celler (*Univ. of Western Ontario*), R. Henderson (*TRIUMF-Univ. of Melbourne*) R. Jeppesen (*Los Alamos National Lab*)
485. $^{15}\text{N}(n, p)^{15}\text{C}$: An investigation of single particle spin dipole transitions [completed], W.P. Alford, A. Celler (*Univ. of Western Ontario*), R. Abegg*, D. Frekers, R. Helmer, K.P. Jackson, S. Yen (*TRIUMF*), W.P. Alford (*Univ. of Western Ontario*), O. Häusser* (*SFU-TRIUMF*), A. Trudel, M. Vetterli (*Simon Fraser Univ.*), R. Henderson (*TRIUMF-Univ. of Melbourne*), R. Jeppesen (*Los Alamos National Lab*)
486. Spin isovector giant resonances in deformed nuclei [completed data-taking], S.A. Long, K. Raywood, G.G. Shute, B.M. Spicer (*Univ. of Melbourne*), R. Henderson (*TRIUMF-Univ. of Melbourne*), D. Frekers, R. Helmer, K.P. Jackson, S. Yen (*TRIUMF*), O. Häusser* (*TRIUMF-SFU*), M. Vetterli (*Simon Fraser Univ.*), W.P. Alford, A. Celler (*Univ. of Western Ontario*), M.A. Moinester, A.I. Yavin (*Tel-Aviv Univ.*), R. Jeppesen, N. King (*Los Alamos National Lab*)
488. (n, p) on helium isotopes [completed data-taking], R. Abegg*, D. Frekers, R. Helmer, K.P. Jackson, C.A. Miller, S. Yen (*TRIUMF*), M. Moinester (*Tel-Aviv Univ.*), O. Häusser* (*TRIUMF-SFU*), B. Pointon, A. Trudel, M. Vetterli (*Simon Fraser Univ.*), W.P. Alford, A. Celler (*Univ. of Western Ontario*), R. Henderson (*TRIUMF-Univ. of Melbourne*), K. Hicks (*Ohio Univ.*), R. Jeppesen (*Los Alamos National Lab*)
489. GT-M1 comparison and isovector spin-dipole strength in (sd) shell nuclei [completed data-taking], O. Häusser* (*TRIUMF-SFU*), J. Mildenerger, B. Pointon, A. Trudel, (*Simon Fraser Univ.*), W.P. Alford, A. Celler (*Univ. of Western Ontario*), R. Abegg*, K. Ferguson, R. Helmer, R. Henderson, K.P. Jackson, C.A. Miller, M. Vetterli (*TRIUMF*)
490. Calibration of $\sigma/B(\text{GT})$ at 300 MeV using the (p, n) reaction on ^{27}Al and ^{58}Ni [completed data-taking], B. Larsen, J. Mildenerger, B. Pointon, A. Trudel, M. Vetterli (*Simon Fraser Univ.*), O. Häusser* (*TRIUMF-SFU*), R. Helmer, K.P. Jackson, S. Yen (*TRIUMF*), A. Celler (*Univ. of Western Ontario*), R. Henderson (*TRIUMF-Univ. of Melbourne*), K. Hicks (*Ohio Univ.*), R. Jeppesen (*Los Alamos National Lab*)
491. $^{45}\text{Sc}(n, p)^{45}\text{Ca}$ and $^{45}\text{Sc}(p, n)^{45}\text{Ti}$: A significant test of model calculations in the (fp) shell [completed], W.P. Alford, A. Celler (*Univ. of Western Ontario*), R. Abegg*, K. Ferguson, R. Helmer, K.P. Jackson, S. Yen (*TRIUMF*), S. Long, K. Raywood (*Univ. of Melbourne*), B.A. Brown (*Michigan State Univ.*)
492. Enhancement of the $S = 1, T = 0$ nuclear response in pion scattering [completed data-taking], O. Häusser* (*SFU-TRIUMF*), J. Mildenerger, A. Trudel, M. Vetterli (*Simon Fraser Univ.*), D. Frekers, R. Helmer, K.P. Jackson, C.A. Miller, D. Ottewell, S. Yen (*TRIUMF*), R.R. Johnson (*TRIUMF-UBC*), M. Seviar (*Univ. of British Columbia*), W.P. Alford, A. Celler (*Univ. of Western Ontario*), R. Henderson (*TRIUMF-Univ. of Melbourne*), G.A. Moss (*Univ. of Alberta*), K. Hicks (*Ohio Univ.*), R. Jeppesen (*Los Alamos National Lab*), R. Ristinen (*Univ. of Colorado*)
493. μSR study of exotic single crystal superconductors [completed], G. Aeppli, B. Batlogg, D.R. Harshman, L. Remeika, L. Scheemeyer (*AT&T Bell Laboratories*), E. Bucher (*AT&T Bell Labs & Univ. Konstanz*), R. Kiefl (*TRIUMF*), E.J. Ansaldò (*Univ. of Saskatchewan*), T. Riseman, D.Ll. Williams (*Univ. of British Columbia*), G.M. Luke (*Columbia Univ.*)
494. Superconductivity and magnetism of heavy-fermion and high- T_c related systems: Muon spin rotation study combined with neutron scattering [completed], G.M. Luke, A. Moodenbaugh, Y.J. Uemura (*Columbia Univ.*),

- J.H. Brewer, S.R. Kreitzman, T. Riseman (*Univ. of British Columbia*), R.F. Kiefl (*TRIUMF*), S.D. Dodds (*Rice Univ.*), M.B. Maple, M. Torikachvili (*Univ. of California, San Diego*), D.C. Johnston (*Iowa State Univ. and Ames Lab*), W.J. Kossler, X.H. Yu (*College of William and Mary*), C.E. Stronach (*Virginia State Univ.*), Y. Hidaka, T. Murakami (*Nihon Telephone and Telegraph*), Y. Oonuki (*Tsukuba Univ.*)
495. Studies of oxide superconductors by negative muons [active], R. Kadono, K. Nagamine, K. Nishiyama, T. Yamazaki, H. Yasuoka (*Univ. of Tokyo*), N. Nishida (*Tokyo Inst. of Technology*), J.H. Brewer (*Univ. of British Columbia*), R. Kiefl (*TRIUMF*)
496. Measurements of the angular distribution of the spin transfer parameter D_{LS} in $pp \rightarrow d\pi^+$ [completed data-taking], R. Abegg*, P.W. Green, L.G. Greeniaus, D.A. Hutcheon (*TRIUMF-Univ. of Alberta*), E. Korkmaz, D. Mack, G.A. Moss, W.C. Olsen, Y. Ye (*Univ. of Alberta*), N.R. Stevenson (*TRIUMF*)
497. Measurement of the flavour-conserving hadronic weak interaction [active], J. Birchall, J. Bland, A.A. Hamian, L. Lee, S.A. Page, W.D. Ramsay, W.T.H. van Oers, R.J. Woo (*Univ. of Manitoba*), C.A. Davis, R. Helmer, C.D.P. Levy (*TRIUMF*), P.W. Green, G. Roy, G.M. Stinson (*Univ. of Alberta*), J.D. Bowman, R.E. Mischke (*Los Alamos National Lab*), Y. Kuznetsov, N.A. Titov, A.N. Zelenski (*INR Moscow*)
498. Analysing power zero crossing angles in np elastic scattering below 300 MeV [completed], J. Birchall, C.A. Davis, N.E. Davison, S.A. Page, W.D. Ramsay, W.T.H. van Oers (*Univ. of Manitoba*), L.G. Greeniaus (*TRIUMF*)
500. Formation, relaxation and LCR spectroscopy of muonated radicals in the gas phase [completed data-taking], D.J. Arseneau, D.G. Fleming, J.R. Kempton, M. Senba, K. Venkateswaran (*Univ. of British Columbia*), J.C. Brodovitch, P.W. Percival (*Simon Fraser Univ.*), D.M. Garner (*TRIUMF*), S.F.J. Cox (*Rutherford Appleton Lab*), E. Roduner (*Univ. Zürich*)
501. Study of the $^{16}\text{O}(\pi^+, \pi^+\pi^-)$ reaction at $T_{\pi^+} = 240$ MeV [completed data-taking], N. Grion (*INFN-Trieste*), P. Camerini, R. Rui (*Univ. di Trieste*), E. Oset, M. Vicente-Vacas (*Univ. Valencia*), G.R. Smith (*TRIUMF*), M. Hanna, R. Olszewski, M. Rozon, M. Seviar, V. Sossi (*Univ. of British Columbia*), R.R. Johnson (*TRIUMF-UBC*), R.P. Trelle (*Univ. of Colorado*)
502. Measurement of analysing powers in low-energy πd elastic scattering [completed data-taking], R.B. Schubank, Y.M. Shin, N.R. Stevenson (*Univ. of Saskatchewan*), P. Delheij, D.R. Gill, D. Healey, G.R. Smith, G.D. Wait (*TRIUMF*), R.R. Johnson (*TRIUMF-UBC*), M. Hanna, J. McAlister, V. Sossi, P. Weber (*Univ. of British Columbia*), E.L. Mathie (*Univ. of Regina*), R.A. Ristinen, R.P. Trelle (*Univ. of Colorado*)
503. Search for a πNN bound state [inactive], R.A. Ristinen, R.P. Trelle (*Univ. of Colorado*), R.R. Johnson (*TRIUMF-UBC*), D. Frekers, D.R. Gill, D. Ottewell, G.R. Smith (*TRIUMF*), R. Olszewski, M.F. Rozon, M.E. Seviar, P. Weber (*Univ. of British Columbia*), R. Schubank, N.R. Stevenson (*Univ. of Saskatchewan*), E.L. Mathie (*Univ. of Regina*)
504. Analyzing powers for $\pi^\pm \ ^{13}\vec{\text{C}}$ scattering at $T_\pi=100$ MeV, [completed], D.R. Gill, D. Ottewell, G.R. Smith, G.D. Wait (*TRIUMF*), R.R. Johnson (*TRIUMF-UBC*), J.T. Brack, R. Olszewski, M.E. Seviar (*Univ. of British Columbia*), R. Rui (*INFN Trieste*), E.L. Mathie, V. Pafilis (*Univ. of Regina*), R.B. Schubank, N.R. Stevenson (*Univ. of Saskatchewan*), J.J. Kraushaar, R.J. Peterson, R.A. Ristinen, R.P. Trelle (*Univ. of Colorado*), G.S. Kyle (*New Mexico State Univ.*), D. Dehnhard (*Univ. of Minnesota*)
505. Total absorption cross sections at low energies [completed], E. Friedman, A. Goldring (*Hebrew Univ. Jerusalem*), R.R. Johnson, O. Meirav, D. Vetterli, P. Weber (*Univ. of British Columbia*), A. Altman (*Soreq NRC*)
506. Low energy $\pi + d \rightarrow 2p$ analysing powers [inactive], G.M. Huber, E.L. Mathie, S.I.H. Naqvi, D.M. Yeomans (*Univ. of Regina*), D. Healey, D. Ottewell, R. Tacik (*TRIUMF*), M. Pavan (*Univ. of British Columbia*)
508. Study of the $\pi^+ + d \rightarrow \pi^- + \pi^+ + p + p$ reaction at $T_{\pi^+} = 270$ MeV [inactive], P. Camerini, R. Rui (*Univ. di Trieste*), N. Grion (*INFN Trieste*), E. Oset, M.J. Vicente-Vacas (*Univ. Valencia*), G.R. Smith (*TRIUMF*), R.R. Johnson (*TRIUMF-UBC*), M. Hanna, R. Olszewski, F.M. Rozon, M. Seviar, V. Sossi (*Univ. of British Columbia*), P. Trelle (*Univ. of Colorado*)
510. Cross-section measurements for the production of ^{186}Re from the spallation of ^{197}Au with 425–500 MeV protons [inactive], T.J. Ruth (*TRIUMF*), J.M. D’Auria, S. Gardner (*Simon Fraser Univ.*), C. Schell (*Univ. of British Columbia*)
511. Pion transfer in hydrogenous materials [completed data-taking], D. Armstrong, D.F. Measday, S. Stanislaus (*Univ. of British Columbia*), M. Harston (*Univ. of Surrey*), D. Horváth (*Central Research Inst., Budapest*), K. Aniol (*California State Univ., LA*)
512. Analysing powers in the $^{13}\vec{\text{C}}(\pi, \pi')$ reaction between 100 and 300 MeV [deferred], D.R. Gill, D. Ottewell, G.R. Smith, G.D. Wait (*TRIUMF*), R.R. Johnson (*TRIUMF-UBC*), R. Olszewski, M.E. Seviar (*Univ. of British Columbia*), R. Rui (*INFN Trieste*), E.L. Mathie, V. Pafilis (*Univ. of Regina*), R.B. Schubank, N.R. Stevenson (*Univ. of Saskatchewan*), J. Brack, J.J. Kraushaar, R.J. Peterson, R.A. Ristinen, R.P. Trelle (*Univ. of Colorado*), G.S. Kyle (*New Mexico State Univ.*), D. Dehnhard (*Univ. of Minnesota*)

513. Angular correlations in the $^{12}\text{C}(\pi, \pi'\gamma)$ reaction between 100 and 300 MeV [deferred], D.R. Gill, D. Ottewell, G.R. Smith, G.D. Wait (*TRIUMF*), R. Olszewski, M.E. Sevier (*Univ. of British Columbia*), R.R. Johnson (*TRIUMF-UBC*), R. Rui (*INFN Trieste*), E.L. Mathie, V. Pafilis (*Univ. of Regina*), R.B. Schubank, N.R. Stevenson (*Univ. of Saskatchewan*), J. Brack, J.J. Kraushaar, R.J. Peterson, R.A. Ristinen, R.P. Trelle (*Univ. of Colorado*)
514. The pion-deuteron breaking reaction with CLASS [deferred], G.J. Lolos, E.L. Mathie, S.I.H. Naqvi (*Univ. of Regina*), G.R. Smith (*TRIUMF*)
515. Pion bremsstrahlung with negative pions [deferred], P. Kitching (*TRIUMF-Univ. of Alberta*), F. Farzanpay, P. Fuchs, A.W. Stetz, L.W. Swenson, N. Wen (*Oregon State Univ.*), G.R. Smith (*TRIUMF*), W.C. Olsen (*Univ. of Alberta*), N. Stevenson (*Univ. of Saskatchewan*)
516. Angular distributions and energy dependence for $d(\pi^{+-}, \pi^{-+})\pi NN$ [deferred], R.A. Ristinen, R.P. Trelle (*Univ. of Colorado*), D. Frekers, D.R. Gill, D. Ottewell, G.R. Smith (*TRIUMF*), R.R. Johnson (*TRIUMF-UBC*), R. Olszewski, M.F. Rozon, M.E. Sevier, P. Weber (*Univ. of British Columbia*), E.L. Mathie (*Univ. of Regina*), R. Schubank, N.R. Stevenson (*Univ. of Saskatchewan*), D. Ashery (*Tel-Aviv Univ.*)
517. Cross sections and analysing powers in the $^{14}\vec{\text{N}}(\pi, 2p)$ reaction between 100 and 300 MeV [deferred], D.R. Gill, D. Ottewell, G.R. Smith, G.D. Wait (*TRIUMF*), R.R. Johnson (*TRIUMF-UBC*), R. Olszewski, M.E. Sevier (*Univ. of British Columbia*), R. Rui (*INFN Trieste*), E.L. Mathie, V. Pafilis (*Univ. of Regina*), R.B. Schubank, N.R. Stevenson (*Univ. of Saskatchewan*), J. Brack, J.J. Kraushaar, R.J. Peterson, R.A. Ristinen, R.P. Trelle (*Univ. of Colorado*), G. Kyle (*New Mexico State Univ.*), P. Roos (*Univ. of Maryland*)
518. Pion-induced pion production on ^3He at threshold [deferred], R.A. Ristinen, R.P. Trelle (*Univ. of Colorado*), D. Frekers, D.R. Gill, D. Ottewell, G.R. Smith (*TRIUMF*), R.R. Johnson (*TRIUMF-UBC*), R. Olszewski, M.E. Sevier, P. Weber (*Univ. of British Columbia*), R. Rui (*INFN Trieste*), E.L. Mathie (*Univ. of Regina*), R.B. Schubank, N.R. Stevenson (*Univ. of Saskatchewan*)
519. High dose rate effects in advanced radiation-hardened CMOS microelectronics [completed data-taking], F. Sexton, J.R. Schwank, M.R. Shaneyfelt (*Sandia National Laboratories*),
520. μSR test of mechanisms for high- T_c superconductivity [completed], I. Affleck, J.H. Brewer, J.F. Carolan, A.C.D. Chaklader, R. Cline, W.N. Hardy, J. Kempton, S.R. Kreitzman, T.M. Riseman, G. Roehmer, D.Ll. Williams, B.-X. Yang (*Univ. of British Columbia*), R. Kadono, R. Keitel, R.F. Kiefl (*TRIUMF*), E.J. Ansaldo (*Univ. of Saskatchewan*), J. Greedan (*McMaster Univ.*), M. Ishikawa (*ISSP, Tokyo*), K. Nagamine, K. Nishiyama (*Univ. of Tokyo MSL*), N. Nishida, S. Ohkuma (*Tokyo Inst. of Technology*), T. Yamazaki (*Univ. of Tokyo*), G.M. Luke, Y.J. Uemura (*Columbia Univ.*)
521. μSR studies of $(\text{LaSr})\text{CuO}_4$, $\text{Ba}(\text{PbBi})\text{O}_3$ and $(\text{BaK})\text{BiO}_3$ [completed data-taking], G.M. Luke, B. Sternlieb, Y.J. Uemura (*Columbia Univ.*), J.H. Brewer, J.R. Kempton, S.R. Kreitzman, T.M. Riseman, R. Kiefl (*TRIUMF*), W.J. Kossler, X.H. Yu (*College of William & Mary*), C.E. Stronach (*Virginia State Univ.*), S. Uchida (*Univ. of Tokyo*), K. Kumagai (*Hokkaido Univ.*), A.W. Sleight (*Du Pont Exp. Station*)
523. Pion absorption reactions ^4He , $^6,7\text{Li}$, ^9Be , $^{12}\text{C}(\pi^\pm, nN)$, $n > 1$ with PALAS [deferred], G.J. Lolos, E.L. Mathie, S.I.H. Naqvi (*Univ. of Regina*), M. Comyn, D. Frekers, D. Ottewell (*TRIUMF*), D. Humphrey (*Western Kentucky Univ.*)
524. Muonium reactivity enhancements [completed], G.B. Porter, D.C. Walker, Z. Wu (*Univ. of British Columbia*), M.V. Barnabas (*Argonne National Lab*), K. Venkateswaran (*Hindustan Lever Ltd.*), J.M. Stadlbauer* (*Hood College*), B.W. Ng (*Winona State Univ.*)
525. Muonium studies on copolymerization in micelles [completed], D.C. Walker, Z. Wu (*Univ. of British Columbia*), M.V. Barnabas (*UBC-TRIUMF*), G.B. Porter, K. Venkateswaran (*TRIUMF*), J.M. Stadlbauer* (*Hood College*), B.W. Ng (*Winona State Univ.*)
526. A study of the formation and de-excitation of excited nuclear matter [inactive], J.M. D'Auria, R.G. Korteling (*Simon Fraser Univ.*), K.P. Jackson (*TRIUMF*), V. Viola (*Indiana Univ.*), K. Kwiatkowski (*IUCF*), S. Kaufmann (*Argonne National Lab*)
527. Slowing-down time of muons in gases [complete], D.J. Arseneau, D.G. Fleming, A.C. Gonzalez, J.R. Kempton, J. Pan, M. Senba (*Univ. of British Columbia*), D.M. Garner (*TRIUMF*)
528. Muonium reactions with O_2 , CO and NO in high pressure moderators [completed], D.J. Arseneau, D.G. Fleming, J. Kempton, J. Pan, M. Senba (*Univ. of British Columbia*), A.C. Gonzalez (*Univ. of Southern California*), D.M. Garner (*TRIUMF*)
529. Kinetic isotope effects in the muonium + hydrogen halides (Hx) gas reactions [completed data-taking], D.J. Arseneau, D.G. Fleming, J. Kempton, J.J. Pan, M. Senba, A. Tempelmann (*Univ. of British Columbia*), A.C. Gonzalez (*Univ. of Southern California*), D.M. Garner (*TRIUMF*)

530. π^+ -proton total cross sections at low energies [completed], E. Friedman, A. Goldring (*Hebrew Univ. Jerusalem*), R.R. Johnson, O. Meirav (*Univ. of British Columbia*), B.K. Jennings (*TRIUMF*), G. Wagner (*Univ. Tübingen*), A. Altman (*Soreq NRC*)
531. μ SR study in trans-(CH)_x [completed data-taking], S. Ikehata, K. Nagamine, K. Nishiyama, N. Oda (*Univ. of Tokyo*)
532. Secondary electron emission in μ -foil interactions [active], T. Azuma, Y. Miyake, K. Nishiyama, Y. Watanabe, Y. Yamazaki (*Univ. of Tokyo*), K. Nagamine (*Univ. of Tokyo-RIKEN*), T. Matsuzaki (*RIKEN*), K. Kuroki (*Inst. Police Science, Tokyo*)
533. Studies on formation of mesomolecules by introduction of μ^- in LiH and LiD [completed data-taking], T. Kondow, Y. Miyake, K. Nagamine, T. Nagata, K. Nishiyama (*Univ. of Tokyo*), K. Ishida, T. Matsuzaki (*RIKEN*)
534. Tissue chemical analysis with muonic x-rays [completed data-taking], Y. Hosoi, Y. Kakuto, K. Sakamoto, Y. Takai (*Tohoku Univ. School of Medicine*), K. Nagamine (*Univ. of Tokyo*)
535. Search for deeply bound pionic states in heavy nuclei via pion transfer (n, p) reactions [completed], R.S. Hayano, T. Yamazaki (*Univ. of Tokyo*), H. Toki (*Tokyo Metropolitan Univ.*), H. Sakai (*Osaka Univ.*), O. Häusser* (*SFU-TRIUMF*), K.P. Jackson (*TRIUMF*), A. Trudel, M.C. Vetterli (*Simon Fraser Univ.*)
536. The ${}^6\text{Li}(\mu^-, 2t)\nu_\mu$ reaction [inactive], K. Kletch, T. Langen, C. Rangacharyulu, R.B. Schubank, Y.M. Shin, N.R. Stevenson (*Univ. of Saskatchewan*), C. Kim (*Univ. of Calgary*)
- 537a. Radiative decay of the Δ resonance: Cross sections for $\pi^- p \rightarrow \gamma n$ [completed data-taking], D.F. Measday, A. Noble (*Univ. of British Columbia*), E.C. Booth, D. Delli Carpini, J. Miller (*Boston Univ.*), D. Mack, S. Wood (*CEBAF*), M. Kovash, M. Pickar, M. Wang (*Univ. of Kentucky*), B. Bassalleck, M. Halka (*Univ. of New Mexico*), M. Moinester (*Tel-Aviv Univ.*), R. Jacot-Guillarmod, D. Ottewell (*TRIUMF*), S. Stanislaus (*Los Alamos National Lab*), P. Weber (*CERN*)
- 537b. Radiative decay of the Δ resonance: Analyzing powers for $\pi^- p \rightarrow \gamma n$ [completed data-taking], B. Bassalleck, J. Stasko (*Univ. of New Mexico*), E. Booth, M. Chertok, J. Miller (*Boston Univ.*), R. Jacot-Guillarmod, D. Ottewell (*TRIUMF*), M.A. Kovash, M.A. Pickar (*Univ. of Kentucky*), D. Mack (*CEBAF*), D.F. Measday (*Univ. of British Columbia*), M. Moinester (*Tel Aviv*), P. Weber (*CERN*)
538. Measurement of σ/B_{GT} for ${}^{13}\text{C}$ [completed data-taking], J. Mildenerger, A. Trudel, M. Vetterli (*Simon Fraser Univ.*), O. Häusser* (*SFU-TRIUMF*), W.P. Alford, A. Celler, (*Univ. of Western Ontario*), R. Helmer, S. Yen (*TRIUMF*)
539. Diffusion of light interstitials and the effect of conduction electrons [active], R. Kadono, R.F. Kiefl (*TRIUMF*), J.H. Brewer, S.R. Kreitzman, G.M. Luke, T.M. Riseman, D.L. Williams (*Univ. of British Columbia*), E.J. Ansaldo (*Univ. of Saskatchewan*), T.L. Estle (*Rice Univ.*), M. Celio (*Univ. Zürich*), R. Wäppling (*Univ. of Uppsala*), J. Kondo (*Electrotechnical Lab*)
540. Spin response of magnetic dipole transitions in ${}^{158}\text{Gd}$ [completed data-taking], R. Abegg*, D. Frekers, R. Helmer, C.A. Miller, K.P. Jackson, S. Yen (*TRIUMF*), R. Azuma, C. Chan, T. Drake, J. King (*Univ. of Toronto*), R.B. Schubank (*Univ. of Saskatchewan*), A. Celler (*Univ. of Western Ontario*), M. Vetterli (*Simon Fraser Univ.*), R. Richter, H.J. Stein (*Univ. Darmstadt*)
541. Spin-momentum correlations of nucleons in polarized ${}^3\text{He}$ [completed data-taking], O. Häusser* (*SFU-TRIUMF*), P. Delheij, K.P. Jackson, C.A. Miller (*TRIUMF*), R. Woloshyn (*TRIUMF-SFU*), J. Mildenerger, M. Vetterli (*Simon Fraser Univ.*), R. Henderson (*Univ. of Melbourne-TRIUMF*), T. Chupp (*Harvard Univ.*)
542. Spin-observables from ${}^{28}\text{Si}(p, p'\gamma)$ [completed], K. Hicks (*Ohio Univ.*), A. Trudel, M. Vetterli (*Simon Fraser Univ.*), O. Häusser* (*SFU-TRIUMF*), C.A. Miller, S. Yen (*TRIUMF*), A. Celler (*Univ. of Western Ontario*), R. Jeppesen, N.S.P. King, G. Morgan (*Los Alamos National Lab*), N. Hill (*Oak Ridge National Lab*), M. Kovash (*Univ. of Kentucky*), R. Henderson (*Univ. of Melbourne-TRIUMF*), J. Shepard (*Univ. of Colorado*)
544. A search for an excited pion-bound state of the nucleon via $p(p, n)X^{++}$ [completed data-taking], R. Abegg*, D. Frekers, C.A. Miller, S. Yen (*TRIUMF*), J. Alster, D. Ashery, E. Piasetzky, A.J. Yavin (*Tel-Aviv Univ.*), R. Henderson (*Univ. of Melbourne-TRIUMF*)
545. A study of quasielastic charge exchange [deferred], F.T. Baker (*Univ. of Georgia*), K. Hicks (*Ohio Univ.*), R. Helmer, K.P. Jackson, C.A. Miller, S. Yen (*TRIUMF*), O. Häusser* (*SFU-TRIUMF*), A. Trudel, M. Vetterli (*Simon Fraser Univ.*), A. Celler (*Univ. of Western Ontario*), D. Beatty, R. Ferguson, C. Glashauser, A. Green (*Rutgers Univ.*)
546. Muonium-substituted free radicals [complete], B. Addison-Jones, J.C. Brodovitch, F. Ji, P.W. Percival (*Simon Fraser Univ.*), D.M. Bartels (*Argonne National Lab*)

547. μ^+ SR in exotic single-crystal superconductors [completed data-taking], G. Aeppli, B. Batlogg, D. Bishop, C. Broholm, R.J. Cava, G.P. Espinosa, A.T. Fiory, D.R. Harshman, M. Inui, R.N. Kleiman, L.F. Schneemeyer (*AT&T Bell Labs*), E. Bücher (*AT&T Bell Labs–Univ. Konstanz*), D.Ll. Williams (*Univ. of British Columbia*), E.J. Ansaldo (*Univ. of Saskatchewan*), R.H. Heffner (*Los Alamos National Lab*), D.B. Mitzi (*Stanford Univ.*)
548. μ SR (Condensed matter physics) [completed data-taking], S. Dodds, T.L. Estle (*Rice Univ.*), R. Kadono, R.F. Kiefl (*TRIUMF*), J.H. Brewer, S.R. Kreitzman (*Univ. of British Columbia*), E.J. Ansaldo (*Univ. of Saskatchewan*), M. Celio (*Univ. Zürich*), R.C. DuVarney (*Emory Univ.*), C. Schwab (*CRN, Strasbourg*)
549. Measurement of Gamow-Teller strength in the $^{100}\text{Ru}(n,p)^{100}\text{Tc}$ reaction [inactive], D. Frekers, R. Helmer, K.P. Jackson, C.A. Miller, S. Yen (*TRIUMF*), O. Häusser* (*SFU–TRIUMF*), A. Trudel, M. Vetterli (*Simon Fraser Univ.*), W.P. Alford, A. Celler, (*Univ. of Western Ontario*), W.C. Olsen (*Univ. of Alberta*), J. Engel (*Caltech*), R. Henderson (*Univ. of Melbourne–TRIUMF*)
550. Quasi-free $^{16}\text{O}(\pi^+, \gamma p)^{15}\text{O}$ and non-quasi-free $^{16}\text{O}(\pi^-, \gamma p)^{15}\text{C}$ at 90, 125 and 160 MeV [completed data-taking], K. Choi, N. Kolb, E. Korkmaz, D.J. Mack, W.C. Olsen (*Univ. of Alberta*), J. Miller (*Boston Univ.*), F. Adimi, P. Roos (*Univ. of Maryland*), F. Farzanpay, P. Fuchs, A. Stetz, W. Swenson, J. Zhao, (*Oregon State Univ.*), D.A. Hutcheon, C.A. Miller, D. Ottewell (*TRIUMF*)
552. $pp \rightarrow d\pi^+$ analyzing powers near threshold [completed], R. Abegg*, D.A. Hutcheon, C.A. Miller (*TRIUMF*), L.G. Greeniaus, E. Korkmaz, D. Mack, W.C. Olsen, N.L. Rodning (*Univ. of Alberta*)
553. Ground state correlations and GT strength in ^{16}O [completed], K. Hicks, J. Rapaport (*Ohio Univ.*), D. Frekers, R. Helmer, K.P. Jackson, S. Yen (*TRIUMF*), O. Häusser* (*SFU–TRIUMF*), J. Mildenerger, A. Trudel, M. Vetterli (*Simon Fraser Univ.*), A. Celler (*Univ. of Western Ontario*), R. Jeppesen (*Los Alamos National Lab*), R. Henderson (*Univ. of Melbourne–TRIUMF*)
554. πNN resonances induced by proton nucleus scattering [inactive], R. Abegg*, D. Frekers, R. Helmer, J. Iqbal, K.P. Jackson, B. Jennings, C.A. Miller, S. Yen (*TRIUMF*), R.E. Azuma, C. Chan (*Univ. of Toronto*), R. Schubank (*Univ. of Saskatchewan*), M. Vetterli (*Simon Fraser Univ.*), G. Lolos (*Univ. of Regina*), P. Green (*Univ. of Alberta*), R. Henderson (*Univ. of Melbourne–TRIUMF*)
555. Pion absorption reactions $^{12}\text{C}(\pi^-, pp)X$ and $^{12}\text{C}(\pi^+, ppp)X$ [inactive], G.J. Lolos, E.L. Mathie, S.I.H. Naqvi, M. Yeomans (*Univ. of Regina*), D. Humphrey, G. Vourvopoulos (*Western Kentucky Univ.*), M. Comyn, D. Frekers, D. Ottewell (*TRIUMF*), G. Jones, P. Weber (*Univ. of British Columbia*), G.M. Huber (*Indiana Univ.*), X. Aslanoglou (*Ohio Univ.*)
556. The reaction $\pi^+ + ^4\text{He} \rightarrow \pi^+ + \pi^- + pppn$ [completed data-taking], P. Amaudruz, J. Brack, R.R. Johnson, O. Meirav, D. Ottewell, F.M. Rozon, M. Sevier, G. Sheffer, G. Smith, V. Sossi, D. Vetterli, P. Weber (*Univ. of British Columbia*), P. Camerini, R. Rui (*Univ. di Trieste*), N. Grion (*Univ. di Trieste–INFN*), N.R. Stevenson (*Univ. of Saskatchewan*), M.J. Vicente-Vacas (*Univ. of Valencia*)
557. Elastic scattering of 100 MeV π^+ from a polarized ^3He target [completed data-taking], O. Häusser* (*SFU–TRIUMF*), E.J. Brash, C. Chan, B. Larson, A. Rahav, S. Ram, A. Trudel (*Simon Fraser Univ.*), M. Arbel, P. Delheij, R. Henderson, D.F. Ottewell, A. Mellinger, A. Sadeh, B. Schneiderbauer, M. Vetterli (*TRIUMF*), D. Thiessen (*Univ. of British Columbia*), D.M. Whittal (*NAC South Africa*)
558. Measurement of pion scattering and reactions with polarized ^3H and ^3He [deferred], P. Delheij, D.R. Gill, P. Levy, C.A. Miller, D.F. Ottewell, P. Schmor, G.R. Smith, G.D. Wait (*TRIUMF*), R.B. Schubank, Y.M. Shin, N.R. Stevenson (*Univ. of Saskatchewan*), R.R. Johnson (*TRIUMF–UBC*), M. Hanna, V. Sossi, P. Weber (*Univ. of British Columbia*), O. Häusser* (*SFU–TRIUMF*), M. Law, M. Vetterli (*Simon Fraser Univ.*), N. Grion, R. Rui (*INFN Trieste*), E.L. Mathie, M. Yeomans (*Univ. of Regina*), R. Henderson (*Univ. of Melbourne–TRIUMF*)
559. Coulomb effects in positive and negative pion elastic scattering from polarized deuterons [deferred], P. Delheij, D.R. Gill, D. Healey, D.F. Ottewell, G.R. Smith, G.D. Wait (*TRIUMF*), R.R. Johnson (*TRIUMF–UBC*), M. Hanna, O. Meirav, V. Sossi, D. Vetterli, P. Weber (*Univ. of British Columbia*), R.B. Schubank, Y.M. Shin, N.R. Stevenson (*Univ. of Saskatchewan*), E.L. Mathie (*Univ. of Regina*), N. Grion, R. Rui (*INFN Trieste*), E.T. Boschitz, R. Tacik (*Univ. of Karlsruhe*)
560. Low energy π^+p analyzing powers with CHAOS [active], J. Clark, M.E. Sevier (*Univ. of Melbourne*), B. Jamieson, P. Tagliente (*Univ. of British Columbia*), P. Amaudruz, P. Delheij, L. Felawka, D.F. Ottewell, K. Raywood, G.R. Smith (*TRIUMF*), F. Bonutti, P. Camerini, N. Grion, R. Rui (*Univ. Trieste*), E.L. Mathie, R. Tacik, M. Yeomans (*Univ. of Regina*), J. Brack, G. Hofman, J. Patterson, R.A. Ristinen (*Univ. of Colorado*), E. Gibson (*California State Univ., Sacramento*), H. Staudenmeier (*Univ. of Karlsruhe*), R. Meier, G. Wagner (*Univ. Tübingen*)
561. Threshold measurements of $\text{H}(\pi^-, \pi^+\pi^-)n$ and $\text{H}(\pi^+, \pi^+\pi^+)n$ [completed data-taking], J. Clark, M.E. Sevier (*Univ. of Melbourne*), G. Hofman, M. Kermani, P. Tagliente (*Univ. of British Columbia*), P. Amaudruz, P.

- Delheij, L. Felawka, R. Meier, D.F. Ottewell, K. Raywood, G.R. Smith (*TRIUMF*), F. Bonutti, P. Camerini, R. Rui (*Univ. Trieste*), N. Grion (*INFN, Trieste*), E.L. Mathie, R. Tacik, M. Yeomans (*Univ. of Regina*), J. Brack, R.A. Ristinen (*Univ. of Colorado*), E. Gibson (*California State Univ., Sacramento*), H. Staudenmeier (*Univ. of Karlsruhe*)
562. Spin isovector giant resonances in ^{181}Ta [completed data taking], S.A. Long, G.G. Shute, B.M. Spicer (*Univ. of Melbourne*), R.S. Henderson (*Univ. of Melbourne-TRIUMF*), R. Helmer, K.P. Jackson, C.A. Miller, S. Yen (*TRIUMF*), W.P. Alford (*Univ. of Western Ontario*)
563. Search for the $6^-;1$ stretched state of the mass-20 systems [completed data-taking], M. Munro, G.G. Shute, B.M. Spicer (*Univ. of Melbourne*), R.S. Henderson (*Univ. of Melbourne-TRIUMF*), R. Helmer, K.P. Jackson, C.A. Miller, S. Yen (*TRIUMF*), W.P. Alford (*Univ. of Western Ontario*), J.W. Watson (*Kent State Univ.*)
564. Differential cross sections and analysing powers for the $^4\text{He}(\bar{p}, \pi^+)^5\text{He}$ reaction in the region of the $\Delta(1232)$ resonance [completed], J. Campbell, W.R. Falk, K.M. Furutani, H. Guan (*Univ. of Manitoba*), P. Walden, S. Yen (*TRIUMF*), E.G. Auld, F.A. Duncan (*Univ. of British Columbia*), G.J. Lolos (*Univ. of Regina*), R.D. Bent (*IUCF*), G.M. Huber (*IUCF-Univ. of Regina*), E. Korkmaz (*Univ. of Alberta*), A. Trudel (*Simon Fraser Univ.*), A. Celler (*Univ. of Western Ontario*)
565. Longitudinal spin correlation parameter ($A_{\ell\ell}$) in np elastic scattering at TRIUMF energies [pending], A.R. Berdoz, J. Birchall, J.R. Campbell, N.E. Davison, G. Liping, S.A. Page, W.D. Ramsay, W.T.H. van Oers (*Univ. of Manitoba*), C.A. Davis (*TRIUMF-Univ. of Manitoba*), R. Abegg*, C.A. Miller (*TRIUMF*), P.W. Green, E. Korkmaz, A. Opper (*Univ. of Alberta*), L.G. Greeniaus (*TRIUMF-Univ. of Alberta*)
566. Elastic proton scattering from polarized ^3He [completed data-taking], O. Häusser*, (*SFU-TRIUMF*), P. Delheij, K. Ferguson, K.P. Jackson, C.D.P. Levy, C.A. Miller, B. Morrisette, M. Vetterli, R.M. Woloshyn (*TRIUMF*), R. Henderson (*TRIUMF-Melbourne*), J. Mildemberger, A. Rahav (*Simon Fraser Univ.*), W.P. Alford (*Univ. of Western Ontario*), T.E. Chupp (*Harvard Univ.*)
567. Measurement of the lifetimes of isomeric states during atomic cascade of negative pions in liquid He and Ne [completed data-taking], R.S. Hayano, M. Iwasaki, S. Nakamura, H. Outa (*Univ. of Tokyo*), T. Nagae, Y. Watanabe, T. Yamazaki (*INS, Univ. of Tokyo*), R. Kadono, Y. Kuno, T. Numao (*TRIUMF*), H. Tada (*Univ. Tokyo, Komaba*)
568. The $\pi p \rightarrow \pi\pi N$ reaction at $E = 200\text{--}300$ MeV [completed data-taking], P. Camerini, N. Grion, R. Rui (*INFN, Trieste*), I. Iqbal, R.R. Johnson, O. Meirav, M. Sevier, V. Sossi, D. Vetterli, P. Weber (*Univ. of British Columbia*), G. Smith (*TRIUMF*), M. Rozon (*Carnegie-Mellon Univ.*), M. Vicente (*Univ. Valencia*)
569. Fast outgoing protons and deuterons from muon capture on ^3He nuclei [completed], W.J. Cummings, G.E. Dodge, S.S. Hanna, B.H. King, S.E. Kuhn (*Stanford Univ.*), Y.M. Shin (*Univ. of Saskatchewan*), K-S. Chung, J-M. Lee (*Univ. of Yonsei, Seoul*), R.B. Schubank (*Univ. of British Columbia*), G.R. Mason (*Univ. of Victoria*), R. Helmer, N.R. Stevenson, U. Wienands (*TRIUMF*), Y.K. Lee (*Johns Hopkins Univ.*), D.P. Rosenzweig (*Univ. of Washington*), B.E. King (*Simon Fraser Univ.*)
570. Gamma-neutrino angular correlation in muon capture on ^{28}Si [completed], D.S. Armstrong (*College of William and Mary*), E. Gete, D.F. Measday, B. Mofta (*Univ. of British Columbia*), J. Bauer, T.P. Goringe, B. Johnson, B. Siebels (*Univ. of Kentucky*), S. Stanislaus (*Valparaiso Univ.*)
571. Longitudinal μ^- spin relaxation measurement on high T_c superconductors [active], H. Kojima, J. Tanaka, E. Torikai (*Yamanashi Univ.*), K. Nagamine, K. Nishiyama, T. Yamazaki (*Univ. of Tokyo*), H. Kitazawa (*RIKEN*)
572. μ^+ SR in single-crystal organic superconductors [active], S.V. Chichester, A.T. Fiory, R.C. Haddon, D.R. Harshman, M.L. Kaplan, L.W. Rupp, Jr. (*AT&T Bell Labs*), R.N. Kleiman (*AT&T Bell Labs-Cornell Univ.*), D.B. Mitzi (*Stanford Univ.*), T. Pfiz (*Max Planck Inst.*), D.L.L. Williams (*Univ. of British Columbia*)
573. Temperature dependence of the spin-exchange cross sections between muonium and cesium atoms [active], D.J. Arseneau, D.G. Fleming, A.C. Gonzalez, J.R. Kempton, J. Pan, M. Senba, A. Tempelmann (*Univ. of British Columbia*)
574. Muonium radical yields [completed], G.B. Porter, D.C. Walker, Z. Wu (*Univ. of British Columbia*), M.V. Barnabas (*Argonne National Lab*), K. Venkateswaran (*Hindustan Lever Ltd.*), J.M. Stadlbauer* (*Hood College*), B.W. Ng (*Winona State Univ.*)
575. Ultra-slow μ^- production via muon catalyzed fusion [completed data-taking], M. Iwasaki, N. Kawamura, K. Nagamine, S. Sakamoto, K. Shimomura (*Univ. of Tokyo*), K. Ishida, P. Strasser (*RIKEN*), E. Torikai (*Yamanashi Univ.*), G.M. Marshall (*TRIUMF*)

576. Spin-dependent structure functions of the proton and the neutron [test], P. Delheij, C.A. Miller, M. Vetterli, R. Woloshyn (*TRIUMF*), O. Häusser* (*SFU-TRIUMF*), C. Choi, L.G. Greeniaus, P. Kitching, N.L. Rodning (*Univ. of Alberta*), R. Henderson (*Univ. of Melbourne-TRIUMF*)
578. Negative pion bremsstrahlung [deferred], F. Farzanpay, P. Fuchs, A.W. Stetz, L.W. Swenson, J. Zhao (*Oregon State Univ.*), P. Kitching (*TRIUMF-Univ. of Alberta*), K. Choi, D. Mack, W.C. Olsen (*Univ. of Alberta*), N. Stevenson (*Univ. of Saskatchewan*)
579. Kinetic isotope effects and tunneling contributions to rate constants for hydrogen atom transfer reactions: $\text{Mu}+\text{CH}_4$ and $\text{Mu}+\text{CD}_4$ [deferred], D.J. Arseneau, D.G. Fleming, A.C. Gonzalez, K.D. Hensel, J.R. Kempton, J.J. Pan, M. Senba, A. Tempelmann (*Univ. of British Columbia*), D.M. Garner (*BC Cancer Foundation*)
580. Interaction of muons with incommensurate spin density waves in chromium and Cr alloys [completed data-taking], E. Fawcett (*Univ. of Toronto*), J.H. Brewer (*Univ. of British Columbia*), R.F. Kiefl (*TRIUMF*), E.J. Ansaldo (*Univ. of Saskatchewan*), D.R. Noakes (*Univ. of Alberta*)
581. μSR studies in organic superconductors [active], L.P. Le, G.M. Luke, B.J. Sternlieb, Y.J. Uemura (*Columbia Univ.*), J.H. Brewer, S.R. Kreitzman, T.M. Riseman (*Univ. of British Columbia*), R.F. Kiefl (*TRIUMF*), G. Saito, H. Yamochi (*ISSP-Univ. of Tokyo*)
582. μSR study of the vortex lattice in the mixed state [completed data-taking], E.J. Ansaldo (*Univ. of Saskatchewan*), J.H. Brewer (*Univ. of British Columbia*), D.R. Noakes (*Virginia State Univ.*), Ch. Niedermayer (*Univ. Konstanz*), A. Mawdsley, J. Tallon (*DSIR, New Zealand*), D.C. Johnson (*Ames Univ.*)
583. μSR study of magnetic ordering in oxides [completed data-taking], E.J. Ansaldo (*Univ. of Saskatchewan*), J.H. Brewer, T.M. Riseman (*Univ. of British Columbia*), R.F. Kiefl, J.W. Schneider (*TRIUMF*), D.R. Noakes, C. Stronach (*Virginia State Univ.*), Ch. Niedermayer (*Univ. Konstanz*), A. Fuertes, B. Martinez, X. Obradors (*Univ. of Barcelona*), J.B. Torrance (*IBM*)
584. Muonium in silicon carbide [inactive], R.F. Kiefl, J.W. Schneider (*TRIUMF*), S.A. Dodds, T.L. Estle (*Rice Univ.*), S.R. Kreitzman (*Univ. of British Columbia*), W.J. Choyke (*Univ. of Pittsburgh*), R.C. DuVarney (*Emory Univ.*), R. Lichti (*Texas Tech. Univ.*)
585. Muonium spectroscopy of the silicon suboxides a-SiO_x [completed data-taking], S.F.J. Cox (*Rutherford Appleton Lab*), E.A. Davis, A. Singh (*Leicester Univ.*), S.R. Kreitzman (*TRIUMF*), T.L. Estle, B. Hitti (*Rice Univ.*), D. Lamp, R.L. Lichti (*Texas Tech. Univ.*), R. Duvarney (*Emory Univ.*), D.W. Cooke, M. Paciotti (*LAMPF*), A.C. Wright (*Univ. of Reading*)
586. Muonium-substituted organic free radicals on surfaces [completed data-taking], E. Roduner, M. Schwager (*Univ. Zürich*), I. Reid (*PSI*), J.C. Brodovitch, P. Percival, S.K. Leung, S. Sun-Mack, S. Wlodek (*Simon Fraser Univ.*), D.G. Fleming, A. Gonzalez, K. Hensel, J. Kempton, J. Pan, M. Senba, A. Templemann (*Univ. of British Columbia*), R. Marzke (*Arizona State Univ.*)
587. Study of first forbidden beta transitions using beta-delayed neutron emission [completed data-taking], J. D'Auria, M. Dombisky (*Simon Fraser Univ.*), W. Liu (*SFU-Univ. of Alberta-Univ. of Toronto*), L. Buchmann, K.P. Jackson, J. Vincent (*TRIUMF*), G. Roy (*Univ. of Alberta*), I. Towner (*Chalk River Nuclear Labs*), P. Reeder (*Pacific Northwest Lab*)
588. Muonated thiyl and alkyl free radicals in solution [inactive], M.V. Barnabas (*Argonne National Lab*), G.B. Porter, D.C. Walker, Z. Wu (*Univ. of British Columbia*), J.M. Stadlbauer* (*Hood College*), B.W. Ng (*Winona State Univ.*), K. Venkateswaren (*Hindustan Lever Ltd.*)
589. The $\beta\alpha$ decay of ^{16}N : Parity-forbidden decay and astrophysical application [completed data-taking], L. Buchmann, K.P. Jackson, J. Vincent (*TRIUMF*), J. D'Auria, M. Dombisky, W. Liu (*Simon Fraser Univ.*), R.E. Azuma, J.D. King, S.S. Wong (*Univ. of Toronto*), C.A. Barnes, B. Fillipone, T.R. Wang (*Caltech*)
590. Distribution of 6^- strength in the mass-32 nuclides via the $^{32}\text{S}(n, p)$ reaction [completed data-taking], S. Koutsoliotas, S.A. Long, M. Munro, B.M. Spicer, G.N. Taylor (*Univ. of Melbourne*), R.S. Henderson (*Univ. of Melbourne-TRIUMF*), K.P. Jackson, C.A. Miller, S. Yen (*TRIUMF*), W.P. Alford (*Univ. of Western Ontario*), A.D. Bacher (*Indiana University*)
591. The role of 3NA in $^{12}\text{C}(\pi^+, ppp)X$ and $^{12}\text{C}(\pi^\pm, ppn)X$ reactions [completed data-taking], L. Alexa, P. Barghava, G. Huber, G.J. Lolos, E.L. Mathie, S.I.H. Naqvi, Z. Papandreou, R. Tacik, D. Watts, M. Yoemans (*Univ. of Regina*), M. Comyn, D. Ottewell (*TRIUMF*), G. Jones, P. Weber (*Univ. of British Columbia*), T. Bauer (*Univ. of Utrecht*)
592. Radiative muon capture on ^3He [completed data-taking], C. Chen, P. Gumplinger, J.A. Macdonald, J.-M. Poutissou, R. Poutissou, D.H. Wright (*TRIUMF*), P. Depommier (*Univ. de Montréal*), P. Bergbusch, M.D. Hasinoff, E. Saettler, D. Sample (*Univ. of British Columbia*), D.S. Armstrong (*College of William and Mary*), M. Blecher, C. Sigler (*Virginia Polytechnic Inst. & State Univ.*), B. Doyle, T.P. Gorringer (*Univ. of Kentucky*)

593. Momentum distributions of backward-production protons in proton-nucleus interactions [active], S. Burzynski, A.J. Trudel (*TRIUMF-SFU*), A. Celler (*TRIUMF-Univ. of Western Ontario*), K.P. Jackson, L. Lee, S. Yen (*TRIUMF*), R. Korteling (*Simon Fraser Univ.*), D.M. Seliverstov, I.I. Strakovsky (*St. Petersburg Nuclear Physics Inst.*), Y. Wu (*TRIUMF-Inst. of Atomic Energy, Beijing*)
594. The elastic and inelastic scattering of intermediate energy protons on deuterium at small momentum transfer [completed], S. Burzynski, A. Trudel (*Simon Fraser Univ.*), J.E. Cromer, R. Helmer, K.P. Jackson, B.E. King, S. Yen (*TRIUMF*), I. Slaus (*Rudjer Boškovic Institute, Zagreb*), B. Spicer (*Univ. of Melbourne*)
595. Measurement of iT_{11} in pion absorption on ^3He [completed data-taking], C. Chan, B. Larson, A. Rahav, M. Vetterli (*Simon Fraser Univ.*), O. Häusser* (*SFU-TRIUMF*), P. Delheij, D.R. Gill, P. Levy (*TRIUMF*), G. Jones, M. Pavan (*Univ. of British Columbia*), A. Altman, D. Ashery, S. Ram (*Tel-Aviv Univ.*), R. Henderson (*Univ. of Melbourne-TRIUMF*)
596. Giant spin excitation in deformed nuclei [completed data-taking], D. Frekers, R. Helmer, K.P. Jackson, C.A. Miller, S. Yen (*TRIUMF*), A. Richter, H. Woertche (*TH Darmstadt*), O. Häusser* (*SFU-TRIUMF*), C. Chan, A. Trudel, M. Vetterli (*Simon Fraser Univ.*), A. Celler (*Univ. of Western Ontario*), R. Henderson (*Univ. of Melbourne-TRIUMF*)
597. β -decay branching ratios in ^{26}Ne and ^{27}Ne [inactive], P. McNeely, G. Roy (*Univ. of Alberta*), L. Buchmann, M. Dombbsky, J. Vincent (*TRIUMF*), J. D'Auria (*Simon Fraser Univ.*)
598. Pion-proton integral cross sections in the resonance region [completed data-taking], E. Friedman, A. Goldring, M. Schechter (*Hebrew Univ. of Jerusalem*), A. Altman (*Soreq NRC*), R.R. Johnson, D. Vetterli (*Univ. of British Columbia*), J. Jaki, M. Metzler (*Univ. Karlsruhe*), B.K. Jennings (*TRIUMF*)
599. Muons and muonium in solid hydrogen [completed data-taking], D. Arseneau, J.H. Brewer, K. Chow, T. Duty, D.G. Fleming, W.N. Hardy, M. Montour, G.D. Morris, D. Mould (*Univ. of British Columbia*), C. Ballard, M. Gingras, K. Hoyle, S.R. Kreitzman, M. Senba (*TRIUMF*), V.G. Storchak (*Kurchatov Inst.*)
600. μSR in high- T_c superconductors [active], J.H. Brewer, J.F. Carolan, K. Chow, T. Duty, P. Dosanjh, J. Elzey, W.N. Hardy, S. Johnston, R.F. Kiefl, R. Liang, A. MacFarlane, G.D. Morris, T.M. Riseman, I. Shinkoda, P.C.E. Stamp (*Univ. of British Columbia*), J. Akimitsu, A. Amano (*Aoyama-Gakuin Univ.*), E.J. Ansaldo, J. Boyle (*Univ. of Saskatchewan*), C. Ballard, K. Hoyle, S.R. Kreitzman, J.W. Schneider, M. Senba (*TRIUMF*), H. Zhou (*CTF Systems*), P. Mendels (*Orsay-UBC*), C. Niedermayer (*Univ. Konstanz-TRIUMF*), H. Glückler (*Univ. Konstanz*), G.M. Luke (*Columbia Univ.*), R. Cary, H.P. Cook, M. Davis, D.R. Noakes, M.U. Spurlock, C.E. Stronach (*Virginia State Univ.*), L.J. Campbell, L.L. Daemen (*Los Alamos National Lab*), A. Amato, F.N. Gygax, A. Schenck, M. Weber (*IMP/ETH Zürich*), H. Maletta (*KFA Jülich*), S. Lee (*Univ. of Birmingham*), T. Iwasaki, N. Nishida, S. Okuma, S. Shiratake (*Tokyo Inst. of Tech.*), N. Mohri (*ISSP, Univ. of Tokyo*), K. Nishiyama (*Univ. of Tokyo*) J. Sugiyama, S. Tanaka, H. Yamauchi (*SRL/ISTEC*), B. Martinez (*Univ. Barcelona*), Zhong Ming (*IHEP Beijing*)
601. Properties of the flux lattice in high- T_c superconductors [completed data-taking], J.H. Brewer, J.F. Carolan, K. Chow, T. Duty, P. Dosanjh, J. Elzey, W.N. Hardy, S. Johnston, R.F. Kiefl, R. Liang, A. MacFarlane, G.D. Morris, T.M. Riseman, I. Shinkoda, P.C.E. Stamp (*Univ. of British Columbia*), J. Akimitsu, A. Amano (*Aoyama-Gakuin Univ.*), E.J. Ansaldo, J. Boyle (*Univ. of Saskatchewan*), C. Ballard, K. Hoyle, S.R. Kreitzman, J.W. Schneider, M. Senba (*TRIUMF*), H. Zhou (*CTF Systems*), P. Mendels (*Orsay-UBC*), C. Niedermayer (*Univ. Konstanz-TRIUMF*), H. Glückler (*Univ. Konstanz*), G.M. Luke (*Columbia Univ.*), R. Cary, H.P. Cook, M. Davis, D.R. Noakes, M.U. Spurlock, C.E. Stronach (*Virginia State Univ.*), L.J. Campbell, L.L. Daemen (*Los Alamos National Lab*), A. Amato, F.N. Gygax, A. Schenck, M. Weber (*IMP/ETH Zürich*), H. Maletta (*KFA Jülich*), S. Lee (*Univ. of Birmingham*), T. Iwasaki, N. Nishida, S. Okuma, S. Shiratake (*Tokyo Inst. of Tech.*), N. Mohri (*ISSP, Univ. of Tokyo*), K. Nishiyama (*Univ. of Tokyo*) J. Sugiyama, S. Tanaka, H. Yamauchi (*SRL/ISTEC*), B. Martinez (*Univ. Barcelona*), Zhong Ming (*IHEP Beijing*)
603. $\mu^+\text{SR}$ studies of 1-dimensional magnetic systems [active], L.P. Le, G.M. Luke, B.J. Sternlieb, Y.J. Uemura, W.D. Wu (*Columbia Univ.*), J.H. Brewer, R. Kiefl, T.M. Riseman (*Univ. of British Columbia*), S.R. Kreitzman (*TRIUMF*), M. Mekata (*Fukui Univ.*), Y. Ajiro (*Kyoto Univ.*), K. Kakurai (*Tohoku Univ.*)
604. Slow muon physics (μSOL) [active], G. Aeppli, D. Bishop, A.T. Fiory, D.R. Harshman, R.N. Kleiman, A.P. Mills (*AT&T Bell Laboratories*), A.S. Rupaal, J.H. Turner* (*Western Washington Univ.*), M. Senba, D.Ll. Williams (*Univ. of British Columbia*)
605. Final muon states in semiconductors using rf μSR spectroscopy [completed data-taking], S.A. Dodds, T.L. Estle, B. Hitti (*Rice Univ.*), R.C. DuVarney (*Emory Univ.*), J. Brewer, K. Chow, D.Ll. Williams (*Univ. of British Columbia*), S.R. Kreitzman, J.W. Schneider, M. Senba (*TRIUMF*), C.D. Lamp, R.L. Lichti (*Texas Tech. Univ.*), S.F.J. Cox (*Rutherford Appleton Lab*), T. Pfiz (*Max Planck Inst.*), P. Mendes (*Univ. de Paris Sud*)

606. μ^+ SR studies of exotic superconductors [active], L.P. Le, G.M. Luke, B.J. Sternlieb, Y.J. Uemura, W.D. Wu (*Columbia Univ.*), J.H. Brewer, R. Kiefl, T.M. Riseman (*Univ. of British Columbia*), S.R. Kreitzman (*TRIUMF*), M.B. Maple, C.L. Seaman (*Univ. of California, San Diego*), M. Ishikawa (*Univ. of Tokyo, ISSP*), A.W. Sleight (*Oregon State Univ.*), R. Giannetta (*City Univ. of New York*), J.D. Jorgensen, G.D. Hinks (*Argonne National Lab*)
607. Isomeric muonated radicals [completed data-taking], G.B. Porter, D.C. Walker, Z. Wu (*Univ. of British Columbia*), M.V. Barnabas (*Argonne National Lab*), J.M. Stadlbauer* (*Hood College*), B.W. Ng (*Winona State Univ.*), K. Venkateswaran (*Hindustan Lever Ltd.*)
608. Muonium in GaP and GaAs [completed], E.J. Ansaldo (*Univ. of Saskatchewan*), K. Chow, S.R. Kreitzman, A. MacFarlane, T. Pfiz (*Univ. of British Columbia*), T.L. Estle, B. Hitti (*Rice Univ.*), R.C. DuVarney (*Emory Univ.*), R.F. Kiefl (*UBC-TRIUMF*), R.L. Lichti (*Texas Tech. Univ.*), J.W. Schneider (*TRIUMF*), C. Schwab (*CRN, Strasbourg*)
609. Fluorescence measurement of the vibrational energy distribution of $\text{MuF}(v)$ [active], D.J. Arseneau, S. Baer, D.G. Fleming, J.J. Pan, M. Senba, A. Tempelmann (*Univ. of British Columbia*), G.M. Marshall (*TRIUMF*), J.J. Sloan (*Univ. of Waterloo*)
610. Muonium dynamics and reactivity in Si at high temperature [completed], K. Chow, S.R. Kreitzman, A. MacFarlane (*Univ. of British Columbia*), T.L. Estle, B. Hitti (*Rice Univ.*), R.C. DuVarney (*Emory Univ.*), R.F. Kiefl (*UBC-TRIUMF*), R.L. Lichti (*Texas Tech. Univ.*), J.W. Schneider (*TRIUMF*), C. Schwab (*CRN, Strasbourg*), M. Senba (*TRIUMF-UBC*)
611. μ SR investigations of RT_2 intermetallics (R=rare earth, T=transition metal) [completed data-taking], G.M. Kalvius, A. Kratzer, K-H. Münch, M. Weber (*Tech. Univ. Munich*), L. Asch (*Univ. of Munich*), R. Wäppling (*Univ. Uppsala*), J. Deportes (*CRNS Grenoble*), J.H. Brewer, K. Chow, R.F. Kiefl (*Univ. of British Columbia*), S.R. Kreitzman, J. Schneider (*TRIUMF*)
612. Hyperfine dependence of exclusive muon capture on ^{19}F , ^{23}Na , ^{27}Al , ^{35}Cl , and ^{37}Cl [completed data-taking], D.S. Armstrong (*Virginia Polytech. Inst. & State Univ.*), T.P. Gorrings, B. Johnson, J. Bauer, M. Kovash, M. Pickar (*Univ. of Kentucky*), M. Hasinoff, D. Measday, B. Mofteh (*Univ. of British Columbia*), D. Wright (*TRIUMF*)
613. Reactions of muonic hydrogen isotopes [completed data-taking], G.A. Beer, M. Maier, G.R. Mason, A. Olin, T. Porcelli (*Univ. of Victoria*), G.M. Marshall (*TRIUMF*), M.C. Fujiwara (*Univ. of British Columbia*), R. Jacot-Guillarmod, P.E. Knowles, F. Mulhauser, L.A. Schaller (*Univ. de Fribourg*), T.M. Huber (*Gustavus Adolphus College*), P. Kammel (*Lawrence Berkeley Lab*), J. Zmeskal (*IMEP Vienna*), A.R. Kunselman (*Univ. of Wyoming*), C. Petitjean, V. Markushin (*PSI*), J.M. Bailey (*Chester Technology*), S.K. Kim (*Jeonbuk National Univ.*), A. Adamczak (*Inst. Nuclear Physics, Krakow*), M. Faifman (*RRC Kurchatov Inst.*)
614. Precise measurement of the ρ , σ and $(P_\mu\xi)$ parameters in muon decay [active], M. Comyn, D.R. Gill, P. Gumpinger, R. Helmer, R. Henderson, J.A. Macdonald, A. Olin, D. Ottewell, R. Openshaw, J.-M. Poutissou, R. Poutissou, G. Sheffer, D. Wright (*TRIUMF*), P. Depommier (*Univ. of Montréal*), P. Green, P. Kitching, M. Quraan, N. Rodning, F. Sobratee, J. Soukup, G.M. Stinson (*Univ. of Alberta*), M. Hasinoff (*Univ. of British Columbia*), E.L. Mathie, R. Tacik (*Univ. of Regina*), W. Shin (*Univ. of Saskatchewan*), Y. Davydov (*JINR, Moscow*), C. Gagliardi, J. Hardy, J. Musser, R. Tribble, M. Vasiliev (*Texas A&M Univ.*), D. Koetke, R. Manweiler, P. Nord, S. Stanislaus (*Valparaiso Univ.*), A. Khruchinsky, V. Selivanov, V. Torokhov (*KIAE, Moscow*), E. Korkmaz, T. Porcelli (*Univ. of Northern British Columbia*)
615. Normal and sideways spin observables for the reaction $\bar{p}\bar{n} \rightarrow pp(^1S_0)\pi^-$ [deferred], D. Ashery, H. Han, M. Moinester, S. Ram, A. Yavin (*Tel Aviv Univ.*), C. Chan, O. Häusser*, B. Larson, A. Rahav (*Simon Fraser Univ.*), P. Delheij, D. Hutcheon, P. Levy, M. Vetterli (*TRIUMF*), F. Duncan, G. Jones (*Univ. of British Columbia*), R. Henderson (*TRIUMF-Univ. of Melbourne*),
616. Spin-momentum correlations of nucleons in polarized ^3He [completed data-taking], W.P. Alford, A. Celler (*Univ. of Western Ontario*), C. Chan, B. Larson, A. Rahav, A. Trudel, Bin Xiao (*Simon Fraser Univ.*), T.E. Chupp (*Harvard Univ.*), P. Delheij, K.P. Jackson, P. Levy, M. Vetterli (*TRIUMF*), O. Häusser* (*SFU-TRIUMF*), R. Henderson (*Univ. of Melbourne-TRIUMF*), D.M. Whittall (*NAC South Africa*), R. Woloshyn (*TRIUMF-SFU*)
617. Mass and decay studies of nuclei near the proton dripline [completed data-taking], J. Batchelder, D.M. Moltz, T. Ognibene (*Lawrence Berkeley Lab*), P.L. Reeder (*Pacific Northwest Lab*), J. D'Auria (*SFU-TRIUMF*), M. Dombisky (*Simon Fraser Univ.*), L. Buchmann (*TRIUMF*), P. McNeely (*Univ. of Alberta*), K. Toth (*Oak Ridge National Lab*)
618. pp elastic cross sections at TRIUMF energies [deferred], C. Chan, S. Burzynski, B. Larson, A. Rahav, A. Trudel, Bin Xiao (*Simon Fraser Univ.*), O. Häusser* (*SFU-TRIUMF*), R. Abegg*, R. Helmer, D. Hutcheon,

33

9

- K.P. Jackson, C.A. Miller, D. Ottewell, M. Vetterli, P. Walden, S. Yen (*TRIUMF*), W.P. Alford, A. Celler (*Univ. of Western Ontario*), R. Henderson (*Univ. of Melbourne-TRIUMF*), D.M. Whittal (*NAC South Africa*), A. Yavin (*Tel Aviv Univ.*)
619. Studies on high- T_c superconductor LaSrCuO with (μ^-0) probes [completed data-taking], K. Nishiyama, K. Nagamine (*Univ. of Tokyo*), E. Torikai, H. Kojima, I. Tanaka (*Univ. of Yamanashi*), H. Kitazawa (*RIKEN*), R. Saito (*Univ. of Electro-communications*)
620. μ^- SR study in trans-(CH) x [active], K. Nagamine, K. Nishiyama, S. Ikehata, N. Oda (*Univ. of Tokyo*)
621. Studies on secondary electron emission in μ -foil interactions [active], T. Azuma, Y. Miyake, K. Nishiyama, Y. Watanabe, Y. Yamazaki (*Univ. of Tokyo*), K. Nagamine (*Univ. of Tokyo-RIKEN*), T. Matsuzaki (*RIKEN*), K. Kuroki (*Inst. Police Science, Tokyo*)
622. Normal and anomalous muonium in ^{13}C diamond [active], J.W. Schneider (*TRIUMF*), E.J. Ansaldò (*Univ. of Saskatchewan*), K. Chow, S.R. Kreitzman, A. MacFarlane (*Univ. of British Columbia*), S. Connell, J.P.F. Sellschop, M.C. Stemmet (*Univ. of the Witwatersrand*), T.L. Estle, B. Hitti (*Rice Univ.*), R.C. DuVarney (*Emory Univ.*), R.F. Kiefl (*UBC-TRIUMF*), D. Lamp, R.L. Lichti (*Texas Tech. Univ.*), C. Schwab (*CRN, Strasbourg*)
623. Kinematically complete measurements of quasifree pion-nucleus single and double scattering reactions [inactive], G. Burleson, G. Kyle, S. Mukhopadhyay, M. Rawool, (*New Mexico State Univ.*), P.A. Amaudruz, D. Ottewell, G.R. Smith (*TRIUMF*), N. Chant, P. Roos (*Univ. of Maryland*), A. Klein (*Old Dominion Univ.*), J.T. Brack (*Univ. of British Columbia*)
624. The ($\pi, 2\pi$) reaction, a tool to determine scattering lengths and coupling constants [completed data-taking], F. Bonutti, P. Camerini, E. Fragiaco, N. Grion, R. Rui (*Univ. of Trieste*), S. McFarland, P. Tagliente (*Univ. of British Columbia*), P. Amaudruz, L. Felawka, D. Healey, D. Ottewell, K. Raywood, G. Smith (*TRIUMF*), E. Mathie, R. Tacik, M. Yeomans (*Univ. of Regina*), J. Brack, G. Hofman, R. Ristinen (*Univ. of Colorado*), J. Clark, M. Sevier (*Univ. of Melbourne*), E. Gibson (*California State Univ., Sacramento*), V. Mayorov, O. Patarakin, V. Tikhonov (*Kurchatov Inst.*), R. Meier (*Univ. Tübingen*)
625. Low energy pion-nucleus reaction and total cross sections [completed data-taking], S. Høibråten, M. Kohler, B. Kriss, R.J. Peterson, R.A. Ristinen, J. Wise (*Univ. of Colorado*), J.T. Brack, D. Ottewell (*TRIUMF*), R.R. Johnson (*Univ. of British Columbia*), D. Oakley (*Lewis & Clark Univ.*)
626. The characterization of the emitting source in fragment production [deferred], R. Korteling (*Simon Fraser Univ.*), K.P. Jackson (*TRIUMF*), V. Viola (*Indiana Univ.*), K. Kwiatkowski (*IUCF*), S. Kaufmann (*Argonne National Lab*)
627. A search for narrow resonant-like structures in pp and pA interactions using the polarized proton beam at TRIUMF [completed data-taking], V.V. Avdeichikov, V.A. Nikitin, P.V. Nomokonov, A.V. Pavlik (*JINR*), A. Gafarov, A. Kadishnov, Yu. Koblik, V. Pirogov, B.S. Yuldashev (*Inst. of Nucl. Phys., Tashkent*), S. Kan, A. Khaneles, A. Pak, E. Surin, K. Turdaliev (*Phys. Tech. Inst., Tashkent*), S. Yen (*TRIUMF*), V. Chaloupka, W. Dougherty, G. Liang, H.J. Lubatti, T. Zhao (*Univ. of Washington*)
628. A search for deeply bound pionic states in heavy nuclei via the pion production reaction $^{208}\text{Pb}(n, d)$ [complete], S. Burzynski, D. Frekers, D. Hutcheon, K.P. Jackson, Y. Kuno, O. Häusser*, C.A. Miller, A. Olin, A. Trudel, M. Vetterli, S. Yen (*TRIUMF*), M.H. Tanaka, T. Yamazaki (*INS Tokyo*), N. Matsuoka (*Osaka Univ.*), A. Okihana (*Kyoto Univ. of Education*)
629. GT^+ strength distribution of astrophysical interest in (fp) shell nuclei [completed], W.P. Alford, A. Celler (*Univ. of Western Ontario*), D. Frekers, K.P. Jackson, K. Lee, M. Vetterli (*TRIUMF*), R. Henderson (*TRIUMF-Univ. of Melbourne*), S. Burzynski, A. Rahav, A. Trudel (*Simon Fraser Univ.*), S. El-Kateb (*King Fahd Univ. of Petroleum and Minerals*)
630. Elastic proton scattering from sideways- and longitudinally-polarized ^3He [completed data-taking] D.M. Whittal (*NAC South Africa-SFU*), R. Abegg*, P. Delheij, P. Levy, M. Vetterli (*TRIUMF*), W.P. Alford (*Univ. of Western Ontario*), E.J. Brash, C. Chan, B. Larson, A. Rahav, A. Trudel (*Simon Fraser Univ.*), T.E. Chupp (*Harvard Univ.*), O. Häusser* (*SFU-TRIUMF*), R. Henderson (*Univ. of Melbourne-TRIUMF*), J.P. Svenne (*Univ. of Manitoba*)
631. Giant spin excitation in ^{238}U [completed data-taking], R. Abegg*, A. Celler, D. Frekers, R. Henderson, K.P. Jackson, C.A. Miller, A. Trudel, M. Vetterli, S. Yen (*TRIUMF*), P.W. Green (*TRIUMF-Univ. of Alberta*), A. Richter, H. Woertche (*Univ. of Darmstadt*)
632. Dilepton production in nucleon-nucleus collisions [deferred], A. Stetz, L.W. Swenson (*Oregon State Univ.*), K. Hicks (*Ohio University*), P. Walden (*TRIUMF*), F. Farzanpay, P. Fuchs, J. Zhao (*Ohio State Univ.*)

633. A measurement of $p + p \rightarrow p + n + \pi^+$ at 420 and 500 MeV [active], K. Hicks (*Ohio Univ.*), M. Benjamintz, W.R. Falk, R.G. Pleydon (*Univ. of Manitoba*), R. Abegg*, D. Hutcheon, A. Miller, P. Walden, S. Yen (*TRIUMF*), M. Hartig (*Univ. of Munster*), G. O'Reilly (*Univ. of Northern British Columbia*)
634. Investigation of the $(p, d\pi^+)$ reaction in the quasifree region [active], M. Benjamintz, J.R. Campbell, W.R. Falk, A. Green (*Univ. of Manitoba*), P.L. Walden, S. Yen (*TRIUMF*), E. Korkmaz (*Univ. of Northern British Columbia*), E.G. Auld (*Univ. of British Columbia*)
635. Experimental survey of the (\bar{p}, π^-) reaction in the Δ -region [active], E. Korkmaz (*Univ. of Northern British Columbia*), R. Abegg*, D.A. Hutcheon, A. Lang, P.L. Walden, S. Yen (*TRIUMF*), W.C. Olsen, A.K. Opper, M. Punyasena (*Univ. of Alberta*), E.G. Auld, G. Jones (*Univ. of British Columbia*), R.D. Bent (*IUCF*), J. Campbell, W.R. Falk (*Univ. of Manitoba*)
636. The $^{12}\text{C}(p, p'\pi^\pm)$ reaction to discrete final states [active], A. Celler, D. Frekers, C.A. Miller, A. Trudel, P. Walden, S. Yen (*TRIUMF*), E.G. Auld, G. Jones (*Univ. of British Columbia*), W. Falk (*Univ. of Manitoba*), E. Korkmaz (*Univ. of Alberta*), L. Bland, T. Londergan, R. Mehrem, P. Schwandt, G. Walker (*Indiana Univ.*), B.K. Jain (*Bhabha Inst.*)
637. Nucleon knockout with SASP [active], R. Abegg*, D. Frekers, P.W. Green, D.A. Hutcheon, C.A. Miller, P.L. Walden (*TRIUMF*), N.S. Chant, P. Roos (*Univ. of Maryland*), E.D. Cooper (*Ohio State Univ.*), L.G. Greeniaus (*TRIUMF-Univ. of Alberta*), K. Hicks (*Ohio Univ.*), P. Kitching, W.J. McDonald, W.C. Olsen (*Univ. of Alberta*), D. Mack (*CEBAF*), O. Maxwell (*Florida State Univ.*)
638. $\pi^+ \rightarrow e^+\nu\gamma$ in flight with the high intensity 240 MeV/c pion beam at TRIUMF [deferred], G. Atoyan, V. Bolotov, S. Gninenko, E. Guschin, V. Isakov, A. Kovzelev, V. Marin, Yu. Musienko, A. Poblaguev, V. Postoev, I. Semenjuk, S. Volkov (*INR Moscow*), V. Semenov (*IHEP Protvino*), P. Depommier (*Univ. de Montréal*)
639. Muonium enhancement effects in micelles [completed], G.B. Porter, D.C. Walker, Z. Wu (*Univ. of British Columbia*), M.V. Barnabas (*Argonne National Lab*), J.M. Stadlbauer* (*Hood College*), K. Venkateswaran (*Hindustan Lever Ltd.*), B.W. Ng (*Winona State Univ.*)
640. Search for magnetic correlations in the orthorhombic compounds CeTSn ($T = \text{Ni, Pt, Pd}$) [active], L. Asch, G.M. Kalvius, A. Kratzer, K.-H. Münch, M. Weber (*Tech. Univ. of Munich*), R.F. Kiefl (*UBC-TRIUMF*), R. Wäppling (*Univ. of Uppsala*), T. Takabatake (*Hiroshima Univ.*)
641. Kinetic isotope effects in H-atom abstraction reactions by muonium: $\text{Mu} + \text{CH}_4$ and $\text{Mu} + \text{CD}_4$ [completed], D. Arseneau, D.G. Fleming, J.J. Pan, R. Snooks (*Univ. of British Columbia*), S. Baer, M. Senba (*UBC-TRIUMF*), A. Gonzalez (*Univ. of Southern California, Los Angeles*)
642. μSR studies on doped- C_{60} superconductors [completed data-taking], A. Keren, L.P. Le, G.M. Luke, B. Sternlieb, Y.J. Uemura, W.D. Wu (*Columbia Univ.*), J.H. Brewer, R.F. Kiefl, T.M. Riseman (*Univ. of British Columbia*), G. Gruner, K. Holczer (*UCLA*), S.R. Kreitzman (*TRIUMF*)
643. A test of the low-energy theorem for radiative pion capture [completed data-taking], B. Bassalleck (*Univ. of New Mexico*), C. Gossett (*Univ. of Washington*), D. Hutcheon, R. Jacot-Guillarmod, D. Ottewell, R. Schubank, N.R. Stevenson (*TRIUMF*), M.A. Kovash, K. Liu (*Univ. of Kentucky*), E. Korkmaz, A. Opper (*Univ. of Alberta*), J. Miller (*Boston Univ.*), Y.M. Shin (*Univ. of Saskatchewan*)
645. Absolute differential cross sections in the $\pi^\pm + p \rightarrow \pi^\pm + p$ reaction around the Δ resonance [completed data-taking], F. Duncan, A. Feltham, G. Jones, J. Lange, M.M. Pavan, K. Raywood, M.E. Sevier (*Univ. of British Columbia*), R. Adams, J. Brack, R. Helmer, D.F. Ottewell, G.R. Smith, B. Wells (*TRIUMF*), R.A. Ristinen (*Univ. of Colorado*), I. Strakovski (*Virginia Tech. Inst.*), E.L. Mathie, R. Tacik (*Univ. of Regina*), H. Staudenmaier (*Univ. of Karlsruhe*)
646. μSR study of $\text{GaAs}/\text{Al}_x\text{Ga}_{1-x}\text{As}$ superlattices and 2D electron gases [completed data-taking], J.H. Brewer, K. Chow, R.F. Kiefl, S.R. Kreitzman, A. MacFarlane, T. Tiedje (*Univ. of British Columbia*), S.A. Dodds, T.L. Estle (*Rice Univ.*), R.C. DuVarney (*Emory Univ.*), D. Lamp, R.L. Lichti (*Texas Tech. Univ.*), J.W. Schneider, C. Zhang (*TRIUMF*), C. Schwab (*CRN, Strasbourg*)
647. μ^- transfer and mesomolecule formation in D_2 -He mixture [completed data-taking], M. Iwasaki, S. Sakamoto, P. Strasser (*Univ. of Tokyo*), K. Nagamine (*Univ. of Tokyo-RIKEN*), K. Ishida, T. Matsuzaki, Y. Watanabe (*RIKEN*), M. Kamimura (*Kyushu Univ.*), E. Torikai (*Yamanashi Univ.*)
648. Magnetism and superconductivity in heavy fermion systems [completed data-taking], G.M. Luke, A. Keren, L.P. Le, B.J. Sternlieb, Y.J. Uemura, W.D. Wu (*Columbia Univ.*), J.H. Brewer, R. Kiefl, T.M. Riseman (*Univ. of British Columbia*), S.R. Kreitzman (*TRIUMF*), M.B. Maple, C.L. Seaman (*Univ. of California, San Diego*), Y. Onuki (*Univ. of Tsukuba*)
650. Kinetic isotope effects favouring muonium [active], G.B. Porter, D.C. Walker (*Univ. of British Columbia*), J.M. Stadlbauer* (*Hood College*), K. Venkateswaran (*Hindustan Lever Ltd.*), H.A. Gillis (*St. Francis Xavier Univ.*)

651. Gamow-Teller unit cross section from $^{64}\text{Ni}(n,p)^{64}\text{Co}(\text{g.s.})$ [active], W.P. Alford (*Univ. of Western Ontario*), E.J. Brash, W. Cummings, W. Kielhorn, A. Trudel (*Simon Fraser Univ.*), O. Häusser* (*SFU-TRIUMF*), R. Henderson, K.P. Jackson, M.C. Vetterli, S. Yen (*TRIUMF*), R.L. Boudrie, J. Ullmann (*LAMPF*), S. El-Kateb (*King Fahd Univ. of Petroleum and Minerals*), H.T. Fortune (*Univ. of Pennsylvania*)
652. Spin-momentum distributions of protons in polarized ^3He [completed data-taking], E. Brash, W. Cummings, W. Kielhorn (*Simon Fraser Univ.*), P. Delheij, R. Henderson, M. Vetterli, S. Yen (*TRIUMF*), M. Epstein, D. Margaziotis (*California State Univ.*), O Häusser* (*SFU-TRIUMF*), R. Woloshyn (*TRIUMF-SFU*)
653. Measurement of the $\pi^+\pi^-$ invariant mass in nuclei. A tool for determining the mass distribution of the σ meson [completed data-taking], P. Amaudruz, J. Brack, D. Ottewell, G.R. Smith (*TRIUMF*), G. Jones, R.R. Johnson, M.E. Sevier (*Univ. of British Columbia*), E.L. Mathie, R. Tacik (*Univ. of Regina*), R.A. Ristinen (*Univ. of Colorado*), G.S. Kyle (*New Mexico State Univ.*), P. Schuck (*ISN Grenoble*), G. Chanfray (*IPN Lyon*), P. Camerini, R. Rui (*Univ. di Trieste*), N. Grión (*INFN Trieste*)
654. Muon investigations of fullerene chemistry [complete], B. Addison-Jones, J.-C. Brodovitch, F. Ji, P.W. Percival (*Simon Fraser Univ.*), D.M. Bartels (*Argonne National Lab*)
655. Total cross section for the $p(\pi^+, \pi^+\pi^0)$ reaction near threshold [completed data-taking], R.R. Johnson, N. Suen (*UBC-TRIUMF*), N. Fazel, V. Sossi (*Univ. of British Columbia*), A. Altman (*TRIUMF-Tel Aviv Univ.*), E. Friedman, M. Paul, M. Schechter (*Hebrew Univ. Jerusalem*), G.J. Wagner (*Univ. Tübingen*)
656. A comparison of the (n,p) and (μ^-, ν) reactions on ^{23}Na [completed data-taking], W.P. Alford (*Univ. of Western Ontario*), J. Bauer, J. Evans, T.P. Gorringer, B. Siebels (*Univ. of Kentucky*), S. El-Kateb (*King Fahd Univ. of Petroleum and Minerals*), R. Helmer, K.P. Jackson, S. Yen (*TRIUMF*), A. Trudel (*Simon Fraser Univ.*)
657. Longitudinal μ^- SR studies on high T_c superconductor LaSrCuO [completed data-taking], H. Kojima, I. Tanaka, E. Torikai (*Yamanashi Univ.*), K. Kojima, K. Nagamine, K. Nishiyama (*Univ. of Tokyo*), H. Kitazawa (*RIKEN*)
658. Application of μ SR to the study of solid C_{60} compounds [active], E.J. Ansaldo (*Univ. of Saskatchewan*), J.H. Brewer, K. Chow, T.L. Duty, J. Elzey, R.F. Kiefl, A. MacFarlane (*Univ. of British Columbia*), R.C. DuVarney (*Emory Univ.*), T.L. Estle, B. Hitti (*Rice Univ.*), J. Fischer (*Univ. of Pennsylvania*), D. Lamp, R.L. Lichti (*Texas Tech. Univ.*), J.W. Schneider (*TRIUMF*), C. Schwab (*CRN Strasbourg*)
659. Production of slow and monoenergetic $(^3\text{H} \mu^-)^+$ beam from the decay of $(d^3\text{He} \mu)$ molecule [active], M. Iwasaki, K. Nagamine, S. Sakamoto, P. Strasser (*Univ. of Tokyo*), K. Ishida (*RIKEN*), E. Torikai (*Yamanashi Univ.*)
660. Gamow-Teller strength distributions from $^{13}\text{C}(n,p)^{13}\text{B}$ and $^{27}\text{Al}(n,p)^{27}\text{Mg}$ [completed data-taking], W.P. Alford (*Univ. Western Ontario*), S. Burzynski (*Simon Fraser Univ.*), H.T. Fortune, P. Hui, R. Ivie, M. McKinzie, D.A. Smith, A.L. Williams (*Univ. of Pennsylvania*), O. Häusser* (*SFU-TRIUMF*), R. Henderson, K.P. Jackson, M. Vetterli (*TRIUMF*)
661. The neutron-neutron scattering length via $\pi^-d \rightarrow \gamma nn$ [completed data-taking], B. Bassalleck, H. Fischer, D. Wolfe (*Univ. of New Mexico*), E. Christy, T.P. Gorringer, C. Jiang, M.A. Kovash, K. Liu, (*Univ. of Kentucky*), E. Korkmaz (*Univ. of Northern British Columbia*), D. Measday, M. Saliba, T. Stocki (*Univ. of British Columbia*), D. Ottewell (*TRIUMF*), A. Opper (*Univ. of Alberta*), K.S. Sim (*Korea Univ.*), J. Stasko (*Michigan State Univ.*)
662. Complete beta-delayed one- and two-proton emission study of ^{22}Al [letter of intent], J.C. Batchelder, J. Cerny, D.M. Moltz, T. Ognibene, M.W. Rowe, R.J. Tighe (*Lawrence Berkeley Lab*), J. D'Auria, M. Dombisky (*Simon Fraser Univ.*), L. Buchmann, J. Vincent (*TRIUMF*)
663. Study of the Δ isobar admixture in nuclei and search for exotic states [active], R. Abegg*, L. Lee, S. Yen (*TRIUMF*), G. Jones (*Univ. of British Columbia*), A. Gorelov (*Kurchatov Inst.*), F. Khanna (*Univ. of Alberta*), A. Kotov, D. Seliverstov, I.I. Strakovsky, L. Uvarov (*St. Petersburg Nuclear Physics Inst.*)
664. Muonium formation and reaction on powdered platinum surface [active], R. Kadono, A. Matsushita (*RIKEN*), K. Nishiyama (*Univ. of Tokyo*), K. Nagamine (*Univ. of Tokyo-RIKEN*)
665. Muon spin relaxation in quasicrystals [active], E.J. Ansaldo (*Univ. of Saskatchewan*), J.H. Brewer (*Univ. of British Columbia*), G.M. Luke (*Columbia Univ.*), P. Mendels (*Univ. Paris Sud Orsay*), D.R. Noakes, C.E. Stronach (*Virginia State Univ.*), S.J. Poon (*Univ. of Virginia*)
666. A search for deeply bound pionic atoms via the radiative pion capture reaction $^{208}\text{Pb}(\pi^-, \gamma)$ [completed data-taking], R.R. Johnson, G. Jones, J. Lange, S. McFarland, K.J. Raywood, M.E. Sevier (*Univ. of British Columbia*), A. Altman, D.A. Hutcheon, S. Yen (*TRIUMF*)
667. Interference of Fermi and Gamow-Teller amplitudes in the $^3\text{He}(\bar{n}, p)\text{T}$ reaction [active], R. Abegg*, P. Delheij, E. Henderson, K.P. Jackson, M.C. Vetterli, S. Yen (*TRIUMF*), W.P. Alford (*Univ. of Western Ontario*),

- E.J. Brash, S. Burzinsky, W. Cummings, E. Gete, W.B. Lorenzon (*Simon Fraser Univ.*), O. Häusser* (*SFU-TRIUMF*), C. Horowitz (*Indiana Univ.*), K. Hicks, B.W. Larson, J. Rapaport (*Ohio Univ.*), L. Ray (*Univ. of Texas*)
668. de Haas van Alphen oscillations in the muon Knight shift in antimony metal [active], S. Johnston, R.F. Kiefl, E. Koster, D.Ll. Williams (*Univ. of British Columbia*), S.R. Kreitzman (*TRIUMF*)
669. μ^+ SR in exotic single-crystal superconductors [active], G. Aeppli, B. Batlogg, D. Bishop, C. Broholm, R.J. Cava, G.P. Espinosa, D.R. Harshman, R.N. Kleinman, L.F. Schneemeyer (*AT&T Bell Labs*), E.J. Ansaldo (*Univ. of Saskatchewan*), E. Bucher (*AT&T Bell Labs-Univ. Konstanz*), T.M. Riseman, D.Ll. Williams (*Univ. of British Columbia*)
670. Radiative muon capture on nuclei [active], D.S. Armstrong (*College of William and Mary*), P. Depommier (*Univ. de Montréal*), B. Doyle, T.P. Goringe (*Univ. of Kentucky*), P. Bergbusch, M.D. Hasinoff, D. Sample, E. Saettler (*Univ. of British Columbia*), C. Chen, P. Gumplinger, J.A. Macdonald, J.-M. Poutissou, R. Poutissou, D.H. Wright (*TRIUMF*), M. Blecher, C. Sigler (*Virginia Polytechnic Inst. & State Univ.*)
671. Muonium's pH-dependence [active], G.B. Porter, D.C. Walker (*Univ. of British Columbia*), J.M. Stadlbauer* (*Hood College*), M.V. Barnabas (*Proctor & Gamble Ltd.*), K. Venkateswaran (*Hindustan Lever Ltd.*)
672. μ SR studies of Kagome lattice and other frustrated spin systems [active], A. Keren, L. Le, G. Luke, Y.J. Uemura, W.D. Wu (*Columbia Univ.*) Y. Ajiro, M. Mekata (*Fukui Univ.*), H. Kikuchi (*Tsukuba Univ.*), M. Takano (*Kyoto Univ.*), K. Kakurai (*ISSP, Tokyo Univ.*)
673. μ SR studies of Tl₂201 and infinite layer cuprate high-T_c systems [active], L.P. Le, G.M. Luke, Y.J. Uemura, W.D. Wu (*Columbia Univ.*) K. Kajima, S. Uchida, (*Tokyo Univ.*), Y. Kubo (*NEC Research Inst.*), M. Takano (*Kyoto Univ.*), J.T. Markert (*Univ. of Texas*), J.H. Brewer (*TRIUMF-UBC*)
674. Measurements of exclusive muon capture rates in the 1s-0d shell [active], J. Bauer, J. Evans, T. Goringe, B. Johnson, M. Kovash (*Univ. of Kentucky*), P. Gumplinger, M. Hasinoff, D. Measday, B. Moftah (*Univ. of British Columbia*), D. Armstrong (*Univ. of California, Berkeley*), D. Wright (*TRIUMF*)
675. Irradiation of silicon tracker component [completed data-taking], M. Frautschi, J.A.J. Matthews, S. Seidel (*Univ. of New Mexico*), A. Grillo, K. O'Shaughnessy, W.A. Rowe, H. Sadrozinski, E. Spencer, A. Webster, M. Wilder (*Univ. of California, Santa Cruz*), S.S. Han, A.P.T. Palounek, H. Ziock (*Los Alamos National Lab*), T. Collins, I. Kipnis, H. Spieler (*Lawrence Berkeley Lab*), J. Krizmanic, J. Skarha (*Johns Hopkins Univ.*), M. Cheng, M.-L. Chu, G. Rurngsheng, P.K. Teng (*Academica Sinica*), E. Kajfasz, J. Pawlak, P. Ratzmann, J. Spalding, L. Spiegel (*Fermilab*), T. Ohsugi (*Hiroshima Univ.*), H. Iwasaki, T. Kondo, S. Terada, Y. Unno (*KEK*), J. Boudreau, T. Huffman, P. Shepard (*Univ. of Pittsburgh*), B. Tannenbaum (*Texas A&M Univ.*), D. Benjamin, A. Sill (*Texas Tech. Univ.*)
676. Forward diproton production in deuterium and hydrogen [active], R. Abegg*, K.P. Jackson, C.A. Miller, P. Walden, S. Yen (*TRIUMF*), W.P. Alford (*Univ. of Western Ontario*), S. Burzynski, A. Trudel (*Simon Fraser Univ.*)
677. Surface interactions and motions of radicals in zeolites [active], D.J. Arseneau, D.G. Fleming, C.A. Fyfe, M. Shelley, J. Pan (*Univ. of British Columbia*), E. Roduner (*Univ. of Zürich*), S. Kreitzman, M. Senba (*TRIUMF*)
678. Beta delayed deuteron emission from ⁶He [active], L. Buchmann, K.P. Jackson (*TRIUMF*), J.M. D'Auria, R.G. Korteling (*Simon Fraser Univ.*), M. Dombisky (*SFU-Univ of Alberta*), U. Giessen (*TRIUMF-Univ. of Toronto*), J. King (*Univ. of Toronto*), V.G. Lind, Z.-Y. Zhou (*Utah State Univ.*), P. McNeely, G. Roy (*Univ. of Alberta*), P. Reeder (*Pacific Northwest Lab*)
679. Systematic study of 3D-transition metal oxides by μ SR [active], W. Higemoto, T. Iwasaki, H. Nishida, H. Nishiki, M. Sekino (*Tokyo Inst. of Technology*), P. Birrer, K. Kojima, K. Nishiyama (*Univ. of Tokyo*)
680. Muonium diffusion in ice [active], B. Addison-Jones, J.-C. Brodovitch, F. Ji, P. Percival (*Simon Fraser Univ.*), D.M. Bartels (*Argonne National Lab*)
681. Decay properties of extremely neutron-rich noble-gas nuclides [active], L. Buchmann, U. Giessen (*TRIUMF*), J. D'Auria (*Simon Fraser Univ.*), P.L. Reeder (*Pacific Northwest Lab*), M. Dombisky (*SFU-Univ. of Alberta*), P. McNeely, G. Roy (*Univ. of Alberta*)
682. Nuclear studies of ⁹B, ⁸B, and ⁵Li [completed data-taking], R.E. Azuma, J.D. King, J. Powell (*Univ. of Toronto*), L. Buchmann, C. Iliadis (*TRIUMF*), K.P. Jackson (*TRIUMF-SFU*), J. D'Auria, R. Korteling (*Simon Fraser Univ.*), M. Dombisky (*Univ. of Toronto-Univ. of Alberta*), U. Giesen (*TRIUMF-Univ. of Alberta*), G. Roy (*Univ. of Alberta*)

683. Asymmetries following muon capture by polarized muonic ^3He [active], J. Behr, A. Gorelov, W. Lorenzon (*Simon Fraser University*), W. Cummings, P. Delheij, G.M. Marshall (*TRIUMF*), M. Hasinoff, J.C. Huang, E. Saettler (*Univ. of British Columbia*), O. Häusser* (*SFU-TRIUMF*), K. Hicks (*Ohio Univ.*), P. Bogorad, G.D. Cates, K. Kumar, A. Young (*Princeton Univ.*), R. Holmes, J. McCracken, P. Souder, X. Wang (*Syracuse Univ.*), B. Larson (*Univ. of Minnesota*), D. Tupa (*Los Alamos National Lab*)
684. μSR spin relaxation studies of small molecules in the gas phase [active], D. Arseneau (*TRIUMF*), D. Fleming, J.J. Pan (*UBC-TRIUMF*), M. Senba (*Dalhousie Univ.*), T. Claxton (*Univ. of Leicester*), S.F.J. Cox (*Rutherford Appleton Lab.*), U. Himmer, E. Roduner (*Univ. of Stuttgart*)
685. Muonium in CVD-diamond films [active], R.F. Kiefl, A. MacFarlane (*Univ. of British Columbia*), S.H. Connell, J.P.F. Sellschop, C.G. Smallman (*Univ. of the Witwatersrand*), T.L. Estle, B. Hitti (*Rice Univ.*)
686. ^{18}O PNC [active], P. McNeely, G. Roy (*Univ. of Alberta*), L. Buchmann (*TRIUMF*), J.M. D'Auria (*Simon Fraser Univ.*), M. Dombisky (*Univ. of Alberta-SFU*), U. Giesen (*TRIUMF-Univ. of Toronto*), K.P. Jackson (*TRIUMF-SFU*), J. Powell (*Univ. of Toronto*)
687. μSR investigation of frustrated antiferromagnets $\text{Tb}_2\text{Mo}_2\text{O}_7$, $\text{Y}_2\text{Mo}_2\text{O}_7$ and LiNiO_2 [active], J. Brewer, J. Chakhalian, S. Dunsiger, R. Kiefl, A. MacFarlane, R.I. Miller, J. Sonier (*Univ. of British Columbia*), J. Gardner, B. Gaulin, J. Greedan (*McMaster Univ.*), M. Gingras (*TRIUMF*), G. Luke, Y.J. Uemura (*Columbia Univ.*), K. Kojima (*Univ. of Tokyo*)
688. Pion production through $n+p \rightarrow ^2\text{He}+\pi^-$ [active], R. Abegg*, D.A. Hutcheon, W. Kellner, A. Ling, C.A. Miller, P. Walden, S. Yen (*TRIUMF*), D. Frekers, W. Garske, V. Hennen, M. Hartig, H.J. Wörtche (*Westfälische-Wilhelms Univ. at Münster*), A.K. Opper (*Univ. of Ohio*), J.A. Niskanen (*Univ. of Helsinki*), H. Machner (*KFA Jülich*)
691. TF- μ^+ SR lineshape in high- T_c superconductors [active], D.A. Bonn, J.H. Brewer, J. Chakhalian, S. Dunsiger, W.N. Hardy, R.F. Kiefl, R. Liang, R.I. Miller, A. Price (*Univ. of British Columbia*), D.R. Noakes, C.E. Stronach (*Virginia State Univ.*), S.R. Kreitzman (*TRIUMF*), J.E. Sonier (*Los Alamos National Lab*)
692. Quantum diffusion of muonium in cryocrystals: probing microscopic crystalline defects with muons [active], A. Benbasat, J.H. Brewer, D.G. Fleming, W.N. Hardy, G. Morris (*Univ. of British Columbia*), D. Arseneau, C. Ballard, M. Good, B. Hitti, S.R. Kreitzman (*TRIUMF*), E.J. Ansaldo (*Univ. of Saskatchewan*), N.V. Prokof'ev, V.G. Storchak (*Kurchatov Inst.*), S.P. Cottrell, S.F.J. Cox (*Rutherford Appleton Lab*)
693. Fast chemistry of μ^+ and muonium in van der Waals crystals and liquids [active], A. Benbasat, J.H. Brewer, D.G. Fleming, W.N. Hardy, G. Morris (*Univ. of British Columbia*), D. Arseneau, C. Ballard, M. Good, B. Hitti, S.R. Kreitzman (*TRIUMF*), E.J. Ansaldo (*Univ. of Saskatchewan*), N.V. Prokof'ev, V.G. Storchak (*Kurchatov Inst.*), S.P. Cottrell, S.F.J. Cox (*Rutherford Appleton Lab*)
694. Charge states and sites of muonium in (heavily-doped) GaAs [active], K.H. Chow, R.F. Kiefl, W.A. MacFarlane, J. Sonier (*Univ. of British Columbia*), S.F.J. Cox (*Rutherford Appleton Lab*), E.A. Davis, A. Singh (*Leicester Univ.*), R.C. DuVarney, R.L. Lichti (*Texas Tech. Univ.*), T.L. Estle, B. Hitti (*Rice Univ.*), C. Schwab (*CRN, Strasbourg*)
695. μSR in porous Si [active], K.H. Chow, R.F. Kiefl, W.A. MacFarlane, J. Sonier, T. Tiedje, T. van Buuren (*Univ. of British Columbia*), S.F.J. Cox (*Rutherford Appleton Lab*), E.A. Davis, A. Singh (*Leicester Univ.*), R.C. DuVarney (*Emory Univ.*), T.L. Estle, B. Hitti (*Rice Univ.*), R.L. Lichti (*Texas Tech. Univ.*), C. Schwab (*CRN, Strasbourg*)
696. Hyperfine dependence of exclusive μ^- capture on ^{35}Cl [completed data-taking], D.S. Armstrong (*Univ. of California, Berkeley*), J. Bauer, T.P. Gorringer, B. Johnson, M. Kovash, R. Sedlar, B. Siebels (*Univ. of Kentucky*), M. Hasinoff, D. Measday, B. Moftah (*Univ. of British Columbia*), D. Wright (*TRIUMF*)
697. μSR investigation of the effects of overdoping hole carriers, varying chain filling, and Zn-substitution, on T_c and m_{eff} of high- T superconductors [active], E.J. Ansaldo, D. Harrington (*Univ. of Saskatchewan*), C. Bernhard, U. Binniger, A. Hofer, Ch. Niedermayer (*Univ. Konstanz*), J. Tallon (*New Zealand Inst. for Industrial R&D*), J. Brewer (*Univ. of British Columbia*), D.R. Noakes, C. Stronach (*Virginia State Univ.*), P. Mendels (*Univ. Paris Sud*)
698. Gamow-Teller and $L = 2$ strength in $^{31}\text{P}(n,p)^{31}\text{Si}$ [completed data-taking], D. Beatty, H.T. Fortune, P.P. Hui, R.B. Ivie, M.G. McKinzie, Z. Mao, D.A. Smith (*Univ. of Pennsylvania*), S. Arole, T.P. Gorringer, R. Sedlar, B. Siebels (*Univ. of Kentucky*), J. Campbell, K.P. Jackson, A.G. Ling, P. Walden, S. Yen (*TRIUMF*)
699. Spin-flip isovector quadrupole in $^{27}\text{Al}(n,p)^{27}\text{Mg}$ and $^{56}\text{Fe}(n,p)^{56}\text{Mn}$ [active], D.P. Beatty, H.T. Fortune, P.P. Hui, R.B. Ivie, Z. Mao, M.G. McKinzie, Y.-X. Ren, D.A. Smith (*Univ. of Pennsylvania*), R. Abegg*, A.G. Ling, S. Yen (*TRIUMF*), R. Sedlar, B. Siebels (*Univ. of Kentucky*)

65

66

700. Measuring cross sections of long-lived radionuclides produced by 200-500 MeV protons in elements found in meteorites and lunar rocks [active], J. Vincent (*TRIUMF*), J.M. Sisterson (*Harvard Univ.*), K. Kim (*San Jose State Univ.*), A.J.T. Jull (*Univ. of Arizona*), M.W. Caffee (*Lawrence Livermore National Lab*), R.C. Reedy (*Los Alamos National Lab*) 37
702. Measurement of kaon-nucleon elastic scattering at 16 MeV [active], G.A. Beer, P. Knowles, G.R. Mason, A. Olin, L.P. Robertson (*Univ. of Victoria*), P. Amaudruz, D.R. Gill, G. Smith, S. Yen (*TRIUMF*), L. Lee (*Univ. of Manitoba*), G. Tagliente (*Univ. of British Columbia*)
703. Study of the decay $\pi^+ \rightarrow e^+ \nu$ phase I – lifetime measurement of the pion [active], D.A. Bryman, T. Numao, A. Olin (*TRIUMF*)
704. Charge symmetry breaking in $np \rightarrow d\pi^0$ close to threshold [active], R. Abegg*, P.W. Green, D.A. Hutcheon (*TRIUMF–Univ. of Alberta*), L.G. Greeniaus (*Univ. of Alberta–TRIUMF*), R.W. Finlay, K. Hicks, A.K. Opper, S.D. Reitzner (*Ohio Univ.*), E. Korkmaz, G.V. O’Rielly (*Univ. of Northern British Columbia*), J.A. Niskanen (*Univ. of Helsinki*), P. Walden (*TRIUMF–UBC*), S. Yen (*TRIUMF*), C.A. Davis (*TRIUMF–Univ. of Manitoba*), D.V. Jordan (*Ohio Univ.–Univ. of Alberta*), E. Auld (*Univ. of British Columbia*) 37
705. Development of modular gas microstrip chambers as in-target tracking devices for an experiment to detect $\Lambda\Lambda$ hypernuclei at the BNL AGS (BNL885) [active], C.A. Davis (*TRIUMF–Univ. of Manitoba*), B. Bassalleck, H. Fischer, J. Lowe, A. Rusek, R. Stotzer, D. Wolfe (*Univ. of New Mexico*), A. Berdoz, A. Biglan, G. Franklin, P. Koran, R. Magahiz, R. McCrady, F. Merrill, C. Meyer, B. Quinn, R.A. Schumacher, I.R. Sukaton (*Carnegie Mellon Univ.*), J. Birchall, L. Gan, M.R. Landry, L. Lee, S.A. Page, W.D. Ramsay, W.T.H. van Oers (*Univ. of Manitoba*), T. Buerger, M. Bürger, M. Eggers, J. Franz, E. Roessle, H. Schmitt (*Univ. of Freiburg*), R. Chrien, M. May, P.H. Pile, R. Sawafta, R. Sutter (*Brookhaven National Lab*), J. Doornbos, D.R. Gill (*TRIUMF*), H. Enyo, T. Iijima, K. Imai, Y. Kondo, A. Masaike, N. Saito, S. Yokkaichi, M. Yosoi (*Kyoto Univ.*), J. Nelson, R. Zybert (*Univ. of Birmingham*), K. Okada, F. Takeutchi (*Kyoto Sangyo Univ.*), R.L. Stearns (*Vassar College*), V.J. Zeps (*Univ. of Kentucky*), J. Szymanski (*IUCF*) 13
706. μ SR studies of spin fluctuations in CePt_2Sn_2 and other Kondo spin systems [active], A. Keren, K. Kojima, G.M. Luke, Y.J. Uemura, W.D. Wu (*Columbia Univ.*), K. Andres, G.M. Kalvius (*Tech. Univ. Munich*), H. Fujii, G. Nakamoto, T. Takabatake, H. Tanaka (*Hiroshima Univ.*), M. Ishikawa (*ISSP, Univ. of Tokyo*), B. Andraka (*Univ. of Florida*), D.L. Cox (*Ohio State Univ.*)
707. μ SR measurements on two-dimensional site-diluted antiferromagnets [active], K. Kojima (*Columbia Univ.–Univ. of Tokyo*), A. Keren, G.M. Luke, Y.J. Uemura, W.D. Wu (*Columbia Univ.*), H. Ikeda (*KEK–KENS*), R.J. Birgeneau (*MIT*), K. Nagamine (*Univ. of Tokyo*)
708. The spin relaxation and chemical reactivity of muonium-substituted organic radicals in the gas phase [active], D.G. Fleming, J.J. Pan, M. Shelley (*Univ. of British Columbia*), D.J. Arseneau (*TRIUMF–UBC*), M. Senba (*TRIUMF*), J.C. Brodovitch, P.W. Percival (*Simon Fraser Univ.*), H. Dilger, E. Roduner (*Univ. of Zürich*), S.F.J. Cox (*Rutherford Appleton Lab*)
709. $^{90,92,94,96}\text{Zr}(n, p)^{90,92,94,96}\text{Y}$ reaction at 200 MeV [active], A.G. Ling, P.L. Walden (*TRIUMF*), J. Rapaport (*Ohio Univ.*), D.A. Cooper, D.L. Prout, E.R. Sugarbaker (*Ohio State Univ.*), M. Halbert (*Oak Ridge National Lab*), D. Mercer (*Univ. of Colorado*), J. Campbell (*Univ. of Manitoba–TRIUMF*), M. Hartig (*Univ. Muenster*)
710. Dynamics of muonium in Ge and GaAs [completed data-taking], R.L. Lichti (*Texas Tech. Univ.*), S.F.J. Cox (*Rutherford Appleton Lab*), R.F. Kiefl (*Univ. of British Columbia*), K.H. Chow (*Lehigh Univ.*), T.L. Estle (*Rice Univ.*), B. Hitti (*TRIUMF*), E.A. Davis (*Leicester Univ.*), C.R. Schwab (*CNRS, Strasbourg*)
712. μ SR study of superconducting spin glasses [active], V. McMullen, D.R. Noakes, C.E. Stronach (*Virginia State Univ.*), E.J. Ansaldo (*Univ. of Saskatchewan*), J.H. Brewer (*Univ. of British Columbia*), G. Cao, J.E. Crow (*NHMFL*), S. McCall (*Florida State Univ.–NHMFL*)
713. Muonium chemistry in supercritical water [active], B. Addison-Jones, J.-C. Brodovitch, K. Ghandi, I. McKenzie, P. Percival (*Simon Fraser Univ.*), J. Schüth (*Univ. of Bonn*) 67
714. Atomic PNC in francium: preparations [active], J.A. Behr, L. Buchmann, M. Dombisky, P. Jackson, C.D.P. Levy (*TRIUMF*), J.M. D’Auria, P. Dubé, A. Gorelov, D. Melconian, T. Swanson, M. Trinczek (*Simon Fraser Univ.*), O. Häusser (*SFU–TRIUMF*), U. Giesen (*Univ. of Alberta*), I. Kelson, A.I. Yavin (*Tel Aviv Univ.*), J. Deutsch (*Univ. Catholique de Louvain*), J. Dilling (*SFU–Heidelberg*)
715. Spin correlations in β^+ decay of optically trapped ^{37}K [active], J.M. D’Auria, P. Dubé, A. Gorelov, O. Häusser*, D. Melconian, M. Trinczek (*Simon Fraser Univ.*), G. Ball, J.A. Behr, L. Buchmann, M. Dombisky, K.P. Jackson, B.K. Jennings (*TRIUMF*), U. Giesen (*Univ. Notre Dame*), W.P. Alford (*Univ. of Western Ontario*), J. Deutsch (*Univ. Catholique de Louvain*) 45

716. Complete beta-delayed particle emission study of ^{31}Ar [deferred], J. Cerny, D.M. Moltz, T. Ognibene, M.W. Rowe, R.J. Tighe (*Lawrence Berkeley Lab*), L. Buchmann (*TRIUMF*), J. D'Auria (*Simon Fraser Univ.*), M. Dombisky (*SFU-Univ. of Alberta*), G. Roy (*Univ. of Alberta*)
717. Muon hyperfine transition rates in light nuclei [completed], J.H. Brewer, E. Gete, M.C. Fujiwara, J. Lange, D.F. Measday, B.A. Moftah, M.A. Saliba, T. Stocki (*Univ. of British Columbia*), T.P. Gorringe (*Univ. of Kentucky*) 68
718. Superconductivity and magnetism in quaternary boron carbides [active], A. Keren, G.M. Luke, Y.J. Uemura, W.D. Wu (*Columbia Univ.*), K. Kojima (*Columbia Univ-Univ. of Tokyo*), S. Uchida (*Univ. of Tokyo*)
719. $^4\text{He}(\pi^+, \pi^- pp)$ invariant mass measurement with CHAOS [completed data-taking], P. Amaudruz, L. Felawka, R. Meier, D. Ottewell, G. Smith (*TRIUMF*), T. Mathie, R. Tacik, M. Yeomans (*Univ. of Regina*), J. Graeter, G. Wagner (*Univ. Tübingen*), J. Clark, M. Seviar (*Univ. of Melbourne*), G. Hofman, M. Kermani, P. Tagliente (*Univ. of British Columbia*), F. Bonutti, P. Camerini, N. Grion, R. Rui (*Univ. di Trieste*), J. Brack, R. Ristinen (*Univ. of Colorado*), E. Gibson (*California State Univ., Sacramento*), O. Patarakin (*Kurchatov Inst.*), E. Friedman (*Hebrew Univ. of Jerusalem*) 47
720. Muonium's nucleophilicity [active], G.B. Porter, D.C. Walker (*Univ. of British Columbia*), J.M. Stadlbauer* (*Hood College*), K. Venkateswaran (*Hindustan Lever Ltd.*), M.V. Barnabas (*Proctor & Gamble Ltd.*) 69
721. The delta nucleon reaction in CHAOS [completed data-taking], F. Farzanpay, P. Hong, E.L. Mathie, N. Mobed (*Univ. of Regina*), R. Tacik (*TRIUMF-Univ. of Regina*), P.A. Amaudruz, L. Felawka, R. Meier, D. Ottewell, G.R. Smith (*TRIUMF*), N. Grion (*INFN, Trieste*), P. Camerini, R. Rui (*Univ. di Trieste*), E. Gibson (*California State Univ., Sacramento*), G. Hofman, G. Jones, M. Kermani (*Univ. of British Columbia*), M.E. Seviar (*Univ. of Melbourne*), J.T. Brack, R.A. Ristinen (*Univ. of Colorado*)
722. Pion initial state interactions in the $^{12}\text{C}(\pi^+, ppp)$ reaction [completed data-taking], T. Mathie, R. Tacik (*Univ. of Regina*), P.A. Amaudruz, L. Felawka, D. Ottewell, K. Raywood, G.R. Smith (*TRIUMF*) M. Kermani, S. McFarland (*Univ. of British Columbia*), F. Bonutti, P. Camerini, R. Rui (*Univ. di Trieste*), N. Grion (*INFN, Trieste*), E.F. Gibson (*California State Univ., Sacramento*), M. Seviar (*Univ. of Melbourne*), J. Brack, G. Hofman (*Univ. of Colorado*), R. Meier (*Univ. of Tübingen*)
723. Study of pion-nucleus double-scattering reactions [completed data-taking], R. Tacik (*TRIUMF-Univ. of Regina*), T. Mathie (*Univ. of Regina*), L. Felawka, R. Meier, D. Ottewell, G. Smith (*TRIUMF*), G. Hofman, M. Kermani, M. Seviar (*Univ. of British Columbia*), F. Bonutti, P. Camerini, R. Rui (*Univ. di Trieste*), N. Grion (*INFN, Trieste*)
724. μSR measurements on spin ladder systems [active], A. Keren, G.M. Luke, Y.J. Uemura, W.D. Wu (*Columbia Univ.*), K. Kojima (*Columbia Univ.-Univ. of Tokyo*), M. Takano (*Kyoto Univ.*), K. Nagamine (*Univ. of Tokyo*) 70
725. Pion double charge exchange reactions on $^3,^4\text{He}$ in the energy range 50–100 MeV [completed], P. Amaudruz, L. Felawka, R. Meier, D. Ottewell, G. Smith (*TRIUMF*), T. Mathie, R. Tacik, M. Yeomans (*Univ. of Regina*), J. Graeter, G. Wagner (*Univ. Tübingen*), J. Clark, M. Seviar (*Univ. of Melbourne*), G. Hofman, M. Kermani, P. Tagliente (*Univ. of British Columbia*), F. Bonutti, P. Camerini, N. Grion, R. Rui (*Univ. di Trieste*), J. Brack, R. Ristinen (*Univ. of Colorado*), E. Gibson (*California State Univ., Sacramento*), O. Patarakin (*Kurchatov Inst.*), E. Friedman (*Hebrew Univ. of Jerusalem*) 49
726. Beta-delayed proton and γ -decay of ^{65}Se , ^{69}Kr and ^{73}Sr [active], D. Anthony, J. D'Auria, M. Trinczek (*Simon Fraser Univ.*), R.E. Azuma, J.D. King (*Univ. of Toronto*), L. Buchmann, K.P. Jackson, J. Vincent (*TRIUMF*), M. Dombisky (*SFU-Univ. of Alberta*), U. Giesen (*TRIUMF-Univ. of Alberta*), J. Görres, H. Schatz, M. Wiescher (*Univ. of Notre Dame*), C. Iliadis (*TRIUMF-Univ. of Toronto*), G. Roy (*Univ. of Alberta*)
728. Search for population and de-excitation of low-spin superdeformed states in Po-Hg region via β^+ and α decays [active], Y.A. Akovali, M. Brinkman (*Oak Ridge National Lab*), J.M. D'Auria (*TRIUMF-SFU*), J.A. Becker, E.A. Henry (*Lawrence Livermore National Lab*), M. Dombisky (*Simon Fraser Univ.*), P.F. Mantica (*UNISOR*), W. Nazarewicz (*Joint Inst. for Heavy Ion*), J. Rikovsky, N.J. Stone (*Oxford Univ.*), M.A. Stoyer (*Lawrence Berkeley National Lab*), R.A. Wyss (*MSI, Sweden*)
729. Gamow-Teller and spin-dipole strengths from $^{17,18}\text{O}(n, p)$ [active], D.P. Beatty, H.T. Fortune, P.P. Hui, R.B. Ivie, Z.Q. Mao, M.G. McKinzie, D.A. Smith (*Univ. of Pennsylvania*), W.P. Alford (*Univ. of Western Ontario*), K.P. Jackson, A.G. Ling, C.A. Miller, P. Walden, S. Yen (*TRIUMF*)
730. The solar neutrino problem and a new measurement of $^7\text{Be}(p, \gamma)^8\text{B}$ [deferred], R.E. Azuma, J.D. King (*Univ. of Toronto*), P. Bricault, L. Buchmann, T. Ruth, H. Schneider, J. Vincent, S. Zeisler (*TRIUMF*), J. D'Auria, R. Korteling (*Simon Fraser Univ.*), M. Dombisky (*SFU-Univ. of Alberta*), U. Giesen (*TRIUMF-Univ. of Alberta*), C. Iliadis (*TRIUMF-Univ. of Toronto*), G. Roy (*Univ. of Alberta*), M. Wiescher (*Univ. of Notre Dame*)

731. Investigation of spin-polarized muonium in metallic semiconductors [active] K.H. Chow, S. Dunsiger, R.F. Kiefl, W.A. MacFarlane, J. Sonier (*Univ. of British Columbia*), S.F.J. Cox (*Rutherford Appleton Lab*), E.A. Davis, A. Singh (*Leicester Univ.*), T.L. Estle, B. Hitti (*Rice Univ.*), R.L. Lichti (*Texas Tech. Univ.*), P. Mendels (*Orsay Univ.*), C. Schwab (*CRN, Strasbourg*)
732. Quantum impurities in one dimensional spin 1/2 chains [active], I. Affleck, J.H. Brewer, K. Chow, S. Dunsiger, S. Eggert, R.F. Kiefl, A. MacFarlane, J. Sonier (*Univ. of British Columbia*), A. Keren, Y.J. Uemura (*Columbia Univ.*)
733. Probing high T_c superconductor with “paramagnetic” (μ^-O) system [active], H. Kojima, I. Tanaka, E. Torikai (*Yamanashi Univ.*), K. Nishiyama (*Univ. of Tokyo*), K. Nagamine (*Univ. of Tokyo-RIKEN*), I. Watanabe (*RIKEN*), T.P. Das (*State Univ. of New York*), S. Maekawa (*Nagoya Univ.*)
734. Radiative muon capture on nickel isotopes [active], D.S. Armstrong, P. McKenzie (*College of William and Mary*), G. Azuelos, P. Depommier (*Univ. de Montréal*), P. Bergbusch, P. Gumplinger, M. Hasinoff, E. Saettler (*Univ. of British Columbia*), B. Doyle, T.P. Gorringer, R. Sedlar (*Univ. of Kentucky*), M. Blecher, C. Sigler (*Virginia Polytechnic Inst.*), J.A. MacDonald, J.-M. Poutissou, R. Poutissou, D. Wright (*TRIUMF*)
735. Studies of single layer cuprate superconductors [active], G.M. Luke, B. Nachumi, Y.J. Uemura (*Columbia Univ.*), K. Kojima (*Columbia Univ.-Univ. of Tokyo*), S. Uchida (*Univ. of Tokyo*), R.H. Heffner, L.P. Le (*Los Alamos Nat. Lab.*), R. MacLaughlin (*Univ. of California, Riverside*), M.B. Maple (*Univ. of California, San Diego*)
736. Tests of electro-weak theory using ^{14}O beam [deferred], M. Bahtacharya, A. Garcia, R. Rutchi, M. Wayne (*Univ. of Notre Dame*), L. Buchmann (*TRIUMF*), C. Iliadis (*TRIUMF-Univ. of Toronto*), B. Fujikawa (*Lawrence Berkeley Lab.*), S.J. Freedman, J. Mortara (*Univ. of California, Berkeley*)
737. Magnetic and superconducting behaviour in selected oxide materials [active], R.H. Heffner, L.P. Le (*Los Alamos National Lab*), D.E. Maclaughlin (*Univ. of California, Riverside*), G. Luke, B. Nachuma, Y.J. Uemura (*Columbia Univ.*), K. Kojima (*Columbia Univ.-Univ. of Tokyo*)
740. Irradiation of silicon tracker components [active], R. Lipton, L. Spiegel (*Fermilab*), K.F. O’Shaughnessy (*Univ. of California, Santa Cruz*), B. Barnett, J. Cameratta, J. Škarha (*Johns Hopkins Univ.*), N. Brunner, M. Frautschi, M. Gold, Y. Ling, J. Matthews, S. Seidel (*Univ. of New Mexico*), D. Bortoletto, A. Garfinkel, A. Hardman, K. Hoffman, T. Keaffaber, N.M. Shaw (*Purdue Univ.*)
741. Beta-delayed proton decay of ^{17}Ne to α -emitting states in ^{16}O [active], J. Chow, J.D. King, A.C. Morton (*Univ. of Toronto*), L. Buchmann, M. Dombisky, K.P. Jackson, T. Shoppa, P. Wrean (*TRIUMF*), J.M. D’Auria (*Simon Fraser Univ.*), U. Giesen, G. Roy (*Univ. of Alberta*), N. Bateman (*TRIUMF-Univ. of Toronto-SFU*), W. Galster (*Univ. Catholique de Louvain*), T. Davinson, A.C. Shotter (*Univ. of Edinburgh*), R.N. Boyd (*Ohio State Univ.*), C. Iliadis (*Univ. of North Carolina*), J. Powell (*Univ. of California, Berkeley*) 49
742. Scattering of muonic hydrogen isotopes [active], V.M. Bystritsky, V.A. Stolupin (*JINR*), R. Jacot-Guillarmod, P.E. Knowles, F. Mulhauser (*Univ. of Fribourg*), G.M. Marshall (*TRIUMF*), M. Filipowicz, J. Wozniak (*Fac. Phys., Nucl. Tech., Krakow*), A. Adamczak (*Inst. Nucl. Physics, Krakow*), A.R. Kunselman (*Univ. of Wyoming*), V.E. Markushin, C. Petitjean (*PSI*), T.M. Huber (*Gustavus Adolphus College*), G.A. Beer, M. Maier, A. Olin, T.A. Porcelli (*Univ. of Victoria*), P. Kammel (*Univ. of California, Berkeley*), M.C. Fujiwara (*Univ. of British Columbia*), J. Zmeskal (*IMEP Vienna*), S.K. Kim (*Jeonbuk National Univ.*) 52
743. Gamow-Teller strength in $^{64,66,68}Zn$ and $^{63,65}Cu(n,p)$ [active], W.P. Alford (*Univ. of Western Ontario*), D. Beatty, H.T. Fortune, P.P. Hui, R.B. Ivie, Z. Mao, M.G. McKinzie, D.A. Smith (*Univ. of Pennsylvania*), S. Yen (*TRIUMF*)
744. Hadronic weak and electromagnetic form factors via $\pi^-p \rightarrow e^+e^-n$ [active], D. Armstrong (*College of William and Mary*), P. Gumplinger, M.D. Hasinoff, D.H. Wright (*Univ. of British Columbia*), M. Blecher (*Virginia Polytech. Inst. & State Univ.*), E. Christy, B.C. Doyle, T.P. Gorringer, M.A. Kovash (*Univ. of Kentucky*), J.A. Macdonald (*TRIUMF*)
745. μ^-SR measurements on one-dimensional spin systems [active], K. Kojima (*Columbia Univ.-Univ. of Tokyo*), K. Nagamine, K. Nishiyama, S. Uchida (*Univ. of Tokyo*), G.M. Luke, B. Nachumi, Y.J. Uemura (*Columbia Univ.*), I. Affleck, S. Dunsiger, S. Eggert, R.F. Kiefl (*Univ. of British Columbia*)
746. Muonium dynamics in Si, Ge and GaAs studied by RF- μSR and μW - μSR [active], S.R. Kreitzman (*TRIUMF*), T.L. Estle, B. Hitti (*Rice Univ.*), R. Lichti (*Texas Tech.*), K. Chow (*Univ. of British Columbia*), S.F.J. Cox (*Rutherford Appleton Lab*), E.A. Davis (*Leicester Univ.*), C. Schwab (*CRN Strasbourg*) 71
747. μSR study of re-entrant spin glasses a-FeMn, AuFe, and $Fe_{70}Al_{30}$ [active], I.A. Campbell (*Univ. Paris Sud Orsay*), S. Dunsiger, R.F. Kiefl (*Univ. of British Columbia*), M.J.P. Gingras (*TRIUMF*), M. Hennion, I. Mirebeau (*Saclay, LLB*), K. Kojima, G.M. Luke, B. Nachumi, Y.J. Uemura, W.D. Wu (*Columbia Univ.*)

749. Muonium-substituted free radicals [active], B. Addison-Jones, J.-C. Brodovitch, K. Ghandi, I. McKenzie, P.W. Percival (*Simon Fraser Univ.*), J. Schüth (*Univ. of Bonn*) 71
750. Liquid chemistry μ SR [active], G.B. Porter, D.C. Walker (*Univ. of British Columbia*), J.M. Stadlbauer* (*Hood College*), K. Venkateswaran (*Lever Hindustan Ltd.*), M.V. Barnabas Procter & Gamble Ltd.) 69
751. Tests in preparation for μ SR measurements of off-axis internal magnetic fields in anisotropic superconductors [active], E. Csomortani, W.J. Kossler, X. Wan (*College of William and Mary*), D.R. Harshman (*Physikon*), A. Greer (*Gonzaga Univ.*), E. Koster, D.L. Williams (*Univ. of British Columbia*), C.E. Stronach (*Virginia State Univ.*) 73
752. Muonium centres in Si and GaAs [active], K.H. Chow (*Oxford Univ.*), S.F.J. Cox (*Rutherford Appleton Lab*), E.A. Davis (*Leicester Univ.*), S. Dunsiger, R.F. Kiefl, W.A. MacFarlane (*Univ. of British Columbia*), T.L. Estle (*Rice Univ.*), B. Hitti (*TRIUMF*), R.L. Lichti (*Texas Tech.*), C. Schwab (*CRN Strasbourg*)
753. Studies of magnetic correlations in planar oxides [active], K. Kojima (*Columbia Univ.–Univ. of Tokyo*), M. Larkin, G.M. Luke, J. Merrin, B. Nachumi, Y.J. Uemura (*Columbia Univ.*), B.J. Sternlieb (*Brookhaven Nat. Lab*), S. Uchida (*Univ. of Tokyo*)
754. A search for the muonium substituted hydroxyl radical [deferred], T.A. Claxton, G. Marston (*Leicester Univ.*), S.F.J. Cox (*Rutherford Appleton Lab*), D. Arseneau, D. Fleming, M. Senba, P. Wassell (*Univ. of British Columbia*), J.-C. Brodovitch, P.W. Percival (*Simon Fraser Univ.*)
755. Muonium formation in Zn-spinels [deferred], G.M. Kalvius, A. Kratzer, W. Potzel (*Tech. Univ. Munich*), R. Wäppling (*Univ. of Uppsala*), D.R. Noakes (*Virginia State Univ.*), S.R. Kreitzman (*TRIUMF*), A. Martin (*Univ. of Jena*), M.K. Krause (*Univ. of Leipzig*)
756. Mu+NO spin relaxation: electron exchange or paramagnetism? [deferred], D.G. Fleming, J.J. Pan, M. Senba, M. Shelley (*Univ. of British Columbia*), D.J. Arseneau (*TRIUMF*), E. Roduner (*Univ. of Zürich*)
757. Study of muon dynamics in ferroelectric materials and proton ionic conductors – comparison with proton dynamics [active], W.K. Dawson, K. Nishiyama, S. Ohira, K. Shimomura (*Univ. of Tokyo*), K. Nagamine (*Univ. of Tokyo–RIKEN*), S. Ikeda (*KEK*), S. Shin (*Univ. of Tokyo –ISSP*), N. Sata (*Tohoku Univ.*)
758. Electronic structure of muonium and muonium-lithium complexes in graphite and related compounds [active], J. Brewer, J. Chakhalian, S. Dunsiger, R.F. Kiefl, W.A. MacFarlane, R. Miller, J. Sonier (*Univ. of British Columbia*), J. Dahn (*Dalhousie Univ.*), J. Fischer (*Univ. of Pennsylvania*), B. Hitti, S.R. Kreitzman (*TRIUMF*)
759. Study of the isotropic hyperfine coupling constant of muonium at high temperature and under uniaxial pressure [active], W.K. Dawson, K. Nishiyama, S. Ohira, K. Shimomura (*Univ. of Tokyo*), K. Nagamine (*Univ. of Tokyo–RIKEN*), T.P. Das (*Univ. of New York, Albany*)
761. Parity violation in $p-p$ scattering at 450 MeV [deferred], J. Birchall, J.R. Campbell, A.A. Green, A.A. Hamian, L. Lee, S.A. Page, W.D. Ramsay, S.D. Reitzner, W.T.H. van Oers (*Univ. of Manitoba*), C.A. Davis (*TRIUMF–Univ. of Manitoba*), P.W. Green, G. Roy, J. Soukup, G.M. Stinson (*Univ. of Alberta*), D.C. Healey, R. Helmer, C.D.P. Levy, P.W. Schmor (*TRIUMF*), N.A. Titov, A.N. Zelenskii (*INR, Moscow*)
762. Gamow-Teller and spin-flip dipole strengths near $A = 90$ [active], W.P. Alford (*Univ. of Western Ontario*), D.P. Beatty, H.T. Fortune, P.P. Hui, R.B. Ivie, D. Koltenuk, J. Yu (*Univ. of Pennsylvania*), A. Ling, S. Yen (*TRIUMF*), S. El-Kateb (*King Fahd Univ.*)
763. Muon cooling and acceleration in an undulating crystal channel [deferred], S.A. Bogacz, D.B. Cline, D.A. Sanders (*UCLA*), L.M. Cremaldi, B. Denardo, Q. Jie, D.J. Summers (*Univ. of Mississippi–Oxford*), G.M. Marshall (*TRIUMF*)
764. Calibration of a segmented neutron detector [active], E. Korkmaz, G. O’Rielly (*Univ. of Northern British Columbia*), D.A. Hutcheon (*TRIUMF*), A.K. Opper (*Univ. of Alberta*), G. Feldman, N.R. Kolb (*Univ. of Saskatchewan*)
766. The ortho-para transition rate in muonic molecular hydrogen [active], D.S. Armstrong, J.H.D. Clark (*College of William and Mary*), T.P. Gorringer, S. Tripathi (*Univ. of Kentucky*), E. Gete, M.D. Hasinoff, D.F. Measday, B.A. Moftah, T. Stocki (*Univ. of British Columbia*), D.H. Wright (*TRIUMF*), R. Woo (*Univ. of Manitoba*)
767. Direct measurement of sticking in muon catalyzed $d-t$ fusion [active], J.M. Bailey (*Chester Technology, UK*), G.A. Beer, M. Maier, G.R. Mason, T.A. Porcelli (*Univ. of Victoria*), K.M. Crowe, P. Kammel (*Univ. of California, Berkeley–LBL*), M.C. Fujiwara, E. Gete, T.J. Stocki (*Univ. of British Columbia*), T.M. Huber (*Gustavus Adolphus College*), S.K. Kim (*Jeonbuk National Univ.*), A.R. Kunselman (*Univ. of Wyoming*), G.M. Marshall, A. Olin (*TRIUMF*), C.J. Martoff (*Temple Univ.*), V.S. Melezhik (*JINR, Dubna*), F. Mulhauser (*Univ. of Fribourg*), C. Petitjean (*PSI*), J. Zmeskal (*IMEP Vienna*)

768. Generalized Fulde-Ferrell-Larkin-Ovchinnikov state in heavy fermion and intermediate valence systems [active], J. Akimitsu, K. Ishii, A. Yamashita, T. Yokoo (*Aoyama Gakuin Univ.*), R. Kadono (*RIKEN*), K. Nishiyama (*Univ. of Tokyo*)
769. Effects of uniaxial stress on muonium in semiconductors [active], K.H. Chow (*Oxford*), B. Hitti (*TRIUMF*), R.F. Kiefl (*Univ. of British Columbia*), T.L. Estle (*Rice Univ.*), R. Lichti (*Texas Tech. Univ.*)
770. μ SR studies of organic conductors: (BEDT-TTF)₂-X and (TMTTF)₂Br [active], K. Kojima, M. Larkin, G.M. Luke, J. Merrin, B. Nachumi, Y.J. Uemura (*Columbia Univ.*), P.M. Chaikin (*Princeton Univ.*), G. Saito (*Kyoto Univ.*)
771. μ SR studies of geometrically frustrated S = 1/2 spin systems [active], K. Kojima, M. Larkin, G.M. Luke, J. Merrin, B. Nachumi, Y.J. Uemura (*Columbia Univ.*), M.J.P. Gingras (*TRIUMF*), S. Dunsiger, R.F. Kiefl (*Univ. of British Columbia*), D.C. Johnston, S. Kondo (*Iowa State Univ.*), S. Uchida (*Univ. of Tokyo*), R.J. Cava (*AT&T Bell Labs*)
772. Search for the Δ - Δ dibaryon [active], R. Abegg*, C.A. Miller, P. Walden, S. Yen (*TRIUMF*), R. Bent (*Indiana Univ.*), T.Y. Chen, F. Wang, C.H. Ye (*Nanjing Univ.*), W. Falk (*Univ. of Manitoba*), D. Frekers, M. Hartig (*Univ. Muenster*), T. Goldman (*Los Alamos National Lab*), M. Heyrat, C.W. Wong (*UCLA*), G. Jones (*Univ. of British Columbia*), E. Korkmaz, G. O’Rielly (*Univ. of Northern British Columbia*), C. Rangacharyulu (*Univ. of Saskatchewan*), I. Strakovsky (*Virginia Tech. Inst.*), Z.X. Sun, J.C. Xu (*Inst. Atomic Energy, China*), T. Walton (*Cariboo Univ. College*)
773. Muon-electron interaction in n-type silicon [active], D. Arseneau, B. Hitti, S.R. Kreitzman (*TRIUMF*), J.H. Brewer, R.F. Kiefl, G. Morris (*Univ. of British Columbia*), K. Chow (*Oxford Univ.*), S.F.J. Cox (*Rutherford Appleton Lab*), D.G. Eshchenko (*INR, Moscow*), T.L. Estle (*Rice Univ.*), R. Lichti (*Texas Tech. Univ.*), V.G. Storchak, (*Kurchatov Inst.*)
774. Muonium dynamics in GaAs studied by rf and μ -wave μ SR [active], B. Hitti, S.R. Kreitzman (*TRIUMF*), T.L. Estle (*Rice Univ.*), R. Lichti (*Texas Tech. Univ.*) 75
775. Electron transport in insulators, semiconductors and magnetic materials [active], A. Benbasat, J.H. Brewer, D.G. Fleming, W.N. Hardy, G. Morris (*Univ. of British Columbia*), D. Arseneau, C. Ballard, M. Good, B. Hitti, S.R. Kreitzman (*TRIUMF*), E.J. Ansaldo (*Univ. of Saskatchewan*), N.V. Prokof’ev, V.G. Storchak (*Kurchatov Inst.*), S.P. Cottrell, S.F.J. Cox (*Rutherford Appleton Lab*)
776. Rare earth materials with disordered spin structures [active], J.H. Brewer (*Univ. of British Columbia*), K. Fukamichi (*Tohoku Univ.*), G.M. Kalvius (*Tech. Univ. Munich*), C.U. Jackson, D.R. Noakes, C.E. Stronach, M.F. White, Jr. (*Virginia State Univ.*), R. Wäppling (*Uppsala Univ.*) 76
777. Vortex state of s-wave superconductors investigated by muon spin rotation [active], J.H. Brewer, J. Chakhalian, S. Dunsiger, R.F. Kiefl, R. Miller, A. Price (*Univ. of British Columbia*), J. Sonier (*Los Alamos National Lab*), M. Larkin, Y.J. Uemura (*Columbia Univ.*), G.M. Luke (*McMaster Univ.*), J.W. Brill (*Univ. of Kentucky*), J. Akimitsu, K. Kakuta, K. Ohishi (*Aoyama Gakuin Univ.*), P. Canfield (*Ames Lab*), W. Higemoto, R. Kadono (*KEK-IMSS*), M. Nohara (*ISSP, Univ. of Tokyo*), T. Yokoo (*CREST*) 77
778. $\pi^\pm p$ differential cross sections in the Coulomb-nuclear interference region [active], P. Amaudruz, L. Felawka, D. Healey, D. Ottewell, K. Raywood, G. Smith (*TRIUMF*), P. Camerini, E. Fragiaco, A. Fumagalli, N. Grion, R. Rui (*Univ. di Trieste*), B. Jamieson, G. Tagliente (*Univ. of British Columbia*), E. Mathie, R. Tacik, M. Yeomans (*Univ. of Regina*), H. Denz, J. Pätzold, R. Meier, G. Wagner (*Univ. Tübingen*), J. Clark, M. Seviar (*Univ. of Melbourne*), J. Brack, J. Patterson, R. Ristinen (*Univ. of Colorado*), E. Gibson (*California State Univ., Sacramento*), M. Pavan (*MIT*), O. Patarakin (*Kurchatov Inst.*) 56
779. Accelerator mass spectrometry experiments at ISAC [active], S. Calvert, A. Glass, R.R. Johnson, T. Petersen (*Univ. of British Columbia*), Z. Gelbart, D. Ottewell (*TRIUMF*), R. Schubank (*unaffiliated*), C.S. Wong (*Inst. of Ocean Sciences*), J. Clague (*Geological Survey Canada*), M. Paul (*Hebrew Univ. of Jerusalem*)
780. Deeply bound pionic states through $^{208}\text{Pb}(p, ^3\text{He})^{206}\text{Pb} \otimes \pi^-$ [active], D. Frekers, W. Garske, K. Grewer, M. Hartig, H. Wörtche (*Univ. Muenster*), H. Machner (*KFA, Jülich*), D. Hutcheon, P. Walden, S. Yen (*TRIUMF*), A. Opper (*Univ. of Ohio*)
781. Investigations of the $\pi\pi$ invariant mass distributions of nuclear (π^+ , $\pi^-\pi^+$) reactions with the CHAOS detector [completed data-taking], J. Clark, M.E. Seviar (*Univ. of Melbourne*), G. Hofman, M. Kermani, P. Tagliente (*Univ. of British Columbia*), P. Amaudruz, P. Delheij, L. Felawka, R. Meier, D.F. Ottewell, K. Raywood, G.R. Smith (*TRIUMF*), F. Bonutti, P. Camerini, R. Rui (*Univ. Trieste*), N. Grion (*INFN, Trieste*), E.L. Mathie, R. Tacik, M. Yeomans (*Univ. of Regina*), J. Brack, R.A. Ristinen (*Univ. of Colorado*), E. Gibson (*California State Univ., Sacramento*), H. Staudenmeier (*Univ. of Karlsruhe*) 58

782. Non-fermi-liquid behaviour and other novel phenomena in heavy-fermion alloys [active], W.P. Beyermann, D.E. MacLaughlin (*Univ. of California, Riverside*), R.H. Heffner (*Los Alamos National Lab*), G.M. Luke, Y.J. Uemura (*Columbia Univ.*), G.J. Nieuwenhuys (*Univ. of Leiden*), P.C. Canfield (*Iowa State Univ.*), Z. Fisk (*Florida State Univ.*), M.B. Maple (*Univ. of California, San Diego*), G.R. Stewart (*Univ. of Florida–Univ. of Augsburg*) 78
783. Paramagnetic frequency shifts in unconventional superconductors [active], R.H. Heffner (*Los Alamos National Lab*), W.P. Beyermann, D.E. MacLaughlin (*Univ. of California, Riverside*), G.J. Nieuwenhuys (*Univ. of Leiden*), Y.J. Uemura (*Columbia Univ.*), G.R. Stewart (*Univ. of Florida–Univ. of Augsburg*), G.M. Luke (*McMaster Univ.*), B. Andraka (*Univ. of Florida*), P.C. Canfield (*Ames Lab, Iowa State Univ.*), Z. Fisk (*Florida State Univ.*), M.B. Maple (*Univ. of California, San Diego*)
784. μ SR studies of spin singlet states in oxides [active], Y. Fudamoto, K. Kojima, M. Larkin, G.M. Luke, J. Merrin, B. Nachumi, Y.J. Uemura (*Columbia Univ.*), S. Dunsiger, R.F. Kiefl (*Univ. of British Columbia*), M. Gingras (*Univ. of Waterloo*), M. Sato (*Nagoya Univ.*), H. Hase (*RIKEN*), K. Uchinokura, K. Ueda, Y. Ueda (*Univ. of Tokyo*) 80
785. Pion double charge exchange on ^3He with CHAOS [completed data-taking], R. Tacik (*TRIUMF–Univ. of Regina*), E.L. Mathie, M. Yeomans (*Univ. of Regina*), H. Clement, J. Graeter, R. Meier, J. Petzold, G.J. Wagner (*Univ. of Tübingen*), E. Friedman (*Hebrew Univ. of Jerusalem*), N. Grion (*INFN Trieste*), P. Camerini, E. Fragiaco, R. Rui (*Univ. of Trieste*), L. Felawka, D. Ottewell, K. Raywood, G.R. Smith (*TRIUMF*), G. Hofman, B. Jamieson, G. Tagliente (*Univ. of British Columbia*), J. Clark, G. Molony, M.E. Sevier (*Univ. of Melbourne*), E. Gibson (*California State Univ. Sacramento*), H. Staudenmeyer (*Univ. of Karlsruhe*), S. Filippov, Y. Gavrilov, T. Karavicheva (*Moscow Meson Factory*) 59
786. Low energy structures in the β -delayed particle decays of ^9C , ^{12}N and ^{17}Ne [active], N. Bateman (*TRIUMF–SFU–Univ. of Toronto*), L. Buchmann, K.P. Jackson, T. Shoppa (*TRIUMF*), J. Chow, J.D. King, C. Mortin (*Univ. of Toronto*), T. Davison, A. Ostrowski, A. Shotter (*Univ. of Edinburgh*), J. D’Auria (*Simon Fraser Univ.*), E. Gete, D. Measday (*Univ. of British Columbia*), U. Giesen (*Univ. of Alberta*)
788. Nuclear and atomic physics with the CPT spectrometer [active], B. Barber, K.S. Sharma (*Univ. of Manitoba*), X. Feng (*Univ. of Manitoba–McGill Univ.*), F. Buchinger, J. Crawford, S. Gulick, J. Lee, B. Moore (*McGill Univ.*), E. Hagberg, J. Hardy, V. Koslowsky, G. Savard (*Chalk River Nuclear Lab*)
789. μ SR studies of magnetic fluctuations in hydronium jarosites, model Kagomé antiferromagnets [active], A. Harrison, A.S. Wills (*Univ. of Edinburgh*), Y. Fudamoto, K. Kojima, M. Larkin, G.M. Luke, J. Merrin, B. Nachumi, Y.J. Uemura (*Columbia Univ.*), T. Mason (*Univ. of Toronto*)
790. μ SR studies of stripe order in $\text{La}_{1.6-x}\text{Sr}_x\text{Nd}_{0.4}\text{CuO}_4$ modified cuprate superconductors [active], Y. Fudamoto, K. Kojima, M. Larkin, G.M. Luke, J. Merrin, B. Nachumi, Y.J. Uemura (*Columbia Univ.*), M. Crawford (*Du Pont*), A. Moodenbaugh (*Brookhaven National Lab*), S. Uchida (*Univ. of Tokyo*)
791. Electronic structure and dynamics of charged muonium and muonium-dopant centers in semiconductors [active], K.H. Chow (*Oxford Univ.*), R.F. Kiefl (*Univ. of British Columbia*), B. Hitti (*TRIUMF*), T.L. Estle (*Rice Univ.*), R. Lichti (*Texas Tech. Univ.*), S.F.J. Cox (*Rutherford Appleton Lab*), C. Schwab (*CRN, Strasbourg*) 81
792. Muonium in III-V semiconductors: identification of states and transitions [active], K.H. Chow (*Oxford Univ.*), S.F.J. Cox (*Rutherford Appleton Lab*), B. Hitti (*TRIUMF*), T.L. Estle (*Rice Univ.*), R.L. Lichti (*Texas Tech. Univ.*), C. Schwab (*CRN, Strasbourg*) 82
793. Production of an intense ^{15}O beam for ISAC [active], J. D’Auria, R. Lange (*Simon Fraser Univ.*), M. Domsbky, T. Ruth, J. Vincent (*TRIUMF*), K. Carter (*Oak Ridge National Lab*), B. Zhuikov (*INR, Moscow*)
794. μ^+ SR study on the magnetic properties of LaCoO_3 and $\text{La}_{1-x}\text{Sr}_x\text{CoO}_3$ [active], V.V. Krishnamurthy, I. Watanabe (*RIKEN*), K. Asai, N. Yamada (*Univ. of Electro-communications*), K. Nagamine (*Univ. of Tokyo–RIKEN*)
795. μ SR study on non fermi liquid behaviour [active], Y. Miyako, Y. Yamamoto (*Osaka Univ.*), S. Murayama (*Muroran Inst. of Tech.*), K. Nagamine (*Univ. of Tokyo*), K. Nishiyama (*Univ. of Tokyo–RIKEN*)
796. μ SR studies in ionic crystals doped with either colour centres or impurity [deferred], Y. Miyake, K. Nagamine, K. Nishiyama, K. Shimomura (*Univ. of Tokyo*), A. Matsusita (*RIKEN*)
797. Magnetic correlations in the ternary equiatomic Ce compounds CeT_3Sn [active], L. Asch, G.M. Kalvius A. Kratzer (*Tech. Univ. Munich*), R.F. Kiefl (*UBC–TRIUMF*), R. Wäppling (*Univ. of Uppsala*), T. Takabatake (*Hiroshima Univ.*), D.R. Noakes (*Virginia State Univ.*)
798. μ SR studies on the competition of RKKY exchange and Kondo effect in CeT_2X_2 compounds (T=transition metal, X=Si,Ge) [active], H.-H. Klauss, W. Kopmann, F.J. Litterst, W. Wagener, H. Walf (*Tech. Univ. Braunschweig*), E. Baggio Saitovitch, M.B. Fontes (*CBPF Rio de Janeiro*), A. Krimmel, A. Loidl (*Univ. of Augsburg*)

799. Hyperfine structure and site determination of (μ^- -O) system in LaSuCuO high T_c superconductors [active], H. Kojima, I. Tanaka, E. Torikai (*Yamanashi Univ.*), K. Nishiyama (*Univ. of Tokyo-RIKEN*), K. Nagamine, K. Shimomura (*Univ. of Tokyo*), I. Watanabe (*RIKEN*), T.P. Das (*State Univ. of New York*)
801. Studies of multi-phonon states via β -decay [active], R.F. Casten, G. Cata-Danil, B. Liu, N.V. Zamfir (*Yale Univ.*), C. Barton, D.S. Brenner (*Clark Univ.*), R.L. Gill (*Brookhaven National Lab*)
802. Superdeformation and smooth band termination on and near the $N = Z$ line: Part 1 ^{60}Zn [active], J.A. Cameron, S. Flibotte, D.S. Haslip, J. Nieminen, C. Svensson, J.C. Waddington, J.N. Wilson (*McMaster Univ.*), G. Ball (*TRIUMF*), A. Galindo-Uribarri, D.C. Radford (*Oak Ridge National Lab*), D. Ward (*Lawrence Berkeley National Lab*)
803. Experimental studies of interaction and properties of neutron-rich nuclei at ISAC [active], A.S. Iljinov, A.V. Klyachko, E.S. Konobeevsky, M.V. Morodovskoy, M.A. Prohvatilov, A.I. Reshetin, Yu.V. Ryabov, K.A. Shileev, V.A. Simonov, V.M. Skorkin, S.V. Zuyev (*INR RAS*)
804. Muonium in gallium nitride [active], E.S. Bates, M.R. Dawdy, T.L. Head, R.L. Lichti (*Texas Tech. Univ.*), B. Hitti (*TRIUMF*), T.L. Estle (*Rice Univ.*), C. Schwab (*CNRS Strasbourg*)
805. A study of the $^{13}\text{N}(p, \gamma)^{14}\text{O}$ reaction with a ^{13}N beam [active], R.E. Azuma, J. Chow, J.D. King, A.C. Morton (*Univ. of Toronto*), N. Bateman (*TRIUMF-Toronto*), L. Buchmann, K.P. Jackson, T. Shoppa (*TRIUMF*), J.M. D'Auria (*Simon Fraser Univ.*), U. Giesen (*SFU-TRIUMF*), G. Roy (*Univ. of Alberta*), W. Galster (*Univ. Catholique de Louvain*), A.C. Shotter (*Univ. of Edinburgh*), R.N. Boyd (*Ohio State Univ.*), U. Greife, C. Rolfs, F. Strieder, H.-P. Trautvetter (*Ruhr Univ. of Bochum*)
806. Excitation of high-spin isomeric states and compound nucleus formation by intermediate energy protons and stopped pions [active], A.S. Iljinov, V.M. Kokhanyuk, B.L. Zhuikov (*INR RAS*), I. Liu, J. Vincent, A.Z. Zyuzin (*TRIUMF*)
807. Study of the vortex-state in highly anisotropic single crystalline high- T_c superconductors [active], Th. Blasius, Ch. Niedermayer (*Univ. Konstanz*), E.J. Ansaldò (*Univ. of Saskatchewan*), D. Pooke, J. Tallon (*NZIRD*), J.I. Budnick (*Univ. of Connecticut*), C. Bernhard (*Max Planck Inst.*), D.R. Noakes, C. Stronach (*Virginia State Univ.*), K. Kishio (*Univ. of Tokyo*)
808. Spin glass order in magnets frustrated by competing ferro- and antiferromagnetic exchange [active], G.M. Kalvius, A. Kratzer, W. Potzel (*Techn. Univ. Munich*), R. Wäppling (*Univ. of Uppsala*), D.R. Noakes (*Virginia State Univ.*), J. Gal (*Beer Sheva Univ.*), W. Schäfer (*Bonn Univ.*), S. Kreitzman (*TRIUMF*)
809. Quantum diffusion of muonium in crystals with orientational degrees of freedom [active], D. Arseneau, B. Hitti, S.R. Kreitzman (*TRIUMF*), J.H. Brewer, A. Izadi, G.D. Morris (*Univ. of British Columbia*), D.G. Eshchenko (*INR, Moscow*), V.G. Storchak (*Kurchatov Inst.*), J.D. Brewer (*Simon Fraser Univ.*)
810. First direct study of the $^{23}\text{Mg}(p, \gamma)^{24}\text{Al}$ reaction with a recoil mass separator (DRAGON) [active], N.P.T. Bateman, J.M. D'Auria, D. Hunter, R. Korteling (*Simon Fraser Univ.*), R.N. Boyd (*Ohio State Univ.*), L. Buchmann, R. Helmer, D. Hutcheon, K.P. Jackson, A. Olin, J. Rogers (*TRIUMF*), U. Giesen, G. Roy (*Univ. of Alberta*), L. Gialanella, U. Greife, C. Rolfs, F. Strieder, H.-P. Trautvetter (*Ruhr-Univ. Bochum*), A. Hussein (*Univ. of Northern British Columbia*), M. Junker (*INFN Gran Sasso*), J.D. King (*Univ. of Toronto*), P.D. Parker (*Yale Univ.*), A. Shotter (*Univ. of Edinburgh*), M. Wiescher (*Univ. of Notre Dame*)
811. A direct study of the $^{19}\text{Ne}(p, \gamma)^{20}\text{Na}$ reaction with a recoil mass separator (DRAGON) [active], N.P.T. Bateman, J.M. D'Auria, D. Hunter, R. Korteling (*Simon Fraser Univ.*), R.N. Boyd (*Ohio State Univ.*), L. Buchmann, R. Helmer, D. Hutcheon, K.P. Jackson, A. Olin, J. Rogers (*TRIUMF*), U. Giesen, G. Roy (*Univ. of Alberta*), L. Gialanella, U. Greife, C. Rolfs, F. Strieder, H.-P. Trautvetter (*Ruhr-Univ. Bochum*), A. Hussein (*Univ. of Northern British Columbia*), M. Junker (*INFN Gran Sasso*), J.D. King (*Univ. of Toronto*), P.D. Parker (*Yale Univ.*), A. Shotter (*Univ. of Edinburgh*), M. Wiescher (*Univ. of Notre Dame*)
812. Proposed study of the $^8\text{Li}(\alpha, n)^{11}\text{B}$ reaction [active] R.N. Boyd (*Ohio State Univ.*), L. Buchmann (*TRIUMF*), J.M. D'Auria (*Simon Fraser Univ.*), J.D. King (*Univ. of Toronto*), I. Tanihata (*RIKEN*)
813. A study of the $^{15}\text{O}(\alpha, \gamma)^{19}\text{Ne}$ reaction at the astrophysically important energy [active], N.P.T. Bateman, J.M. D'Auria, D. Hunter, R. Korteling (*Simon Fraser Univ.*), R.N. Boyd (*Ohio State Univ.*), L. Buchmann, R. Helmer, D. Hutcheon, K.P. Jackson, A. Olin, J. Rogers (*TRIUMF*), U. Giesen, G. Roy (*Univ. of Alberta*), U. Greife, C. Rolfs, F. Strieder, H.-P. Trautvetter (*Ruhr-Univ. Bochum*), A. Hussein (*Univ. of Northern British Columbia*), J.D. King (*Univ. of Toronto*), P.D. Parker (*Yale Univ.*), A. Shotter (*Univ. of Edinburgh*), M. Wiescher (*Univ. of Notre Dame*)
814. μSR studies of unconventional superconductivity in Sr_2RuO_4 [active], Y. Fudamoto, K.M. Kojima, M. Larkin, G.M. Luke, J. Merrin, B. Nachumi, Y.J. Uemura (*Columbia Univ.*), Y. Maeno (*Kyoto Univ.*), R.J. Cava (*Princeton Univ.*)

84

86

88

815. β -NMR investigation of magnetic multilayers and giant magnetoresistance [active], J.C. Chakhalian, S. Dunsiger, W.A. MacFarlane, R. Miller, J. Pond, J. Sonier, B. Turrell (*Univ. of British Columbia*), R.F. Kiefl (*UBC-TRIUMF*), B.D. Gaulin (*McMaster Univ.*), M. Gingras (*Univ. of Waterloo*), R. Heffner (*Los Alamos National Lab*), B. Heinrich (*Simon Fraser Univ.*), B. Ittermann (*Univ. of Marburg*)
816. Semiconductor quantum wells investigated by β -NMR [active], J.H. Brewer, J.C. Chakhalian, S. Dunsiger, R. Miller, T. Tiedje (*Univ. of British Columbia*), M. Gingras (*Univ. of Waterloo*), B. Ittermann (*Univ. of Marburg*), B. Hitti, P. Levy, S.R. Kreitzman, A. Zelenski (*TRIUMF*), R.F. Kiefl (*TRIUMF-UBC*)
817. β -NMR investigation of type II superconductors [active], D. Bonn, J.H. Brewer, J.C. Chakhalian, S. Dunsiger, W. Hardy, R. Liang, R.F. Kiefl, W.A. MacFarlane, R. Miller, J. Sonier (*Univ. of British Columbia*), M. Gingras (*Univ. of Waterloo*), R. Heffner (*Los Alamos National Lab*), B. Ittermann (*Univ. of Marburg*), B. Hitti, P. Levy, S.R. Kreitzman, A. Zelenski (*TRIUMF*), G.M. Luke (*Columbia Univ.*), J.W. Brill (*Univ. of Kentucky*)
818. μ^+ SR study of magnetic ordering in the one-dimensional spin-1/2 antiferromagnet copper benzoate [active], J.C. Chakhalian, S. Dunsiger, R.F. Kiefl, W.A. MacFarlane, R. Miller, J. Sonier (*Univ. of British Columbia*), C. Broholm, D.C. Dender, P. Hammar, D. Reich (*Johns-Hopkins Univ.*), G. Luke, T. Uemura (*Columbia Univ.*)
819. μ^+ SR studies of the antiferromagnetic instability and metastable state in colossal magnetoresistance system $(\text{Nd}_{1-y}\text{Sm}_y)_{1/2}\text{Sr}_{1/2}\text{MnO}_3$ ($y = 0.875$) [active], W. Higemoto, I. Watanabe (*RIKEN*), K. Nishiyama (*KEK*), K. Nagamine (*RIKEN-KEK*), A. Asamitsu, H. Kuwahara, Y. Tokura (*JRCAT, Univ. of Tokyo*)
821. Shape coexistence and shape mixing in neutron-deficient platinum isotopes: on-line nuclear orientation studies of the decays of ^{182}Au and ^{186}Au [active], K.S. Krane (*Oregon State Univ.*), J.L. Wood (*Georgia Inst. of Tech.*), J. D'Auria (*Simon Fraser Univ.*)
822. Effect of disorder on quantum spin liquid state [active], J. Akimitsu, K. Ishii, K. Oishi, T. Yokoo (*Aoyama Gakuin Univ.*), R. Kadono, K. Nagamine (*RIKEN*), K. Nishiyama (*KEK*)
823. Pure fermi decay in medium mass nuclei [active], J. Cerny, D.M. Moltz, J. Powell (*Lawrence Berkeley Lab*), G. Savard (*Argonne National Lab*), J.C. Hardy (*Texas A&M Univ.*), S. Bishop, J. D'Auria (*Simon Fraser Univ.*), G.C. Ball, P. Bricault, J.A. Macdonald (*TRIUMF*), J.R. Leslie, H.-B. Mak, I.S. Towner (*Queen's Univ.*) 60
824. Measurement of the astrophysical rate of the $^{21}\text{Na}(p,\gamma)^{22}\text{Mg}$ reaction [active], N.P.T. Bateman, J.M. D'Auria, U. Giesen, D. Hunter, R. Korteling (*Simon Fraser Univ.*), R.N. Boyd (*Ohio State Univ.*), L. Buchmann, R. Helmer, D. Hutcheon, K.P. Jackson, A. Olin, J. Rogers (*TRIUMF*), U. Giesen (*SFU-TRIUMF*), G. Roy (*Univ. of Alberta*), U. Greife, C. Rolfs, F. Strieder, H.-P. Trautvetter (*Ruhr-Univ. Bochum*), A. Hussein (*Univ. of Northern British Columbia*), J.D. King (*Univ. of Toronto*), P.D. Parker (*Yale Univ.*), A. Shotter (*Univ. of Edinburgh*), M. Wiescher (*Univ. of Notre Dame*), S. Kubono (*Univ. of Tokyo*), T. Motobayashi (*Rikkyo Univ.*) 62
825. Equilibrium defects and order in intermetallic compounds studied using isomeric probes [active], G.S. Collins (*Washington State Univ.*)
826. Studies of ultrathin magnetic films with implanted isotopes [active], R. Kiefl, A. Kotlicki, J. Pond, B.G. Turrell (*Univ. of British Columbia*), R.C.C. Ward, M.R. Wells (*Oxford Univ.*), J.M. D'Auria, B. Heinrich (*Simon Fraser Univ.*), C.A. Davis, P.P.J. Delheij (*TRIUMF*), K. Krane (*Oregon State Univ.*), P. Mantica (*Michigan State Univ.*), J.L. Wood, (*Georgia Inst. of Tech.*)
827. Parity violation in ^{182}W [active], J. D'Auria (*TRIUMF-SFU*), C.A. Davis P.P.J. Delheij (*TRIUMF*), R. Kiefl, A. Kotlicki, J. Pond, B. Turrell (*Univ. of British Columbia*), K.S. Krane (*Oregon State Univ.*)
828. Nuclear moments in the mass-100 region [active], K.S. Krane (*Oregon State Univ.*), J.L. Wood (*Georgia Inst. of Tech.*), J.M. D'Auria, B. Heinrich (*Simon Fraser Univ.*), C.A. Davis, P.P.J. Delheij (*TRIUMF*), P. Mantica (*Michigan State Univ.*), R. Kiefl, A. Kotlicki, J. Pond, B.G. Turrell (*Univ. of British Columbia*), R.C.C. Ward, M.R. Wells (*Oxford Univ.*)
829. Muonium as a hydrogen isotope: reactions in solution [active], D.P. Chong, G.B. Porter, D.C. Walker (*Univ. of British Columbia*), K. Venkateswaran (*Hindustan Lever Ltd.*), H.A. Gillis (*St. Francis Xavier Univ.*)
830. The hot entropy bubble and the decay of ^9Li [active], N. Bateman (*TRIUMF-SFU-Toronto*), L. Buchmann, K.P. Jackson, S. Karataglidis, T. Shoppa, E. Vogt (*TRIUMF*), J. Chow, J.D. King, C. Martin (*Univ. of Toronto*), T. Davison, A. Ostrowski, A. Shotter (*Univ. of Edinburgh*), J. D'Auria, U. Giesen (*Simon Fraser Univ.*), E. Gete, D. Measday (*Univ. of British Columbia*)
831. Magnetic properties of $\text{REBa}_2\text{Cu}_3\text{O}_x$ [active], D. Andreica, F.N. Gygax, M. Pinkpank, A. Schenck (*ETH Zürich*), B. Hitti (*TRIUMF*), A. Amato (*PSI*), J.H. Brewer (*UBC-TRIUMF*) 89
832. Study of the non-magnetic-magnetic transition in the $\text{Yb}(\text{Cu}_{1-x}\text{Ni}_x)_2\text{Si}_2$ system [active], D. Andreica, F. Gygax, M. Pinkpank, A. Schenck (*ETH Zürich-PSI*), A. Amato (*PSI*), B. Hitti (*TRIUMF*) 90

833. μ SR studies of doped MnSi and $V_{2-y}O_3$: non-fermi-liquid behaviour, spin fluctuations and itinerant magnetism [active], Y. Fudamoto, K. Kojima, M. Larkin, G.M. Luke, B. Nachumi, O. Tchernyshyov, Y.J. Uemura (*Columbia Univ.*), R.H. Heffner, J. Sorrao (*Los Alamos National Lab*), D.E. MacLaughlin (*Univ. of California, Riverside*), M. Isobe, K. Ueda, Y. Ueda (*Univ. of Tokyo*), Z. Fisk (*Florida State Univ.*), J.H. Brewer (*Columbia Univ.-UBC*)
834. μ SR study of transverse spin freezing in bond-frustrated magnets [active], A. Kuprin, D.H. Ryan, J. van Lierop (*McGill Univ.*), J.M. Cadogan (*UNSW*)
835. μ SR studies of intercalated HfN and Bi2212 superconductors [active], Y. Fudamoto, I. Gat, M. Larkin, B. Nachumi, Y.J. Uemura (*Columbia Univ.*), G.M. Luke (*McMaster Univ.*), K. Kojima (*Univ. of Tokyo*), R.H. Heffner (*Los Alamos National Lab*), D.E. MacLaughlin (*Univ. of California, Riverside*), S. Yamanaka (*Hiroshima Univ.*)
836. Elasticks [active], R.E. Azuma, J.D. King (*Univ. of Toronto*), G. Ball, L. Buchmann, K.P. Jackson, B. Jennings, S. Karataglidis, E. Vogt (*TRIUMF*), N. Bateman (*TRIUMF-SFU-Univ. of Toronto*), T. Davison, A. Ostrowski, A. Shotter (*Univ. of Edinburgh*), J. D'Auria (*Simon Fraser Univ.*), W. Galster (*Univ. Catholique de Louvain*), G. Roy (*Univ. of Alberta*)
837. Pion-induced errors in memory chips [active], J.T. Brack, G. Hofman, J. Patterson R.J. Peterson, R.A. Ristinen (*Univ. of Colorado*), J.F. Ziegler (*IBM*), M.E. Nelson (*US Naval Academy*), G. Smith (*TRIUMF*) 63
838. Measurement of the $\pi^- p \rightarrow \gamma \gamma n$ capture mode of pionic hydrogen [active], S. Arole, T. Gorringer, M. Kovash, S. Tripathi, P. Zolnierczuk (*Univ. of Kentucky*), D. Armstrong, J. Clark (*College of William and Mary*), M. Hasinoff (*Univ. of British Columbia*), D. Wright (*TRIUMF*) 64
839. Thermal test of prototype high power ISAC target [active], D. Drake, D. Liska, W.L. Talbert, M. Wilson (*Amparo Corp.*), P. Bricault, M. Dombisky, P. Schmor (*TRIUMF*), E. Dalder, C. Landram, K. Sale, D. Slaughter (*Lawrence Livermore National Lab*), J. Nolen, G. Savard (*Argonne National Lab*), G. Alton (*Oak Ridge National Lab*)
840. Muon transfer from excited states of muonic hydrogen with x-ray measurement [active], S. Sakamoto, K. Shimomura (*KEK*), K. Nagamine (*KEK-RIKEN*), K. Ishida, N. Kawamura, Y. Matsuda, T. Matsuzaki, S.N. Nakamura, P. Strasser (*RIKEN*)
841. ISAC beam and target development [active], P. Bricault, M. Dombisky (*TRIUMF*)
842. Muonium-substituted free radicals in sub- and supercritical water [active], B. Addison-Jones, J.-C. Brodovitch, K. Ghandi, P.W. Percival (*Simon Fraser Univ.*), J. Schüth (*Univ. Bonn*)
843. Quadrupole ordering in dense Kondo system studied by μ LCR [active], J. Akimitsu, K. Kakuta, K. Ohishi (*Aoyama Gakuin Univ.*), W. Higemoto, R. Kadono (*KEK-IMSS*), T. Yokoo (*CREST*)
844. Quantum impurities in one dimensional spin 1/2 chains [active], I. Affleck, J. Brewer, J. Chakhalian, S. Dunsiger, R.F. Kiefl, R. Miller, A. Price (*Univ. of British Columbia*), S. Eggert (*Chalmers Univ.*), B. Hitti (*TRIUMF*), A.A. Keren (*Israel Inst. of Tech.*), W.A. MacFarlane (*Univ. Paris-Sud*), G. Morris (*UBC-TRIUMF*), Y.J. Uemura (*Columbia Univ.*), M. Verdagner (*CNRS*), I. Yamada (*Chiba Univ.*)
845. μ SR studies of vortex phases in (Ba,K)BiO₃ [active], G.M. Luke, M.A. Lumsden (*McMaster Univ.*), Y. Fudamoto, M.I. Larkin, Y.J. Uemura (*Columbia Univ.*), K.M. Kojima (*Univ. of Tokyo*), M. Gingras (*Univ. of Waterloo*), I. Joumard, T. Klein, J. Marcus (*Univ. of Grenoble*)
846. Complex order parameter symmetry in YB₂Cu₃O_{7- δ} at low T and high magnetic field [active], I. Affleck, D.A. Bonn, J.H. Brewer, J.F. Carolan, W.N. Hardy, R.F. Kiefl, R.-X. Liang, R.I. Miller, P.C.E. Stamp (*Univ. of British Columbia*), A.V. Balatsky, R.H. Heffner, J.E. Sonier (*Los Alamos National Lab*), G.M. Luke (*McMaster Univ.*), D.R. Noakes, C.E. Stronach (*Virginia State Univ.*)
847. Electron-doped high- T_c superconductors [active], R.H. Heffner, J. Sarrao, J.E. Sonier (*Los Alamos National Lab*), G.M. Luke (*McMaster Univ.*), J.H. Brewer, R.F. Kiefl, A. Price (*Univ. of British Columbia*), A. Yaouanc (*CEADRF Grenoble*)
848. μ SR investigation of the vortex state of YBa₂Cu₃O_{6+x} [active], D. Bonn, J.C. Chakhalian, S. Dunsiger, W.N. Hardy, R.X. Liang, R. Miller, A. Price (*Univ. of British Columbia*), J.H. Brewer, R.F. Kiefl (*UBC-TRIUMF*), J. Sonier (*Los Alamos National Lab*)
849. Spin structure and magnetic volume fraction of La214 systems: revisiting “1/8”, “stripes”, “spin glass”, and “swiss cheese” [active], T. Kakeshita, K.M. Kojima, T. Ono, S. Uchida (*Univ. of Tokyo*), Y. Fudamoto, I. Gat, M. Larkin, Y.J. Uemura (*Columbia Univ.*), G.M. Luke (*McMaster Univ.*), B. Nachumi (*NIST*), R.H. Heffner (*Los Alamos National Lab*), D.E. MacLaughlin (*Univ. of California, Riverside*)

850. Effects of dilute (Cu,Zn) substitution in spin gap systems SrCu_2O_3 and CuGeO_3 [active], Y. Fudamoto, I. Gat, M.I. Larkin, Y.J. Uemura (*Columbia Univ.*), K.M. Kojima, K. Manabe, K. Uchinokura (*Univ. of Tokyo*), G.M. Luke (*McMaster Univ.*), M. Azuma, M. Takano (*Kyoto Univ.*)
852. Magnetic phases in geometrically frustrated rare earth pyrochlores [active], R. Kiefl (*UBC-TRIUMF*), B.D. Gaulin, G. Luke, M.A. Lumsden (*McMaster Univ.*), M.J.P. Gingras (*Univ. of Waterloo*), J.S. Gardner, J.M. Roper (*Los Alamos National Lab*), J. Chakhalian, S. Dunsiger, R. Miller, A. Price (*Univ. of British Columbia*), W.A. MacFarlane, P. Mendels (*Univ. Paris-Sud*)
856. μSR study on CuO [active], W. Higemoto, K. Nishiyama, K. Shimomura (*KEK*), M. Suzuki, S. Tanaka, N. Tsutsumi, X.G. Zheng (*Saga Univ.*)
857. Investigation of the magnetic properties of the cerium compound probed by negative muon [active], W. Higemoto, K. Nagamine, K. Nishiyama, K. Shimomura (*KEK*), V.V. Krishnamurthy (*RIKEN*)
858. Repolarization of muonic atom in semiconductors by laser optical pumping in solids [active], W. Higemoto, R. Kadono, K. Nagamine, K. Nishiyama K. Shimomura (*KEK*)

*deceased

LIFE SCIENCES PROJECT PROPOSALS

	Page
LS0. PET facilities [active], <u>K.R. Buckley</u> , E.T. Hurtado (<i>TRIUMF</i>), S. Jivan (<i>UBC-TRIUMF</i>)	92
LS1. Attenuation maps for quantitative SPECT [completed], <u>A. Celler</u> (<i>UBC-VHHSC</i>), S. McFarland (<i>Univ. of British Columbia</i>), S. Barney, M. Limber (<i>Simon Fraser Univ.</i>)	
LS2. Synthesis of ^{18}F -glycosides as potential imaging agents for the study of glycosidase activity in the brain [active], <u>M.J. Adam</u> (<i>TRIUMF</i>), D. Lyster (<i>Vancouver Hospital & Health Sciences Centre</i>), G. Matte (<i>Saskatoon Hospital</i>)	93
LS3. Synthesis of radiopharmaceuticals for positron emission tomography [active], <u>M.J. Adam</u> , K.R. Buckley, E.T. Hurtado, J. Huser, S. Jivan, J.-M. Lu, T.J. Ruth (<i>TRIUMF</i>)	93
LS4. TR13 targets for PET radioisotope production [active], K. Buckley, T. Hurtado, <u>T.J. Ruth</u> , S.K. Zeisler (<i>TRIUMF</i>)	93
LS5. Production and on-line separation of ^{124}I from enriched tellurium [active], W.Z. Gelbart, E.T. Hurtado, <u>T.J. Ruth</u> , N.R. Stevenson, S.K. Zeisler (<i>TRIUMF</i>), R.R. Johnson (<i>Univ. of British Columbia</i>)	
LS6. Bone calcium resorption studies in pre- and peri-menopausal women using accelerator mass spectrometry [completed], <u>R.R. Johnson</u> , A. Priestman, J.C. Prior (<i>Univ. of British Columbia</i>), A. Altman, W.Z. Gelbart, V. Sossi (<i>TRIUMF</i>), D. Berkovits, S. Ghelberg, M. Paul (<i>Racah Inst., Hebrew Univ. Jerusalem</i>), L.M. Shulman (<i>Chaim Sheba Med. Centre</i>), R. Chechik (<i>WI</i>), E. Venzel (<i>Simon Fraser Univ.</i>)	95
LS7. PET 3D data quantification and integration into a research clinical environment [completed], K.S. Morrison, T.J. Ruth, <u>V. Sossi</u> , M.W. Stazyk (<i>UBC-TRIUMF</i>), K.R. Buckley (<i>TRIUMF</i>), J.S. Barney (<i>Vancouver Hospital & Health Sciences Centre</i>), D. Sirota, B.J. Snow (<i>Univ. of British Columbia</i>)	
LS8. Radiotracers for the physical and biosciences [active], L. Buchmann, T.J. Ruth, S.K. Zeisler (<i>TRIUMF</i>), A.D.M. Glass, R.R. Johnson, M. Lowe, C.E.R. Orvig (<i>Univ. of British Columbia</i>), T.F. Budinger (<i>Lawrence Berkeley Lab.</i>)	94
LS10. Biological evaluation of radiohalogenated DNA aptamers [active], <u>H. Dougan</u> (<i>TRIUMF</i>), J.B. Hobbs, D.M. Lyster (<i>Univ. of British Columbia</i>), J.I. Weitz (<i>McMaster Univ.</i>)	95
LS11. Development of single photon imaging agents [active], <u>D. Lyster</u> (<i>UBC-VHHSC</i>), L. Alcorn, M. Hampong, T. Lutz, C. Vo (<i>Univ. of British Columbia</i>)	
LS12. A simulation platform for the design of position encoding multicrystal detectors [completed], A. Altman, <u>C. Moisan</u> , <u>J.G. Rogers</u> (<i>TRIUMF</i>), E. Hoskinson, G. Tsang (<i>Univ. of British Columbia</i>)	
LS13. Utility of 2-[F-18]-fluoro-2-deoxy-d-glucose SPECT imaging in the evaluation of patients with solitary pulmonary nodules [completed], A. Celler, D. Lyster, <u>D. Worsley</u> (<i>Univ. of British Columbia</i>), M. Adam (<i>TRIUMF</i>)	
LS14. Production of ^{127}Xe from cesium with 90–110 MeV protons [active], D. Pearce, <u>J. Vincent</u> (<i>TRIUMF</i>)	
LS15. Investigation of frame realignment on the reproducibility of ^{18}F -6-fluorodopa positron emission tomography [active], <u>K.S. Morrison</u> , T.J. Ruth (<i>UBC-TRIUMF</i>), B.J. Snow (<i>Univ. of British Columbia</i>)	
LS17. Table-top radiocarbon facility [active], W. Gelbart, <u>R.B. Schubank</u> (<i>TRIUMF</i>), E. Venczel (<i>UBC-SFU</i>), S. Calvert, R.R. Johnson, J. Nagel, T. Peterson, V. Sossi (<i>Univ. of British Columbia</i>), D.E. Nelson (<i>Simon Fraser Univ.</i>), J. Prior, K. Schoenholzer, R. Sutton, V. Walker (<i>UBC/VHHSC</i>), R. Middleton (<i>Univ. of Pennsylvania</i>), M. Paul (<i>Hebrew Univ. of Jerusalem</i>), J. Clague, L. Jackson, J. Lutenuer, D. Templeman-Kluit (<i>Geological Survey of Canada</i>), R.N. McNeely, J.-S. Vincent (<i>GSC Ottawa</i>), V. Barrie (<i>Pacific Geoscience Center</i>), D. Prior, K.R. Robertson, G. Vilks (<i>Bedford Inst. of Oceanography</i>), R. Brown, S. Wang (<i>Elemental Research Inc.</i>), J. Vogel (<i>Lawrence Livermore National Lab</i>), A.E. Litherland (<i>Univ. of Toronto</i>), S. Dias, S. Sood (<i>Ontario Hydro</i>), H.R. Andrews, R.M. Brown, R.J. Cornett (<i>AECL</i>), D.B. Carlisle (<i>Environment Canada</i>), J. Carron, A. Kabir, R.C.J. Wilkinson (<i>Canadian Centre for Inland Waters</i>), R. Gephart, P. Molton, D. Robertson (<i>Batelle Pacific Northwest Labs</i>)	
LS18. Cooperative development of ^{82}Sr -Rb generators for human use in Canada [completed], <u>J. Vincent</u> (<i>TRIUMF</i>), R. Beanlands (<i>Univ. of Ottawa Heart Inst.</i>), B. Bowen (<i>McMaster Univ.</i>), W. Dickie (<i>Nordion Int.</i>)	

- LS19. An ^{15}O -water generator: a feasibility study [active], K.R. Buckley, T.J. Ruth (*TRIUMF*)
- LS20. Prototype heat-pipe water target for ^{18}F -production [active], K.R. Buckley, E.T. Hurtado, T.J. Ruth (*TRIUMF*), J.W. Lenz (*private consultant*)
- LS21. Aluminum kinetics in plants [active], A. Glass, R.R. Johnson, L. Oliveira (*Univ. of British Columbia*), K. Buckley, Z. Gelbart (*TRIUMF*), D. Berkovitz, M. Paul (*Hebrew Univ. Jerusalem*), E. Venczel (*Simon Fraser Univ.*) 95
- LS22. Virtual national biomedical tracer facility [active], T.J. Ruth, J.S. Vincent (*TRIUMF*), E.J. Peterson, D. Phillips (*Los Alamos National Lab*)
- LS24. Scanning for early detection and staging of breast cancer: a comparative study using FDG PET and MIBI SPECT [active], P.F. Cohen, P. Klimo (*Lions Gate Hospital-UBC*), M. Cackette (*Ebco Industries Ltd.*), J. Whiffen (*JALORN*), V. Sossi (*TRIUMF-UBC*), J. Porter (*Nordion Int.*), R.R. Johnson (*Univ. of British Columbia*) 95
- LS25. 3D PET in human neuroreceptor studies: quantification and reconstruction [completed], K.S. Morrison, T. Oakes, T.J. Ruth, V. Sossi (*UBC-TRIUMF*), K.R. Buckley (*TRIUMF*), M. Krzywinski, M. Schulzer, J. Stoessel (*Univ. of British Columbia*) 96
- LS26. A gaseous planar positron source for routine 3D PET normalization [active], T. Oakes, T.J. Ruth, V. Sossi (*UBC-TRIUMF*), K. Buckley, S. Jivan, R. MacDonald (*TRIUMF*) 97
- LS27. The feasibility and efficacy of using 2-(F-18)-fluoro-2-deoxy-D-glucose (18-FDG) to evaluate children with musculoskeletal neoplasm [active], R. Anderson, J. Davis, D. Lyster, H.R. Nadel, T.J. Ruth, M. Stilwell, D. Worsley (*Univ. of British Columbia*)
- LS28. Evaluation of potentially viable myocardium with dobutamine myocardial SPECT imaging [active], H. Abbey, A.-Y. Fung, L. Hook, D.M. Lyster, D.F. Worsley (*Vancouver Hospital & Health Sciences Centre*), M. Adam, S. Jivan (*TRIUMF*) 97
- LS29. Production and distribution of FDG for clinical studies [active], D. Lyster, D. Worsley (*Vancouver Hospital & Health Sciences Centre*), P. Cohen (*Lions Gate Hospital*), H. Nadel (*Children's Hospital*), M.J. Adam, S. Jivan, T.J. Ruth, V. Sossi (*TRIUMF*) 97
- LS30. Life Sciences five year plan contribution [active], J.-M. Poutissou, T.J. Ruth, V. Sossi (*TRIUMF*), L. Robertson (*Univ. of Victoria*) 97
- LS31. Auger electron emitters for therapy-physics and chemistry [active], D. Pearce, T.J. Ruth, J. Vincent, A. Zyuzin (*TRIUMF*), V. Kokhanyuk, V. Kravchuk, B.L. Zhuikov (*INR Moscow*)
- LS32. ^{18}F - H_2 ^{18}O supply to the University of Alberta [active], S.A. McQuarrie, J.R. Mercer (*Univ. of Alberta*), A.J.B. McEwan (*CCI*), R.R. Johnson (*UBC-Ebco*), T.J. Ruth (*Univ. of British Columbia*)
- LS33. Evaluation and improvement of a dual head coincidence camera [active], K.S. Morrison, T.J. Ruth, V. Sossi (*UBC-TRIUMF*), M. Krzywinski (*Univ. of British Columbia*), P. Cohen (*Lions Gate Hospital*), P. Klimo (*Lions Gate Hospital-UBC*), T.K. Lewellen, D.A. Mankoff (*Univ. of Washington*) 98
- LS34. Production of ^{103}Pd [active], R.R. Johnson, R. Pavan (*Univ. of British Columbia*), M. Cackette, K.L. Erdman (*Ebco Industries Ltd.*), Z. Gelbart (*TRIUMF*) 95
- LS35. Development of F-18 labelled nitroimidazole PET imaging agents for tissue hypoxia [active], M.J. Adam (*TRIUMF*), K. Skov (*B.C. Cancer Research Centre-UBC*), S. Evans, C. Koch, A. Kuchera (*Univ. of Pennsylvania*), I. Baird (*Univ. of British Columbia*) 99